The Puu Oo Eruption of Kilauea Volcano, Hawaii: Episodes 1 Through 20, January 3, 1983, Through June 8, 1984

U.S. GEOLOGICAL SURVEY PROFESSIONAL PAPER 1463

COVER

Lava pond and low fountain within Puu Oo Crater shortly before onset of vigorous lava fountaining during episode 9. Lava was overflowing spillway, which is outside photograph at lower left. View approximately southward; photograph taken at 1559 H.s.t. September 15, 1983.

THE PUU OO ERUPTION OF KILAUEA VOLCANO, HAWAII: EPISODES 1 THROUGH 20, JANUARY 3, 1983, THOUGH JUNE 8, 1984

Fountain (approx 200 m high) emanating from Puu Oo vent, 6.5 hours after beginning of episode 10. Most voluminous flow, composed of sluggish pahoehoe, has traveled 300 to 400 m southeastward (toward lower left) from vent. An additional aa-flow lobe (lower right) heads northeast, directly toward camera, within evacuated episode 9 channel, and spatter-fed flows blanket north side of cone. Fountain produced a significant tephra deposit around much of Puu Oo. View southwestward; photograph by R.W. Decker, taken at 0730 H.s.t. October 5, 1983.

The Puu Oo Eruption of Kilauea Volcano, Hawaii: Episodes 1 Through 20, January 3, 1983, Through June 8, 1984

EDWARD W. WOLFE, *Editor*

U.S. GEOLOGICAL SURVEY PROFESSIONAL PAPER 1463

A comprehensive study of the first 1½ years of the most voluminous eruption of Kilauea Volcano in historical time

UNITED STATES GOVERNMENT PRINTING OFFICE, WASHINGTON : 1988

DEPARTMENT OF THE INTERIOR

DONALD PAUL HODEL, *Secretary*

U.S. GEOLOGICAL SURVEY

Dallas L. Peck, *Director*

Library of Congress Cataloging-in-Publication Data

The Puu OO eruption of Kilauea Volcano, Hawaii.

(U.S. Geological Survey professional paper ; 1463)
"A comprehensive study of the first 1 1/2 years of the most voluminous eruption of Kilauea Volcano in historical time."
Bibliography: p.
Supt. of Docs.: 19.16:1463
1. Kilauea Volcano (Hawaii)—Eruptions. I. Wolfe, Edward W. II. Series.
QE523.K5P88 1988 551.2'2'099691 86-600300

**For sale by the Books and Open-File Reports Section,
U.S. Geological Survey, Federal Center, Box 25425, Denver, CO 80225**

PREFACE

In contrast to many other of the world's active volcanoes, Kilauea erupts frequently and with relatively little danger to human life. Furthermore, access to much of the volcano is relatively easy. For these reasons, Kilauea Volcano is an unrivaled location for volcanologic research. Studies of basaltic volcanism there have been carried out for the past 75 years by the staff of the Hawaiian Volcano Observatory (HVO), which has been operated continuously by the U.S. Geological Survey since 1948. This tradition of volcanic studies was continued during the Puu Oo eruption, abetted by increasingly comprehensive and sophisticated instrumentation, a continuously developing understanding of Kilauean magmatic processes, and a level of logistic support, provided by helicopters, that was unprecedented.

The eruptive activity, which began on January 3, 1983, was episodic: Relatively brief periods of vigorous fountaining and high-volume flow production alternated with longer repose periods. By early June 1984, 20 distinct eruptive episodes had occurred. (At the time of this writing in June 1985, a total of 33 episodes had occurred, and the continuing Puu Oo eruption had become Kilauea's most voluminous in historical time.)

The Puu Oo eruption was intensely monitored by HVO during the first 1½ years, and a wealth of observational, instrumental, and analytical data were collected. The repetitive style of the eruption provided a superb opportunity to assess a range of eruptive-episode and repose-period behavior. This volume presents the results of the first year and a half of comprehensive geologic, geophysical, geochemical, and petrologic monitoring and study.

Note added in proof.—Episodic lava-fountain eruptions continued at Puu Oo through episode 47, in June 1986. In July 1986, as episode 48 was anticipated, a new vent opened approximately 3 km downrift from Puu Oo, and lava discharge from the Puu Oo vent ceased. Relatively slow, quiet lava discharge from the new vent has continued almost without interruption to the present time (June 22, 1988), building a broad lava shield and an apron of pahoehoe flows that extends across the south flank of Kilauea Volcano to the ocean.

CONTENTS

[Numbers designate chapters]

ILLUSTRATIONS

[Plates are in pocket]

1. GEOLOGIC OBSERVATIONS AND CHRONOLOGY OF ERUPTIVE EVENTS

By Edward W. Wolfe, Christina A. Neal, Norman G. Banks, and Toni J. Duggan

CONTENTS

ABSTRACT

The Puu Oo eruption began at Napau Crater in the east rift zone of Kilauea Volcano on January 3, 1983. In its first 1½ years, the eruption produced nearly 240×10^6 m^3 of new basalt, built a new 130-m-high cone (Puu Oo) at the principal vent, and spread basalt flows over more than 30×10^6 m^2 of the rift zone and south flank of the volcano. Several flows entered sparsely populated areas and destroyed 18 dwellings. The Puu Oo eruption continues unabated as of May 1985.

The initial outbreak was a fissure eruption. In sporadic eruptions over a 4-day period, the fissure system extended progressively farther downrift nearly 8 km, from Napau at the uprift end to the vicinity of the prehistoric cinder cone Kalalua at the downrift end. Extrusive activity then became localized south of Puu Kahaualea along a 1-km-long segment of the fissure system that erupted intermittently through mid-January.

During the next 17 months, 19 brief (9 hours to 12 days) episodes of vigorous fountaining and high-volume emission of lava flows alternated with longer (8–65 days) repose periods. During eruptive episodes, harmonic tremor was at high levels, and rapid subsidence occurred at Kilauea's summit. During repose periods, harmonic tremor was continuous but low, and Kilauea's summit inflated. New flows and vent deposits accumulated at a fairly steady rate that averaged 13×10^6 to 14×10^6 m^3/mo. Although the volume of lava produced in individual episodes ranged from 2×10^6 to 38×10^6 m^3, most episodes produced from 8×10^6 to 14×10^6 m^3. Lava-production rate increased through the series of eruptive episodes, and so comparable volumes of lava were discharged in progressively less time.

After episode 1, central-vent eruptions dominated. The primary vent during episodes 2 and 3 was south of Puu Kahaualea. Beginning with episode 4, Puu Oo, 1.5 km farther uprift, became the sole eruptive locus. From episodes 2 through 20, the dominant style was one in which a steep pipelike conduit delivered gas and disrupted lava through a vent in the floor of a broad crater within a growing cone of agglutinated spatter. This process formed a fountain that played above the surface of a pond formed of lava that had coalesced from the disrupted and degassed melt. The pond overflowed through a low point in the crater rim to feed one or more long, relatively narrow flows by way of a vigorous, channelized river of pahoehoe that underwent a transition to aa several kilometers from the vent. Most such flows were 4 to 8 km long and 100 to 500 m wide; a few were longer, and the longest extended more than 13 km from the vent.

The height of the fountain, which reached a maximum of nearly 400 m, was related in part to the lava-discharge rate but was strongly influenced by other factors that may have included changing conduit conditions, entrapment of gas during repose periods, and damping by coalesced melt in the pond and, possibly, in the conduit beneath. High, broad-based fountains that maintained a high level of turbulent effervescence across the entire crater impeded development of the pond and the efficient lava-delivery system that it supplied. Thus, during periods of higher fountaining, flows were more likely to be relatively disorganized and short; at such times, thick, spatter-fed flows were common.

The average velocity of the main, river-fed flows normally ranged from about 50 to 300 m/h, and a few times was from 400 to 500 m/h. The average velocity increased through the series of eruptive episodes, possibly in response to both decreased viscosity and increased discharge rate, which resulted in an increased supply of lava to the individual flows.

A tendency toward decreasing average flow thickness through the series of eruptive episodes also suggests that viscosity may have decreased as the Puu Oo eruption proceeded. Concomitantly increasing lava temperature, decreasing phenocryst content, and changing lava composition may all have been related to this apparent change in viscosity.

Low-level extrusive activity was common during repose periods. It was dominated by gradual ascent of the column of magma within the open pipe at Puu Oo Crater, and was punctuated by numerous occurrences of gas-piston activity.

INTRODUCTION

OVERVIEW OF THE FIRST 20 EPISODES

The Puu Oo eruption, in the middle part of Kilauea's east rift zone, began at 0031 H.s.t. January 3, 1983, at Napau Crater (fig. 1.1). Over the next few days, the eruptive-fissure system extended progressively farther northeastward, and the eruptive locus migrated downrift to the vicinity of the prehistoric cinder cone Kalalua. These events were preceded and accompanied by a large subsidence of Kilauea's summit (see chap. 6) and a swarm of shallow earthquakes that migrated northeastward to the vicinity of Kalalua (see chap. 7) as the eruptive dike worked its way downrift through the shallow rocks of the rift zone. Extrusive activity then became localized south of Puu Kahaualea along a 1-km-long segment of the fissure system that erupted intermittently through mid-January. During this first episode, the style was dominated by fissure eruptions that produced linear fountains as much as several hundred meters long. Spatter from these fountains built low ramparts adjacent to the eruptive fissures, and fluid sheets of pahoehoe, which converted locally to aa, spread from the erupting vents.

After the January fissure eruptions, repetitious central-vent eruptions dominated, first at the 1123 vent (designated by the time of its first eruptive activity) and subsequently at Puu Oo (fig. 1.1). Over the next 17 months (through the period covered by this chapter), there were 19 such eruptive episodes (fig. 1.2; table 1.1). Most were relatively brief occurrences of vigorous fountaining and high-volume production of lava flows, separated by longer periods of relative quiescence. During the eruptive episodes, harmonic tremor was at high levels, and rapid subsidence occurred at Kilauea's summit; during the repose periods, harmonic tremor was continuous but low, and Kilauea's summit inflated. Low-level eruptive activity precursory to the major eruptive episodes occurred during most of the repose periods.

Although both the spacing between eruptive episodes and the volume of lava discharged in successive episodes varied somewhat (fig. 1.3), a striking regularity developed. Repose periods ranged in length from 8 to 65 days, but more than 60 percent were from 2 to 4 weeks long. New flow and vent deposits accumulated in the rift zone at an average rate of 13×10^6 to 14×10^6 m^3/mo (value uncorrected for vesicularity). Although the monthly average was fairly steady, over time the durations of individual episodes tended to decrease, and the lava-discharge rates to increase (fig. 1.4; table 1.1). By the end of episode 20, approximately 240×10^6 m^3 of new flows and vent deposits covered 31×10^6 m^2 of the central part of the rift zone and south flank of Kilauea.

The flows of episodes 2 through 5 overran 15 dwellings in a sparsely populated subdivision, completely crushing and burying them after initially setting them on fire. Three more dwellings were destroyed by the episode 18 lava flow, which passed east of the subdivision and reached another sparsely populated area about a kilometer inland from the coast (pl. 1).

The central-vent eruptions built large pyroclastic cones at the 1123 vent and at Puu Oo. Subsequently, elders of the Hawaiian community at Kalapana named the 1123 vent "Pu'u Halulu," in reference to the chantlike sound they heard at Kalapana from the erupting vents. Informal names, "Puu O," and "O vent," for the nearby major episode 3 vent (see figs. 1.8, 1.29), were coined because of its proximity in map position to the letter "O" in the label "Lava Flow of 1965" on the topographic map then in use. The Kalapana elders subsequently chose "Pu'u 'O'o" as the name for the very large new cone that grew at this locality, northeast of Puu Kamoamoa within Hawaii Volcanoes National Park. The 'o'o is a native Hawaiian bird, now extinct, that once lived in the eruption area.

SIGNIFICANCE OF THE PUU OO ERUPTION

For most of its length, the eruptive-fissure system for the Puu Oo eruption is at the south edge of a 1- to 2-km-wide zone in which repeated eruptions occurred (pl. 1) from 1961 through 1969 (Richter and others, 1964; Wright and others, 1968; Moore and Koyanagi, 1969; Jackson and others, 1975; Swanson and others, 1979). Among the historical fissure systems of the middle east rift, only that of 1977 (Moore and others, 1980), which barely overlaps the east end of the Puu Oo system, is farther south. Through episode 1, the 1983 eruption was largely similar in style, duration, and eruptive products to these recent predecessors.

The episodic style of central-vent eruption that developed after episode 1 is unique in historical time in the middle east rift zone. However, it is strikingly similar to

FIGURE 1.1.—Index map of Kilauea area, showing locations of features described in text. UTM, Uwekahuna tiltmeter; bh, borehole tiltmeters KMM (near Puu Kamoamoa) and KLU (near Kalalua). Inset shows locations of observation stations, designated camps A through E.

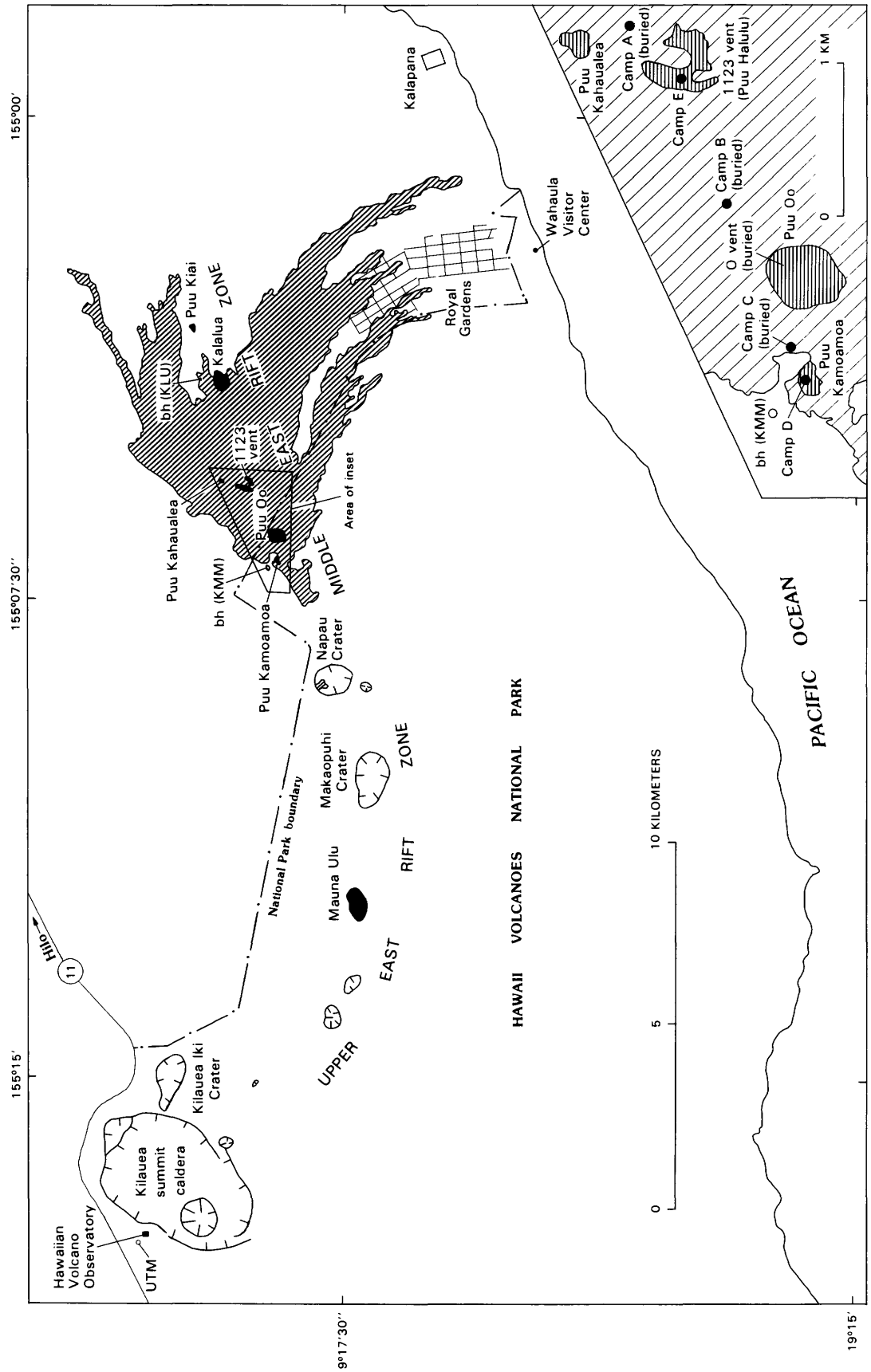
155°00'
155°07'30"
155°15'
19°17'30"
19°15'
Hilo
11
Hawaiian Volcano Observatory
UTM
Kilauea summit caldera
Kilauea Iki Crater
National Park boundary
UPPER EAST RIFT ZONE
Mauna Ulu
Makaopuhi Crater
Napau Crater
Puu Kamoamoa
bh (KMM)
Puu Kahaualea
MIDDLE EAST RIFT ZONE
1123 vent
Puu Oo
Area of inset
bh (KLU)
Puu Kiai
Kalalua
Royal Gardens
Kalapana
Wahaula Visitor Center
HAWAII VOLCANOES NATIONAL PARK
PACIFIC OCEAN
0 5 10 KILOMETERS
Puu Kahaualea
Camp A (buried)
Camp E
1123 vent (Puu Halulu)
Camp B (buried)
O vent (buried)
Puu Oo
Camp C (buried)
bh (KMM)
Camp D
Puu Kamoamoa
0 1 KM

the first stage of the 1969–71 Mauna Ulu eruption (Swanson and others, 1979), which took place in the upper part of the rift zone. In 12 episodes during a period of slightly more than 7 months, from May through December 1969, Mauna Ulu produced an estimated 69×10^6 m^3 of lava at a fairly steady average rate of approximately 10×10^6 m^3/mo (value uncorrected for vesicularity; Swanson, 1972). As at Puu Oo, the eruptive episodes at Mauna Ulu were characterized by high fountaining and rapid lava discharge. However, average volumes, average recurrence intervals, and average monthly lava-supply rates were smaller for Mauna Ulu (fig. 1.3). In addition, Mauna Ulu produced more pahoehoe than aa, whereas aa dominated after episode 1 at Puu Oo. After 12 episodes with high or sustained fountaining, the Mauna Ulu eruption became dominated by a steady slow discharge that built the Mauna Ulu shield and transported large volumes of pahoehoe to relatively great distances from the vent by way of a system of lava tubes (Peterson and Swanson, 1974; Peterson, 1976; Tilling and others, 1987). In contrast, the episodic style of the Puu Oo eruption has continued through episode 20 and beyond, producing one of the largest vent structures of Kilauea Volcano and creating an extraordinary complex of interleaved aa flows. Like the Mauna Ulu eruption, the Puu Oo eruption has given us an unusual opportunity for systematic study of magmatic and eruptive processes.

The Puu Oo eruption continued with remarkable indifference to tectonic and eruptive events on nearby Mauna Loa Volcano. A large ($M = 6.7$) earthquake (Koyanagi and others, 1984; Buchanan-Banks, 1987) occurred beneath Mauna Loa's southeast flank on November 16, 1983, between episodes 11 and 12 of the Puu Oo eruption. Although this earthquake caused a displacement of nearly 300 microradians at the Uwekahuna tiltmeter (fig. 1.2), it did not recognizably affect the continuing events at Puu Oo. A major Mauna Loa eruption occurred from March 25 to April 15, 1984 (Lockwood and others, 1985), and, for the first time since 1919, the two volcanoes were erupting simultaneously. Episode 17, which occurred on March 30–31 during the Mauna Loa eruption, and episode 18, which occurred on April 18–21 after the Mauna Loa eruption, followed the normal pattern.

SCOPE AND APPROACH

Our intent is to provide a systematic and thorough account of our observations of the eruptive processes and products during the first 1½ years of the Puu Oo eruption. Other chapters in this volume present concurrent

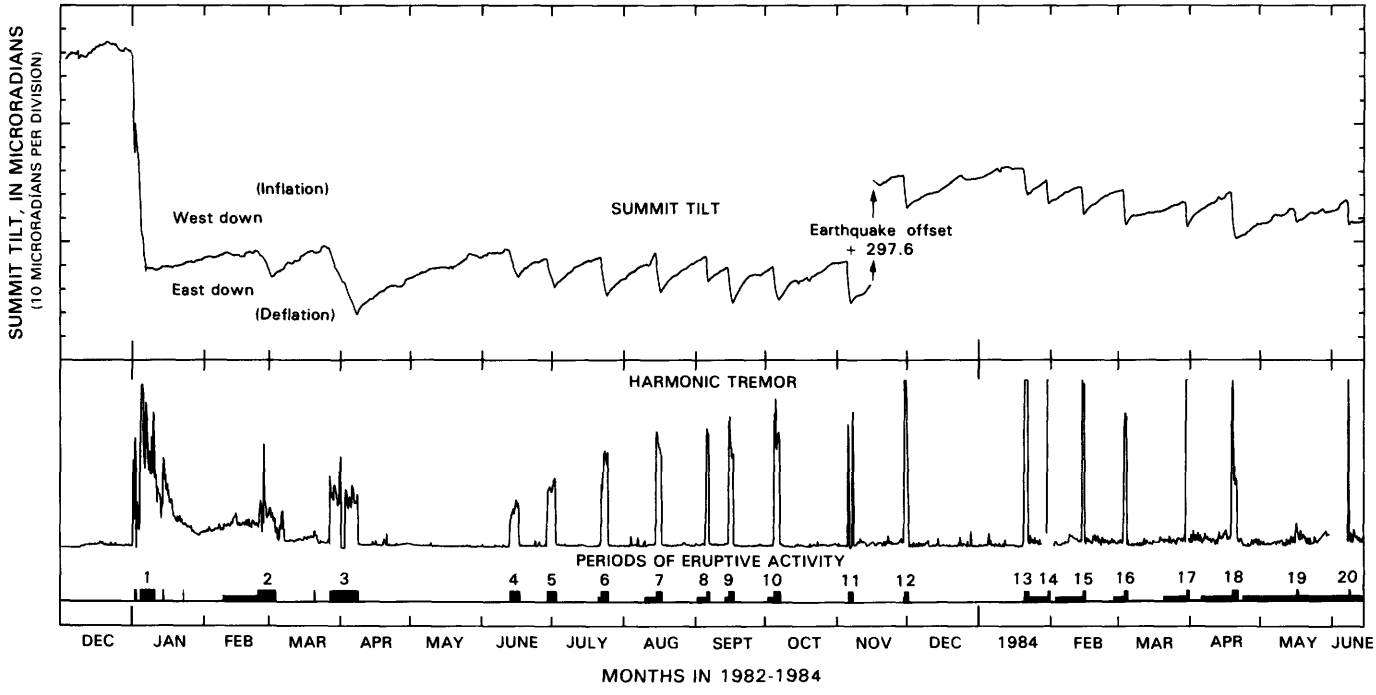

FIGURE 1.2.—Relations of Kilauea summit tilt and middle-east-rift-zone harmonic tremor and eruptive activity from December 1982 through June 1984. Summit tilt measured by Uwekahuna tiltmeter; note brief period of reinflation during the large summit subsidence in early January 1983. Relative amplitude of harmonic tremor was approximated by averaging signal from a seismic station near eruption site for a 10-minute period once every 6 hours; breaks in plot record data gaps. During episode 19, brief periods of high tremor did not coincide with programmed sampling intervals. Occurrences of major eruptive episodes (solid, full-height bars) and low-level volcanic activity (half-height bars) are shown for Puu Oo eruption, episodes 1 through 20 (numbers).

TABLE 1.1.—*Times of occurrence, durations, areas covered, volumes erupted, and lava-discharge rates for episodes 1 through 20 of the Puu Oo eruption, 1983–84*

[For episode 2, "low-level eruption" refers to a period of prolonged slow lava discharge (avg approx 1,400 m^3/h) from February 10 to 25, 1983. For episodes 3 through 20, it refers to a period, preceding a major eruption, during which any or all of the following phenomena were observed at the active vent: intermittent gas-piston activity, intermittent spattering, occasional emission of small pahoehoe flows, and presence of a visible lava surface (sometimes partly crusted) in the conduit extending downward from the crater floor. Normally, low-level eruptive activity was confined to the interior of the crater; however, on rare occasions, short-lived pahoehoe flows spilled from Puu Oo. The "beginning of vigorous eruption" was recognized in the following ways (order indicates priority): (1) direct observation of continuous emission of lava from the crater; (2) time-lapse camera record of beginning of continuous emission of lava from the crater; (3) where spillway activity was not recorded, time-lapse camera record of first appearance of fountaining above the crater rim; (4) beginning of rapid increase in harmonic-tremor amplitude. The "end of vigorous eruption" was recognized in the following ways (order indicates priority): (1) direct observation of cessation of lava discharge; (2) time-lapse camera record of cessation of fountaining; (3) rapid decay of harmonic-tremor amplitude. Lava-discharge rate is calculated only for period of vigorous eruption. Except for episode 2, the volume of lava erupted during periods of low-level activity was negligible]

Episode	First report of low-level eruption (H.s.t.)	Beginning of vigorous eruption (H.s.t.)	End of vigorous eruption (H.s.t.)	Duration of vigorous eruption (h)	Area covered (10^6 m^2)	Volume erupted (10^6 m^3)	Lava-discharge rate (10^3 m^3/h)
			1983				
[1]1	---	0031 Jan. 3	---	---	4.8	14	---
[2]2	1030 Feb. 10	0900 Feb. 25	1451 Mar. 4	174	2.7	14	80
3	0600 Mar. 21	0100 Mar. 28	0257 Apr. 9	290	7.9	38	130
4	---	1025 June 13	1413 June 17	100	2.2	11	110
5	1000 June 29	1251 June 29	0715 July 3	90	3.4	13	140
6	0600 July 21	1530 July 22	1630 July 25	73	2.0	9	120
7	1610 Aug. 8	0741 Aug. 15	1600 Aug. 17	56	3.7	14	250
[3]8	0900 Sept. 2	0511 Sept. 6	0526 Sept. 7	24	2.0	8	330
[3]9	0009 Sept. 14	1541 Sept. 15	1920 Sept. 17	52	2.1	8	150
10	0800 Oct. 2	0106 Oct. 5	1650 Oct. 7	64	2.7	14	220
11	---	2350 Nov. 5	1845 Nov. 7	43	4.3	12	280
12	1600 Nov. 29	0447 Nov. 30	1545 Dec. 1	35	3.0	8	230
			1984				
[3,4]13	1100 Jan. 20	1724 Jan. 20	1123 Jan. 22	42	2.6	10	230
[3]14	1123 Jan. 22	1745 Jan. 30	1318 Jan. 31	19	2.1	6	320
15	1000 Feb. 3	1940 Feb. 14	1501 Feb. 15	19	2.2	8	420
16	1900 Feb. 27	1450 Mar. 3	2231 Mar. 4	32	3.2	12	380
17	0910 Mar. 20	0448 Mar. 30	0324 Mar. 31	23	3.0	10	430
18	1340 Apr. 5	1800 Apr. 18	0533 Apr. 21	60	6.6	24	410
[5]19	0830 Apr. 23	0500 May 16	0050 May 18	44	1.4	2	50
20	0800 May 18	2104 June 7	0625 June 8	9	1.6	4	480

[1]Episode 1 was characterized by intermittent eruptive activity for nearly 3 weeks. Periods of active eruption totaled approximately 99 hours. The last sizable event occurred on January 15; a minor one occurred on January 23.

[2]During episode 2, approximately 0.5×10^6 m^3 of basalt was discharged during low-level eruption from February 10 to 25. The remaining 13.6×10^6 m^3 was discharged during the period of vigorous eruption at a rate of approximately 70,000 m^3/h.

[3]Flow was partly buried by younger basalt before it could be mapped in detail. Thus, uncertainty is greater in estimates of area, volume, and lava-discharge rate.

[4]Fountaining and flow production during episode 13 occurred in two main periods. The first, approximately 31 hours long, was separated by about 5 hours from the 6-hour-long second period.

[5]Episode 19 was characterized by low fountain activity and intermittent low-volume overflows from the lava pond within Puu Oo Crater. This activity was interrupted by four 1- to 3-hour-long periods, totaling about 7 hours altogether, of higher fountaining and increased lava discharge estimated at about 100,000 to 200,000 m^3/h.

geophysical, geochemical, and petrologic studies of the eruptive series, and an interpretative synthesis is given by Wolfe and others (1987).

The section below entitled "General Observations" is a topical treatment of eruptive phenomena and products, dealing mainly with the central-vent eruptions of episodes 2 through 20; it is followed by a chronologic narrative of the first 20 episodes. Plates 2 through 20 show the vent deposits and the distribution, thickness, and sequential flow-front positions for the flows produced during each eruptive episode. In addition, graphic summaries of flow progress are given on plates 1 through 5.

METHODOLOGY

The eruptive zone is in a relatively inaccessible part of Kilauea's east rift zone. Thus, we relied heavily on helicopters for monitoring eruptive episodes and repose-period activity. Because of the high cost of helicopter support, we visited the eruption area only intermittently during repose periods, and many times we were not on site at the beginnings of major episodes.

We made intensive use of time-lapse cameras, which were kept running most of the time, to supplement our first-hand observations. The resulting film record was helpful in reconstructing the style and timing of activity at the erupting vents, and it provided the basis for the fountain-height summary plots (see figs. 1.21–1.24). Fountain heights were measured from images projected onto a computerized digitizing tablet. Scaling for the plots came from measurements made periodically by transit or theodolite, from calibration of the cameras with a target of known size and distance, or from measurement in 35-mm frames from a camera with a lens of known focal length. The timing of such events as the beginning of an eruptive episode varies in quality for several reasons: (1) poor visibility due to inclement weather sometimes interfered with the camera view; (2) not all timing marks were adequately recorded at both the beginning and end of a roll of film; and (3) at longer frame intervals (more than a minute), the camera timing mechanism was sub-

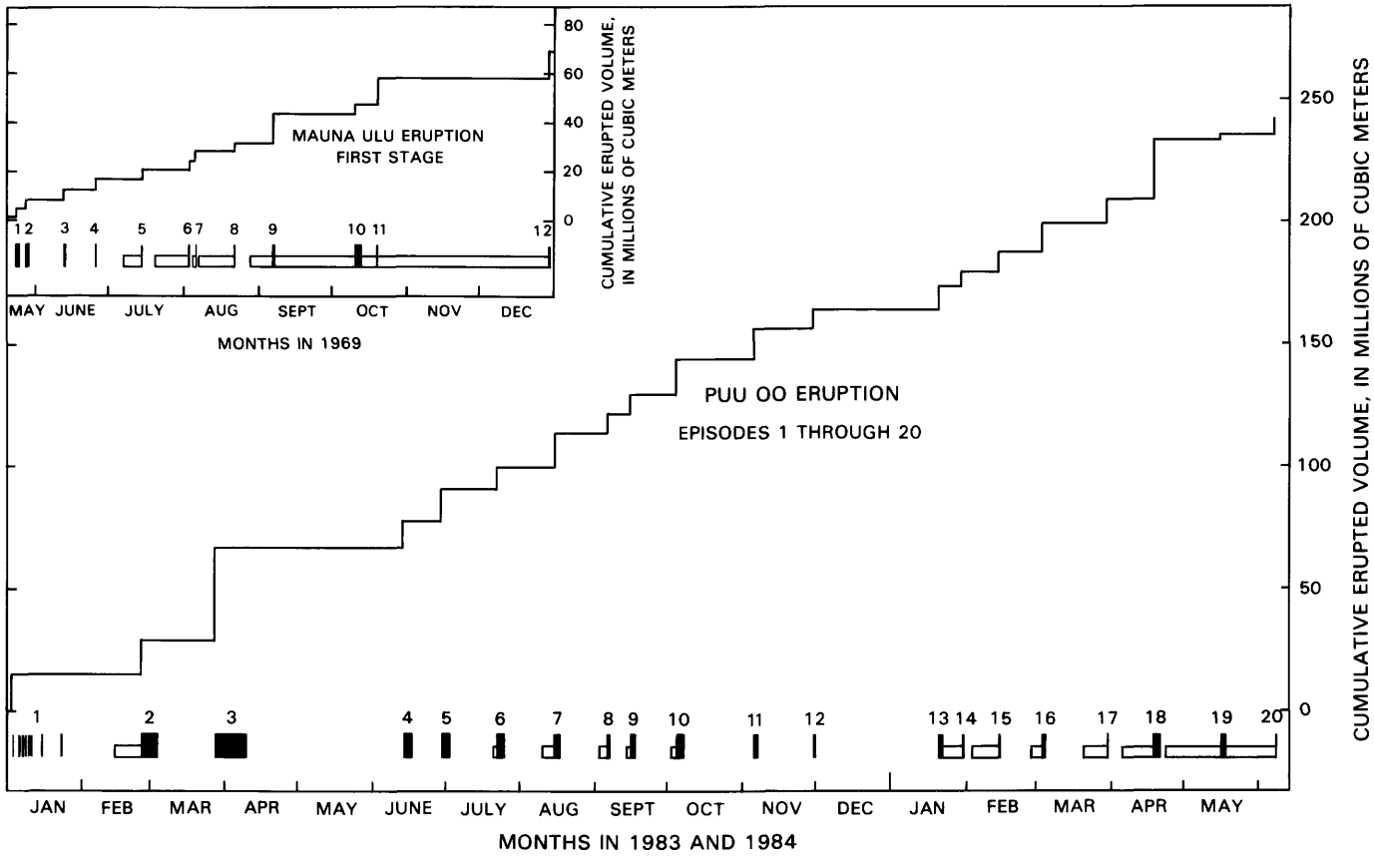

FIGURE 1.3.—Cumulative erupted volume, occurrence of major eruptive episodes (numbered solid blocks), and occurrence of low-level volcanic activity (open, half-height blocks) during first stage of 1969–71 Mauna Ulu eruption (Swanson and others, 1979) and episodes 1 through 20 of Puu Oo eruption.

ject to drift that may have led to cumulative errors of several minutes over periods as long as 7 days. Although the times of events recorded in many time-lapse frames are accurate to within a minute or less, reasons 2 and 3 may have led to errors that we surmise could be as large as 10 minutes.

A major effort was made to measure lava temperatures and to sample comprehensively. For the most part, we collected samples of melt and quenched them in water to minimize groundmass crystallization. During episode 1, many samples were of molten spatter from the fissure fountains. Later, the central-vent fountains were too difficult to approach, and most samples came from active pahoehoe. Air-fall lapilli were also collected. Details of temperature measurements, sample collection, and chemical analyses are presented in chapter 2, and sample studies in chapter 3.

During eruptive episodes, the flow-front progress was monitored periodically by helicopter surveillance. Sketches of the flows at these times, many made under conditions of poor visibility because of smoke from the burning forest and, at times, bad weather, are the basis for the successive flow-front positions shown in plates 1 through 5. Within the Royal Gardens subdivision, observers on the paved streets tracked the flow-front progress directly.

Flows and vent deposits were mapped with the help of aerial photographs taken as soon as possible after each major episode. In a few cases, one or two subsequent episodes occurred before the weather was suitable for aerial photography. The photographs were not of photogrammetric-mapping quality, and frames from several different flightlines were commonly required to create a single "pass" relatively free of clouds. Contacts were mapped on the photographs and transferred with an optical comparator to orthophotoquads. Because of planimetric distortions that resulted largely from imperfect plumb of the camera and the paucity of distinct photoidentifiable features in some of the rain forest, mapped contacts may be locally in error, probably by no more than 100 m at worst and normally much less. The mapping was field checked and is represented in the detailed maps of plates 1 through 5; these maps have been fitted to the published 1:24,000-scale topographic quadrangle maps.

Thicknesses were measured by handlevel at many points along the flow margins. We tried to avoid places where the observed thickness seemed abnormal—for example, where the flow edge had preferentially piled up against a kipuka, or where there was a large evacuated central channel. The measured thicknesses are shown on plates 1 through 5; they have been omitted for episode 1 because the episode 1 flows in the rift zone are a complex of overlapping flows that are not sorted out on plate 1.

The area covered during each episode was measured from the detailed 1:24,000-scale map, and the volume of lava was calculated using the measured thicknesses. The lava-discharge rate listed in table 1.1 is the measured volume divided by the number of hours of vigorous eruption.

Acknowledgments.—The entire staff of the Hawaiian Volcano Observatory (HVO) were involved in field observations, operational support, and other studies (reported elsewhere in this volume) related to the ongoing eruptive activity. We especially thank Jim Griggs, indefatigable staff photographer, for his extraordinary helpfulness and skill in aerial photography, eruption photography, endless darkroom work, and preparation of illustrations. U.S. Geological Survey (USGS) colleagues Jane Buchanan-Banks, John P. Lockwood, Richard B. Moore, and George E. Ulrich, delaying their own project work, each spent many days observing and sampling during eruptive episodes or assisting in eruption-related work during repose periods. Other USGS colleagues from the mainland, as well as university students and professors, in particular from the University of Hawaii, came to help, study, and learn. Our helicopter pilots brought a high level of skill, enthusiasm, and professionalism that contributed immeasurably to the ease of our work. We also received continuing cooperation and assistance from the personnel of Hawaii Volcanoes National Park. Lu Setnicka's clerical skill, attention to detail, and unending willingness and good humor were indispensable in completing the manuscript. Many friends invested long days and nights; their enthusiastic support helped us and made our work more fun, and we thank them. Continuing discussion with L.P. Greenland has been invaluable in focusing our thoughts and clarifying our ideas about some of the eruptive phenomena.

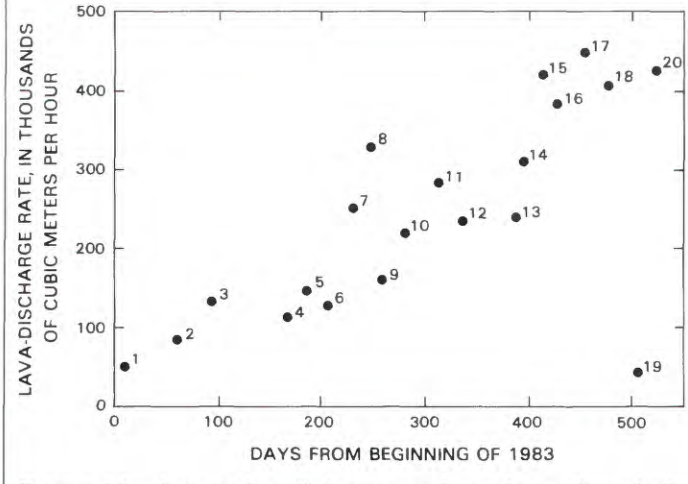

FIGURE 1.4.—Average lava-discharge rate for each eruptive episode (numbers) versus time since the beginning of 1983.

GENERAL OBSERVATIONS

DEVELOPMENT OF VENT STRUCTURES

In contrast to the low, linear spatter ramparts that formed during the fissure eruptions of episode 1, the central-vent eruptions of episodes 2 through 20 built large, cratered cones composed of agglutinated spatter, cinders, and rootless flows. The dominant eruptive style was one in which a broad columnar fountain or one or more small fountains rose above a lava pond within the crater. The major flow was fed by a lava river overflowing from the pond through a low point in the crater rim (fig. 1.5).

The central vents quickly became at least partly encircled by spatter rings built of fallout from the fountain, and further development of the vent structures through successive eruptive episodes resulted largely from upward and outward growth of the original ring structure. Asymmetry occurred, mostly because the prevailing northeast wind tended to concentrate the fallout on the leeward side of the fountain.

Growth of the cones resulted primarily from accumulation of molten spatter fragments, commonly as large as 1 m in diameter, that formed a fragile agglutinate which built steep and commonly unstable crater walls and cone flanks. Fountains higher than about 100 m produced abundant fine-grained tephra. At these times, accumulating, highly vesicular air-fall lapilli and bombs (fig. 1.6) formed thick local deposits that mantled the leeward flanks of the cones and extended as thin sheets a kilometer or more downwind. Fine tephra wafted upward by thermal currents commonly ascended hundreds of meters above the higher fountains, and Pele's hair was carried as far as 45 km from the vent.

FIGURE 1.5.—1123 vent erupting during episode 2. Fountains are erupting through a nearly circular lava pond, about 60 m in diameter. A thin nonincandescent skin covers most of pond surface. Base of main fountain is about 40 m wide. High part of enclosing rim is a steep rampart of agglutinated spatter, formed from fallout that accumulated on downwind side of fountain. Low part of ring, though partly of pyroclastic origin, is mainly a pahoehoe bulwark built by overflows and by lava that leaked from enclosed pond through short lava tubes. A voluminous lava river debouches from pond through a low place in south rim of enclosing levee. Western part of recently active 0740 cones (at left) is glowing and emitting fume. Fume near right edge of photograph is from easternmost of a discontinuous line of small vents extending uprift from main vent. View southward; photograph by J.P. Lockwood, taken during the afternoon of March 1, 1983.

Changing fountain trajectories commonly caused brief, intense bombardment of a sector of the cone's flank by spatter. Short-lived, spatter-fed pahoehoe flows normally resulted (fig. 1.7), most of which were subsequently buried by agglutinated spatter or loose tephra.

GROWTH OF PUU OO

Although fissure vents had erupted at or near the site of Puu Oo during episodes 1 and 2, Puu Oo emerged as a distinct central-vent edifice during episode 3. The progenitor of Puu Oo was a pair of juxtaposed spatter rings enclosing low fountains (fig. 1.8) about 50 m west of the vigorously erupting O vent, which had also been active in this area for part of episode 2. By the second day of episode 3 (March 29, 1983), these two spatter rings had coalesced to form a single crater with a low fountain that erupted weakly along with the more vigorous O vent until both shut off on March 30. Episode 3 activity continued for several more days at the 1123 vent.

Beginning with episode 4, the newly formed Puu Oo was the sole eruptive locus except for nearby, short-lived fissure vents that erupted weakly along with Puu Oo during episodes 4 and 11. By the end of episode 4, the main part of Puu Oo was a steep-sided, truncated cone, about 20 to 30 m high and 100 m wide (fig. 1.9); a smaller, satellitic cone had formed on its west flank, where episode 4 fissure vents impinged on the main cone. A steep-walled crater, about 20 m deep, was enclosed within the main cone. During episodes 4 and 5, lava overflowed the crater through a narrow breach that formed a spillway in the south rim and fed flows that extended into the western part of the Royal Gardens subdivision. Near the end of episode 5, part of the northeast rim slumped sufficiently to create a low point over which episode 6 lava spilled. This initiated the development of a deep, steep-walled breach that for many months provided egress for lava during eruptions and ingress for geologists between major eruptive episodes.

With each successive episode, the cone grew higher and broader (fig. 1.10). Asymmetry was perpetuated by maintenance of the breach, which formed a low place in the northeast rim (fig. 1.11), and by preferential accumulation of spatter and air-fall deposits to the southwest,

FIGURE 1.6.—Puu Oo vent during episode 16. Fountain is 300 to 400 m high. Dark tephra, falling out to northeast, raises a cloud of dust where it strikes flank of Puu Oo. Additional fine tephra, visibly incandescent at night, is wafted above denser fountain by updrafts. Pulsating supply to fountain produced upward-surging fronts marked by zones of brighter incandescence. View eastward from camp D; photograph taken at 1659 H.s.t. March 3, 1984.

elongating the cone in that direction and forming a topographic peak in the southwestern part of the rim crest. In addition, production of thick spatter-fed flows created a prominent shoulder adjacent to the south flank of the cone (fig. 1.12). Occasionally, gravitational collapse resulted in a net decrease in height in some sections of the cone from one eruptive episode to the next. At the end of episode 19, the crater-rim crest was about 120 m above the local preeruption surface (fig. 1.11). The steep-walled cone, with average outer slopes of about 30°, was approximately 320 m in maximum diameter and surmounted a broad, more gently sloping apron composed of flows and local air-fall deposits. Visible from many distant vantage points, Puu Oo had become the most imposing topographic feature in the central part of Kilauea's east rift zone.

As the cone grew during successive eruptive episodes, the enclosed crater broadened. Normally, it was approximately circular in plan (fig. 1.13), except for a pronounced northeastward bulge during the later episodes from accentuated flaring of the rim adjacent to the spillway. After episode 4, the nearly circular rim crest was 40 to 50 m in diameter. After episode 19 (fig. 1.11), the maximum diameter of the rim, measured northwest-southeast, was about 120 m, and the distance from the southwest rim crest to the spillway was about 150 m.

Episodes 5 through 10 each left a main crater with a relatively flat floor, about 30 m in diameter. (A satellitic crater on the west flank of Puu Oo erupted during episode 5, in addition to the main crater.) The floor was covered with coarse breccia (fig. 1.14) composed of angular blocks from the walls, which rose steeply upward.

FIGURE 1.7.—Molten spatter fragments falling from episode 9 fountain and a thin, fluid, transient spatter-fed flow that formed moments earlier when fountain trajectory was inclined over northwest (right) flank. A still-cooling, earlier spatter-fed flow armors north flank (center). Older thick, spatter-fed aa that extends outward from base of cone forms steep flow front in foreground. Photograph taken at 1400 September 17, 1983, from 100 m north of the cone. Numerals (lower right) indicate date and time.

FIGURE 1.8.—Fountains and flows at and near O vent early in episode 3. Line of fountains is 100 to 150 m long. O vent is at left. Pair of spatter rings in center, each with a low fountain, is at site of Puu Oo; they coalesced within a day to form a single cone and crater. View southward; photograph taken at 0811 H.s.t. March 28, 1983.

FIGURE 1.9.—Puu Oo from floor of evacuated southeastern channel after episode 4. Main Puu Oo vent is marked by large spatter cone that stands about 20 m high and encloses a crater about 40 m in diameter. Lava feeding main flow spilled through narrow breach visible in south crater rim and formed steep-walled channel in foreground. Satellitic, western Puu Oo cone is visible on left shoulder of main Puu Oo cone. View northward; photograph taken at 1045 H.s.t. June 29, 1983.

Our impression was that superficial collapse of the steep walls must have occurred as lava withdrew into the conduit at the end of an eruptive episode. Normally, after these early episodes, no conduit opening was visible through the rubble. However, two closely spaced, open, vertical pipes, 3 to 4 m in diameter, were visible descending from the crater floor after episodes 8 and 9. Their walls exposed the edges of thin layers of platy and rubbly basalt that probably record successively buried levels of the crater floor (fig. 1.14).

The most profound intracrater collapse occurred at the end of episode 10. The resulting crater interior was a complex of blocks, including slices as much as tens of meters long, of the crater walls that had collapsed into the depres-

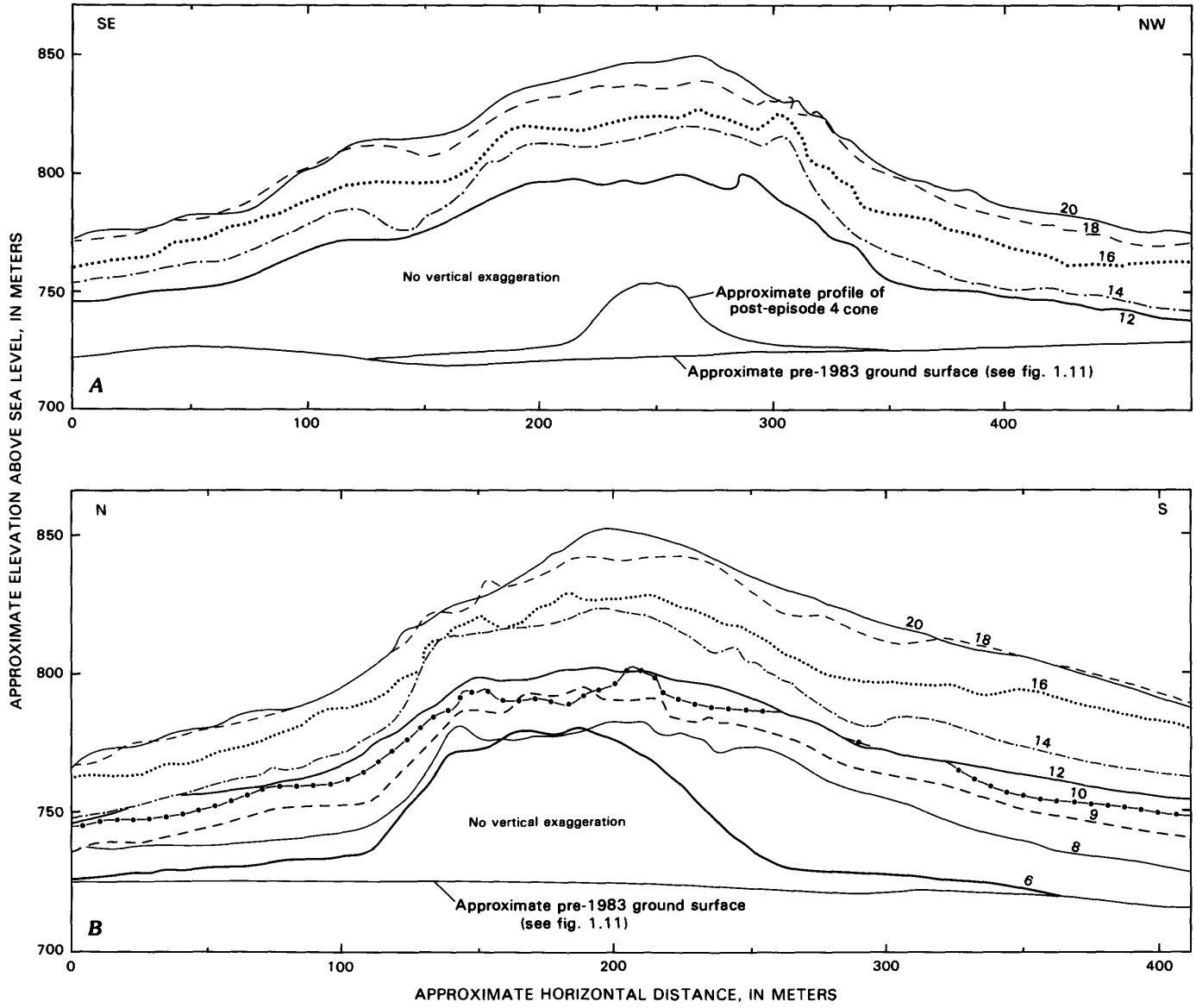

FIGURE 1.10.—Superimposed profiles of Puu Oo. *A*, Viewed from the northeast after episodes 12, 14, 16, 18, and 20. Profiles (identified by episode number) were traced from photographs taken from camp E, located 1.3 km northeast of Puu Oo (see fig. 1.1). After episode 20, summit of Puu Oo stood approximately 130 m above preexisting ground level. *B*, Viewed from the west after episodes 6, 8, 9, 10, 12, 14, 16, 18, and 20. (Profiles identified by episode number; additional profiles were omitted to preserve clarity of outlines.) Profiles were traced from time-lapse-film frames taken from near camp D, located 750 m west of Puu Oo (see fig. 1.1). Owing to frequent camera moves and several camera focal-length changes, perspective and scale control vary. Thus, control is weak for the precise placement of episode 9 profile relative to episode 8 profile, of episode 14 profile relative to episode 12 profile, and of episode 18 profile relative to episode 16 profile. Scale was determined from photographs of known focal length and distance from cone. In addition, periodic transit measurements of maximum cone height and two detailed topographic surveys served to constrain superpositions.

sion (fig. 1.15). Grooved and slickensided surfaces low on the inner crater walls indicated that the crater floor had undergone at least 5 to 10 m of subsidence at the end of episode 10.

Episode 10 marked a temporary change in the style of venting at Puu Oo. The conduit system, which had been delivering lava through the floor of Puu Oo Crater, increased in complexity by developing distinct secondary vents at the base of the northwest crater wall and on the west rim. Still greater complexity developed during episodes 11 and 12, when several vents erupted on the rims and flanks of Puu Oo, as well as within the crater (fig. 1.16). In addition, lava was slowly erupted during episode 11 from fissures that extended about 200 m uprift and downrift from Puu Oo (pl. 3). The complexity of vent distribution may reflect partial blockage of the shallow crater-floor conduit. Apparently, the blockage began during episode 10 and was compounded by subsidence of the crater floor and collapse of the interior walls at the end of that episode. Thus, an enlarged, compartmented, and distorted crater formed (fig. 1.17).

Episode 13 reestablished a single bowl-shaped, open crater (fig. 1.18). An open conduit that was to remain a permanent feature through subsequent episodes descended from the crater floor. After episode 13, this conduit tapered from about 20 m in diameter at the top to about 10 m in diameter at a depth of 25 m, where further visibility was blocked by lava standing in the pipe. From episode 14 on, as much of the pipe as we could see (approx 50 m at most) was vertical, nearly cylindrical, and about 20 m in diameter.

The crater floor was broader and more basinlike after episode 14 (fig. 1.13) than in earlier episodes. The basin was largely enclosed by steep crater walls, which, until

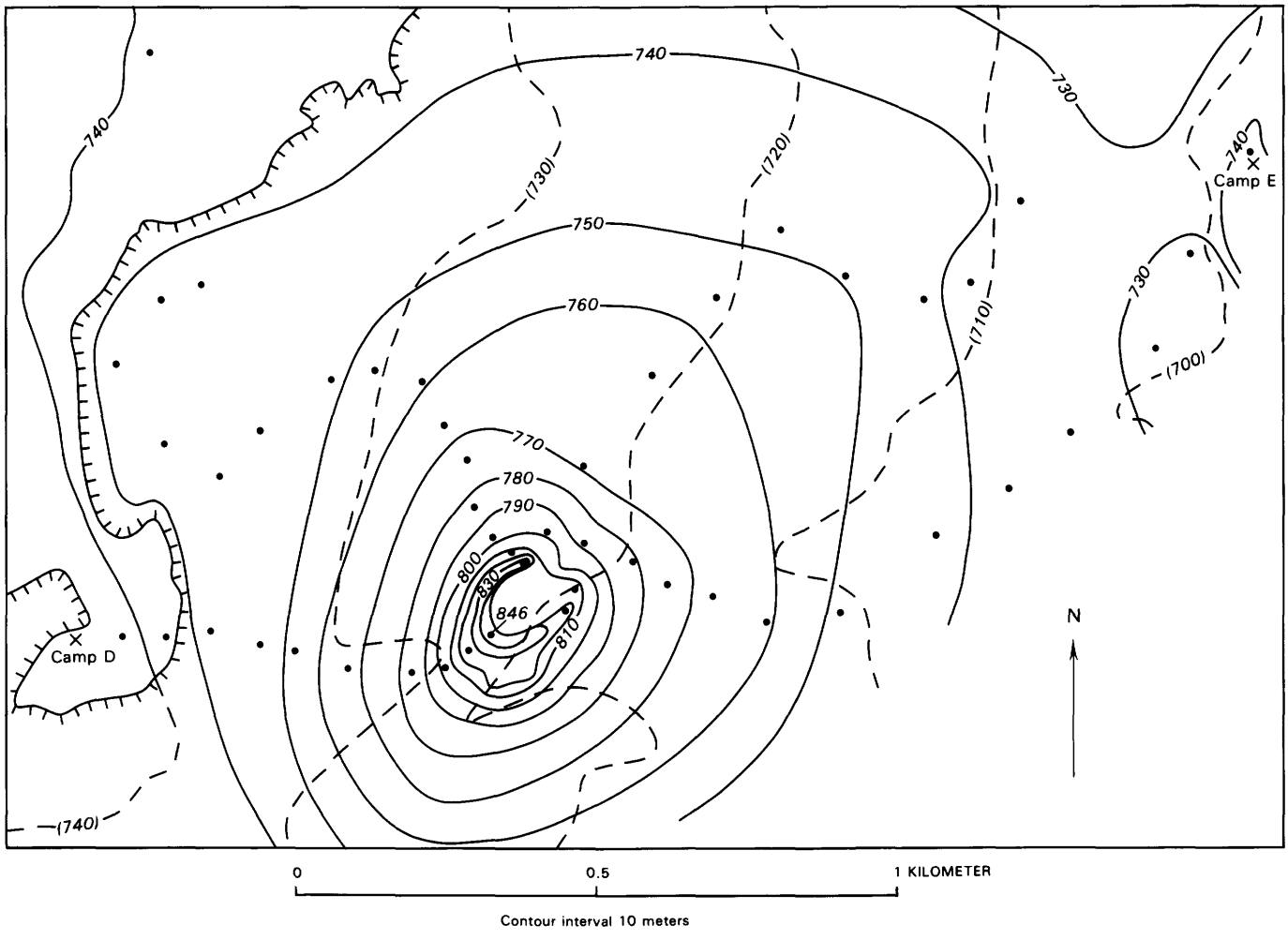

FIGURE 1.11.—Topographic map of Puu Oo after episode 19. Map was compiled by R.Y. Hanatani from a survey on May 22, 1984. Dots denote locations of surveyed control points. Hachured line is edge of 1983–84 basalt at time of survey; hachures are on 1983–84 basalt side. Contours on buried pre-1983 surface (dashed, values in parentheses) modified from U.S. Geological Survey Kalalua 7.5-minute quadrangle, 1982. For location, compare with figure 1.1.

episode 19, towered about 40 m above the crater floor. The spillway through the northeast crater rim persisted, and a low arcuate ridge, about 5 m high, separated the shallow basin from the spillway (fig. 1.13). The remarkable persistence of the geometry and general dimensions of the crater, with almost no change from one repose period to the next until episode 19, suggests that a relatively stable equilibrium between eruptive processes and crater formation had been attained. Minimal collapse of the crater walls after some of these later eruptive episodes reinforces this suggestion. Although significant failure of the walls followed episodes 16 and 18, the walls and floor

FIGURE 1.12.—Puu Oo between episodes 17 and 18. Cone is about 100 m high. Pronounced bulge at right reflects repeated deposition of spatter and air-fall deposits and development of thick, spatter-fed flows. View eastward from camp D; photograph taken at 1046 H.s.t. April 15, 1984.

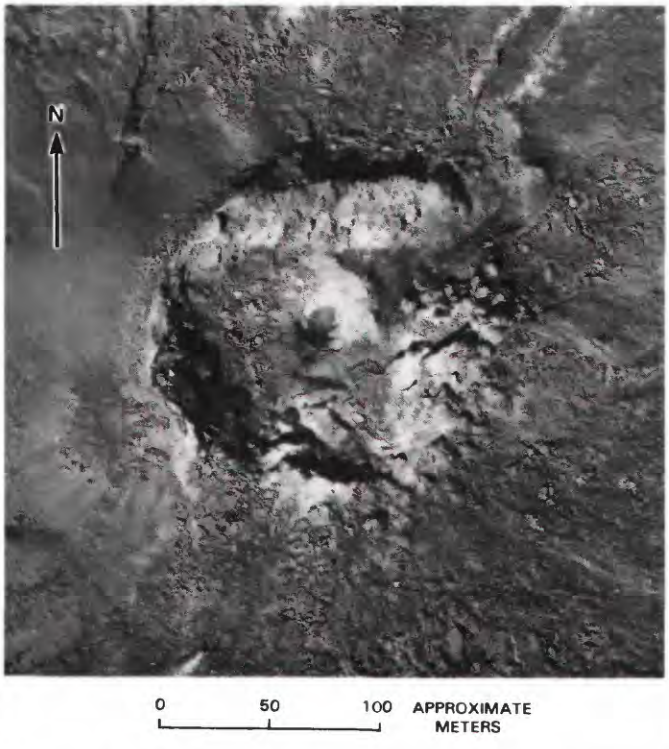

FIGURE 1.13.—Puu Oo after episode 14. Bowl-like crater is about 40 m deep. Open, nearly circular, vertical conduit intersecting crater floor is about 20 m in diameter; after episode 13, it was a permanent feature. Photograph by Jay Whiteford, Air Survey Hawaii, taken February 11, 1984.

FIGURE 1.14.—Angular blocks of oxidized agglutinate from crater walls surround an open vertical, 4-m-diameter pipe descending from floor of Puu Oo Crater after episode 9. Photograph taken at about 1000 H.s.t. September 23, 1983.

FIGURE 1.15.—Post-episode 10 crater, about 90 m in diameter at the rim. Floor of crater is covered with rubble and collapsed blocks from walls and rim of cone. Fuming areas at base of north crater wall (foreground) and crest of west rim (right) were near sites of prominent secondary fountains during episode 10. Open cracks in fuming area high on west rim remained incandescent between episodes 10 and 11. Spillway (S), crossing northeast rim, is choked with rubble that was apparently transported into spillway by last lava exiting crater. View southeastward; photograph taken at 1501 H.s.t. October 30, 1983. Faint numerals (lower right) indicate date and time.

were largely mantled with smooth, glassy basalt after episodes 13 through 15, and 17.

Unlike the preceding episodes that had been characterized by steady, voluminous lava emission and continuous vigorous fountaining, episode 19 was characterized by intermittent, low-volume overflows from the basin within Puu Oo and only a few brief periods of increased lava emission and vigorous fountaining. The effect of this relatively low level eruptive episode was to nearly fill the crater of Puu Oo with solidified basalt (fig. 1.19), a change that led to elimination of the basin and the associated long, lava-river-fed flows. For months thereafter, higher fountains and shorter, thicker, spatter-fed aa flows dominated.

LAVA PONDS AT THE CENTRAL VENTS

During the central-vent eruptions, lava supplied from beneath the crater floor commonly formed a pond (figs. 1.5, 1.20) that, along with one or more fountains, filled the shallow closed basin within the growing pyroclastic ring. Between eruptive episodes, when no lava was in the crater, we could see that the low point in this ring, which formed a spillway through which the pond overflowed, generally was about 5 to 15 m above the crater floor. At Puu Oo, the breach through the crater rim formed a narrow constriction, so that the surface of the overflowing pond was several meters higher than the rock floor of the spillway, and at times the pond surface appeared to incline gently toward the spillway. We estimate that the pond was normally at least 10 to 20 m deep. As Puu Oo slowly grew larger during successive eruptive episodes, the diameter of the enclosing basin, which, measured at the level of the spillway, gives an approximate limiting diameter for the pond, increased from about 20 to 100 m.

FIGURE 1.16.—Puu Oo vent erupting during episode 12. Four general loci of fountaining are visible: (1) spillway area, on northeastern flank; (2) southeast rim of crater; (3) high in northwest sector of Puu Oo (the most vigorous, partly obscured by fume); and (4) low fountain within crater. View westward; photograph taken at 0952 H.s.t. November 30, 1983. Numerals (lower right) indicate date and time.

FIGURE 1.17.—Puu Oo after episode 12. Irregular shape and compartmentation of crater were caused by simultaneous eruption of several distinct fountains (fig. 1.16) within crater and on its rims and flanks. Spillway and adjacent evacuated channel are at upper right (arrows). Episode 13 eruption began with gradual filling and overflow of deep compartment adjacent to spillway. View southwestward; photograph taken at 0942 H.s.t. January 10, 1984. Numerals (lower right) indicate date and time.

FIGURE 1.18.—Puu Oo after episode 13. Simple, nearly circular crater contrasts markedly with complex crater that preceded episode 13 (fig. 1.17). Lava surface is visible about 25 m down open vertical conduit, which tapers from about 20 m in diameter at the crater floor to 10 m in diameter at lava surface. View southwestward; photograph taken at 1156 H.s.t. January 24, 1984.

During vigorous eruption, lava poured through the breach in the crater wall and normally fed a well-channelized river of pahoehoe. When fountaining was relatively low, we could sometimes see that the smooth lava surface of the spillway extended without disruption into the crater interior (fig. 1.20), so that the immediate source of the pahoehoe river was the lava pond within the crater. The relative peacefulness of this pond surface where not turbulently disrupted by the fountain indicated that little, if any, effervescence was occurring and that the pond lava had sufficient strength to maintain its shape adjacent to the vigorously turbulent fountain. Apparently, the lava in the quiet part of the pond had lost most of its dissolved magmatic gas.

At times, high, broad, ash-laden fountains issued from the Puu Oo Crater (fig. 1.6), particularly during the early stages of some eruptive episodes. Because of the breadth of these fountains, we could not see the pond at such times. Continuing passage of the lava river through the spillway indicated that melt was accumulating in the basin, but flows produced under such conditions were sometimes more sluggish than when a well-developed pond was present (see subsection below entitled "River-Fed Flows").

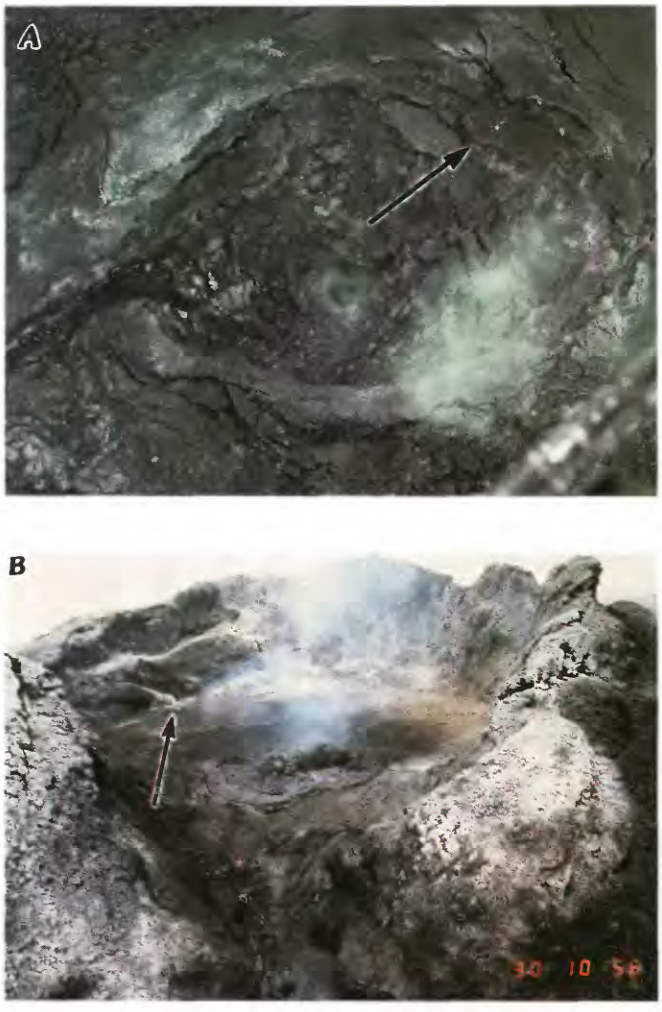

FIGURE 1.19.—Puu Oo Crater before and after filling by episode 19 pahoehoe. *A*, Deep, bowl-shaped crater after episode 18. Walls and floor are mantled by slumped debris that had temporarily plugged the open, 20-m-diameter pipe. Spillway and steeply inclined chute (see fig. 1.91) descending outer flank of cone are at left. Shorter crater diameter is about 100 m. Arrow marks level to which solid basalt filled crater during episode 19. Helicopter strut and skid visible in lower right corner. View southeastward; photograph taken at 1355 H.s.t. April 23, 1984. *B*, Puu Oo after episode 19. Deep crater and breach in northeast rim were largely filled during episode 19 by successive pahoehoe overflows from central conduit. Arrow denotes same slumped ledge of crater-rim material as in figure 1.19*A*. View southeastward; photograph taken at 1056 H.s.t. May 30, 1984. Numerals (lower right) indicate date and time.

FOUNTAINS AT EPISODE 1 FISSURE VENTS

Linear fountains, from tens to several hundreds of meters long, erupted from the episode 1 fissure vents. The

FIGURE 1.20.—Puu Oo erupting during episode 7. Smooth surface of pond fills crater from base of fountain to spillway, where lava cascades down outer flank (lower left) and supplies main flow. A small tube-fed flow, apparently also fed by lava of the pond, issues from north base of Puu Oo (bottom center). Spatter from 50-m-high fountain feeds flows to southwest (upper right) and northwest (right center). A satellitic crater on west flank is partly visible at upper right; it contained an active vent during episode 5 but is not actually erupting here. At times, spatter falling into satellitic crater was so voluminous that a temporary pond formed and overflowed to supply additional lava to southwestern flow. View southward; photograph taken at 0850 H.s.t. August 15, 1983. Numerals (lower right) indicate date and time.

fountains were mostly low, about 5 to 30 m high. A notable exception occurred at midday on January 7, 1983, when a fountain, 60 to 100 m high, issued steadily from a 500-m-long fissure for a period of about 2 hours. This high fissure fountain occurred simultaneously with extraordinarily voluminous lava discharge that was estimated later from the measured flow volume to be 1×10^6 to 1.5×10^6 m^3/h. In contrast, normal episode 1 discharge rates ranged from about 0.06×10^6 to 0.3×10^6 m^3/h and averaged about 0.1×10^6 m^3/h. Clots of molten spatter, as large as 1 or 2 m in diameter, fell out of the episode 1 fissure fountains and built low ramparts adjacent to the vents. Very little tephra was transported downwind away from the erupting fissure vents.

FOUNTAINS AT CENTRAL VENTS

After episode 1, most of the eruptive activity was localized at central vents. The main locus of eruption during episodes 2 and 3 was the 1123 vent; from episode 4 on, Puu Oo, including, on a few occasions, nearby fissure vents, was the sole eruptive locus. In an attempt to characterize the central-vent fountain behavior and in hope of gaining insight into the relations between fountain behavior and other eruptive parameters, such as discharge rate and vent geometry, we measured the fountain heights in time-lapse film records of the central-vent eruptions (figs. 1.21–1.24).

EPISODES 2 AND 3: FOUNTAINS AT THE 1123 VENT

Eruption at the 1123 vent during episode 2 began during the afternoon of February 25, 1983. A spatter ring enclosing a pond with a conspicuous main fountain and a line of discontinuous low fountains (fig. 1.5) quickly formed. For the first 2 days of its activity, this main fountain was relatively low, generally about 20 to 40 m above the surface of the lava pond (fig. 1.21). By the morning of February 26, one short flow had been erupted, at a lava-discharge rate of about 40,000 m^3/h. The major eruptive activity, mostly accompanied by a 60- to 80-m-high fountain at the 1123 vent, began on February 27 and continued until March 4, when episode 2 ended. Lava was discharged at an average rate of about 90,000 m^3/h, double that for the earlier flow accompanied by a low fountain. Apparently, this change in fountain vigor reflected a change in the rate of delivery of magma and, thus, of newly exsolved gas to the vent.

During episode 3, two major vents were active at the 1123 cone. The northeastern fountain, which was by far the higher (fig. 1.25), was the source of our fountain-height record (fig. 1.23). It erupted within a reentrant in the growing cone but for most of episode 3 was not contained within a distinct crater. There seemed to be little, if any, development of a lava pond. Much of the time, the lower, southwestern fountain, which was within a bowllike crater, was obscured from our view by the growing cone. Generally, the two fountains seemed to behave independently. We saw no correlation or anticorrelation between them in relative vigor except for a 24-hour period, ending at 2100 H.s.t. April 3, during which emission of spatter was interrupted for short intervals at both vents (see subsection below on episode 3).

Lava from the northeastern vent supplied a massive aa flow throughout episode 3 at an average rate of about 75,000 m^3/h. Through April 3, little significant lava production occurred at the southwestern vent. Early on April 4, however, the southwestern vent began to discharge lava flows at an average rate of about 130,000 m^3/h, continuing until the end of this eruptive episode. A vigorous, well-channelized lava river issued from the crater at the southwestern vent, and although we never got a direct view, we believe that the flow originated from a lava pond within the crater. We judge from the continued steady advance of the flow from the northeastern vent (pl. 1) that the discharge rate there was not significantly affected by the change at the adjacent southwestern vent, which resulted in a more than twofold increase in the combined discharge rate. In spite of this striking increase in discharge at the southwestern vent, the fountain there remained low. The northeastern fountain, however, greatly increased in vigor (fig. 1.23). Whereas it seldom exceeded 100 m in height before April 4, from April 4 through 7 the fountain was higher than 100 m most of the time, with peaks exceeding 200 m, and tephra falls extending more than a kilometer from the vent. This increase in fountain height at the northeastern vent apparently reflected increasing overall supply of magma and, thus, increasing delivery of newly exsolved gas to the shallow part of the conduit. As discussed below, we believe that the low fountain within the bowllike crater at the southwestern vent may have resulted from damping by the degassed lava that formed a pond within the crater.

EPISODES 4 THROUGH 20: FOUNTAINS AT PUU OO

The fountains at Puu Oo generally emanated from the basin in the lower part of the crater within the growing pyroclastic cone. Exceptions, described below, occurred during episodes 4, 5, and 10 through 12. The range in fountain height was large, from a few tens of meters to nearly 400 m.

Unlike the fountains at the 1123 vent during episodes 2 and 3 (figs. 1.21, 1.23), the Puu Oo fountains were com-

monly highest in the early hours of an eruptive episode (fig. 1.24). As recorded in the fountain data for episodes 4, 6, 9, 10, 14 through 18, and 20, the general height, though sometimes varying widely, decayed after the initial hours. Many of the early high fountains, as well as intermittently high fountains later in an episode (such as those on October 6, 1983, during episode 10 or on March 3, 1984, during episode 16) were nearly vertical and broad

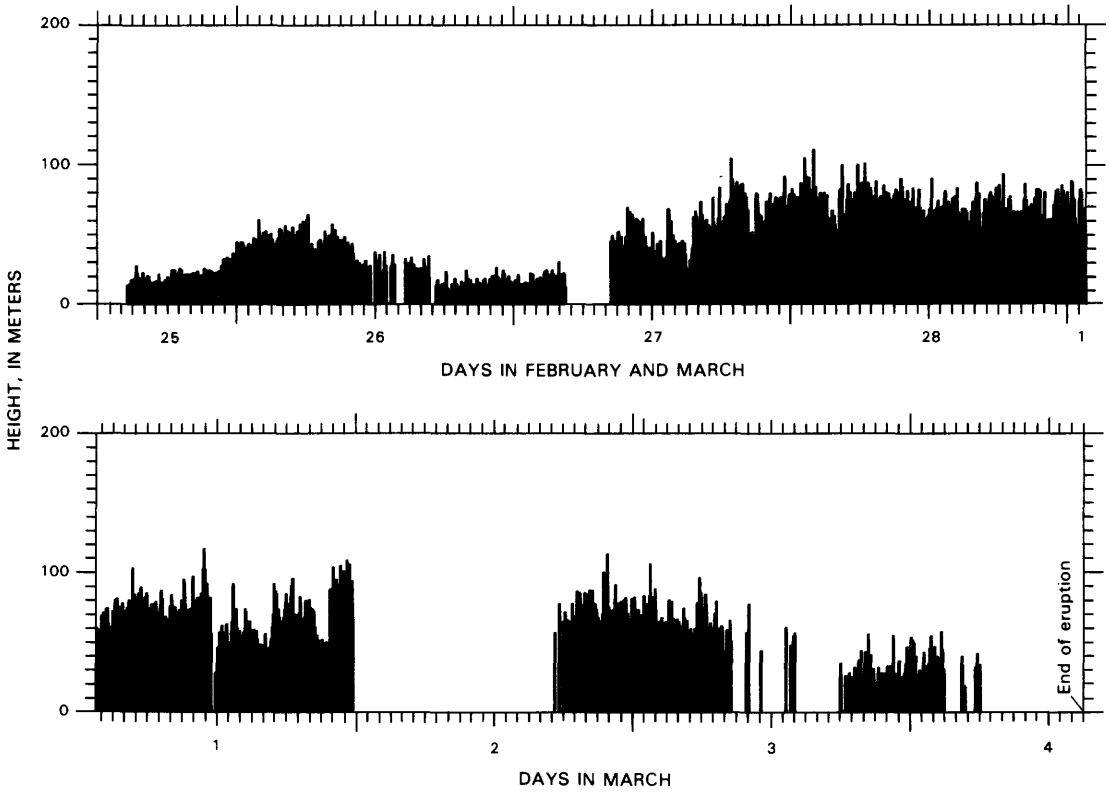

FIGURE 1.21.—Fountain heights of main fountain at 1123 vent during episode 2. Data from a time-lapse camera located at camp A, about 500 m northeast of vent. Datum is approximate base of fountain. Apparent zero values normally reflect data gaps resulting from bad visibility or an inoperative camera; however, they include intermittent cessations in fountain activity on March 4. Data plotted continuously from 1200 H.s.t. February 25 to 1500 H.s.t. March 4, 1983.

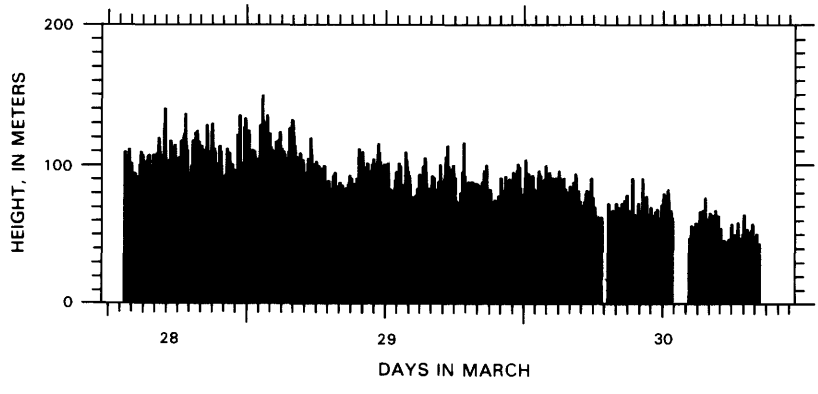

FIGURE 1.22.—Fountain heights at O vent during episode 3. Record begins at 1322 H.s.t. March 28, approximately half a day after beginning of episode 3. Data from a telephoto time-lapse camera at camp A. Datum is approximate base of fountain. Apparent zero values reflect data gaps resulting from bad visibility or an inoperative camera. Data plotted from 1130 H.s.t. March 28 to 2330 H.s.t. March 30, 1983.

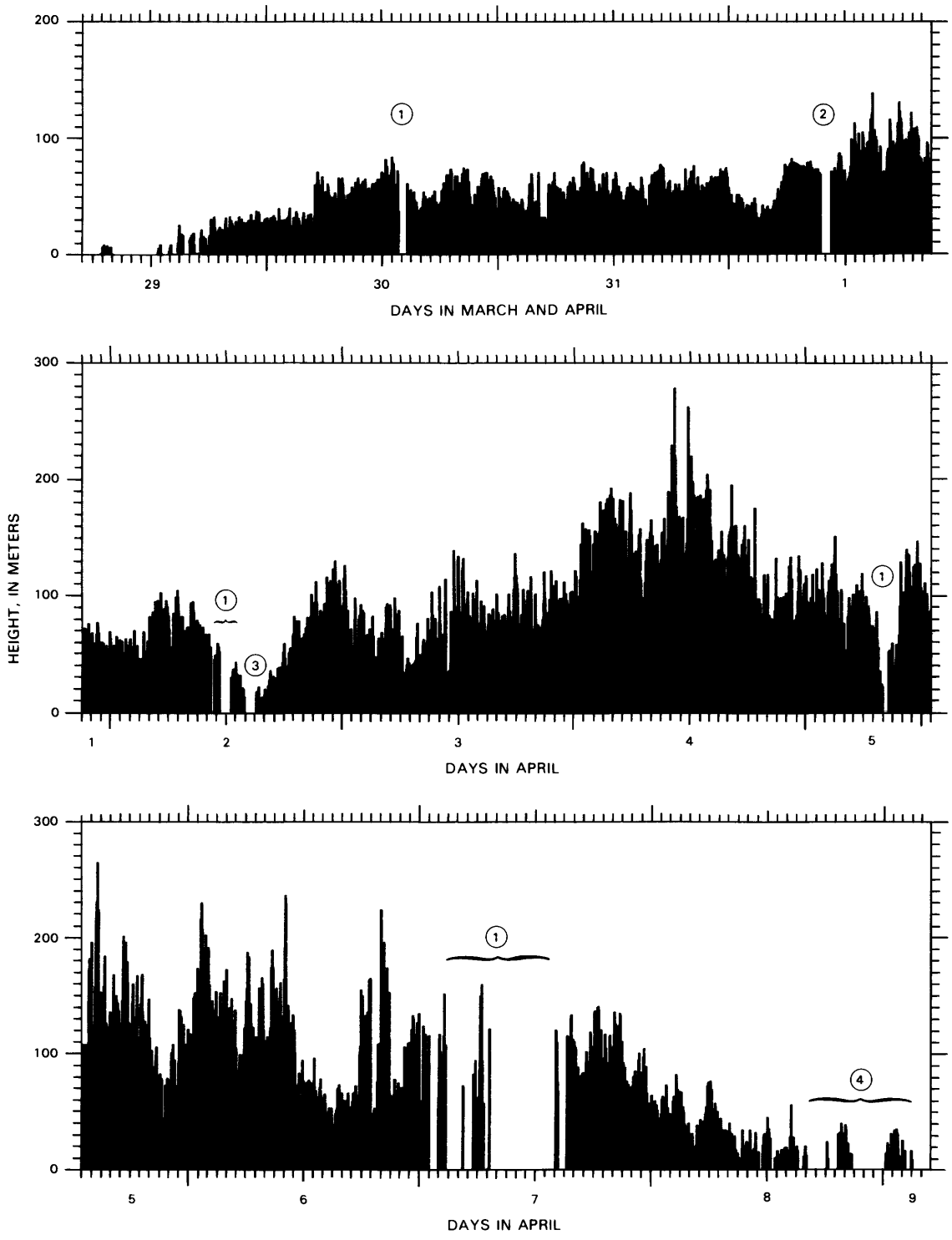

FIGURE 1.23.—Fountain heights of northeastern fountain at 1123 vent during episode 3. Data from a time-lapse camera located initially at camp A and later at camp B. Datum from camp A is approximate base of fountain. Base of fountain was not visible from camp B, and so fountain heights shown after 1000 H.s.t. April 1 are minimums. Fountaining was intermittent before 1800 H.s.t. March 29. Other data gaps (circled numbers) are explained as follows: 1, Data were lost because of poor visibility or inoperative camera. 2, Camera was moved from camp A to camp B. 3, Fountain was very low, and visibility was partly obscured by fume or water vapor; record of a nearby telephoto camera indicates that low spatter was continuously visible. 4, Fountain was so low that it was out of view at times, and visibility was partly obscured by bad weather. Data plotted continuously from 0500 H.s.t. March 29 to 0500 H.s.t. April 9, 1983.

based. The highest ones, generally at least about 200 m high, formed majestic, candlelike pillars that commonly were partly shrouded in a conspicuous cloud of fine tephra (fig. 1.6). Although such fountains generally remained steadily high, the incandescent ejecta that supplied them was emitted in pulses. The spacing between pulses was approximately 1 s; thus, several successive, more brightly incandescent fronts could be seen rising upward through the fountain at any one time. Occasionally, the high fountains became abruptly inclined, or they rapidly disintegrated in a confusion of erratic inclined jets that sprayed ejecta over the outer flanks of Puu Oo—as if an obstacle interfering with the upward trajectory had deflected or fragmented the fountain.

The lower fountains, typical through the greater part of each episode, generally behaved more irregularly. Many of them seemed to be a composite of short-lived individual jets (fig. 1.26) originating in bursts from different parts of the lava pond that was sometimes visible within the crater. At times, these bursts seemed rhythmic, with new jets rising at intervals from about 1 to 3 s. Possibly because of alternating interference and reinforcement among the jets, the overall fountain height commonly oscillated several times per minute over a large vertical range.

Average and maximum fountain heights determined at Puu Oo are shown (fig. 1.27) from the data plotted in figure 1.24. With significant exceptions, discussed below, both values increased during the series of eruptive episodes, and the production of a fountain several hundred meters high continued long past episode 20 as a hallmark of the Puu Oo eruptions.

Fountain height increased fairly steadily from episodes 4 through 10. The extremely low heights for episodes 4 and 5 may partly reflect the fact that the main Puu Oo Crater was not the sole eruptive locus in those episodes. A line of erupting fissure vents extended a short distance uprift from Puu Oo during the early part of episode 4. Discharge from the westernmost vents soon ceased, and the more easterly ones formed a satellitic vent that was active on the west flank of Puu Oo through episode 5.

During the second day of episode 10, high fountaining was abruptly curtailed (fig. 1.24), and new discrete vents formed at the base of the northwest interior crater wall and on the high west rim of the crater. As already suggested above in the subsection entitled "Growth of Puu Oo," this event may have recorded partial blockage of the established vent through the crater floor, and the effect may have been exacerbated at the end of episode 10, when subsidence of the crater floor and profound collapse of its walls occurred. Low fountains and complex vent distribution in and near Puu Oo during episodes 11 and 12 indicated that the inferred blockage continued at least through those episodes. Conduit blockage and development of a complex of subsidiary passages for transmission of lava to the surface seem adequate to explain the diminished fountain heights during and after episode 10.

Episode 13 marked a return to a single vent within the crater, as represented by the open pipe that we could see descending from the central part of the crater floor during all the repose periods after episode 13. Fountain vigor increased from episode 13 through 16, and early high, tephra-laden fountains like those of episodes 9 and 10 resumed in episodes 15 and 16.

One could speculate (fig. 1.27) that episodes 15 and 16 marked a return to the trend of evolving fountain behavior that was established during episodes 4 through 10 and interrupted in the later part of episode 10. If so, other perturbations apparently followed episodes 16 and 18, although they are less readily explained. As in episode 10, the crater walls failed markedly at the ends of episodes 16 and 18. However, the disruption within the crater was less severe than after episode 10; and in the ensuing episodes, no subordinate vents opened to suggest that the shallow conduit had been blocked. Whether collapse of the episode 16 and 18 crater walls was a coincidental, superficial event or was somehow related to diminished fountain height in the ensuing episode is unclear. Furthermore, the episode 19 eruption was abnormal in both volume and style. It was unusually small: Only 2×10^6 m^3 of lava was discharged. Unlike the other episodes, episode 19 was characterized by repeated intermittent, low-volume overflows from Puu Oo Crater; these were punctuated by four brief periods of higher volume lava production and moderate fountaining that were, in turn, interrupted by repeated, brief, abrupt pauses in discharge—it seemed like an eruptive episode that could not get fully under way.

The trend toward increasing fountain vigor through the series of eruptive episodes at Puu Oo probably reflects evolution of the lava-delivery system. Generally, the rate of lava discharge increased through the 20 episodes (fig. 1.4). Although the relation is complex in detail, we conclude that increasing fountain vigor at Puu Oo was related, at least in part, to increasing discharge rate. We concluded similarly for the episode 2 and 3 fountains at the 1123 vent. L.P. Greenland (oral commun., 1985; see chap. 4) sampled vent-gas emissions from episode 1 through the repose period between episodes 15 and 16. He found that the composition of erupted magmatic gas was constant during that period and inferred that the initial concentration of volatile constituents dissolved in the magma was also constant. Therefore, changes from one episode to the next in the general height of the fountain were apparently not related to changes in initial magmatic-gas content. Variation in fountain height might also have been related to changing geometry of the eruptive orifice. For episodes 14 through 20, however, dur-

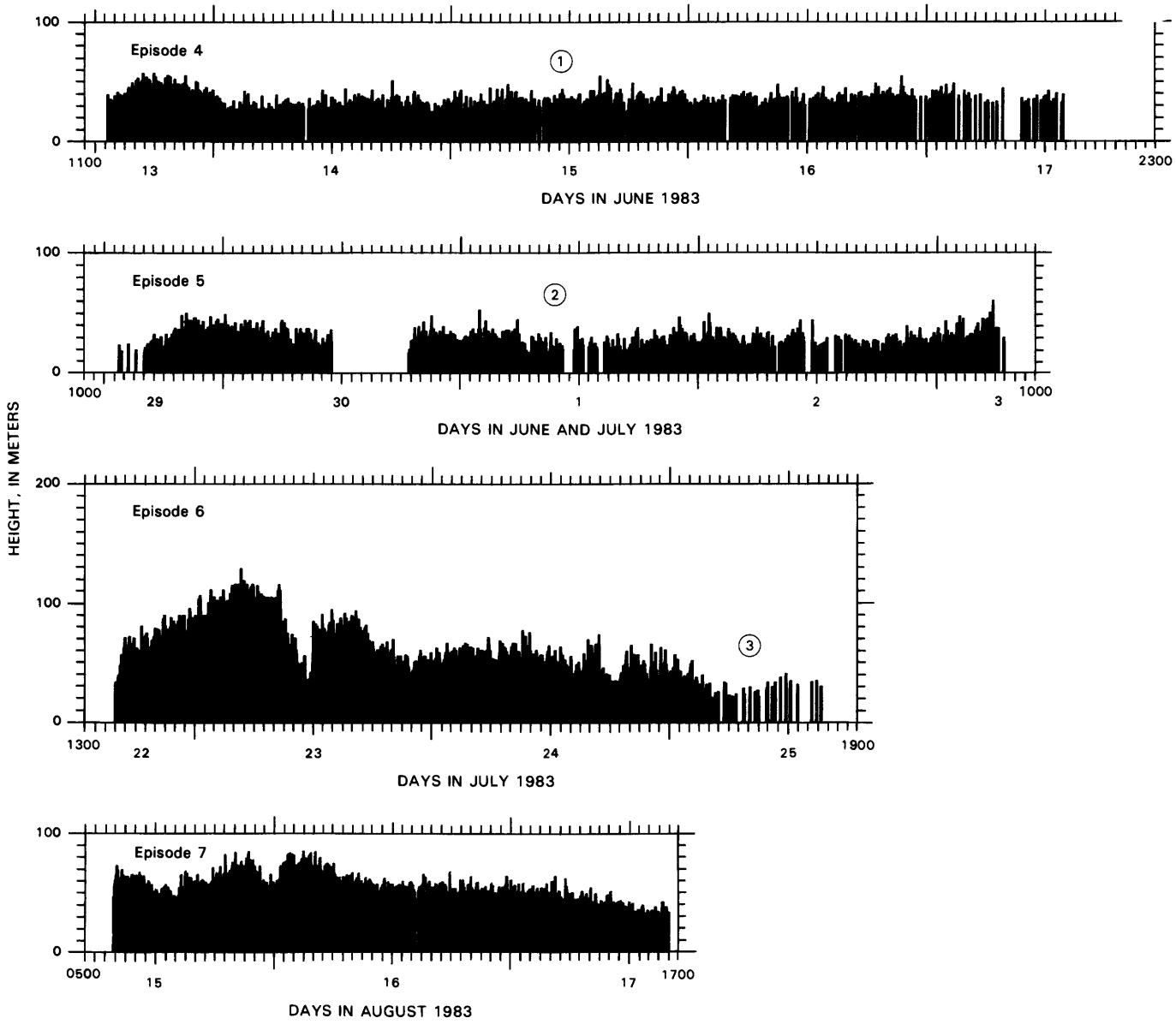

FIGURE 1.24.—Fountain heights at Puu Oo during episodes 4 through 20. Data from a time-lapse camera located at camp B for episode 4 and early part of episode 5, at camp C for later part of episode 5 and episodes 6 and 7, at camp D for episodes 8 through 10, and at camp E for episodes 11 through 20 (see fig. 1.1 for camp locations). From camps B, C, and D, height was measured with respect to a reference point on Puu Oo rim. A correction, ranging from 10 m for episode 4 to 25 m for episode 10, was added to compensate for difference in elevation between pond surface and reference point. For each episode, ending and starting times of fountain record are shown in Hawaiian standard time. Except as noted (circled numbers), gaps in the data record periods of bad visibility or an inoperative camera. 1, Data for main (eastern) fountain; camera was activated at 1305 H.s.t. June 13, 1983, at least 2.5 hours after the eruption began. 2, Data for main (eastern) fountain. Apparent zero values during first 3 hours resulted in part from bad weather and in part from fountain being entirely below crater rim. Large data gap on June 30 records transfer of camera from camp B to camp C. 3, Gaps in record of last day reflect concealment of low fountain by crater wall and intermittent bad visibility. 4, Period of apparent low fountaining at about 0700 H.s.t. September 6, 1983, reflects poor visibility caused as Sun rose directly behind fountain. 5, During periods of multiple fountains, only height of main jet was recorded. 6, Values record highest part of a complex of low fountains within Puu Oo. 7, First 4.5 hours of record is missing because of inoperative camera. 8, Wide gap records temporary cessation of eruption. 9, Heights of highest fountains, in early part of record, are uncertain because dense tephra, which sometimes extended above camera field of view, prevented direct observation of dense, incandescent fountain. 10, Fountaining was intermittent; there are no gaps reflecting bad visibility or camera inoperativeness. Data are shown only for periods of high fountaining.

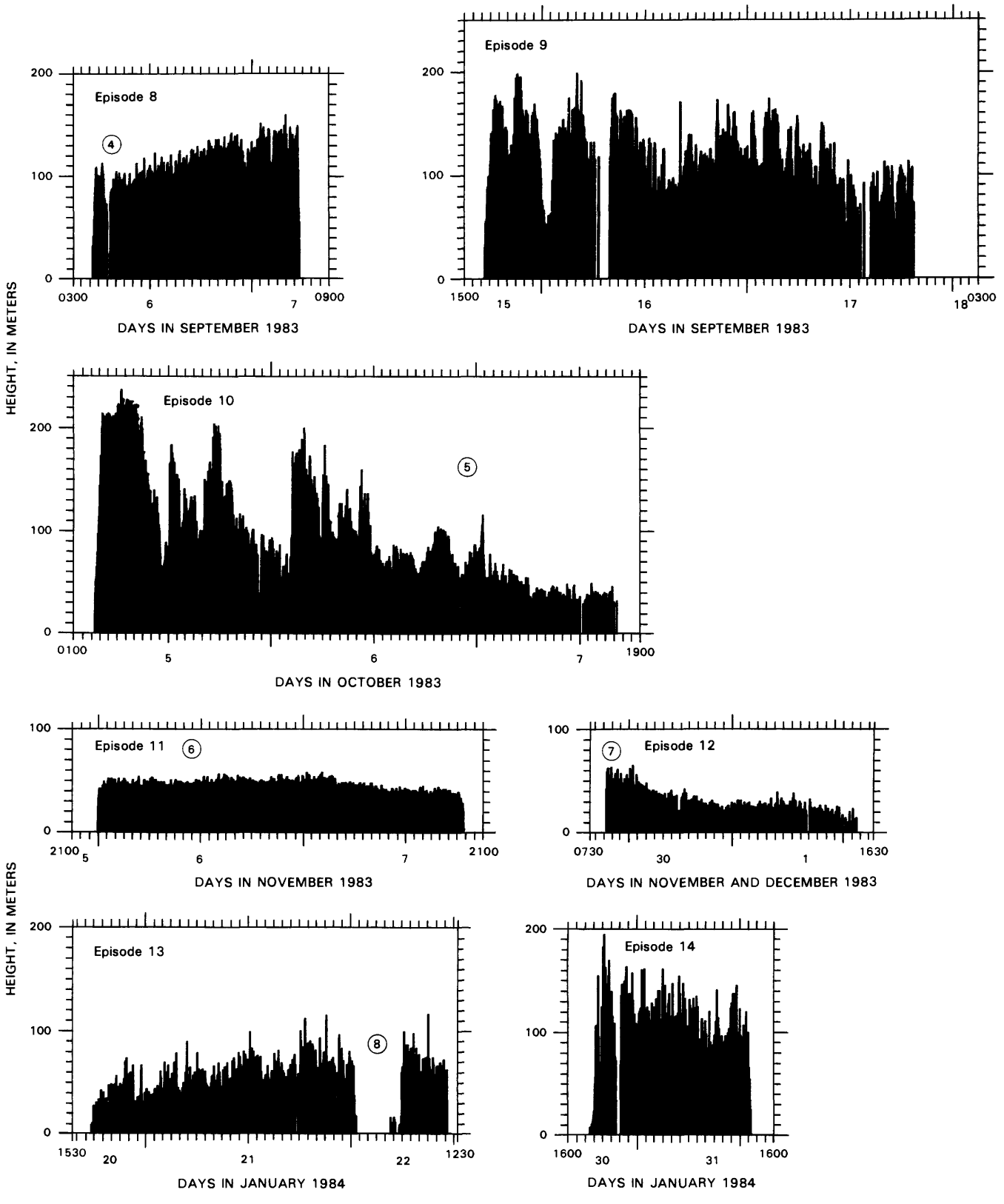

FIGURE 1.24.—Continued

ing which the fountain height varied widely, the visible part of the eruptive orifice was an unchanging vertical, nearly cylindrical, 20-m-diameter pipe descending from the crater floor.

Superimposed on the general trend toward increasing fountain height was a tendency for higher and generally more tephra laden fountains to occur in the early hours of the eruptive episodes and for fountain vigor to show a progressive decay during the episode. This pattern suggests that the lava delivered to the surface early in many of the episodes was slightly more gas rich. Such a phenomenon might be explainable by upward migration and entrapment of exsolved gas during repose periods within the upper part of the magma column in the conduit system beneath Puu Oo. Escape of the gas would have been inhibited by a cap of relatively dense melt. This cap could have formed when degassed fountain and pond melt drained back into the conduit at the end of an eruptive episode (see chap. 5). Elimination of the cap at the onset of an eruptive episode, either by simple extrusion or by erosion and dissemination as new melt rose upward through it, permitted escalating eruption of the melt from the underlying column, the most gas rich first.

Maximum fountain height generally increased more rapidly than average fountain height through the series of eruptive episodes at Puu Oo (fig. 1.27). This trend could reflect either increasing effectiveness of the degassed-magma cap as a seal in inhibiting repose-period gas loss from the underlying magma column, or increasing volume of the gas-enriched melt that supplied the early high foun-

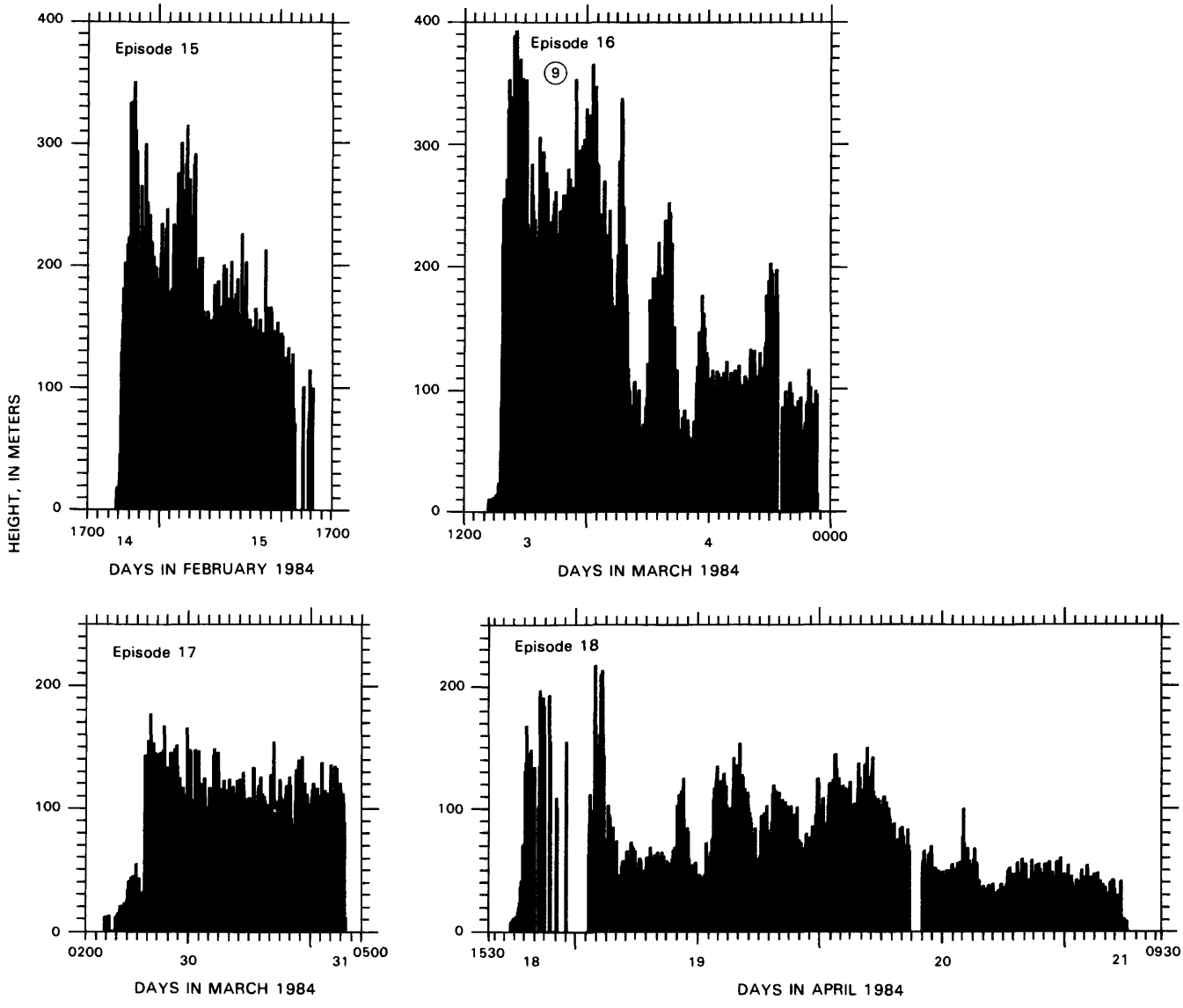

FIGURE 1.24.—Continued

tains. The first mechanism is not supported by available measurements of repose-period SO_2 emissions, and examination of the second mechanism is inconclusive.

Average SO_2 flux was determined at Puu Oo for the repose periods preceding episodes 15 through 20 (see chap. 5). This average flux varied by a factor of about 2 from one repose period to another; however, it showed no correlation, direct or inverse, with the vigor of early fountaining in the next eruptive episode. An anticorrelation might be expected if the degree of gas concentration in the upper part of the magma column at the beginning of an eruptive episode reflected the degree of impermeability of the seal separating the gas-rich melt from the atmosphere between episodes.

The eruption data are inadequate for us to confidently and specifically evaluate changes in the volume of the gas-enriched portion of the magma column, because of uncertainties that include conduit geometry, distribution of exsolved gas at the time of eruption, perturbation of the shallow reservoir during eruption, and applicability of the average lava-discharge rate to the early, high-fountaining hours of an eruptive episode. Nevertheless, the data permit us to speculate about the volume of gas-enriched melt and the theoretical diameter of the conduit that contained it. Greenland and others (see chap. 5) show that most of the exsolved gas present in the magma column at the start of repose periods was in the upper 1,700 m of the column. If we arbitrarily select the upper kilometer of the column as the reservoir in which upward-migrating gas accumulated during repose periods, and assume that the volume of magma involved in the early, high-fountaining part of an eruptive episode represents the volume of gas-enriched magma in an approximately cylindrical conduit before the beginning of eruption, we can calculate a hypothetical average reservoir diameter. The best defined early high fountains occurred in episodes 4, 6, 10, 15, 16, 18, and 20; the results for those episodes are listed in table 1.2. Overall, the resulting conduit diameters range from 21 m (episode 10) to 82 m (episode 20). The high-fountaining activity of episode 10 was unusually lengthy and complex (fig. 1.24). For episode 20, it was unusually brief. Because the episode 20 fountain was relatively high throughout the entire episode, we present a second calculation for which all 9 hours of episode 20 eruption are considered to represent early high fountaining. Eliminating the two extremes gives a limited range of 1.1×10^6 to 3.4×10^6 m^3 for the volume of magma involved in the early high fountains, and an estimated conduit diameter ranging from 38 to 66 m—a result agreeing closely with the 50 ± 30-m diameter inferred by Greenland and others (see chap. 5) from interpretation of gas-flux and geodetic measurements.

Overall, then, we recognize a primary pattern of increasing fountain vigor that correlates in part with increasing lava-discharge rate, and a secondary pattern of increasingly high, early, tephra-laden fountains that we suspect were supplied by a limited volume of magma in which exsolved gas became concentrated above initial levels during repose. Major perturbations, incompletely understood, occurred in these patterns after episodes 10, 16, and 18.

We suppose that the crater-floor subsidence and crater-wall collapse at the end of episode 10 reflected a disruption of the shallow part of the conduit system; this

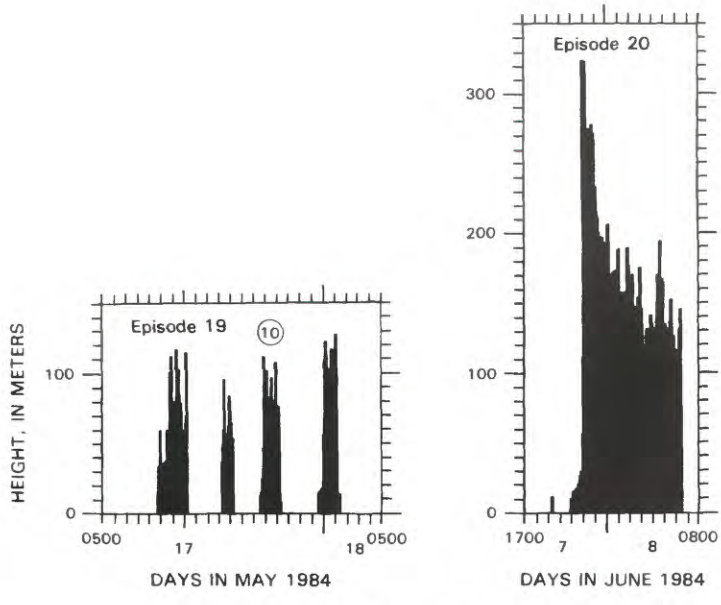

FIGURE 1.24.—Continued

disruption led to the ensuing low fountains and the complexity of the the episode 11 and 12 vents. Unlike most of the other repose periods, in which lava was visible in the pipe or evident just beneath the crater floor for at least one and sometimes many days, visible repose-period activity was minimal or nonexistent before episodes 11 through 13; and the rate of magmatic-gas emission approached zero in the later part of the long repose period preceding episode 13. Collapse within an upper part of the conduit system, reflected by the surficial disruption seen in the crater at the end of episode 10, may have created a plug of porous rubble that impeded the upward rise of erupting magma and forced it to find alternative shallow pathways to the surface. In addition, the permeable rubble may have occupied the zone normally filled during repose periods by relatively impermeable degassed melt. Thus, gas rising through the underlying magma column may have escaped to the surface more easily than was common during repose periods, and the early high fountains normally driven by trapped gas were minimized or eliminated.

The repeated occurrence of a lava pond in the basin, with its surface undisrupted by boiling, and the rapid extrusion from the pond of a voluminous pahoehoe river emitting relatively little magmatic gas indicate that magmatic gas was largely depleted in the lava of the pond.

FIGURE 1.25.—1123 vent erupting during episode 3. Prominent northeastern fountain (at right) is about 150 m high. Tephra fallout raises a dust cloud as it strikes surface of growing cone. Southwestern fountain (center) is barely higher than its crater rim. Nearly 4 hours earlier, steady, voluminous lava emission began at the southwestern vent, producing southeast-flowing pahoehoe river visible at far left. At about 0830 H.s.t., lava flow breached south rim of crater by rafting away part of cone's flank. Part of rafted cone, still slowly moving when photograph was taken, is to left of center in middle ground; small, active, tube-fed pahoehoe flows issue from its base. View northwestward; photograph by J.D. Griggs, taken at 1113 H.s.t. April 4, 1983. Numerals (lower right) indicate date and time.

Greenland and others (see chap. 5) show on theoretical grounds that all newly erupting magma rising within the upper few hundred meters of the conduit was disrupted by exsolving gas to form a low-density spray of vesiculating melt and gas that constituted the fountain. Furthermore, they conclude that dense, relatively degassed magma in the basin formed only from coalescence of disrupted melt that had been degassed by fountaining. Once a body of denser, reaggregated melt became a significant element, it may have interacted with the low-density, gas-rich mixture within the conduit and the basin, damping the overall vigor of fountain activity and producing the more chaotic low fountaining (fig. 1.26) that characterized much Puu Oo activity.

Presence of a continually changing body of coalesced melt in the basin and, possibly, at times in part of the pipe may have caused the transient deflections and disintegrations of high fountains that we sometimes observed. It also provides a means to account for the seemingly disparate behavior of adjacent fountains. For example, at times during the early hours of episode 10, a high, tephra-laden fountain played side by side in the crater with a much lower, intermittent dome fountain (fig. 1.28). Similarly disparate activity occurred at adjacent but separate vents at the 1123 cone during episode 3 (fig. 1.25); the emission from one vent was gas rich and lava poor, and from the other gas poor and lava rich. Such apparent anomalies may have reflected either temporary or prolonged incursions of coalesced melt from the crater into the upper reaches of the erupting conduit system.

FISSURE-VENT FLOWS

Low to moderate rates of lava-discharge that averaged about 0.1×10^6 m^3/h during the episode 1 fissure eruptions normally produced thin (1–3 m thick) sheets of pahoehoe, few of which extended more than a few hundred meters from the vents (pl. 1). Much of the pahoehoe was shelly (Swanson, 1973), and its solidifying surface crust became brecciated locally to form slab pahoehoe. In a few cases, longer, more channelized flows converted to aa and produced lobes that extended as far as 2 km from their vents.

Some of the lava ponded, forming a crust of relatively smooth surfaced, strong, subhorizontal pahoehoe over areas of commonly 10^4 to 10^5 m^2. Lava flowing in tubes beneath the surface slab issued slowly at the edge, forming a short, steep flow front that normally persisted as a high-standing, encircling rampart when the pond-surface slab subsided after termination of supply.

The only high-discharge-rate fissure eruption occurred on January 7, 1983, during episode 1. Over a period of about 3.5 hours, discharge from the easternmost part of

FIGURE 1.26.—Complex of relatively low (max approx 40 m high) fountains, consisting of transient individual jets, within Puu Oo Crater during episode 18. Note ponded lava in crater interior near spillway. View southwestward; photograph by J.D. Griggs, taken at about 1200 H.s.t. April 20, 1984.

the 1983 fissure system (pl. 1) produced a broad, thin flow that extended 5.5 km down the south flank of Kilauea. For 2 to 3 hours at the peak of this eruption, the lava-discharge rate was 1.0×10^6 to 1.5×10^6 m^3/h; during this period, the flow front, recognized from the air as pahoehoe, sped down the average 3° slope at a rate averaging 1.5 to 2.0 km/h. (These were the greatest discharge rate and greatest sustained flow-advance rate of the 20 eruptive episodes discussed in this chapter.) As the flow advance slowed down after supply from the vent stopped, the front converted to slab pahoehoe and aa. Observed after it had stopped moving, the flow was aa for most of its length. It had evidently been emplaced in a relatively fluid state; its thickness averaged about 2 m, and it had enveloped standing ohia trees and preserved open tree molds where the trees had burned away.

CENTRAL-VENT FLOWS

Normally, each central-vent episode produced an elongate major aa flow fed by the lava river that debouched steadily through the lowest part of the crater rim (figs. 1.5, 1.26). Subordinate flows were common. Some originated where an overflow from the lava river, generally near its source, persisted; others were supplied by rapid or persistent accumulation of molten spatter on the flanks of the cone; some, particularly during episodes 4 and 5 and again during episodes 11 and 12, originated at subordinate vents. During episode 3, lava issuing from tubes through the growing 1123 cone formed an apron of pahoehoe adjacent to one sector of the cone. Another apron, of thin sheets of relatively dense, smooth pahoehoe, formed adjacent to the east base of Puu Oo, owing to repeated low-volume overflows from the crater during episode 19.

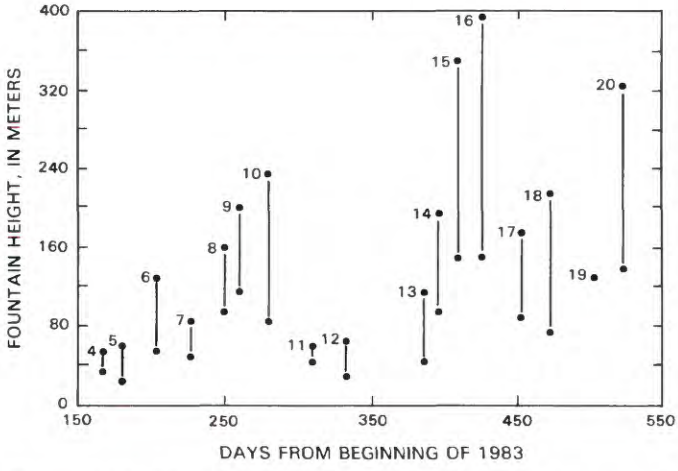

FIGURE 1.27.—Maximum and average fountain heights (average calculated from fountain-height data in fig. 1.24) versus time for episodes 4 through 20 (numbered). For episode 19, only maximum is shown.

The Kilauea central-vent flows described herein share many features in common with the aa lobes produced by the 1984 eruption of Mauna Loa (Lockwood and others, 1985; Lipman and Banks, 1987). In comparison with an average Puu Oo episode (table 1.1), the Mauna Loa eruption was lengthy (approx 3 weeks), about 20 times more voluminous (220×10^6 m^3), and had a generally higher lava-discharge rate (0.5×10^6 to 1.0×10^6 m^3/h through the major period of aa-flow production). The Mauna Loa aa extended approximately twice as far (27 km) from the vent as the longest Kilauea flow and about 4 times as far as the major flow in a typical Kilauea episode (table 1.3). Lipman and Banks (1987) concluded that at Mauna Loa, advance of the major flow lobes was terminated by midflow blockages and diversions that resulted from interrelated phenomena, including declining rate of discharge, increasing viscosity of the erupting melt, and physical maturation of the distributary-channel system. In contrast, discharge was generally steady through normal Kilauea episodes, and most of the major Kilauea flows advanced steadily until they were beheaded, most commonly by the abrupt termination of discharge at the vent. A few major flows stopped advancing because the lava supply was diverted near the vent to a new flow.

RIVER-FED FLOWS

River-fed aa flows, each one much like its predecessors, were the dominant eruptive product of the central-vent episodes. We recognize in them many of the same formative processes, as well as the same aa-flowage zones (with increasing distance downstream, the stabilized channel zone, transitional channel zone, and zone of dispersed flow) described by Lipman and Banks (1987) for the 1984 Mauna Loa eruption. Generally, the Kilauea flows were from 4 to 8 km long and from 100 to 500 m wide; the average width of most of the main flows was 200 to 350 m. A few flows were significantly longer; the longest, produced during episode 18, extended more than 13 km from the vent. The average thickness of the river-fed aa flows ranged from about 3 to 5 m. However, the variation in measured thicknesses was much greater; locally, in the distal part, some flows were as thick as 10 m.

A major river-fed flow was normally initiated as a lobe of fluid pahoeohoe (fig. 1.29) advancing from its source, the lava river pouring through the breach in the crater rim. Initial levees (Sparks and others, 1976), which formed as lateral spreading diminished away from the axis of the lengthening pahoehoe lobe, quickly localized a central lava channel. Repeated overflows added successive pahoehoe layers to these levees, so that a lava river (fig. 1.30) con-

TABLE 1.2.—*Eruption parameters for early high fountains of episodes 4, 6, 10, 15, 16, 18, and 20, and calculated average diameter of a hypothetical 1-km-long cylindrical conduit*

[Durations of high fountaining from data in figure 1.24. Average lava-discharge rates adjusted from data in table 1.1 to approximate dense-rock equivalence, assuming that average porosity of flows was 25 percent. Volume is product of duration of high fountaining times average lava-discharge rate. Reservoir diameter = $2(\text{volume}/1{,}000\pi)^{1/2}$]

Episode	Duration of high fountaining (h)	Average lava-discharge rate (10^3 m^3/h)	Volume of lava erupted during high fountaining (10^6 m^3)	Proportion of total volume of erupted lava (percent)	Calculated reservoir diameter (m)
4	14	82	1.1	14	38
6	25	90	2.3	33	54
10	32	165	5.3	50	82
15	8	315	2.5	42	57
16	12	285	3.4	38	66
18	8	308	2.5	14	56
[1]20	1	360	.4	12	21
20	9	360	3.2	100	64

[1]Episode 20 is considered both for early 1-hour-long period of highest fountaining and for entire episode.

fined within a channel of its own making (stabilized channel zone) steadily delivered lava downflow. Such channels, when seen after an eruptive episode, were shaped like box canyons (fig. 1.9); their depth was generally 2 to 5 m, and their width 5 to 25 m. Oftentimes, the evacuated channel from an earlier eruptive episode channelized the flow during its initial advance (fig. 1.31). The reoccupied channel would soon be bank full, with new overflow levees building along the channel margins, and the new flow front seeking its own path downhill.

Within a few tens of meters of the vent, maximum velocities measured in the lava river were as much as 10 to 15 m/s, and all estimates of lava discharge were several times larger than those determined from measured lava-flow volumes, apparently owing to the low density of lava near the vent. At 1 km from the vent, the maximum flow velocities were normally about 1 to 3 m/s, and estimated discharge was generally within 1 to 2 times the subsequently calculated flux. Standing waves were normally present in the zone of high velocity near the vent, and tearing of the thin, incipient pahoehoe skin as it stretched during passage through the waves sometimes revealed a network of large (tens of centimeters in size), vesicle-like openings (fig. 1.32), suggesting that the near-vent lava was a foam honeycombed with voids. Lipman and Banks (1987) noted similar effects at Mauna Loa and documented a downstream increase in the specific gravity of solidified lava samples from about 0.5 near the vent to 1.5–2.5 in the lower reaches of the flows. L.P. Greenland (written commun., 1985) determined porosities of 57 and 46 percent for samples dipped from the Kilauea lava river during episode 18 at distances of 70 and 1,000 m, respectively, from the vent. At both volcanoes, the flows became progressively depleted in gas with increasing distance from the vent. At Kilauea, our noses indicated that SO_2 flux from the flows was minimal; Greenland (see chap. 4) concludes that vent and upper-conduit processes had largely

FIGURE 1.28.—Puu Oo vent erupting during episode 10. Main fountain is about 60 m high, leans northeastward, and is bombarding spillway with spatter. Just to west of it, a much lower dome fountain, which evolved later to a high jet, also rises from crater. The two fountains may have issued from separate orifices that existed side by side in crater floor before episode 10. View southward; photograph taken at 1058 H.s.t. October 5, 1983.

TABLE 1.3.—*Characteristics of the major episode 1 fissure flow of January 7, 1983, and of the river- and spatter-fed central-vent flows of episodes 2 through 18*

[Average thickness = volume/area; average width = area/length. M, lava-river-fed primary flow of eruptive episode; S, spatter-fed flow]

Episode	Area (10^6 m^2)	Volume (10^6 m^3)	Length from vent (m)	Average lava flux (10^3 m^3/h)	Average thickness (m)	Average width (m)	Average velocity (m/h)	Identification
1	2.0	4.0	5,460	1,110	2.0	370	1,400	Fissure flow, January 7, 1983.
2	.3	.9	2,700	40	3.0	110	140	Northeastern flow.
2(M)	1.8	10.7	7,660	90	5.9	240	50	Southeastern flow.
3(M)	1.4	5.4	4,900	80	3.9	290	60	O vent flow.
3(S)	2.2	11.7	3,860	75	5.3	570	30	Northeastern 1123 vent flow, northeastern lobe.
3(S)	1.4	7.0	4,660	75	5.0	370	20	Northeastern 1123 vent flow, southeastern lobe.[1]
3(M)	.8	4.0	3,360	130	5.0	240	100	Southwestern 1123 vent flow, lobe 1.
3(M)	.3	1.4	1,460	130	4.7	210	---	Southwestern 1123 vent flow, lobe 2.
3(M)	1.9	9.2	7,640	130	4.8	250	90	Southwestern 1123 vent flow, lobe 3.
4(M)	1.8	9.7	7,760	97	5.4	230	90	---
5(M)	1.9	8.4	8,420	93	4.4	230	90	Eastern flow.
5	1.1	3.2	5,960	37	2.9	180	80	Western flow.
6(M)	1.7	8.3	6,480	114	4.9	260	80	---
7(M)	2.7	9.8	6,680	175	3.6	400	110	Northeastern flow.
7(S)	.8	3.2	3,320	80	4.0	240	90	Southeastern flow.
8(M)	1.2	4.7	4,360	196	3.9	280	210	---
9(M)	1.8	7.7	5,260	148	4.3	340	100	---
10(M)	1.4	5.8	4,060	91	4.1	340	60	Northeastern flow.
10(S)	1.3	7.5	3,380	117	5.8	380	50	Eastern flow.
11(M)	3.4	10.4	9,570	242	3.0	360	210	---
12(M)	1.6	5.0	8,360	143	3.2	190	250	Northeastern flow.
12	.5	1.1	2,300	32	2.1	220	60	Northern flow.
12	.8	1.7	4,440	49	2.1	180	320	Eastern flow.
13(M)	2.3	6.4	7,350	205	2.8	310	210	First flow.
13(M)	1.1	3.2	3,110	525	2.9	350	480	Second flow.[2]
14(M)	1.1	2.5	4,720	129	2.3	230	200	Eastern flow.
14(S)	.4	1.2	1,540	64	2.8	260	80	Southeastern flow.
15(M)	1.4	4.9	4,700	257	3.5	300	240	Northeastern flow.
15	.6	1.8	2,940	93	3.2	200	260	Eastern flow.
16(M)	2.2	7.5	7,930	232	3.3	280	240	---
17(M)	2.4	7.4	10,780	338	3.1	220	490	Eastern flow.
17(S)	.4	1.6	1,540	71	4.0	260	150	Southeastern flow.
18	.8	3.0	5,340	123	3.9	150	280	Northeastern flow.
18(M)	3.1	13.6	13,230	226	4.4	230	270	Eastern flow.
18(M)	1.3	3.4	7,350	249	2.5	180	430	Southeastern flow.
18	.8	2.2	4,710	58	2.7	170	130	Southern flow.

[1]Northeastern 1123 vent, southeastern lobe: area, volume, average thickness, and average width calculated from intersection with northeastern lobe.

[2]Distinction between first and second episode 13 flows was uncertain in mapping. Consequently, area and, thus, volume, flux, and average width of the second flow may have been incorrectly estimated. We have, therefore, omitted the second flow from plots showing those variables (figs. 1.43, 1.44, 1.46, 1.47).

depleted the original magmatic gas in the lava and that the gases of the flows were mainly plume gases and air that had been trapped and mixed with coalescing fragments of melt in the fountaining process. The sustained cascade of spatter fragments and the turbulent disruption where the fountain issued from the pond (fig. 1.20) must have churned these gases into the lava supplying the pond, much as an eggbeater whips air into cream or egg white. Thus, as long as the eruption lasted, the pond in its closed basin was a continuing source of fluid, gas-inflated melt.

During some periods of more vigorous fountaining—for example, the early parts of episodes 6 and 10—a high, broad fountain issued across much or all of Puu Oo Crater, and the lava overflowing the spillway seemed less fluid than normal. At such times, wide flows of spiny pahoehoe grading to aa spread near Puu Oo. Only after fountaining had diminished, pahoehoe issuing through the spillway

established the typical throughgoing channel system, and the normal elongate, river-fed aa flow then developed. Apparently, lava issuing from the crater was less fluid when a high, broad-based fountain prevented development of a stable pond into which air and vent gases could be whipped. As discussed in the next subsection, supply from the fountain with no basin or pond commonly produced thick, slow-moving aa directly. An additional effect of high fountains was to distribute more tephra outside of the crater, reducing the volume of lava available to supply a river-fed flow.

Transient pahoehoe overflows and local sustained leaks from the lava river created a pahoehoe-dominated envelope of levees and thin adjacent flows in the near-vent

FIGURE 1.29.—Pahoehoe flows extending from Puu Oo and fissure vents (to right of Puu Oo) immediately uprift shortly after beginning of episode 4. Growing spatter ring, enclosing a lava pond and fountain at Puu Oo, is approximately 20 to 30 m in diameter. Large, open crater with locally altered rocks, at bottom center just east of Puu Oo, is remnant of O vent, which was active during episode 3. View southward; photograph by J.D. Griggs, taken at 1318 H.s.t. June 13, 1983. Numerals (lower right) indicate date and time.

FIGURE 1.30.—Lava river in episode 2 channel, slightly less than 1 km from 1123 vent. Here, channel is about 15 m wide, and maximum velocity, at channel center, is approximately 2.4 m/s. Banks are pahoehoe overflow levees that slope away from channel on their outer flanks. Plates of smooth pahoehoe crust are carried along on moving lava surface. View westward; photograph taken at 1545 H.s.t. March 3, 1983. Numerals (lower right) indicate date and time.

FIGURE 1.31.—Flow from Puu Oo at beginning of episode 9. Pahoehoe has spilled through breach in crater rim and is advancing down evacuated episode 8 channel. A small distributary rejoins main flow at right. Lava flux is estimated at about 10,000 to 20,000 m^3/h. View northeastward from crater rim; photograph taken at 1603 H.s.t. September 15, 1983. Numerals (lower right) indicate date and time.

FIGURE 1.32.—Standing wave in lava river immediately downstream from Puu Oo during episode 18. Flow is from left to right; wave is probably about 2 m high. Rents in darker pahoehoe skin, formed by stretching during passage across standing wave, reveal large cavities in fluid incandescent lava beneath that give it a honeycombed aspect. Numbers in lower right indicate date and time. View northeastward; photograph taken at 1252 H.s.t. April 18, 1984.

region (fig. 1.33). Farther downstream, generally 1 or 2 km from the vent, this pahoehoe envelope gave way to an envelope of stagnating aa that contained the still-fluid lava river (fig. 1.34). At times, brief overflows locally mantled the aa adjacent to the river with thin pahoehoe.

At a distance generally of about 2 to 5 km from the vent, the river surface underwent a gradual transition to aa (fig. 1.34). Commonly, the position of the pahoehoe-aa transition, once established in the channel, did not migrate appreciably upflow or downflow, and so the toe of the flow tended to extend an increasingly greater distance from the transition as an eruptive episode continued. As at Mauna Loa, a visibly incandescent central channel, of the transitional channel zone, continued its passage within stagnant aa-flow margins (fig. 1.35), although it differed in appearance from the lava of the stable channel upstream. Floating plates of smooth pahoehoe crust (fig. 1.30) within the stable channel zone gave way to abrading clots of basalt; the river surface became more rubbly (fig. 1.36), its velocity slowed, and its incandescence decreased downstream within the transitional channel zone.

We had a few opportunities, when the transitional channel zone extended into the Royal Gardens subdivision, to observe slow downflow movement in which the entire central part of the flow appeared to move as a unit, separated by a narrow boundary zone from the lateral margin. Where continued movement left a partly evacuated channel within the aa at the end of an episode, we noted that the steep, interior channel walls consisted of aa locally plastered with compacted and smoothed gouge that was grooved parallel to the channel axis (fig. 1.37). In addition to evacuated aa channels in which the walls had obviously been shear boundaries, we commonly found arrays of longitudinal ridges of blocky aa, equivalent to the marginal shear ridges documented by Lipman and Banks (1987) within the transitional channel zone on Mauna Loa.

FIGURE 1.33.—Proximal part of bank-full episode 11 lava river, with enclosing envelope of new pahoehoe formed by overflows. Distance to Puu Oo is nearly 2 km. Darker aa at flow margins is from an earlier eruptive episode. View southwestard; photograph by J.D. Griggs, taken at approximately 1100 H.s.t. November 7, 1983.

FIGURE 1.34.—Distal part of episode 11 flow. Fluid pahoehoe river (stabilized channel zone) is enclosed within an envelope of stagnating aa, approximately 200 m wide at bottom center. Flow margin in near and middle ground, about 4 km from the vent, underwent essentially no change during remaining 7 hours of eruption. Transition within channel from pahoehoe to aa, visible here where shiny pahoehoe surface loses its identity, is approximately 5 km from vent. Advancing flow terminus, obscure in distance at upper left, is about 8 km from vent. View eastward; photograph by J.D. Griggs, taken at approximately 1100 H.s.t. November 7, 1983.

FIGURE 1.35.—Incandescent aa channel within transitional channel zone of eastern episode 18 flow. Full width of flow in near ground is 300 to 500 m. Between lower right corner of view (approx 8.7 km from vent) and area where incandescent channel loses its identity (approx 1 km distant), enclosing aa is stagnating. Beyond that, in zone of dispersed flow, active zone widens, and flow perimeter becomes increasingly active toward flow front, out of view in distance, 11 to 12 km from vent. View southward; photograph by J.D. Griggs, taken at approximately 1142 H.s.t. April 20, 1984.

At the downstream end, the transitional channel zone lost its identity (fig. 1.35) as it graded into the zone of dispersed flow behind the active flow front, which normally advanced at average rates ranging from about 50 to 300 m/h. Unlike the upper flowage zones, in which the active lava passed through an axial region bounded by relatively stagnant, largely solidified lava, the active region widened within the zone of dispersed flow. Thus, the perimeter of this zone became increasingly active in the downstream direction, and some lateral spreading occurred near the front. The major activity, however, was concentrated at the front, and the entire front, tens to hundreds of meters wide and representing nearly the full final width of the flow lobe, advanced more or less uniformly. Sometimes the front divided, forming two or more lobes that advanced separately. At times, one of these lobes captured the bulk of the supply, and progress on the other diminished or stopped. Sometimes the lobes rejoined leaving a kipuka within the flow.

Flows of episodes 2 through 5 invaded the Royal Gardens subdivision. More continuous observation of the flow-front advance was possible in the subdivision than in the rain forest between the rift zone and the subdivision. These observations showed that the flow front advanced in pronounced surges (Neal and Decker, 1983), with velocities ranging from about 2 to 30 m/min. Surges at Royal Gardens lasted as long as about an hour, although most were briefer. They were separated by intervals as long as 8 hours during which the flow front advanced more slowly or was virtually stagnant.

Surging also occurred in flatter terrain closer to the vent. During close monitoring of the episode 16 flow advance, from 4 to 5 km from the vent, brief surges originating across only part of the flow front moved as rapidly as 60 m/min.

Advancing surges could commonly be seen from a suitable vantage point while they were still several hundred meters upflow of the flow front. Seen from the front, with line-of-sight parallel to the flow surface, an approaching surge appeared as a rapidly advancing wall of incandescent aa, rising several meters above the normal level of the flow surface. With a downward perspective that gave a view of the flow surface (fig. 1.38), a surge was seen as a tapering sheet of highly incandescent lava, emerging upstream from the axial region of the flow and advancing rapidly over the surface of slow-moving, much less incandescent aa. When not accelerated by a surge, the aa-flow front showed only minor incandescence (fig. 1.39*A*) and advanced slowly as blocks and finer fragments sporadically avalanched down the continually oversteepening front. As the surge approached, however, the front rapidly thickened (fig. 1.39*B*), and its advance accelerated. Subsequently, the advancing front thinned, commonly as

FIGURE 1.36.—Distal part of the advancing northeastern episode 12 flow. Zone of transitional flow, with its rubbly, incandescent central channel, extends virtually to flow terminus, about 5 km from vent. In near to middle ground, flow is 30 to 50 m wide. Except for avalanching of a few blocks, rubbly aa levees are stagnant; they underwent no further recognizable lateral spreading as flow advance continued. On its north (left) flank, episode 12 aa impinges on episode 7 aa. Bare, weathered lava at right was erupted in 1963. View northeastward; photograph by R.B. Moore, taken about 1700 H.s.t. November 30, 1983.

FIGURE 1.37.—Wall of evacuated channel of episode 4 aa flow near Royal Gardens. Steep wall is plastered by striated gouge composed of finely comminuted basalt left at sheared boundary between more active aa channel fill and bounding levee. Backpack for scale. Photograph taken November 25, 1983.

a short-lived, more fluid flow broke out of it (fig. 1.39*C*), or as a rapidly moving sheet of thinner, more fluid lava overtook the thickened aa margin, spilled over it, and became the flow front.

During episode 4, collapse of part of the cone at the vent caused a surge that produced overflows in the stabilized channel zone. Approximately 1½ hours later, a large surge occurred near the distal end of the flow at Royal Gardens about 7 km from the vent. On the supposition that these two events were related, we infer that the pulse of melt traveled the length of the flow at an average velocity of 1.3 m/s, a value in agreement with the lower range of velocities we determined in the stabilized channel zone. Such a transmission would be possible only if a fluid core truly extended through the entire length of the flow. Production of fluid lava at the flow front during surge events supports this idea. In addition, after each eruptive episode, we invariably found small lobes of dense, spiny pahoehoe that had been extruded from the aa-flow margins or, in some cases, from the flow tip.

Normally, however, we saw no specific upstream events that we could relate to the surges in Royal Gardens. We suspect, therefore, that melt tended to pond beneath the carapace of aa in the middle or lower parts of the flow until the thickness of ponded lava was sufficient for gravitational stress to overcome the yield strength; then, a transient lava surge swept downstream to the flow front. Supporting evidence for such a mechanism comes from the observation, during the Mauna Loa eruption, that the belts of shear ridges adjacent to the obvious transitional aa channel inflated and subsided as much as several meters vertically in response to changes of lava level in the channel (Lipman and Banks, 1987).

FIGURE 1.38.—Nighttime surge at Royal Gardens during episode 5. Fluid surge advanced at estimated rate of 21 m/min over preexisting, nearly stagnant aa (lower left, with small points of incandescence.). Photograph by R. Seibert, taken at 1821 H.s.t. July 2, 1983.

SPATTER-FED (ROOTLESS) FLOWS

Brief, intense spatter falls on the steep flanks of the cone produced thin sheets of pahoehoe that armored the cone surface (fig. 1.7). More prolonged falls on the steep flanks produced pahoehoe or aa flows that extended away from the cone. Pahoehoe apparently occurred where intense falls of fluid spatter were rapidly mobilized on the steep slope. During episode 7, intense spatter fall on the west flank of Puu Oo (fig. 1.20) at times filled a nonerupting satellitic crater with a pond that overflowed and supplied a channelized lava river.

A prolonged spatter fall on one sector of the cone's flank sometimes produced a broad and thick spatter-fed aa flow (fig. 1.40) that advanced as much as 3 km from the cone. Such flows did not have well-developed central channel systems and consisted throughout of slowly advancing aa. Near the source, their surfaces were commonly fractured to form slivers elongate perpendicular to the direction of flow; individual slivers could be as large as 5 m across and 50 m long. With continued movement, these slivers broke up to form smaller, more nearly equant blocks. The large fractures are analogous to the tears created by slumping (fig. 1.40), and on the steep cinder-cone flanks, there is probably a continuum from simple slumping to generation of major spatter-fed flows. Likewise, because these spatter-fed flows originate from mobilization of accumulating spatter deposits on the flank of the cone, the flows are continuous with the flanks, and so the distinction between the cone and the flows may be obscure.

The most voluminous (approx 19×10^6 m^3) spatter-fed aa flow was produced during episode 3 at the northeastern vent of the 1123 cone. During approximately 10 days of eruption, the high fountain at this vent produced a multilobed aa flow (pl. 1) that ponderously advanced 4 to 5 km from the vent at an average rate of 25 m/h (table 1.3). On average, the flow was about 5 m thick, but locally it was at least 12 m thick where it buried a preexisting spatter cone at camp A (fig. 1.41). For most of the eruption,

FIGURE 1.39.—Evolution of a surge at Royal Gardens during episode 5. *A*, Surge, which forms low ridge visible through haze behind aa-flow front, approaches nearly stagnant flow front. Rate of approach was estimated at approximately 30 m/min. Photograph by R.W. Decker, taken at 1454 H.s.t. July 2, 1983. *B*, Just 4 minutes later, flow front has doubled in height, incandescence at its front has increased, and accelerated advance has begun. Before it thinned to a fluid lobe, high advancing front shoved truck to vicinity of light-gray sedan before burying them both. Photograph by R.W. Decker, taken at 1458 H.s.t. July 2, 1983. *C*, After surge overtook aa front, a 1- to 2-m-thick fluid breakout continued down paved street at a rate of 15 m/min. View from farther downslope; photograph by R.W. Decker, taken at 1510 H.s.t. July 2, 1983.


A


B


C


CHANNEL
N
0
50
100 METERS

the fountain and the flow issued from a reentrant in the growing 1123 cone (fig. 1.42); after the initial 1 to 2 days, there was no closed basin with a lava pond like those that typified most central-vent episodes and produced the river-fed flows. Pahoehoe, that seemed more like a slurry on the aa-flow surface, occurred only within a few hundred meters of the vent (fig. 1.42); and a short transitional channel, probably contained entirely within a kilometer of the vent, passed, for at least a few days, on the north side of the slowly disappearing camp A spatter cone (fig. 1.41). Otherwise, we saw no evidence of the well-developed channel system that we would see at so many later times, and the resulting flow consisted of coarse, blocky aa throughout.

The massive spatter-fed aa flows apparently formed where spatter accumulating from prolonged falls remained above solidus temperatures but, unlike the more rapidly mobilized spatter-fed flows discussed earlier, formed a mass with too high a yield strength to flow as thin fluid sheets or lobes on the available slope. This slower mobilization could have resulted from lower rates of accumulation, partial cooling during a high-fountaining trajectory, or lower slope angles. As spatter accumulated in a pile some meters thick, it probably lost part of its entrained gas and became denser, but eventually its mass caused sufficient gravitational stress to overcome its increased yield strength. It then began to flow and continued to do so as long as gravitational instability was maintained by continuing spatter accumulation at the source.

NUMERICAL FLOW PARAMETERS

Data obtained from our real-time observations and postepisode flow mapping include measured length, area, and thickness, and calculated flow-advance rate, volume, average thickness, and lava-flux rate for most of the individual flow lobes produced during the central-vent eruptions. The fundamental data are given below in the chronologic narrative and in plates 1 through 5, and, along with derived parameters, are summarized in table 1.3. Note that we use the term "lava-flux rate" for the rate of lava supply to individual flow lobes to distinguish that from the overall lava-discharge rate for each episode (table 1.1).

Flow length versus volume is plotted in figure 1.43 for the central-vent flows of episodes 2 through 18. Although there is significant scatter, the data show that these two parameters are clearly related. As recognized by Malin (1980) for other historical Hawaiian lava flows, the correlation occurs because the flows have a limited range in cross-sectional area. The major flows provide most of the data spread: They range from 2 to 6 m in average thickness and mostly from 200 to 350 m in average width (table 1.3). Thickness was probably controlled primarily by viscosity, and width was limited by the dynamics of levee development and channel formation as the flow extended from its point source at the central vent. Commonly, wider river-fed flows, such as the episode 7 flow (pl. 2), resulted from division of the flow toe into subordinate lobes that traveled along nearly parallel paths. Figure 1.43 also implies that the spatter-fed flows have relatively greater cross-sectional areas than other flows of comparable volume.

Other workers (Walker, 1973; Wadge, 1978; Malin, 1980) have found, in Hawaii and elsewhere, that flow length is correlated with lava-flux rate. The same is true for these central-vent flows (fig. 1.44). In accord with Malin's (1980) conclusion for other historical Hawaiian flows, we found that the amount of scatter in the length-flux relation is greater than in the length-volume relation. For central-vent flows of the Puu Oo eruption, the length-flux correlation results primarily from the limited range of flow widths and thicknesses, as does the length-volume correlation. The additional scatter in the length-flux relation apparently reflects largely the relatively great range (from less than 10 to about 200 hours) in the duration of lava supply. Apparent viscosity, discussed subsequently, probably also played a role in controlling flow morphology and, thus, the length-flux relation.

Flow-advance plots for each eruptive episode are included on plates 1 through 5. Except for brief periods in the early hours of some eruptive episodes, the flows tended to have fairly uniform advance rates. Short-term variations in slope in the diagrams are difficult to evaluate; they may reflect either temporary fluctuations in advance rate or errors in flow-front position that resulted from the sometimes-difficult conditions of flow-front reconnaissance. Our overall impression was that normally during an episode, overall discharge rate varied

FIGURE 1.40.—Puu Oo (top center) and spatter-fed flows to north, southeast, and west after episode 16. Evacuated and rubbly channel (labeled) for main flow is in upper right. Coarse, blocky, spatter-fed flows originated on flanks of cone, where accumulating viscous spatter began moving downslope (arrows indicate direction of movement), deforming under its own weight. More brittle upper part of deforming mass fractured into slivers elongated transverse to direction of flow, and continued movement broke the slivers into smaller, more equant fragments. Near-vent parts of small spatter-fed flows at upper left have been buried by subsequent continued accumulation of pyroclastic materials on flank of cone. Gashes that reflect slumping of the accumulating pyroclastic deposits are conspicuous in south sector. Landscape at left has been smoothed by deposition of an air-fall pyroclastic deposit. Photograph 84.3.16JG120#7 by J.D. Griggs, taken March 16, 1984.

little, if at all. Therefore, the fairly steady advance of the flow front during an episode reflects generally steady lava discharge and the effectiveness of the channelized flow system in delivering lava to the active distal region of the flow. Short-term variations like those represented by the surges witnessed at Royal Gardens probably occurred, but most were averaged out by the intermittency of the flow-front determinations (pls. 1–5).

The flow-advance diagrams also show no clear effect of differing topographic slope on the advance rate.

FIGURE 1.41.—Spatter cone at camp A surrounded by episode 3 aa. Cone, formed in 1965, was 12 m high. Coarse, rubbly aa on south rim (far side) is virtually stagnant. More active lava on north side (in near ground) overtopped north rim of the 1965 cone 2 days later. Subsequently, cone was completely buried by episode 3 aa. View southeastward; photograph by R.B. Moore, taken on the afternoon of April 1, 1983.

FIGURE 1.42.—Erupting 1123 vent during episode 3. Pahoehoe distributary system, which extends about 200 m from vent, issues from base of 40- to 50-m-high northeastern fountain. Small tube-fed flows issue from base of 1123 vent at lower left. Episode 2 cones, of 0740 vent, and pahoehoe are visible at lower right. View northwestward; photograph by J.D. Griggs, taken at approximately 1230 H.s.t. March 31, 1983.

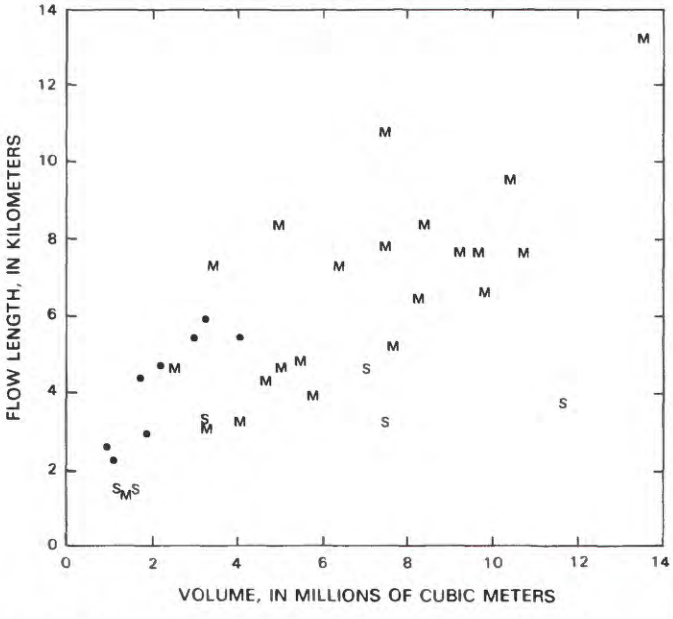

FIGURE 1.43.—Flow length versus volume for central-vent flows of episodes 2 through 18. Data from table 1.3. M, major river-fed flow(s) of each eruptive episode; S, spatter-fed flow; dots, subordinate river-fed flow.

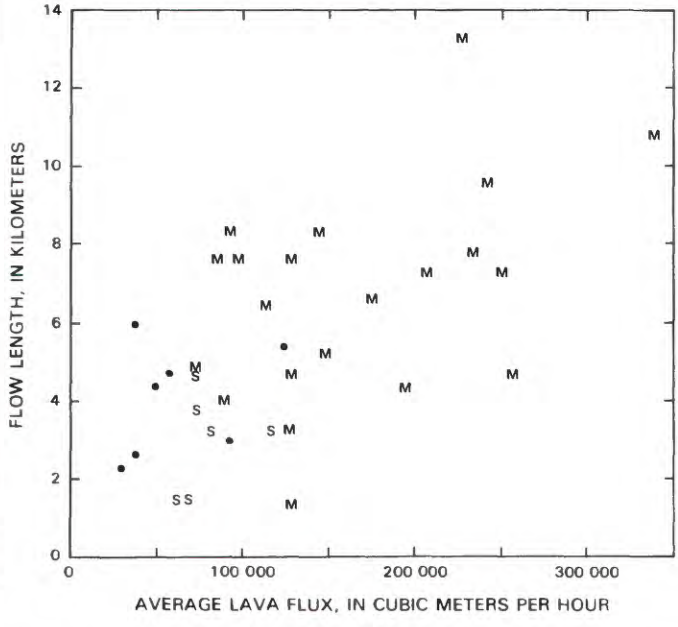

FIGURE 1.44.—Flow length versus average lava-flux rate for central-vent flows of episodes 2 through 18. Same symbols as in figure 1.43.

Average slope angles range from approximately 1.5° along the axis of the rift zone to about 6° in the Royal Gardens area.

Higher than normal early advance rates—for example, in episode 8—reflect rapid advance of the main flow as an elongate lobe of pahoehoe during the early part of an episode before the transition to aa became established. Slower than normal early advance, however, as in episode 16, may reflect lower fluidity of the lava that issued from the crater during periods when the fountain was high and broadly based (see subsection above entitled "River-Fed Flows"), or significant diversion of part of the lava supply to rapidly accumulating tephra deposits from high fountains during the early part of an episode.

Comparison of the flow-advance diagrams for early episodes with those for later episodes shows that the main flows advanced at higher rates during the later episodes. This relation is summarized in figure 1.45, in which the average advance rate versus date is shown. Also shown is the generally lower velocity of the spatter-fed flows.

Three of the later main flows advanced at unusually high average velocities of 400 to 500 m/h. One main flow, which extended from the Puu Oo area to Royal Gardens over a single night during episode 18, was recognized as pahoehoe as its toe moved into the subdivision. Another, the second episode 13 flow, was active for only about 6 hours; its rapid advance rate almost certainly reflects extension of the channelized-pahoehoe channel virtually to the advancing toe. The unusually rapid average advance rate of the third, which was the main flow of episode 17, apparently does not reflect sustained prolongation of fluid channelized pahoehoe to the distal part of the flow. Late in the afternoon of March 30, 1984, after nearly half a day of eruption, the toe of the episode 17 flow was about 5 km from the vent (pl. 5), and the pahoehoe-aa transition in the channel was 1 to 2 km from the vent. By daybreak the next morning, after the eruption's end, the aa toe was more than 10 km from the vent; overflows draping the aa-channel margins showed that fluid pahoehoe within the channel had extended as far as 4 km from the vent, but there was no evidence of its having been within the distal half of the flow. For three-quarters of its length, the episode 17 flow followed the axis of the episode 16 flow, and the rapid advance of the episode 17 flow may reflect its containment, over at least part of its length, within episode 16 levees. Thus, inhibition of lateral spreading at the advancing toe may have resulted in an accelerated forward advance.

The average velocity of the main flows is correlative with the average lava flux (fig. 1.46), which increased through the series of eruptive episodes (fig. 1.47) in apparent response to increasing overall discharge rate (fig. 1.4). These changes probably reflect progressive enlargement and streamlining of the conduit between the summit reservoir and the vent, as well as progressively decreasing viscosity of the melt in transit to the vent.

Unexpectedly, we found that the average flow thickness progressively decreased through the series of central-vent episodes (fig. 1.48). The most likely explanation is that the decreasing average thickness, as well as the increasing average velocity, records a decrease over time in the viscosity of the lava. Thermal, compositional, and petrographic data support this explanation.

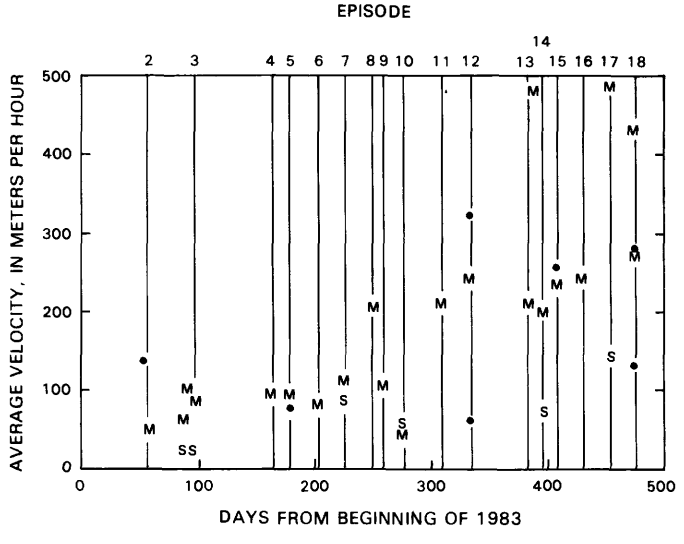

FIGURE 1.45.—Average flow-advance rate versus time of eruption for central-vent flows of episodes 2 through 18 (numbered). Same symbols as in figure 1.43.

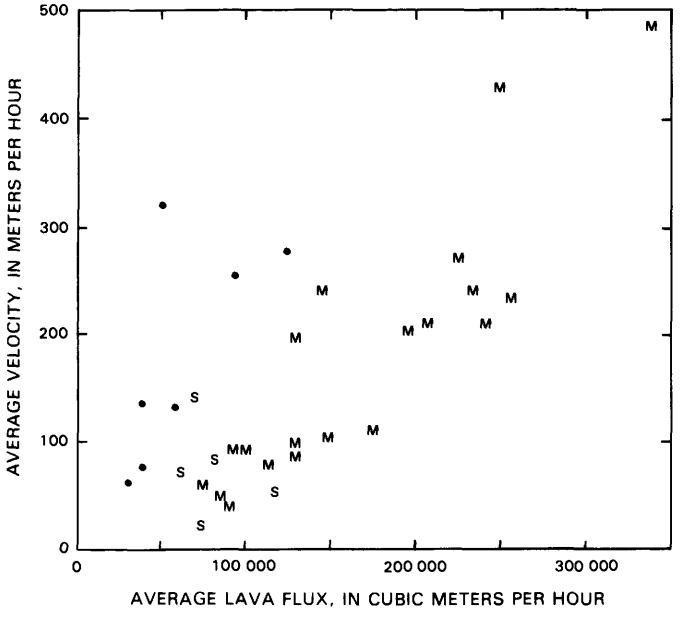

FIGURE 1.46.—Average flow-advance rate versus average lava flux for central-vent flows of episodes 2 through 18. Same symbols as in figure 1.43.

Lava temperatures measured through episode 18 are plotted in figure 2.2 (see chap. 2); most are pahoehoe temperatures measured within 1 or 2 km of the vent. Although these data show scatter for each eruptive episode, an unmistakable progressive increase of about 20 °C is indicated. A concomitant compositional change from distinctly differentiated lava in the early episodes to more mafic lava in the later episodes is illustrated in figure 2.3*B*, which plots analyzed $Na_2O + K_2O$ content versus the time of eruption. A similar plot (fig. 1.49) of the abundance of phenocrysts, which are enclosed in a groundmass of glass (see chap. 3), shows that the proportion of crystals to melt decreased through the early episodes from a high of about 9 percent; after episode 10, the erupting lava was nearly aphyric. The complete analyses are given in chapter 2, and the petrology is discussed in chapter 3.

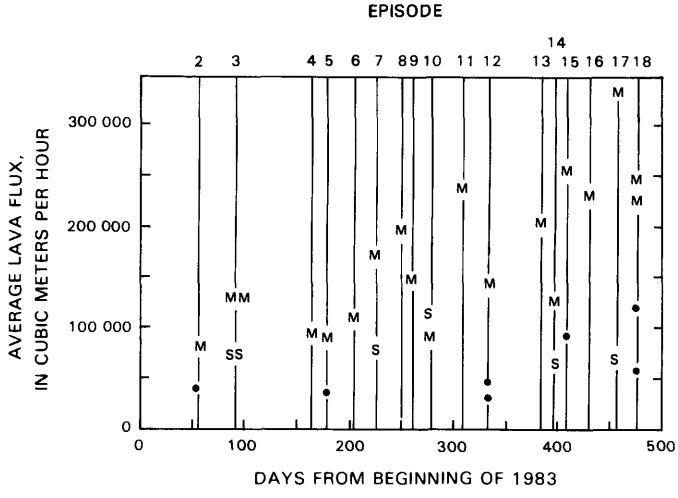

FIGURE 1.47.—Average lava flux versus time of eruption for central-vent flows of episodes 2 through 18 (numbered). Same symbols as in figure 1.43.

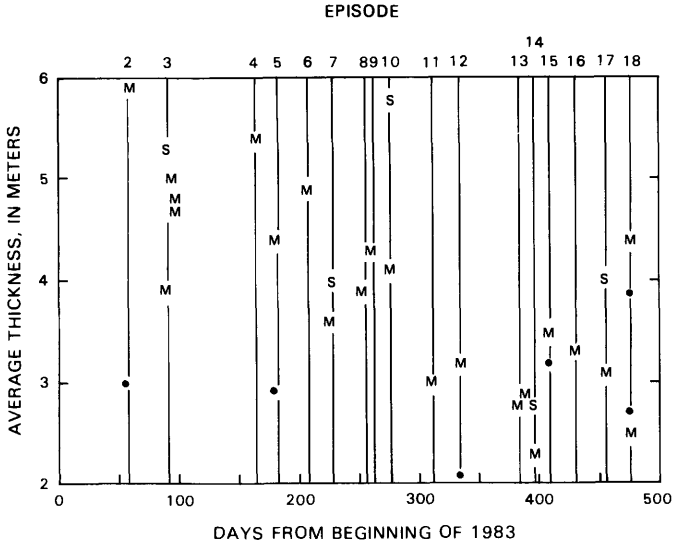

FIGURE 1.48.—Average flow thickness versus time of eruption for central-vent flows of episodes 2 through 18. Same symbols as in figure 1.43.

Field and laboratory studies by Shaw and others (1968) and Shaw (1969) of viscosity relations in Kilauea tholeiite of Makaopuhi lava lake indicate that a 20-°C change within the temperature range of the 1983–84 Kilauea lavas would be expected to yield an inverse change of about 40 percent in viscosity if the melt is crystal free. Addition of crystals with progressive cooling, from none at the 1,200-°C liquidus temperature to about 25 volume percent at 1,120 °C in the solidifying lava lake, greatly exaggerated the viscosity change in the lava lake; a decrease in viscosity, between 1,145 and 1,125 °C, of about an order of magnitude is indicated. In addition, Shaw recognized that the melt itself increased in viscosity as its composition changed in response to progressive crystallization. All three effects operated simultaneously during the first 20 episodes as temperature increased, crystallinity decreased, and the bulk composition became less evolved. The ensuing decrease in viscosity, which is recorded by the increasing average velocity and decreasing average thickness of the main flows, may be responsible in part for the increase in overall rate of lava discharge, which, as discussed above, apparently also contributed to the increasing average advance rates of the main flows.

Comparison with the 1984 Mauna Loa lava is interesting. During that approximately 3 week long eruption, the Mauna Loa lava changed neither in composition nor in its eruptive temperature of about 1,140 °C. Increasing apparent viscosity during the eruption, however, may have reflected increasing crystallinity (Lipman and Banks, 1987), as the microphenocryst abundance increased from less than 0.5 volume percent in the early part of the eruption to 20–30 volume percent in the later part.

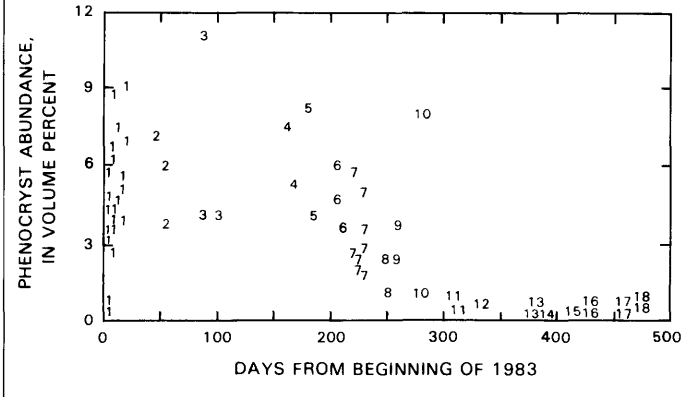

FIGURE 1.49.—Phenocryst content of lava samples versus time of eruption for episodes 1 through 18 (indicated by numbers). Data from Garcia and Wolfe (see chap. 3).

REPOSE-PERIOD ACTIVITY

Low-level eruptive activity was visible between many of the major eruptive episodes. For approximately 2 weeks before the main activity of episode 2, slow and sporadic effusion of about 0.5×10^6 m^3 of lava built a low shield and a line of small spatter cones northeast of the 1123 vent (see subsection below on episode 2). Very slow eruption of spatter and pahoehoe also occurred within and near the 1123-vent spatter ring about a week before episode 3 (see subsection below on episode 3). Thereafter, we observed repeated repose-period occurrences of low-level eruptive activity within Puu Oo Crater or, after episode 13, within the open pipe that descended from the crater floor. This activity was dominated by two phenomena: gas-piston activity and gradual ascent of the magma column toward the surface within the conduit below the crater floor. As in the first stage of the 1969–71 Mauna Ulu eruption, the low-level activity at Puu Oo became more continuous with succeeding eruptive episodes (fig. 1.3).

A general pattern of summit inflation persisted throughout the repose periods. However, the rate of inflation varied (fig. 1.2), and at times inflation was interrupted by brief periods of deflationary tilt change. Harmonic tremor of low amplitude continued in the Puu Oo area through the repose periods.

Gas-piston activity much like that described during repose periods in the first stage of the 1969–71 Mauna Ulu eruption (Swanson and others, 1979) was evident many times during the low-level activity at Puu Oo, although the volume of rising and falling melt was about a tenth of that typically observed at Mauna Ulu. Sometimes we could observe the gas-piston events directly, either in the lower part of the crater between the early episodes or, between the later episodes, within a bowllike inner crater set into the partly crusted top of the lava-filled pipe.

The lava surface, covered by a thin, flexible crust, would gradually rise about 10 to 20 m in the bowl or pipe. The lava was apparently uplifted by a gas accumulation buoyantly rising through the upper part of the magma column (Swanson and others, 1979). At times, a low (max 4 m high) dome fountain played on the lava surface, above the conduit that was exposed when the pond drained. Otherwise, this surface was smooth and undisrupted, suggesting that the rising lava was relatively depleted in gas. At its maximum elevation, when about 2,000 m^3 of melt had accumulated in the bowl, the distended lava surface would be momentarily poised. Then, as the accumulated rising gas pierced the lava surface and began to escape, the lava became agitated and drained rapidly out of sight into the conduit below. Simultaneously, a roaring rush of SO_2-rich gas that commonly carried spatter and Pele's hair was emitted from the collapsing pond and the glowing conduit into which it drained. A distinctive burst in harmonic tremor accompanied each brief episode of rapid draining and gas emission. Lava would then reappear, slowly rising in the stem of the funnel, and the process would begin again. The cycles that we observed ranged from about 4 to 20 minutes in duration and, at times, were strongly periodic. Figure 1.50 illustrates this phenomenon.

Once the single open pipe became a permanent feature, after episode 13, we could see that the magma-column surface within the pipe (fig. 1.51) rose gradually and sometimes spasmodically toward the crater floor during each repose period. Our visits to the remote vent during repose periods were intermittent, and visibility down the pipe was commonly limited by blinding fume and, on damp days, dense water vapor. Under the best conditions, we would first see the top of the magma column when it was about 50 m down the pipe; this first sighting generally occurred days to weeks before the next major episode. Following episodes 13, 19, and 20, the top of the column was immediately visible in the pipe (see representation of low-level volcanic activity in fig. 1.2).

Sometimes the gently roiled magma surface would be open (fig. 1.51); at other times, it would be crusted, but there was always at least one small glowing vent that emitted gas, spatter, and a few small pahoehoe flows (fig. 1.52). Normally, flows or spatter were emitted periodically from such small vents along with a rush of gas and a burst of harmonic tremor that suggested gas-piston activity below the crust. During the repose periods between the early episodes, when the conduit beneath the crater floor was choked with rubble, similar activity at small vents in the crater floor indicated that the magma column was near the level of the crater floor and that more vigorous eruptive activity was imminent.

ERUPTIVE-EPISODE ONSETS, ENDINGS, AND PAUSES

We were able to watch firsthand the beginnings of several major eruptive episodes at Puu Oo. The crater would fill with lava sufficient to steadily overflow the spillway. If gas-piston activity had been occurring, it gave way to an open, roiled pond with a low dome fountain. Over a period ranging in length from tens of minutes to about 2 hours, the rate of overflow would progressively increase from 10^3–10^4 m^3/h to normal lava-discharge rates of at least 10^5 m^3/h. Simultaneously, the fountain would expand from an initial height of less than 10 m to the tens or hundreds of meters typical of vigorous eruption. Because of the quiet, relatively slow extrusion and the minimal fountaining during the early part of the eruption onset, we had the repeated impression that probably 10^4 to 10^5 m^3 of degassed magma was normally expelled

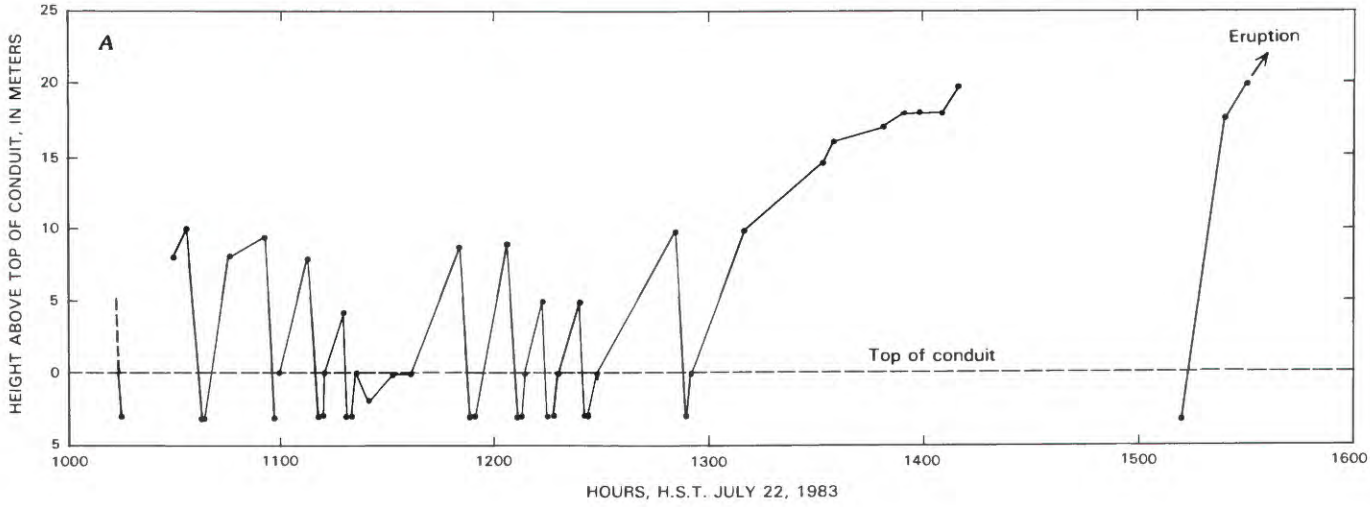
A
Eruption
Top of conduit
HEIGHT ABOVE TOP OF CONDUIT, IN METERS
25
20
15
10
5
0
5
1000
1100
1200
1300
1400
1500
1600
HOURS, H.S.T. JULY 22, 1983

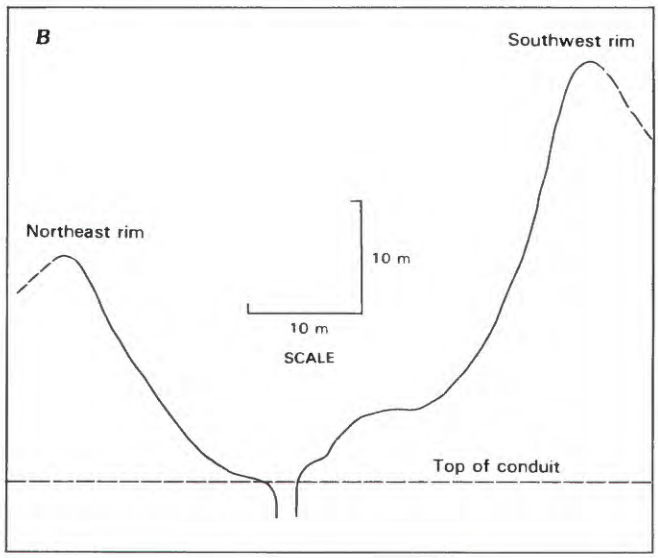
B
Southwest rim
Northeast rim
10 m
10 m
SCALE
Top of conduit


C


D


E

from the subsurface conduit before the typical vigorous lava discharge and fountaining began.

Most individual fissure-eruption events of episode 1 ended gradually over a period of tens of minutes to several hours. The elongate fountain would diminish in height and become less steady, and discharge would stop along some segments, so that the remaining fountain activity was concentrated at separated segments or nodes along the eruptive fissure. Continuous eruption along a segment of the fissure gradually gave way to intermittent eruption that, in the last stages, generally consisted of a series of loud, intermittent gas bursts. These bursts ejected curved, elongate ribbons of lava, several meters long, that spread upward and outward, as if a large bubble had burst within ponded lava in the vent.

The central-vent eruptions at the 1123 vent during episodes 2 and 3 also died gradually, as indicated by the progressive decrease in fountain vigor during the last day of each episode (figs. 1.21, 1.23). During this decay, the fountain became so low at times that it disappeared briefly from view. In addition, during the last hour of episode 2, we saw brief cessations of fountaining and lava-flow production.

In contrast to the gradual endings of episodes 2 and 3 at the 1123 vent, the endings of eruptive episodes at Puu Oo were relatively abrupt. During some episodes, discharge stopped suddenly with no premonitory warning. At least once, we missed the end of an eruptive episode when our attention was briefly diverted from the vent. Ordinarily, however, the fountain diminished in height and became less steady in the last 3 to 10 minutes of the episode, and sometimes during that short period we saw pauses of a few seconds or tens of seconds in fountaining and flow production. Brief gas-bursting events like those that commonly ended the episode 1 fissure eruptions sometimes occurred in Puu Oo Crater during the last moments of an eruptive episode.

Normally, the output of lava from Puu Oo was steady until the terminating moments of the episode, after which no further discharge occurred. Significant exceptions, in episodes 13 and 19, are described in detail in the subsections below on these two episodes. In each case, discharge rapidly waxed and waned, often pausing momentarily, so that high fountaining and flow production would abruptly stop and then resume again. In addition, episode 13 discharge stopped for several hours and then resumed. Many such pauses occurred during episode 19, which included periods of intermittent slow discharge and gentle overflows of lava from Puu Oo Crater. A series of brief pauses was also recorded during a 24-hour period in the middle of episode 3 (see subsection below on episode 3).

The repeated brief, abrupt interruptions and resumptions of vigorous fountaining and flow production seen in episodes 3, 13, and 19 almost certainly reflected interference with subsurface magma transport close to the vent rather than in the summit region. The abrupt or briefly oscillating terminations of eruptive episodes at Puu Oo resembled the pauses that occurred within episodes and, like them, probably were controlled by conditions in the vent region. Furthermore, the onset and ending of deflation at the summit, as recorded by the Uwekahuna tiltmeter, commonly lagged by as much as several hours behind the onset and ending of each eruptive episode at Puu Oo (Wolfe and others, 1987); this relation suggests that the major inflections in the summit tilt record, after the vent became established at Puu Oo, were responses to changes manifested first at the vent.

LATER DEVELOPMENTS

Prolonged pond activity and low discharge during episode 19 largely filled Puu Oo Crater with solidified pahoehoe and led to eventual elimination of the lava pond and the stream of fluid pahoehoe that had issued from it so regularly. Episode 20 was brief and occurred during the night without our witnessing it. Later mapping showed that nearly half of the erupted volume supplied a massive spatter-fed flow, and the rest formed a lava-

FIGURE 1.50.—Gas-piston activity preceding episode 6 at Puu Oo. *A*, Estimated pond depth versus time for July 22, 1983. *B*, Schematic cross section of crater. Observers on northeast rim of crater recorded 11 filling and draining cycles between 1015 H.s.t. and onset of episode 6 at 1530 H.s.t. Breaks in plot reflect gaps in observation. During draining of crater, lava disappeared from view at a depth of 3 m within a 2-m-diameter pipe that extended downward from crater floor. It then quickly reappeared in pipe and slowly refilled bowllike crater. Filling normally occurred over an interval of 5 to 22 minutes, draining took 1 to 3 minutes, and lava was out of view in pipe for 1 to 3 minutes. Prolonged filling that began just before 1300 H.s.t. flooded a low point in northeastern part of crater rim. Pond then drained at least once more before a rapid final filling that led to onset of eruptive episode. Low bench at base of southwest crater wall marks buried site of a vent that built a mound of spatter on preceding day. *C*, Lava pond near end of filling. Solidified, fresh lava adhering to crater wall just above pond surface records one or more deeper previous ponds. Pond is about 30 m in diameter and 10 m deep. A 1- to 2-m-high dome fountain plays on pond surface above conduit. Photograph taken at 1108 H.s.t. July 22, 1983. Numerals (lower right) indicate date and time. *D*, Lava pond beginning to drain. Crusted surface has become concave and is stretching and pulling apart as lava rapidly withdraws from beneath it. Abruptly increased gas emission has disrupted dome fountain and transformed it into a chaotic spray of spatter fragments. Photograph taken at 1110 H.s.t. July 22, 1983. Numerals (lower right) indicate date and time. *E*, Floor of evacuated crater after draining. Lava surface is momentarily out of view in glowing 2-m-diameter conduit descending from floor. Photograph taken at 1059 H.s.t. July 22, 1983. Numerals (lower right) indicate date and time.

river system that fed three small channelized flows to the northeast. Additional filling of the crater occurred during episode 20; thereafter, at least through May 1985, the lava-pond, lava-river style of eruption did not recur. Consistently high fountains since episode 19 have greatly increased the size of Puu Oo and resulted in the accumulation of thick air-fall deposits beyond its downwind flanks. Vestiges of the crater were soon obliterated, and spatter-fed flows developed a thick wedgelike apron of aa surrounding the cone.

CHRONOLOGIC NARRATIVE

EPISODE 1 (JANUARY 3–23, 1983)

SUMMARY OF EPISODE 1

After a 24-hour-long earthquake swarm that migrated from the Mauna Ulu-Makaopuhi Crater area to the vicinity of Puu Kamoamoa (see chap. 7), eruptive activity began within Napau Crater at 0031 H.s.t. January 3, 1983. Eruption continued for 9.5 hours in the early morning of January 3. During that episode, a 6-km-long, discontinuous line of erupting fissures extended progressively downrift from Napau Crater to the 0740 vent (pl. 1), then contracted to the vicinity of Puu Kamoamoa, and finally stopped erupting at 1000 H.s.t. Except for a brief eruption at the 0740 vent during the afternoon of January 3, no further discharge of lava occurred on January 3 or 4.

Subsequent eruptive activity during episode 1 consisted of intermittent events at several different vents (pl. 1; table 1.4). On January 5 and 6, eruptive activity was mainly concentrated at the 0740, 1123, and 1708 vents south of Puu Kahaualea. Fountain activity and minor lava production also occurred uprift at Puu Kamoamoa and at two vents uprift of Kamoamoa. Closely following an extension of the earthquake swarm downrift to the vicinity of Kalalua, vents 1 to 2 km northeast of the 0740 vent opened during the morning of January 7 and erupted until the early morning hours of January 8. They produced a spectacular fissure-fed fountain and a voluminous lava flow that advanced down Kilauea's south flank. From January 8 through 15, eruptive activity was localized south of Puu Kahaualea, mostly at the 1123 and 1708 vents. Finally, a brief, very small eruptive outbreak occurred about 500 m downrift of Puu Kamoamoa on January 23. Altogether, during a total of approximately 99 hours of eruptive activity over a period of 20 days, episode 1 produced an estimated 14×10^6 m^3 of new basalt that covered an area of 4.8×10^6 m^2.

JANUARY 3, 1983

Guided by earthquake locations determined during the premonitory swarm, a crew of observers arrived early on January 2 at a point midway between Napau Crater and Puu Kamoamoa. There, they awaited the eruptive outbreak and were rewarded when fountaining began at the base of the north crater wall of Napau Crater at 0031 H.s.t. January 3. The fountains, however, must have been

FIGURE 1.51.—Open pipe intersecting floor of Puu Oo Crater, approximately 1½ days before onset of episode 15. Lava surface is visible about 15 m down pipe. Accumulating spatter has built a 2- to 3-m-wide collar just above lava surface. View to upper right is across spillway and through deep breach in northeast rim of crater. Spillway surface is about 5 m above top of pipe. View northward; photograph taken at 1126 H.s.t. February 13, 1984. Numerals (lower right) indicate date and time.

FIGURE 1.52.—Floor of Puu Oo Crater, approximately 5 hours before onset of episode 14. Lava welling upward in open pipe (similar to that shown in figure 1.51) flooded crater floor and buried top of pipe shown in figure 1.18. Solid lava surface is about 30 m in diameter. Gas (being sampled here), spatter, and intermittently oozing pahoehoe escape from underlying magma column through a 0.5-m-diameter vent penetrating crust. Most emission takes place during brief episodic bursts that suggest gas-piston activity beneath crust. View southwestward; photograph taken at 1239 H.s.t. January 30, 1984.

TABLE 1.4.—*Summary of episode 1 eruptive activity*

Beginning (H.s.t.)	End (H.s.t)	Vent(s)	Duration (h)	Area covered (km^2)	Volume (10^6 m^3)
0031 Jan. 3	1000 Jan. 3	Napau to 0740	9.48	1.52	3.0
1425 Jan. 3	1521 Jan. 3	0740	.93	.03(?)	.05(?)
1123 Jan. 5	1125 Jan. 5	1123	.03	---	---
1214 Jan. 5	0955 Jan. 6	0740, 1123, 1708.	21.68	---	---
		Puu Kamoamoa----------		.03	.05
		Uprift of Puu Kamoamoa.	---	.21	.3
1011 Jan. 6	2049 Jan. 6	0740	10.63	[1]∿0.5	∿1.5 on ground[1], ≥0.5 in crevice[1].
0957 Jan. 7	0959 Jan. 7	January 7	.03	---	---
1030 Jan. 7	1104 Jan. 7	January 7	.57	---	---
1111 Jan. 7	1558 Jan. 7	January 7	4.78	---	---
		0740	---	Minor	Minor.
1623 Jan. 7	1634 Jan. 7	0740	.18	Minor	Minor.
1642 Jan. 7	1647 Jan. 7	0740	.08	Minor	Minor.
1715 Jan. 7	0432 Jan. 8	January 7	11.28	[2]2.33	[2]5.5
0432 Jan. 8	0502 Jan. 8	0740	.50	Minor	Minor.
1443 Jan. 8	1504 Jan. 8	0740	.35	Minor	Minor.
1957 Jan. 8	2322 Jan. 8	1708	3.42	---	---
0041 Jan. 9	0330-0730 Jan. 9	1708	5(?)	---	---
1713 Jan. 9	2100 Jan. 9	1708	3.78	---	---
0502 Jan. 10	0625 Jan. 10	1708	1.38	---	---
0759 Jan. 10	1450 Jan. 10	1708	6.85	---	---
0130 Jan. 11	∿1230 Jan. 11	1708	∿11	---	---
0312 Jan. 15	0855 Jan. 15	1123, 1708	5.72	[3]∿0.7	[3]∿3
1830(?) Jan. 23	1930(?) Jan. 23	January 23	1(?)	.004	.01

[1]Estimated total area and volume on January 5 and 6 for the 0740, 1123, and 1708 vents combined.
[2]Area and volume for total production of lava from the January 7 vents.
[3]Estimated total area and volume from January 8 through 15 for the 1708 and 1123 vents combined.

less than 30 m high; the observers, looking uprift to the southwest, could see only brightly illuminated fume above the Napau vents.

Beginning at 0155 H.s.t., the vent system extended northeastward, forming a progressively lengthening line of segmented eruptive fissures parallel to the axis of the rift zone (fig. 1.53). Although the overall tendency was for downrift (northeastward) extension of the vent system (fig. 1.54), the sequence of vent opening was complicated in detail. In some places, new vents opened uprift of already-active ones. Where less active, the erupting vents spattered weakly; where more active, they produced low, linear fountains, generally about 10 to 30 m high, and fluid lava flows that spread mainly southeastward (fig. 1.55).

By 0300 H.s.t., the line of erupting vents was more than 4 km long and had transected the prehistoric cinder cone, Puu Kamoamoa. By 0428 H.s.t., the line had extended more than 5 km northeastward from the initial vent at Napau Crater. At 0740 H.s.t., the easternmost vent of January 3, approximately 6 km downrift from the Napau vents, erupted briefly in dense rain forest south of Puu Kahaualea. By the end of this initial eruptive event, the zone of shallow earthquake activity had extended downrift to the vicinity of Puu Kahaualea; from then through midday January 6, shallow earthquakes were concentrated in a zone extending from between Napau Crater and Puu Kamoamoa on the west to the vicinity of the 0740 vent on the east.

Although the final extrusive activity on the morning of January 3 was concentrated near the center of the line of erupting vents, the sequence in which the vents stopped erupting was irregular. By the time the easternmost vent began to erupt at 0740 H.s.t., active eruption elsewhere was confined to a 900-m-long stretch centered on Puu Kamoamoa (fig. 1.55). The 0740 vent erupted for only 20 minutes before shutting down at 0800 H.s.t. The vents immediately uprift and downrift of Kamoamoa died at 0850 and 0939 H.s.t., respectively, and by 1000 H.s.t. the first eruptive event of episode 1 was over when the vent at Puu Kamoamoa also stopped erupting.

Most of the lava produced in this first event, during the morning of January 3, flowed over basalt from eruptions in the 1960's (fig. 1.56). The flows of January 3 were short; the longest advanced about 2 km from its vent. The lava was predominantly pahoehoe, although the longer, more channelized flows formed aa (pl. 1). Measured flow thickness ranged from about 1 to 3 m; an estimated 3×10^6 m^3 of new basalt was emplaced over an area of 1.5×10^6 m^2. The vents were marked by deposits of spatter, ranging from a thin veneer where activity was weak and extrusion minimal, to linear ramparts several meters high in areas of prolonged vigorous eruption.

Shortly after 1200 H.s.t. January 3, production of profuse, hot, SO_2-rich fume was observed along newly lengthening cracks about 1 km east of the 0740 vent in a locality where new vents would erupt about 4 days later

on January 7. Also, from 1425 to 1521 H.s.t., the 0740 vent erupted for a second time, producing a 20- to 30-m-high fissure fountain and a small amount of pahoehoe. No further eruptive activity occurred until January 5.

JANUARY 5 AND 6, 1983

For nearly 2 days after the eruptive activity of January 3, Kilauea was in repose, and the summit reservoir reinflated slightly. During this period, many of the vents of January 3 emitted copious visible fume and burning gas flares. After summit deflation resumed, accompanied by increasing harmonic-tremor amplitude, the eruption itself resumed on January 5. The major eruptive activity of January 5 and 6 occurred along a 1.1-km-long system of fissure vents south of Puu Kahaualea. This system included two new fissure vents that filled the gap between the 0740 vent and the nearest January 3 vent to the southwest. The more easterly of these new vents first erupted at 1123 H.s.t. January 5, and the more westerly at 1708 H.s.t. (fig. 1.57). Minor amounts of lava were also discharged several kilometers uprift.

The initial eruptive event of January 5 was a 2-minute fissure eruption that began at 1123 H.s.t. at one of the new vents. Then, after a 49-minute respite, vigorous eruption began at the 0740 vent, and for more than 32 hours (table 1.4) the rift zone was in nearly continuous eruption. For most of that time, the 0740, 1123, and 1708 vents erupted, sometimes singly and, at other times, in concert (fig. 1.54). Intermittent, relatively low fountaining and

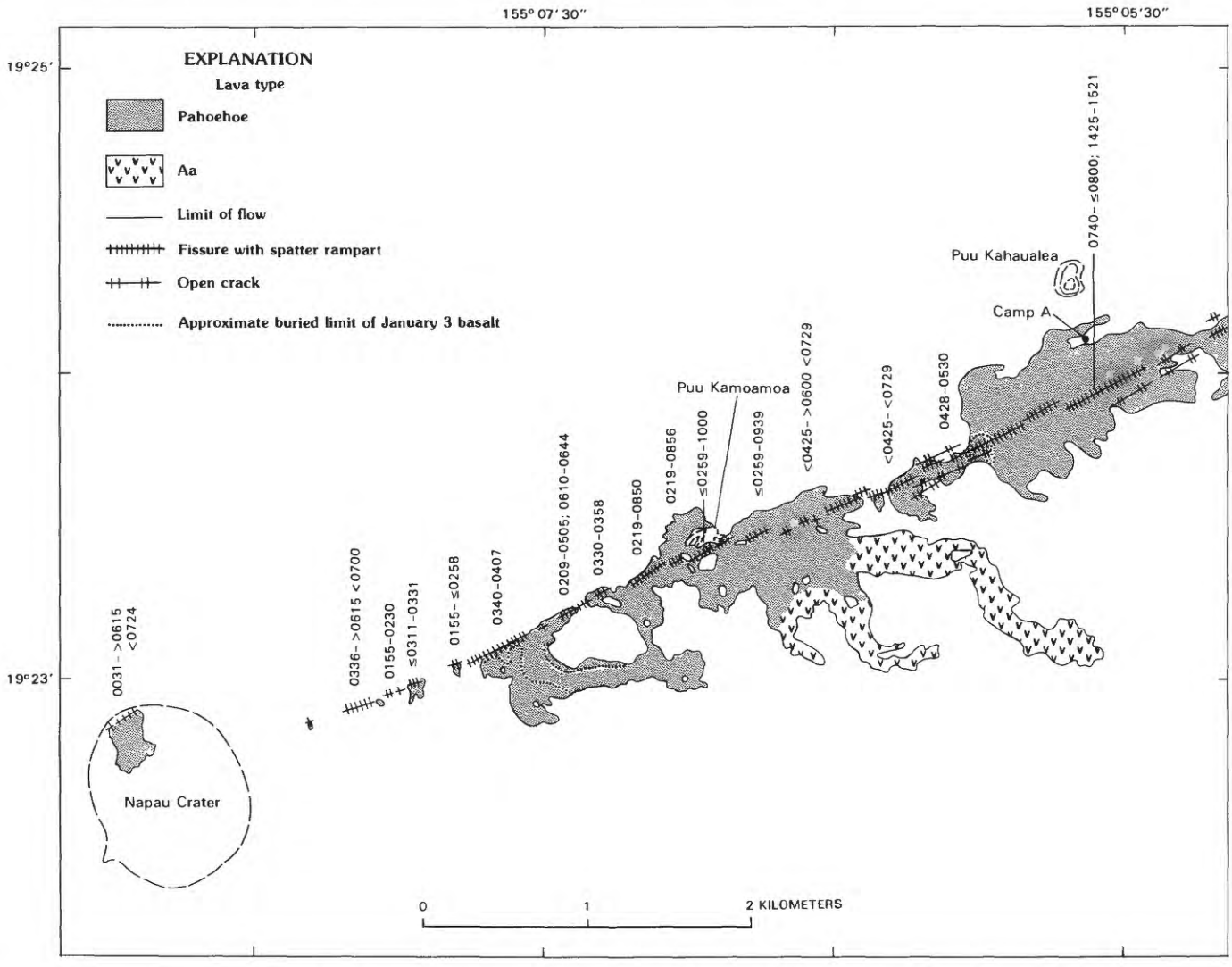

FIGURE 1.53.—Episode 1 vents and flows, from Napau Crater to vicinity of Puu Kahaualea, with times (H.s.t.) and locations, deduced from field notes, verbal reports, video tapes, time-lapse film, and photographs, for beginning and end of eruptive activity for each vent active on January 3, 1983. Flows from vent that opened at 0428 H.s.t. and from vents uprift (southwest) of it were mostly emplaced on January 3. Small volume of lava (estimated at max 0.1×10^6 m^3) emplaced northeast (downrift) of 0428 vent was buried by lava erupted during later parts of episode 1.

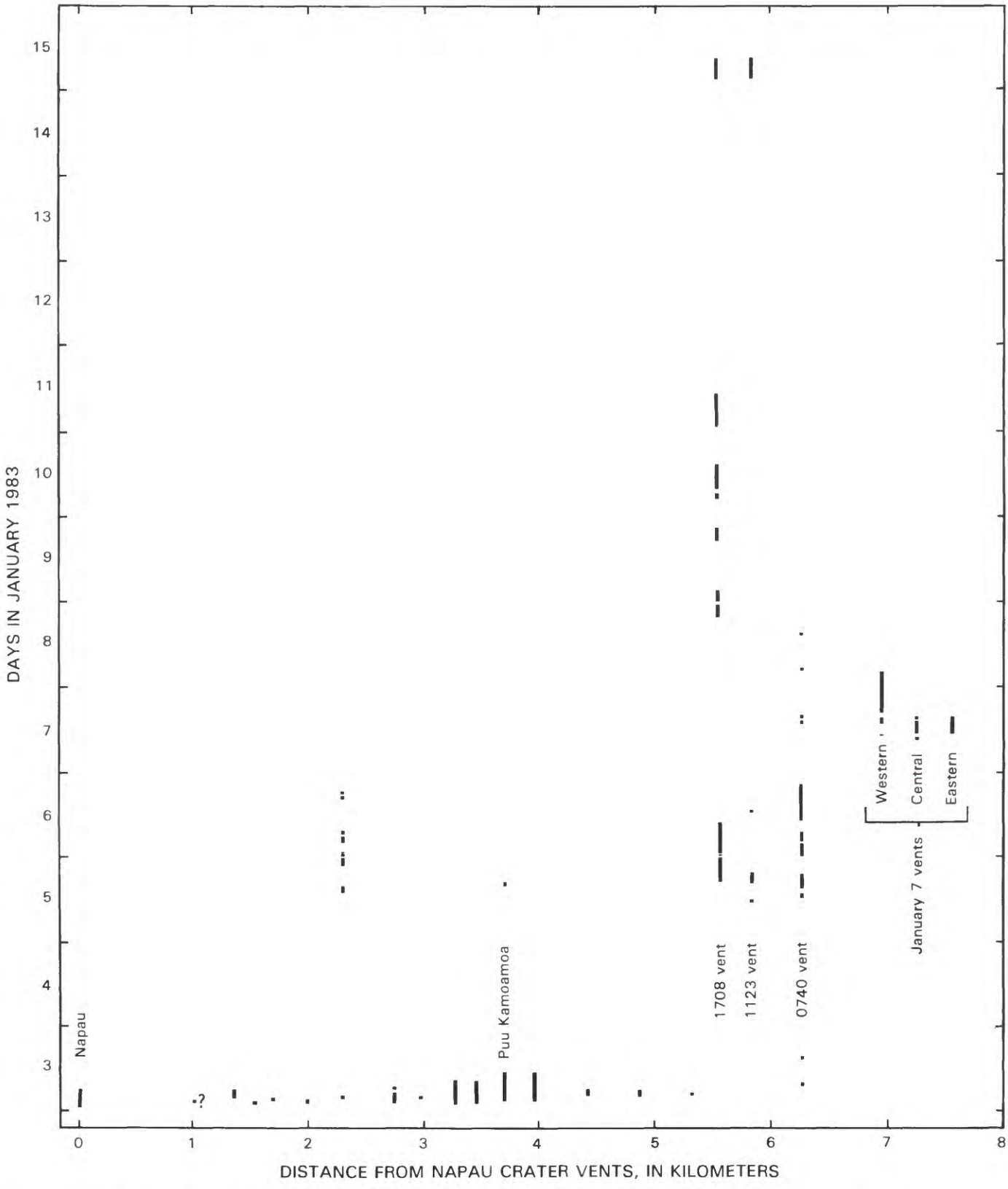

FIGURE 1.54.—Periods of episode 1 vent activity for January 3-15. On x-axis, approximate centers of individual eruptive-fissure segments are scaled downrift from Napau Crater vents. Query indicates uncertainty in time of eruption.

FIGURE 1.55.—Erupting vents and lava flows in vicinity of Puu Kamoamoa (tree covered). Line of erupting vents is about 0.9 km long. View southeastward; photograph by J.D. Griggs, taken at 0729 H.s.t. January 3, 1983. Numerals (lower right) indicate date and time.

minor flow production also occurred during this period at Puu Kamoamoa and at vents approximately 0.6 and 1.2 km uprift of Kamoamoa (figs. 1.54, 1.57).

The vigor of the eruption, as indicated by the intensity of fountain activity, varied, and the major eruptive locus shifted from place to place along the line of erupting vents. Sometimes, in an apparently reciprocal relation, increase in fountain activity on one part of the fissure system would be simultaneous with decrease on another part. At other times, activity on disparate parts of the system would increase or decrease together. On any erupting segment, the more or less continuous fountain line commonly ranged from 1–5 m high along the less active parts to 10–30 m high along the more active parts. Bursts of more distinctly fragmented spatter rose as much as twice the height of the more continuous fountain. Occasionally, part of the fountain was conspicuously higher—50 m or more at the 0740 vent.

As activity ceased on individual segments of the vent system, the waning segment would begin to produce a

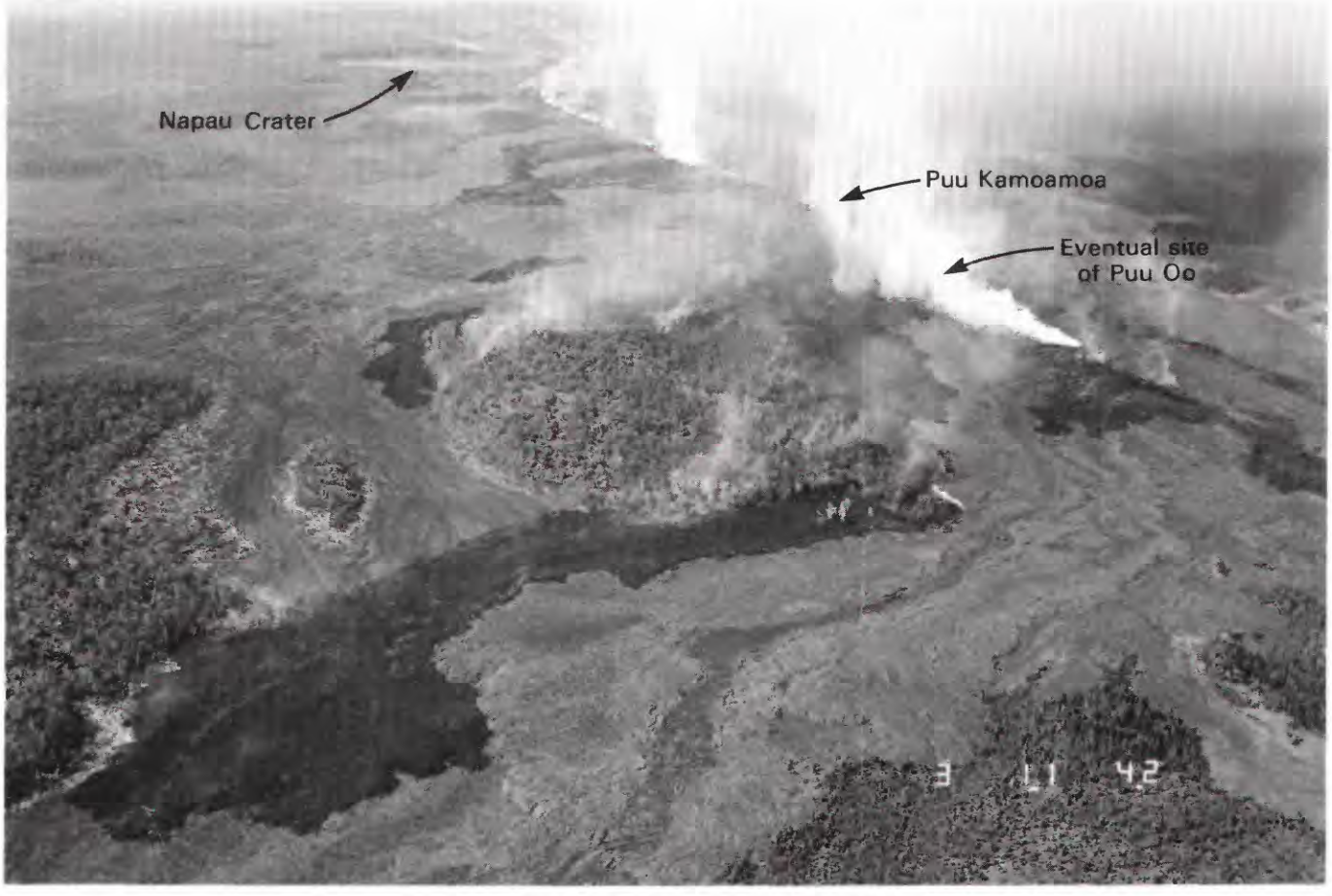

FIGURE 1.56.—Most of the vents (fuming) and flows (dark) that were active on January 3. Lighter colored flows, weathered and treeless, date from the 1960's. 0740 vent is out of view to right. View westward; photograph 83.1.3.JG135E#33A by J.D. Griggs, taken at 1142 H.s.t. January 3, 1983. Numerals (lower right) indicate date and time.

roaring sound similar to that of a large multiengine jet aircraft. The roar was caused by heated air and burning gas being expelled at high velocity through the inactive vent orifices. The gas flares were yellowish orange to reddish orange, and the gas was largely organic in origin (L.P. Greenland, oral commun., 1983). The vents apparently behaved as chimneys, fed by air, pyrolyzed organic matter, and water drawn through the porous rocks of the volcanic edifice. Temperatures in the roaring vents were high enough (1,065–1,070 °C by thermocouple and two-wavelength infrared radiometer) to keep the walls partly molten, and fragments of partially melted wall material were occasionally ejected. Almost invisible in bright daylight, the flaring gas created an eerie glow at night (fig. 1.58).

Much of the lava from the 0740 vent flowed into a gaping crack ("crevice," fig. 1.57), several meters wide, that was approximately parallel to the vent but about 100 m to the south. The crevice was at the base of a 10-m-high, south-facing scarp over which the lava cascaded before disappearing from view (fig. 1.59). At times, the flowing lava bridged part of the crevice, presumably because of having locally filled it, so that lava was supplied to the opening from both sides.

Visual estimates during the eruption suggest that the maximum rate of lava flow into the crevice was about 60,000 m^3/h, and sometimes it was much less. An unmeasurable, but large (possibly approx 0.5×10^6 m^3), volume of lava disappeared into the crevice on January 5 and 6. Subsequent observation of features that have since been buried under newer lava suggested that the large volume of ingested lava was accommodated by extension of at least 2 to 3 m across the crevice. Just downrift of the crevice, lava of January 5–6 (A, fig. 1.60) was cut by a shallow, 10-m-wide graben on strike with the crevice. The bounding faults, though complex, showed an aggregate of 2 to 3 m of dilation, measured perpendicular to the strike of the graben. Unbroken lava of January 8–9 had buried the faults to the southwest (B, fig. 1.60) and separated them from remnants of the

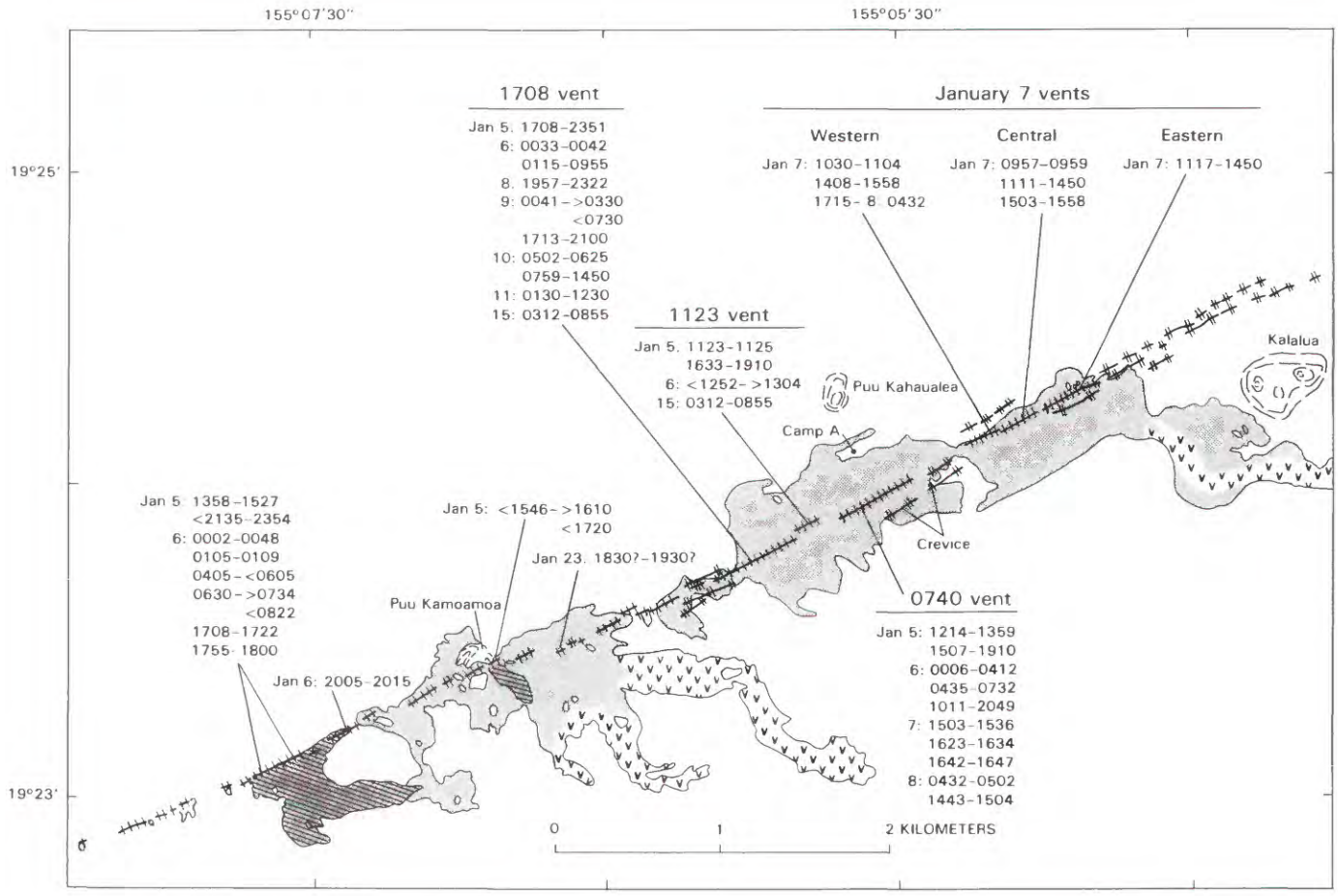

FIGURE 1.57.—Episode 1 vents and flows, with times (H.s.t) and locations, deduced from field notes, verbal reports, time-lapse film, and photographs of eruptive events, January 5–23, 1983. Closely spaced diagonal pattern shows approximate locations of January 5–6 basalt erupted at Puu Kamoamoa and uprift of Puu Kamoamoa; otherwise, symbols are same as in figure 1.53.

FIGURE 1.58.—Incandescent vents emitting burning gas. West end of 0740 vent is at far left, and 1123 vent is at center and right center. Cone at far right, about 15 m high, is at east end of 1708 vent. View southwestward; photograph taken at 1814 H.s.t. January 14, 1983. Numerals (lower right) indicate date and time.

FIGURE 1.59.—Lava from 0740 vent, cascading over 10-m-high scarp and disappearing in open crevice. Eastern part of 0740 vent was inactive at this time. Low fountains at 1123 vent, partly obscured by smoke and volcanic fume, are beyond trees at left. Mauna Loa is on skyline. View westward; photograph by J.P. Lockwood, taken at 1304 H.s.t. January 6, 1983.

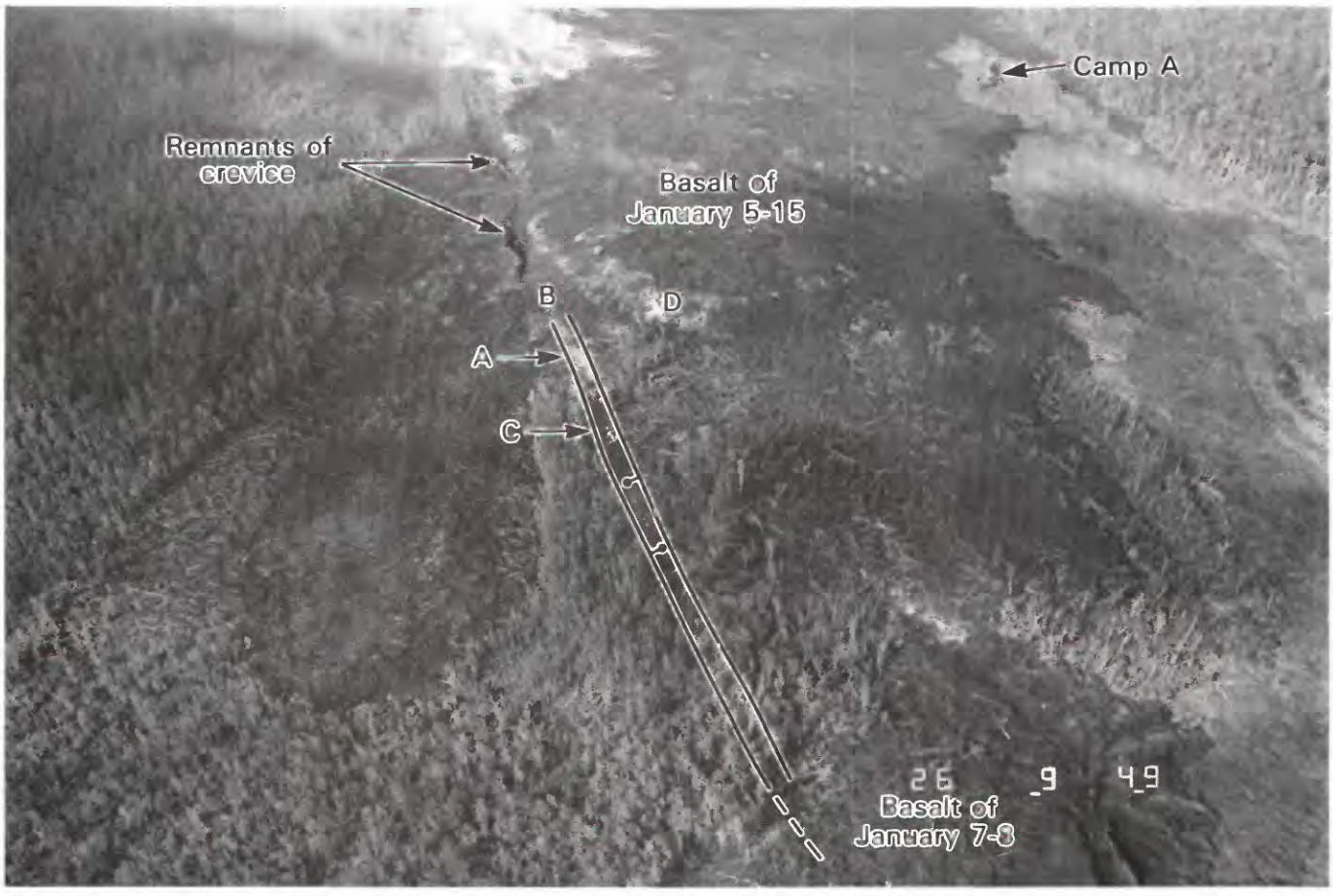

FIGURE 1.60.—Basalt flows of January 5-15, remnants of open crevice, and trace of graben that extended northeastward from it. Solid line, graben boundary; bar and ball on downthrown side. Dashed line, open crack. Letters A–D identify features described in text. Hill at camp A is a 1965 spatter cone, about 12 m high. Narrow lobe of January 11 basalt separates cone from rain forest to north (upper right). View westward; photograph 83.1.26JG135A#34 by J.D. Griggs, taken at 0949 January 26, 1983. Numerals (lower right) indicate date and time.

crevice that were still exposed at the end of episode 1. About 100 m to the northeast (C, fig. 1.60), the graben transected January 5–6 basalt with sufficient throw that prehistoric basalt was exposed in the graben walls beneath the new basalt. About 50 m to the north, at locality D (fig. 1.60), a 1-m-wide, open crack, also cutting January 5–6 basalt, disappeared beneath unbroken basalt of January 8–9. Basalt of January 7–8, unbroken except for a narrow crack, with about 20 cm of dilation, on the northeastward extension of the northern graben-bounding fault, buried the downrift end of the graben.

Extension normal to the rift-zone axis probably also occurred as the feeder dike for the 1708 vent approached the surface. New extension cracks were observed cutting January 3 basalt near the uprift end of the 1708 vent late in the evening of January 5. Cracks mapped later in this area (pl. 1) transected January 3 basalt and are visible in photographs taken at about 1100 H.s.t. January 9.

The lava flows of January 5–6 consisted of fluid pahoehoe that spread in a sheet surrounding the vents south of Puu Kahaualea and that formed thin flows extending southeastward from the vents farther uprift (fig. 1.57). These thin flows, partly on top of January 3 basalt, covered an area of 0.2×10^6 to 0.3×10^6 m^2; their estimated volume was 0.3×10^6 to 0.4×10^6 m^3 (table 1.4). Basalt from the 1708, 1123, and 0740 vents was almost completely buried by younger flows during the period January 8–15; it covered an estimated area of 0.5×10^6 m^2, and its volume on the ground was probably about 1.5×10^6 m^3. An additional 0.5×10^6 m^3 is estimated to have disappeared into the crevice.

JANUARY 7 AND 8, 1983

Shallow earthquakes, which had been persistent in the eruptive area most of the time since January 2, diminished in frequency at midday January 6. They became abundant again just after 0000 H.s.t. January 7 in the vicinity of Kalalua, farther downrift than the swarm had previously extended. The swarm died late on January 7, and no further abundant shallow earthquakes were recorded in the rift zone through the entire period discussed in this report. Accelerated surface deformation in the same general area began during the evening of January 6 and, by midnight, had caused profound disturbance of a borehole tiltmeter (KLU) about 300 m north of Kalalua (fig. 1.1). Daylight on January 7 showed that this tiltmeter was within a northeast-trending zone of new cracks. Immediate remeasurement of a horizontal line crossing the zone of cracks north of Kalalua indicated that approximately 2 m of extension normal to the trend of the rift zone had occurred since the last measurement on January 5. These events apparently recorded emplacement of the easternmost segment of the new dike system that had been delivering lava to the surface farther uprift since January 3.

Observers stationed between Puu Kahaualea and the 0740 vent felt some of the earthquakes and noticed heavy steaming downrift toward Kalalua during the early hours of January 7. Beginning at about 0230 H.s.t., a glow was recognized in the same area, and minor spattering was seen at about 0430 H.s.t. When daylight came, direct observation showed burned vegetation and a glowing fissure that was emitting fume, but no new flows or vent deposits were found. The eastern part of this new fissure system was in the center of a shallow, 100- to 150-m-wide graben with fresh bounding cracks that gaped at least 1 m.

A minor eruption on the central part of the new fissure system began at 0957 H.s.t. January 7 (figs. 1.54, 1.57). This eruption was brief, probably no longer than 2 minutes, and produced a low, 60-m-long spatter rampart. Eruption began in earnest on the January 7 vents at 1030 H.s.t. From then until 1104 H.s.t., the western part formed a low (3–10 m high) fountain, about 300 m long. Beginning at about 1115 H.s.t., the central and eastern vents began to erupt. Within the first hour, the 500-m-long fountain at these vents grew to a height of 60 to 100 m, forming a spectacular display; intense fountaining continued until 1347 H.s.t., when the high-level activity began to wane rapidly. By 1400 H.s.t., fountain heights decreased to no more than 6 m on the central and eastern vents.

At 1408 H.s.t., the western vent, which had been inactive since its initial eruption about 3 hours earlier, began erupting again. Within the first few minutes, the western fountain line grew to a height of 50 to 60 m, which soon waned; by 1440 H.s.t., it had decreased in height to no more than 10 m and continued thus. Activity on the still-diminishing central and eastern vents stopped at 1450 H.s.t. At 1503 H.s.t., low fountaining resumed on the central vent and continued there, as well as on the still-erupting western vent, until 1558 H.s.t., when both vents shut down.

The massive midday eruption of the central and eastern vents produced a wide, rapidly advancing flow that extended 5.5 km southeastward (pl. 1) through rain forest on the south flank of Kilauea. For most of its advance, the flow, seen from the air, was wide and consisted of pahoehoe. At 1440 H.s.t., it was about 4.7 km from the vents. Averaged from the time the central and eastern vents began to erupt, about 2.5 hours earlier, the rate of flow-front advance was 1.3 to 1.4 km/h. However, the eruption did not begin at full vigor but was increasing over the first hour, and aerial observations of the flow-front position (pl. 1) during and shortly after the most vigorous part of the eruption suggest that the average advance rate down the south flank at that time was 1.5 to 2.0 km/h; the maximum rate was probably greater than 2.0 km/h.

When seen again, at 1520 H.s.t., the front had advanced only another 400 m; the rate was slower, and the front consisted of aa and slab pahoehoe. Observed after it had stopped moving, the flow consisted of aa from the area south of Kalalua to the terminus. The aa was thin, generally 1.5 to 2.5 m thick; it had enveloped still-standing ohia trees, and it contained vertical molds where the trees had been burned away.

No further eruption occurred on the central and eastern vents. However, the western vent erupted at a low to moderate level for an additional 11 hours, from 1715 H.s.t. January 7 to 0432 H.s.t. January 8. The fountain line was relatively low during that period; it was commonly 5 to 15 m high and occasionally reached a height of 20 to 30 m. The line of continuous fountains reached a maximum length of 200 m for a brief period early in the evening. For much of this episode, however, the line was discontinuous and the activity sporadic except in the central part, which was the most steady and vigorous. A minor flow, pahoehoe near the vent and aa to the southeast, extended eastward and southeastward on top of the earlier flow from the January 7 vents; it terminated in the area south of Kalalua, about 2 km from its vent.

Flows produced by the January 7 vents spread across relatively flat country bounded by a narrow graben, 300 to 400 m southeast of the vents (Holcomb, 1980). These flows crossed the graben west of Kalalua and extended from there down the south flank of the volcano. They covered an area of 2.33×10^6 m^2 and had a volume of 5×10^6 to 6×10^6 m^3. We estimate that about 4×10^6 m^3 of new basalt was emplaced by the midday eruption on January 7 from the central and eastern vents. That event lasted for nearly 5 hours (table 1.4), at an average lava-discharge rate of about 0.8×10^6 m^3/h. However, because the greater part of that voluminous flow to the southeast was erupted over a 2- to 3-hr period, the maximum lava-discharge rate was well in excess of 10^6 m^3/h and could have been as high as 1.5×10^6 m^3/h. In contrast, we estimate that the later eruption, from the western vent during the night of January 7–8, produced lava at a rate of less than 10^5 m^3/h.

Intermittent, brief (5–34 minute long) eruptions with very low production of spatter and flows occurred several times on January 7 and 8 at the 0740 vent (figs. 1.54, 1.57). Hot, air-rich gases jetting from the 0740 vent also caused occasional minor ejection of spatter and, at one orifice, created a roar that was audible 20 km to the west in Kilauea's summit region.

JANUARY 8–15, 1983

After the last minor eruption from the 0740 vent during the early afternoon of January 8, no further episode 1 lava emission occurred there; nor did the January 7 vents, farther downrift, ever erupt again. Intermittent eruptive activity, however, occurred from late on January 8 through early January 15 at the 1708 vent and, in part, at the 1123 vent (figs. 1.54, 1.57; table 1.4). Heated gases, occasionally carrying fragments of incandescent ejecta, continued to jet from the recently active vents.

The main activity of the 1708 vent during this period took place in a series of moderate eruptions that occurred between 1957 H.s.t. January 8 and approximately 1230 H.s.t. January 11. During this 62.5-hour interval, individual eruptive events ranged in length from about 1.4 to 11 hours, and the 1708 vent was erupting about 50 percent of the time. Eruptions were characterized by low fountains, generally less than 15 m high. At the east end of the vent, spatter from the fountain built a prominent, 15-m-high cone (fig. 1.58). Pahoehoe or, on occasion, slab-pahoehoe flows moved northward and southward from the vent. Flows to the north tended to be more voluminous; some flowed eastward on the north side of the 0740 vent and covered much of the area of the January 5–6 basalt.

On the night of January 8–9, northeast-moving flows onlapped the base of the small 1965 spatter cone at camp A, 300 m north of the 0740 vent. Intense radiant heat from the active pahoehoe-flow edge and concern that camp A might become surrounded by active lava led to a middle-of-the-night evacuation by helicopter, and so no one observed the end of this eruption, which occurred sometime between 0330 and 0730 H.s.t. January 9.

A later flow from the same vent on January 11 produced a lobe that passed on the north side of the camp A spatter cone, so that all but the northeast base of the 12-m-high hill was surrounded by new basalt (fig. 1.60). Visibility was so poor during that event that we could estimate only an approximate time, 1230 H.s.t. January 11, for its end.

After slightly more than 3½ days of repose, a final episode 1 eruption in the area south of Puu Kahaualea occurred on January 15. The 1123 vent was the primary lava producer, but the 1708 vent also erupted. At about 0215 H.s.t. January 15, showers of incandescent fragments began to be ejected from the 15-m-high spatter cone that had formed previously at the east end of the 1708 vent. Reaching heights of 30 to 50 m above the top of the cone, they formed a spectacular fireworks display. After about 15 minutes, the style of eruptive activity evolved from a more or less continuous shower of small glowing fragments to intermittent bursts, accompanied by loud reports, that ejected large chunks and ribbons of spatter, as if large gas bubbles were bursting violently within lava pooled at a shallow level in the vent. Such gas-burst activity with ejection of clots and ribbons of spatter was typical throughout episode 1 at the end of eruptive events when lava production had largely waned or stopped. The gas-burst activity, alternating with renewed showers of

small incandescent fragments, continued at the 1708 vent and extended eastward along the 1123 vent, where the activity earlier in the evening had consisted only of continuous emission of flaring gas (fig. 1.58).

By 0312 H.s.t., the volcano was truly erupting. A low fountain, about 100 m long, had formed at the 1123 vent, and a low, sustained fountain was also playing at the 1708 vent. By 0315 H.s.t., we could recognize that a lava flow was beginning to move northward from the 1123 vent. This moderately vigorous eruption, with the most prominent fountains as much as 20 to 25 m high, continued through the night, producing a pahoehoe sheet that spread southward, eastward, and northeastward. It surrounded the 0740 vent and covered much of the basalt that had been emplaced in previous days between the 0740 vent and camp A.

In the days following the January 15 eruptive activity, the vents south of Puu Kahaualea continued to emit gas that formed burning yellowish-orange flares and, at times, small fragments of incandescent ejecta. However, no further episode 1 eruptive activity occurred in that area, and the 1708 vent never erupted again.

The volume of lava produced by the 1708 and 1123 vents during the period January 8–15 is difficult to estimate because we were unable to map the flows carefully between eruptions. Measurements around the flow edges and in empty tree molds indicate that 2 m is reasonable for the average thickness of any one of these pahoehoe flows. Flows erupted on January 8 and 9 were partly superimposed and formed a widespread sheet that probably covered an area of about 0.5×10^5 m^2. The area covered by superimposed flows is uncertain, but we estimate that 1.5×10^6 m^3 of basalt may have been emplaced on January 8–9. The January 15 eruption produced a pahoehoe sheet that covered an area of about 0.4×10^6 m^2; a reasonable volume estimate for that flow is 0.8×10^6 m^3. Although the areal extent of flows produced on January 10 and 11 is the least certain, they did not extend far enough eastward to reach the area between the 0740 vent and camp A. Sketch maps and mapping done after the January 15 eruption suggest that the areas of the January 10 and 11 flows may have been about 0.1×10^6 and 0.2×10^6 to 0.3×10^6 m^2, respectively. An estimated volume of 0.7×10^6 m^3 seems reasonable and leads to an approximate total of 3×10^6 m^3 of new basalt for the period January 8–15.

JANUARY 23, 1983

A final, minor eruptive event that occurred on January 23 is included with episode 1. Photographers at camp A, north of the 0740 vent, reported glow and fountaining uprift at about 1910 H.s.t. January 23; a tour-plane pilot also reported seeing eruptive activity from the air at about 1830 and 1930 H.s.t. Reconnaissance the next day showed a small, new vent and flow superimposed on one of the January 3 fissures about 400 m northeast of Puu Kamoamoa (fig. 1.57). Approximately 9,000 m^3 of new lava had been erupted to form a 55- by 70-m pad. Possibly only coincidentally, this event followed an $M=4.4$ earthquake that occurred at 1800 H.s.t. beneath Kilauea's south flank.

EPISODE 2 (FEBRUARY 10–MARCH 4,1983)

During the 2½ weeks between the final eruptive activity of episode 1 on January 23 and the onset of episode 2 eruption on February 10, 1983, no measurable volume of new lava was discharged on Kilauea. However, the new vents south of Puu Kahaualea remained incandescent, continued to emit burning gases, and, on occasion, ejected small amounts of spatter. In addition to these conspicuous signs of continuing shallow magmatic activity, low-amplitude harmonic tremor persisted in the eruptive zone (see chap. 7), and extension of about 1 cm/d was measured on a line across the trace of the 0740 vent (see chap. 6). New flows emplaced between February 12 and 14 obstructed this line and ended the measurements.

Increased production of spatter was first noticed on February 10. That morning, we discovered two weakly spattering vents at the west end of the 0740 fissure (pl. 1), which was also emitting copious dirty-brown fume. The more active vent had built a new, 6-m-high spatter cone. Less conspicuous fume was also issuing from the eastern 50 m of the 1123 fissure, and the easternmost part of that fuming fissure was incandescent. Additional fume was being emitted from an incandescent fissure east of Puu Kamoamoa in the approximate area where Puu Oo would eventually develop. Except for emission of water vapor, the rest of the episode 1 fissure system appeared to be inactive.

By February 12, a second small cone had formed at the west end of the 0740 vent, and a new glowing crack extended tens of meters northeastward of these two cones. The rate of growth of the cones was low; small pieces as well as larger chunks and ribbons of spatter, several tens of centimeters in diameter, were being ejected a few fragments at a time in small intermittent bursts. The glowing crack at the east end of the 1123 vent still persisted, and the zone of fume emission had extended uprift along the 1123 fissure so as to include the western part as well. Time-lapse film shows that a brief, low-level spattering event occurred at the 1123 vent during the evening of February 12.

By February 14, continuing intermittent low-level eruption along the 0740 fissure had extended the line of low spatter cones northeastward over the glowing crack seen on February 12. The cones surmounted a low shield (fig.

1.61) formed by slow discharge of pahoehoe that spilled from the vents onto the surface of the shield or leaked through lava tubes into its interior. Similar activity continued until February 25, by which time the individual cones, generally about 10 to 15 m high, were juxtaposed in a 170-m-long line that formed a cockscomb-like crest on the flat-topped, 10-m-high shield. We estimate that, over the 15-day period from February 10 to 25, about 0.5×10^6 m^3 of lava was extruded to form the cones, the shield, and thin, short pahoehoe flows that extended beyond the limits of the shield.

The intensity of eruptive activity increased markedly at about 0900 H.s.t. February 25 and became localized at two vents that formed in the western part of the line of cones (fig. 1.62). The central and eastern parts, which had been active during the preceding night, never erupted again. Steady eruption continued until midafternoon, producing a pahoehoe flow that quickly extended northward toward camp A and then turned northeastward. Although the estimated lava-discharge rate was about 50,000 m^3/h, relatively little spatter was ejected. Lava seemed to well out of the more easterly of the two vents, and at the western one, it erupted in a continuous, but somewhat varying, northwest-directed stream (fig. 1.62) that played for hours and resembled a stream of water issuing under slight pressure from a pipe or hose with no nozzle. The style of lava emission at these two vents suggested that the erupting lava was gas poor, possibly owing to shallow subsurface degassing, as indicated by abundant emission of SO_2-rich fume at nearby nonerupting vents (fig. 1.61).

At about 1430 H.s.t., new fountain activity broke out 100 to 200 m uprift at the 1123 vent (pl. 1), where a 50- to 100-m-long line of fountains formed. The most vigorous part was at the uprift end, where the fountain was about

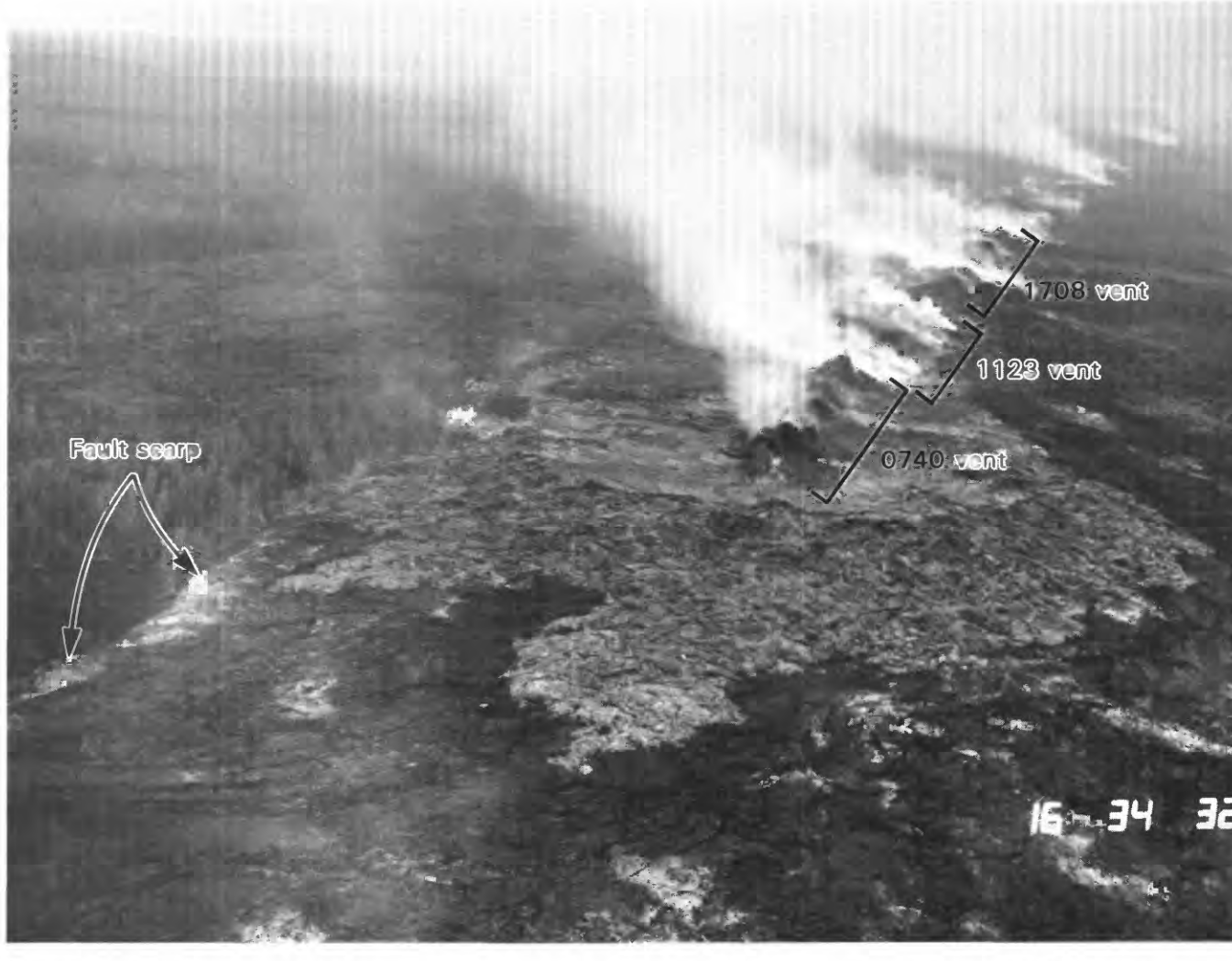

FIGURE 1.61.—Weakly erupting 0740 vent spatter cones surmounting low pahoehoe shield during early part of episode 2. Dark basalt in foreground is from episode 1. Fault scarp (lower left), with crevice at base, faces south. Numbers in lower right indicate date and time. View southwestward; photograph 83.2.14NB135B#34A, taken at 1634 H.s.t. February 14, 1983.

20 m high (fig. 1.21). In the rest of the line, to the northeast, the fountains were no more than a few meters high.

At 1518 H.s.t., a new fountain line became active about 900 m uprift of the 0740 vent. Simultaneously, the western part of the 0740 vent stopped erupting and, except for occasional bursts of spatter during the next 2 days, never erupted again. The vent openings, however, continued to glow and to emit fume throughout episode 2. The new uprift vent formed a line of low fountains, estimated at 5 to 10 m high, that erupted until sometime between 0930 and 1100 H.s.t. February 26, producing a pahoehoe flow that advanced slowly eastward for several hundred meters.

An additional erupting vent, the O vent, which was even farther uprift (pl. 1), was first observed at 0140 H.s.t. February 26. Because the O vent was nearly 2 km from camp A, its activity was difficult to watch closely. At first, the activity was probably low and sporadic. However, the O vent was seen erupting vigorously during the early evening of February 26, during the predawn hours of February 27, and at midafternoon on February 27. Observers in passing aircraft estimated that the fountains were 40 to 50 m high. In addition, time-lapse film data indicate that intermittent activity continued until at least about 1900 H.s.t. February 27. As far as we know, the O vent did not erupt at any later time during episode 2. Its eruption formed a 300- to 400-m-wide pad of pahoehoe (pl. 1).

The main activity of episode 2 was centered at the 1123 vent. A nearly circular lava pond (fig. 1.5) quickly formed. This pond enveloped the line of fountains erupting from the eastern part of the 1123 vent and initiated the central-fountain, lava-pond, lava-river style of activity that would characterize this series of eruptions for months to come. The main fountain, which dominated the activity, played in the western part of the pond. Its fallout quickly built a prominent rampart of spatter and cinders that enclosed the pond on the south and southwest; by the end of episode 2, this rampart was about 25 m high. The rest of the enclosing levee, though partly of pyroclastic origin, consisted largely of a bulwark of pahoehoe built by overflows and by lava that had leaked from the pond through short lava tubes. The more northeasterly fountains, which were initially low and in a continuous line with the main fountain, soon evolved to a discontinuous line of fountains barely rising above the surface of the pond. In addition, a discontinuous line of small fountains opened uprift from the pond at about 0100 H.s.t. February 26 and erupted intermittently and at low levels thereafter.

For the first 2 days of its activity, the main fountain at the 1123 vent was relatively low; its height ranged from about 20 to 60 m above the surface of the pond (fig. 1.21) and was at the low end of this range on February 26. On February 27, the vigor of the fountain increased, and, for about 4 days, the main body of the fountain formed a broad column that was about 60 to 80 m tall most of the time. The intensity of fountaining waned on March 3 (fig. 1.21); the erupting column, when it could be seen through the mist and the volcanic fume that was being blown toward camp A by southerly winds, was about 30 to 50 m tall. Poor visibility on March 4 virtually eliminated any useful time-lapse-camera record. Occasional glimpses showed onsite observers that the fountain was low and varied in behavior, and several times, from about 1000 H.s.t. until it finally shut off permanently at 1451 H.s.t., the fountain apparently shut off or at least dropped to a level so low that it could not be seen, and diminished lava production was reported. Beginning at about 1200 H.s.t., observation of the channel near the vent showed that occasional temporary cessations of fountaining coincided with temporary cessations in the supply of lava to the lava river south of the vent. When fountaining would resume, the lava pond would refill to overflowing and reactivate the river.

Two successive river-fed lava flows advanced from the 1123 vent (pl. 1). Initially, the lava flowed southward from the vent and then turned northeastward along the same narrow graben that formed a local southeast boundary for episode 1 flows on January 7–8. The episode 2 lava flowed partly on top of episode 1 basalt to the vicinity of Kalalua. In about 19 hours, from the time the 1123 vent opened on February 25 until the active flow terminus was near Kalalua at 0915 H.s.t. the next morning, the flow

FIGURE 1.62.—"Firehose" fountain at west end of 0740 vent during episode 2. Line of spatter cones is 170 m long. At left (east) end, tallest cone, which is closest to camera, is about 17 m high and 330 m distant. West end of line is about 400 m from camera. Shiny pahoehoe in foreground is at edge of an active flow from erupting vents. Photograph by J.D. Griggs, taken at 1105 February 25, 1983. Numerals (lower right) indicate date and time.

extended about 2.7 km along a relatively flat course at an average rate of approximately 140 m/h.

Between the mornings of February 26 and 27, the lava river was diverted about 1 km from the vent, possibly owing to a decrease in lava-discharge rate that permitted the northeastward-flowing lava river partly to freeze. No major active flow lobe was seen between the mornings of February 26, when the northeastern lobe was in place, and February 27, when the southeastern lobe was first recognized (pl. 1). The fountain height at the 1123 vent was also low during that interval (fig. 1.21). In addition, the rate of summit deflation and the amplitude of harmonic tremor were lower during about the same period.

The new distributary lobe, first recognized at 0830 H.s.t. February 27, became the main flow; it was supplied by the channelized pahoehoe river shown in figure 1.5. About 1 km from the vent on March 3, we estimated lava flux in the approximately 15-m-wide channel (fig. 1.30). Maximum velocity (2.4 m/s) was determined by timing the passage, through a measured distance (30 m), of a distinctive pahoehoe slab or an object tossed into the most rapidly moving, central part of the lava river. Because velocity decreased to zero at the edges of the channel, we made the simplifying assumption for volume calculations that the average velocity in the channel was half the maximum velocity. For an assumed depth of 2 m, the estimated lava flux was about 130,000 m^3/h. Similar estimates of flux close to the vent during the main part of the eruption ranged as high as about 3 times this value.

At average velocities of 40 to 70 m/h, the toe of the southeastern flow extended through the rain forest to Royal Gardens, which it reached at 1720 H.s.t. March 2. During its advance through the northwestern part of this sparsely populated subdivision, the aa-flow front burned and crushed one house. The advance rate decreased toward the end of the eruption. Average advance rates of approximately 30 m/h and then 20 m/h are indicated for the last 21 hours of episode 2 (pl. 1). During the 24 hours after the eruption finally stopped, at 1451 H.s.t. March 4, the flow front advanced about another 8 m.

Three surges were recognized as the episode 2 flow traversed the corner of the subdivision: at 1745 H.s.t. March 2, 2230 H.s.t. March 3, and about 0730 H.s.t. March 4. The second surge was the best documented. At 2200 H.s.t., a 2-m-high flow front was moving down Queen Street (pl. 1) at only a small fraction of a meter per minute. This flow front slowly thickened to about 6 m and began to move more rapidly. From 2230 to 2300 H.s.t., it surged ahead about 200 m in 30 minutes and simultaneously thinned to about 2 m. After this surge, the flow resumed slow movement in the forest northeast of the street.

In total, vigorous eruption during episode 2 continued from 0900 H.s.t. February 25 to 1451 H.s.t. March 4, a period of nearly 174 hours. In the early part, February 25 to 27, relatively small amounts of basalt, predominantly pahoehoe, issued from the 0740 vent, the O vent, and an additional vent between these two (pl. 1). The main production, from the 1123 vent, produced a flow, mostly aa, with a small early lobe to the northeast and a major later lobe to the southeast. The total volume of new basalt erupted during the 7¼ days of vigorous eruption was approximately 13.6×10^6 m^3, a value suggesting an overall lava-discharge rate of 70,000 m^3/h. An estimated 11.3×10^6 m^3 of basalt composed the major lobe to the southeast, which ranged in thickness from approximately 3 to 10 m. An average lava-discharge rate of about 90,000 m^3/h is indicated for the 1123 vent during the 5¼-day period from 0830 H.s.t. February 27, when the southeastern lobe was first recognized, to the end of the episode.

This vigorous episode was preceded by 15 days of slow, intermittent eruption of the 0740 vent that produced about 0.5×10^6 m^3 of pahoehoe; an average lava-discharge rate of about 1,400 m^3/h is indicated. The total volume of basalt produced during episode 2 was approximately 14×10^6 m^3 over an area of 2.7×10^6 m^2.

EPISODE 3 (MARCH 21–APRIL 9, 1983)

The repose period between episodes 2 and 3 lasted 23 to 24 days, during which time the O vent glowed and emitted fume. This repose period was briefly interrupted about a week before the beginning of episode 3 by low-level eruptive activity at the 1123 vent on March 21. Harmonic-tremor amplitude gradually doubled in the eruptive zone from 0430 to 0630 H.s.t. that morning, and glow reportedly was seen over the vent area between 0530 and 0600 H.s.t. Aerial reconnaissance from 1030 to 1100 H.s.t. showed intermittently active fountains, a few meters high, feeding short (max 20 m long) pahoehoe flows within and just west of the ring of spatter that had formed at the 1123 vent during episode 2. Reconnaissance early the next morning showed that the vents were still glowing but that eruptive activity had stopped. As far as we know, it did not resume before the onset of episode 3.

Episode 3 began in the early morning hours of March 28. The first report of intense glow in the eruption area was at 0230 H.s.t., and at 0300 H.s.t., the glow was visible from HVO. Harmonic-tremor amplitude had increased slightly above the normal repose-period background on March 27, and early on March 28 it began to increase rapidly. By 0100 H.s.t., the amplitude had increased about fivefold, and episode 3 was probably under way.

Initially, the dominant activity was localized in the vicinity of the O vent, which erupted steadily for nearly 3 days. When we first arrived, just after 0800 H.s.t., March 28, fountains there were issuing along a 100- to

150-m-long line (fig. 1.8), and active pahoehoe flows extended 50 to 100 m northward and several hundred meters southward.

The most voluminous lava production was at the O vent itself (pl. 1), where a columnar fountain rose from a circular lava pond bordered on the west by a rampart of accumulating spatter (fig. 1.8). The fountain ranged in height from about 90 to 130 m into the early hours of March 29 (fig. 1.22); subsequently, it gradually diminished in height to about 50 m before eruption at the O vent stopped at 2019 H.s.t. March 30.

Near the center of the line of erupting vents on March 28, two smaller fountains were building a pair of juxtaposed spatter rings containing craters with lava ponds (fig. 1.8). In addition, very small fountains were erupting between this pair and the large eastern vent, and still another small fountain was erupting at the west end of the line of vents. By March 29, the two vents at the center of the line had coalesced to form a single crater within a rim of agglutinated spatter; this crater was the progenitor of Puu Oo. It continued erupting at a relatively low level until the O vent stopped erupting on March 30; much of the time, its fountain was barely as high as the encircling spatter rampart.

The main flow produced at the O vent was a narrow lobe of aa that extended approximately 5 km southeastward and advanced at an average rate of about 60 m/h (pl. 1). Its sources were two pahoehoe rivers from the line of vents. The larger river issued from the O vent, at the east end of the line, and the smaller river from the coalesced pair of craters near the center. The flow covered an area of 1.4×10^6 m^2 and was mostly 3 to 5 m thick (pl. 1); we calculate its volume to be about 5.4×10^6 m^3. For an approximate eruption time of 67 hours, this volume gives an average lava-discharge rate of about 80,000 m^3/h.

Although the O vent was initially dominant, the 1123 vent became the main vent and the biggest lava producer of episode 3. After a hesitant start, the 1123 vent began erupting steadily, forming a spectacular fountain that at times was more than 200 m high (fig. 1.23). For part of episode 3, these two vents erupted together (fig. 1.63). The 1123 vent also produced several thick aa flows, one of which devastated a part of the Royal Gardens subdivision (pl. 1).

When we arrived on the first morning of episode 3, shortly after 0800 H.s.t. March 28, two vents immediately west of the ring of agglutinated spatter that had formed at the 1123 vent during episode 2 were glowing and slowly issuing short (approx 20 m long) pahoehoe flows. These same vents, within 30 m of the west base of the spatter ring, had been active during the minor eruption of March 21. In addition, the vent that had erupted within the spatter ring on March 21 was also glowing, but no new lava was seen then.

The vents just west of the spatter ring, as well as a vent within the ring, erupted sporadically on March 28 and throughout the morning and afternoon of March 29. During that time, they produced intermittent low fountains that gradually increased in vigor, so that by late afternoon of March 29, the fountains were about 10 to 20 m high when active (fig. 1.23). Only small flows, close to the vents, were produced. Also during this period of intermittent activity, the vents outside of the episode 2 spatter ring built a cone of spatter that coalesced with the west flank of the spatter ring to form a single irregular, growing cone. The two western vents coalesced either late on March 30 or early on March 31. Thereafter, for the rest of episode 3, the ever-growing 1123 cone included two craters, each of which contained an active vent and produced separate flows (pl. 1).

Throughout episode 3, the northeastern fountain was the higher of the two (fig. 1.25). Much of the time, the southwestern fountain was low and was obscured from view by the growing cone of spatter and cinder. Thus, our data on fountain activity (fig. 1.23) record the activity only of the northeastern fountain. Except for a unique period on April 2–3, when both fountains apparently went through repeated simultaneous pauses in activity, we recognized no systematic relation, either sympathetic or reciprocal, in their relative vigor.

Production of lava became steady at the 1123 vent at about 1800 H.s.t. March 29. Throughout that night until about 0500 H.s.t. March 30, the northeastern fountain

FIGURE 1.63.—Simultaneously erupting 1123 vent (near) and O vent (distant). Distance between two active vents is about 1.5 km. Line of low, inactive spatter cones in foreground was built during episode 2 at 0740 vent. Growing 1123 vent buried west two-thirds of this line of cones by end of episode 3. View westward; photograph by J.D. Griggs, taken at 1136 H.s.t. March 30, 1983. Numerals (lower right) indicate date and time.

was low and steady; its general height gradually increased from about 20 to 30 m, and it fed an aa flow that advanced steadily northeastward (pl. 1). At about 0500 H.s.t. March 30, the fountain increased abruptly in height, and, through March 31, the northeastern fountain was generally from 40 to 80 m high. On April 1, the northeastern fountain at the 1123 vent developed an episodic style of behavior in which its average height gradually rose and fell; intervals between the major maximums or minimums ranged from a few hours to more than half a day. Maximum crescendos in vigor of the northeastern fountain occurred on April 4, 5, and 6, when average fountain heights of 150 to 200 m persisted for hours at a time, and occasional peak heights were from 200 to 300 m. Subsequently, the vigor of the fountain gradually diminished, such that by the last day the average height measured during periods of maximum vigor was about 20 to 30 m. During minimums late on April 8, the fountain was so low as to be out of view at times; bad visibility also eliminated part of the record. Observers near the vent reported the end of episode 3 activity at 0257 H.s.t. April 9.

Except for a 24-hour period on April 2 and 3, the northeastern fountain played nearly continuously from the time that it became steady on March 29 through the end of episode 3. It became so low as to nearly disappear from view during the early afternoon of April 2 (fig. 1.23). During the last day of episode 3, the fountain was so low that at times we could not see it over the flank of the large 1123 cone, although continuing steady harmonic tremor of high amplitude suggests that no break in lava production occurred. However, from about 2100 H.s.t. April 2 to 2100 H.s.t. April 3, both the northeastern and southwestern vents were inactive simultaneously, or at least spatter disappeared from view, 26 times for periods that generally ranged from about 2 to 6 minutes, separated by intervals of normal activity ranging from 20 minutes to 3 hours in length. The northeastern fountain was mostly 50 to 100 m high during that 24-hour period, and its disappearances and reappearances were abrupt.

Although this behavior was not remarkable for the southwestern fountain, which was generally low and normally visible to us only intermittently, it was unusual for the northeastern fountain. Harmonic tremor in the eruption zone, which was normally strong and steady, was erratic. Although a one-for-one correlation with the observed pauses in fountaining is not apparent, the tremor behavior was much like the observed fountain behavior. Tremor amplitude repeatedly diminished to very low levels for periods ranging from about 2 to 18 minutes in length. Both of these phenomena suggest episodic interference with the supply of magma to the vent. In addition, the rate of summit deflation on April 3 was temporarily diminished. The average rate of summit deflation on that day, measured in an east-west direction by the Uwekahuna tiltmeter, was about 0.03 microradians per hour, about one-third the normal episode 3 deflation rate of 0.1 microradians per hour. This difference suggests that normal downrift transfer of magma along the conduit from the summit reservoir to the vent was partly impeded.

Steady eruptive activity, steady and intense harmonic tremor, and normally rapid summit deflation resumed in the late evening of April 3. The highest fountaining of the northeastern vent ensued in the following days (fig. 1.23), with tephra falls that extended more than a kilometer from the vent. The sporadic activity of April 3 may have been related to an adjustment in the conduit between the summit reservoir and the 1123 vent; steady, rapid discharge from the southwestern vent began early on April 4, and the overall production of lava increased markedly.

From the beginning of steady eruption of the northeastern vent at approximately 1800 H.s.t. March 29, a thick, ponderously moving aa flow advanced steadily. Unlike the episode 2 situation, in which the fountain erupted through a lava pond that, in turn, overflowed to supply a well-channelized pahoehoe river, the northeastern vent, for much of episode 3, appeared to contain relatively little ponded lava. Instead, the flow may have been largely spatter fed. A short pahoehoe river or distributary system that converted to aa within a few hundred meters of the vent (fig. 1.42), appeared to issue from the base of the fountain.

During the night of March 29–30, aa supplied by the northeastern vent almost completely surrounded the small 1965 spatter rampart that we had been using as a site for camp A (pl. 1). Over the next several days, the aa continued to thicken against the flanks of the 12-m-high hill (fig. 1.41). We last saw the hill late on April 3; subsequently, it was completely buried by episode 3 lava.

The flow from the northeastern vent advanced steadily northeastward through April 2 at an average rate of about 30 m/h (pl. 1; table 1.3). This northeasterly advance apparently slowed on April 3, and stopped on April 4 nearly 4 km from the vent after emplacement of a slender lobe northeast of Kalalua. On April 3, some of the lava moving northeastward was diverted to form a small lobe west and south of Kalalua. Advancing at about 10 to 15 m/h, this lobe was in place by late afternoon on April 5.

The supply from the northeastern vent was wholly diverted on April 5 to a new lobe of aa that extended nearly 4 km southeastward between the episode 1 and 2 flows. It advanced at an average rate of about 20 m/h for the rest of episode 3.

Lava production at the southwestern vent was minimal before April 4. Early that morning, the vent became steadily active. At about 0725 H.s.t., the crater filled with lava, and a flow poured steadily over the south crater rim (fig. 1.64*A*). About an hour later, at approximately 0830

H.s.t., a segment of the southern crater wall began to collapse, and a narrow breach quickly formed (fig. 1.64*B*) as the detached sector began moving south. Time-lapse film records show that the collapsing section of the cone was rafted slowly southward during the next several hours. The major portion stopped within 150 m of the cone's flank (fig. 1.25), but one 50-m-diameter block was transported 400 m (fig. 1.65).

The southwestern vent promptly became the source of a well-channelized lava-river system feeding a sequence of flows that advanced southeastward (pl. 1) from April 4 to 9. The first flow extended southward and then southeastward during April 4 and 5; its front stopped about 3.4 km from the vent. Apparently, the flow was beheaded, probably late on April 5, by a second flow that followed the southwest edge of the first. A third flow then broke out near the vent on the east side of the previous two. It captured the lava river and followed the southwest edge of the episode 2 flow toward the Royal Gardens subdivision, which it reached in 2 days. A minor additional flow, pahoehoe instead of the normal aa, was emplaced along the west edge of the previous episode 3 flows early on April 7. It extended about a kilometer south of the vent; most likely it formed from a temporary overflow of the lava river near the vent.

The two long flows extending southeastward from the southwestern vent advanced at average rates of 90 to 100 m/h. The last and longest flow reached the northwest end of King Street in the Royal Gardens subdivision at 0956 H.s.t. April 8; the flow front was then about 5.6 km from the vent. A detailed record of the flow-front advance southeastward along that paved street is shown in figure 1.66. A complexity arises because the sector of the flow front on the street stagnated temporarily on April 8, while lobes in the forest on either side continued to advance (pl. 1). The detailed record shows that the rate of flow-front advance before the end of the eruption (excluding the temporary stagnation, which resulted in a short-lived reentrant in the flow front) changed episodically over a measured range of about 40 to 360 m/h. On the pavement, surges with velocities of approximately 150 to 360 m/h were recorded. The data do not rigorously limit the durations of these surges, but a range from about half an hour to more than an hour is suggested. Periods of slower advance, approximately 40 to 100 m/h, alternated with the surges. The highest recorded surge velocities, 183 to 360 m/h, occurred early on April 9, after the flow front had narrowed distinctly (pl. 1).

The height of the flow front as it advanced along the paved street was determined from time to time by visual estimate by one of several observers. Most of the time, the flow front was 3 to 5 m high; however, as the sector on the pavement became the locus of most rapid advance after its late-afternoon stagnation on April 8, its front was about 6 m high. During the period of highest velocity, at about 0100 H.s.t. April 9, the narrow advancing front was about 10 m high; subsequently, it decreased in height to approximately 3 to 5 m.

The episode 3 lava flow advanced altogether about 2 km southeastward along King Street, and its front came to

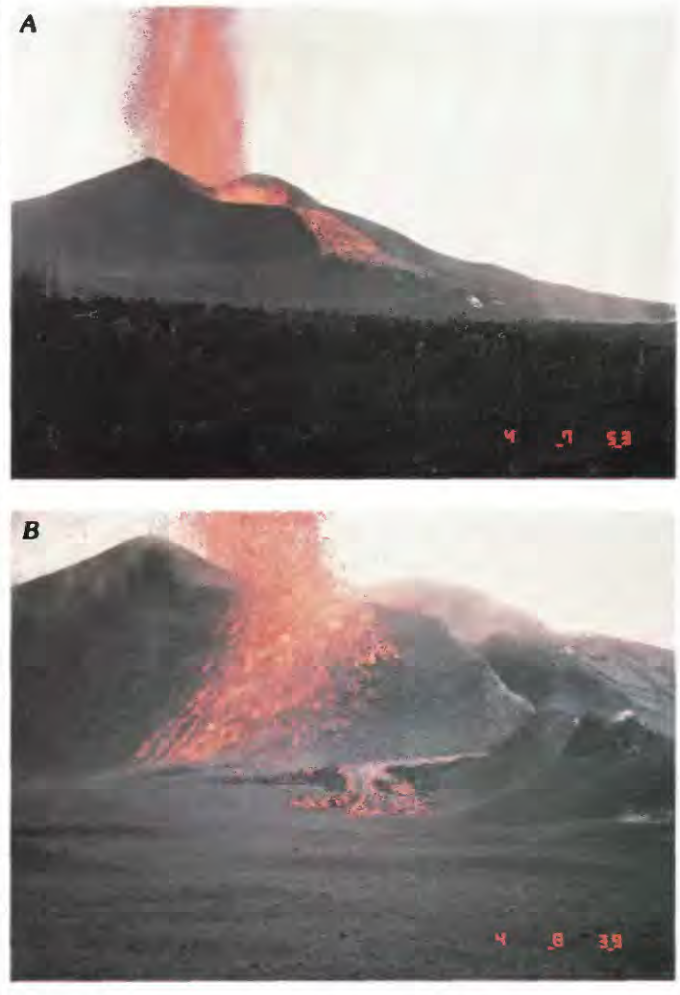

FIGURE 1.64.—Initial displacement of south flank of southwestern crater of 1123 vent during episode 3. *A*, 1123 cone shortly after beginning of steady lava production at southwestern vent. Low southwestern fountain plays within crater to right front of prominent northeastern fountain. Lava has filled crater at southwestern vent and is cascading over unbroken rim. View eastward from camp B; photograph by J.P. Lockwood, taken at 0753 H.s.t. April 4, 1983. Numerals (lower right) indicate date and time. *B*, 1123 vent, ¾ hour later. Narrow, steep breach transects wall of southwestern crater along boundary between stable and failing sectors of crater rim. Segment of cone flank to right of breach is moving slowly southward. Shiny pahoehoe from overflow in figure 1.64*A* mantles cone on both sides of breach. Small pahoehoe flow advancing over episode 3 tephra is probably an overflow from lava river flowing through breach. Low cones, a few meters high, in right center, formed during episodes 1 or 2. View eastward; photograph by J.P. Lockwood, taken at 0839 April 4, 1983. Numerals (lower right) indicate date and time.

rest about 7.6 km from the vent after destroying six dwellings. As a consequence of forming at least one and, possibly, two lobes west of King Street, in addition to the primary lobe on and east of King Street, the flow attained a maximum width of 600 m within the subdivision. After eruptive activity stopped at the vent at 0257 H.s.t. April 9, the flow front advanced an additional 350 m over the next 14 hours (fig. 1.66). Progressively slowing, it advanced another 20 m more over the next 3 to 4 days.

In addition to the major flows from the northeastern and southwestern vents, intermittent slow emission from lava tubes occurred along the south and west base of the 1123 cone. This activity produced a thin apron of pahoehoe flanking the west base of the cone (pl. 1). Tephra, primarily from the high northeastern fountain, completely buried this pahoehoe apron.

During episode 3, the 1123 vent produced a massive cone (fig. 1.67) about 60 m high, composed of agglutinated

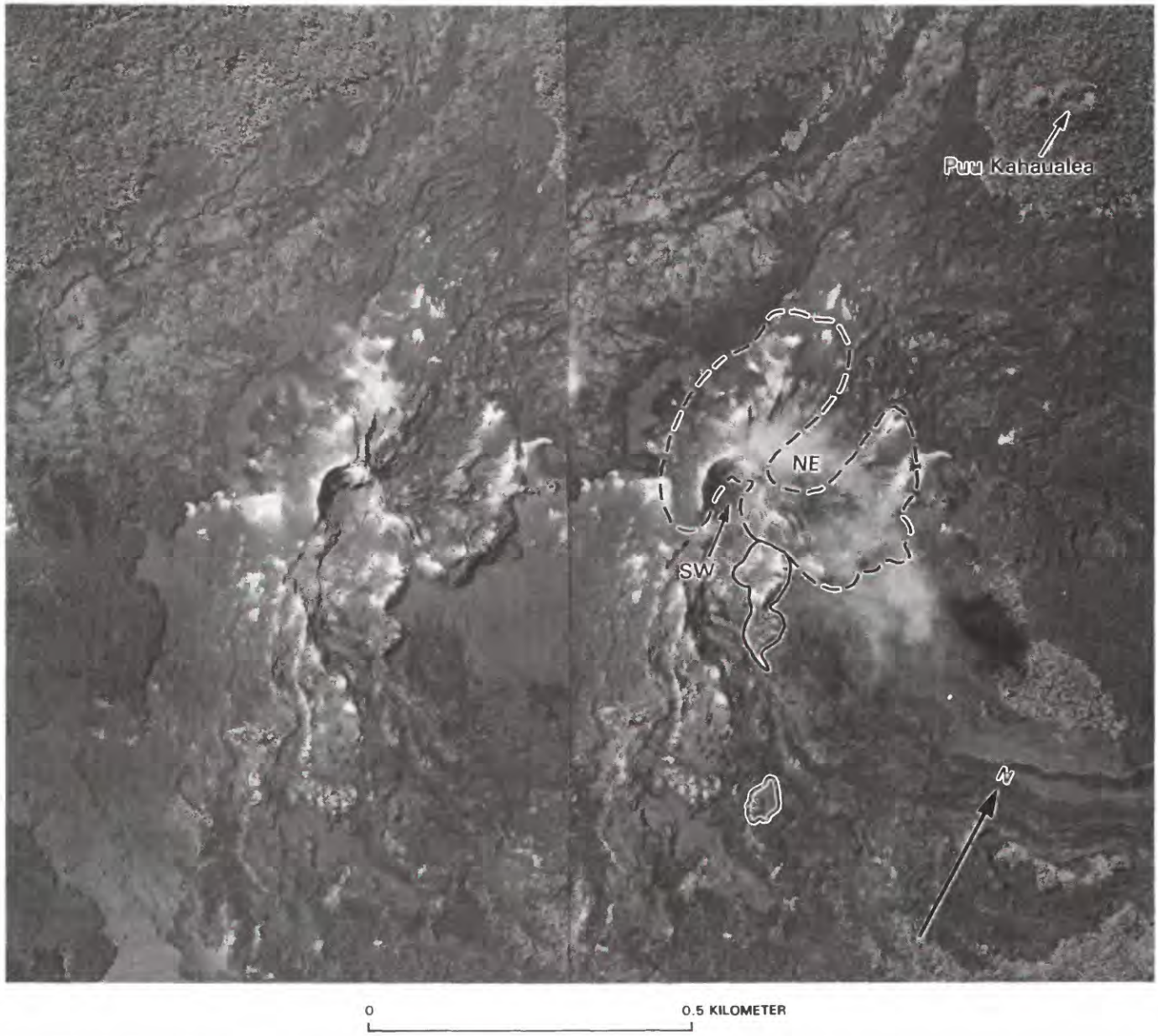

FIGURE 1.65.—Stereophotographs showing 1123 cone (dashed line) and rafted portions of cone (solid line). Southwestern crater (SW) is partly filled by talus from steep crater walls. Northeastern vent (NE), which has no distinct crater, is covered by its own aa. Rootless flows drape west flank of cone. Photographs 83.8.3JG120G#5 and 83.8.3JG120G#6 by J.D. Griggs, taken August 3, 1983.

spatter, rootless flows, and cinders. Figure 1.65 shows that no distinct crater remained at the northeastern vent and that the vent area was covered by aa. These characteristics seem compatible with the observation during this episode that relatively little lava ponded at the northeastern vent. Apparently, the thick northeastern aa flow was supplied directly, or nearly so, by the high northeastern fountain. The southwestern vent, which supplied a well-developed lava-river system, contrasts strikingly: A distinct bowl-shaped crater, which must have contained a lava pond, remained there.

The thick aa flow from the northeastern vent covered an area of 3.5×10^6 m^2; using the thickness data of plate 1 as a guide, we estimate a volume of about 19×10^6 m^3. For the 249-hour period from 1800 H.s.t. March 29, when the northeastern vent became steadily active, to the end of episode 3 at approximately 0300 H.s.t. April 9, the average lava-discharge rate from the northeastern vent was about 75,000 m^3/h. No significant change in that rate occurred, even in response to the high-volume discharge from the southwest vent from April 4 to 9.

Flows from the southwestern vent, also predominantly of thick aa, covered an area of about 2.9×10^6 m^2; we estimate their aggregate volume at about 15×10^6 m^3. The southwestern vent was erupting steadily from about 0730 H.s.t. April 4 to 0300 H.s.t. April 9, a period of 115.5 hours. Thus, its average lava-discharge rate was about 130,000 m^3/h, and the combined rate for the 1123 vent from April 4 to the end of episode 3 was about 200,000 m^3/h.

Including the initial eruptive activity at the O vent, episode 3 continued for approximately 290 hours. Its lavas, almost all aa, covered a total area of 7.9×10^6 m^2 and had an aggregate volume of about 38×10^6 m^3. The average lava-discharge rate was 134,000 m^3/h, but the actual rate ranged from approximately 80,000 m^3/h in the early part of episode 3 to 200,000 m^3/h in the later part.

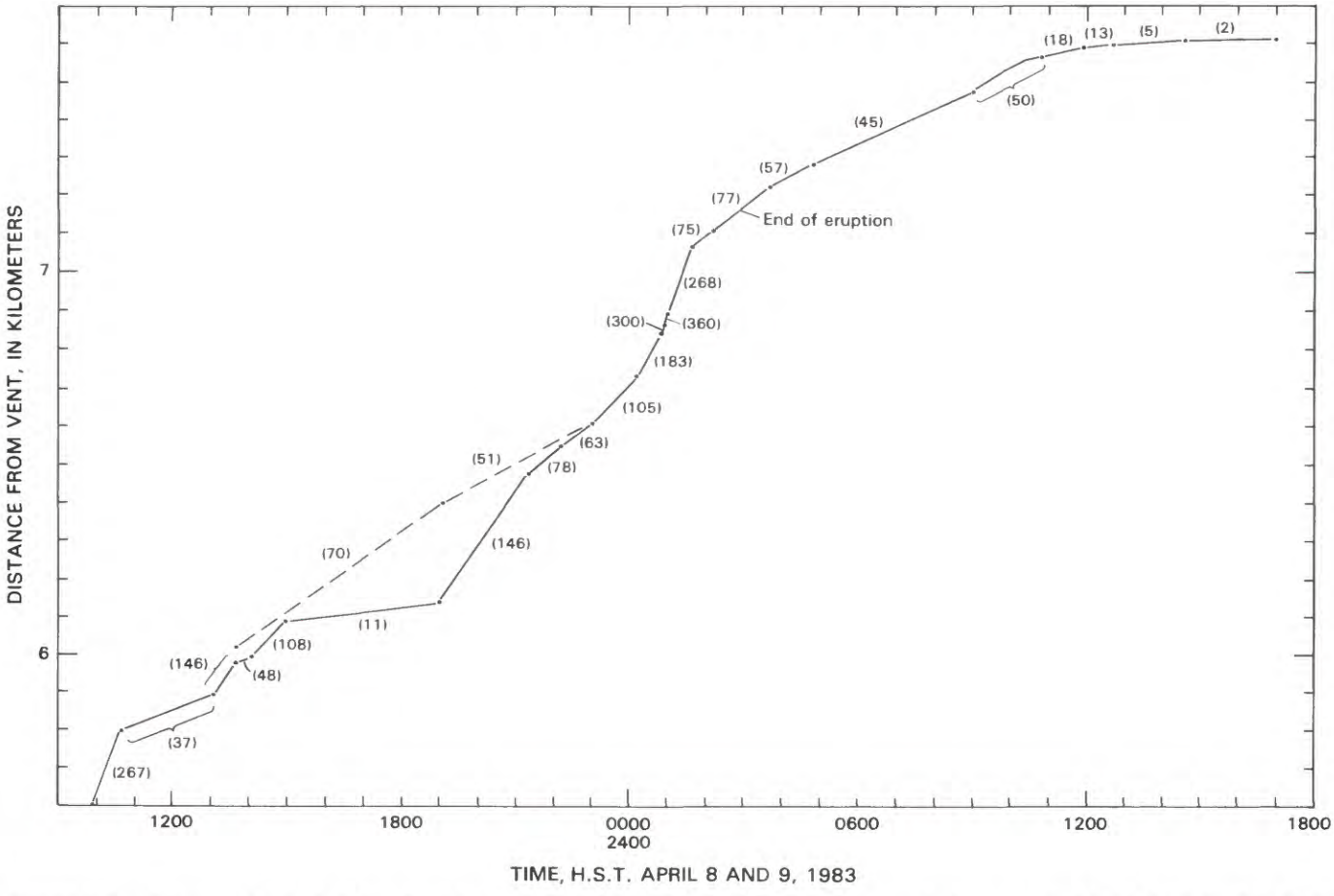

FIGURE 1.66.—Advance of episode 3 flow front in Royal Gardens subdivision from time flow reached pavement at 0956 H.s.t. April 8, 1983, to 1703 H.s.t. April 9, approximately 14 hours after end of eruptive activity. Solid line records advance of flow front southeastward along King Street. Dashed line shows continuing advance of eastern lobe when sector of flow front on King Street temporarily stagnated. Numbers in parentheses are calculated flow-front velocities (in meters per hour) between pairs of data points.

EPISODE 4 (JUNE 13–17,1983)

For 64 days after the end of episode 3, activity in the eruptive zone was characterized by weak harmonic tremor and emission of oxidized magmatic gases from fissures, fumaroles, and spatter cones. Slowly diminishing incandescence persisted in a gaping crack high in the 1123 cone, and by the time episode 4 began, a horizontal distance-measurement line established on Puu Kahaualea on April 21 had shown about 4 cm of extension across the trend of the eruptive fissure just downrift of the 1123 vent. In the succeeding months, no further significant extension across the fissure occurred at this locality.

At 1025 H.s.t. June 13, we received a report of fountaining in the eruptive area from observers in a fixed-wing aircraft. Harmonic-tremor amplitude recorded on a seismometer near Puu Kamoamoa had begun gradually to increase over low repose-period levels, beginning at about 0500 H.s.t. that morning; tremor amplitude peaked at 1100 H.s.t. Arriving at the site at 1145 H.s.t., we found a line of discontinuous fountains, 20 to 40 m high and about 100 to 150 m long, just downrift of Puu Kamoamoa. New vents at the west end of this line were observed opening at 1315 H.s.t. At that time, Puu Oo, a steep-sided spatter cone at the east end of the active vents, approximately 750 m downrift of Puu Kamoamoa, stood 15 to 20 m high and marked the locus of major fountaining and lava discharge (fig. 1.29). A line of less active fissure vents with low spatter ramparts extended uprift 100 m or so from the growing cone. Three pahoehoe flows, the longest of which had traveled about 500 m from the vent (pl. 2), were being fed by the line of erupting vents.

FIGURE 1.67.—60-m-high cone (Puu Halulu) built at 1123 vent during episode 3. Distance to cone is about 1 km. Rootless flows mantle cone's near flank. Flat, smooth surface adjacent to base of cone is formed of an apron of tube-fed pahoehoe erupted from base of cone and then mantled by tephra. Episode 3 tephra mantles hummocky pre-1983 lava in foreground. Small building in foreground was used for storage and shelter. View eastward from camp B; photograph taken at 1036 H.s.t. April 29, 1983. Numerals (lower right) indicate date and time.

The Puu Oo cone enclosed a crater that was partly filled with a lava pond. Fountains rose 30 to 50 m above the pond surface and were visible above the crater rim throughout the 100-hour-long eruption (fig 1.24).

The major lava flow to the southeast (pl. 2) was fed by a lava river that exited the crater where the pond overflowed through a low point in the crater rim. This breach, situated in the south-southeast wall of the crater, was 3 to 5 m wide and extended from one-half to one-third of the way down from the rim of Puu Oo. The lava cascaded over a fall, coalesced at the base of the cone, and commonly produced a spectacular standing wave.

By late afternoon on June 13, the lava river had established a well-developed channel that ranged from about 6 to 20 m in width and was bounded by smooth, stable levees of pahoehoe. Access across the levees to the edge of the lava river was good throughout the entire eruption, and estimates of the width and surface velocity of the river could be made in relative comfort. Lava flux was calculated (table 1.5) as described for the episode 2 channel. On the basis of the appearance of the evacuated channel after episode 4, we use an estimated depth of 3 m near the vent (fig. 1.9) and of 1.5 to 2.0 m 1 km downstream. In addition, observations of large rafted blocks during episode 4 suggest that the 1.5–2.0-m estimate is reasonable. At 1 km downstream, the observed lava flux, 90,000 m^3/h, agrees with that determined from mapping (table 1.3). Near the vent, an estimated flux several times larger suggests that there the lava contained a higher proportion of entrained gas.

In addition to the main flow, two small pahoehoe flows extended northward and southward from the fissure vents immediately uprift of Puu Oo (fig. 1.29). The more active of these two flows extended southward and southeastward from the entire line of low fountains. It began as a broad pahoehoe sheetflow with a maximum width of 150 m and was rapidly developing a central channel and lateral levees when observers first arrived. By late morning on June 15, a lobe of this flow had turned eastward to impinge against the main southeastern flow from Puu Oo (pl. 2). A second, slow-moving pahoehoe flow progressed 150 to 250 m northwestward of the eruptive fissure; this flow was fed primarily by low-level fountaining and emission of lava from the easternmost of the fissure vents. Over the course of episode 4, the flow developed into a nearly flat roofed, 250-m-diameter lava pond or reservoir. Such roofed ponds commonly formed where pahoehoe was slowly supplied by the vent; they apparently contained an interior complex of lava tubes that delivered lava in small streams to the margins or the roof. Pahoehoe buds at the edges of this particular roofed pond

TABLE 1.5.—*Episode 4 lava-river measurements*

[Width estimated visually during episode 4. Depth estimated in evacuated channel after episode 4]

Distance from vent (m)	Width (m)	Depth (m)	Maximum velocity (m/s)	Calculated lava flux (10^3 m^3/h)
10-20	6-8	3	15	570
30	15	3	3	240
130	20	3	3	320
1,000	7-9	1.5-2	3-4	90

supplied many of the measured temperatures and samples for episode 4 (see chap. 2).

For much of episode 4, fountain activity along the fissure vents was characterized by repeated low bursts of fragmented spatter rather than by sustained fountains. Whereas the easternmost fissure vent grew steadily over the first 3 days of episode 4, activity at the other fissure vents decreased rapidly. By the morning of June 15, the cone growing at the eastern fissure vent was similar in size to the cone east of it at the adjacent main vent, and the two had coalesced to form a double cone at Puu Oo. During that afternoon, all but two of the fissure vents were gradually buried by flows from the Puu Oo vent. Low bursts of spatter and low-level flow production continued at the more westerly Puu Oo cone until late afternoon of June 15, when the cone became partly roofed and its lava production apparently stopped.

The main episode 4 flow, aa except for the proximal 1 to 2 km, advanced at an average rate of 90 m/h (pl. 2). By 1600 H.s.t. June 15, the flow had traveled 5.7 km, and its front was west of the Royal Gardens subdivision opposite the end of Ekaha Street. For the next 2 days, the flow advanced westward of the subdivision, entering it only locally and causing no property damage.

Advance rates while the 2- to 12-m-high aa-flow front traveled downslope just west of Royal Gardens averaged about 1 m/min. As in episodes 2 and 3, however, large fluctuations in velocity and thickness were observed as intervals of surging alternated with periods of near-stagnation of the flow front.

A particularly well observed large surge occurred at 1828 H.s.t. June 16. From 1500 until 1828 H.s.t., the front of the episode 4 aa flow at the west edge of the Royal Gardens subdivision was nearly stagnant; the flow itself was approximately 100 m across and was bounded by rubble levees, about 6 m high. Lava output at the vent, 7 km upstream, had been steady until 1700 H.s.t., when partial collapse of the cone caused a temporary but significant increase in the flux observed in the near-vent channel. At 1828 H.s.t., a large pulse of lava was observed moving rapidly down the deep, nearly stagnant axial channel of the flow just west of Pakalana Street. The surge consisted of a wedge-shaped body of brightly incandescent aa, capped by a layer of dark rubble (fig. 1.68). Its surface was 6 to 7 m higher than the tops of the marginal levees, which apparently confined it. Between Pakalana and Pikake Streets, the surge, still within the aa-flow channel, advanced a distance of 420 m in about 12 minutes, at a rate of 33 m/min. The front of the surge was estimated at about 12 m thick and 70 m wide; over its total estimated length of 1 km, it tapered in thickness to about 1 m. These dimensions suggest a volume of about 400,000 m^3 for the observed part of the surge—equivalent, if correct, to about 4 hours of supply from the vent (table 1.3).

Subsequent advance of the flow front was confined to a narrow lobe that advanced slowly down the steep slope west of the subdivision. A final small surge occurred at 1700 H.s.t. June 17, nearly 3 hours after the end of episode 4.

Draining of the central channel, possibly as surges waned or as the flow front continued to advance at the end of episode 4, left high-standing aa levees west of the subdivision. Locally, the interior walls (fig. 1.37) were plastered by finely comminuted basalt striated parallel to the channel axis.

Episode 4 ended suddenly at 1413 H.s.t. on June 17, approximately 100 hours after it began, with little apparent premonitory decay of fountaining or lava output. At the episode's end, the Puu Oo spatter cone stood about 20 m high. The eastern part of the cone contained a rubble-floored crater, approximately 40 to 50 m in diameter at its crest (fig. 1.69), bounded by steep, smooth walls.

FIGURE 1.68.—Surge west of Royal Gardens, traveling approximately 33 m/min down central channel of episode 4 aa flow at west end of Pakalana Street. Note stop-sign standard partly buried by stagnant aa at edge of episode 4 flow. Photograph by R.W. Decker, taken at 1828 H.s.t. June 16, 1983.

FIGURE 1.69.—Eastern (EV) and western (WV) craters within Puu Oo spatter cone (4s), remaining fissure vents (FV) uprift of Puu Oo, and remnant of O vent (3V) of episode 3 and its partial ring of spatter (3s) after episode 4. Vent deposits are delineated by solid lines, dashed where uncertain. Crater rims are delineated by hachured lines; hachures point inward. Active lava flows of episode 5 are visible heading northwestward and southeastward from Puu Oo, and heavy fume issues from both eastern and western Puu Oo vents. Photograph 83.6.29JG120A#7 by J.D. Griggs, taken June 29, 1983, several hours after onset of episode 5.

The southeast wall was still partly breached by a V-shaped notch, 3 to 4 m wide at its narrowest point and extending 8 to 10 m down the side of the cone. The floor of the crater was bisected by a crudely linear opening of unknown depth. Fume emanated from this elongate hole, which was oriented subparallel to the axis of the rift zone. On the uprift shoulder of Puu Oo, the western vent, approximately 15 m high, was also a steep-walled but partly roofed crater. Two small spatter cones marked the sites of part of the surviving fissure vents that had been active until the afternoon of June 15.

Extending southeastward from the eastern Puu Oo vent was an evacuated lava channel, box shaped in cross section and approximately 2 to 4 m deep and 10 m wide (fig. 1.9). The floor of this channel was generally smooth; in places, large sections of the wall had collapsed inward. About 1 km downstream, the average depth decreased to 1 to 2 m, and the width increased to about 15 to 20 m. Because the rate of lava discharge from the fissure vents and western Puu Oo vent was relatively low, those vents did not feed vigorous lava rivers, and so no conspicuous evacuated channels remained in the flows that had traveled northward and southward from them.

Episode 4 produced approximately 11×10^6 m^3 of basalt that covered an area of 2.2×10^6 m^2; the average lava-discharge rate was 110,000 m^3/h. Most of the main, 7.8-km-long southeastern flow was aa, 2.5 to 10.7 m thick and 40 to 400 m wide. A well-defined aa channel persisted for almost the entire aa portion of the flow. The minor flow north of the fissure vents was primarily pahoehoe, several meters thick. The southern fissure-vent flow ultimately extended 2.4 km from the vent and consisted of both aa and pahoehoe, averaging 3.0 m in thickness.

EPISODE 5 (JUNE 29–JULY 3, 1983)

Observers camped near the site of Puu Oo on the night of June 28–29 noticed a strong glow over the vent. At 1000 H.s.t. June 29, as we remeasured a newly established horizontal distance-measurement line across the eruptive fissure just east of Puu Oo,[1] helicopter pilot Bill Lacy, Jr., reported seeing lava ponding inside the crater. Climbing to the southeast rim of the main crater, we saw a thin-crusted pond of lava, like that shown in figure 1.50*B*, slowly rising inside the crater. A 1- to 2-m-high dome fountain played intermittently in the center of the pond. Fresh high-lava marks visible on the inner crater walls indicated that the pond surface had been about 2 m higher at some recent time.

At 1214 H.s.t., lava began to ooze from a small hole about 1 to 2 m below the spillway crest. The narrow lava tongue froze, however, before reaching the channel floor, as the pond inside the crater subsided temporarily. The final breakthrough occurred at 1245 H.s.t., when a 1-m-wide pahoehoe cascade appeared at the same opening and reached the evacuated episode 4 channel floor within 1 to 2 minutes. By 1254 H.s.t., a fluid pahoehoe flow, 30 cm thick at the front and thickening upstream, was spilling through the breach in the crater rim and reoccupying the empty episode 4 channel. Advance rates were slow enough for us to sample the first lava down the channel. An increase in harmonic tremor in the eruptive area began at approximately 1251 H.s.t., followed by an acceleration of lava discharge and development of a low fountain that rose 5 to 10 m from the pond surface.

Activity stabilized by 1300 H.s.t., and the lava channel near the vent was full and often overflowing. A fountain, 10 to 35 m high, with rare bursts to 50 m, played from the surface of the lava pond within the crater. The pond surface was estimated from aerial views to be at the level of the spillway; the pond was probably 20 to 30 m deep. By evening, the fountain had increased in height to about 40 m, and it remained approximately 20 to 40 m high throughout the 90-hour eruption (fig. 1.24).

By 1558 H.s.t. June 29, the western vent, high on the uprift flank of Puu Oo (fig. 1.69), became active with low fountaining through a lava pond and production of small flows. Examination of this vent at 1430 H.s.t. had shown no sign of lava; however, very hot air and fume pulsing from an opening at the top of this partly crusted over spatter cone had been detected at 1055 H.s.t. At the uprift base of the western Puu Oo vent, approximately at the site of one of the episode 4 fissure vents, a small pahoehoe flow issued to the south. Whether this was a separate vent or merely a passive outlet for the western Puu Oo vent is uncertain. By the morning of June 30, the small lava and spatter mound that grew around this minor outlet was buried by pyroclastic deposits from the more active western Puu Oo vent.

A small pahoehoe flow from the western Puu Oo vent ponded north of the vent during the late afternoon and evening of June 29. In the early morning hours of June 30, it developed a throughgoing channel feeding a local pahoehoe flow that extended northeastward, overrunning camp B (pl. 2).

The western Puu Oo vent stopped feeding the northeastern flow during the afternoon of June 30, after it had traveled 800 m, and began, instead, to feed a well-channelized flow that extended southeastward along the southwest edge of the episode 3 and 4 flows (western flow, pl. 2). This flow advanced at an average rate of about 80

[1]Only two sets of measurements were ever made on this short-lived line, which did not survive episode 5. The first was on June 24, and the second just before the onset of episode 5 on the morning of June 29. Approximately 2 cm of extension occurred during that time interval between targets at the ends of a 400-m-long line centered over the eruptive fissure. However, it was impossible to determine whether this deformation was due to lateral extension or to local uplift near the eruptive fissure where the measuring instrument was located.

m/h and took about a third of the total lava discharge of the active vents. By the early evening of July 1, the flow had turned eastward and impinged against the main southeastern flow from the Puu Oo vent. At that time, relatively fluid paheoehoe extended along the channel for approximately three-fourths of the length of the flow. Subsequently, the flow turned southeastward again and continued downslope through the rain forest.

The main flow (eastern flow, pl. 2) followed a path toward Royal Gardens just east of the episode 4 flow. It developed a long, stable pahoehoe channel, with a startling hairpin bend 1.5 km from the vent (fig. 1.70). The vigor of the channel seemed nearly identical to that observed during episode 4. The channel was bank full, and no long-lived changes in velocity or flux were observed during the eruption. About 100 m downstream from Puu Oo, we estimated a channel width of 7 m and an average surface velocity of 1.25 to 1.5 m/s. For an assumed depth of 3 m, these values suggest a flux of 100,000 m^3/h, identical to that determined for the eastern flow later when it was mapped (table 1.3).

The transition from pahoehoe to aa in the channel of the eastern flow occurred downstream from the vent at distances of approximately 3.5, 3.5, and 4.2 km for 1325 H.s.t. June 30, 1100 H.s.t. July 1, and 0910 H.s.t. July 2, respectively, translating to 88, 63, and 58 percent of the total flow length at each successive time. For the first 4.5 km, the toe advanced at an average rate of about 170 m/h; it then slowed down to an average rate of 60 m/h. The higher early rate probably reflects rapid extension of the flow during the first day, when pahoehoe extended nearly to the toe.

The eastern flow approached the subdivision as a 300-m-wide, flat-topped aa front, 3 to 4 m high and moving at about 1 m/min. Just northwest of the subdivision, the flow became confined to a gully, and a narrower lobe, 100 to 200 m wide, accelerated toward the upper end of the subdivision; it reached Ekaha Street at 1950 H.s.t. (fig. 1.71). After traveling approximately 170 m at an average velocity of 3.9 m/min, the flow began an extended period of very sluggish advance. During the night of July 1–2, its average forward velocity was 0.5 m/min, and at 0500 H.s.t. July 2 the flow front was essentially stagnant. Movement was sufficiently slight to allow an observer to walk across the entire flow, which was 120 m wide, 2 to 3 m thick, and had a central channel 15 m wide.

The lull in activity at the flow front ended at 0620 H.s.t. as a surge reactivated the front, which then advanced across Tuberose Street (fig. 1.71) at a rate of 5.0 m/min. The sudden advance related to this surge, like many others observed in Royal Gardens, lasted less than an hour. Between 0730 and 1500 H.s.t. July 2, at least five surges with durations of approximately 25 to 55 minutes were reported. The most impressive surge occurred at 1453 H.s.t. July 2, following a period of slow advance between Pikake and Plumeria Streets. This surge was first observed 300 m upstream of the front and was advancing at a rate of 30 m/min. Viewed from the front, it appeared to be a wall of aa, about 6 m above the level of the 4-m-high, 100-m-wide preexisting flow (fig. 1.39*A*). Responding to the approaching surge, the front doubled in thickness, steepened, and became unstable, and its forward motion accelerated (fig. 1.39*B*). An abandoned truck was overrun in minutes; before burying it, however, the flow pushed it forward as a bulldozer would for a distance of 40 to 50 m. This thickening and acceleration was followed by breakout of a fluid, thin (1–2 m thick) flow of scoriaceous aa (Lipman and Banks, 1987) from near the base of the main flow (fig. 1.39*C*). This thin lobe moved down Hoku Street at a rate of 15 m/min, destroying another abandoned car and decelerating to signal the end of the surge by 1525 H.s.t. The main body of the flow had thinned to 2 to 3 m and continued to advance at less than 1.0 m/min. One home of the total of eight engulfed in Royal Gardens during episode 5 was destroyed during this surge.

The long interval of slow advance that followed the 1453 surge was interrupted at 1821 H.s.t. by another large surge observed passing Pakalana Street. This surge, witnessed primarily from helicopter at night, was a broad sheet of fluid, brightly incandescent lava, about 50 m across and 4 to 5 m high at the front, thinning upstream over a distance of about 800 m (fig. 1.38). As the surge reached the front of the primary flow, a breakout over the lateral levee occurred, sending a short-lived, fluid, thin flow downslope at a rate of 25 m/min. This overflow decelerated rapidly and thickened from 1 to 8 m in 5 minutes.

At least three additional surges of smaller magnitude separated by 3- to 7-hour intervals were reported over the next 13 hours in the subdivision. By 0618 H.s.t. July 3, one of these surges had formed a new lobe that traveled just eastward of Hoku Street (fig. 1.71).

Fountaining and local harmonic tremor dropped abruptly and concurrently between 0713 and 0720 H.s.t. July 3, approximately 90 hours after episode 5 lava production began. Perceptible movement of the flow toe continued for more than 3 additional hours. A small surge occurred at 0930 H.s.t., and the front continued to creep forward slowly until at least 1030 H.s.t.

The vent complex, much like its configuration at the beginning of episode 5 (fig. 1.69), consisted of two juxtaposed spatter cones separated by a wall of spatter. Both cones were steep sided and had bowl-shaped craters. Evacuated, box-shaped lava channels, 3 to 4.5 m deep, extended from the southeast base of the eastern Puu Oo cone and the southwest base of the western cone (see fig. 1.74). The rims of these cones had approximately doubled in height to 40 m during episode 5, and each cone was partly transected by a steep cleft through which the

FIGURE 1.70.—Upper reaches of sinuous episode 5 lava river. Erupting eastern vent at Puu Oo is visible at top, 1.5 km from hairpin bend. Western vent and its flow to southeast are also visible. Apparent gap in river, where smoke originates at upper right, is a short roofed segment that developed where river narrowed and accelerated as it flowed over a southeast-facing escarpment. View northwestward; photograph by J.D. Griggs, taken at approximately 1800 H.s.t. July 1, 1983.

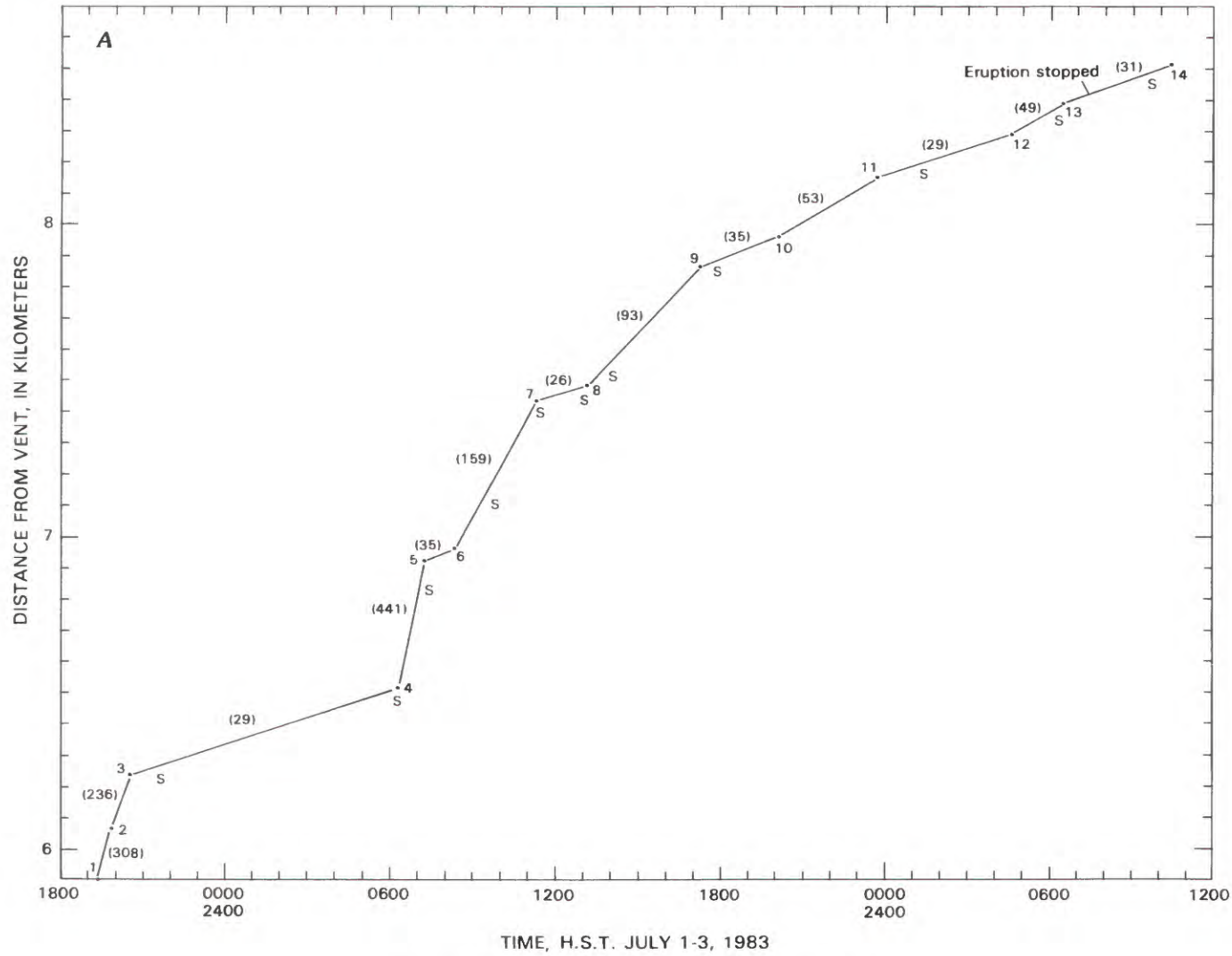
A
DISTANCE FROM VENT, IN KILOMETERS
8
7
6
Eruption stopped
(31)
S
14
(49)
S
13
(29)
S
12
11
(53)
(35)
10
9
S
(93)
(26)
S
8
S
7
S
(159)
S
(35)
6
5
S
(441)
4
S
(29)
3
S
(236)
2
(308)
1
1800
0000
2400
0600
1200
1800
0000
2400
0600
1200
TIME, H.S.T. JULY 1-3, 1983

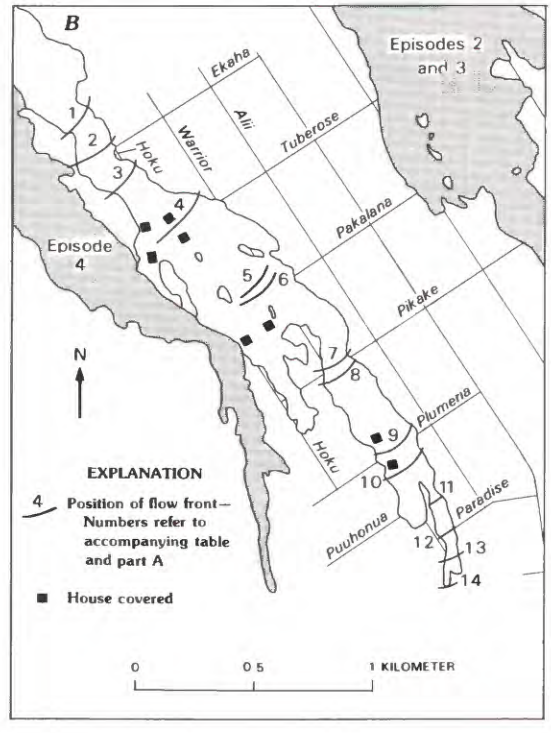
B
Episodes 2
and 3
Ekaha
Alii
Tuberose
Warrior
Hoku
Pakalana
Pikake
Plumeria
Hoku
Puuhonua
Paradise
Episode
4
1
2
3
4
5
6
7
8
9
10
11
12
13
14
N
EXPLANATION
4 Position of flow front—Numbers refer to accompanying table and part A
House covered
0
0 5
1 KILOMETER

respective lava rivers had exited. During heavy bombardment by spatter late in episode 5, outward slumping of the northeastern flank of the eastern cone created a low area in the rim. Although we did not realize it then, this low part of the rim was to become the persistent spillway of subsequent episodes. At that time, however, the breach on the southeast side was considered the most likely spot for the next spillover if eruptive activity resumed.

Approximately 13×10^6 m^3 of basalt was erupted during episode 5; it covered an area of 3.4×10^6 m^2, at an average lava-discharge rate of 140,000 m^3/h. The main flow destroyed eight dwellings in the Royal Gardens subdivision, and four other dwellings were cut off from road access.

FIGURE 1.71.—Summary of episode 5 flow advance in Royal Gardens. *A*, Flow-front advance versus time. Numbers 1 through 14 correspond to successive flow-front positions keyed in figure 1.71*B*. Numbers in parentheses are average velocities (in meters per hour). S, surge reported by flow-front observers. Data points do not necessarily correspond to beginning or end of surges. Thus, plot shows episodicity of flow advance but not necessarily maximum and minimum flow rates. *B*, Part of Royal Gardens subdivision, showing flows of episodes 2 through 5 and houses destroyed by episode 5 lava flow. Table below refers to numbered flow-front positions shown in figure (dashes indicate no data). Average velocity was computed from distance traveled (as measured from preceding flow-front position along line on map connecting successive flow-front positions) divided by elapsed time. Observed velocity was estimated by flow-front observers at indicated time.

Locality	Time (H.s.t.)	Thickness (m)	Average velocity (m/min)	Observed velocity (m/min)	Comments
			July 1		
1	1919	4–5	0.8	5.0	One lobe out of several had become dominant; flow accelerated.
2	1950	—	5.1	—	Reaches Ekaha.
3	2033	2.5–4	3.9	—	Very sluggish (<<1 m/min) most of the night.
			July 2		
4	0620	2.5	0.5	5.0	Surge crosses Tuberose after long stagnant interval; entire flow front 120 m wide.
5	0716	—	7.4	—	Surge and then deceleration.
6	0824	—	.6	—	Surge followed by slow advance.
7	1121	1–2	2.7	8.0	Surge crosses Pikake, then flow thickens to 2–3 m.
8	1315	—	.4	.7	Surge after long interval of sluggish advance.
9	1720	3	1.6	.3	Crosses Plumeria.
10	2009	5	.6	1.0	—
11	2345	8–10	.9	.5	Flow thickens as it slows.
			July 3		
12	0433	—	0.5	0.1	Crosses Paradise, 20–30 m wide.
13	0635	—	.8	.9	Eruption stops at 0715 H.s.t.
14	1030	—	.5	—	Flow essentially halted.

EPISODE 6 (JULY 22–25, 1983)

At 0700 H.s.t. July 20, astronomers on Mauna Kea reported seeing intermittent fountains in the middle east rift zone of Kilauea. Their reports went unsubstantiated and were followed at 0900 H.s.t. by an aircraft observation of fume but no lava at Puu Oo. At approximately 0600 H.s.t. July 21, lava was sighted from a passing aircraft inside the eastern crater at Puu Oo. At 0900 H.s.t., an HVO observer reported a 5- to 10-m-deep lava pond in the eastern vent. For the next 33.5 hours, low-level eruptive activity occurred within the crater, accompanied by a fluctuating increase in harmonic tremor and episodic gas-piston activity (fig. 1.50).

At approximately 1410 H.s.t. July 22, an extended filling event (fig. 1.50*A*) progressed so far that overflow seemed imminent. Observers, who had been watching the gas-piston activity from a low area on the northeastern part of the crater rim, left their vantage point, certain that lava would begin its cascade through the breach in the southeast rim of the crater. When they reached a new observation point high on the southeast side of the cone at 1511 H.s.t., however, they found that the pond was completely drained. From this new vantage point, they saw that their former perch on the northeast rim was covered with new cooling lava from the previous high stand of the pond. Lava reappeared on the crater floor after about a minute, and at 1515 H.s.t. a steady, more rapid filling of the pond commenced (fig. 1.50*A*), accompanied by a fountain of accelerating vigor which soon indicated that a second retreat would be advisable. At approximately 1530 H.s.t., the 20-m-deep pond began to overflow, first on the northeast side and then, briefly, through the breach in the southeast rim. Fountaining and flow production rapidly increased. Soon lava pouring over the low sector of the northeast rim was supplying a flow to the northeast, and spatter cascading over the north rim, with possibly some pond overflow as well, was feeding a broad, thick, slow-moving, spiny pahoehoe flow that advanced northward and northwestward from Puu Oo (fig. 1.72). A short-lived pahoehoe flow reoccupied the evacuated episode 5 channel to the southeast for 200 m, but supply from the southeastern spillway was soon terminated. The flow to the north and northwest became stagnant after several hours, and, thereafter, all the lava discharged from the crater overflowed the northeast rim and fed the northeastern flow.

During episode 6, the early fountain, which rapidly reached 60 m above the surface of the lava pond (fig. 1.24), was strikingly more energetic and sustained than those of episodes 4 and 5. At times, the fountain was directed to the northeast, and heavy spatter fell directly into the pahoehoe river exiting the crater. By 1645 H.s.t., when last seen that day, the flow front had traveled less than

500 m and appeared to be headed into remote rain forest, where it posed no immediate threat to inhabited areas.

The eruption continued steadily throughout the night of July 22–23. At 0300 H.s.t., a strong glow in the direction of Puu Oo was visible from HVO, and the roar of the vent, nearly 20 km away, was audible. There were reports that the fountain was visible from the airport in Hilo, nearly 40 km north of the vent.

Fountain height increased through the first night, reaching a peak of more than 100 m in the early morning hours of July 23 (fig. 1.24). High, steady fountaining continued until about 0830 H.s.t. July 23. The fountain then declined in height sporadically during the rest of the day to a general height of 30 to 60 m that was maintained, with a gradual long-term decline, throughout the rest of the episode. When it was high, the single, vigorous fountain was broad and was commonly inclined to the northeast as much as 10°–35° from vertical. The high fountain produced a tephra blanket that fell to the southwest (downwind), mantling the flank of the cone and partly filling the remnant southwestern episode 5 channel adjacent to the southwest flank of Puu Oo.

During the period of high fountaining, the northeastern flow, mainly aa, continued to be sluggish and failed to develop a throughgoing centralized channel system, even though the lava flux over the northeast crater rim was high. Visual estimates of the flux ranged from 1 to 3 times that seen spilling from Puu Oo during episodes 4 and 5. During the early morning of July 23, the flow was broad, and lobes extended short distances eastward, northeastward, and southeastward in the area between Puu Oo and the 1123 cone. At about 1030 H.s.t., after the fountain height had greatly diminished, more rapidly advancing pahoehoe was seen overriding the sluggish aa. A stable channel system developed, and a lobe of this flow continued northeastward to become the major flow of episode 6 (pl. 2).

The spillway area on the northeast rim of Puu Oo was a broad zone where lava poured continually from the lava pond. Output consisted of two lava rivers separated by a large pinnacle on the rim (fig. 1.73); they coalesced after descending the steep outer slope of the cone. By the last day of episode 6, the smaller, more northerly spillway had been dammed, and the vent geometry was like that shown in figure 1.20.

Supply of lava to the channelized river remained steady, and the flow advanced through the rain forest north of Puu Kahaualea at an average rate of about 80 m/h. During the night of July 24–25, the flow front divided into two major lobes that advanced in parallel (pl. 2). At the episode's end, they were each nearly 6 km from the vent; subsequently, they merged and flowed another half-kilometer.

The eruption stopped at about 1630 H.s.t. July 25. Tremor began gradually to decrease at about 1620 H.s.t. and by 1630 H.s.t. had dropped significantly, coincident with shutdown at the vent. In the last few minutes of the eruption, fountain activity became noticeably lower and more intermittent, with loud, pulsing bursts of fragmented spatter.

Episode 6 lava was predominantly aa at the end of the episode. The two-lobed major northeastern flow had ex-

FIGURE 1.72.—Vigorous fountaining and flow production from Puu Oo 1 hour after beginning of episode 6. Spiny pahoehoe in foreground is fed primarily by voluminous spatter cascading down north flank of cone. To left of fountain, lava overflowing low northeast rim supplies a flow to northeast. Fountain is approximately 60 m high. View southward; photograph taken at 1637 H.s.t. July 22, 1983.

FIGURE 1.73.—Two spillways and lava cascade feeding flow to northeast during episode 6. Fountain height is approximately 40 m above lava-pond surface. By next day, smaller, more northerly spillway was inactive. View southwestward; photograph taken at 1641 H.s.t. July 24, 1983. Numerals (lower right) indicate date and time.

tended a total of 6.5 km into heavy rain forest, establishing a pathway that was to be followed in many subsequent episodes. Remnants of a well-defined central channel were discernible along nearly the entire length of the flow. Pahoehoe overflows as far as 2.75 km from the vent indicated that the fluid pahoehoe portion of the channel had extended about 40 percent of the overall flow length. Additional, spatter-fed aa flows with evacuated central channels extended 0.55 km southward and 1.25 km southeastward (pl. 2).

In total, episode 6 lava covered an area of about 2.0×10^6 m^2 and had a volume of 9×10^6 m^3. The episode lasted 73 hours, and thus the calculated lava-discharge rate was about 120,000 m^3/h.

The Puu Oo cinder and spatter cone had increased its girth and height strikingly during episode 6. The southwest flank was mantled by a thin blanket of tephra (fig. 1.74) from the high fountaining early in the episode. Puu Oo contained a steep-walled, bowl-shaped crater (fig. 1.75*A*), about 50 m in diameter at its rim crest and 30 to 40 m in diameter at the level of the spillway. An interior bench or terrace, about 10 to 15 m above the floor, skirted the north, east, and south walls. The west wall was steep, unstable, and approximately 25 m high from the floor to the rimtop. At the base of this wall was a fuming, incandescent crack and a 5- by 20-m elongate block, about 8 m high, that was mantled by spatter on its top and slickensided on its sides (fig. 1.75*B*). The vertical striations imply that the block was left standing high as lava and rubble of the crater floor subsided at the end of episode 6.

The western Puu Oo vent (fig. 1.74), active in episode 5, remained quiet during episode 6; it received only occasional spatter-fed flows from the episode 6 fountain. It retained definition after episode 6 but was only one-fourth as large as the main part of Puu Oo.

The Puu Oo spillway was a broad, low area on the northeast crater rim. About 15 m wide (fig. 1.75*A*), it was smooth and wide enough to use as a landing area for small helicopters.

EPISODE 7 (AUGUST 15-17, 1983)

On August 8, a pilot reported lava "deep" in the vent. On August 10, observers on the rim and inside Puu Oo Crater saw a small glowing hole at the west edge of the crater floor, where an incandescent crack had been noted on July 26 just after episode 6. A small pahoehoe flow had issued from the vicinity of this hole, and a low collar of spatter surrounded it. By the afternoon of August 11, the floor of the crater was completely repaved with thin new pahoehoe (fig. 1.75*A*). Sporadic production of small lava flows, accompanied by low-level spattering and occasional cyclic rise and fall of lava visible within the hole, continued for the next 4 days. Throughout this period, activity was mild enough to permit direct sampling of gases and small lava flows on the crater floor.

Observers were absent for the beginning of vigorous lava production on the morning of August 15. An increase in harmonic tremor was recorded at 0709 H.s.t. by a seismometer near Puu Oo, and time-lapse film recorded fountains rising above the crater rim by 0741 H.s.t. At 0850 H.s.t., when we arrived at the site, a fountain 60 m high emanated from Puu Oo Crater, which was filled by a lava pond about 20 m deep. The low northeastern part of the rim was again the spillway, and lava from the overflowing pond (fig. 1.20) fed a rapidly advancing pahoehoe flow that followed the path of the episode 6 lava to the northeast.

The remnant of the western crater at Puu Oo, which had last been active in episode 5, accumulated falling spatter so rapidly that it contained an overflowing pond. Thus, a moderately voluminous pond- and spatter-fed flow advanced southwestward from the vicinity of the nonerupting western crater, and a smaller spatter-fed flow traveled northwestward from the north side of Puu Oo (fig. 1.20). The northwestern flow advanced slowly and eventually turned northeastward, traveling a total of 600 m (pl. 2). The southwestern flow received a significant but varying component of overflow from the secondary pond and traveled more rapidly, at rates of about 50 to 150 m/h. By morning on August 17, after turning southeastward and traveling approximately 3 km from the vent, this flow had been beheaded, and it slowly halted.

During the heavy spatter fall that produced the rootless northwestern flow, the north rim of Puu Oo became deeply furrowed (fig. 1.76). As we watched, individual pinnacles seemed to grow upward and simultaneously become better defined by development of the bounding furrows, as if the falling fragments were accreting to the pinnacles or eroding the furrows, or both. Eventually the pinnacles became unstable and broke off, falling into the crater or rolling down the outside of the cone.

The main, northeastern flow received the major part of the lava output (table 1.3). As in previous episodes, this flow was fed by a vigorous pahoehoe river with narrow overflow levees for approximately the first kilometer. A broad, unimpeded cascade of lava down the spillway on the northeastern flank of Puu Oo Crater supplied this river with overflow from the lava pond. After traveling approximately 1 km over episode 6 basalt during the first hour of the eruption, the flow widened, became aa at its front, and decelerated. It then continued to advance into rain forest south of the episode 6 basalt and, in places, over 1963 basalt, at an average rate of about 100 m/h.

The advance of the northeastern flow was complicated by repeated division of the flow front to form subordinate lobes (pl. 2). By the morning of August 16, the front had

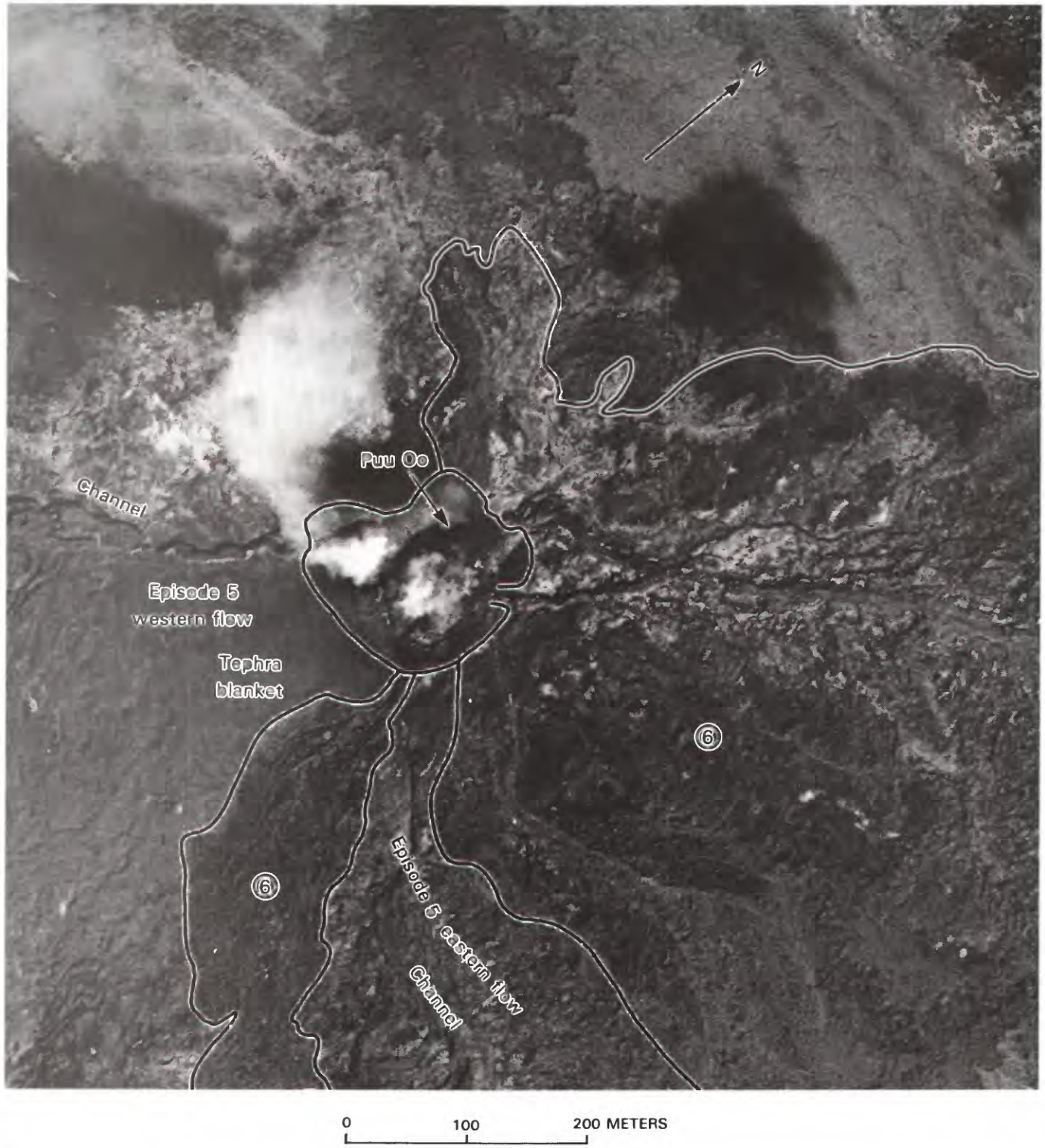

FIGURE 1.74.—Puu Oo and nearby episode 6 flows (6) after episode 6. Evacuated episode 6 channel is conspicuous northeast (to right) of Puu Oo. Though fuming heavily, western Puu Oo Crater remained inactive during episode 6. Photograph 83.8.3JG120F#7 by J.D. Griggs, taken August 8, 1983.

divided to form the southern and middle lobes, which traveled side by side, although the southern lobe received more lava supply and advanced more rapidly. Subsequently, each lobe divided again. A slow-moving (approx 30 m/h) northern lobe separated from the middle lobe, and a more rapidly moving (approx 120 m/h) northeastern lobe separated from the southern lobe. Thus, at the episode's end, the complex northeastern flow was advancing along each of four distinct fronts.

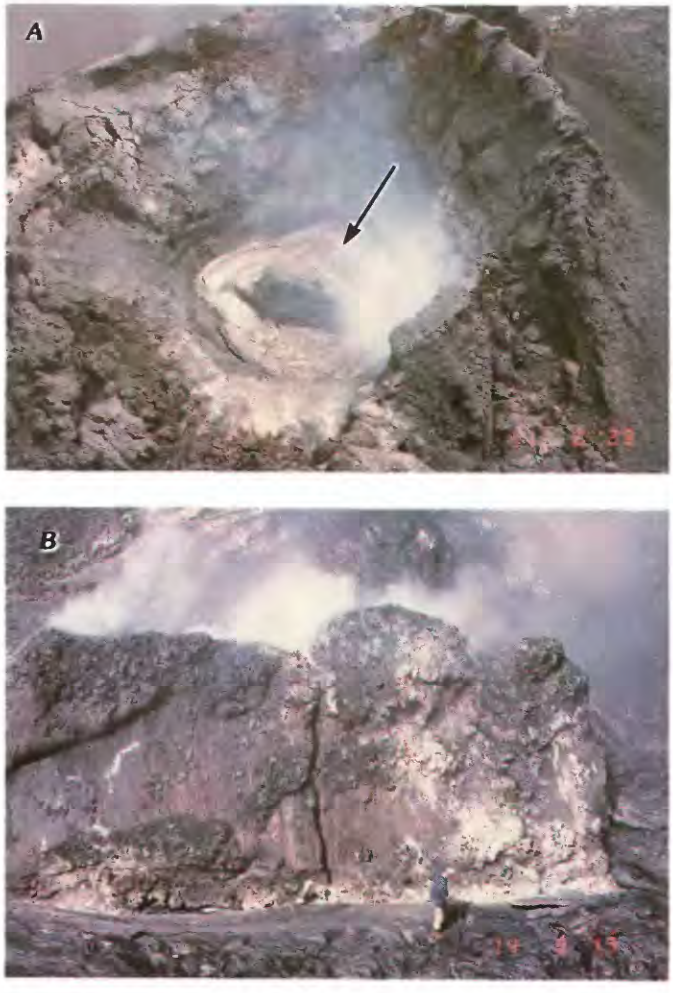

FIGURE 1.75.—Interior of Puu Oo between episodes 6 and 7. *A*, New pahoehoe flows, erupted after episode 6, cover crater floor. Glowing hole (arrow) marks vent at base of steep west wall. Spillway, mantled by shiny episode 6 pahoehoe, is smooth surface near bottom edge of photograph. Large block on crater floor, surrounded by new flows, is 20 m wide. Smaller western crater, which did not erupt after episode 5, is partly visible at upper right. View southwestward; photograph taken at 1429 H.s.t. August 11, 1983. Numerals (lower right) indicate date and time. *B*, Large slickensided block on floor of Puu Oo Crater. Person is standing on pahoehoe erupted within Puu Oo between episodes 6 and 7. View southwestward from Puu Oo spillway; photograph taken at 0917 H.s.t. August 14, 1983. Numerals (lower right) indicate date and time.

Fountain height varied little during episode 7 (see fig. 1.24); it ranged from about 40 to 80 m over the first day and, thereafter, diminished slowly but steadily to about 30 m near the episode's end. As in episode 6, fountaining commonly was broadly distributed over the lava pond in the style illustrated in figure 1.26. The fountaining was characterized by irregular jets, many distinctly inclined from vertical.

Lava output and fountaining stopped abruptly at approximately 1600 H.s.t. August 17. The episode had produced 14×10^6 m^3 of basalt, which covered an area of 3.7×10^6 m^2. A duration of 57 hours indicates an average lava-discharge rate of about 250,000 m^3/h, then the highest average rate determined for any episode.

At the end of episode 7, Puu Oo was a steep-walled cone, almost circular in plan view, containing a bowl-shaped crater, approximately 90 m in diameter at the top (fig. 1.77). The interior walls, partly of rubble, extended downward into a deep, steep-walled hole with little, if any, crater floor. An incandescent crack persisted low in the west wall. A low spillway area again transected the northeast rim of the crater; it led, by way of a steeply inclined notch, down the outside of the cone to an evacuated pahoehoe channel, 8 to 15 m wide. At the base of the cone, where this channel began, a 10- to 15-m-long segment was roofed to form a short tube. The channel retained sharp definition for 600 m downstream, where it evolved into an aa channel that extended nearly to the ends of the

FIGURE 1.76.—Furrowing of north rim of Puu Oo by falling spatter during episode 7. Fountain height is approximately 70 m (fig. 1.24). View southeastward from near camp C; photograph taken at 0541 H.s.t. August 16, 1983. Numerals (lower right) indicate date and time.

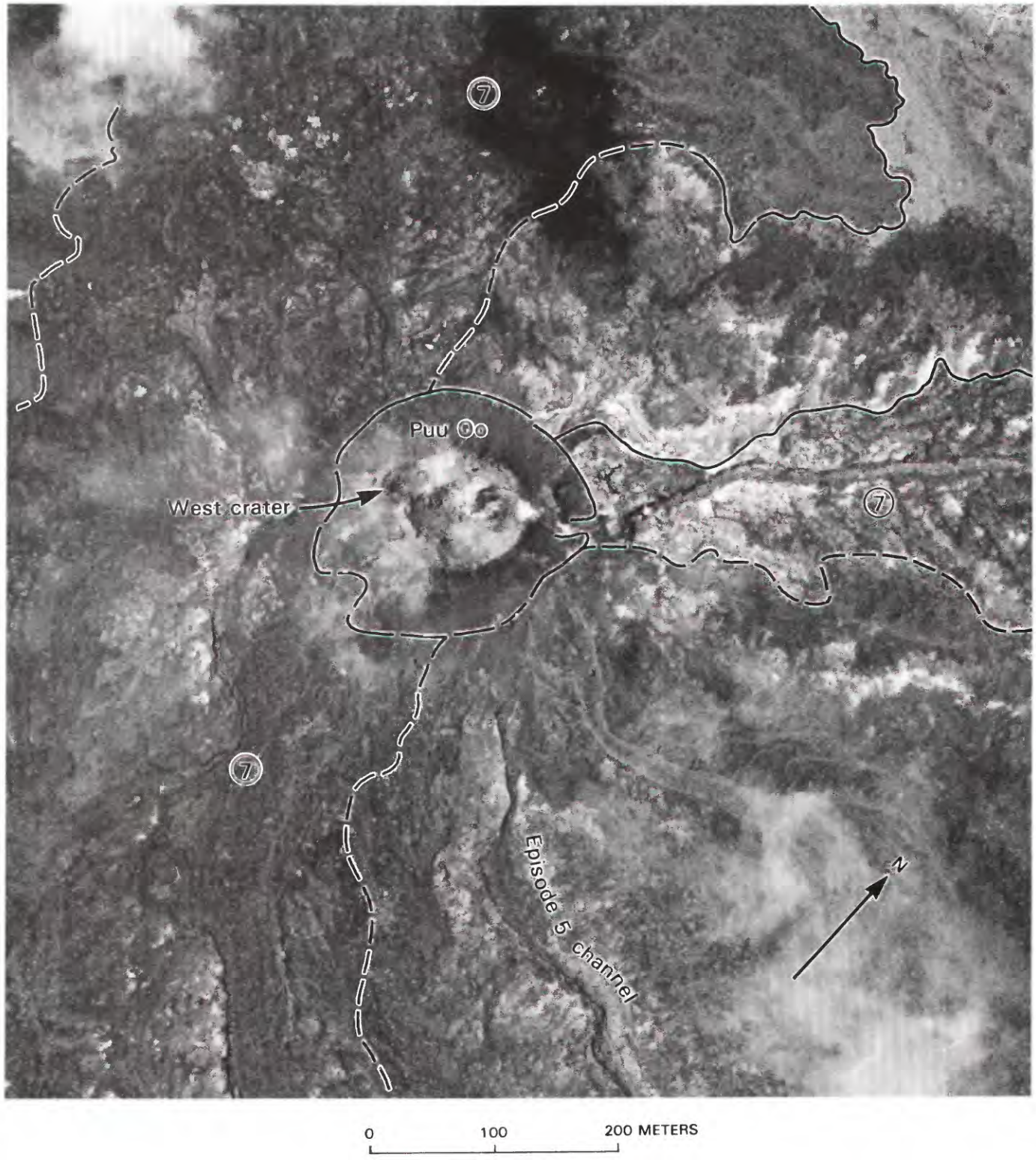

FIGURE 1.77.—Puu Oo and nearby episode 7 lava flows (7). Photograph 83.9.2JG120A#1 by J.D. Griggs, taken September 2, 1983.

flows. Pahoehoe overflow levees and islands persisted downflow to beyond Puu Kahaualea, 2.7 km from the vent. For the first 2 km, the flow ranged in width from about 100 to 500 m; farther northeast, the maximum width was about 700 m, but individual flow lobes were narrower, generally 150 to 300 m wide. The longest of the four lobes ultimately extended 6.7 km from Puu Oo.

The western crater at Puu Oo, last an active vent during episode 5, was partly obliterated during episode 7; however, it was still recognizable on the uprift shoulder of Puu Oo. The southeastern aa flow, with a broad, poorly defined central channel, extended southward and then southeastward 3.3 km from the vicinity of the western crater.

EPISODE 8 (SEPTEMBER 6–7, 1983)

We became aware of renewed low-level eruptive activity within Puu Oo Crater on September 2. Spatter and small flows from two vents had filled in the deep central depression, forming a crater floor about 12 m below the level of the spillway. One vent had produced a 4-m-high and 6- to 7-m-wide cone of spatter (fig. 1.78) near the center of the smooth and nearly flat new crater floor. A 4-m-diameter opening in the top of the cone was incandescent near the surface and occasionally emitted small spatter fragments to heights of a few meters. Near the west edge of the crater floor, at the site of the incandescent crack, a second vent had produced several short (less than 25 m long) pahoehoe flows and a small amount of spatter. In the process, it had built a rounded lava mound with a transient central hole that was an excellent site for sampling both magmatic gas and melt. This mound was incandescent just below a superficial accumulation of agglutinated spatter and small flows. Episodic, vigorous degassing and minor spatter ejection may have reflected the occurrence of gas-piston activity beneath the vent. The vigorously exiting hot gases bulged the cap of agglutinated spatter upward, and small flows were sometimes extruded. In addition, local gas jets occasionally mobilized melt from within the spatter mound to produce small, steep-sided driblet cones.

By September 4, continued intermittent low-level eruption had filled in parts of the crater floor with approximately 300 m^3 of small pahoehoe flows. The vent at the west end of the crater floor had grown 3 to 4 m through the accumulation of short flows and spatter. The more central spatter cone continued to emit fragments of spatter (max 30 cm diam) to heights of several meters at a rate of a few fragments per minute.

On September 5, we discovered an active lava pond, approximately 5 m deep, extending across the entire crater floor. The pond was almost completely covered with a thin crust; in places, small pahoehoe lobes with still-incandescent cracks had flowed over the crust. A high-lava mark on the crater walls and spillway indicated that sometime before 0850 H.s.t. September 5, the pond had reached a depth of about 12 m. No lava, however, had reached above the level of the spillway and exited the crater. A 15-m-long, 1- to 3-m-wide lava stream, estimated to be carrying about 1,000 to 3,000 m^3/h, issued from the nearly flooded western vent and traveled across the crusted surface of the lava pond. It disappeared down a hole near the center of the pond at the approximate site of the central intracrater vent of September 2–4. Occasionally, the adjacent crusted-pond surface would be broken open or overrun by pahoehoe oozes fed by this lava stream. No net change in the volume of the lava pond or in the vigor of the lava stream was seen during 6 hours of continuous observation. Spattering at the western vent, where the stream originated, was minimal, implying that the lava was relatively degassed. Apparently, deeply stored, gas-rich melt was not participating in this lava circulation, which was apparently confined to the upper part of the conduit and storage system beneath Puu Oo.

At 0511 H.s.t. September 6, the time-lapse camera at camp D recorded the onset of vigorous eruptive activity as fountaining became visible above the rim of Puu Oo. By 0730 H.s.t., when observers reached the eruption site, a vigorous fountain was rising approximately 100 m from within Puu Oo. It was broadly based, fluctuated little in height, and filled the entire crater. Time-lapse data show a slow but continual increase in fountain height throughout the 24-hour eruption (see fig. 1.24).

FIGURE 1.78.—Interior of Puu Oo during low-level activity preceding episode 8. Spatter cone at right is approximately 4 m high. Lava mound at left (circled person for scale) marks a vent that is actively degassing, intermittently producing spatter and small pahoehoe flows, and building little driblet cones. Spillway (out of view to right) is approximately 12 m above level of crater floor. View northward; photograph taken at 1920 H.s.t. September 2, 1983.

The northeastern spillway was once again the locus of overflow from the pond inside Puu Oo. The cascade from the spillway supplied a well-channelized river that carried the lava northeastward on top of earlier 1983 flows. When we arrived at 0730 H.s.t. September 6, the flow, entirely of pahoehoe, had reached 1,200 m from the vent, a distance indicating an average advance of more than 500 m/h. This value is a minimum; instead of continuing to advance, the lava had ponded, forming a broad, inflating, roofed pahoehoe pond or reservoir about 1 km northeast of Puu Oo. Minor flows broke out to the north from the ponded lava, and by early afternoon on September 6, a more vigorous pahoehoe front had developed from the northeast end of the roofed pahoehoe pond. It traveled north-northeastward into thick rain forest and, for the rest of episode 8, followed the north edge of episode 6 and 7 flows (pl. 3). By about 1600 H.s.t. September 6, the ponded part of the flow was collapsing, apparently being drained as the fluid flow front advanced rapidly northwestward of Puu Kahaualea. The presence of standing trees surrounded by lava as much as 500 m upstream of the front attested to the fluidity of the flow. The front was estimated from helicopter overflights to be about 1 m thick and 80 m wide, traveling at rates of 100 to 160 m/h.

An additional flow traveled southeastward from Puu Oo during episode 8. It was primarily spatter fed and, by 1615 H.s.t. September 6, had traveled only 250 m from Puu Oo.

A moderate tephra fallout carried by tradewinds smoothed the southwest flank of the Puu Oo cone. The upper flank, however, was disturbed between midnight and 0200 H.s.t. September 7, when a section of the southwest rim and flank began to creep downslope, producing a wedge-shaped rootless flow. Though moving primarily as a gravity slide, the flow was partly fed by occasional falls of heavy fluid spatter. The event left a 30-m-deep scar in the southwest rim and a pronounced bulge in the profile of the southwest flank of the cone (see fig. 1.10*B*).

After nearly 24 hours of vigorous lava production, fountains began to diminish in height and density at approximately 0518 H.s.t. September 7. For the next 7 minutes, a few erratic fountains, reaching 20 to 30 m above the cone, alternated with sporadic, dispersed sprays of ejecta; by approximately 0526 H.s.t., all fountaining had ceased.

According to the final aerial reconnaissance, the northeastern lava flow extended approximately 4.4 km from the vent. At the episode's end, the flow was largely aa. Owing to poor weather, a comprehensive set of aerial photographs was not obtained until after episode 10, and by then much of the episode 8 flow was buried. Thus, the areal extent and volume of episode 8 lavas are only approximate. Aa thicknesses measured in the episode 8 flow to the northeast ranged from 3.5 to 5.5 m (pl. 3). The proximal part of the flow contained a well-developed evacuated channel, 10 to 20 m wide and 2 to 4 m deep, bounded primarily by aa levees; pahoehoe overflow levees occurred locally. The southeastern rootless flow had apparently received an increased volume of spatter during the night of September 6–7. By the episode's end, the flow had extended approximately 1.7 km southeast of Puu Oo and was primarily aa, 2.7 to 4.0 m thick. An additional small, spatter-fed flow extended 300 m westward of the cone.

We estimate that the volume of episode 8 lava was approximately 8×10^6 m^3, which covered an area of 2.0×10^6 m^2. This was the smallest volume yet erupted in a single episode during the entire 1983 series. Episode 8 was also the shortest single eruptive episode yet observed, lasting just more than 24 hours. A calculated average lava-discharge rate of about 330,000 m^3/h was the highest determined since eruptive activity localized at Puu Oo in June 1983.

After episode 8, the vent complex consisted again of a steep-walled cone enclosing a nearly circular crater, approximately 90 m in diameter at its rim crest (fig. 1.79). The base of this cone was draped with talus and fractured spatter-fed flows. Although continued slumping rejuvenated the scar in the southwest rim, the primary breach was still in the northeast wall. This breach consisted of a vertical cleft or notch, approximately 10 m wide and 5 m above the level of the crater floor. It led downslope outside the crater into an evacuated channel

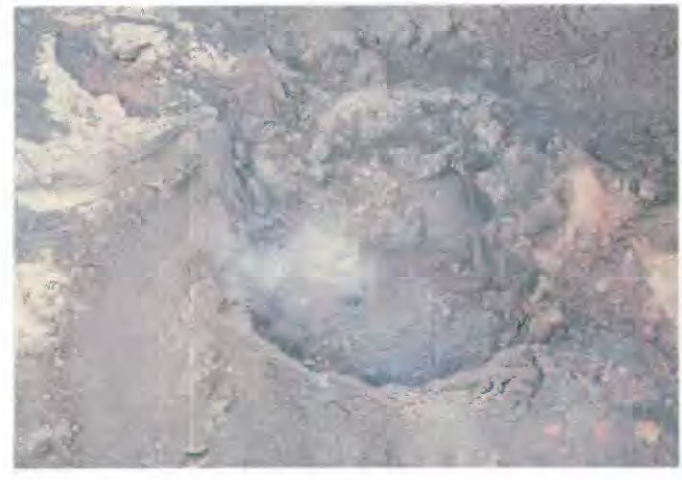

FIGURE 1.79.—Puu Oo after episode 8. Crater diameter is approximately 90 m at rim crest. Spillway is visible in upper left. Two open conduits, about 3 m in diameter, extend steeply downward from crater floor. Steep outer walls of Puu Oo are surrounded in part by talus (lower left) and fractured, spatter-fed flows (top). Fresh scars at right record continued slumping of southwest rim and flank. View eastward; photograph taken at 1416 H.s.t. September 9, 1983. Numerals (lower right) indicate date and time.

that followed the axis of the northeastern episode 8 flow. The interior crater walls, except for the southwest sector, which was slumped inside as well as outside, were smooth, spatter mantled, and relatively uniform in height. Two nearly circular conduits, about 3 m in diameter, extended steeply downward from the rough, blocky crater floor.

EPISODE 9 (SEPTEMBER 15-17, 1983)

Only one week separated episode 8 and the onset of low-level eruptive activity within Puu Oo Crater before episode 9. Shortly after midnight on September 14, a time-lapse camera on the northeast rim of Puu Oo recorded a brief occurrence of low-level spatter emission from the more easterly of the two open conduits on the crater floor (fig. 1.79). At about 1713 H.s.t. September 14, sporadic but slowly accelerating spatter production began again and continued into the morning of September 15. Fragments of lava were thrown to maximum heights of about 10 m above the crater floor. At no time during this period was any activity from the more western conduit recorded on film.

At 1026 H.s.t. September 15, lava began to well up and out of the central conduit, forming a pond in Puu Oo Crater. By 1132 H.s.t., the pond stood 5 m deep, high enough to send a small pahoehoe flow (total volume, approx 300 m^3) cascading over the spillway. It traveled 20 to 30 m before the pond began to drain back into the conduit and the flow was beheaded. By 1312 H.s.t., lava was no longer visible in the crater; only occasional spatter and glow in the conduit opening are recorded on film. A second pond began to fill the crater at about 1450 H.s.t.; this time, observers were present on the rim. The low vigor of fountain activity suggests that the lava filling the crater was degassed; a small amount of spatter was being ejected from a 3-m-diameter dome fountain that played on the surface of the thin-crusted lava pond. A drainback began at approximately 1512 H.s.t., and lava poured back down the central conduit in 6 minutes. By 1527 H.s.t., lava reappeared, and the pond again began to rise. At 1541 H.s.t., for the second time, the level of the pond rose high enough to send a small pahoehoe flow over the northeastern spillway and into the evacuated episode 8 channel (see fig. 1.31). On the basis of estimated channel width, depth, and average surface velocity of 4 m, 1 m, and 1 m/s, respectively, a flux of 10,000 to 20,000 m^3/h was estimated for this small flow. The lava pond maintained a fairly constant depth of 5 m, while a 3- to 8-m-high dome fountain played continuously above the site of the central conduit. By 1610 H.s.t., the slow-moving flow had traveled 150 to 175 m down the channel and was easily sampled. The dome fountain remained active and doubled in average height by 1624 H.s.t. Activity steadily increased in vigor, and by 1711 H.s.t., after observers left, a camera located 750 m west of Puu Oo at camp D recorded spatter rising above the crater rim.

During the night of September 15-16, time-lapse film recorded a fountain emanating from Puu Oo Crater and reaching heights of as much as 200 m (see fig. 1.24). In the early morning, the roar of the fountain was audible 20 km away at HVO, and a large brown fume cloud, visible from HVO during most eruptive episodes, drifted southwestward with the trade wind. Throughout the morning, the fountain was visible from along Hawaii Highway 11 between Hilo and Kilauea's summit.

Although the fountain height varied appreciably throughout episode 9, it tended gradually to decay from general levels of 150 to 200 m in the early part of the episode to about 100 m in the later part. The fountain was broad and commonly erratic in trajectory. At times, two or more separate jets were clearly visible that emerged from the crater in a V-shaped pattern, as if originating from the same point but diverted by some obstacle. Because of the vigorous, low-trajectory fountain jets, spatter bombarded almost the entire outside surface of the cone, armoring the flanks with thin sheets of fluid spatter-fed flows (see fig. 1.7). Heavy spatter fall to the west produced short-lived rootless flows that moved over tephra from earlier episodes as well as from episode 9. Lightweight tephra fell in abundance on the southwest flank of Puu Oo—possibly the heaviest observed since the episode 3 tephra fall at the 1123 vent. It smoothed the bulge left after episode 8 but added preferentially to that sector of the cone (see fig. 1.10*B*).

The major lava flow of episode 9 exited the spillway and continued northeastward on top of week-old episode 8 basalt. About 1.5 km from the vent, the flow veered slightly northward and followed the northwest edge of the episode 8 lava into the rain forest (pl. 3). Although a vigorous, channelized pahoehoe river traced the axis of the flow to the northeast, early lava exiting the vent must have traveled as a broad, thin sheet of pahoehoe; attempts to reach the channel edge on the morning of September 15 were thwarted by a wide area of still-hot pahoehoe, extending several hundred meters northward from the river.

By 1200 H.s.t. September 16, the flow had developed two lobes that were traveling northeastward, parallel to each other. The more southerly lobe advanced only 200 to 300 m before stagnating; for the rest of the episode, only the more northern of these two lobes was active. Between 1200 H.s.t. September 26 and 0930 H.s.t. September 17, this lobe traveled at average rates ranging from about 40 to 160 m/h along the northwest edge of the episode 8 lava flow (pl. 3). The episode 9 flow was predominantly aa, except for the proximal pahoehoe river.

The eruption stopped at 1920 H.s.t. September 17. The conspicuous flow to the northeast, primarily aa, extended

a total of 5.3 km from Puu Oo (pl. 3). Poor weather again prevented systematic coverage of the eruption area with aerial photography after episode 9. Thus, a volume of 8×10^6 m^3 over an area of 2.1×10^6 m^2 is based on a combination of aerial-reconnaissance sketch maps made during the eruption and mapping from post-episode 10 photographs, which showed exposed parts of the episode 9 basalt. The estimated average lava-discharge rate based on these numbers is 150,000 m^3/h.

For several days after the eruption, numerous reports of black clouds or dense black fume emanating from Puu Oo were received at HVO. However, no unusual activity at the vent was ever confirmed.

Inspection of the vent on September 23 revealed two open conduits, strikingly similar in position and appearance to those observed before episode 9, extending downward from the rubble-strewn floor of Puu Oo Crater. The more conspicuous of these two conduits was a cylindrical vertical pipe, 4 m in diameter except for the upper few meters, where it flared outward to a diameter of 6 to 7 m. We could see only 15 to 20 m down the conduit (see fig. 1.14). The upper few meters was partly smoothed and plastered with a thin covering of lava that may have formed during the later stages of drainback at the end of episode 9. Elsewhere in the pipe, the walls exhibited thin, horizontally layered, partly oxidized, platy to rubbly basalt. Although we heard intermittent low-pitched, rumbling exhalations, and heavy fume issued from the conduit, no glow was observed from helicopter or the ground.

About 10 m west of this open conduit, a second open hole, elongate in an east-west direction, extended downward from the crater floor. This hole was about 1 by 2–3 m at the surface and was brightly incandescent at a depth of about 5 m. Heavy fume also issued from this western conduit.

The crater itself was nearly bowl shaped and circular in plan view; its diameter ranged from 30 m at the level of the floor to 100 m at the rim crest, and the spillway stood about 4 m above the general level of the floor. The interior walls of the cone were a combination of steep, primarily smooth, spatter-mantled surfaces to the north and south, and a gentler, slumped, blocky slope on the west. The spillway persisted as a narrow V-shaped notch in the northeast wall, and the rim of the cone descended gradually toward the spillway from either side; thus, the northeast sector of the cone was significantly lower than other sections. An additional low area persisted in the southwest rim, where previous late-stage collapse had been localized.

The outer flanks of Puu Oo were mostly steep. Locally, they were a chaotic jumble of slumped blocks below exposed headwalls of agglutinate. Elsewhere, they were smoothed by coherent spatter-fed flows or by tephra deposits that were situated preferentially to the west and southwest.

EPISODE 10 (OCTOBER 5–7, 1983)

Copious amounts of steam and fume were seen at Puu Oo after episode 9, but no eruptive activity was recognized until October 2, when a small new lava flow, estimated at 300 to 500 m^3 in volume, was observed on the floor of the crater, surrounding a brightly incandescent central conduit (open pipe, fig. 1.14). This flow had apparently issued from the vent between 0750 and 0800 H.s.t., when an electric tripwire in the crater was cut. When we arrived at 1000 H.s.t., the flow surface was slowly collapsing as lava drained back from beneath it into the open conduit.

After that initial small flow was extruded, the vent was relatively quiet through October 4. Observers saw intermittent low-level spattering in the open conduit, varying fume production, and a few occurrences of glow over the cone at night. Sometimes the top of the magma column was visible a few meters below the top of the conduit.

Harmonic-tremor amplitude and intensity of glow over Puu Oo increased together just after midnight on October 5. At about 0106 H.s.t., several minutes after low-level fountaining had commenced inside the crater, lava began to spill through the deep breach in the northeast rim. By 0200 H.s.t., sporadic fountaining had increased in vigor sufficiently to be occasionally visible over the crater rim from camp D; by 0400 H.s.t., a roar from the eruptive area was audible at HVO, accompanied by a strong glow in the predawn sky.

When we arrived at 0730 H.s.t. October 5, we saw the most spectacular fountain thus far at Puu Oo—a single, vertical jet, more than 200 m high (see frontispiece). The fountain was broad, and its base filled nearly the entire bowl-shaped depression within the cinder and spatter cone. Fountaining was high enough that spatter and tephra bombarded almost all sides of the cone, but it was concentrated in the north, northeast, and southeast sectors. The only lava flow of significant volume was a multilobed, tacky pahoehoe flow that had traveled 300 to 400 m southeastward from the northeast base of Puu Oo. An additional sluggish aa lobe advanced northeast along the path of the episode 9 pahoehoe channel; slow-moving spatter-fed flows covered a large part of the north flank of Puu Oo. We were struck by the low apparent flow output and limited flow progress in comparison with previous episodes. The spillway contained a vigorous lava river with an intermittent standing wave near the base of Puu Oo. The spillway lava and nearby spatter-fed lava coalesced near the base of the cone and fed the flows to the southeast (eastern flow, pl. 3) and northeast.

Unobserved from the air at 0730 H.s.t. but unmistakable on the ground was still-hot pahoehoe, extending at

least 1 km to the north and northeast of Puu Oo. No longer active, these flows were being overrun by the more sluggish flow advancing northeastward. Time-lapse-camera data show that an early pahoehoe flow to the north and northeast had occurred.

At about 0900 H.s.t., the fountain began decreasing in height, declining by 1100 H.s.t. from more than 200 m to a low of about 40 m. During this interval, the appearance of the northeastern flow also changed. By 1000 H.s.t, a broad, complex pahoehoe flow with an incipient central channel and many anastamosing distributaries was traveling northward and northeastward on top of the earlier aa.

Fountain activity began to fluctuate markedly and became more complex after its pronounced diminution between 0900 and 1100 H.s.t. October 5. Although the fountain subsequently was as high as 200 m for some periods, large variations in height and trajectory were superimposed on an overall trend of steadily decaying height (see fig. 1.24), and the development of several distinct fountains within Puu Oo Crater made episode 10 fountain activity some of the more complex observed at Puu Oo up to that time.

Shortly before 1100 H.s.t. October 5, a second fountain developed just west of the main jet, then about 60 m high. Initially, it was a smaller dome fountain (see fig. 1.28) that repeatedly disintegrated in low bursts of spatter. For much of the day, however, until just after 0000 H.s.t. October 6, the two fountains fluctuated greatly in height, trajectory, and degree of separation. At times, a single, tall fountain rose vertically for hours, followed abruptly by a rapid decay and appearance of two energetic jets emanating from what appeared to be the central conduit and diverging in a V-shaped trajectory. Commonly, though not in every case, a decrease in the height of the combined fountain was accompanied by a sudden increase in apparent lava output over the spillway.

The complexity of fountaining continued to increase. Early on October 6, a third small and possibly independent fountain emerged adjacent to the northwest interior wall of the crater. This fountain grew rapidly in height to overtake the main fountain. After about 10 minutes, the new fountain lost its identity as the entire crater became filled with low, chaotic fountains, rarely reaching 40 to 70 m above the rim. In harmony with the transition to low, chaotic fountains, the time-lapse film record clearly shows an increase in the flux of lava pouring over the spillway and feeding the northeastern flow.

After about an hour, fountaining returned, between 0200 and 0300 H.s.t. October 6, to the simpler system of a single and, at times, double jet that reached a maximum height of 200 m. An apparent decrease in the flow of lava through the spillway accompanied the return to high fountaining.

Varyingly high fountaining persisted until nearly midday October 6, after which the fountain height decreased and the small, separate fountain returned at the base of the northwest interior wall. This time it was unquestionably distinct from the other fountains in the crater: It clearly represented a separate new vent. Shortly thereafter, another new vent, with its own fountain, opened high on the west interior wall of the crater. These secondary fountains remained small, generally rising to less than 10 to 20 m above the cone, and built subdued local spatter ramparts on the preexisting Puu Oo cone rim. Generally low fountains, partly on the rim and also in a chaotic array within the crater, persisted with little variation until the eruption's end on October 7. During this period of low, multiple fountains, output over the spillway, as recorded on time-lapse film, was again higher than during earlier periods of higher fountaining.

The lava-channel system for the northeastern flow was slow in becoming well established, and for the first 2 days the flow was mainly sluggish aa that advanced, largely on top of the episode 9 flow, at an average rate of about 50 m/h. The flow was relatively thick and broad, and much lava spread out near Puu Oo (pl. 3). During that time, much of the erupting lava was supplied as fluid spatter, which, along with intermittent overflows from the northeastern lava river, fed the predominantly spatter fed eastern flow. It, too, advanced slowly, at about 50 m/h.

Lower fountain heights in the later part of episode 10 led to a diminished supply of fluid spatter feeding the southeastern flow; the supply of lava to the river feeding the northeastern flow increased concomitantly, and the southeastern flow slowed. The increased supply invigorated the lava-channel system, and when we reconnoitered the northeastern flow front at 0730 H.s.t. October 7, the fluid pahoehoe channel had extended to the toe, almost 3 km from the vent. Thus, the flow then extended more rapidly, at more than 100 m/h, as a narrow lobe pushing through the rain forest at the northwest edge of the episode 9 flow. Increased supply to the northeastern lava river also resulted in the formation of a series of standing waves that were conspicuous within 200 m of the vent on October 7. Formed in the 10- to 15-m-wide river, the waves were several meters in amplitude and separated by 15 to 20 m.

Low fountaining within Puu Oo continued until at least 1633 H.s.t. October 7, according to a time-lapse-camera record. However, poor weather obscured the view, and we have neither a good film record nor a direct observation of the episode's end. Harmonic tremor in the eruptive zone decreased in amplitude rapidly at about 1650 H.s.t., nearly 64 hours after the start of the eruption; we infer that the eruption ended then.

Lava from Puu Oo covered an area of 2.7×10^6 m^2 with approximately 14×10^6 m^3 of basalt during episode 10;

the average lava-discharge rate was about 220,000 m^3/h. The northeastern flow extended a total of 4.1 km. Like most long flows from Puu Oo, it consisted predominantly of aa; its average thickness was about 4 m. A central channel was discernible from the vent to 2.5 km downflow, and pahoehoe overflows from the channel occurred along much of this distance. Beyond the point where the central channel was recognizable, the flow was entirely aa, and no discernible channel structure was preserved. The southeastern flow, which had been most active during the first 2 days of episode 10, consisted of two lobes, the longest of which extended a total of 3.4 km from the vent. Both lobes were entirely aa, averaging about 6 m thick. In the zone between the two major flows of episode 10, a broad lava delta extended 900 m eastward and northeastward of Puu Oo. The delta was composed of a complex stack of aa and pahoehoe flows emplaced primarily during the first 2 days of the eruption before a channel was well established in the northeastern flow. For the last day of episode 10, this delta was intermittently enlarged by transient spatter-fed flows and a few overflows from the northeastern pahoehoe channel.

After episode 10, the Puu Oo edifice was an imposing, broad cinder and spatter cone, 150 to 200 m wide by 300 m long, elongate southward and rising about 80 m above the preeruption surface. The circular crater and slopes that defined Puu Oo were characterized by extremely rough and chaotic terrain (fig. 1.80). Large, wedge-shaped stacks of fractured spatter-fed flows, more than 10 m thick, extended northward and northwestward from the cone. A complex of spatter-fed flows interbedded with and mantled by a thick tephra deposit that had been accumulating since episode 8 caused the southward elongation. The spillway was a broad, rubble-covered low spot still on the northeast rim of the cone. A chute led down the northeast flank of Puu Oo and bifurcated around a large block of cone material that may have been partially rafted; the two distributaries then coalesced into a single aa-floored channel that wound its way toward the northeast.

The complex interior of Puu Oo Crater was choked with rubble consisting of both boulder-size material and whole slivers of the cone's walls and rim that had collapsed into the depression after the eruption (see fig. 1.15). Grooved and slickensided surfaces on the inner crater walls indicated that the floor of the crater had undergone 5 to 10 m of subsidence at the end of episode 10. One especially large, coherent section of the west and southwest wall had slumped toward the interior of the crater. Its toe formed a steep wall running approximately northwest-southeast through the crater. At the northwest end of the wall, where it intersected the floor of the crater, a low area of intense heat and fume, near the position of one of the secondary fountains during episode 10, persisted throughout the subsequent repose period. A second area of localized fuming and heat emission, near another of the secondary fountains observed during the later part of episode 10, was high on the west-southwest rim of the cone in the zone of detachment of the large collapsed section. Fuming and incandescence in open cracks persisted there throughout the subsequent repose period. The crater rim above both sites of secondary fountaining had been modified by falling spatter to form subtle, local spatter ramparts.

Uprift of the crater, running down the tephra-covered west flank of Puu Oo along the strike of the January 1983 eruptive fissure, isolated areas of persistent fuming were visible for most of the repose period following episode 10. This phenomenon occurred after many eruptive episodes, and sometimes incandescent cracks persisted high on the cone.

EPISODE 11 (NOVEMBER 5-7, 1983)

The repose interval between episodes 10 and 11 lasted 30 days, the longest repose since eruptive activity became localized at Puu Oo in June 1983. During this period, fume was emitted at low levels from the vent complex. Although minor glow was reported over the south side of the cone on the nights of October 30 and November 1, no eruptive activity was observed during the repose period. Unlike the previous six episodes, when vigorous eruption was preceeded by hours to days of low-level eruptive activity within the crater, episode 11 discharge began suddenly.

The electric tripwire in Puu Oo Crater was cut between 2350 and 2400 H.s.t. November 5, coincident with the onset of lava emission in the crater. Eruption of lava first signaling the onset of episode 11, however, was not from vents within the Puu Oo cone. The camp D time-lapse camera recorded the initial outbreak west of the main Puu Oo edifice at approximately 2350 H.s.t. It occurred along a 30- to 40-m-long segment in the vicinity of the January 23, 1983, vent (pl. 1), about 200 m northeast of Puu Kamoamoa and about 200 m uprift of the west base of Puu Oo. Activity along this zone was weak, consisting of discontinuous low fountains, less than 5 m high, and low to moderate levels of lava emission. Fountaining then began high on the west flank of Puu Oo at about 2356 H.s.t.; nearly simultaneously, fountaining broke out within Puu Oo Crater. A general downrift migration of activating vents continued as at least three distinct vents opened east of Puu Oo. This activity culminated at approximately 0107 H.s.t. November 6 as a final small fissure vent opened about 150 m northeast of Puu Oo. Most of the extracrater vents paralleled or coincided with the 1983 eruptive fissure. Fountaining associated with eruptive activity at all vents outside of Puu Oo remained relatively

FIGURE 1.80.—Puu Oo and nearby episode 10 flows (10) after episode 10. Solid line, flow boundary; dashed where approximate. Crater is approximately 90 to 100 m in diameter. Conspicuous evacuated channel heading northeast from Puu Oo (arrows) fed northeastern flow of episode 10. Eastern flow was mostly spatter fed. South quadrant of Puu Oo is smoothed owing to tephra accumulation since episode 8. Thick pile of spatter-fed flows is visible on northwest flank. Photograph 83.10.11JG120A#8 by J.D. Griggs, taken October 11, 1983.

weak throughout the night. Inside Puu Oo Crater, the fountain height quickly reached and was sustained at a maximum of about 50 m (see fig. 1.24).

By 0010 H.s.t. November 6, glow over the eruption site was visible from HVO. Broad fountaining was reported from Mountain View (18 km north of Puu Oo) at 0200 H.s.t., and fountains remained visible from Kalapana (14 km southeast of Puu Oo) and Mountain View through dawn.

At 0730 H.s.t. November 6, when we arrived at the site, active vents extended discontinuously from about 200 m uprift of Puu Oo, over the crest and through the crater, and to about 300 m downrift of the cone (fig. 1.81). These vents produced flows that traveled in several directions from the cone (pl. 3). The major flow, supplied by way of the spillway, was traveling northeastward along the path of the episode 10 northeastern flow. It had advanced rapidly since the beginning of episode 11, and at 0730 H.s.t. November 6 it was composed of pahoehoe nearly to its terminus, which was 3.7 km from the vent. For the rest of the day, the flow gradually slowed, widened, and locally entered the rain forest north of the episode 10 flow. Lava discharge into the northeastern pahoehoe river represented about 80 to 90 percent of the total output; the remaining 10 to 20 percent was accounted for by lava discharge from the subordinate vents uprift and downrift of Puu Oo Crater.

The small vents east of Puu Oo had low fountains (max 5–10 m high). Lava welled out of these small vents and, along with overflow from the main lava river, fed a slow-moving pahoehoe flow that traveled eastward. Uprift of Puu Oo, at least six extracrater vents erupted more vigorously than those downrift. Activity at the smaller of these vents was characterized by repeated bursts that sent fragments to heights of less than 10 m, forming small, coalescing, conical spatter cones. Low-level emission of lava generally occurred from small openings in the bases of these growing spatter structures. The westernmost vent (farthest right, fig. 1.81) contained a low (3–5 m high) dome fountain that occasionally disintegrated, constructing a spatter shell around itself that was open to the north. Lava issuing from these small western vents and, in part, from a more active one high on the west flank of Puu Oo fed overlapping short sheetflows of pahoehoe to the north and west.

High on the west flank of Puu Oo, the most energetic extracrater vent originated from near the site of the fuming and intermittently incandescent area observed there after episode 10. It produced moderately vigorous fountains, possibly as much as 20 m high, and fed a cascade that was the primary source for the southern flow (pl. 3), pahoehoe fed by way of a central channel. In addition, occasional northward flows from this vent produced transient, overlapping sheets and tongues of pahoehoe (fig. 1.81). Fountaining from the vent was rapidly constructing its own enclosing spatter rim that eventually grew into a separate crater on the Puu Oo cone.

The bulk of the fountain activity and lava production, however, was confined to the main Puu Oo Crater. There, multiple fountains, possibly as many as four or more, played from separate vents on the crater floor and interior walls. One prominent fountain at the base of the north interior wall intermittently fed a rootless flow down the north flank of Puu Oo. In addition, for the entire episode,

FIGURE 1.81.—Discontinuous, 700-m-long line of erupting vents with low fountains during episode 11. Line transects Puu Oo (center) and extends both uprift (right) and downrift (left). Small red spots at far left represent most northeasterly vents. Photographs taken at 0730 H.s.t. November 6, 1983.

several small fountains erupted through the channelized lava river on the northeast flank of the cone below the spillway. Throughout episode 11, fountaining from within Puu Oo remained low (see fig. 1.24), and lava output remained steady and high. Owing to the dense jumble of fountains, it was difficult to distinguish a coherent lava pond inside Puu Oo. The steady volume of lava spilling down the northeast side of the cone, however, suggested that a significant surface reservoir of lava was contained within the crater.

The vigorous pahoehoe river that traveled northeastward from Puu Oo contained a remarkable set of standing waves over a zone about 150 to 200 m long (fig. 1.82). The waves first appeared in a stretch of the river about 100 m from the base of Puu Oo. At least five major waveforms were visible along this stretch, separated by 20 to 40 m; amplitudes of the waves ranged from approximately 1 to 3 m. In the middle of the zone of standing waves, the gradient of the surface of the flowing lava and the enclosing levees changed sharply. The smaller waves were nearer the vent, where the gradient was estimated at 10°. Larger waves occurred at and below the point where this gradient became gentler, possibly 2°. About 90 m downstream of this inflection, the lava river widened and slowed considerably, and waveforms disappeared. In the zone of standing waves, maximum surface velocities of 8 to 10 m/s and a relatively constant average width of 15 m were estimated. Using an assumed depth of 2 to 4 m and an approximate average surface velocity of 4 to 5 m/s, we calculate a flux of about 500,000 to 1,000,000 m^3/h. These values are 2 to 4 times that of the average lava flux calculated from the mapped volume (table 1.3), and they presumably represent inflation of the lava by air and vent gases. Posteruption measurements of channel geometry indicated that the real-time estimates of width and depth were minimums.

Although the vigor of fountaining within Puu Oo Crater remained steady, the level of activity at the eastern extracrater vents diminished during the night of November 6–7. By dawn on November 7, only low fountains eman-

FIGURE 1.82.—Episode 11 lava river, flowing from right to left, showing part of series of 1- to 3-m-high standing waves described in text. Downstream of waves, lava river widened and slowed significantly as it swung northeastward. Geologist is standing on episode 10 basalt; new overflow levees are visible adjacent to active river. View northeastward; photograph by M.L. Summers, taken November 6, 1983.

ating from vents near the northeast base of the cone continued to be active and to contribute, along with the vents inside Puu Oo, to the northeastern lava river. During the night of November 6–7, the western extracrater vents also shut down gradually. The dome fountain at the westernmost vent (fig. 1.81) remained active until about 0200 H.s.t. November 7. The moderately vigorous vent high on the west flank of Puu Oo shut down at about 0400 H.s.t. November 7 but continued to emit small bursts of spatter intermittently until daylight. Thus, supply to the southern flow was terminated. For most of November 7, fountaining was confined to those vents active within Puu Oo and at its northeastern base; the only active flow was the elongate aa flow that advanced to the northeast.

At approximately 1915 H.s.t. November 6, a crack opened in the area west-northwest of Puu Oo (pl. 3) with a report audible to nearby observers over the roar of the fountaining. Although the observers, who were about 30 m from the crack, felt no movement, the borehole tiltmeter (KMM, fig. 1.1), located about 200 m north of the new crack, was jarred off scale. This new crack steamed profusely at first. Oriented N. 60 °E., it was at least 360 m long and recorded a maximum of 0.5 m of extension perpendicular to its strike. The amount of extension and the surface expression of cracking diminished westward and disappeared altogether within episode 1 lava north of Puu Kamoamoa and camp D (pl. 3). To the east, the crack was buried by new lava of episode 11. No subsequent displacement occurred.

Episode 11 ended at 1841 H.s.t. November 7 as the remaining vents gradually shut down over a period of several minutes. Fountaining on the northeast flank of Puu Oo stopped first. Then, after several diffuse sprays of fragmental material were emitted, the more central fountains inside Puu Oo stopped erupting.

One major flow to the northeast and two minor flows to the east and southeast were produced during episode 11 (pl. 3). The northeastern flow was 9.6 km long and split into two distinct lobes approximately 5 km downflow. The bulk of this flow was aa; however, pahoehoe overflow levees from the active central lava river persisted about 3 km along its length. Likewise, the 2-km-long southeastern flow was predominantly pahoehoe in its upper reaches, thickening downstream and evolving into aa in its last 1-km stretch. The eastern flow, 1.4 km long, also consisted primarily of pahoehoe in its proximal part and of aa in the last 600 m. During 43 hours of eruption, 12×10^6 m^3 of new basalt covered an area of 4.3×10^6 m^3; the average lava-discharge rate was 280,000 m^3/h.

Puu Oo changed strikingly in shape during episode 11 (figs. 1.80, 1.83). Spatter deposits from vents erupting on and near the northeast flank had extended the flank more than 100 m northeastward. In addition, separate craters had grown high on the north and west flanks of Puu Oo. Dense fume emanated from the northern satellitic crater; thus, it is not distinguished in figure 1.83. Incandescent cracks were visible at several places in the spillway corridor that transected the northeast flank of Puu Oo. The spillway was no longer a narrow, steep notch; it had become a broad, elongate breach in the northeastern wall of Puu Oo, floored by a smooth, easily scaled ramp of pahoehoe.

The vents that had been active uprift and downrift of Puu Oo were marked by 5- to 10-m-high spatter cones or ramparts overlooking the new flows. These vents remained hot for many days, but no interior incandescence was ever seen.

EPISODE 12 (NOVEMBER 30–DECEMBER 1, 1983)

Between episodes 11 and 12, copious hot, oxidized fume issued from the interior of Puu Oo. Incandescent openings persisted in many places throughout the cone complex, although the intensity of glow diminished somewhat over the course of the repose period. Most conspicuous of these incandescent areas were those in and near the Puu Oo spillway. The crater rim and internal septa composed of agglutinate delineated several chambers within the larger crater.

Except for causing some minor collapse within Puu Oo Crater, the $M=6.7$ Mauna Loa earthquake of November 16, 1983 (Koyanagi and others, 1984; Buchanan-Banks, 1987) had no significant effect on Puu Oo or on the low-amplitude harmonic tremor in the eruption area during this repose period.

Disturbance of the tripwire between 1600 and 1610 H.s.t. November 29, in addition to reports of glow over Puu Oo between 2200 and 2310 H.s.t., suggests that low-level activity preceded the onset of vigorous episode 12 eruption by 6 to 11 hours. Harmonic-tremor amplitude in the eruptive zone began to fluctuate at about 0730 H.s.t. November 29 and remained irregular throughout the day. After a gradual but steady increase beginning at 2300 H.s.t., tremor amplitude increased significantly at 0445 H.s.t., and by 0450 H.s.t., fountaining at Puu Oo was visible from Hilo.

Observers arrived at Puu Oo at 0750 H.s.t. November 30. At least four loci of fountaining, all within the crater or high on its rim, could be identified (see fig. 1.16). The northwestern fountain of the group, which was the most vigorous, rose an estimated 50 to 60 m. A second fountain, less vigorous than the first, played from a site approximately in the center of the crater. A third major fountain emanated from the spillway, at the northeast end of Puu Oo Crater; this fountain appeared to be erupting from a level lower than the other vents. The fourth major fountain was actually a group of fountains erupting from the southern part of the Puu Oo rim and crater. Good

views into the crater revealed a complex, multilevel lava pond, supplying a cascade northeastward over the spillway. Each of the four active vents apparently contributed to this pond.

Several separate flows issued from Puu Oo that morning (pl. 4); all were pahoehoe during our first reconnaissance at 0845 H.s.t. The major flow traveled northeastward for the first few hundred meters as a high-

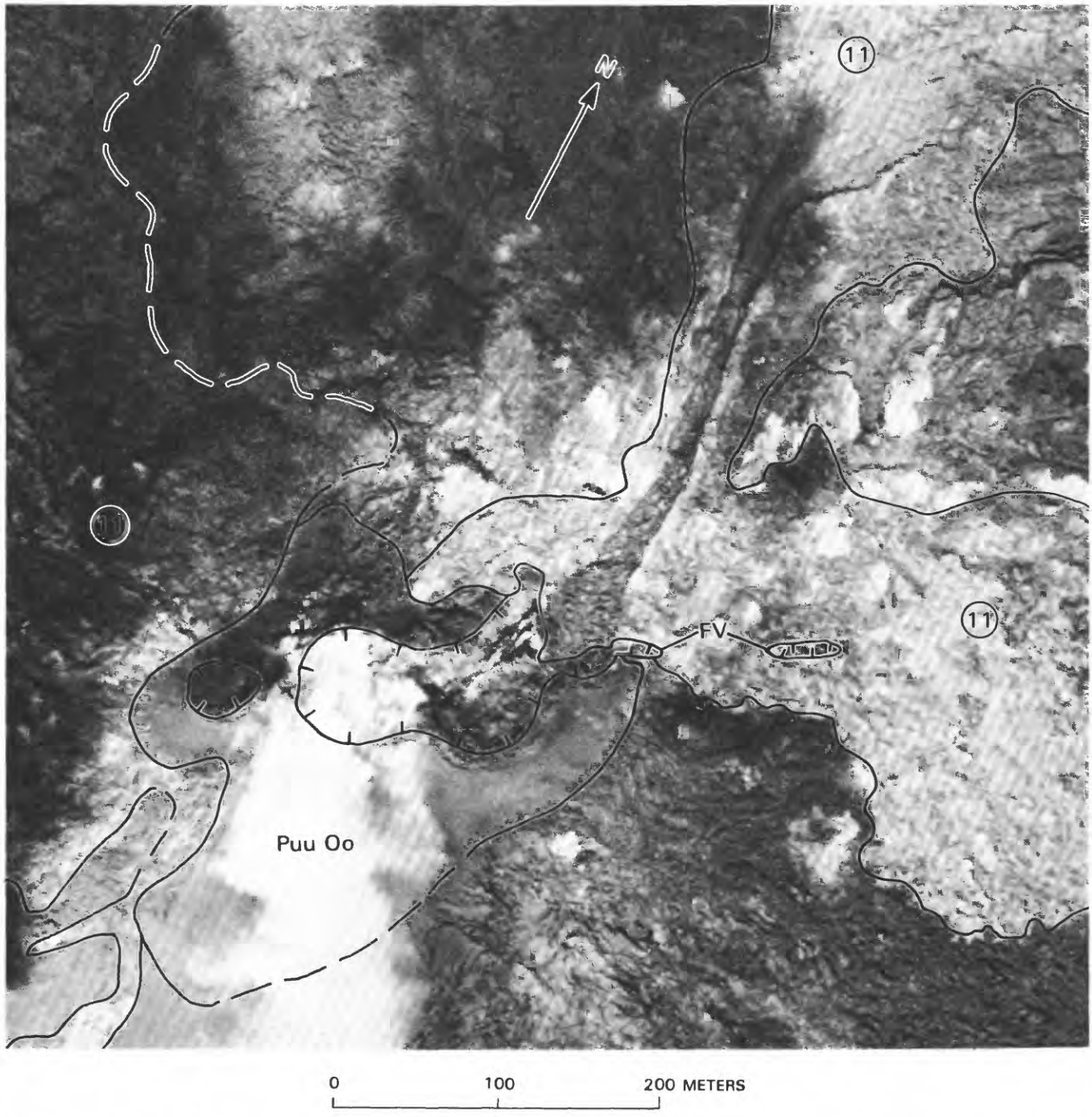

FIGURE 1.83.—Puu Oo after episode 11, showing nearby parts of episode 11 flows (11) and spatter ramparts built by small episode 11 vents (FV) to northeast. Solid line, flow boundary; dashed where approximate. Hachured line, crater rim; hachures point inward. Photograph 83.11.14JG120A#11 by J.D. Griggs, taken November 14, 1983.

velocity, vigorous pahoehoe river confined within the evacuated episode 11 channel; beyond that it slowed and broadened. Spatter from the northwestern fountain and pond overflow fed a pahoehoe flow that advanced north and northeast from the cone. The less vigorous, southern fountains fed several narrow spatter- and pond-fed flows that traveled southward and eastward from Puu Oo.

The general height of the array of low fountains gradually decreased through November 30 to about 20 to 30 m, and that level was maintained through the rest of episode 12 (see fig. 1.24). A unique variation in Puu Oo fountain behavior occurred on December 1. Beginning at about 0040 H.s.t., a vigorous jet of gas, possibly steam, with entrained tephra became conspicuous at the northwestern vent, where, earlier in the eruption, a vigorous lava fountain had played. This jet, about 50 m high, persisted throughout the rest of the episode. Periodically, southeast winds caused fallout from the jet to pelt camp D with 2- to 3-cm-diameter tephra.

Early on December 1, both the level of the pond inside Puu Oo and the general vigor of fountaining had decreased. The local fountaining centers had developed individual spatter walls around themselves, so that Puu Oo appeared distinctly chambered (see fig. 1.17). Most of the erupting lava continued to feed the northeastern flow; a lesser amount fed the northern flow, and the eastern flow was stagnant. The average rate of advance of the northeastern flow had declined to about 160 m/h from about 400 m/h on the preceding day, but a reduction in supply to the flow is not implied; the advancing front was 2 to 5 times as wide as on the previous day (pl. 4).

At 1545 H.s.t. December 1, after 35 hours of lava production, a rapid reduction in harmonic-tremor amplitude in the eruptive zone accompanied the cessation of fountaining at Puu Oo. Seen from the air, Puu Oo was an elongate cone, irregular in outline, enclosing at least five distinct chambers separated by conspicuous septa (see fig. 1.17). Incandescence was immediately visible in numerous cracks and holes inside some of the chambers; over the succeeding weeks, the openings gradually cooled, and the incandescence diminished. In the northeastern part of the edifice, one large chamber extended downward to a steep-walled pipe, about 30 m across and open for at least 90 m. The walls of this pipe consisted of thin-layered, platy and rubbly basalt that was partially oxidized. No drainback textures could be identified. Spatter and drainback features were, however, identifiable in some of the smaller vent structures clustered inside Puu Oo. Numerous rockfalls within the crater occurred immediately after the eruption and continued well into the subsequent repose period. As was typical of posteruption periods, varying amounts of oxidized fume issued from many parts of the crater. The spillway was an elongate, slightly sinuous, wide chute that ran down the northeast rim of the cone.

The main, northeastern flow of episode 12 was extraordinarily narrow (less than 100 m) over much of its length (pl. 4). Broad overflow levees composed of pahoehoe occurred along much of the first 4.7 km; beyond that, the flow was entirely aa. The 2-km-long northern flow was characterized by a similar distribution, with a broad pahoehoe field near the vent evolving downflow into aa only. The eastern flows, also pahoehoe evolving downstream to aa, advanced more than half the distance to Royal Gardens during episode 12. Altogether, 8×10^6 m^3 of lava had been erupted at an average rate of 230,000 m^3/h.

Between 7 and 8 km northeast of Puu Oo, near the terminus of the major, northeastern flow of episode 12, a zone of new, steaming cracks parallel to the east-rift-zone axis was discovered on December 17 by a passing pilot (pl. 4). Subsequent investigation on the ground showed that about 1 m of extension had occurred perpendicular to the strike of the rift zone. At the uprift end, the new cracks disappeared under episode 12 lava; evidence suggests that the episode 12 flow may have been broken locally by propagation of the new cracks. The lava, however, also was apparently emplaced against crack-related, 1- to 2-m-high fault scarps that did not move subsequently; thus, cracking may have spanned a period of time that encompassed emplacement of the episode 12 flow. The new cracks are within a zone in which numerous older cracks have cut prehistoric basalt. Although these new cracks are approximately on strike with the 1983 eruptive fissure, they are entirely downrift of the region of shallow earthquakes associated with the January 1983 dike emplacement. Subsequent monitoring near the uprift end of the new cracks showed no further movement.

EPISODE 13 (JANUARY 20–22, 1984)

Seven weeks of repose separated episodes 12 and 13. The first suggestion of pre-episode 13 low-level activity was a report at 2130 H.s.t. January 12 of a slight orange glow reflected on fume over Puu Oo. At 1117 H.s.t. January 20, an HVO observer spotted incandescent cracks in the surface of crusted lava about 50 m down the near-vertical open pipe descending from the large northeastern crater shown in figure 1.17. Between 1300 and 1400 H.s.t., observation from the rim of this crater as well as from a helicopter revealed what was apparently a cascade of lava from an opening in the north wall, deep within the pipe. At about 1545 H.s.t., the lava column began to slowly rise, and by 1724 H.s.t. it had reached the level of the spillway and had begun to flow northeastward out of the crater at a rate of approximately 10,000 m^3/h. Concurrently, a 5-m-high dome fountain played discontinuously over the center of the overflowing pond within the crater. The pond surface was roiled, as in a rolling boil in a

saucepan. The vigor of surface agitation and rate of overflow gradually increased, and by 1740 H.s.t. observers had to retreat from the crater rim.

Unlike some previous episodes that reached their maximum output and fountain height near the start of flow production, episode 13 activity accelerated gradually. By about 2000 H.s.t. January 20, lava output was estimated to be at least 100,000 m^3/h in a lava river that flowed northeastward from Puu Oo, and the fountain height had slowly increased to 40 to 50 m above the pond (see fig. 1.24). Much different from the complex fountains of the recent previous episodes, this fountain consisted of a single column approximately centered over the position of the large open pipe. None of the peripheral vents of recent episodes was active. This single fountain remained relatively low throughout episode 13 (fig. 1.24), although its height gradually increased to a general maximum of 80 to 90 m.

For much of episode 13, the fountain height and the lava flux within the channel close to Puu Oo oscillated in a style we had not seen in earlier episodes. At intervals of about 0.5 to 1 minute, the fountain would diminish to about half its full height and then quickly rebuild to full height. Thus, the general level recorded in fig. 1.24 probably represents neither the maximum nor the minimum but some intermediate fountain height. In rapid response to the fountain changes, the lava river in the channel near the base of Puu Oo rose and fell. At times, flow through the spillway actually stopped for 10 to 15 seconds. Recovery was always rapid, and surges that filled the channel repeatedly advanced through the first 100 m at about 10 m/s. The surging lava would often overflow the confining banks to produce rapidly moving overflows. Fragments of melt thrown out of the surging river on the outsides of sharp bends built ramparts of spatter. Visual estimates suggest that the lava-river flux may have undergone rapid changes as great as threefold.

The oscillation in fountain height and lava-river flux apparently recorded repetitive brief interruption in the supply of melt to the vent. It was distinct from more rapid pulsing, at intervals of about a second, that we also saw in the fountain jets.

The pulsing output fed a single lava river and flow that moved northeastward (pl. 4), as had all the major flows beginning with episode 6. The flow bifurcated around Puu Kahaualea but rejoined into a single advancing front by midmorning January 21.

At 0027 H.s.t. January 22, after 31 hours of eruption, the fountain became intermittent and low for a period of about 10 minutes; eruption stopped entirely at 0041 H.s.t., and the flows were cut off. Eruptive activity resumed at about 0432 H.s.t. with low, intermittent fountaining that lasted until 0502 H.s.t. After another 34 minutes of inactivity, fountaining began anew at 0536 H.s.t. and reached preshutdown levels within about 15 minutes (see fig. 1.24). Output northeastward over the spillway, the only locus of overflow from the lava pond in Puu Oo Crater throughout episode 13, was quickly reestablished and remained vigorous for the rest of the eruption. New lava advanced directly over the earlier episode 13 flow, and the major lobe again traveled in a northeasterly direction. This resumption of activity also resulted in a breakout to the southeast from the northeastern lava river about 700 m from the vent (pl. 4).

Beginning at about 1115 H.s.t. January 22, a spasmodic decay of fountaining and output began again at Puu Oo, heralding the end of episode 13, which occurred at 1123 H.s.t. At least five off-on cycles were observed before activity finally ceased; each cycle lasted about a minute. Off periods were characterized by relative quiet and emission of blue-brown fume from the crater. Helicopter views into the crater immediately after the final disappearance of fountain activity revealed the boiling top of a magma column in a vertical pipe extending downward from the center of the crater floor. Partly crusted at times, the active column remained 0 to 25 m below the level of the crater floor that surrounded the open pipe for the ensuing repose period (see fig. 1.18).

The open pipe within the crater (fig. 1.84) was much like the one left after episode 12 that had filled with lava at the beginning of episode 13. About 25 m wide at the top, the post-episode 13 pipe narrowed downward to about 10 m across at a depth of 20 to 25 m. The crater floor surrounding this conduit was mantled with episode 13 pahoehoe and was generally inclined toward the center of the crater. The interior walls of the crater steepened

FIGURE 1.84.—Interior of Puu Oo Crater after episode 13. Top of vertical conduit is approximately 20 m in diameter where person (circle) is standing. Light fume emanating from conduit is visible in shadowed area at lower left. Spillway, out of view to right, is 5 m higher than ledge on which person stands. View northwestward from southeast crater rim; photograph taken January 25, 1984.

upward, and the spillway was a steep chute down the northeast side of the cone (see fig. 1.18). Immediately after episode 13, the chute was smoothly paved by pahoehoe (fig. 1.85*A*), but shortly after the eruption ended, blocks and rubble fell into it from the walls (fig. 1.85*B*). In fact, after most eruptions, avalanching of coarse talus into the spillway chute made it a dangerous avenue into the crater. Otherwise, the post-episode 13 crater remained relatively free of rubble for the ensuing repose period.

Puu Oo changed significantly in gross shape during episode 13 (see figs. 1.17, 1.18). Tephra fallout from periods of higher fountaining had added some bulk to the south and southwest sides of the cone, healing slump scars and irregularities inherited from episodes 11 and 12. The most radical change, however, was in plan view. After episode 13, Puu Oo was a nearly circular cone enclosing a single central crater. The exterior walls steepened upward from the base of the cone, which was largely surrounded by an apron of flows.

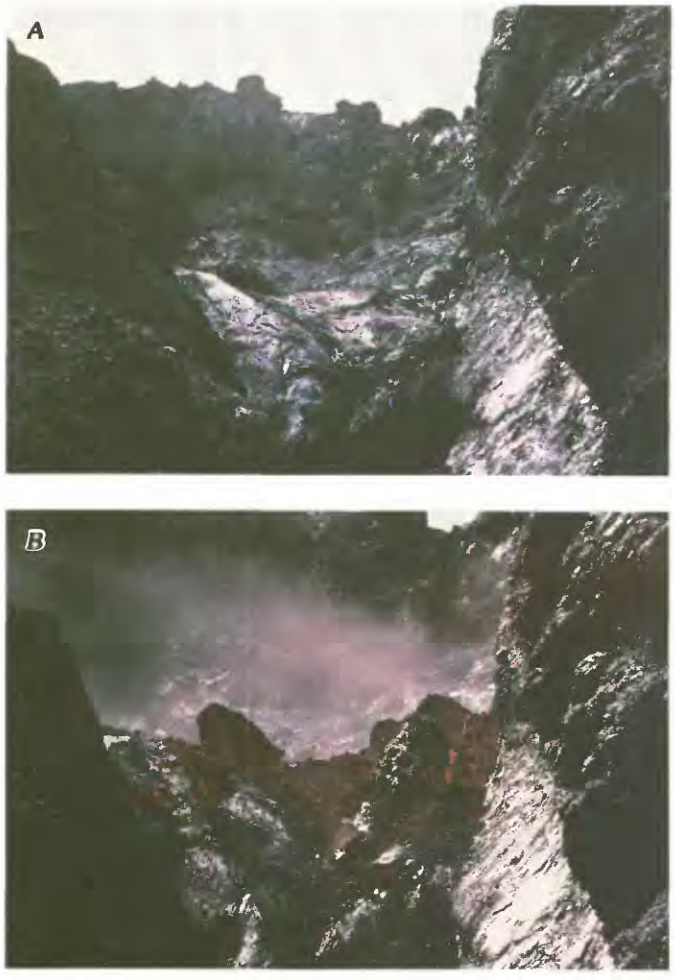

FIGURE 1.85.—Puu Oo spillway and rockfall, approximately 2.5 hours after episode 13. *A*, Spillway transecting rim of Puu Oo Crater. High-lava mark, which forms a linear boundary between smooth, highly reflective pahoehoe and rougher, less reflective spatter deposits to right of spillway, presumably reflects level of lava that flowed out of crater and down spillway during episode 13. Position of this mark suggests that stream of lava was about 10 m thick as it exited crater. Spillway is about 30 m wide. View westward toward crater interior; photograph taken at about 1400 H.s.t. January 22, 1983. *B*, Similar view to figure 1.86*A*, several minutes later, showing incandescent blocks that fell from steep north wall. Spillway is about 30 m wide, and so largest of these blocks is about 7 m across.

A deep, sinuous evacuated channel with partly overhanging levees along its first several hundred meters led away from the northeast base of Puu Oo. Its channelized pahoehoe river had supplied the main, northeastern flow during episode 13 (pl. 4). This flow was a composite of the flows produced during each of the two eruptive periods of episode 13. The first flow, emplaced between 1724 H.s.t. January 20 and 0041 H.s.t. January 22, had traveled 7.4 km; it was predominantly pahoehoe for the first 3.5 km and entirely aa for the rest of its length. The second eruptive pulse produced another flow that traveled northeastward on top of the first (pl. 4) for a total distance of approximately 3.1 km. Local aa flows that extended northward and southeastward from the second flow formed as breakouts, on January 22, from the reactivated lava river. Aerial photographs were not obtained until after two additional eruptive episodes had occurred; thus, mapping of the episode 13 lava flow is based in part on helicopter sketch maps made during the eruption.

EPISODE 14 (JANUARY 30–31, 1984)

Throughout the short, 8-day repose period between episodes 13 and 14, the surface of the magma column remained visible at depths of 0 to 25 m below the top of the open pipe (figs. 1.18, 1.84) extending downward from the floor of Puu Oo Crater. At times, molten to barely crusted lava was exposed at the surface of this column. However, much of the time the column was capped by a crust of basalt, generally composed of a combination of agglutinated spatter and smooth pahoehoe. A small irregular orifice, generally from 0.5 to 3 m across, pierced the crust and served as the vent for minor amounts of spatter, a few small pahoehoe flows, and varying amounts of gas, all emitted episodically in response to gas-piston activity in the magma column. For hours at a time, the gas-piston cycles were rhythmic and brief, 4 to 6 minutes long, although longer, irregularly spaced events also occurred.

The overall rise of the magma column led to flooding of the crater floor sometime between January 27 and 30. This flooding produced a solid crust (fig. 1.52) about 30 m in diameter and 4 m below the level of the spillway. Emission of short (1–3 m long), glassy pahoehoe flows and spatter from a 0.5-m-wide vent through the crust near the northeast edge of the pond surface had built a small mound of lava, about 4 m wide and 1 m high. The vent

itself was incandescent, and as we watched it, roaring pulses of gas and minor spatter issued intermittently.

At about 1030 H.s.t. January 30, harmonic tremor began a gradual increase that peaked at about 1830 H.s.t. as fountaining from Puu Oo became visible to sailors off the south coast of the island. By 1951 H.s.t., fountaining was visible from the Wahaula visitor center (see fig. 1.1) and from high points in the upper east rift zone. Although a clear view into the spillway was obstructed by vent deposits, time-lapse film from camp E shows that the lava filling Puu Oo Crater reached the level of the spillway and probably began to overflow between 1739 and 1745 H.s.t. The vigor of fountaining gradually accelerated, and by 1848 H.s.t., broad bursts were reaching the top of the cone. The fountain was broad, filling nearly the entire crater.

On the morning of January 31, when we arrived at Puu Oo, the single broad fountain, approximately centered over the site of the conduit, was about 100 m high. The time-lapse film record (see fig. 1.24) indicates that the fountain quickly built to 200 m in height early in episode 14 and then generally decreased gradually to about 100 m in height at the end of the brief eruption. During that decline, the fountain height fluctuated rapidly. The field observation was that fountain heights fluctuated at intervals of 10 to 20 seconds from low levels (10–20 m above the rim of the cone) to higher levels (80–100 m above the rim of the cone). The higher bursts produced short-lived spatter-fed flows down the flanks of Puu Oo. Nearly continuous bombardment of the south rim and flank of the cone by spatter produced a large, rootless aa flow that ultimately traveled 1.5 km southeastward of Puu Oo (pl. 4). A smaller spatter-fed flow extended 0.7 km southward.

The lava river exiting from the crater over the spillway carried nearly three-fourths of the lava flux. Near the base of the cone, a distributary of the river, diverted northwestward, fed a thick, ponded pahoehoe flow that spread northwest of Puu Oo. The main channel fed a complex flow advancing eastward. This time, instead of a single lava river evolving downstream into an aa lobe, a complex network of distributary pahoehoe channels emerged from the main channel within a kilometer of the vent and spread in several directions (fig. 1.86). Several distributaries, however, merged near the southwest base of the 1123 cone to produce a flow to the east that evolved downstream to aa and was the most active. By the episode's end, it had extended 4.7 km from Puu Oo (pl. 4). Other distributaries merged to supply a shorter lobe on the north side of the 1123 cone.

After only 19 hours of eruption, lava emission deteriorated spasmodically between about 1315 and 1318 H.s.t. January 31. Immediately after activity stopped, we had a clear view of the crater interior (fig. 1.87). An incandescent circular opening, emitting fume and fine brown particulate matter, marked the central conduit; except for the beheaded flow draining from the spillway chute and glowing collapse along the walls of the cone, no movement was visible. After several minutes, fume filling the conduit and the interior of the crater obscured the view.

Aerial photographs were unavailable until after episode 15; thus, the distribution of episode 14 flows as mapped on plate 4 is approximate in places. When mapped after episode 15, all the exposed episode 14 lava flows were aa except for the thick pahoehoe lobe northwest of Puu Oo. The new basalt covered an area of about 2.1×10^6 m^2 and had a volume of 6×10^6 m^3, with an average lava-discharge rate of 320,000 m^3/h.

After episode 14, Puu Oo again contained a steep-walled, bowl-shaped crater, approximately 40 to 45 m across at the level of the spillway. Extending downward from the floor was a nearly vertical open conduit, about 20 m in diameter, almost an exact replica of the pre-episode 14 conduit (fig. 1.84). The edges of thin lava layers were exposed in its walls. At the top it flared to merge with the sloping crater floor, and the flaring lip was mantled with drainback lava.

The interior walls of the crater were lined with a beautiful, delicate, glassy pahoehoe coat and glassy spatter bombs. Parts of the wall were furrowed (fig. 1.88), forming a parapet at the rim like that seen on the episode 7 rim (fig. 1.76). A bench that may have represented the high-lava mark of the pond inside the crater during episode 14 was visible on parts of the interior walls (fig. 1.88). Its position suggests that the pond surface stood about 10 m higher than the rock floor of the spillway.

In the northeast wall of the crater, the spillway was now a broad, 30- to 40-m-wide cleft. Northeastward, it led down into an evacuated channel that retained definition for about 200 m. The south rim of Puu Oo had been degraded by spatter bombardment into a low, smoothed terrace (fig. 1.87) that would persist through several episodes, providing us with a convenient and safe point of entry and exit.

EPISODE 15 (FEBRUARY 14–15, 1984)

Although we heard low-pitched, rumbling exhalations from deep within the open pipe on February 1, the day after episode 14 ended, we could see no lava. However, lava was seen deep in the pipe during aerial reconnaissance flights on February 3 and 5. Ground observation on February 7 revealed that a partly crusted magma column stood 45 m below the crest of the spillway. For the next 6 days, this column rose at an average rate of about 4 to 5 m/d. Its crusted surface was broken by a small opening through which spatter was intermittently thrown; the active, roiled lava surface was commonly visible just

FIGURE 1.86.—Puu Oo erupting during episode 14. Complex of distributaries transports fluid lava to north, northeast, and southeast. Fountain at Puu Oo is approximately 100 m high. Altered cinder and spatter cone in foreground is 1123 cone (Puu Halulu); camp E is on right shoulder of this cone. View southwestward; photograph by J.D. Griggs, taken at 1115 H.s.t. January 31, 1984.

FIGURE 1.87.—Puu Oo vent, about 8 minutes after end of episode 14. Glowing, 20-m-diameter hole marks location of conduit. Note beheaded lava flow draining from spillway chute and incandescence where local collapse of walls is occurring. Part of helicopter is visible at lower left. View westward; photograph taken at 1326 H.s.t. January 31, 1984. Numerals (lower right) indicate date and time.

FIGURE 1.88.—Furrowed, spatter-mantled north interior wall of Puu Oo after episode 14 (compare fig. 1.76). Wall towers steeply 30 to 40 m above general level of crater floor. Bench visible in lower part of frame may represent a high-lava mark of ponded lava during episode 14; if so, pond surface was about 10 m higher than the rock floor of the spillway. Photograph taken February 1, 1984.

beneath the crust. By the morning of February 13, the column surface, which was then free of crust, had risen to within 20 m of the lip of the spillway (fig. 1.51). Between 0700 and 0710 H.s.t. February 14, according to time-lapse film data, the column briefly rose sufficiently high to send a 100- to 150-m-long pahoehoe flow over the spillway and down the evacuated episode 14 channel.

Time-lapse film data indicated that low-level fountaining commenced inside Puu Oo at about 1940 H.s.t. February 14. Between 1940 and 1943 H.s.t., lava reached the level of the spillway, and sustained overflow began. Fountaining accelerated quickly along with output. Within an hour, peak fountain heights exceeded 200 m; and in less than 2 hours, at 2133 H.s.t., the maximum height for the episode (350 m) was attained. Thereafter, the single broad fountain centered over the crater declined spasmodically to about 100 m in height at the end of the episode (see fig. 1.24). As in episode 14, the fountain height oscillated widely.

High fountains and strong tradewinds combined to produce an extensive tephra fallout downwind of Puu Oo. Tephra fell at least as far southwest as Napau Crater, 4 km uprift of Puu Oo (see fig. 1.1), and evidence of the early high fountains and heavy tephra fall at camp D was conspicuous when we arrived at 0730 H.s.t. February 15. Lightweight, frothy bombs, as large as 50 cm across, littered the ground around the camp, and the canvas tarp covering our shed was still smoldering; it had been burned completely through in places.

The major lava flow, fed by lava pouring through the spillway, traveled northeastward from Puu Oo. When we first saw it, early on February 15, it was about 2 km long (pl. 4) and almost entirely aa; the pahoehoe-aa transition in the channel was within a few hundred meters of the vent. Subsequently, as the fluid pahoehoe channel lengthened, its envelopment in hot, fresh aa made approach to the central channel difficult. Occasional overflows from the channel were our only source of active pahoehoe for temperature measurements and sampling.

An additional aa flow extended eastward. Time-lapse-camera records indicated that this flow had been fed vigorously during the night of February 14–15 both by spatter and by overflow from the lava cascade down the northeast face of Puu Oo. By dawn, however, the flow was being fed only intermittently and was essentially at its final length when we first saw it early on February 15 (pl. 4).

The eruption continued steadily until 1458 H.s.t. February 15. Then, over the next 3 minutes, fountaining spasmodically stopped and restarted three times before finally shutting down at 1501 H.s.t.

Two conspicuous flows of episode 15 extended northeastward and eastward (pl. 4) 4.7 km and 2.9 km, respectively; both were predominantly aa. In addition, relatively short, thick, spatter-fed aa flows flanked Puu Oo on the west, south, and southeast. The high fountains of episode 15 had deposited much tephra on the southwest flank of the cone. The geometry and general appearance of the bowl-shaped crater were virtually unchanged from its pre-episode 15 condition. Approximately 8×10^6 m^3 of new basalt had been erupted over a period of 19 hours, giving the highest average lava-discharge rate thus far—420,000 m^3/h.

EPISODE 16 (MARCH 3–4, 1984)

Conditions at Puu Oo remained relatively stable during the first 13 days of repose between episodes 15 and 16. High levels of SO_2-rich fume emanated from the open pipe, and, except for sighting of incandescence at a depth of 40 to 50 m on February 22 and hearing of low-pitched, rumbling exhalations that may have indicated lava at depth on February 24, no activity was directly observed until February 28. (People camped near the eruption site on February 27 reported glow over Puu Oo at 1900 H.s.t., but this event was not confirmed in the time-lapse film record.) At 1200 H.s.t. February 28, we saw active, partly crusted lava within the pipe, about 30 m below the level of the spillway. Over the ensuing 5 hours, the column rose at a rate of about 1 m/h. By 1700 H.s.t., the lava surface was completely open and vigorously churning. Small amounts of spatter were occasionally emitted from its disturbed surface. During the next 4 days, the column was partly crusted at times. Its behavior alternated between quiescence and rhythmic gas pistoning in which the surface rose and fell 10 to 15 m.

The lava filled the crater, formed a pond, and began to overflow the spillway at about 1450 H.s.t. March 3. Initially, the fountain was low, 10 to 20 m above the pond surface. The vigor and height of the fountain accelerated gradually, and by 1519 H.s.t., fountaining was high enough to be visible over the rim (about 40 m above the surface of the lava pond) from camp D. At 1700 H.s.t., fountaining peaked at a new record height for Puu Oo—approximately 390 m (see fig. 1.24). As in episode 15, the fountain height declined spasmodically through episode 16, although it remained generally high through the first night. By the end of episode 16, the general height was less than 100 m.

Glowing tephra, carried by hot updrafts over the vent, was at times wafted to twice the height of the denser part of the fountain. This tephra was especially visible at night, when it caused severe overestimation of fountain heights by observers at distant vantage points. Erratic winds distributed tephra on all sides of the vent. Intermittently, for periods of 10 to 30 minutes during the night of March 3–4, easterly winds dropped incandescent bombs, as large as 20 cm in diameter, on camp D, 750 m west

of the vent. These periods of bombardment made systematic sampling of tephra easy. However, the aluminum roof of our shed was repeatedly dented and sometimes punctured by the larger fragments, and the general clatter of pyroclasts hitting the roof reminded us of an aluminum corn popper at its peak of activity.

When high, the single fountain was a broadly based jet of varying trajectory. Within it, at any one time we could see the more brightly incandescent fronts of several distinct pulses rising upward through the fountain (see fig. 1.6). The effect was particularly striking at night. During periods of lower fountaining, the fountain decayed into multiple jets of spatter, also varying in trajectory. For several hours before dawn on March 4, the high fountain appeared, on time-lapse film, to be split into two: One fountain was a high, energetic column that leaned to the north, and the other a low, dense fountain that did not rise above the rim of the cone. The situation was similar to one witnessed during episode 10 (see fig. 1.28).

Early high fountains produced a thick, broad, spatter-fed aa flow that advanced more than 1 km northward, and several smaller rootless flows that extended southeastward and westward (fig. 1.40). The major flow was fed by a vigorous cascade of lava overflowing from the crater through the spillway. This cascade funneled into a narrow channel for the first several hundred meters, beyond which the pahoehoe river broadened and slowed, heading east and then southeast toward Royal Gardens (pl. 5). The flow advanced mostly on top of earlier 1983-84 flows. Approximately 6 km from its source, the flow split into two lobes, the longer of which extended another 1.6 km across the northeast corner of the Royal Gardens subdivision. This lobe, however, was almost entirely confined to the evacuated aa channel of an episode 2 flow, and so it caused no additional damage to property.

Availability of additional assistance during episode 16 gave us the opportunity to monitor the front of the main flow in the middle distance between Puu Oo and the steeper slopes of Kilauea's south flank at Royal Gardens. In general, the flow front remained relatively fluid and thin (generally less than 4–5 m thick) during this part of its passage. Advance rates measured over short time intervals indicated a typical range in advance rate from 55 to 510 m/h. The faster rates coincided with temporary surges in the flow; these surges were generally accompanied by thinning of the flow front and commonly by thin (1–2 m thick) breakouts of more fluid lava from the interior of the flow. These breakouts would advance for several minutes; briefly, one advanced at a rate of 1 m/s.

Fountaining stopped temporarily at 2228 H.s.t. March 4. After a brief renewal of activity, it halted finally at 2231 H.s.t. For the next 10 to 15 minutes, small, diffuse bursts of spatter issued from the open pipe in the crater floor. Burning gases were also seen flaring at the top of the pipe.

The main flow, one of the longer in the series, extended nearly 8 km from the vent. It was nearly all aa, although pahoehoe overflows mantled the levees locally within 2 km of the vent. The main flow constituted about 60 percent of the total erupted volume, which was 12×10^6 m^3, and thick, spatter-fed flows accounted for nearly 40 percent. Altogether, episode 16 lasted 32 hours; the average lava-discharge rate was 380,000 m^3/h.

On March 8, ground crews entered Puu Oo to find that the bowl-shaped crater interior had the same general form as before. Its appearance differed, however, because coarse rubble from superficial collapse of the walls mantled the walls and floor; broad, delicate pahoehoe surfaces like those that characterized the crater interior after episodes 14 and 15 were absent. No lava or incandescence was sighted in the conduit until March 20; a significant layer of rubble may have capped the magma column.

EPISODE 17 (MARCH 30–31, 1984)

During the 25-day repose period between episodes 16 and 17, lava was first sighted in the open pipe at Puu Oo on March 20 at a depth of about 60 m below the level of the spillway. The magma column was largely crusted, and churning lava was visible through a 3- to 4-m-diameter hole in the crust. Intermittent observations for the next 10 days indicated that the column rose slowly, and some gas-piston activity occurred. The major outbreak of Mauna Loa that began early on March 25 had no apparent effect on the activity at Puu Oo.

The rising lava filled the crater and began overflowing the spillway between 0330 and 0350 H.s.t. March 30, accompanied by intermittent dome fountaining, about 10 to 15 m high. In tandem, harmonic-tremor amplitude in the eruption zone increased slightly at 0330 H.s.t. After four aborted overflows, a final steady overflow of the lava pond occurred at approximately 0448 H.s.t. March 30. Simultaneously, fountaining began to increase, and by 0611 H.s.t. the fountain was visible above the rim of Puu Oo from camp D. Glow over the eruption site had been observed as early as 0515 H.s.t. from HVO, 20 km away. For the first time in 65 years, Mauna Loa and Kilauea were in simultaneous eruption.

We arrived at the eruption site at about 1000 H.s.t. March 30. By that time, the fountain centered over the crater was 100 to 140 m high (fig. 1.89). It consisted of a broad complex of short-lived jets of spatter, produced at a rate of about 20 per minute, which created a general impression of rapid pulsation in the overall fountain height. Strong trade winds blew most of the tephra to the southwest and deposited it on the elongate southwest flank of the cone. After a slow initial increase in fountain height during the first 7 hours of the eruption, the height increased abruptly to about 150 m at approximately 0740

H.s.t. and then diminished gradually to about 100 m, which was maintained until the episode's end (see fig. 1.24).

When we first saw it at 1000 H.s.t. March 30, a narrow lava flow, fed by a voluminous torrent of lava cascading over the spillway (fig. 1.89), extended 1.5 km east-northeastward from the base of Puu Oo (pl. 5). In addition, spatter spilling over the south rim of the crater had initiated a spatter-fed flow to the southeast that was then 0.5 km long. Later in the morning, about 2 km from the vent, the main flow turned east-southeastward and began extending in the general direction of the Royal Gardens subdivision. Aa for most of its length, the flow advanced at the extraordinarily high (for Puu Oo flows) average rate of 490 m/h (table 1.3). Along individual segments between our helicopter reconnaissances, average advance rates ranged from about 300 to more than 700 m/h. This high rate may reflect confinement of the flow, for much of its advance, to the topographically confined, axial-channel part of the episode 16 flow. The stable, pahoehoe-bearing channel zone of the episode 17 flow was of normal length. When the flow was 4 to 5 km long, the transition to aa in the channel occurred about 1.5 km from Puu Oo; after the episode's end, we found pahoehoe overflow levees as far as 3.8 km from the vent.

Fountaining and flow production ceased together at 0324 H.s.t. March 31, less than 23 hours after episode 17 had begun. At about that time, reports of a shooting star traveling in the direction of Mauna Loa Volcano from the middle east rift of Kilauea reached the media, reviving discussion of Pele's divided attentions during the dual eruption. The main flow extended 10.8 km from the vent; it passed northeast of Royal Gardens and came within 1.7 km of the highway near the coast. Spatter accumulating high on the south flank of Puu Oo fed small flows to the west and a 1.5-km-long flow to the southeast (pl. 5; fig. 1.90). About 10×10^6 m^3 of new basalt was erupted at an average rate of about 430,000 m^3/h.

FIGURE 1.89.—Puu Oo erupting during episode 17. Fountain height is approximately 100 m. Torrent of lava cascades over spillway, feeding a lava river that is locally perturbed by large blocks grounded in channel. Near base of Puu Oo within lava river, standing wave (arrow) several meters high may record presence of another channel obstruction. A second flow, at left, originates from spatter ejected over south rim of crater. View southwestward; photograph taken at 1008 H.s.t. March 30, 1984. Numerals (lower right) indicate date and time.

After episode 17, Puu Oo Crater was about the same size and shape as after episodes 14 through 16. The south wall, over which spatter had poured, feeding flows westward and eastward (fig. 1.90), remained smooth and gently sloping; the adjacent part of the rim was relatively low. The north and west walls were high and steep; they funneled directly into the open pipe that was now a permanent feature of the crater floor. The walls and floor, relatively free of rubble, were largely lined with pahoehoe, as they had been after episodes 13 through 15. New airfall-tephra deposits mantled the outer flanks of the cone on the south and southwest.

EPISODE 18 (APRIL 18–21, 1984)

After episode 17, we first detected lava deep in the open pipe on April 5. For the next week, the lava level fluctuated between depths of about 10 and 50 m in the pipe, and we were aware of some gas-piston activity. From April 12 to 17, the lava stabilized at shallower depths of 10 to 25 m down the pipe, and intermittent gas-piston activity continued.

Time-lapse film recorded the first occurrence of low fountain activity within Puu Oo Crater at 1751 H.s.t. April 18. By 1800 H.s.t., lava had begun to overflow through the deep breach in the northeast rim of the crater. The intensity of both fountaining and overflow increased gradually. Over the first hour, fountain height increased to about 70 m; it then doubled abruptly at 1859 H.s.t. Thereafter, typically moist east-rift-zone weather obscured the camera's view, but a few clear frames record a very narrow, high fountain reaching more than 200 m above the level of the spillway (see fig. 1.24). At times, this vigorous high fountain fluctuated wildly in inclination and trajectory, showering large sections of the cone with spatter. A heavy tephra fall during the night deposited 10 to 20 cm of lapilli and small bombs in the vicinity of Puu Kamoamoa and camp D, and Pele's hair fell 20 km west of the vent at HVO. At about 0240 H.s.t. April 19, the fountain height decreased dramatically and, for the rest of the eruption, fluctuated irregularly between about 30 and 150 m. During periods of higher fountaining, tephra fallout from the single high, columnar fountain was significant, especially on the west and north sides of the vent. Higher fountaining was characterized by a single dominant jet, although at times the fountain split

into two divergent jets. At other times, adjacent to the main jet, a lower, less energetic fountain played. During periods of lower fountaining, a more complex assemblage of multiple jets was observed (see fig. 1.26).

We arrived at the eruption site at 0700 H.s.t. April 19 to find that our aluminum shelter at camp D had been ripped apart and scattered over several hundred meters downwind. We had often noticed dust devils over the hot tephra accumulating on the flanks of Puu Oo; apparently one had traveled through camp D during the night, tearing our metal shed to pieces. During the ensuing day, several more dust devils passed through camp. We subsequently moved to camp E, on the 1123 cone.

Episode 18 produced four long, river-fed aa flows (pl. 5); short, thick spatter-fed flows also advanced northward and westward from the vent. The river-fed flows were all fed by branches of a wide, sinuous pahoehoe river that issued from the spillway in the northeast rim of Puu Oo

FIGURE 1.90.—Puu Oo cone (c) and nearby parts of episode 17 lava flows (17m, main, river-fed flow; 17s, spatter-fed flows). Glowing lava (arrow), seen through hole in crusted surface of magma column, is visible within shadowed, 20-m-diameter open pipe. Thick air-fall tephra, locally overlain by spatter-fed flows, mantles southern part of cone. Solid line, boundaries of cone and flows; dashed where approximate. Photograph 84.4.13JG120D#6 by J.D. Griggs, taken April 13, 1984.

Crater. When we arrived at 0700 H.s.t. April 19, a massive spatter-fed flow, apparently fed by high fountains during the night, was slowly extending northward nearly a kilometer from the vent. The lava flux through the spillway seemed high relative to our recollections of most previous eruptions. The river supplied three major flows at that time, and two of them, extending rapidly northeastward and eastward from the vent, were entirely pahoehoe. The third, a small flow that extended southeastward (south flow, pl. 5), advanced slowly and remained minor for the entire day. Observations on the ground suggested that supply to this south flow varied; the level of pahoehoe flowing in its central channel fluctuated appreciably during the day, decreasing overall. Within the first kilometer of Puu Oo, overflows from the lava-river system were voluminous and frequent, producing broad pahoehoe sheets that surrounded the main flow channels.

During the night of April 19–20, a thick flow, fed by spatter from high inclined fountains, moved toward camp D (pl. 5). By the morning of April 20, some significant changes had occurred in the lava-river system and its flows. The northeastern flow had been beheaded and was stagnant. The southern flow also was nearly stagnant; the meager amount of lava that continued to feed it had begun to pond and spread laterally within 2 km of the vent. The eastern flow, which had veered southeastward after passing to the north of camp E on the 1123 cone, was still vigorously supplied and was advancing steadily adjacent to the episode 17 flow, more than 10 km from the vent. It was completely contained, however, in its upper reaches, below the level of its wide pahoehoe levees. Our visual impression of the spillway and nearby part of the lava river was that the total output from Puu Oo, though still vigorous, appeared to have decreased from the first day.

At the time of our last reconnaissance flight for April 20, at about 1720 H.s.t., the eastern flow extended nearly 12.9 km from the vent and was threatening several houses east of the Royal Gardens subdivision (pls. 1, 5). A minor pahoehoe overflow had diverged from the main channel about 0.5 km from Puu Oo; the resulting pahoehoe lobe extended about 0.5 km from the main flow. After our reconnaissance, this minor overflow apparently beheaded the main flow, taking virtually all of the lava supply (table 1.3) and developing into a rapidly moving flow (southeastern flow, pl. 5) that became the fourth major flow of episode 18. Traveling primarily over earlier 1983–84 flows, this new flow reached Royal Gardens shortly before 0600 H.s.t. April 21. It advanced at a relatively high average rate (430 m/h) during the night, covering 5.4 km in 12.5 hours. Though thin (approx 1.5 m at its edge) and apparently fluid (trees were left standing after its passage, not knocked down as in normal aa flows), the narrow flow was entirely aa when inspected in the morning. It reached 0.7 km into the subdivision adjacent to the southwest edge of the episode 3 flow; fortunately, it destroyed no homes.

Observation of the eastern flow as it entered a sparsely developed rural area east of Royal Gardens showed that its advance slowed significantly (pl. 5) in response to its being beheaded near the source. Nevertheless, it still managed to overrun two houses, two vehicles, and some outbuildings before the eruption stopped at 0533 H.s.t. April 21. The flow front, ranging in thickness from 3 to 10 m when active, continued to creep forward slowly for many hours after the eruption stopped, destroying a third house during the afternoon of April 21.

The eastern flow, the longest thus far of the entire series of eruptive episodes, was predominantly aa. It was 13.2 km long and came within about 1 km of the ocean and 0.6 km of the coast highway (pl. 5). Pahoehoe overflow levees intermittently bracketed the evacuated central channel for the first 3.5 km of its length. The northeastern and southern flows were also primarily aa, with pahoehoe levees in their near-vent channel areas. The surprise southeastern flow that invaded Royal Gardens had broad pahoehoe margins along its first 1.7 km.

After major lava production ceased at 0533 H.s.t. April 21, the time-lapse film record shows that minor bursts of spattering continued at Puu Oo until 0628 H.s.t. At 0830 H.s.t., a crusted lava surface was visible near the top of the pipe, and small amounts of spatter issued from two holes in the crust. Within less than an hour, however, debris collapsing from the oversteepened interior walls of the crater had plugged the pipe opening. It reopened by April 23; apparently, the debris that covered the opening collapsed into the pipe. Numerous small, high-frequency seismic events resembling rockfall signatures were recorded on a seismometer near Puu Oo on April 22, including a brief flurry of about 135 events between 0520 and 0545 H.s.t. This seismic activity may have recorded collapse and clearing of the rubble that blocked the magma-filled pipe on April 21.

The crater shape established during episode 14 still persisted; however, the walls and rim had undergone some superficial collapse, as they had after episode 16. Thus, the floor and walls were a jumble of slumped blocks and finer rubble (see fig. 1.19A). The south crater wall was no longer gently sloping, and entrance into the crater after episode 18 was possible only through the spillway chute, which was a deep, locally overhanging corridor lined with glassy pahoehoe and mantled by debris from posteruption collapse (fig. 1.91). It ran steeply down from the low northeast lip of the crater and abruptly flattened as it emptied into the evacuated channel.

Episode 18 lasted 60 hours; it was the longest since episode 5 in early July 1983. Except for episode 3, episode

18 was the most voluminous: It produced 24×10^6 m^3 of new basalt at an average lava-discharge rate of 410,000 m^3/h.

EPISODE 19 (MAY 16–18, 1984)

After episode 18 and continuing through the first half of May, lava at the top of the magma column was intermittently visible deep in the Puu Oo pipe. Fume often obscured the view. Bursts of gas and spatter, as well as repeated distinctive, low seismic bursts, indicated gas-piston activity.

Beginning at about 0115 H.s.t. May 16, lava apparently rose high enough that intermittent periods of glow and minor spattering within the crater were visible from camp E. At about 0500 H.s.t., the first of a series of short-lived pahoehoe overflows was recorded. For the next 44 hours, overflows lasting from 3 to 30 minutes recurred at irregular intervals ranging in length from 4 minutes to several hours. In general, these overflows carried lava at estimated rates of 10^3 to 10^5 m^3/h. Commonly the rate gradually increased during an individual occurrence. Each overflow was accompanied by coincident higher tremor. The sequence of episode 19 eruptive events is summarized in figure 1.92.

During periods of overflow, a quiet, partly crusted lava pond filled the crater, and an intermittent low dome fountain played over the site of the conduit. The pond would slowly rise until it was high enough to overflow the spillway. At the end of an overflow, the pond would abruptly drop in level, commonly draining completely back into the upper part of the pipe. Such repeated effusive events created a stack of short pahoehoe flows extending eastward from Puu Oo.

FIGURE 1.91.—Spillway chute at Puu Oo after episode 18. Note person (circle), 1.5 m tall, standing in middle ground for scale. Steep, locally overhanging walls are lined with glassy pahoehoe to a height of about 2 to 4 m, presumably reflecting depth of last flowing lava. Above that, walls are mantled by spatter, some of which has fallen into evacuated chute. View southwestward; photograph taken at 1534 H.s.t. April 27, 1984. Numerals (lower right) indicate date and time.

Four separate times, the eruptive activity developed into brief occurrences of high fountaining (fig. 1.92), vigorous flow production, and high tremor, similar to the style more typical of Puu Oo eruptions thus far. During these intervals, a fountain as high as 100 m or more (see fig. 1.24) played in the crater, and estimated output over the spillway was 100,000 to 200,000 m^3/h. Commonly, the fountain height would fluctuate over a period of 40 to 60 seconds from heights of less than 30 or 40 m to 100 m or more. As in episode 13, output of lava over the spillway, changing rapidly by possibly a factor of 2, fluctuated in concert with the changes in fountain height. In addition, brief interruptions in lava discharge and fountaining occurred during longer periods of high fountaining; these interruptions, specifically recorded only during the first high-fountain occurrence, lasted from a few seconds to 4 minutes. Resumption of discharge after each interruption was abrupt, and flow production and fountaining returned to full vigor almost instantaneously. A new flow front would surge rapidly down the channel that had drained moments before. During the high-fountain occurrences, lava coursed down the channel near the vent and then spread eastward, within 1 to 1.5 km of Puu Oo, as broad overlapping sheets, mainly of pahoehoe (pl. 5). Elongate lobes extended 1 to 2 km along the evacuated channels of the eastern and southeastern flows of episode 18.

The fourth and last high-fountain event ended early on May 17 (fig. 1.92). Many low-level lava-discharge events occurred during the ensuing 24 hours. A tube system developed close to the vent, and the flows that issued from it commonly formed thin, fluid pahoehoe sheets that spread rapidly; one of them advanced approximately 1 km in 36 minutes, for an average velocity of 1.6 km/h. In sampling and measuring temperatures in this overflow sheet, we were struck by the dense, degassed nature of the pahoehoe. Within several tens of minutes after its emplacement, we could walk on the pahoehoe toes or on the sheet itself without breaking through shelly spots. Repeated effusion of this type constructed an apron of smooth, firm pahoehoe extending about 1 km eastward of Puu Oo.

During the final hours of episode 19, on the night of May 17–18, overflows and periods of recognizable fountain activity in the vent were smaller in magnitude and more uniform in duration than previously. In fact, the style evolved to one resembling gas-piston activity; the lava column occasionally reached high enough during the rise part of a cycle to produce a short-lived overflow. During nearly 3 hours of careful timing and observation from

camp E between 1930 and 2215 H.s.t., the pattern of activity consisted of the following cycle: Increased glow and spattering over the conduit signaled the rise of the lava column; overflow (when the column rose sufficiently high), accompanied by low spattering and dome fountaining, would last about 2.5 to 7 minutes (the durations of individual events tended to shorten over time), sending short pahoehoe flows within several hundred meters of the vent; drainback of the column would be initiated by vigorous, diffuse bursts of spatter fragments and rapidly weakening glow; lava would then remain out of view for periods of 5 to 14 minutes; and then the cycle would

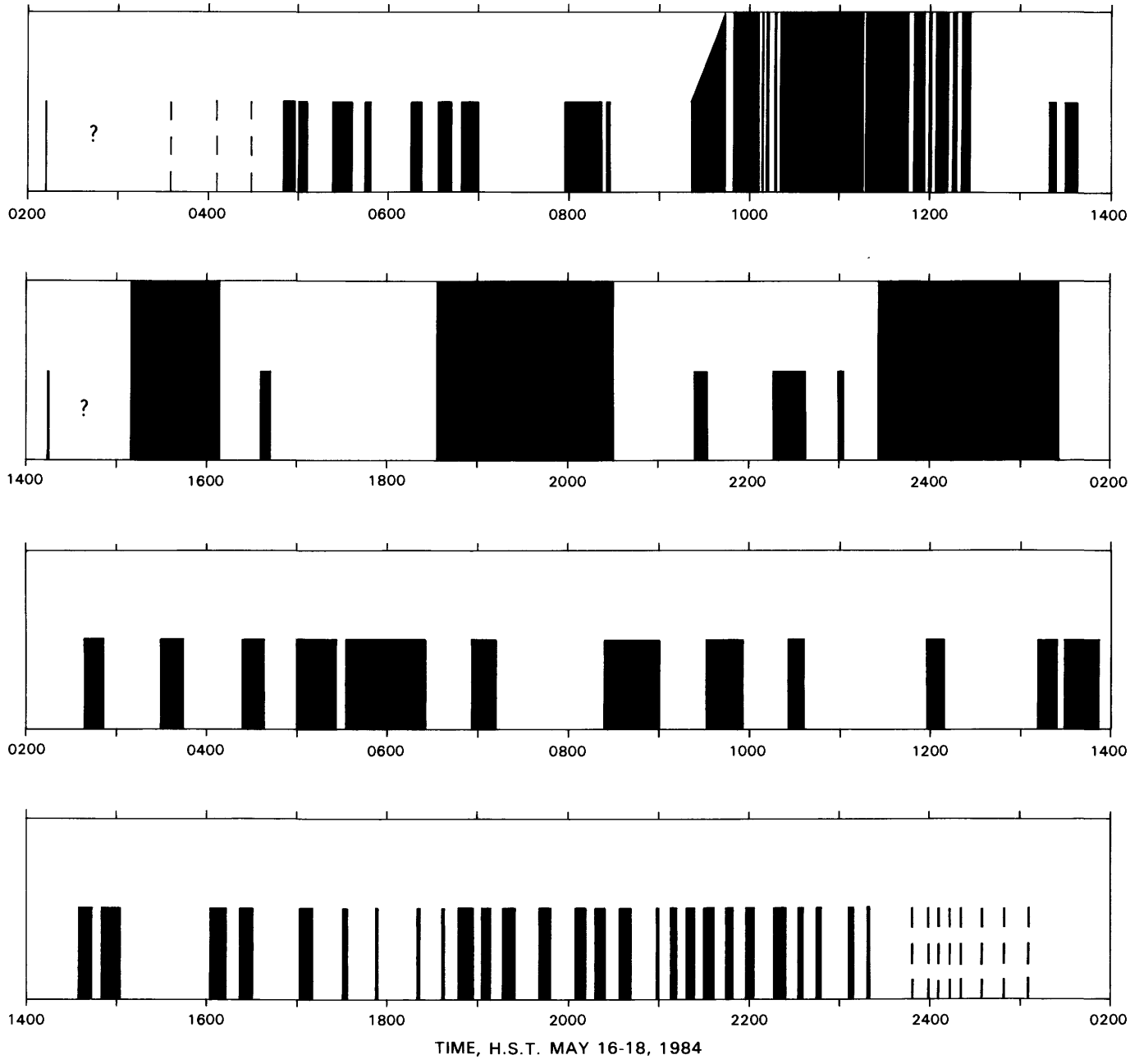

FIGURE 1.92.—Observed periods of eruptive activity during episode 19. Full-height bars, periods of high fountains and high lava output; half-height bars, periods of low-level activity, including dome fountaining and overflow. Dashed bars, individual film frames of strong glow only that may or may not reflect actual overflows from the crater. Data are from onsite observations, when available, and from time-lapse camera records (of lesser quality in terms of time control and completeness) otherwise; queried periods are times of questionable records.

begin anew. Episodic bursts of low tremor seen in the seismic record support the interpretation of this type of behavior as reflective of gas pistoning. At about 0030 H.s.t., tremor bursts associated with cyclic rise and fall of the lava column diminished and became highly irregular. The final overflow, marking the last gasp of episode 19, occurred at about 0049 H.s.t. May 18.

A helicopter overflight on the morning of May 18 revealed the surface of an active magma column about 30 m down the pipe. This column persisted at shallow levels in the pipe until episode 20.

Although fountains during episode 19 were never vigorous or sustained enough to significantly affect the exterior of Puu Oo, this new style of generally slow discharge with prolonged rise and fall of a body of lava within the crater drastically modified the shape of the crater (see fig. 1.19). The deep, bowl- to funnel-shaped interior was largely filled by new basalt. Its new raised crater floor was smooth and sloped gently inward toward the open conduit (see fig. 1.19*B*).

Episode 19 lava flows were thin where we could measure them. They covered an area of about 1.4×10^6 m^2 and had an estimated volume of about 2×10^6 m^3—a minimum value because we may have underestimated the aggregate thickness of episode 19 lava flows near the vent. However, this value agrees reasonably well with the volume we would estimate from our observation of lava discharge during the episode.

EPISODE 20 (JUNE 7-8, 1984)

An active magma column remained at shallow depths in the open conduit for the entire repose period following episode 19. For the first 10 days, most overflights and ground checks revealed a nearly continuous crust stretching across the conduit at a depth of about 15 m. A 3- to 4-m-wide opening emitted intermittent spatter, Pele's hair, and bursts of fume and burning gas as gas-piston activity proceeded. On May 29, we thought that lava-pond activity like that of episode 19 might be recurring. Accompanied by increased harmonic-tremor amplitude in the eruptive zone and slight deflation of Kilauea's summit, gas-piston activity stopped, and the magma column apparently assimilated any existing crust and rose to within 2 m of the top of the conduit. Its surface was open and actively roiled. Occasionally, it overflowed to produce short pahoehoe flows on the adjacent crater floor, and it built a low rampart of spatter around the pipe opening. On May 30, however, the column withdrew a short distance back into the pipe, and the harmonic tremor decayed into the pattern of cyclic bursts indicative of gas-piston activity. Fairly continuous gas-piston activity at shallow levels in the pipe continued through the rest of the repose period.

Episode 20 occurred almost entirely at night, and the only direct record of the eruptive activity is on time-lapse film. Continuous, low-level spattering began at 1911 H.s.t. June 7; at 2016 H.s.t., sporadic fountaining, 10 to 30 m high, became visible and slowly increased in vigor. Lava first overflowed the northeast rim and cascaded down the steep spillway chute at 2104 H.s.t.; the fountain was still low, about 15 m. At 2200 H.s.t., with dramatic suddenness, the level of output increased markedly; the fountain height increased by a factor of 20 to 30, to more than 300 m, flooding the north and northeast sides of the cone with heavy, fountain-fed spatter and pond overflow. A high but steadily decaying (see fig. 1.24), broad fountain and strong flow production continued uninterrupted until 0624 H.s.t. June 8, minutes after the first HVO observers arrived on the scene. The dying fountain sputtered back on at 0624:30 H.s.t. for 2.5 minutes before ceasing entirely. At 0925 H.s.t., 3 hours after the end of the eruption, several small bursts of spatter occurred. A helicopter overflight at 1100 H.s.t. revealed an open lava surface about 30 m down the open pipe; intermittent puffs of fume and bursts of tremor indicated that gas-piston activity had resumed.

Episode 20 lasted 9 hours and produced four distinct flows that traveled northwestward and northeastward from the Puu Oo cone (pl. 5). The northwestern flow, of spatter-fed aa, was broad and extended about a kilometer from Puu Oo. The three flows to the northeast were river fed. The two longest flows extended to the northeast as narrow lobes consisting of near-vent pahoehoe and distal aa. The longest of these northeastern flows traveled 3.8 km; its evacuated channel was floored with pahoehoe for much of its length. A smaller, bilobed flow to the northeast on top of episode 19 basalt was relatively narrow and predominantly aa. The erupted volume, distributed over an area of 1.6×10^6 m^2, was 4×10^6 m^3. Although episode 20 was brief and its volume small in comparison with most of its predecessors (table 1.3), it had the greatest average lava-discharge rate, 480,000 m^3/h.

Episode 20 raised the level of the crater floor about 5 to 10 m relative to the north rim, which had not changed significantly in elevation since episode 18 (see fig. 1.10*A*). The north rim was about 10 m above the level of the spillway, which was now a broad low in the northeast rim rather than a deep cleft (fig. 1.93). The west and south rims grew upward appreciably during episode 20 (fig. 1.10; compare figs. 1.19B and 1.93). The west rim, which formed the high point, was about 30 m higher than the floor at the spillway; it was about 130 m above the pre-1983 ground surface. The floor still formed a shallow basin; the top of the 20-m-diameter open pipe was about 10 m lower than the spillway surface. Episode 20 added more air-fall tephra to the southwest sector of the Puu Oo cone.

FIGURE 1.93.—Puu Oo after episode 20. Spillway, mantled with pahoehoe, is a broad low in northeast rim of crater. Top of 20-m-diameter open pipe is about 10 m lower than spillway surface. Steep west (distant) and south (left) walls grew upward appreciably during episode 20 and partly collapsed afterward, spilling talus onto smooth pahoehoe crater floor. High point on west rim is about 30 m higher than level of spillway and 130 m above pre-1983 ground surface. Spatter falling on north flank of Puu Oo (right) fed a massive flow in that sector. Air-fall tephra deposit on southwest flank is partly visible beyond rim and steep southeast flank of cone. View southwestward; photograph by G.E. Ulrich, taken June 14, 1984. Numerals (lower right) indicate year, month, and day.

REFERENCES

Buchanan-Banks, J.M., 1987, Structural damage and ground failures from the November 16, 1983, Kaoiki earthquake, Island of Hawaii, chap. 44 *of* Decker, R.W., Wright, T.L., and Stauffer, P.H., eds., Volcanism in Hawaii: U.S. Geological Survey Professional Paper 1350, v. 2, p. 1187–1220.

Holcomb, R.T., 1980, Preliminary geologic map of Kilauea volcano, Hawaii: U.S. Geological Survey Open-File Report 80-796, scale 1:50,000, 2 sheets.

Jackson, D.B., Swanson, D.A., Koyanagi, R.Y., and Wright, T.L., 1975, The August and October 1968 east rift eruptions of Kilauea Volcano, Hawaii: U.S. Geological Survey Professional Paper 890, 33 p.

Koyanagi, R.Y., Endo, E.T., Tanigawa, W.R., Nakata, J.S., Tomori, A.H., and Tamura, P.N., 1984, Kaoiki, Hawaii earthquake of November 16, 1983: A preliminary compilation of seismographic data at the Hawaiian Volcano Observatory: U.S. Geological Survey Open-File Report 84-798, 35 p.

Lipman, P.W., and Banks, N.G., 1987, Aa flow dynamics, Mauna Loa 1984, chap. 57 *of* Decker, R.W., Wright, T.L., and Stauffer, P.H., eds., Volcanism in Hawaii: U.S. Geological Survey Professional Paper 1350, v. 2, p. 1527–1567.

Lockwood, J.P., Banks, N.G., English, T.T., Greenland, L.P., Jackson, D.B., Johnson, D.J., Koyanagi, R.Y., McGee, K.A., Okamura, A.T., and Rhodes, J.M., 1985, The 1984 eruption of Mauna Loa Volcano, Hawaii: Eos (American Geophysical Union Transactions), v. 66, no. 16, p. 169–171.

Malin, M.C., 1980, Lengths of Hawaiian lava flows: Geology, v. 8, no. 7, p. 306–308.

Moore, J.G., and Koyanagi, R.Y., 1969, The October 1963 eruption of Kilauea Volcano, Hawaii: U.S. Geological Survey Professional Paper 614-C, p. C1–C13.

Moore, R.B., Helz, R.T., Dzurisin, Daniel, Eaton, G.P., Koyanagi, R.Y., Lipman, P.W., Lockwood, J.P., and Puniwai, G.S., 1980, The 1977 eruption of Kilauea volcano, Hawaii: Journal of Volcanology and Geothermal Research, v. 7, no. 3-4, p. 189–210.

Neal, C.A., and Decker, R.W., 1983, Surging of lava flows at Kilauea volcano, Hawaii [abs.]: Eos (American Geophysical Union Transactions), v. 64, no. 5, p. 904.

Peterson, D.W., 1976, Processes of volcanic island growth, Kilauea volcano, Hawaii, 1969–1973: International Association of Volcanology and Chemistry of the Earth's Interior, Symposium on Andean and Antarctic Volcanology Problems, Santiago, Chile, 1974, Proceedings, p. 172–189.

Peterson, D.W., and Swanson, D.A., 1974, Observed formation of lava tubes during 1970–71 at Kilauea volcano, Hawaii: Studies in Speleology, v. 2, p. 209–222.

Richter, D.H., Ault, W.U., Eaton, J.P., and Moore, J.G., 1964, The 1961 eruption of Kilauea Volcano, Hawaii: U.S. Geological Survey Professional Paper 474-D, p. D1–D34.

Shaw, H.R., 1969, Rheology of basalt in the melting range: Journal of Petrology, v. 10, no. 3, p. 510–535.

Shaw, H.R., Peck, D.L., Wright, T.L., and Okamura, R., 1968, The viscosity of basaltic magma: An analysis of field measurements in Makaopuhi lava lake, Hawaii: American Journal of Science, v. 266, no. 4, p. 225–264.

Sparks, R.S.J., Pinkerton, H., and Hulme, G., 1976, Classification and formation of lava levees on Mount Etna, Sicily: Geology, v. 4, no. 5, p. 269–271.

Swanson, D.A., 1972, Magma supply rate at Kilauea volcano, 1952–1971: Science, v. 175, no. 4018, p. 169–170.

——— 1973, Pahoehoe flows from the 1969–71 Mauna Ulu eruption, Kilauea Volcano, Hawaii: Geological Society of America Bulletin, v. 84, no. 2, p. 615–626.

Swanson, D.A., Duffield, W.A., Jackson, D.B., and Peterson, D.W., 1979, Chronological narrative of the 1969–71 Mauna Ulu eruption of Kilauea Volcano, Hawaii: U.S. Geological Survey Professional Paper 1056, 55 p.

Tilling, R.I., Christiansen, R.L., Duffield, W.A., Endo, E.T., Holcomb, R.T., Koyanagi, R.Y., Peterson, D.W., and Unger, J.D., 1987, The 1972–74 Mauna Ulu eruption, Kilauea Volcano: An example of quasi-steady-state magma transfer, chap. 16 *of* Decker, R.W., Wright, T.L., and Stauffer, P.H., eds., Volcanism in Hawaii: U.S. Geological Survey Professional Paper 1350, v. 1, p. 405–469.

Wadge, G., 1978, Effusion rate and the shape of aa lava flow-fields on Mount Etna: Geology, v. 6, no. 8, p. 503–506.

Walker, G.P.L, 1973, Lengths of lava flows, *in* Guest, J.E., and Skelhorn, R.R., eds., Mount Etna and the 1971 eruption: Royal Society of London Philosophical Transactions, ser. A., v. 274, no. 1238, p. 107–118.

Wolfe, E.W., Garcia, M.O., Jackson, D.B., Koyanagi, R.Y., Neal, C.A., and Okamura, A.T., 1987, The Puu Oo eruption of Kilauea Volcano, episodes 1–20, January 3, 1983 to June 8, 1984, chap. 17 *of* Decker, R.W., Wright, T.L., and Stauffer, P.H., eds., Volcanism in Hawaii: U.S. Geological Survey Professional Paper 1350, v. 1, p. 471–508.

Wright, T.L., Kinoshita, W.T., and Peck, D.L., 1968, March 1965 eruption of Kilauea volcano and the formation of Makaopuhi lava lake: Journal of Geophysical Research, v. 73, no. 10, p. 3181–3205.

2. LAVA SAMPLES, TEMPERATURES, AND COMPOSITIONS

By CHRISTINA A. NEAL, TONI J. DUGGAN, EDWARD W. WOLFE, and ELAINE L. BRANDT

CONTENTS

ABSTRACT

A total of 173 lava temperatures were measured and 346 samples were collected during the first 20 episodes of the Puu Oo eruption of Kilauea. Of these samples, 43 were selected for classical chemical analysis. This chapter lists these data and briefly discusses field techniques and results. During the first 11 eruptive episodes, equilibrium temperatures in pahoehoe increased steadily from a range of 1,098–1,125 °C during episode 1 to 1,133–1,144 °C during episode 11. Subsequent measured lava temperatures through episode 20 remained fairly steady within the range of 1,129–1,147 °C. Chemical analyses show a general correspondence between progressively changing composition and measured temperatures.

INTRODUCTION

The Puu Oo eruption of Kilauea Volcano's middle east rift zone began on January 3, 1983. By June 8, 1984, 20 episodes in the continuing eruption had produced approximately 240×10^6 m^3 of basalt. Though strikingly similar in style to the first stage of the Mauna Ulu eruption (Swanson and others, 1979), the Puu Oo eruption is unique in Kilauea's historical record because of the duration of its episodic series, the nature of the resulting lava field, and the size of the principal vent structure. One important part of the monitoring effort by the Hawaiian Volcano Observatory has been to systematically measure lava temperatures and to collect samples of successive lava flows and other eruptive products. In addition, the major-element composition of samples representing each episode has been determined by classical wet chemical methods (Peck, 1964). This chapter presents a compilation of these data sets along with pertinent supporting information. Its purpose is to provide the reader with: (1) a discussion of our strategy, methods, and the conditions of sampling and temperature measurements; (2) a careful documentation and listing of all sample, temperature, and compositional data from episodes 1 through 20; and (3) a summary of the results. For more detailed discussion of each eruptive episode and the geologic context of specific samples and temperatures, the reader is referred to the eruption narrative and discussion of geologic observations in chapter 1. The petrology of the lavas is discussed in chapter 3.

Acknowledgments.—Many individuals have generously shared their time, energy, and enthusiasm in the Hawaiian Volcano Observatory's monitoring program at Puu Oo. We thank them all for their assistance. We especially thank Norman G. Banks for his leadership and instruction in thermocouple techniques.

METHODS

LAVA TEMPERATURES

All the lava temperatures reported in this chapter (tables 2.1, 2.2) were obtained using Inconel-clad Chromel-Alumel thermocouples. These probes worked well under the difficult conditions of flowing lava, active vents, and field transport. All episode 1 temperatures and all temperatures in aa flows were measured with ¼-in.-diameter thermocouples. From episode 2 on, pahoehoe temperatures were measured with a 1/16-in.-diameter thermocouple, normally preferred because of its minimal thermal mass and, thus, rapid equilibration. Generally, the 1/16-in.-thermocouple was wound around a light steel bar for support, with the tip of the thermocouple extended 10 to 20 cm beyond the end of the supporting bar. Temperatures were read from a direct-reading digital thermometer attached to the thermocouple. Previous use of thermocouple equipment to measure temperatures of basaltic melt was discussed by, for example, Wright and others (1968), Wright and Okamura (1977), and Peck (1978). Techniques for similar temperature measurements in pyroclastic products were described by Banks and Hoblitt (1982). For a more detailed description of specific thermocouple hardware, see the report by Lipman and Banks (1987).

After several measurements were made with the Inconel sheath intact, thermal and mechanical stress commonly rendered the thermocouple useless. However, after we discarded 3 to 6 cm of the faulty end and exposed the internal wires with a pair of strippers, the wires could be

TABLE 2.1.—*Summary of equilibrium temperatures measured during the vigorous parts of episodes 1 through 20 of the Puu Oo eruption of Kilauea Volcano*

[Temperatures measured in melt during low-level activity between eruptive episodes and in cool, spatter-fed flows are omitted. Two equilibrium temperatures measured in blocky aa 6 km from the vent during episode 3, both lower than 1,000 °C, are also omitted]

Episode	Number of equilibrium temperatures	Average measured temperature (°C)	Range of measured temperatures (°C)
1	8	1,117	1,098-1,125
2	18	1,115	1,111-1,120
3	28	1,120	1,111-1,129
4	9	1,125	1,115-1,132
5	4	1,127	1,125-1,129
6	4	1,132	1,126-1,138
7	10	1,135	1,130-1,141
8	2	1,129	1,128-1,130
[1]9	---	---	---
10	6	1,138	1,134-1,142
11	5	1,140	1,133-1,144
12	3	1,136	1,135-1,137
13	12	1,139	1,129-1,147
14	2	1,137	1,136-1,137
15	2	1,138	1,136-1,139
16	8	1,139	1,135-1,142
17	4	1,133	1,131-1,137
18	6	1,139	1,136-1,144
19	2	1,140	1,138-1,141
[1]20	---	---	---

[1]No equilibrium melt temperatures were obtained during episodes 9 and 20.

twisted together by hand and immersed in melt with a high degree of success. This vastly lengthened the life of a single thermocouple wire and made repeated measurements of temperatures possible. Also, bare-wire thermocouples generally equilibrated more quickly than sheathed thermocouples, a trait preferred by most workers. Sheathed and bared thermocouple wires recorded identical temperatures when tested in a furnace over a temperature range comparable to those of our field measurements. Contamination problems leading to erroneous temperatures, such as those documented by Wright and Okamura (1977), were probably eliminated by the short immersion times (generally several minutes for the ¼-in.-diameter thermocouple but less than 1 minute for the 1/16-in.-diameter thermocouple).

Temperature measurements were most successful in pahoehoe melt that was slow moving and well insulated from exposure to the atmosphere. Thus, ideal situations included oozes through cracks in accretionary levees forming at the edges of lava rivers and short, tube-fed toes at pahoehoe flow fronts or margins. These conditions consistently resulted in the highest temperatures obtained in episodes 1 through 20, and presumably most closely approximate true eruption temperatures. A variation of about 5 °C in the temperatures measured in pahoehoe toes at the same locations over periods of several hours probably reflects heterogeneities in the temperatures of melt erupted; no obvious systematic change in subaerial conditions (degree of insulation or rate of transport through the evolving network of channels and tubes) can be isolated to explain this variation. However, differing rates, durations, and conditions of transport, superimposed on possible eruptive thermal heterogeneities, may explain observed variations of 5 to 15 °C in measured pahoehoe temperatures over a period of days.

Temperatures of spatter-fed flows, of thin, rapidly cooling overflows from lava rivers, and of rapidly moving melt in the highly sheared zone at the edges of leveed lava rivers were all consistently lower than those measured in insulated pahoehoe. For the purposes of this report, a "short-lived overflow from a lava river" is defined as a transient overbank deposit of pahoehoe, generally less than 1 m thick and mobile for periods of no more than a few minutes. "Long-lived overflows" or "breakouts" refer to major spills from the lava river that endured for tens of minutes to several hours. Most of these flows were active long enough to develop into a widespread, locally tube-fed pahoehoe flow.

Three temperatures were measured inside vents that were actively degassing and incandescent. Low-level, repose-period eruptive activity that produced short pahoehoe flows or active lava ponds inside the Puu Oo vent was also the source of some of the temperature measurements listed in tables 2.1 and 2.2.

In nearly all these situations, the technique for obtaining temperatures of melt was similar. After several seconds of preheating by holding the thermocouple adjacent to exposed melt (several minutes for the ¼-in.-diameter thermocouples), 3 to 10 cm of the wire was immersed in melt (fig. 2.1) and worked back and forth slowly to maintain fluid-wire contact and to prevent a sheath of solidified lava from forming on the wire. The larger thermocouple was particularly prone to accumulate such a sheath, which would insulate the thermocouple and prevent it from reaching equilibrium with the melt during the measurement. It was generally easiest to have a team of two people working together to obtain a temperature measurement. A thin shield of corrugated aluminum (approximately 3 by 4 ft, with two nylon-rope loops for handles; see fig. 2.1) was effective in reflecting enough heat to protect workers and permit a close approach to the molten lava. One person would immerse and maneuver the thermocouple, attempting to avoid hitting any developing crust that might damage or break the wire,

while the other person would read aloud the increasing temperature values. After many minutes with the large thermocouple but commonly within tens of seconds after immersion for the thin one, the thermometer would settle on a single reading or fluctuate within 1 °C in either direction from a single temperature value. The temperature recorded was the value at which the thermometer appeared to stabilize, defined in this chapter as the equilibrium temperature. In some cases, the thermocouple wire would break, or conditions around the probe would deteriorate, and stable temperatures were not obtained. Here, recorded temperatures are considered nonequilibrium, minimum values, denoted with the ≥ symbol in table 2.2.

Temperatures of aa flows were measured with the more rigid ¼-in.-diameter thermocouple. For these measurements, the probe was preheated, again by holding the thermocouple inches from the flow surface to lessen the thermal contrast, and inserted into the incandescent matrix between the cooler aa fragments. The thermocouple was then held in place to be gradually engulfed by the advancing flow. In some cases, at penetrations ranging from 0.2–0.3 to 2–3 m, the probe apparently broke through the aa carapace into more continuous melt. During episode 3, temperatures of 1,094 and 1,099 °C were determined in an aa flow 6 km from the vent by this means. Those temperatures were 10 to 30 °C lower than those measured within 1 km of the vent earlier in episode 3.

During episode 16, temperatures were measured in short-lived breakouts from aa flows. Here, the lava was commonly fluid enough to allow us to use the 1/16-in.-diameter thermocouple; at times, the thermocouple was worked successfully through a relatively thin aa carapace

FIGURE 2.1.—Geologists measure temperature of pahoehoe toe about 250 m northeast of Puu Oo. Toe is fed by sluggish pahoehoe flow that branched from main lava river. Flexible, 1/16-in.-diameter thermocouple is supported by thin but rigid steel rod. Aluminum shield protects workers from radiant heat. Photograph by J.D. Griggs, taken approximately 1200 m. H.s.t. January 31, 1984.

into the more plastic flow interior. Temperatures measured under these conditions ranged from 1,135 to 1,138 °C (table 2.2), even at distances as far as 6 to 7 km from the vent. These high temperatures were only 4 to 7 °C lower than the pahoehoe temperatures measured within 2 km of Puu Oo during the same eruptive episode.

SAMPLING

Samples were collected as soon as possible after temperatures were measured, so as to closely correlate the data in space and time. Most samples were taken by using a rock hammer. Pahoehoe could easily be scooped with the hammer, placed in an empty coffee can or similar container, and quenched with water. Water served the dual purpose of minimizing groundmass crystallization and cooling the glassy sample so that it could be detached from the hammer and handled. Once in the can, the water was allowed to cool the sample and then poured off; the sample was bagged in a heavy canvas sample bag and labeled. At times, a bent steel bar or steel pipe was used to sample melt too difficult to approach within arm's reach. Aa flows were sampled similarly, although samples were not strictly melt but rather fragments hacked loose with a hammer. Early in the eruption, spatter bombs from low-fountaining fissure vents were collected regularly. Most bombs were collected while still molten and were promptly quenched with water. As the Puu Oo vent became established and the fountains more difficult to approach, hot samples of molten spatter were collected less frequently, and the emphasis in sampling shifted to pahoehoe river and flow samples.

We tried to be as comprehensive as possible in sampling melt from successive episodes. Specifically, our objective was to collect samples of each of the following: (1) low-volume, intermittent flows and spatter produced within the vent between most of the major eruptive episodes; (2) lava erupted early in each episode; (3) representative samples throughout the episode; and (4) some of the last melt to be erupted. Our success varied. For most of episode 9, broad, hot, newly solidified sheets of pahoehoe prevented safe access to the lava river, and so we had to settle for samples of air-cooled, solidified basalt. During episode 13, however, we had sufficient help to sample day and night, as well as good access to melt, and we were thus able to measure temperatures and sample overflows from the lava river approximately every 2 hours.

In addition to samples of melt or spatter, relatively dense, slowly cooled samples ("dense-rock samples," table 2.2) from lava flows of each episode were taken for petrographic study. Samples of lightweight tephra produced during high-fountaining events were collected several times during episode 3 and after episodes 9, 12, and 14 through 18. Systematic, repetitive sampling of tephra during episode 16 was reported elsewhere (Paces and Rose, 1984).

CHEMICAL ANALYSES

RESULTS

A plot of lava temperatures against time (fig. 2.2) for episodes 1 through 19 reveals a simple trend. In general, between episodes 1 and 11, average equilibrium temperatures gradually but steadily increased from 1,117 °C during episode 1 to 1,140 °C during episode 11 in November 1983 (table 2.1). Thereafter, although our total range of measured temperatures was from 1,129 to 1,147 °C, average eruptive-episode temperatures of 1,133 to 1,140 °C dominated, with little variation.

Compositional trends of the erupted lavas, recorded in the variation of major oxides, show a general pattern of progressive enrichment over time of CaO and MgO, with correlative depletion of Fe and incompatible elements. For CaO and $Na_2O + K_2O$ (fig. 2.3), this compositional change displays a striking, qualitative similarity to the pattern of temperature changes discussed above. Thus, changes over time in lava temperature apparently reflect progressive compositional change of the erupting melt. The implications of this apparently sympathetic evolution of temperature and composition are discussed by Wolfe and others (1987).

EXPLANATION OF TABLES

Most of the information listed in table 2.2 is self-explanatory. The sample identification (for example, 1/84KE14-231F) consists of the following: month and year collected (1/84), the designation "KE", which indicates Kilauea's east rift zone, the number of the episode during which the sample was erupted (14), a unique identifying number (231), and either an "F" for flow sample or an "S" for a sample of spatter or air-fall tephra. Underlined sample identifications flag samples for which classical chemical analyses are listed in table 2.3. In most cases, all the samples from a particular episode are sequential; exceptions are noted, and additional sample identifications cited. Samples collected during low-level activity between eruptive periods bear the number of the succeeding eruptive episode. "Quench" refers to whether or not the molten sample was cooled rapidly in water. "Location and comments" contains a brief description of the conditions, setting, and source of the sample or temperature. Information presented under this heading is of varying quality and comprehensiveness; we have

attempted here to be concise and yet as complete as the record allows. Further details are provided in chapter 1.

VENT NOMENCLATURE

Episode 1 eruptive vents referred to in table 2.2 were named after the time or date of their initial activation (for example, 1708, 1123, January 23). The locations of these and other episode 1 vents are shown in figure 2.4.

The O vent of episode 3 was named for its proximity on the topographic map to the letter "O" in the word "flow." Beginning with episode 4, the principle vent structure was Puu O, a cinder and spatter cone that grew just uprift of the O vent and eventually buried it completely (fig. 2.4). Subsequently, elders of the Hawaiian community in Kalapana renamed the two large vent structures of the 1983–84 eruption. The 1123 vent became Puu Halulu, a name which refers to the chanting sound heard in Kalapana during eruptions. Puu O became Puu Oo, after an extinct native bird, the ʻoʻo, that once lived in the area.

REFERENCES CITED

Banks, N.G. and Hoblitt, R.P., 1982, Summary of temperature studies of 1980 deposits, *in* Lipman, P.W., and Mullineaux, D.R., eds., The 1980 eruptions of Mount St. Helens, Washington: U.S. Geological Survey Professional Paper 1250, p. 295–313.

Lipman, P.W., and Banks, N.G., 1987, Aa flow dynamics, Mauna Loa 1984, chap. 57 *of* Decker, R.W., Wright, T.L., and Stauffer, P.H., eds., Volcanism in Hawaii: U.S. Geological Survey Professional Paper 1350, v. 2, p. 1527–1567.

Paces, J.B., and Rose, W.I., Jr., 1984, Hourly volatile and chemical evolution during Phase 16 of the 1983–84 Kilauea east rift zone eruption [abs.]: Eos (American Geophysical Union Transactions), v. 65, no. 45, p. 1130–1131.

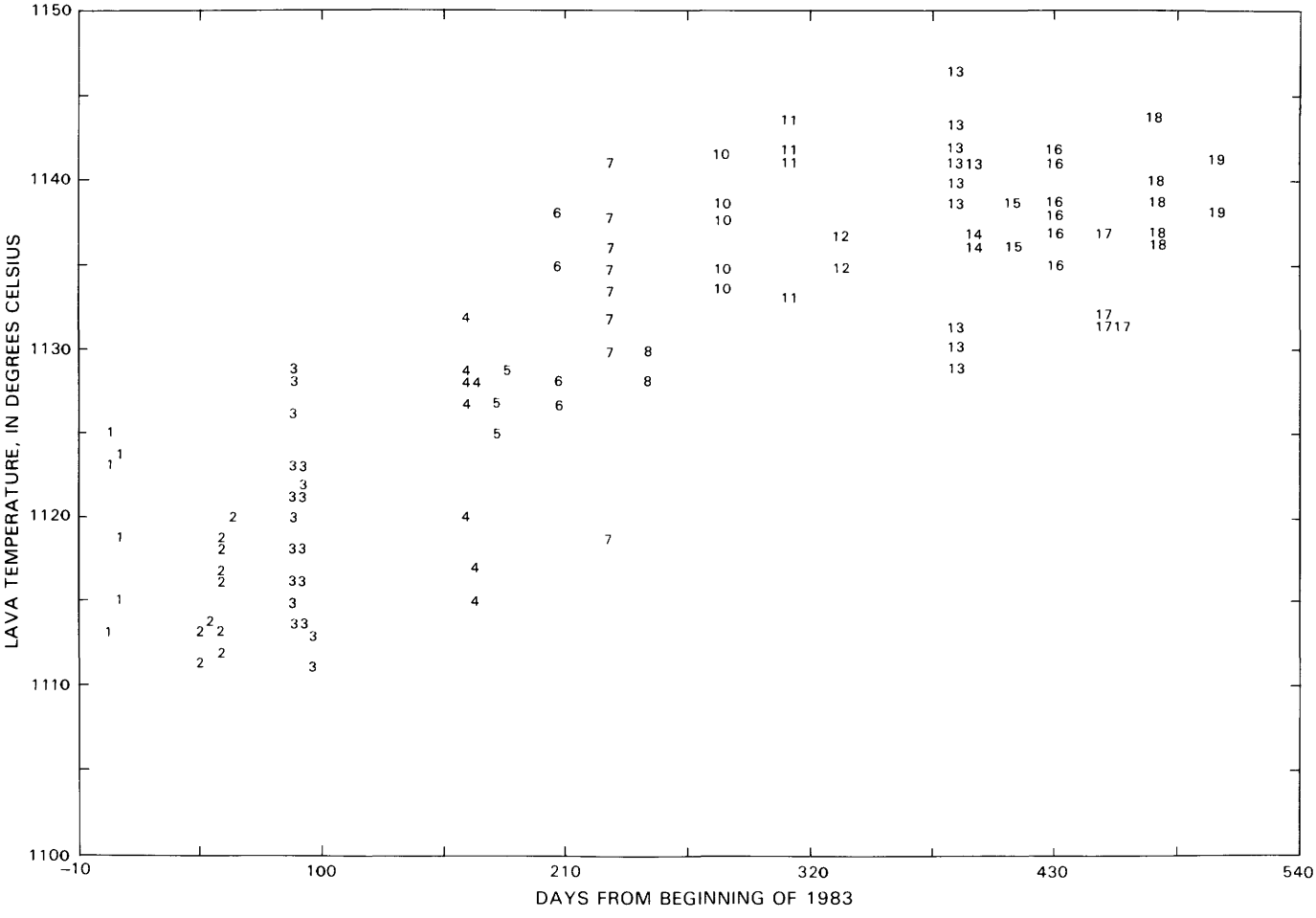

FIGURE 2.2.—Equilibrium lava temperatures ≥1,100 °C measured during vigorous parts of episodes 1 through 19 (no equilibrium temperatures were measured during episodes 9 and 20). Numbers correspond to episodes.

Peck, D.L., 1978, Cooling and vesiculation of Alae lava lake, Hawaii: U.S. Geological Survey Professional Paper 935-B, 59 p.

Peck, L.C., 1964, Systematic analyses of silicates: U.S. Geological Survey Bulletin 1170, 89 p.

Swanson, D.A., Duffield, W.A., Jackson, D.B., and Peterson, D.W., 1979, Chronologic narrative of the 1969-71 Mauna Ulu eruption of Kilauea Volcano, Hawaii: U.S. Geological Survey Professional Paper 1056, 55 p.

Wolfe, E.W., Garcia, M.O., Jackson, D.B., Koyanagi, R.Y., Neal, C.A., and Okamura, A.T., 1987, The Puu Oo eruption of Kilauea Volcano, episodes 1-20, January 3, 1983 to June 8, 1984, chap. 17 *of* Decker, R.W., Wright, T.L., and Stauffer, P.H., eds., Volcanism in Hawaii: U.S. Geological Survey Professional Paper 1350, v. 1, p. 471-508.

Wright, T.L., Kinoshita, W.T., and Peck, D.L., 1968, March 1965 eruption of Kilauea volcano and the formation of Makaopuhi lava lake: Journal of Geophysical Research, v. 73, no. 10, p. 3181-3205.

Wright, T.L., and Okamura, R.T., 1977, Cooling and crystallization of tholeiitic basalt, 1965, Makaopuhi lava lake, Hawaii: U.S. Geological Survey Professional Paper 1004, 78 p.

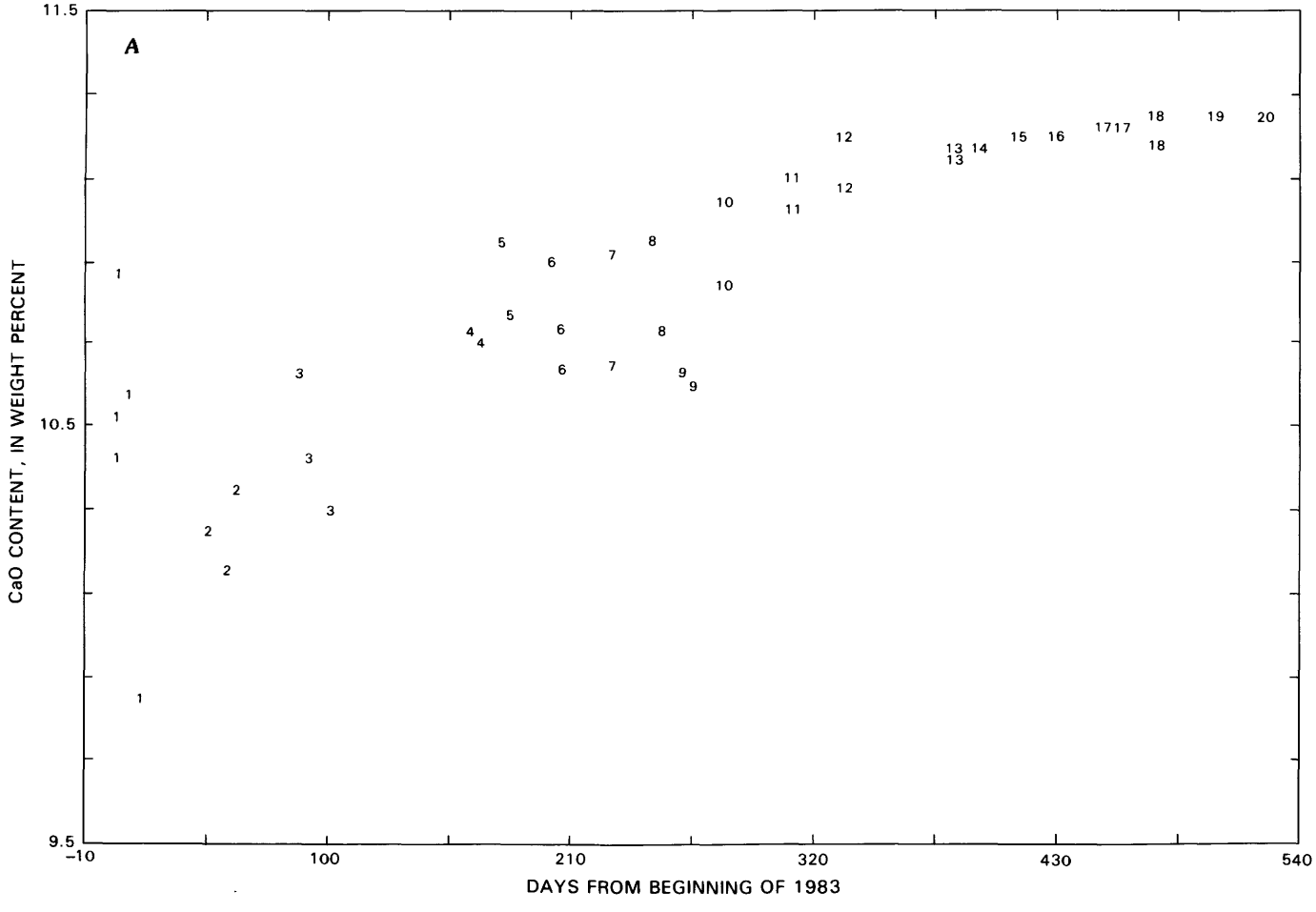

FIGURE 2.3.—Weight percent CaO (*A*) and $Na_2O + K_2O$ (*B*) versus time for 41 samples analyzed from episodes 1 through 20. Complete wet chemical analyses are listed in table 2.3. Numbers correspond to episodes.

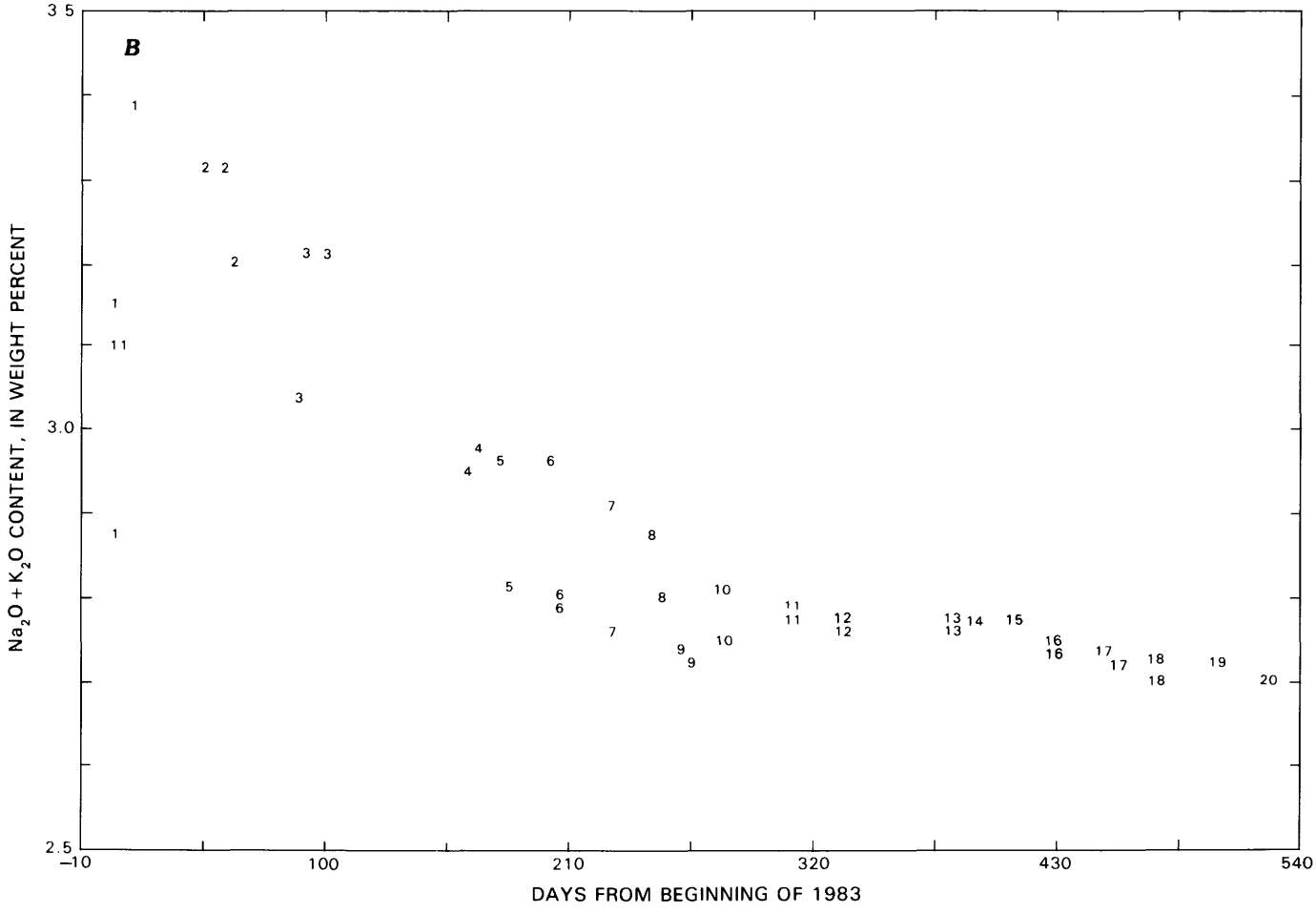

FIGURE 2.3.—Continued

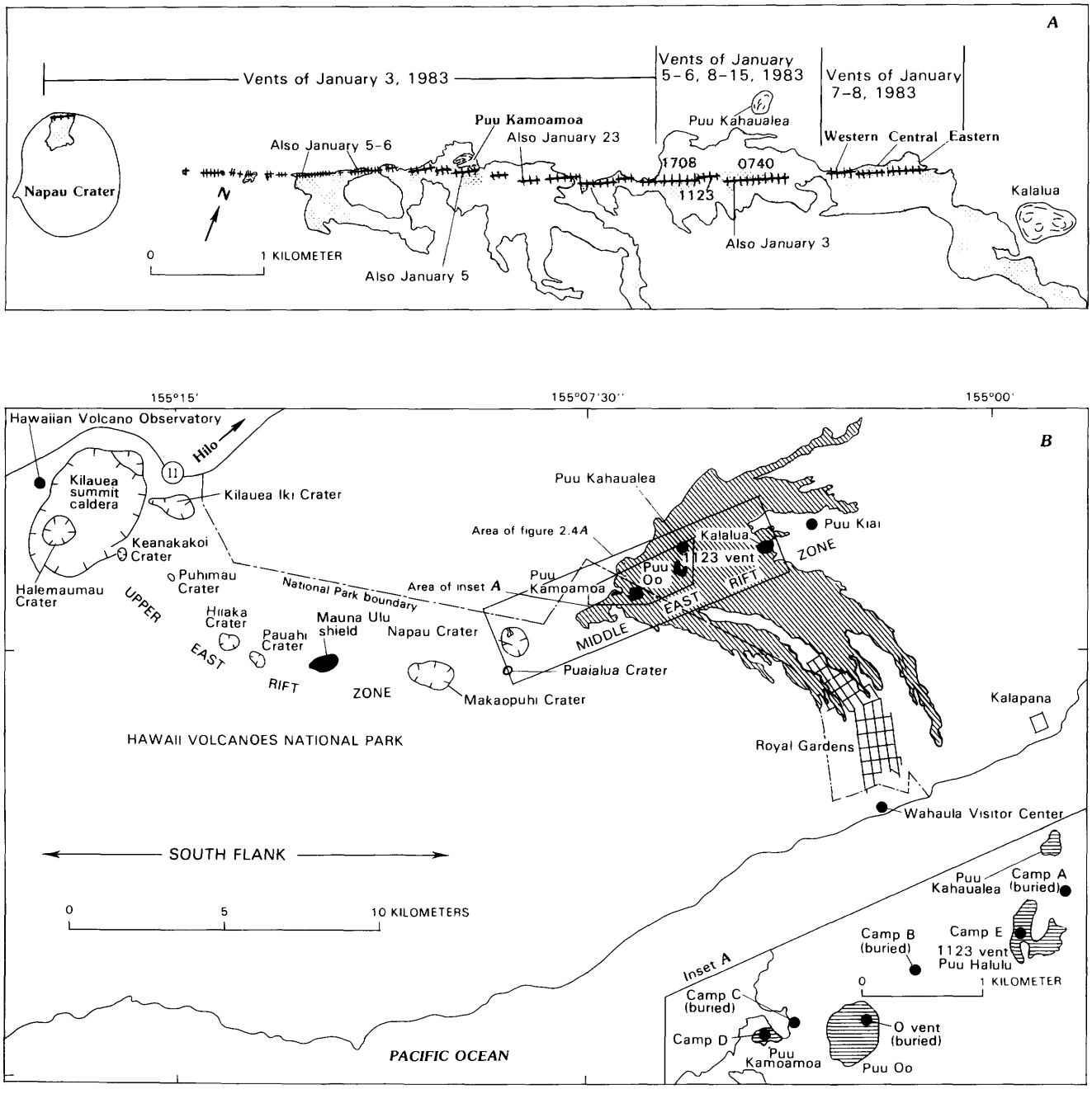

FIGURE 2.4.—Locations of vents and features referred to in table 2.2. *A*, Vents of episode 1 (hachured line) and generalized parts of episode 1 lava flows (shaded). *B*, Index map of Kilauea's summit, south flank, and upper and middle east rift zones. Selected prominent historical and prehistoric vents of the east rift zone are shown in black. Area covered by lava flows of episodes 1 through 20 is shown by lined pattern. Locations of principal vents of episodes 3 through 20 are shown in inset *A*: 1123 vent (Puu Halulu), O vent (buried), and Puu Oo (post-episode 20).

TABLES 2.2, 2.3

TABLE 2.2.—*Samples collected and temperatures measured during episodes 1 through 20 of the Puu Oo eruption of Kilauea Volcano*

[Underlined sample identifications are those for which analyses are listed in table 2.3; ---, sample not collected, time not recorded, or temperature not measured; ?, collector, date, or quench history unknown; do., ditto]

Sample	Collector	Date	Time (H.s.t.)	Temperature (°C)	Quench	Location and comments
1/83KE1-1F	E. Wolfe---------	01-03-83	0230	---	yes	Small, spiny pahoehoe flow from vent 1 km northeast of northeastern part of Napau Crater rim. Sample collected when solid but still incandescent.
1/83KE1-2F	J. Lockwood, R. Moore.	01-03-83	0508	---	?	Active flow, 20 m northwest of Puu Kamoamoa, approximately 120 m from vent.
1/83KE1-3S	R. Moore---------	01-03-83	0548	---	?	Spatter from small vent on east side of Puu Kamoamoa.
1/83KE1-4S	E. Wolfe---------	01-03-83	0605	---	yes	Molten spatter from vent 2.6 km northeast of northeastern part of Napau Crater rim.
---	do----------	01-03-83	0630	1,113	---	Pahoehoe from west end of erupting vent, sampled at 0605 H.s.t. (above).
1/83KE1-5S	do----------	01-03-83	0704	---	yes	Molten spatter from vent 2.6 km northeast of northeastern part of Napau Crater rim.
1/83KE1-6S	J. Lockwood------	01-03-83	0958	---	yes	Spatter from vent on west flank of Puu Kamoamoa. Sample collected as vent was dying.
1/83KE1-7S	N. Banks---------	01-05-83	1140	---	no	Spatter from 1123 vent.
1/83KE1-8F	do----------	01-05-83	1240	≥1,108	yes	Flow from 0740 vent, 30-80 m north of vent.
1/83KE1-9F	do----------	01-03-83	1515	1,125	yes	Flow from 0740 vent, 50 m north of vent.
1/83KE1-10F	E. Wolfe, N. Banks.	01-05-83	1530	1,123	yes	Flow from 0740 vent, 100 m north of vent.
1/83KE1-11S	N. Banks---------	01-05-83	2159	---	yes	Molten spatter from west end of 1708 vent.
1/83KE1-12S	E. Wolfe---------	01-06-83	1000	---	?	Spatter ejected from 1708 vent during vigorous gas emission.
1/83KE1-13F	do----------	01-06-83	1058	---	yes	Spiny pahoehoe flow from 0740 vent, north of vent.
1/83KE1-14F	do----------	01-06-83	1240	≥1,116	yes	Pahoehoe flow from 0740 vent, 250 m north of vent. Lava froze to thermocouple.
1/83KE1-15F	do----------	01-06-83	1736	---	yes	Pahoehoe flow near northeast end of 0740 vent.
1/83KE1-16S	N. Banks---------	01-07-83	0930	---	yes	Spatter ejected from 0740 vent during vigorous gas emission.
1/83KE1-17S	N. Banks, J. Buchanan-Banks.	01-07-83	1100	---	yes	Molten spatter from western January 7 vent.
1/83KE1-18S	N. Banks, T. Duggan, J. Buchanan-Banks.	01-07-83	1500	---	yes	Molten spatter from western part of western January 7 vent.
1/83KE1-19S	E. Wolfe---------	01-07-83	1735	---	yes	Molten spatter from western January 7 vent.
1/83KE1-20S	do----------	01-07-83	2005	---	yes	Molten spatter from western January 7 vent, from center of 100-m-long fissure fountain.
1/83KE1-21S	do----------	01-07-83	2230	---	yes	Do.
1/83KE1-22F	do----------	01-08-83	0240	1,124	yes	Pahoehoe toe from west end of western January 7 vent, 25 m from vent.

TABLE 2.2.—*Samples collected and temperatures measured during episodes 1 through 20 of the Puu Oo eruption of Kilauea Volcano*—Continued

Sample	Collector	Date	Time (H.s.t.)	Temperature (°C)	Quench	Location and comments
1/83KE1-23S	N. Banks---------	01-08-83	0918	---	yes	Spatter ejected from 0740 vent during vigorous gas emission.
1/83KE1-24S	do----------	01-08-83	1214	---	yes	Do.
1/83KE1-25S	do----------	01-08-83	1454	---	yes	Do.
1/83KE1-26S	D. Jackson-------	01-08-83	2104	---	yes	Molten spatter from 1708 vent.
1/83KE1-27F	do----------	01-08-83	2230	---	yes	Pahoehoe toe of flow from 1708 vent.
1/83KE1-28F	do----------	01-08-83	2249	---	yes	Do.
1/83KE1-29F	do----------	01-09-83	0153	---	yes	Do.
1/83KE1-30F	J. Lockwood------	01-10-83	0600	---	no	Inactive flow, about 300 m north of 0740 vent. Flow probably came from 1708 vent early on January 9. Sample collected when cold.
1/83KE1-31S	do----------	01-10-83	0720	---	?	Spindle bomb ejected from 1708 vent during vigorous gas emission.
1/83KE1-32S	N. Banks---------	01-10-83	1137	---	yes	Molten spatter from 1708 vent.
1/83KE1-33S	J. Buchanan-Banks.	01-10-83	1346	---	yes	Do.
1/83KE1-34F	N. Banks---------	01-11-83	0315	1,115	yes	Flow from 1708 vent, 30 m north of vent.
---	do----------	01-11-83	0420	1,119	---	Do.
1/83KE1-35F	do----------	01-11-83	0730	1,115	yes	Slabby pahoehoe flow from 1708 vent, about 600 m northeast of vent.
1/83KE1-36F	E. Wolfe---------	01-11-83	0920	---	yes	Spiny to slabby pahoehoe flow from 1708 vent, 100 m north of vent.
---	do----------	01-11-83	1220	1,098	---	Sluggish (1 m/s) flow from 1708 vent, in shallow (few tens of centimeters), 2-m-wide channel about 400 m north of vent.
1/83KE1-37F	do----------	01-11-83	1240	---	?	Do.
1/83KE1-38F	do----------	01-15-83	0430	---	yes	Slabby pahoehoe flow from 1123 and 1708 vents, about 500 m north of vents.
1/83KE1-39F	do----------	01-15-83	0706	---	yes	Pahoehoe flow from west end of 1123 vent, 10 m north of vent.
1/83KE1-40F	do----------	01-15-83	0840	≥1,110	yes	Pahoehoe flow from west end of 1123 vent, 30 to 40 m north of vent. Thermocouple froze into flow, reached maximum temperature of 1,110 °C.
1/83KE1-41S	do----------	01-17-83	0145	---	yes	Spatter ejected from 1708 vent during vigorous gas emission.
1/83KE1-42S	R. Moore---------	01-17-83	1050	---	yes	Do.
1/83KE1-43S	J. Judd, R. Moore.	01-17-83	1140	---	yes	Do.
1/83KE1-44S	J. Judd, R. Moore, T. Duggan	01-17-83	1220	---	yes	Do.
1/83KE1-45S	do----------	01-17-83	1510	---	yes	Do.
1/83KE1-46S	L. McBroome, C. Finn, J. Lockwood.	01-18-83	0425	---	yes	Spatter ejected from 0740 vent during vigorous gas emission.

TABLE 2.2.—*Samples collected and temperatures measured during episodes 1 through 20 of the Puu Oo eruption of Kilauea Volcano*—Continued

Sample	Collector	Date	Time (H.s.t.)	Temperature (°C)	Quench	Location and comments
1/83KE1-47S	N. Banks	01-20-83	1145	---	yes	Spatter ejected from 0740 vent during vigorous gas emission.
1/83KE1-48S	L. McBroome	01-21-83	2000	---	no	Do.
1/83KE1-49S	N. Banks	01-12-83	---	---	no	Spatter erupted on January 3 from Napau Crater vent.
1/83KE1-50S	do	01-12-83	---	---	no	Spatter erupted on January 3 from first vent east of Napau Crater, 0.5 km northeast of northeastern part of Napau Crater rim.
1/83KE1-51S	J. Buchanan-Banks.	01-12-83	---	---	no	Spatter erupted on January 3 from second vent east of Napau Crater, 0.8 km northeast of northeastern part of Napau Crater rim.
1/83KE1-52S	do	01-12-83	---	---	no	Spatter erupted on January 3 from vent 1.4 km northeast of northeastern part of Napau Crater rim.
1/83KE1-53S	do	01-12-83	---	---	no	Spatter erupted on January 3 from vent 1.2 km northeast of northeastern part of Napau Crater rim.
1/83KE1-54S	N. Banks	01-24-83	---	---	no	Spatter erupted on January 23 from January 23 vent.
1/83KE1-55S	do	01-28-83	---	---	no	Spatter erupted on January 5-6 from westernmost January 5 vent, approximately 1.5 km northeast of northeastern part of Napau Crater rim.
1/83KE1-56S	do	01-28-83	---	---	no	Spatter erupted on January 5 from January 5 vent at Puu Kamoamoa.
1/83KE1-57S	do	02-01-83	---	---	no	Spatter erupted on January 3 from vent approximately 0.8 km northeast of Puu Kamoamoa.
1/83KE1-58S	do	02-01-83	---	---	no	Spatter erupted on January 3 from vent approximately 1.1 km northeast of Puu Kamoamoa.
			(see sample 6/84KE1-276F)			
2/83KE2-59S	E. Wolfe	02-10-83	1030	---	no	Fresh, glassy spatter from new 6-m-high spatter cone at west end of 0740 vent.
2/83KE2-60S	do	02-12-83	1100	---	yes	Molten spatter from west end of 0740 vent.
2/83KE2-61S	do	02-12-83	1230	---	yes	Do.
2/83KE2-62F	do	02-14-83	1120	≥1,113	yes	Pahoehoe toe from 0740 vent, within 100 m of vent.
---	do	02-14-83	1145	≥1,111	---	Do.
2/83KE2-63S	do	02-14-83	1440	---	yes	Molten spatter from west end of 0740 vent.
---	N. Banks	02-14-83	1525	1,111	---	Pahoehoe toe from central part of 0740 vent, 30 m south of vent.
---	E. Wolfe	02-14-83	1535	1,113	---	Do.
---	do	02-14-83	1550	1,111	---	Do.
2/83KE2-64F	do	02-14-83	1610	1,113	yes	Do.
---	N. Banks	02-14-83	1612	1,113	---	Do.
2/83KE2-65F	E. Wolfe	02-15-83	0924	1,113	yes	Pahoehoe toe from 0740 vent, within 100 m of vent.

TABLE 2.2.—*Samples collected and temperatures measured during episodes 1 through 20 of the Puu Oo eruption of Kilauea Volcano*—Continued

Sample	Collector	Date	Time (H.s.t.)	Temperature (°C)	Quench	Location and comments
---	N. Banks---------	02-16-83	0912	1,113	---	Pahoehoe from 0740 vent, 40 m north of vent.
2/83KE2-66F	E. Wolfe, R. Moore.	02-16-83	1037	≥1,109	yes	Pahoehoe toe from 0740 vent, 30 m from vent.
2/83KE2-67S	do----------	02-17-83	1020	---	yes	Molten spatter from 0740 vent, 30 m west of east end. Sample may include some older, cold 1983 spatter.
2/83KE2-68F	do----------	02-17-83	1038	1,114	yes	Pahoehoe toe from 0740 vent, approximately 90 m north of vent.
2/83KE2-69S	E. Wolfe---------	02-18-83	1452	---	yes	Molten spatter from 0740 vent, 30 m west of east end. Sample includes some older, cold 1983 spatter.
2/83KE2-70S	N. Banks---------	02-22-83	1318	1,113	yes	Molten spatter from east end of 0740 vent. Temperature measured in spatter-fed pahoehoe flow.
---	do----------	02-22-83	1343	1,113	---	Pahoehoe toe from 0740 vent, near east end of vent.
2/83KE2-71F	do----------	02-22-83	1415	1,113	yes	Pahoehoe toe from 0740 vent, 100 m from vent.
---	do----------	02-22-83	1425	1,112	---	Pahoehoe from 0740 vent, 100 m from vent.
---	do----------	02-22-83	1444	1,119	---	Pahoehoe from 0740 vent, 180 m north of vent.
---	do----------	02-22-83	1457	1,117	---	Pahoehoe from 0740 vent, 50 m from vent.
2/83KE2-72S	do----------	02-23-83	0945	---	yes	Molten spatter from 0740 vent.
2/83KE2-73S	E. Wolfe---------	02-23-83	1338	---	yes	Molten spatter from east end of 0740 vent. Sample includes some older, cold, 1983 spatter.
2/83KE2-74F	C. Milholland, D. Jackson.	02-25-83	0741	---	yes	Pahoehoe from west end of 0740 vent.
2/83KE2-75F	do----------	02-25-83	1100	---	yes	Pahoehoe from western part of 0740 vent.
2/83KE2-76F	N. Banks---------	02-25-83	1456	1,118	yes	Pahoehoe flow from west end of 0740 vent, north of vent.
2/83KE2-77F	E. Wolfe---------	02-25-83	2129	1,116	yes	Pahoehoe from 1123 vent, 120 m north of vent.
2/83KE2-78F	do----------	02-26-83	0110	1,112	yes	Pahoehoe toe from 1123 vent, 50 m east of vent.
2/83KE2-79F	R. Moore---------	02-27-83	1335	1,120	yes	Pahoehoe toe from western part of 1123 vent, second small vent uprift of main fountain, 20 m north of vent.
3/83KE2-80F	do----------	03-01-83	0756	1,120	yes	Pahoehoe toe in flow from pond, 300 m northeast of 1123 vent.
3/83KE2-81S	J. Lockwood, D. Sundeen.	03-01-83	2146	---	yes	Molten spatter from 1123 vent.
3/83KE2-82S	J. Lockwood------	03-02-83	2053	---	yes	Do.
3/83KE2-83F	E. Wolfe---------	03-03-82	1830	---	no	Aa from 1123 vent, from east edge of flow on Tuberose Street in Royal Gardens, 6 km from vent.
3/83KE3-84F	do----------	03-22-83	---	---	no	Small pahoehoe flow erupted the previous morning within episode 2 spatter ring at 1123 vent.
3/83KE3-85S	N. Banks---------	03-28-83	1100	---	?	Spatter from O vent.

TABLE 2.2.—*Samples collected and temperatures measured during episodes 1 through 20 of the Puu Oo eruption of Kilauea Volcano*—Continued

Sample	Collector	Date	Time (H.s.t.)	Temperature (°C)	Quench	Location and comments
3/83KE3-86F	N. Banks	03-28-83	1150	1,126	yes	Pahoehoe, 150 to 200 m north of O vent.
---	do	03-28-83	1211	1,126	---	Pahoehoe toe, 100 m north of O vent.
3/83KE3-87S	do	03-28-83	1238	---	yes	Spatter from O vent, north of vent.
---	do	03-28-83	1300	1,120	---	Pahoehoe, 350 m north of O vent.
---	do	03-28-83	1309	1,126	---	Pahoehoe, 150 m north of O vent.
3/83KE3-88F	do	03-28-83	1515	1,129	yes	Pahoehoe toe, 150 m west of O vent.
---	do	03-28-83	1525	1,128	---	Pahoehoe, west of O vent.
---	do	03-28-83	1622	1,123	---	Pahoehoe, 140 m north of O vent.
---	do	03-28-83	1640	1,123	---	Pahoehoe toe, 130 m north of O vent.
3/83KE3-89F	E. Wolfe	03-29-83	1320	1,118	yes	Pahoehoe toe, 150 m west of O vent.
---	do	03-29-83	1330	1,114	---	Spiny pahoehoe toe, 150 m west of O vent.
---	do	03-29-83	1332	1,116	---	Do.
---	do	03-29-83	1347	1,118	---	Pahoehoe toe, 150 m west of O vent.
---	do	03-29-83	1403	1,115	---	Do.
3/83KE3-90F	do	03-29-83	1505	1,114	yes	Spiny pahoehoe toe, 150 m west of O vent.
3/83KE3-91F	do	03-29-83	1644	---	yes	Spiny pahoehoe flow from lava pond at northeastern 1123 vent, 150 m north of vent.
3/83KE3-92F	R. Moore, F. Trusdell.	03-29-83	2340	≥1,109	yes	Spiny pahoehoe, transitional to aa, from northeastern 1123 vent, 300 m northeast of vent.
3/83KE3-93F	E. Wolfe, M. Sako.	03-30-83	1201	1,121	yes	Pahoehoe toe, 80 to 100 m south of 1123 vent.
3/83KE3-94F	do	03-30-83	1515	---	no	Aa from northeastern 1123 vent, 300 m northeast of vent.
---	do	03-31-83	1021	1,118	---	Pahoehoe toe, 300 m northwest of 1123 cone.
3/83KE3-95F	E. Wolfe, B. Stokes.	03-31-83	1028	---	yes	Do.
---	E. Wolfe	03-31-83	1107	1,116	---	Do.
---	do	03-31-83	1130	1,116	---	Do.
3/83KE3-96F	E. Wolfe, B. Stokes.	03-31-83	1145	1,122	yes	Do.
3/83KE3-97F	do	03-31-83	1335	1,123	yes	Do.
---	E. Wolfe	03-31-83	1425	1,121	---	Do.
3/83KE3-98F	E. Wolfe, B. Stokes.	03-31-83	1535	1,118	yes	Pahoehoe toe, 80 m northwest of 1123 cone.
4/83KE3-99S	J. Lockwood, L. Petersen.	04-02-83	1005	---	no	Air-fall lapilli (1-2 cm across) that accumulated 1 km west of 1123 vent between 0945 and 1005 H.s.t.
4/83KE3-100F	do	04-02-83	1229	1,122	yes	Pahoehoe flow from southwestern 1123 vent.
4/83KE3-101F	E. Wolfe, N. Banks.	04-02-83	1325	1,121	yes	Slabby pahoehoe from southwestern 1123 vent, 150 m from vent.

TABLE 2.2.—*Samples collected and temperatures measured during episodes 1 through 20 of the Puu Oo eruption of Kilauea Volcano*—Continued

Sample	Collector	Date	Time (H.s.t.)	Temperature (°C)	Quench	Location and comments
4/83KE3-102S	E. Wolfe, N. Banks.	04-02-83	1400	---	yes	Spatter from southwestern 1123 vent.
4/83KE3-103F	do	04-02-83	1420	1,114	yes	Slabby pahoehoe from southwestern 1123 vent; from 20-m-long flow issuing from south base of 1123 cone.
4/83KE3-104F	E. Wolfe	04-02-83	1448	---	yes	Pahoehoe from southwestern 1123 vent; from channel exiting crater to west.
4/83KE3-105F	J. Lockwood, L. Petersen.	04-02-83	2127	1,118	yes	Flow from southwestern 1123 vent, 300 m northwest of vent.
4/83KE3-106S	J. Lockwood	04-03-83	0600	---	no	Air-fall lapilli (1-2 cm across) that accumulated 1 km west of 1123 vent between 0100 and 0600 H.s.t.
4/83KE3-107F	J. Lockwood, L. Petersen, B. Pedit.	04-04-83	0901	≥1,108	?	Flow from southwestern 1123 vent, 150 m northwest of vent.
4/83KE3-108F	E. Wolfe	04-04-83	1400	1,113	yes	Terminus of small spiny to slabby pahoehoe flow from southwestern 1123 vent, 100 m southwest of vent.
4/83KE3-109F	do	04-04-83	1500	1,111	yes	Small viscous, spiny pahoehoe flow of southwestern 1123 vent, 150 to 200 m south of vent; issuing from base of cone.
4/83KE3-110S	J. Lockwood	04-04-83	1900	---	---	Air-fall lapilli (1-3 cm across) that accumulated 1 km west of 1123 vent between 1800 and 1900 H.s.t.
4/83KE3-111S	do	04-04-83	0700	---	---	Air-fall lapilli (1-2 cm across) that accumulated 1 km west of 1123 vent between 0330 and 0700 H.s.t.
4/83KE3-112S	do	04-05-83	1430	---	---	Air-fall lapilli (1-2 cm across) that accumulated 1 km west of 1123 vent between 1230 and 1430 H.s.t.
4/83KE3-113F	E. Wolfe	04-05-83	1520	---	yes	Cooling but still-incandescent aa from overflow of pahoehoe river from southwestern 1123 vent, 300 m south of vent.
4/83KE3-114F	do	04-05-83	1550	---	no	Dense aa; same overflow, same locality as for preceding sample.
4/83KE3-115F	E. Wolfe, D. Jackson.	04-07-83	1400	---	no	Spiny pahoehoe flow from southwestern 1123 vent, emplaced at about 0500 H.s.t. Sample collected about 1 km south of vent.
---	N. Banks	04-08-83	1230	1,094	---	Aa-flow front in Royal Gardens, from southwestern 1123 vent, 5.9 km from vent.
---	do	04-08-83	1515	1,099	---	Aa-flow front in Royal Gardens, from southwestern 1123 vent, 6.1 km from vent.
4/83KE3-116F	E. Wolfe	04-09-83	0850	---	no	Aa-flow front in Royal Gardens, from southwestern 1123 vent, 7.5 km from vent.
4/83KE3-117F	R. Moore, F. Trusdell, D. Jackson.	04-09-83	1115	---	?	Hot (not molten) pahoehoe from evacuated channel of southwestern 1123 vent, 200 m south of vent.
6/83KE4-118F	T. Duggan, B. Talai.	06-13-83	1530	---	yes	Pahoehoe toe of northern flow from fissure vents west of Puu Oo, 40 m from vent.
6/83KE4-119F	do	06-13-83	1558	---	yes	Pahoehoe toe of northern flow from fissure vents west of Puu Oo, 50 to 60 m from vent.

TABLE 2.2.—*Samples collected and temperatures measured during episodes 1 through 20 of the Puu Oo eruption of Kilauea Volcano*—Continued

Sample	Collector	Date	Time (H.s.t.)	Temperature (°C)	Quench	Location and comments
6/83KE4-120F	E. Wolfe---------	06-13-83	1809	1,127	yes	Tube-fed pahoehoe toe from fissure vents west of Puu Oo, 30 to 40 m northwest of vent.
---	do----------	06-13-83	1830	1,120	---	Crusted pahoehoe toe from fissure vents west of Puu Oo, 30 to 40 m northwest of vent. Toe 2 to 3 m long, 20 cm thick, and 60 cm wide. Crust had to be broken to sample melt.
6/83KE4-121F	do----------	06-13-83	2345	1,129	yes	Tube-fed pahoehoe from fissure vents west of Puu Oo, 30 m north of vent.
6/83KE4-122F	do----------	06-14-83	0940	1,132	yes	Tube-fed pahoehoe toe from fissure vents uprift of Puu Oo, 40 to 50 m north of vents. Flow issued from crusted pahoehoe pond developing in flow on north side of vent.
6/83KE4-123F	do----------	06-14-83	1030	1,127	yes	Tube-fed pahoehoe bud from fissure vents uprift of Puu Oo, 40 m from Puu Oo; from east edge of crusted pahoehoe pond in flow on north side of vent.
6/83KE4-124F	do----------	06-14-83	1420	1,128	yes	Tube-fed pahoehoe bud from fissure vents uprift of Puu Oo, 80 m from Puu Oo; from northeast edge of crusted pahoehoe pond in flow on north side of vent.
6/83KE4-125F	do----------	06-15-83	1500	---	yes	Overflow from lava river, Puu Oo vent flow to southeast, 70 m downstream from cascade over a 5- to 10-m-high scarp, 1.1 km from vent.
6/83KE4-126F	do----------	06-16-83	1030	---	yes	Lava-river sample from Puu Oo vent flow to southeast, 500 m from vent.
6/83KE4-127F	do----------	06-16-83	1110	≥1,120	yes	Lava-river sample from Puu Oo vent flow to southeast, 1.1 km from vent. Thick sheath of solidified basalt grew on probe after temperature reached 1,120 °C.
6/83KE4-128F	do----------	06-16-83	1155	1,128	yes	Overflow from lava river in Puu Oo vent flow to southeast, 1 km downstream from vent at base of cascade over preexisting 5- to 10-m-high scarp.
6/83KE4-129F	do----------	06-16-83	1625	---	yes	Lava-river sample from Puu Oo vent flow to southeast, 70 m downstream of cascade over preexisting 5- to 10-m-high scarp, 1.1 km from vent.
6/83KE4-130F	do----------	06-17-83	1200	1,115	yes	Lava-river sample from Puu Oo vent flow to southeast, 80 m downstream of cascade over preexisting 5- to 10-m-high scarp, 1.1 km from vent.
---	do----------	06-17-83	1200	1,117	---	Do.
6/83KE4-131F	do----------	06-22-83	---	---	no	Pahoehoe crust from spillway on southeast flank of Puu Oo.
6/83KE4-132S	do----------	06-22-83	---	---	no	Spatter from floor of eastern crater at Puu Oo, erupted late in episode 4.
			(see sample 1/84KE4-207F)			
6/83KE5-133F	do----------	06-29-83	1302	---	yes	Pahoehoe bud from flow front of eastern flow from Puu Oo at start of episode 5, 60 m southeast of vent in evacuated episode 4 channel.
---	do----------	06-29-83	1332	1,127	---	Pahoehoe bud from flow front of eastern flow from Puu Oo, 300 m southeast of vent.

TABLE 2.2.—*Samples collected and temperatures measured during episodes 1 through 20 of the Puu Oo eruption of Kilauea Volcano*—Continued

Sample	Collector	Date	Time (H.s.t.)	Temperature (°C)	Quench	Location and comments
6/83KE5-134F	E. Wolfe----------	06-29-83	1335	1,127	yes	Pahoehoe bud from flow front of eastern flow from Puu Oo, 300 m southeast of vent.
6/83KE5-135F	do----------	06-29-83	1552	≥1,127	yes	Pahoehoe overflow from lava river, eastern flow from Puu Oo, 400 to 500 m southeast of vent.
6/83KE5-136F	do----------	06-29-83	1735	1,125	yes	Pahoehoe bud in northern flow from western Puu Oo vent, 70 m from vent.
7/83KE5-137F	do----------	07-01-83	1750	≥1,120	yes	Pahoehoe overflow, 150 m from lava river, western flow from western Puu Oo vent. Overflow was thin and froze quickly.
7/83KE5-138F	R. Moore, D. Clague, J. Eaby.	07-02-83	1105	1,129	yes	Pahoehoe ooze, west side of Puu Oo cone. Temperature measurement was repeated once.
7/83KE5-139F	do----------	07-03-83	0900	---	no	Rootless flow from west base of Puu Oo.
7/83KE5-140F	J. Judd----------	07-07-83	---	---	no	Cold aa from channel sample of western flow from western Puu Oo vent, 3 km southeast of vent.
7/83KE5-141F	E. Wolfe---------	?	---	---	no	Aa flow from northwest side of eastern Puu Oo vent, 50 m north of vent; probably erupted late in episode 5.
7/83KE5-142F	do----------	07-13-83	---	---	no	Pahoehoe from north edge of ponded northern flow from western Puu Oo vent, 200 m north of vent; erupted June 29 or 30.
7/83KE5-143F	do----------	07-13-83	---	---	no	Pahoehoe from flow to north and northeast from western Puu Oo vent, 100 m north of vent; erupted June 30.
7/83KE5-144F	do----------	07-21-83	---	---	no	Pahoehoe from terminus of flow to north and northeast from western Puu Oo vent, 800 m northeast of vent; erupted June 30.
			(see sample 7/83KE5-204F)			
7/83KE6-145S	P. Greenland, R. Tilling.	07-21-83	---	---	no	Spatter in eastern crater at Puu Oo; erupted during low-level activity between 1237 and 1304 H.s.t.
7/83KE6-146F	R. Moore, C. Neal.	07-22-83	1400	1,128	yes	Edge of rising lava pond in eastern crater at Puu Oo.
7/83KE6-147F	do----------	07-23-83	0935	---	yes	Terminus of viscous, spiny pahoehoe flow, 250 to 350 m northeast of Puu Oo.
7/83KE6-148F	R. Moore, C. Neal, L. Petersen.	07-23-83	1215	1,126	yes	Pahoehoe flow moving eastward on top of primary aa flow, 1 km from Puu Oo.
---	R. Moore, C. Neal.	07-23-83	1338	1,128	---	Pahoehoe flow moving eastward, 1 km from Puu Oo.
7/83KE6-149F	E. Wolfe----------	07-24-83	1107	1,138	yes	Pahoehoe overflow from lava river, northeastern flow from Puu Oo, 700 m northeast of vent.
7/83KE6-150F	do----------	07-24-83	1058	≥1,136	yes	Pahoehoe overflow from lava river, northeastern flow from Puu Oo, 700 m northeast of vent. Thermocouple quickly developed a sheath of solidified basalt.
7/83KE6-151F	do----------	07-24-83	1250	≥1,138	yes	Pahoehoe overflow from lava river, northeastern flow from Puu Oo, 700 m northeast of vent.

TABLE 2.2.—*Samples collected and temperatures measured during episodes 1 through 20 of the Puu Oo eruption of Kilauea Volcano*—Continued

Sample	Collector	Date	Time (H.s.t.)	Temperature (°C)	Quench	Location and comments
7/83KE6-152S	J. Judd----------	07-25-83	0656	---	yes	Spatter from Puu Oo.
7/83KE6-153S	do----------	07-25-83	0730	---	yes	Do.
---	E. Wolfe---------	07-25-83	1300	1,135	---	Pahoehoe in northeastern flow from Puu Oo, 800 m northeast of vent.
7/83KE6-154F	do----------	07-26-83	0800	---	no	Pahoehoe from small channel on north side of Puu Oo that had been draining Puu Oo Crater at 1630 H.s.t. July 25 after the eruption stopped.
			(see samples 11/83KE6-205F and 11/83KE6-238F)			
8/83KE7-155S	P. Greenland-----	08-10-83	---	---	no	Spatter fragments on floor of Puu Oo Crater, possibly containing some oxidized post-episode 6 rubble. From low-level activity before episode 7.
8/83KE7-156F	E. Wolfe---------	08-10-83	1645	---	yes	Small pahoehoe flow on floor of Puu Oo Crater, erupted at 1630 H.s.t. Sample collected from molten interior of crusted toe.
---	do----------	08-14-83	1322	≥1,125	---	Temperature measured directly in vent within Puu Oo, 10 minutes before emission of small pahoehoe flow between 1330 and 1332 H.s.t. Probe may not have been in melt.
8/83KE7-157F	do----------	08-14-83	1332	---	yes	Small, thin pahoehoe flow on floor of Puu Oo Crater; erupted between 1330 and 1332 H.s.t.
8/83KE7-158F	do----------	08-15-83	0930	1,119	yes	Viscous, spiny pahoehoe overflow from channel of spatter-fed southwestern flow from Puu Oo, in evacuated episode 5 channel, 200 m from vent. Sample collected from different toe 5 minutes after temperature measurement.
8/83KE7-159F	do----------	08-15-83	1110	1,134	yes	Pahoehoe overflow on north side of lava river in northeastern flow from Puu Oo, 1 km northeast of vent.
---	do----------	08-15-83	1141	1,135	---	Pahoehoe toe in overflow on north side of lava river in northeastern flow from Puu Oo, 1 km northeast of vent.
8/83KE7-160F	do----------	08-15-83	1245	1,134	yes	Do.
8/83KE7-161F	do----------	08-15-83	1615	1,130	yes	Pahoehoe toe in overflow on north side of lava river, northeastern flow from Puu Oo, 300 m northeast of vent.
8/83KE7-162F	do----------	08-15-83	1645	1,136	yes	Do.
8/83KE7-163F	do----------	08-16-83	0755	1,132	yes	Pahoehoe toe at front of flow fed by spatter and, in part, from a secondary pond also supplied by spatter, 200 to 300 m north of Puu Oo.
8/83KE7-164F	do----------	08-16-83	1305	1,136	yes	Spiny pahoehoe toe from same flow as above sample, 200 m north of Puu Oo.
8/83KE7-165F	do----------	08-16-83	1503	1,135	yes	Viscous tube-fed pahoehoe toe from same flow as above sample, 200 to 300 m from vent.
8/83KE7-166F	do----------	08-17-83	1200	1,138	yes	Pahoehoe ooze through accretionary levee at north side of lava river, northeastern flow from Puu Oo, 800 to 900 m northeast of vent.

TABLE 2.2.—*Samples collected and temperatures measured during episodes 1 through 20 of the Puu Oo eruption of Kilauea Volcano*—Continued

Sample	Collector	Date	Time (H.s.t.)	Temperature (°C)	Quench	Location and comments
8/83KE7-167F	E. Wolfe---------	08-17-83	1225	1,141	yes	Slow-moving pahoehoe ooze through accretionary levee at north edge of lava river, northeastern flow from Puu Oo, 900 m northeast of vent.
			(see sample 11/83KE7-239F)			
9/83KE8-168S	do----------	09-02-83	0900	---	no	Spatter from low-level eruption within Puu Oo. Sample collected adjacent to new 4-m-high spatter cone on floor of crater.
9/83KE8-169F	do----------	09-03-83	1030	---	no	Pahoehoe flow on floor of Puu Oo Crater, from western intracrater vent.
9/83KE8-170F	do----------	09-04-83	0856	1,102	yes	Temperature inside actively degassing spatter cone over western intracrater vent. Thermocouple may not have been immersed in melt; sample may be of remelted material.
9/83KE8-171F	do----------	09-04-83	0917	1,120	yes	Same as above sample; thermocouple in melt. Temperature measurement was repeated several times. Sample from inside spatter cone, possibly of remelted material.
9/83KE8-172F	do----------	09-06-83	0910	1,128	yes	Spiny pahoehoe toe in overflow 100 m from lava river; flow heading northeast from Puu Oo, 800 to 900 m from vent.
9/83KE8-173F	do----------	09-06-83	1220	1,130	yes	Viscous, spiny tube-fed pahoehoe from northeast edge of crusted pahoehoe pond developing within northeastern flow, 1 km from Puu Oo. Pahoehoe issued from base of 7-m-high levee enclosing pond.
9/83KE8-174F	do----------	09-07-83	1550	---	no	Pahoehoe from spillway of Puu Oo, 30 m from conduit. Sample was still hot when collected 10.5 hours after eruption.
			(see sample 11/83KE8-240F)			
9/83KE9-175F	do----------	09-15-83	1630	---	yes	Small overflow from lava river just below a lava fall; flow heading northeast from Puu Oo, 30 m from vent.
9/83KE9-176S	K. Yamashita-----	09-16-83	---	---	no	Pele's hair from Puu Oo on Chain of Craters Road, 9.5 km from vent.
9/83KE9-177F	E. Wolfe---------	09-17-83	1400	---	no	Pahoehoe from north edge of crusted pahoehoe pond in northeastern flow, 1 km from Puu Oo. Dense rock sample, still warm.
9/83KE9-178F	do----------	09-23-83	1100	---	no	Late episode 9 basalt from channel wall, 20 to 30 m northeast of Puu Oo.
			(see sample 9/83KE9-340S)			
10/83KE10-179F	do----------	10-02-83	1000	---	?	Pahoehoe flow erupted about 0750 H.s.t. on floor of Puu Oo Crater. Some lava from flow interior was draining back into conduit when sample was collected.
10/83KE10-180S	P. Greenland-----	10-02-83	1000	---	no	Spatter on floor of Puu Oo Crater, probably erupted about 0750 H.s.t. Sample may contain contaminants of episode 9 rock.
10/83KE10-181F	E. Wolfe---------	10-05-83	1030	---	yes	Spiny pahoehoe/aa from spatter-fed flow, 300 m north of Puu Oo. Flow had been active 30 minutes earlier.

TABLE 2.2.—*Samples collected and temperatures measured during episodes 1 through 20 of the Puu Oo eruption of Kilauea Volcano*—Continued

Sample	Collector	Date	Time (H.s.t.)	Temperature (°C)	Quench	Location and comments
10/83KE10-182F	E. Wolfe---------	10-05-83	1319	≥1,137	yes	Pahoehoe toe in overflow from lava river, northeastern flow from Puu Oo, 400 to 500 m north of vent.
10/83KE10-183F	do----------	10-05-83	1407	1,138	yes	Pahoehoe toe in broad sheet overflow from lava river, northeastern flow from Puu Oo, 1.2 km northeast of vent.
---	do----------	10-05-83	1438	1,138	---	Do.
10/83KE10-184F	do----------	10-05-83	1610	1,139	yes	Pahoehoe at north edge of sheet overflow from lava river, northeastern flow from Puu Oo, 1.3 km northeast of vent.
10/83KE10-185F	do----------	10-06-83	1341	1,135	yes	Spiny pahoehoe at northwest edge of overflows moving north from lava river, northeastern flow from Puu Oo, 500 to 600 m north-northeast of vent.
10/83KE10-186F	do----------	10-06-83	1420	1,134	yes	Viscous pahoehoe bud in overflow from lava river, northeastern flow from Puu Oo, 500 m north-northeast of vent.
---	do----------	10-06-83	---	≥1,139	---	Pahoehoe in fast-moving overflow from lava river, northeastern flow from Puu Oo, 500 to 600 m north-northeast of vent. Temperature measurement was repeated several times.
10/83KE10-187F	do----------	10-07-83	1050	1,142	yes	Pahoehoe ooze through accretionary levee at north edge of lava river, northeastern flow from Puu Oo, 1.6 km northeast of vent.
			(see sample 11/83KE10-241F)			
11/83KE11-188F	do----------	11-06-83	0920	1,142	yes	Active pahoehoe toe on surface of crusted pahoehoe sheet flow from westernmost extracrater vent, 80 m west of source vent.
11/83KE11-189F	do----------	11-06-83	0950	1,141	yes	Pahoehoe toe erupting from beneath crust at edge of broad, crusted pahoehoe sheet flow, 600 m north of vent. Flow was fed by spatter cascading over north rim of Puu Oo from vent within northern part of crater.
11/83KE11-190F	E. Wolfe, C. Neal, M. Summers.	11-06-83	1135	1,144	yes	Pahoehoe toe oozing from under solid crust of overflow or seepage from lava river, 50 m from edge of lava river, northeastern flow, 200 to 250 m northeast of Puu Oo.
---	do----------	11-06-83	1140	1,144	---	Do.
11/83KE11-191F	E. Wolfe, C. Neal.	11-06-83	1503	1,141	yes	Pahoehoe toe at leading edge of rapidly moving, crusted pahoehoe sheet flow from western extracrater vents. Temperature measured as flow decelerated 125 m uprift of westernmost vents.
---	E. Wolfe---------	11-07-83	1000	≥1,135	---	Pahoehoe from edge of lava river, northeastern flow, 300 m northeast of Puu Oo.
11/83KE11-192F	do----------	11-07-83	1030	≥1,123	yes	Pahoehoe from edge of lava river, northeastern flow, 300 m northeast of Puu Oo. Large sheath of solidified basalt prevented equilibrium temperature from being reached.
11/83KE11-193F	do----------	11-07-83	1150	1,133	yes	Rapidly moving thin pahoehoe overflow, 5 m from lava river, northeastern flow, 300 m northeast of Puu Oo.
11/83KE11-194F	do----------	11-07-83	1405	---	yes	Pahoehoe from edge of lava river, northeastern flow, 4.5 km northeast of Puu Oo.

TABLE 2.2.—*Samples collected and temperatures measured during episodes 1 through 20 of the Puu Oo eruption of Kilauea Volcano*—Continued

Sample	Collector	Date	Time (H.s.t.)	Temperature (°C)	Quench	Location and comments
11/83KE11-195F	E. Wolfe	11-08-83	1130	---	no	Slightly oxidized pahoehoe from floor of evacuated channel, northeastern flow, 250 m northeast of Puu Oo. Sample collected 17 hours after eruption.
			(see sample 11/83KE11-242F)			
11/83KE12-196F	C. Neal	11-30-83	1030	1,135	yes	Edge of thin viscous pahoehoe sheet flow on northwest flank of Puu Oo, both pond and spatter fed, 250 m north of Puu Oo.
11/83KE12-197F	E. Wolfe	11-30-83	1140	≥1,140	yes	Spiny tube-fed pahoehoe, 600 m north of Puu Oo.
11/83KE12-198F	do	11-30-83	1300	1,137	yes	Spiny tube-fed pahoehoe toe, 600 m north of Puu Oo. Temperature of 1,138 °C measured at same locality at 1255 H.s.t.
11/83KE12-199F	do	11-30-83	1450	1,135	yes	Pahoehoe toe at edge of wide, spreading pahoehoe sheet flow fed by fountains and pond overflow at southeast rim of Puu Oo, 200 m east of Puu Oo.
11/83KE12-200F	do	11-30-83	1600	≥1,135	yes	Sheet overflow from lava river, eastern flow from Puu Oo, 20 to 25 m from channel, 400 m east of Puu Oo. Average channel velocity, 2 m/s.
---	do	12-01-83	1110	≥1,144	---	Pahoehoe sheet flow heading north from Puu Oo, 300 m from vent. Temperature of ≥1,141 °C also recorded.
12/83KE12-201F	do	12-01-83	1130	---	yes	Pahoehoe sheet flow heading north from Puu Oo, 200 m north of Puu Oo.
12/83KE12-202F	do	12-01-83	1300	---	no	Solidified pahoehoe pond, 600 m north-northwest of Puu Oo. Dense-rock sample, collected while still hot.
12/83KE12-203F	do	12-01-83	1440	≥1,141	yes	Tube-fed pahoehoe toe issuing from edge of crusted lava pond, 600 to 700 m north of Puu Oo. Flow from northern vent of Puu Oo.
			(see samples 1/84KE12-206F and 1/84KE12-341S)			
7/83KE5-204F	C. Neal	07-29-83	---	---	no	Dense aa interior of Puu Oo flow in Royal Gardens, 7.4 km from source.
11/83KE6-205F	E. Wolfe	11-26-83	---	---	no	Spiny pahoehoe outcrop in aa flow, 6.3 km northeast of Puu Oo. Dense-rock sample.
1/84KE12-206F	do	01-06-84	---	---	no	Spiny pahoehoe that issued from terminus of aa flow, 7 km northeast of Puu Oo. Dense-rock sample.
1/84KE4-207F	do	01-10-84	---	---	no	Spiny pahoehoe outcrop in aa flow, 7.4 km southeast of Puu Oo. Dense-rock sample.
1/84KE13-208F	do	01-20-84	1759	---	yes	Spiny pahoehoe, solid but incandescent, from 350-m-long flow. Sample collected 250 m northeast of Puu Oo.
1/84KE13-209F	do	01-20-84	2032	---	yes	Pahoehoe oozing through levee at margin of lava river, 300 m northeast of Puu Oo.
---	do	01-20-84	2038	1,131	---	Temperature measured in same locality as previous sample.
1/84KE13-210F	do	01-20-84	2230	1,129	yes	Long-lived pahoehoe overflow, 25 m from lava river, 300 m northeast of Puu Oo.

TABLE 2.2.—*Samples collected and temperatures measured during episodes 1 through 20 of the Puu Oo eruption of Kilauea Volcano*—Continued

Sample	Collector	Date	Time (H.s.t.)	Temperature (°C)	Quench	Location and comments
1/84KE13-211F	E. Wolfe---------	01-21-84	0015	≥1,131	yes	Long-lived pahoehoe overflow, 30 m from lava river, 250 m northeast of Puu Oo.
1/84KE13-212F	do----------	01-21-84	0345	1,140	yes	Long-lived pahoehoe overflow, 75 m from lava river, 250 m northeast of Puu Oo.
1/84KE13-213F	do----------	01-21-84	0545	---	yes	Molten spatter from lava river as it banked high on channel wall, 30 m northeast of spillway.
1/84KE13-214F	do----------	01-21-84	0635	1,142	yes	Front of active, long-lived pahoehoe-sheet breakout from lava river, 300 to 400 m north of lava river, 500 m northeast of Puu Oo.
1/84KE13-215F	do----------	01-21-84	0834	1,141	yes	Tube-fed pahoehoe toe in long-lived breakout from lava river, 300 m from lava river, 500 m northeast of Puu Oo.
1/84KE13-216F	C. Byers, M. Garcia.	01-21-84	0912	1,147	yes	Tube-fed pahoehoe toe in long-lived breakout from lava river, 200 m from lava river, 700 m northeast of Puu Oo.
1/84KE13-217F	E. Wolfe---------	01-21-84	1055	---	yes	Pahoehoe overflow at edge of lava river, 100 m northeast of Puu Oo.
1/84KE13-218F	C. Byers, M. Garcia, R. Moore, M. Caress.	01-21-84	1206	1,130	yes	Tube-fed pahoehoe toe in long-lived breakout from lava river, 300 m from lava river, 3.5 km northeast of Puu Oo.
1/84KE13-219F	do----------	01-21-84	1215	1,139	yes	Do.
1/84KE13-220F	do----------	01-21-84	1329	1,140	yes	Do.
1/84KE13-221F	M. Garcia--------	01-21-84	1620	---	yes	Pahoehoe overflow from lava river, 300 m northeast of Puu Oo.
1/84KE13-222F	C. Byers, M. Garcia.	01-21-84	2016	---	yes	Pahoehoe overflow, 30 m from lava river, 300 m northeast of Puu Oo.
1/84KE13-223F	C. Byers, M. Garcia, M. Caress.	01-21-84	2208	---	no	Molten spatter from lava river, 250 m northeast of Puu Oo.
1/84KE13-224F	do----------	01-22-84	0002	---	yes	Pahoehoe overflow from lava river, 300 m northeast of Puu Oo.
1/84KE13-225F	E. Wolfe, C. Neal, M. Garcia, C. Byers.	01-22-84	0845	1,144	yes	Tube-fed pahoehoe toe in several-hour-old breakout from proximal part of lava river produced during second eruptive period, 250 m north of Puu Oo.
1/84KE13-226F	E. Wolfe---------	01-22-84	1050	1,144	yes	Pahoehoe toe issuing from under crusted surface of actively expanding, long-lived pahoehoe sheet overflow from proximal part of lava river, 250 m from Puu Oo.
1/84KE13-227F	do----------	01-22-84	1200	≥1,140	yes	Tube-fed pahoehoe toe in long-lived breakout from lava river, 300 m north of Puu Oo.
---	do----------	01-22-84	1212	1,141	---	Do.
			(see sample 2/84KE13-233F)			
1/84KE14-228F	do----------	01-26-84	---	---	no	Remnant pahoehoe crust from highstand of lava pond inside Puu Oo Crater, erupted between 1700 H.s.t. January 25 and 0900 H.s.t. January 26.

TABLE 2.2.—*Samples collected and temperatures measured during episodes 1 through 20 of the Puu Oo eruption of Kilauea Volcano*—Continued

Sample	Collector	Date	Time (H.s.t.)	Temperature (°C)	Quench	Location and comments
1/84KE14-229F	E. Wolfe---------	01-30-84	1300	---	no	2-m-long pahoehoe flow on floor of Puu Oo Crater, from 0.5-m-wide vent through crusted surface of lava pond. Sample was incandescent and water cooled.
1/84KE14-230F	do----------	01-31-84	0950	1,136	yes	Spiny pahoehoe toe from edge of broad, slow-moving pahoehoe sheet flow supplied by distributary flowing northwest from lava river, 600 m north of Puu Oo. Temperature measurement was repeated several times.
1/84KE14-231F	E. Wolfe, C. Neal.	01-31-84	1125	1,137	yes	Tube-fed spiny pahoehoe toe from overflow of lava river in eastern flow, 200 m north of lava river, 500 m northeast of Puu Oo.
1/84KE14-232F	E. Wolfe---------	01-31-84	1340	---	yes	Pahoehoe toe in still-active flow that had been supplied by distributary flowing northwest from lava river, 150 m northwest of Puu Oo. Sample was taken 30 minutes after eruption stopped.
2/84KE13-233F	do----------	02-10-84	---	---	no	Spiny pahoehoe at edge of aa flow, 6 km from Puu Oo. Dense-rock sample.
2/84KE14-234F	do----------	02-10-84	---	---	no	Thick ponded pahoehoe, 300 m northwest of Puu Oo. Dense-rock sample.
			(see sample 2/84KE14-342S)			
2/84KE15-235F	do----------	02-15-84	0915	≥1,129	yes	Viscous, spiny pahoehoe toe oozing from edge of aa of northeastern flow from Puu Oo, 800 m north of Puu Oo.
2/84KE15-236F	do----------	02-15-84	1130	≥1,132	yes	Viscous, thin pahoehoe overflow, 30 m from lava river, northeastern flow, 500 m northeast of Puu Oo.
---	do----------	02-15-84	1145	1,136	---	Do.
2/84KE15-237F	do----------	02-15-84	1245	1,139	yes	Front of viscous, thin pahoehoe sheet overflow, 40 m from lava river, northeastern flow, 1 km northeast of Puu Oo.
			(see samples 2/84KE15-243F and 2/84KE15-343S)			
11/83KE6-238F	do----------	11-26-83	---	---	no	Aa boulder, 5.2 km northeast of Puu Oo. Dense-rock sample.
11/83KE7-239F	do----------	11-26-83	---	---	no	Spiny pahoehoe at margin of aa flow, 5.9 km northeast of Puu Oo. Dense-rock sample.
11/83KE8-240F	do----------	11-26-83	---	---	no	Pahoehoe from ponded area, 200 to 300 m northwest of 1123 vent, 1.2 km from Puu Oo. Dense-rock sample.
11/83KE10-241F	do----------	11-26-83	---	---	no	Spiny pahoehoe at edge of aa flow, just south of 1123 vent, 1.3 km from Puu Oo. Dense-rock sample.
11/83KE11-242F	do----------	11-26-83	---	---	no	Spiny pahoehoe surrounded by aa, 5.3 km northeast of Puu Oo. Dense-rock sample.
2/84KE15-243F	do----------	02-28-84	---	---	no	Spiny pahoehoe at edge of aa flow, 3.6 km northeast of Puu Oo. Dense-rock sample.
2/84KE16-244S	?	02-28-84	---	---	?	Spatter collected within Puu Oo during low-level eruptive activity before episode 16.
3/84KE16-245S	E. Wolfe---------	03-01-84	---	---	no	Spatter emitted during the night of February 29-March 1. Sample collected on floor of Puu Oo Crater.

TABLE 2.2.—*Samples collected and temperatures measured during episodes 1 through 20 of the Puu Oo eruption of Kilauea Volcano*—Continued

Sample	Collector	Date	Time (H.s.t.)	Temperature (°C)	Quench	Location and comments
3/84KE16-246S	E. Wolfe	03-02-84	0830	---	no	Spatter emitted during the night of March 1-2. Sample collected from terrace 4 m above crusted lava pond in conduit inside Puu Oo.
3/84KE16-247F	E. Wolfe, C. Neal.	03-03-84	1818	---	yes	Spatter-fed aa flow, 300 m north of Puu Oo.
3/84KE16-248F	E. Wolfe	03-04-84	0755	≥1,120	yes	Pahoehoe toe from stagnating flow, 500 m north of Puu Oo, that was active between 0600 and 0630 H.s.t., probably spatter fed. First temperature measurement was followed by a second of ≥1127 °C in a similar locality.
3/84KE16-249F	do	03-04-84	0810	1,139	yes	Same toe as for previous sample.
3/84KE16-250F	N. Banks	03-04-84	1015	1,135	yes	Aa-flow terminus, 2.8 km east of Puu Oo. Temperature measured and sample collected in breakouts from molten central zone.
3/84KE16-251F	E. Wolfe	03-04-84	1020	1,142	yes	Fast-moving pahoehoe-sheet overflow from lava river, 80 m from lava river, 1.5 km east of Puu Oo.
3/84KE16-252F	N. Banks	03-04-84	1205	1,138	?	Fluid breakout, aa-flow terminus, 3.9 km east of Puu Oo. Thermocouple penetrated 1.5 m into flow interior.
3/84KE16-253F	E. Wolfe	03-04-84	1258	1,141	yes	Pahoehoe overflow, 20 to 30 m from lava river, 1.5 km northeast of Puu Oo.
3/84KE16-254F	do	03-04-84	1525	1,141	yes	Pahoehoe ooze through crusted pahoehoe at edge of lava river, 1.5 km east of Puu Oo. First temperature measurement was followed by others of 1,134 and 1,136 °C at same locality.
3/84KE16-255F	N. Banks, R. Moore.	03-04-84	1613	1,137	yes	Edge of aa-flow from Puu Oo, 4.9 km east of Puu Oo. Temperature measured in and sample collected from 5- to 7-m-thick flow. Probe was worked into plastic interior beneath thin aa carapace.
---	do	03-04-84	1830	1,137	---	Fluid breakout, aa-flow terminus, 6.3 km east of Puu Oo.
---	do	03-04-84	2331	≥1,135	---	Fluid, 1-m-thick breakout from aa-flow terminus, 7.5 km from Puu Oo. Probe penetrated 1 m into flow interior.
			(see samples 3/84KE16-262F and 3/84KE16-344S)			
3/84KE17-256F	E. Wolfe	03-30-84	1050	---	yes	Viscous incandescent aa, eastern flow, 1 km northeast of Puu Oo.
3/84KE17-257F	C. Neal	03-30-84	1120	---	no	Spatter-fed aa, flow terminus, 100 m west of Puu Oo. Flow 1 m thick and moving 0.7 m/min. Sample was water cooled.
3/84KE17-258F	E. Wolfe	03-30-84	1310	1,131	yes	Transitional slabby pahoehoe/aa overflow from central channel of southeastern flow, 1.5 km southeast of Puu Oo.
---	do	03-30-84	1415	1,132	---	Slabby pahoehoe ooze in overflow at edge of lava river. Same locality as for previous sample.
3/84KE17-259F	do	03-30-84	1700	1,137	yes	Pahoehoe overflowing edge of lava river, eastern flow, 300 m northeast of Puu Oo.
3/84KE17-260F	do	03-31-84	0745	1,131	yes	Spiny pahoehoe oozing from underneath crust on evacuated channel floor, eastern flow, 2.0 km northeast of Puu Oo.

TABLE 2.2.—*Samples collected and temperatures measured during episodes 1 through 20 of the Puu Oo eruption of Kilauea Volcano*—Continued

Sample	Collector	Date	Time (H.s.t.)	Temperature (°C)	Quench	Location and comments
3/84KE17-261F	E. Wolfe---------	03-31-84	0747	---	no	Spiny pahoehoe outcrop in eastern aa flow, 2.0 km northeast of Puu Oo. Dense-rock sample.
			(see sample 3/84KE17-345S)			
3/84KE16-262F	do----------	03-23-84	---	---	no	Spiny pahoehoe outcrop in aa flow, 2.2 km east of Puu Oo. Dense-rock sample, collected while still hot.
4/84KE18-263F	do----------	04-19-84	0825	1,139	yes	Tube-fed pahoehoe from crusted pahoehoe pond formed of overflows from lava river in northeastern flow, 40 m north of lava river, 500 m northeast of Puu Oo.
---	do----------	04-19-84	0845	≥1,143	---	Same locality as for previous sample.
4/84KE18-264F	do----------	04-19-84	0955	1,137	yes	Tube-fed pahoehoe from crusted pahoehoe pond formed of overflows from lava river in northeastern flow, 100 m north of lava river, 600 m northeast of Puu Oo.
4/84KE18-265F	do----------	04-19-84	1355	1,140	yes	Pahoehoe toe issuing from edge of crusted pahoehoe pond formed of overflows from lava river in northeastern flow, 100 m north of lava river, 750 m northeast of Puu Oo.
4/84KE18-266F	do----------	04-19-84	1520	1,136	yes	Front of 0.5-m-thick, fluid pahoehoe sheet overflow, 150 m north of lava river in northeastern flow, 1 km northeast of Puu Oo.
4/84KE18-267F	do----------	04-20-84	1130	1,144	yes	Pahoehoe ooze from crusted overflow of lava river in eastern flow, 40 m north of lava river, 1.1 km northeast of Puu Oo.
4/84KE18-268F	do----------	04-20-84	1432	1,136	yes	Thin, rapidly freezing pahoehoe overflow of lava river in eastern flow, 3 m north of lava river, 1.5 km northeast of Puu Oo. Crust had to be broken to sample melt.
---	N. Banks----------	04-20-84	2038	≥1,098	---	Aa-flow front, eastern flow, approximately 13 km from vent. Thermocouple inserted 20 to 30 cm into plastic interior.
---	do----------	04-20-84	2220	≥1,106	---	Temperature measured in moving aa, eastern flow, approximately 13 km from vent.
---	do----------	04-21-84	0038	≥1,109	---	Aa-flow front, eastern flow, approximately 13 km from vent. Thermocouple inserted 20 cm but did not penetrate plastic interior.
4/84KE18-269F	E. Wolfe---------	04-21-84	1040	---	no	Spiny pahoehoe surface on floor of evacuated channel of eastern flow, still viscous in cracks, 2.0 km northeast of Puu Oo. Dense-rock sample, water cooled.
			(see sample 4/84KE18-346S)			
5/84KE19-270F	do----------	05-16-84	0830	---	yes	Pahoehoe discharged from Puu Oo during pond overflow between 0757 and 0822 H.s.t., 150 m northeast of Puu Oo.
5/84KE19-271F	do----------	05-16-84	1215	≥1,133	yes	Front of thin (30 cm thick) pahoehoe overflow from active channel formed during high fountaining between 0930 and 1230 H.s.t., 10 m from channel, 1 km northeast of Puu Oo.
5/84KE19-272F	C. Neal, R. Moore, B. Pedit.	05-17-84	1009	1,138	yes	Dense pahoehoe toe at front of flow discharged from Puu Oo during pond overflow between 0937 and 0953 H.s.t., 1 km northeast of Puu Oo.

TABLE 2.2.—*Samples collected and temperatures measured during episodes 1 through 20 of the Puu Oo eruption of Kilauea Volcano*—Continued

Sample	Collector	Date	Time (H.s.t.)	Temperature (°C)	Quench	Location and comments
---	R. Moore---------	05-17-84	1013	1,141	---	Same flow and locality as for previous sample.
5/84KE19-273F	E. Wolfe---------	05-28-84	---	---	no	Thick pahoehoe slab on channel floor, 100 m east of Puu Oo, from last(?) lava overflow from Puu Oo during episode 19. Dense-rock sample.
6/84KE20-274F	do----------	06-08-84	0715	---	yes	Tube-fed, slabby pahoehoe toe at terminus of northern flow, 3.5 km northeast of Puu Oo.
---	do----------	06-08-84	0750	≥1,137	---	Do.
6/84KE20-275F	do----------	06-14-84	1100	---	no	Block in Puu Oo spillway. Dense-rock sample.
6/84KE1-276F	G. Ulrich--------	06-26-84	---	---	no	Pahoehoe buried in tephra, 20 m north of west end of Puu Kamoamoa. Dense-rock sample.
9/83KE9-340S	C. Neal----------	09-27-83	---	---	no	Lightweight tephra (4-10 cm across) collected at surface, approximately 200 m southwest of Puu Oo.
1/84KE12-341S	do----------	01-10-84	---	---	no	Do.
2/84KE14-342S	do----------	02-07-84	---	---	no	Do.
2/84KE15-343S	do----------	02-21-84	---	---	no	Lightweight tephra, large and small fragments, collected at surface, 600 m uprift of Puu Oo. Not on main dispersal axis.
3/84KE16-344S	do----------	03-08-84	---	---	no	Lightweight tephra collected at camp D, 750 m west of Puu Oo.
3/84KE17-345S	do----------	03-30-84	1123	---	no	Lightweight part of 40-cm-diameter bomb, probably a product of high fountaining early in episode. Sample collected 100 m southwest of Puu Oo during the episode.
4/84KE18-346S	do----------	04-19-84	1700	---	no	Lightweight tephra, including large bomb fragments from early high fountains and small fragments from later fountaining. Sample collected approximately 900 m uprift of Puu Oo.

TABLE 2.3.—*Classical chemical analyses of 43 lava samples from episodes 1 through 20 of the Puu Oo eruption of Kilauea Volcano*

[Analyses in weight percent, determined by the techniques of Peck (1964); analyst, Elaine L. Brandt, U.S. Geological Survey, Denver, Colo.]

Field No.	1/83KE1-5S	1/83KE1-10F	1/83KE1-17S	1/83KE1-39F	1/83KE1-49S	2/83KE2-66F	2/83KE2-77F	3/83KE2-81S	3/83KE3-88F	3/83KE3-96F	4/83KE3-117F	6/83KE4-121F
Laboratory No.	D-252970	D-252971	D-252972	D-252973	D-252974	D-252975	D-252976	D-252977	D-252978	D-252979	D-252980	D-252981
SiO_2	50.76	51.14	50.83	50.93	50.88	51.08	50.89	50.90	50.68	50.84	50.63	50.67
Al_2O_3	14.37	14.36	14.41	14.14	14.10	14.19	14.06	14.29	14.25	14.50	14.37	14.17
Fe_2O_3	1.38	1.25	1.33	1.58	1.20	1.32	1.44	1.54	1.25	1.48	3.79	1.37
FeO	10.22	10.08	10.06	10.53	10.08	10.51	10.42	10.08	10.17	10.09	8.06	9.91
MgO	6.28	6.28	6.34	5.74	6.72	5.97	5.96	6.04	6.59	6.08	6.02	7.00
CaO	10.53	10.43	10.57	9.86	10.88	10.25	10.14	10.34	10.62	10.42	10.29	10.72
Na_2O	2.53	2.55	2.51	2.70	2.38	2.66	2.65	2.59	2.49	2.60	2.59	2.43
K_2O	.57	.60	.59	.69	.50	.65	.66	.61	.55	.61	.62	.52
H_2O^+	.03	.04	.03	.04	.05	.04	.04	.06	.06	.06	.04	.05
H_2O^-	<.01	<.01	<.01	<.01	<.01	<.01	<.01	<.01	<.01	<.01	<.01	<.01
TiO_2	2.77	2.66	2.71	3.16	2.66	3.12	3.11	3.01	2.82	2.99	3.00	2.73
P_2O_5	.29	.31	.29	.35	.27	.33	.33	.32	.29	.31	.31	.28
MnO	.17	.17	.17	.18	.17	.17	.18	.17	.17	.17	.17	.17
CO_2	<.01	<.01	<.01	.01	<.01	<.01	<.01	<.01	<.01	<.01	<.01	<.01
Cl	.01	.01	.01	.01	.01	.01	.01	.01	.01	.01	.01	.01
F	.04	.04	.04	.05	.03	.06	.06	.05	.05	.05	.05	.04
Total S	<.01	<.01	<.01	<.01	.01	<.01	<.01	.01	<.01	<.01	.01	<.01
Subtotal	99.95	99.92	99.89	99.97	99.94	100.36	99.95	100.02	100.00	100.21	99.96	100.07
Less O	.02	.02	.02	.02	.02	.03	.03	.03	.02	.02	.03	.02
Total	99.93	99.90	99.87	99.95	99.92	100.33	99.92	99.99	99.98	100.19	99.93	100.05

TABLE 2.3.—*Classical chemical analyses of 43 lava samples from episodes 1 through 20 of the Puu Oo eruption of Kilauea Volcano*—Continued

Field No.	6/83KE4-130F	6/83KE5-136F	6/83KE5-139F	7/83KE6-146F	7/83KE6-149F	7/83KE6-154F	8/83KE7-159F	8/83KE7-167F	9/83KE8-172F	9/83KE8-174F	9/83KE9-177F
Laboratory No.	D-252982	D-252983	D-252984	D-254064	D-254065	D-254066	D-254067	D-254068	D-256017	D-256018	D-256019
SiO_2	50.64	50.86	50.43	50.70	50.47	50.18	50.75	50.27	50.85	50.33	50.19
Al_2O_3	14.01	14.16	13.52	14.19	13.42	13.52	14.26	13.56	14.12	13.23	13.23
Fe_2O_3	1.29	1.24	1.53	1.42	1.82	2.30	1.42	1.26	1.50	2.97	4.21
FeO	9.99	9.99	9.88	9.79	9.79	9.17	9.81	10.07	9.63	8.53	7.37
MgO	7.06	7.01	7.86	6.79	7.99	8.26	6.85	8.29	6.97	8.21	8.46
CaO	10.70	10.95	10.77	10.89	10.73	10.62	10.92	10.66	10.95	10.73	10.62
Na_2O	2.42	2.42	2.31	2.42	2.30	2.30	2.39	2.27	2.36	2.29	2.24
K_2O	.56	.54	.50	.54	.50	.49	.52	.49	.52	.51	.50
H_2O^+	.07	.03	.03	.07	.07	.08	.07	.05	.07	.01	.03
H_2O^-	<.01	<.01	<.01	<.01	<.01	<.01	<.01	<.01	<.01	<.01	<.01
TiO_2	2.73	2.73	2.60	2.72	2.57	2.57	2.67	2.56	2.71	2.61	2.59
P_2O_5	.28	.27	.26	.27	.26	.26	.27	.25	.26	.25	.25
MnO	.17	.16	.17	.17	.17	.17	.17	.17	.17	.17	.17
CO_2	<.01	<.01	<.01	<.01	<.01	.01	<.01	<.01	<.01	.01	<.01
Cl	.01	.01	.01	.01	.01	.01	.01	.01	.01	<.01	<.01
F	.03	.03	.04	.04	.04	.03	.04	.04	.04	.03	.03
Total S	<.01	<.01	<.01	<.01	<.01	<.01	<.01	<.01	<.01	<.01	.01
Subtotal	99.96	100.40	99.91	100.02	100.14	99.97	100.15	99.95	100.16	99.88	99.90
Less O	.01	.01	.02	.02	.02	.01	.02	.02	.02	.01	.02
Total	99.95	100.39	99.89	100.00	100.12	99.96	100.13	99.93	100.14	99.87	99.88

TABLE 2.3.—*Classical chemical analyses of 43 lava samples from episodes 1 through 20 of the Puu Oo eruption of Kilauea Volcano*—Continued

Field No.	9/83KE9-178F	10/83KE10-183F	10/83KE10-187F	11/83KE11-190F	11/83KE11-195F	11/83KE12-197F	12/83KE12-203F	1/84KE13-209F	1/84KE13-216F	1/84KE13-226F
Laboratory No.	D-256020	D-256932	D-256933	D-256934	D-256935	D-256936	D-256937	D-257689	D-257690	D-257691
SiO_2	50.21	50.72	50.49	50.78	50.53	50.80	50.81	50.74	50.72	50.91
Al_2O_3	13.12	13.66	13.49	13.76	13.71	13.81	13.84	13.79	13.77	13.67
Fe_2O_3	2.58	1.48	1.35	1.21	2.61	1.30	1.27	1.32	1.18	1.36
FeO	8.93	9.74	9.94	9.85	8.62	9.77	9.83	9.75	9.88	9.75
MgO	8.61	7.27	8.33	7.26	7.38	7.31	7.46	7.29	7.27	7.27
CaO	10.60	11.05	10.84	11.09	11.03	11.07	11.21	11.17	11.17	11.14
Na_2O	2.23	2.31	2.26	2.30	2.28	2.28	2.29	2.29	2.29	2.28
K_2O	.49	.50	.49	.49	.49	.48	.48	.49	.49	.48
H_2O^+	.05	.04	.05	.05	.08	.10	.08	.07	.09	.05
H_2O^-	<.01	<.01	<.01	<.01	<.01	<.01	<.01	<.01	<.01	<.01
TiO_2	2.57	2.63	2.58	2.61	2.58	2.60	2.60	2.60	2.60	2.58
P_2O_5	.25	.25	.24	.25	.25	.25	.25	.25	.25	.25
MnO	.17	.17	.17	.17	.17	.17	.16	.17	.16	.17
CO_2	<.01	<.01	<.01	<.01	.01	.01	<.01	<.01	<.01	<.01
Cl	.01	<.01	<.01	<.01	.01	<.01	<.01	.01	.01	.01
F	.03	.03	.03	.03	.03	.03	.03	.03	.04	.03
Total S	<.01	<.01	<.01	<.01	<.01	<.01	<.01	<.01	<.01	<.01
Subtotal	99.85	99.85	100.26	99.85	99.78	99.98	100.31	99.97	99.92	99.95
Less O	.01	.01	.01	.01	.01	.01	.01	.01	.02	.01
Total	99.84	99.84	100.25	99.84	99.77	99.97	100.30	99.96	99.90	99.94

TABLE 2.3.—*Classical chemical analyses of 43 lava samples from episodes 1 through 20 of the Puu Oo eruption of Kilauea Volcano*—Continued

Field No.	1/84KE14-231F	2/84KE15-237F	3/84KE16-247F	3/84KE16-254F	3/84KE17-256F	3/84KE17-260F	4/84KE18-263F	4/84KE18-269F	6/84KE19-272F	6/84KE20-274F
Laboratory No.	D-257692	D-257693	D-258029	D-258030	D-258031	D-258032	D-258033	D-258034	D-258932	D-258933
SiO_2	50.77	50.78	50.85	50.81	50.87	50.84	50.73	50.51	50.78	50.67
Al_2O_3	13.70	13.65	13.47	13.56	13.52	13.58	13.74	13.57	13.66	13.61
Fe_2O_3	1.45	1.77	2.36	1.39	2.33	1.61	1.22	2.03	1.20	1.47
FeO	9.63	9.34	8.91	9.76	8.88	9.54	9.90	9.18	9.88	9.63
MgO	7.33	7.39	7.46	7.47	7.51	7.48	7.48	7.89	7.59	7.61
CaO	11.18	11.19	11.20	11.19	11.23	11.23	11.25	11.18	11.24	11.25
Na_2O	2.28	2.27	2.28	2.27	2.26	2.26	2.26	2.23	2.26	2.24
K_2O	.49	.50	.47	.47	.48	.47	.46	.47	.46	.46
H_2O^+	.04	.04	.03	.03	.03	.05	.05	.06	.11	.13
H_2O^-	<.01	<.01	<.01	<.01	<.01	<.01	<.01	<.01	<.01	<.01
TiO_2	2.57	2.55	2.57	2.55	2.56	2.56	2.57	2.48	2.53	2.51
P_2O_5	.25	.25	.25	.25	.26	.25	.25	.24	.24	.24
MnO	.16	.17	.17	.17	.17	.17	.17	.17	.17	.16
CO_2	<.01	<.01	<.01	<.01	<.01	<.01	<.01	.01	<.01	<.01
Cl	.01	.01	.01	.01	.01	.01	<.01	.01	.01	.01
F	.04	.03	.02	.03	.02	.03	.03	.02	.03	.03
Total S	<.01	<.01	<.01	<.01	<.01	<.01	<.01	<.01	<.01	<.01
Subtotal	99.90	99.94	100.05	99.96	100.13	100.08	100.11	100.05	100.16	100.02
Less O	.02	.01	.01	.01	.01	.01	.01	.01	.01	.01
Total	99.88	99.93	100.04	99.95	100.12	100.07	100.10	100.04	100.15	100.01

3. PETROLOGY OF THE ERUPTED LAVA

By MICHAEL O. GARCIA[1] and EDWARD W. WOLFE

CONTENTS

ABSTRACT

The mineralogy and whole-rock, major-element composition of lava from episodes 1 through 20 of the Puu Oo eruption of Kilauea Volcano are diagnostic of processes that occurred during this eruption. Lava from episodes 1 through 3 was produced by crystal fractionation of magma stored in isolated pockets in the rift zone. Lava from episodes 4 through 20 has a composition typical of summit lava, indicating that summit-type magma reached the eruption site by episode 4, nearly 6 months after the start of this eruptive sequence.

Significant chemical and mineralogic changes in the lava of each eruptive episode occurred during episodes 5 through 10. These changes probably resulted from crystal fractionation (involving olivine ± augite) in a shallow reservoir beneath Puu Oo.

Progressive increase in CaO and MgO contents and decrease in TiO_2, Na_2O, K_2O, and P_2O_5 contents in the lava from episodes 4 through 20 may reflect either an increasing proportion of summit magma mixed with differentiated, rift-zone magma, or an increasing degree of partial melting of the mantle leading to an increase in the contribution of clinopyroxene to the melt. These two processes could also have occurred in combination.

INTRODUCTION

The Puu Oo eruption began on January 3, 1983, at Napau Crater (see fig. 1.1), midway along Kilauea's east rift zone. After an initial series of fissure eruptions on an 8-km-long vent system, the eruptive style evolved to one of episodic central-vent eruptions that, as of July 1985, have continued for 2½ years and produced the greatest volume of lava of any historical eruption of Kilauea. The lava shows a significant degree of compositional variation that reflects petrologic processes within Kilauea Volcano and, possibly, within the mantle. This chapter reports petrologic results from the first 20 eruptive episodes, January 3, 1983, through June 8, 1984. The eruptive activity during that 1½-year period is described in chapter 1. Only a brief review of that activity is given here to provide a specific context for the petrologic discussion.

ERUPTIVE ACTIVITY DURING EPISODES 1 THROUGH 3

Episode 1 produced about 14×10^6 m^3 of lava (volume not adjusted to dense-rock equivalent) in a series of short, vigorous fissure eruptions, most of which lasted from about 1 to 12 hours. They occurred intermittently from January 3 through January 23 and were separated by repose periods ranging in duration from a few minutes to 8 days. Sporadic spattering and minor flow production occurred between the more significant periods of lava discharge.

During the first hours of the eruption on January 3, a discontinuous line of eruptive fissures formed that extended 6.3 km from Napau Crater downrift to the 0740 vent (vent designated by time of its first eruptive activity; pl. 1). Lava discharge stopped temporarily at midday on January 3 and resumed at the 1123 vent on January 5. An intense eruption occurred on January 5 and 6 in the 0740–1123 vents area. On January 7, the eruptive fissure system extended an additional 1.5 km downrift (northeastward); these new vents were the site of about 19 hours of intense eruptive activity. Thereafter, sporadic fissure eruptions continued in the 0740–1123 vents area through January 15. Intermittent vigorous gas emission and spattering occurred at the 0740 and 1708 vents between January 15 and 23. Finally, on January 23, episode 1 ended with a brief eruption near Puu Kamoamoa.

Episode 2 began in early February with slow leakage of lava from the 0740 vent; within 2 weeks, an estimated 0.5×10^6 m^3 of lava was extruded. In late February, the eruptive activity abruptly intensified and shifted to the 1123 vent, where voluminous central-vent eruptions ensued during the rest of episode 2 (late February–early March 1983) and during episode 3 (late March–early April). Less voluminous lava discharge also occurred uprift during these episodes at the O vent, which was later buried by Puu Oo (see fig. 1.1). Approximately 53×10^6 m^3 of lava was erupted during episodes 2 and 3.

[1]Hawaii Institute of Geophysics, University of Hawaii, Honolulu.

ERUPTIVE ACTIVITY DURING EPISODES 4 THROUGH 20

After slightly more than 2 months of quiescence, episode 4, in mid-June 1983, initiated a series of intermittent central-vent eruptions in the Puu Oo area. These eruptions formed a large new spatter cone, Puu Oo.

From episode 4 through 20, approximately 173×10^6 m^3 of lava issued from the Puu Oo vent. These episodes lasted from about 1 to 4 days and were characterized by vigorous fountaining and high-volume emission of lava flows. At these times, rapid subsidence occurred at Kilauea's summit. The eruptive episodes were separated by longer periods of relative quiescence, commonly about 2 to 4 weeks long, during which Kilauea's summit gradually inflated. During these repose periods, a magma column apparently persisted beneath the vent; the top of this column was sometimes visible. At times, it supplied lava to an intermittent pond or to pahoehoe flows of small volume on the crater floor.

MAGMA STORAGE AND TRANSPORT WITHIN KILAUEA

Geologic and geophysical study of Kilauea has led to a generalized model of the structure and plumbing of the volcano (see reviews by Ryan and others, 1981, and Dzurisin and others, 1984). Basaltic melt derived from the upper mantle (greater than 60 km depth) migrates upward to a shallow reservoir, 2 to 6 km below the summit of Kilauea. Continuing accumulation of magma causes inflation of the reservoir, which is manifested by uplift and distention of the overlying crust. Eruptions of the volcano or intrusions that transfer magma from the summit to the rift zones give episodic relief from accumulating magmatic stress in the reservoir region; at such times the summit region subsides and contracts.

Petrologic and geophysical evidence suggests that magma is stored in the rift zones. Dzurisin and others (1984) concluded that more than 10^9 m^3 of magma may have intruded the east rift zone and been stored during the period 1956–83. Wright and Fiske (1971) showed that cooling and crystallization of magma stored in the rift zones may result in substantial compositional variation of erupted magma due to effects of crystal fractionation. Such lava has a low Mg number $[100 \times Mg/(Mg + Fe^{2+})]$ and a composition that diverges from olivine control (Wright and Fiske, 1971). Additional variation results from mixing of such differentiated magma with new magma intruded from the summit reservoir. [In this report, we adopt the terminology of Wright and Fiske (1971) in referring to all lava containing less than 6.8 weight percent MgO as differentiated, even though mixing as well as crystal fractionation may have been involved in its origin.] On the basis of geologic mapping and compositional analysis of prehistoric flows and vent deposits in the lower east rift zone, Moore (1983) inferred that, over periods of hundreds of years, long-lived reservoirs have repeatedly produced lava of differentiated or hybrid (mixed) composition. In contrast, lava erupted at the summit has a higher Mg number (greater than 55) and a composition that generally can be explained by olivine control (Wright, 1971). Temporally, subtle changes occur in the composition of the olivine-controlled summit lava that are probably related to small changes in the composition and degree of melting of the mantle source for Kilauea Volcano (Wright, 1984).

Typically, lava erupted early in a sequence of rift-zone eruptions is differentiated, whereas lava erupted later may be of intermediate composition, reflecting mixing of stored magma with new summit magma. During protracted eruptions like that of Mauna Ulu (1969–71, 1972–74), olivine-controlled lava of unmixed, summit-type composition may be erupted. Hofmann and others (1984) attributed small but progressive variation in the composition of olivine-controlled lava of the 1969–71 Mauna Ulu eruption to gradual change in source composition or degree of partial melting.

In summary, the following sequence of events has been inferred for eruptions on Kilauea's east rift zone: (1) Undifferentiated, olivine-controlled magma from the summit reservoir intrudes the east rift; (2) isolated pockets of magma form, and cooling of the magma causes differentiation beyond olivine control; (3) stored rift-zone magma may be diluted by more recently intruded summit magma; and (4) lava of summit composition may be discharged in prolonged eruptions. Its composition may change in response to variation in the composition and (or) degree of melting of the source.

SAMPLING AND ANALYTICAL TECHNIQUES

More than 300 samples were collected during the first 20 episodes of the Puu Oo eruption. Most samples were collected molten from active flows or falling spatter and were quenched in water. Samples of rapidly quenched melt are difficult to study in thin section because they are extremely friable and vesicular. Therefore, at least one sample of relatively dense rock was collected and studied after each eruptive episode. Modes, consisting of at least 1,000 points, were made on both the water-quenched (table 3.1) and dense samples (table 3.2). In most samples, the mineral grains are in a glassy matrix; these grains are referred to as "phenocrysts," regardless of their size. Details of sampling technique and settings for the individual samples are given in chapter 2. The sample numbers used here correspond to the final digits of the sample numbers used in chapter 2. "F" indicates a flow sample, and "S" a spatter sample.

TABLE 3.1.—*Modal mineralogy of lava samples from the Puu Oo eruption*

[All analyses in volume percent, 1,000 counts per sample, vesicle free; analysts, R. Ho and S. Spengler. Vent location for episodes 4 through 20 was Puu Oo. Do., ditto; n.d., not determined]

Vent/ sample	Plagio- clase	Oli- vine	Augite	Matrix	Time (H.s.t)	Date	Comment
			Episode 1				
Napau							
492	2.1	0.1	2.1	95.7	n.d.	01/03	First flow.
Puu Kamoamoa							
2F	.7	.0	.1	99.2	0508	01/03	-----
5S	.6	.0	.2	99.2	0704	01/03	-----
6S	.3	.0	.0	99.7	0958	01/03	-----
1123 vent							
7S	2.1	.3	.8	96.8	1140	01/05	-----
39F	3.1	.3	1.2	95.4	0706	01/15	-----
Western January 7 vent							
17S	2.1	.2	1.3	96.4	1100	01/07	-----
19S	2.4	.3	1.2	96.1	1735	01/07	-----
22F	4.6	.8	.7	93.9	0240	01/08	-----
0740 vent							
10F	1.7	.1	1.5	96.7	1530	01/05	-----
13F	2.8	.5	1.6	95.1	1058	01/06	-----
15F	3.8	.8	1.2	94.2	1736	01/06	-----
25S	2.1	.4	.4	97.1	1454	01/08	-----
46S	2.8	.9	.2	96.1	0425	01/18	Only spatter.
47S	6.5	1.0	1.7	90.8	1145	01/20	Do.
48S	3.7	1.9	1.4	93.0	2000	01/21	Do.
1708 vent							
27F	2.8	.1	.7	96.4	2230	01/08	-----
30F	3.4	.3	.7	95.6	0600	01/10	-----
31S	3.9	.0	2.8	93.3	0720	01/10	-----
34F	4.5	.0	3.3	91.2	0315	01/11	-----
37F	5.0	.0	2.5	92.5	1240	01/11	-----
41S	4.2	.7	.7	94.4	0145	01/17	Only spatter.
45S	3.5	.6	.9	95.0	1510	01/17	Do.
			Episode 2				
0740 vent							
66F	3.9	1.6	1.6	92.9	1037	02/16	-----
1123 vent							
77F	4.3	.1	1.6	94.0	2129	02/25	-----
81S	2.8	.1	.8	96.3	2146	03/01	-----
			Episode 3				
Puu Oo							
88F	5.8	0.3	4.9	89.0	1515	03/28	-----
1123 vent							
96F	3.0	.2	.9	95.9	1145	03/31	-----
117F	3.1	.0	1.1	95.8	1115	04/09	-----
			Episode 4				
121F	3.8	0.3	3.4	92.5	2345	06/13	-----
130F	1.1	1.4	2.8	94.7	1200	06/17	-----
			Episode 5				
136F	4.1	0.5	3.7	91.7	1735	06/29	-----
139F	.6	1.4	2.1	95.9	0900	07/03	-----
			Episode 6				
146F	3.0	1.0	2.0	94.0	1400	07/22	Early.
149F	.0	4.0	.7	95.3	1107	07/24	-----
154F	.2	2.3	1.1	96.4	0800	07/26	Late.
			Episode 7				
155S	2.8	0.6	2.4	94.2	ND	08/10	Pre-episode.
156F	1.4	.0	1.2	96.8	1645	08/10	Do.
158F	.4	.2	1.8	97.6	0930	08/15	Early.
159F	1.1	.2	1.1	97.6	1110	08/15	Do.
162F	.2	1.4	.6	97.8	1645	08/15	-----
163F	.1	2.3	.5	97.1	0755	08/16	-----
165F	.0	1.6	.4	98.0	1530	08/16	-----
166F	.0	2.1	1.4	96.5	1200	08/17	-----
			Episode 7--Continued				
167F	.0	4.3	.8	94.9	1225	08/17	Late.
			Episode 8				
172F	0.1	0.5	0.6	98.8	0910	09/06	Early.
174F	.0	1.6	.8	97.6	1550	09/07	Late.
			Episode 9				
177F	0.0	2.4	1.3	96.2	1400	09/17	Late.
178F	.0	6.6	0.4	93.0	1100	09/17	Do.
			Episode 10				
183F	0.0	0.3	0.8	98.9	1407	10/05	Early.
187F	.0	5.9	2.1	92.0	1050	10/07	Late.
			Episode 11				
190F	0.0	0.6	0.3	99.1	1135	11/06	-----
195F	.0	.0	.3	99.7	1130	11/08	-----
			Episode 12				
197F	0.0	0.3	0.3	99.4	1140	11/30	-----
203F	0	.5	.1	99.4	1440	12/01	-----
			Episode 13				
216F	0.0	0.0	0.1	99.9	0912	01/21	-----
226F	0	.4	.0	99.6	1050	01/22	-----
			Episode 14				
231F	0.0	0.1	0.0	99.9	1125	01/31	-----
			Episode 15				
237F	0.0	0.4	0.0	99.6	1245	02/15	-----
			Episode 16				
247F	0.0	0.2	0.0	99.8	1818	03/03	-----
254F	.0	.6	.1	99.3	1525	03/04	-----
			Episode 17				
256F	0.0	0.0	0.3	99.7	1050	03/30	-----
260F	.0	.6	.2	99.2	0745	03/31	-----
			Episode 18				
263F	0.0	0.9	0.0	99.1	0825	04/19	-----
269F	.0	.5	.0	99.5	1040	04/21	-----
			Episode 19				
272F	0.0	0.8	0.0	99.2	1009	05/17	-----
			Episode 20				
274F	0.0	0.5	0.0	99.5	0715	06/08	-----

TABLE 3.2.—*Modal mineralogy of dense-rock samples from the Puu Oo eruption*

[All analyses in volume percent, 1,000 counts per sample, vesicle free; analysts, R. Ho and S. Spengler. Asterisks, samples from University of Hawaii, Manoa, collection]

Episode	Sample	Plagioclase	Olivine	Augite	Matrix
1	276F	0.6	0.0	0.5	98.9
2	2*	3.1	.2	.2	96.5
3	3*	1.5	.2	.1	98.2
4	207F	4.9	1.9	2.3	90.9
5	5*	1.3	5.3	1.6	91.8
6	6*	.1	5.4	1.3	93.2
7	7*	.0	4.0	1.8	94.2
8	8*	.0	.8	1.0	98.2
9	178F	.0	6.6	.7	92.7
10	10*	.0	.9	.7	98.4
11	11*	.0	.4	.1	99.5
12	202	.0	.2	.2	99.6
13	233	.0	.2	.0	99.8
14	235	.0	.1	.0	99.9
15	243	.0	.8	.0	99.2
16	262	.0	.2	.0	99.8
18	269	.0	.2	.0	99.8
19	273	.0	2.0	.2	97.8

Whole-rock, major-element analyses were done by classical wet chemical methods (Peck, 1964) in the U.S. Geological Survey laboratories in Denver, Colo., and by rapid-fusion, electron-microprobe methods (Jezek and others, 1979) at the University of Hawaii. Wet chemical analyses are of high precision and accuracy but are expensive and time consuming. A total of 43 such analyses (see chap. 2, table 2.3) were done, mostly on samples obtained early and late from each episode. In contrast, microprobe analyses are inexpensive and can be quickly completed. We have analyzed 68 samples (table 3.3) by this method, using the results to investigate details of compositional variation within individual eruptive episodes. Analysis of five samples from episode 1 by each technique shows that results from these two techniques compare favorably (table 3.4). The differences are within 1.5 percent of the amount present except for K_2O (4-percent difference), which is in low concentration (0.5–0.7 weight percent).

Acknowledgments.—We appreciate the assistance in monitoring eruptive episodes and in sampling their products from our colleagues at the University of Hawaii and within the U.S. Geological Survey, from both the mainland and the Hawaiian Volcano Observatory. In particular, we thank N.G. Banks, J. Buchanan-Banks, J.P. Lockwood, R.B. Moore, and C.A. Neal, who were on hand to assist and relieve us, and C.D. Byers for his excellent analytical assistance. Thanks go also to T.A. Duggan, who handled the initial cataloging and all the detailed management of the samples, and to Ritchie Ho, who prepared samples for microprobe analyses and determined most of the modes. This project was supported by U.S. National Science Foundation Grant EAR 84-07763.

COMPOSITION AND MINERALOGY

OVERALL COMPOSITIONAL VARIATION

Lava of episodes 1 through 3 was differentiated beyond olivine control, as indicated by its low (less than 6.8 weight percent) MgO content coupled with relatively low CaO content and relatively high content of TiO_2, FeO_t (total Fe as FeO), Na_2O, K_2O, and P_2O_5 contents (figs. 3.1, 3.2). One of the most and one of the least differentiated samples (25S and 10F, respectively; see chap. 2) were erupted from the same vent (0740) during episode 1. Thus, compositional variation occurred locally in the rift zone. Compositions are less diverse during episodes 2 and 3, intermediate between the extremes of episode 1.

After episode 1, the lava generally contained progressively more CaO and MgO and less K_2O, Na_2O, TiO_2, and FeO_t (fig. 3.1). Superimposed on the gradual, long-term compositional change was a series of short-term changes, evident in episodes 5 through 10 and, to a lesser degree, in episode 18. In each of these eruptive episodes, lava erupted late was enriched in MgO (fig. 3.1) and depleted in CaO, Al_2O_3, and incompatible elements.

OVERALL MINERALOGIC VARIATION

In concert with the large variation in the chemical composition of the lava from the first 20 episodes of the Puu Oo eruption, there was also substantial mineralogic variation (table 3.1). The earliest samples of episode 1 lava (except for Napau Crater sample 49S) are nearly aphyric (less than 1 volume percent phenocrysts; fig. 3.3). Later samples of episode 1 lava are strongly porphyritic (approx 9 volume percent) and contain abundant euhedral plagioclase and augite phenocrysts. Lava of episodes 2 through 10 was somewhat (1–2 volume percent) to strongly (more than 10 volume percent) porphyritic (fig. 3.4). In contrast, lava of episodes 11 through 20 was nearly aphyric (less than 1 volume percent).

The relative proportions of plagioclase, augite, and olivine phenocrysts also vary substantially in samples of lava from episodes 1 through 20. During episodes 1 through 3, plagioclase and augite were the dominant phenocrysts. In all but 1 (sample 48S) of 27 point-counted samples of lava from episodes 1 through 3, olivine composes less than 1 volume percent (table 3.1). It is subordinate to plagioclase in all samples, and subordinate to augite in 20 of the samples.

During episode 4, the relative proportions of minerals changed; plagioclase became subordinate to augite. This change was the first indication that the source of the lava might be changing.

TABLE 3.3.—*Microprobe analyses of fused whole-rock powders*

[All anayses in weight percent; analysts: M. Garcia, C. Byers, and S. Spengler]

Sample	SiO_2	TiO_2	Al_2O_3	FeO_t	MgO	CaO	Na_2O	K_2O	Total
Episode 1									
49S	50.87	2.70	14.01	11.10	6.68	11.09	2.30	0.47	99.22
2F	51.05	2.90	13.85	11.55	6.15	10.45	2.50	.54	98.99
5S	50.91	2.79	14.08	11.45	6.39	10.75	2.41	.56	99.34
6S	50.90	3.00	13.95	11.45	6.20	10.40	2.50	.55	98.95
10F	51.13	2.72	14.41	11.00	6.36	10.45	2.55	.54	99.16
17S	50.83	2.73	14.41	11.32	6.41	10.67	2.58	.57	99.52
25S	51.40	3.10	13.75	11.70	5.75	9.95	2.60	.60	98.65
37F	51.40	3.30	13.75	11.60	5.80	9.90	2.70	.65	99.10
39F	51.36	3.15	13.90	11.65	5.77	9.91	2.61	.69	99.04
40F	51.31	3.21	13.84	11.82	5.80	9.76	2.68	.67	99.09
54S	51.15	3.00	14.01	11.41	6.16	10.13	2.52	.60	98.98
Episode 2									
66F	50.97	3.15	14.00	11.70	5.93	10.01	2.58	0.64	98.98
77F	50.87	3.22	14.12	11.55	5.98	10.27	2.06	.45	98.52
81S	50.86	3.07	14.08	11.57	6.07	10.38	2.52	.58	99.13
Episode 3									
88F	50.81	2.87	14.12	11.17	6.68	10.70	2.45	0.52	99.32
96F	51.02	3.11	14.08	11.53	6.09	10.48	2.49	.58	99.38
117F	50.79	2.94	14.06	11.21	6.74	10.75	2.35	.52	99.36
Episode 4									
121F	51.00	2.75	13.75	11.10	7.00	10.65	2.30	0.50	99.05
130F	51.00	2.80	13.60	11.15	7.05	10.65	2.35	.51	99.11
Episode 5									
136F	51.00	2.80	13.60	11.00	7.00	10.70	2.35	0.49	98.94
139F	50.40	2.60	13.20	11.34	8.27	10.45	2.23	.51	99.00
Episode 6									
146F	51.05	2.78	13.88	11.17	6.75	10.83	2.37	0.52	99.35
149F	50.91	2.60	13.40	11.40	7.90	10.70	2.29	.49	99.69
154F	50.59	2.61	13.29	11.07	8.18	10.55	2.23	.49	99.01
Episode 7									
156F	50.68	2.72	14.17	11.08	6.90	11.00	2.38	0.51	99.44
159F	50.91	2.68	14.01	11.07	6.92	11.06	2.40	.52	99.57
162F	50.58	2.65	13.93	11.06	6.98	10.96	2.39	.54	99.09
163F	50.62	2.63	13.65	11.13	7.73	10.77	2.36	.51	99.43
165F	50.62	2.64	13.43	11.11	7.81	10.78	2.34	.50	99.23
167F	50.83	2.61	13.46	11.04	8.00	10.77	2.31	.50	99.52
Episode 8									
172F	51.15	2.70	13.80	10.70	7.00	10.95	2.40	0.50	99.20
174F	50.90	2.70	13.35	10.90	7.80	10.60	2.20	.48	98.93
Episode 9									
175F	50.85	2.69	13.81	10.99	7.19	10.92	2.33	0.51	99.29
177F	50.70	2.65	13.20	10.95	8.30	10.65	2.15	.46	99.06
178F	50.85	2.65	13.50	11.05	8.15	10.60	2.15	.47	99.42
Episode 10									
179F	50.73	2.68	13.74	10.84	7.11	11.10	2.21	0.50	98.91
Episode 10--Continued									
181F	50.69	2.63	13.55	10.91	7.30	11.09	2.30	0.50	98.97
183F	50.57	2.63	13.67	11.07	7.30	11.13	2.22	.55	99.14
186F	50.63	2.56	13.30	11.13	8.21	10.73	2.13	.48	99.17
187F	50.42	2.57	13.23	11.24	8.59	10.81	2.20	.50	99.56
Episode 11									
188F	50.79	2.61	13.73	10.88	7.24	11.16	2.22	0.50	99.13
190F	50.74	2.63	13.67	10.93	7.29	11.10	2.25	.49	99.10
191F	50.90	2.58	13.59	10.83	7.26	11.11	2.18	.48	98.93
194F	50.65	2.52	13.65	10.80	7.42	11.14	2.17	.50	98.85
195F	50.69	2.59	13.47	10.89	7.26	11.08	2.20	.50	98.68
Episode 12									
197F	50.81	2.56	13.61	10.92	7.22	11.24	2.24	0.49	99.09
200F	50.87	2.60	13.65	10.90	7.23	11.16	2.21	.50	99.12
201F	50.99	2.54	13.66	11.08	7.36	11.16	2.25	.50	99.54
203F	50.68	2.56	13.49	11.04	7.36	11.19	2.24	.50	99.06
Episode 13									
209F	50.91	2.55	13.42	10.96	7.12	11.47	2.30	0.48	99.21
216F	50.88	2.61	13.48	10.90	7.10	11.36	2.31	.49	99.13
224F	50.52	2.58	13.45	11.02	7.21	11.33	2.32	.50	98.93
225F	50.78	2.61	13.42	11.07	7.21	11.35	2.34	.49	99.27
Episode 14									
229F	50.91	2.61	13.48	10.74	7.24	11.30	2.30	0.48	99.06
232F	50.66	2.56	13.38	10.86	7.27	11.31	2.32	.47	98.83
Episode 15									
237F	50.74	2.58	13.49	11.05	7.30	11.10	2.22	0.49	98.97
Episode 16									
246S	50.87	2.57	13.54	10.94	7.27	11.27	2.34	0.47	99.27
247F	50.81	2.58	13.62	10.96	7.34	11.28	2.26	.45	99.30
254F	50.84	2.49	13.46	11.10	7.36	11.15	2.21	.47	99.08
Episode 17									
256F	50.80	2.52	13.49	10.92	7.40	11.18	2.24	0.46	99.01
260F	50.73	2.53	13.50	11.10	7.40	11.31	2.23	.46	99.26
Episode 18									
263F	50.75	2.55	13.68	10.92	7.12	11.13	2.26	0.48	98.89
268F	50.64	2.60	13.72	10.65	7.22	11.17	2.19	.46	98.65
Episode 19									
270F	50.79	2.72	13.82	10.70	7.35	11.01	2.18	0.46	99.03
272F	50.76	2.66	13.70	10.62	7.36	11.18	2.19	.47	98.94
Episode 20									
274F	50.92	2.61	13.90	10.77	7.37	10.98	2.21	0.46	99.22

Episode 5 marked the beginning of a period (episodes 5–10) during which the lava erupted within a single episode showed a large compositional variation (fig. 3.1). Lava samples collected early in episodes 5 through 7 contain common plagioclase and augite (2–4 volume percent each) and minor olivine (max 1 volume percent). Lava collected late in each of these episodes has augite (episode 5) or olivine (episodes 6, 7) as the dominant phenocryst; plagioclase is rare or absent (less than 0.6 volume percent). In samples collected during episodes 8 through 10, augite abundance varies inconsistently; plagioclase is absent in these samples except for rare phenocrysts in an early episode 8 sample (172F). Olivine is the dominant phenocryst phase in samples collected late during episodes

TABLE 3.4.—*Comparison of U.S. Geological Survey wet chemical analyses and University of Hawaii microprobe analyses of samples from episode 1 of the Puu Oo eruption*

[All analyses in weight percent]

Sample-----	5S		10F		17S		30F		49S		Average relative error (percent)
	Wet chemical	Micro-probe	Wet chemical	Micro-probe	Wet chemical	Micro-probe	Wet chemical	Micro-probe	Wet chemical	Micro-probe	
SiO_2-------	50.76	50.91	51.14	51.13	50.83	50.83	50.93	51.05	50.88	50.87	+0.09
Al_2O_3------	14.37	14.08	14.36	14.41	14.41	14.31	14.14	13.90	14.10	14.01	-.94
FeO_t-------	11.46	11.45	11.20	11.00	11.26	11.32	11.91	11.65	11.16	11.10	-.86
MgO--------	6.28	6.39	6.28	6.36	6.34	6.41	5.74	5.77	6.72	6.68	+1.24
CaO--------	10.53	10.75	10.43	10.45	10.57	10.67	9.86	9.91	10.88	11.09	+1.11
Na_2O-------	2.53	2.41	2.55	2.55	2.51	2.58	2.70	2.61	2.38	2.30	-1.42
K_2O--------	.57	.56	.60	.54	.59	.57	.69	.69	.50	.47	-4.07
TiO_2-------	2.77	2.79	2.66	2.72	2.71	2.73	3.16	3.15	2.66	2.70	+.93
Total---	99.27	99.35	99.22	99.16	99.22	99.42	99.13	98.73	99.28	99.22	0.05

8 through 10, and the last sample collected during episode 10 (187F) is the most olivine rich (approximately 6 volume percent) of all the samples collected during episodes 1 through 20.

Samples of the lava of episodes 11 through 20 are nearly aphyric (0.1 through 0.9 volume percent phenocrysts). Olivine is dominant, augite is rare (less than 0.3 volume percent), and plagioclase is absent. Olivine is the only phenocryst phase in lava samples from episodes 14, 15, and 18 through 20.

MINERALOGIC VARIATION WITHIN EPISODE 1

Lava erupted from the 1708, 1123, and 0740 vents shows a substantial increase in plagioclase and olivine abundances during January 5–6 (fig. 3.3). After a pause in lava discharge, this pattern was repeated on January 7–8 at the January 7 vents, which were at the northeast end of the fissure system. During the early morning of January 8, Kilauea's summit stopped subsiding (Wolfe and others, 1987). From January 8 through 11, the abundance of plagioclase phenocrysts again increased, while that of olivine phenocrysts decreased. In contrast to the pattern for January 5–7, augite, like plagioclase, generally increased in abundance during January 8–11.

A major hiatus in lava discharge occurred between January 11 and 15. A 6-hour eruption on January 15 was followed by 8 days of intermittent spatter ejection during which spatter samples were collected. In general, the augite and olivine increased in abundance during this period; plagioclase abundance remained high but varied. The most plagioclase rich sample of episodes 1 through 20 (47S, 6.5 volume percent) was collected during this period.

The cores of olivine phenocrysts from samples of 0740 vent lava discharged on January 5-6 show a trend over time of increasing FeO_t (fig. 3.5; table 3.5). After a brief hiatus, this trend was repeated, as shown in samples of lava discharged first from the January 7 vent and later from the 0740 and 1708 vents during the period January 8–11. The less FeO_t rich olivine phenocrysts, which came from the samples collected earliest in each sequence, have reversely zoned rims (that is, less FeO_t rich than the cores). In addition, distinctly more FeO_t rich olivine crystals, interpreted as xenocrysts because of their resorbed margins and abnormally high FeO_t content, occur in some samples.

In summary, an overall increase in the abundance of phenocrysts occurred during episode 1. The phenocryst phases varied substantially in relative abundance: plagioclase, 0.3 to 6.5 volume percent; augite, less than 0.1 to 3.3 volume percent; olivine, less than 0.1 to 1.4 volume percent. A sharp change occurred in the proportions and abundances of phenocrysts after some brief breaks in lava discharge. The abundance of plagioclase phenocrysts generally increased during individual periods of lava discharge. Olivine cores increased in FeO_t content from January 5 to 6 and again from January 7 to 11.

COMPOSITIONAL VARIATION WITHIN EPISODES 1 THROUGH 3

A total of 10 samples from episode 1 were analyzed. Because of the complexity of episode 1 (as reflected in relatively great compositional variation), its extended duration, and the wide distribution of vents, these samples are insufficient for a detailed analysis of magma sources in the rift zone. Nevertheless, some general observations can be made.

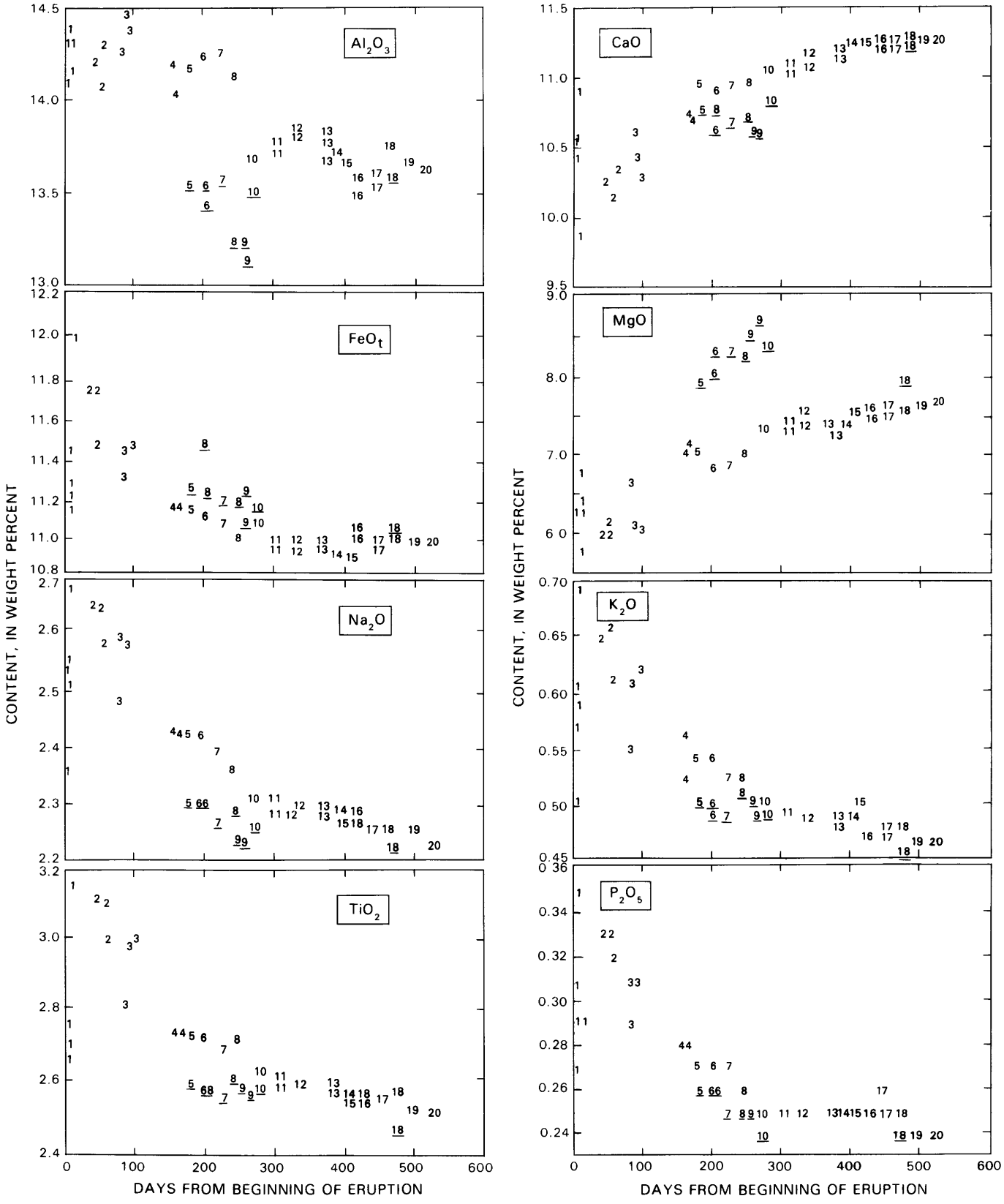

FIGURE 3.1.—Major-oxide contents versus day of eruption. Numbers denote episodes; underscore denotes late, MgO-enriched lava. Data are from wet chemical analyses (see chap. 2).

Two compositional groups are recognized among the samples: less differentiated basalt, containing 6.15 to 6.7 weight percent MgO; and more differentiated basalt, containing approximately 5.8 weight percent MgO (fig. 3.6). The less differentiated lava was erupted along parts of the entire fissure system through January 7. From January 8 through 15, eruptive activity was confined to the area of the 0740, 1123, and 1708 vents, and only more differentiated lava was erupted. This break in composition occurred as Kilauea's summit stopped deflating (fig. 3.6). The last lava erupted during episode 1 was less differentiated in composition. The MgO content of the more differentiated January 1983 lava is similar to that of the most MgO rich lava, erupted 3 to 5 km downrift in 1977 (fig. 3.2; Moore and others, 1980). The 1977 lava, however, contains approximately 0.2 weight percent TiO_2 more at the same K_2O content, indicating that the 1977 lava and the most differentiated January 1983 lava represent distinct magma batches.

Lava of both the less and more differentiated compositions is typical of magma that has been stored in the rift zone, and is unlike summit lava, which is olivine controlled (Wright and Fiske, 1971). The range of compositions observed for lava of episode 1 may be due either to crystal fractionation in isolated pockets or to mixing of magma from pockets. The lava contains mineralogic and textural evidence of mixing (that is, olivine xenocrysts with resorbed grain margins and olivine phenocrysts with reversely zoned rims; fig. 3.5). The lava compositions define linear trends on most element-element plots (figs. 3.2, 3.7). However, the elbow trend on the Al_2O_3-MgO plot indicates that the two lava types are not related by mixing of the compositional extremes. Instead, crystal fractionation involving removal of augite along with plagioclase and olivine is a more plausible mechanism for deriving the more differentiated lava from magma with

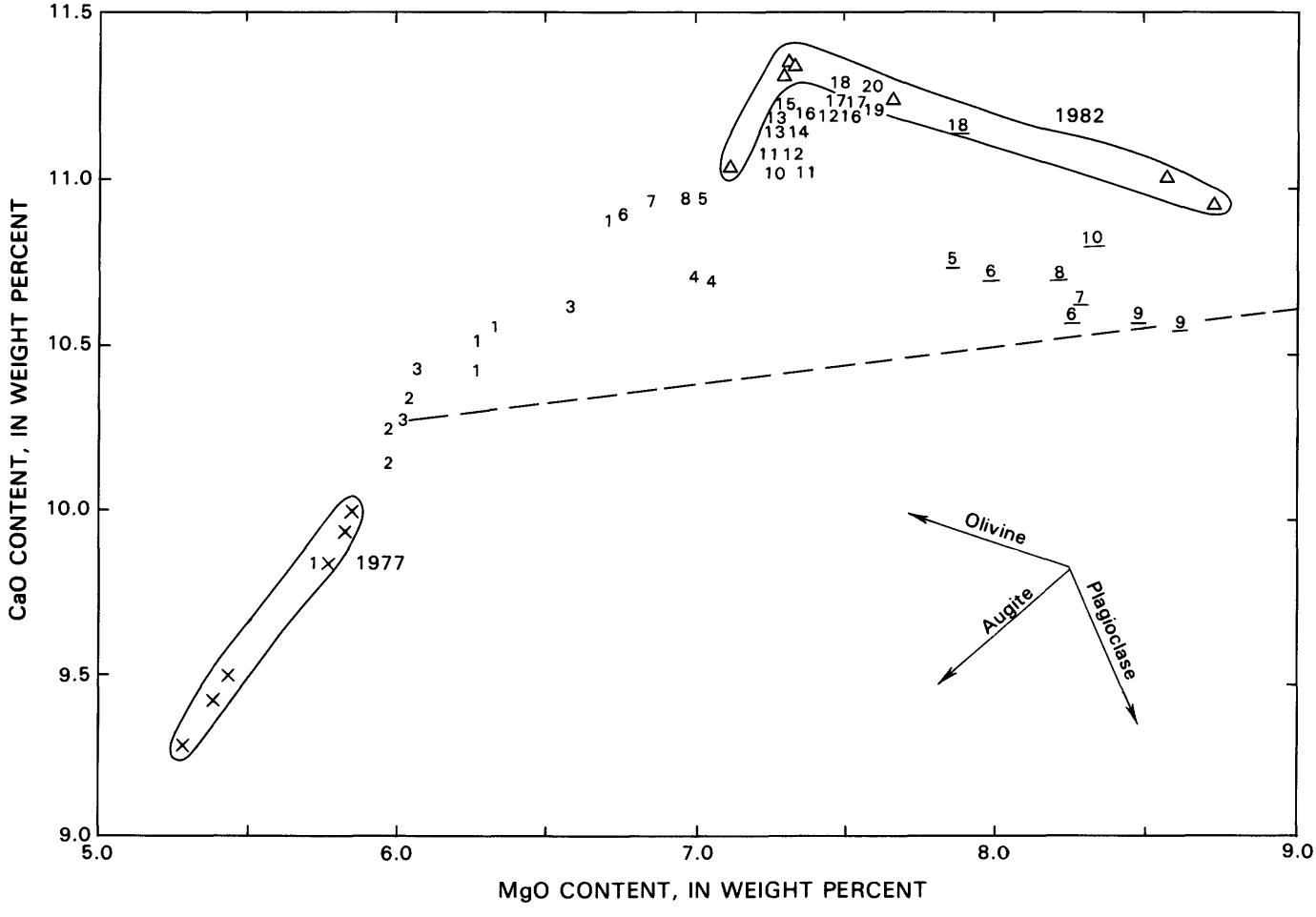

FIGURE 3.2.—CaO versus MgO content for samples from episodes 1 through 20 of the Puu Oo eruption (numbers denote episodes; see chap. 2), 1982 summit eruptions (triangles), and 1977 middle east rift zone, (X's; Moore and others, 1980). Arrows show olivine-, augite-, and plagioclase-control lines. Dashed line is drawn to illustrate a possible mixing line between the average composition for differentiated lava from episodes 1 through 3 (excluding Napau Crater and O vent samples) and the most MgO rich Puu Oo lava. Underscore denotes late lava from episodes 5 through 10 and 18.

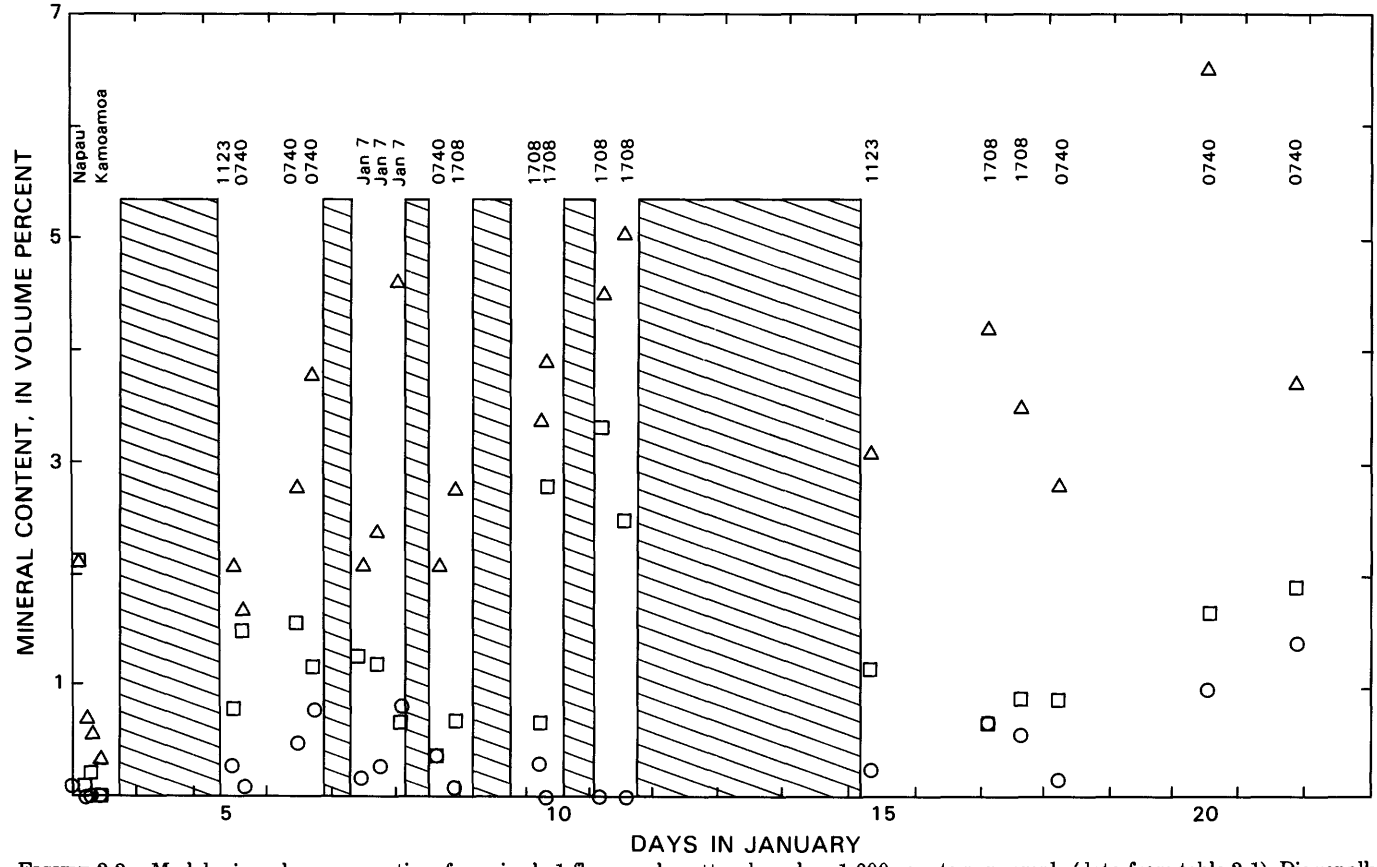

FIGURE 3.3.—Modal mineralogy versus time for episode 1 flows and spatter, based on 1,000 counts per sample (data from table 3.1). Diagonally ruled bars indicate hiatuses in lava discharge between January 3 and 15. Last major lava discharge of episode 1 occurred on January 15; thereafter, through January 22, samples represent sporadic, low-level spattering events. Triangles, plagioclase; circles, olivine; squares, augite. Names and numbers refer to vents (pl. 1).

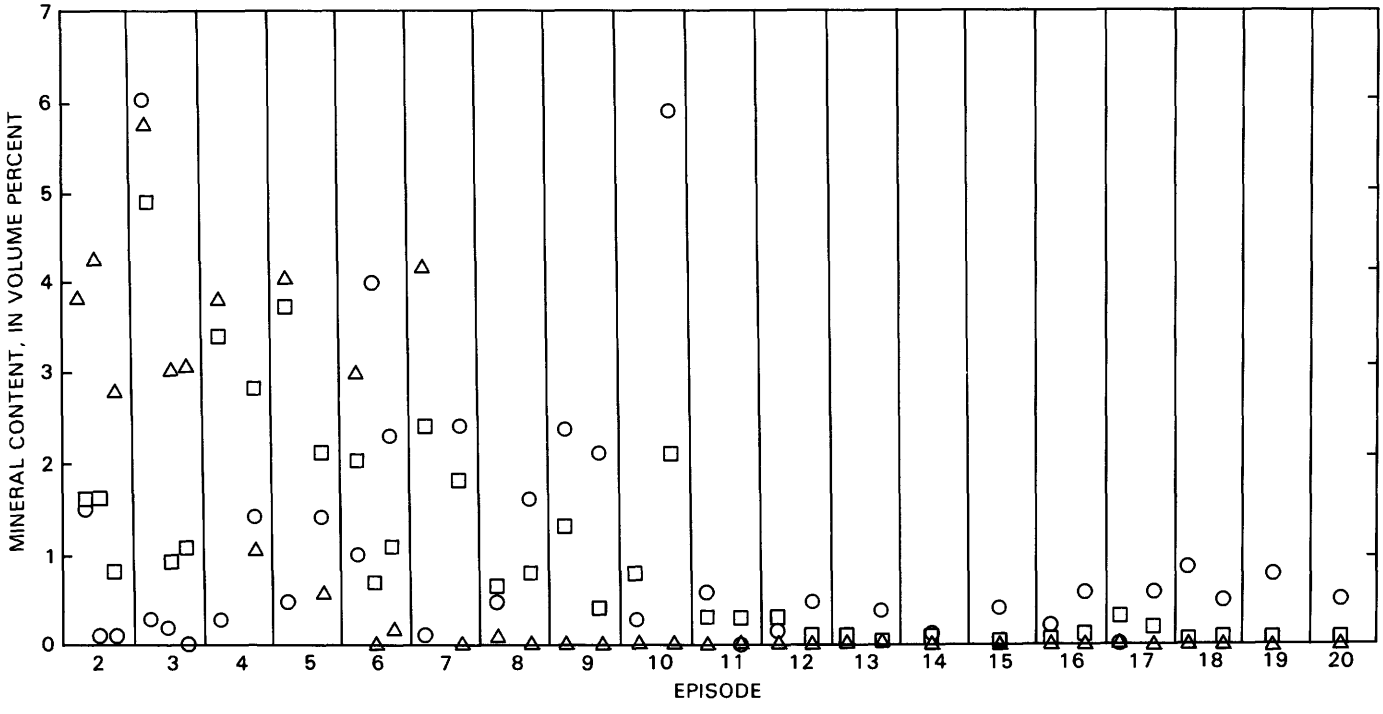

FIGURE 3.4.—Modal mineralogy of samples from episodes 2 through 20. Data from table 3.1. Triangles, plagioclase; circles, olivine; squares, augite.

a composition similar to that of the less differentiated lava. Least-squares mixing calculations support this crystal-fractionation model. Moderate residuals ($r^2 = 0.44$) are obtained for mixing two episode 1 end-member compositions (39F, 49S) to yield an intermediate composition (10F). Low residuals ($r^2 = 0.05$) are obtained for crystal fractionation by using observed mineral compositions (table 3.6) for deriving the most differentiated sample (39F) from the least differentiated sample (49S).

Lava erupted during episodes 2 and 3 may also have evolved by crystal fractionation. Its composition is within the range and trends defined by episode 1 compositions (fig. 3.7).

Wright and Fiske (1971) proposed that the compositional variation in lava erupted from a discontinuous system of fissures in the east rift zone during the early part of the 1955 eruption reflected an origin from pockets of magma which were physically isolated from each other and evolved in composition independently. This process may have produced the observed range in compositions for lavas from episodes 1 through 3. Mixing probably played only a minor role in determining the lava composition.

Note added in proof.—More recent trace-element and mineral analyses indicate that many of the differentiated rocks sampled in episodes 1 through 3 are hybrids.

COMPOSITIONAL VARIATION WITHIN INDIVIDUAL EPISODES (5-10, 18) AT PUU OO

Substantial, systematic variation in the composition of the lava from individual eruptive episodes occurred during episodes 5 through 10 (fig. 3.1). Similar but less extensive variation also occurred in episode 18 lava. Lava erupted late in episodes 5 through 10 contained approximately 1 to 1.5 weight percent MgO more than did the lava erupted early. Increase in MgO content was accompanied by a small but systematic decrease in CaO, Al_2O_3, TiO_2, Na_2O, K_2O, and P_2O_5 contents. Lava of episodes 11 through 17, 19, and 20 did not show this type of variation and was comparable in composition to the lava sampled during the early parts of episodes 8 through 10.

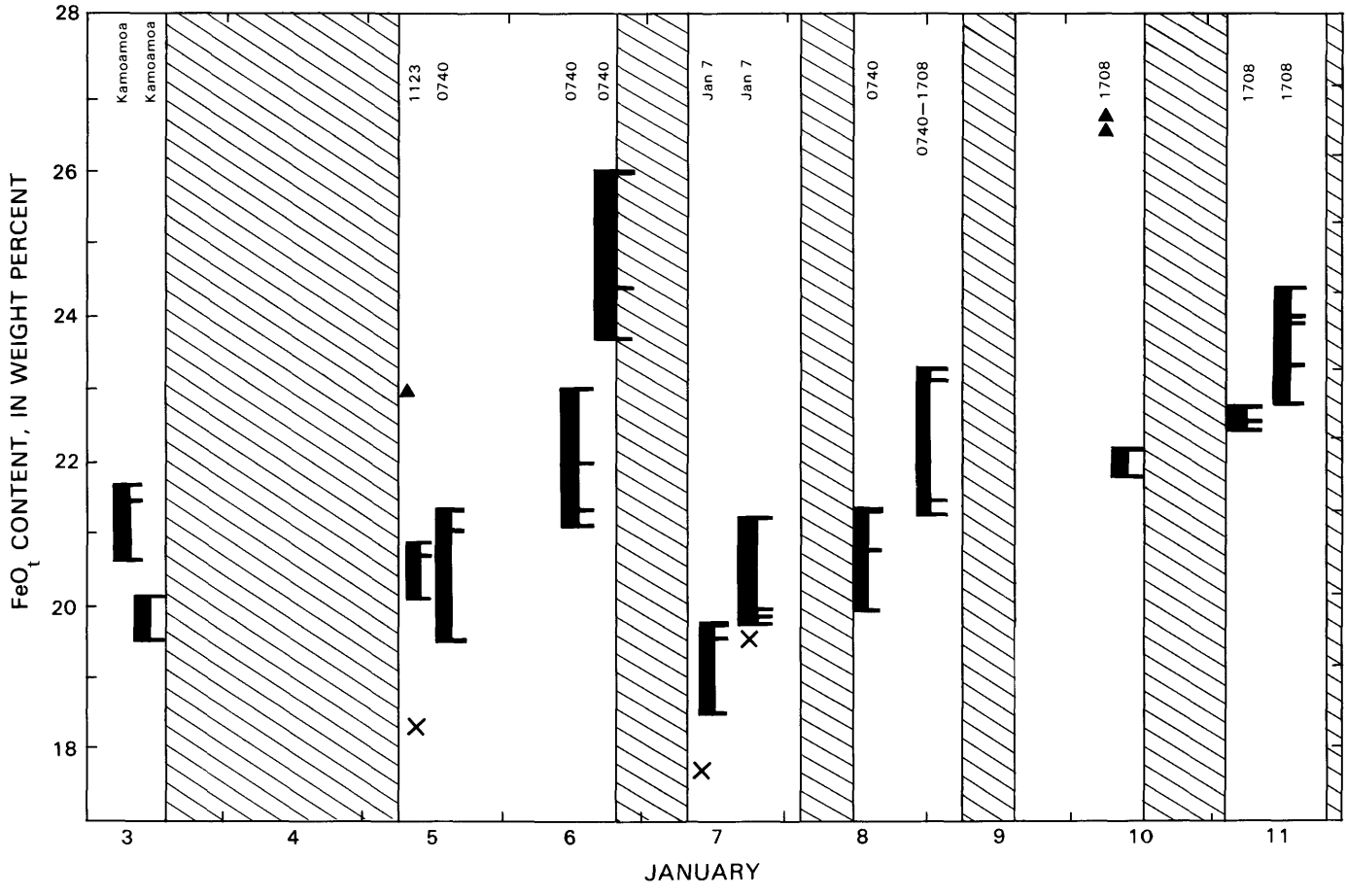

FIGURE 3.5.—FeO_t content of olivine phenocrysts and xenocrysts versus time for episode 1 lava. Solid bars indicate range in composition of phenocryst cores; lines on bars indicate average analyses (3-4 points) of individual grains. Triangles, xenocrysts; X, phenocryst rim. Diagonally ruled bars indicate hiatuses in lava discharge. Data from table 3.5. Names and numbers refer to vents (pl. 1).

The best suite of samples for examining the compositional change within a single episode was collected during episode 7. Even so, this collection contains substantial gaps (fig. 3.8). The suite represents both the period of low-level eruptive activity within the crater before sustained lava discharge, and the 56 hours of sustained lava emission during episode 7.

Lava extruded within the crater before the main episode 7 eruption, as well as lava discharged during the first 12 hours of sustained eruption, was typical of that erupted during the early parts of episodes 5 through 7. It was plagioclase-phyric and contained moderate MgO content (6.8–7.0 weight percent; see fig. 3.10; table 3.3). By hour 25 of the eruptive episode (note a 12-hour sampling gap), its mineralogy and chemistry had changed significantly. The abundance of olivine phenocrysts had increased, plagioclase phenocrysts had virtually disappeared, and augite phenocrysts had decreased (fig. 3.8; table 3.1); MgO content had increased to 7.7 weight percent, and the other oxides except for FeO_t had decreased (table 3.3). From hour 25 to 53, only minor changes occurred in the mineralogy and composition of the lava (fig. 3.8).

The increase in MgO content of late episode 7 lava cannot be explained simply by addition of olivine crystals for the following reasons: (1) Unlike the early episode 7 lava, the late lava contained no plagioclase phenocrysts; (2) 3 to 4 times the volume of augite phenocrysts present in late episode 7 lava would be required to account for the observed change in composition; and (3) the olivine phenocrysts in the late episode 7 lava are in equilibrium with the bulk composition of the lava (partition coefficient $= 0.30 \pm 0.03$; Roeder and Emslie, 1970) as is true for other episode 5–8 samples (fig. 3.9). In fact, the olivine in the late episode 7 lava would be out of equilibrium with the early episode 7 lava composition. Thus, the late episode 7 olivine phenocrysts are not cumulates from a less mafic magma like that erupted early in episode 7.

The chemical variation observed within some single episodes may have been generated in a zoned magma body beneath Puu Oo. A crystal-fractionation model in which 3.5 weight percent olivine plus 1.9 weight percent clinopyroxene of the observed compositions (tables 3.5, 3.7) is subtracted from the composition of late episode 7 lava yields excellent results (sum of squares of residuals, 0.01) in approximating the composition of early episode 7 lava. Thus, the observed compositional variation may have resulted from simple crystal fractionation during the preceding repose period. However, the rate of crystallization required by this model (approx 5.4 volume percent within 21 days) is substantially higher than that proposed by Wright and Tilling (1980) for augite and plagioclase crystallization in magma stored in Kilauea's east rift zone (1–2 percent per year). The difference in these rates of crystallization is probably due to shallower storage (that is, cooler thermal regime) of magma beneath Puu Oo (top of conduit exposed to the surface) and smaller reservoir size, which resulted in a larger ratio of surface area to

TABLE 3.5.—*Olivine phenocryst-core analyses*

[Major-element-oxide analyses in weight percent, averages of three to four points per grains, two to four grains per sample. Cations determined on the basis of four oxygens. Mg number = $100x(Mg/Mg+Fe^{2+})$]

Sample	SiO_2	FeO_t	MgO	Sum	Cations				Mg number
					Si	Fe^{2+}	Mg	Sum	
Episode 1									
2F	38.30	21.20	39.60	99.10	0.999	0.462	1.540	3.001	76.9
6S	38.70	19.80	40.90	99.40	.999	.428	1.574	3.001	78.6
7S	38.63	20.77	40.69	100.09	.995	.447	1.562	3.005	77.7
10F	38.10	21.10	39.90	99.10	.994	.460	1.552	3.006	77.1
13F	38.00	22.70	38.30	99.00	1.000	.499	1.502	3.000	75.0
15F	37.50	24.70	36.80	99.00	.997	.549	1.458	3.003	72.6
17F	38.80	19.60	41.30	99.70	.998	.422	1.583	3.002	79.0
19S	38.30	19.90	41.10	99.30	.992	.431	1.586	3.008	78.6
25S	38.30	20.90	40.30	99.50	.994	.454	1.559	3.006	77.5
27F	38.20	22.80	38.50	99.50	1.000	.499	1.502	3.000	75.1
31S	37.80	23.10	38.40	99.30	.994	.508	1.505	3.006	74.8
34F	38.00	22.80	38.60	99.40	.996	.500	1.508	3.004	75.1
37F	37.90	24.00	37.60	99.50	.998	.528	1.476	3.002	73.6
40F	37.92	23.27	38.49	99.68	.994	.510	1.503	3.006	74.7
49S	38.70	18.52	42.70	99.92	.989	.396	1.626	3.011	80.4
54S	37.71	23.62	38.51	99.84	.989	.518	1.505	3.011	74.4
Episode 2									
66F	38.07	22.66	38.91	99.64	0.995	0.494	1.515	3.005	75.4
77F	37.90	22.69	39.10	99.69	.990	.496	1.523	3.010	75.4
81S	37.87	22.08	39.75	99.70	.987	.481	1.544	3.013	76.2
Episode 3									
88F	37.78	22.34	39.61	99.73	0.986	0.488	1.541	3.014	76.0
96F	37.64	22.59	39.58	99.81	.983	.493	1.541	3.017	75.7
117F	38.51	19.10	42.33	99.94	.987	.409	1.617	3.013	79.8
Episode 4									
130F	38.68	18.44	42.60	99.72	0.990	0.395	1.625	3.010	80.5
Episode 5									
139F	39.57	17.03	43.44	100.04	1.001	0.360	1.638	2.999	82.0
Episode 6									
146F	39.19	19.46	42.04	100.69	0.996	0.414	1.593	3.004	79.4
149F	39.55	17.24	43.30	100.09	1.001	.365	1.633	2.999	81.7
154F	39.54	17.71	42.38	99.63	1.007	.377	1.609	2.993	81.0
Episode 7									
159F	38.00	20.00	42.14	100.14	0.981	0.421	1.617	3.019	79.4
167F	39.44	17.07	43.06	99.57	1.003	.363	1.632	2.997	81.8
Episode 8									
172F	39.47	17.18	42.77	99.42	1.005	0.336	1.624	2.995	81.6
174F	39.57	16.83	42.76	99.16	1.008	.359	1.624	2.992	81.9
Episode 9									
177F	39.74	16.43	43.65	99.82	1.004	0.347	1.644	2.996	82.6
178F	39.60	16.58	43.36	99.54	1.004	.352	1.639	2.996	82.3
Episode 12									
197F	38.66	20.25	39.60	98.51	1.009	0.442	1.540	2.991	77.7
203F	38.71	18.63	40.88	98.22	1.006	.405	1.583	2.994	79.6

TABLE 3.6.—*Mixing calculations for lava from episode 1 of the Puu Oo eruption*

[All analyses in weight percent, normalized to 100 percent. Solutions: mixing, 29.6 percent (sample 39F) + 100.00 percent (sample 49S) = 129.6 percent (sample 10F); fractionation, sample 49S - (8.1 percent augite + 5.8 percent plagioclase + 1.2 percent olivine) = sample 39F]

	Whole rock			Minerals			Residuals (observed - calculated)	
Sample----	Most evolved 39F	Intermediate 10F	Least evolved 49S	Olivine	Augite	Plagioclase	Mixing (r^2=0.44)	Fractionation (r^2=0.05)
SiO_2------	51.08	51.29	51.02	38.30	51.76	49.33	0.33	-0.13
TiO_2------	3.17	2.67	2.67	.00	.77	.00	-.15	.08
Al_2O_3-----	14.18	14.40	14.14	.00	2.46	31.80	.33	-.06
FeO-------	11.99	11.24	11.19	19.90	8.07	.75	.17	-.08
MnO-------	.18	.17	.17	.00	.23	.00	.00	.00
MgO-------	5.76	6.30	6.74	41.10	16.35	.00	-.28	-.04
CaO-------	9.89	10.46	10.91	.00	20.11	15.23	-.28	.00
Na_2O------	2.71	2.56	2.39	.00	.25	2.72	.13	.09
K_2O-------	.69	.60	.50	.00	.00	.18	.07	.10
P_2O_5------	.35	.31	.27	.00	.00	.00	.03	.03

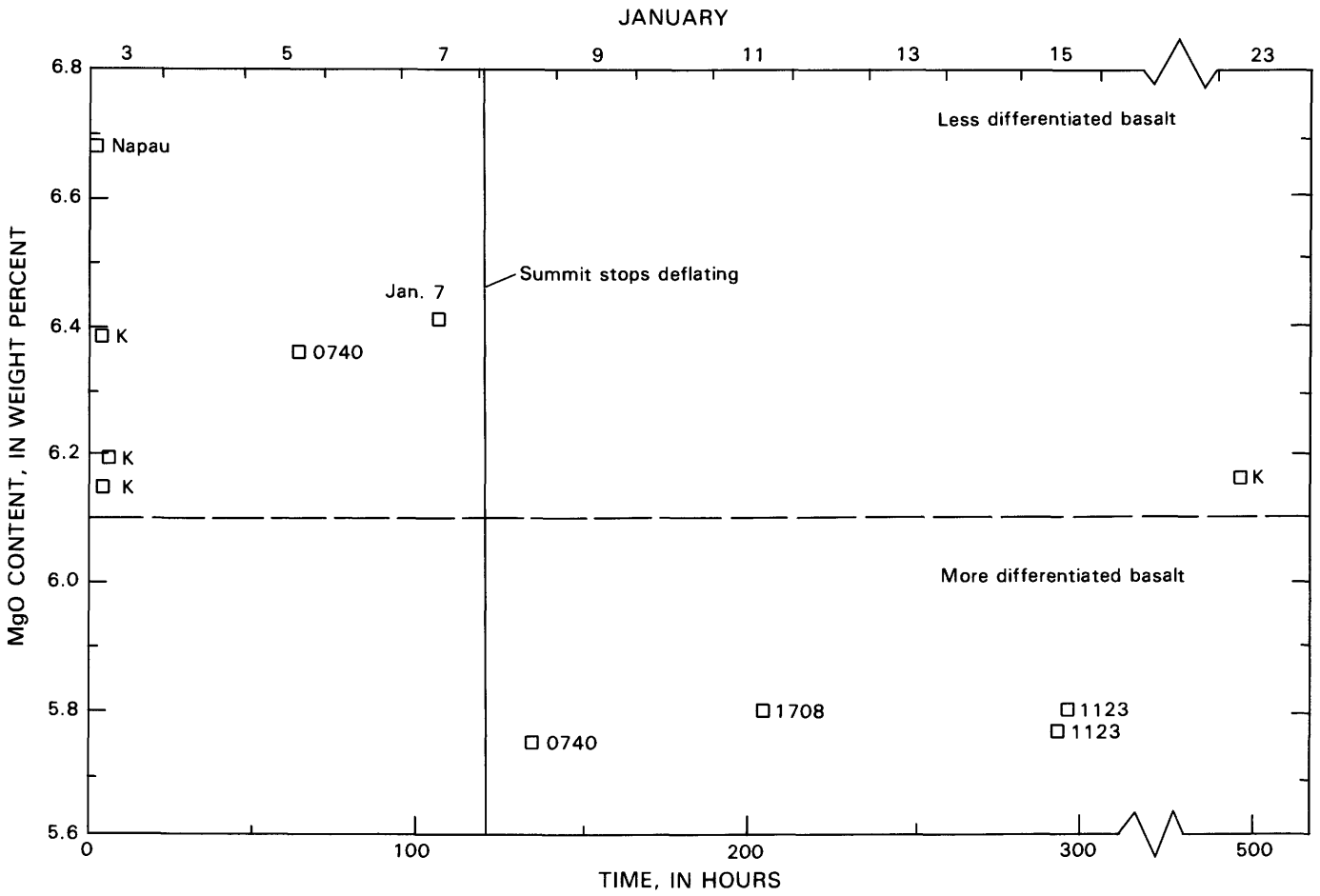

FIGURE 3.6.—MgO content versus time for episode 1 lava. Vent localities: K, Puu Kamoamoa area; others as shown in plate 1. Data from table 3.3. Note break in horizontal scale. Dashed line divides two compositional groups erupted during episode 1.

TABLE 3.7.—*Augite phenocryst-core compositions for lavas from episodes 7 and 8 of the Puu Oo eruption*

[Values for samples are averages of three to four spot analyses; analyst, M. Garcia. Pyroxene end-member components: En, enstatite; Fs, ferrosite; Wo, wollastonite. Mg number= $100xMg/(Mg+Fe^{2+})$]

Episode	7		8	
	Early (sample 159F)	Late (sample 167F)	Early (sample 172F)	Late (sample 174F)
SiO_2	50.8	51.8	50.4	50.8
TiO_2	1.0	.7	1.2	.9
Al_2O_3	2.4	2.8	3.8	3.4
Cr_2O_3	.1	.6	.6	.7
FeO	9.1	6.6	7.5	6.5
MnO	.2	.2	.2	.1
MgO	17.1	17.6	17.2	17.6
CaO	19.0	19.8	18.5	19.4
Na_2O	.4	.2	.2	.2
Total	100.1	100.3	99.6	99.6
En	47.5	49.4	49.3	49.9
Wo	38.0	40.0	38.3	39.5
Fs	14.5	10.6	12.4	10.6
Mg number	76.6	82.3	80.1	82.5

volume of the magma. These features promote faster cooling and crystallization.

LONG-TERM COMPOSITIONAL VARIATION WITHIN EPISODES 4 THROUGH 20

Independent of crystal fractionation effects during repose periods is the continuing increase during episodes 4 through 20 in CaO and MgO contents and the concomitant depletion in FeO_t, TiO_2, Na_2O, K_2O, and P_2O_5 contents in the Puu Oo lava (fig. 3.1). Two possible mechanisms to explain this trend are rift-zone mixing (Wright and Fiske, 1971; Wright and others, 1975) and changing conditions of melting in the mantle (Hofmann and others, 1984).

According to the mixing model, these long-term compositional changes reflect progressive dilution of a reservoir of differentiated, rift-zone magma by fresh magma repeatedly transferred from the summit reservoir to the rift zone during the series of eruptive episodes. Although the end-member compositions are not known, for illustration we have drawn a hypothetical mixing line in figure 3.2 that uses the composition of the most MgO rich lava (late episode 9) erupted at Puu Oo during the first 20 episodes and an average composition calculated from all of the analyzed samples from episodes 1 through 3 except those from Napau Crater and the O vent. Lava represented by the Napau Crater and O vent samples has a significantly higher MgO content (6.72 and 6.59 weight percent, respectively) and may reflect more recent intrusion of summit magma than does the other lava of episodes 1 through 3. The Napau lava is strikingly similar in composition (except in TiO_2 content) to some MgO-poor lava erupted during the early parts of episodes 5 through 8 at Puu Oo. However, because of the remoteness in both space and time of the Napau lava from similar lava erupted later at Puu Oo, we interpret this similarity as a coincidence.

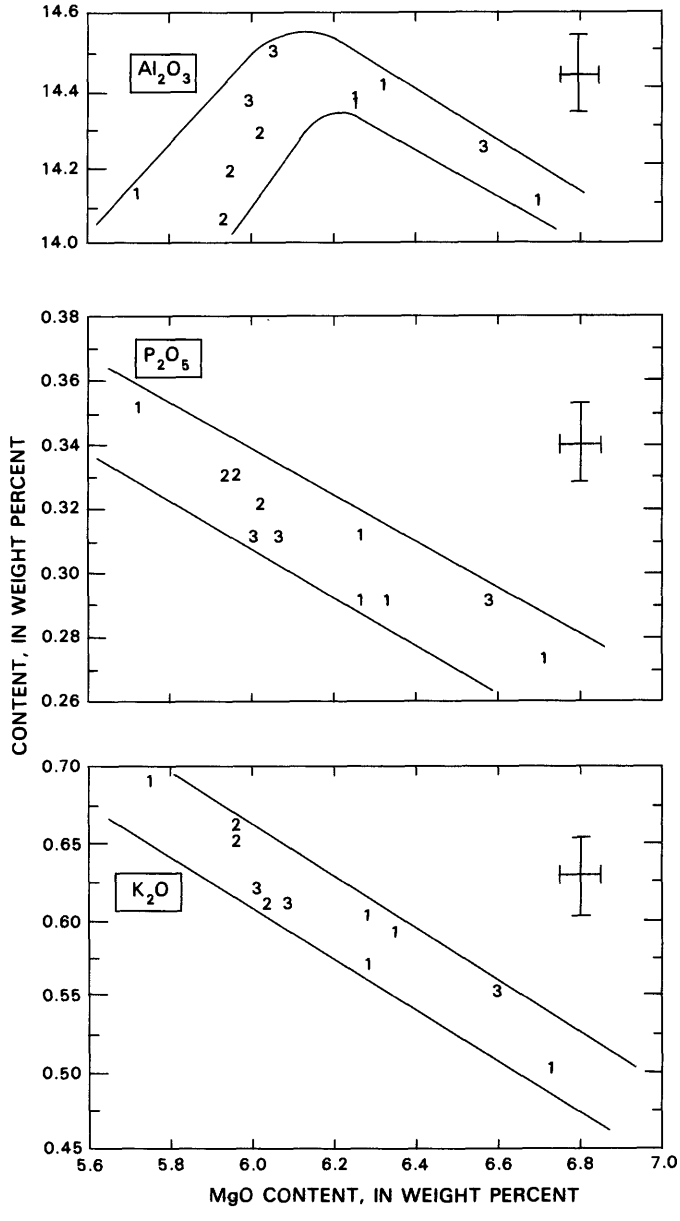

FIGURE 3.7.—Al_2O_3, P_2O_5, and K_2O contents versus MgO content for episodes 1 through 3. Numbers denote episodes. Data from chapter 2; error bars indicate precision estimates from Wright (1971). Parallel lines indicate trend of variation in composition.

In summary, the mixing model is as follows. Summit magma intruding in the rift zone intersected pockets of differentiated magma in storage and provided the impetus for eruption of the early differentiated lava. Lava erupted later at Puu Oo was a hybrid produced by mixing of olivine-controlled magma newly arrived from the summit reservoir with differentiated magma still present in the rift zone. Increasing dilution of the CaO- and MgO-depleted, differentiated magma by summit magma was reflected in a continuing increase in CaO and MgO con-

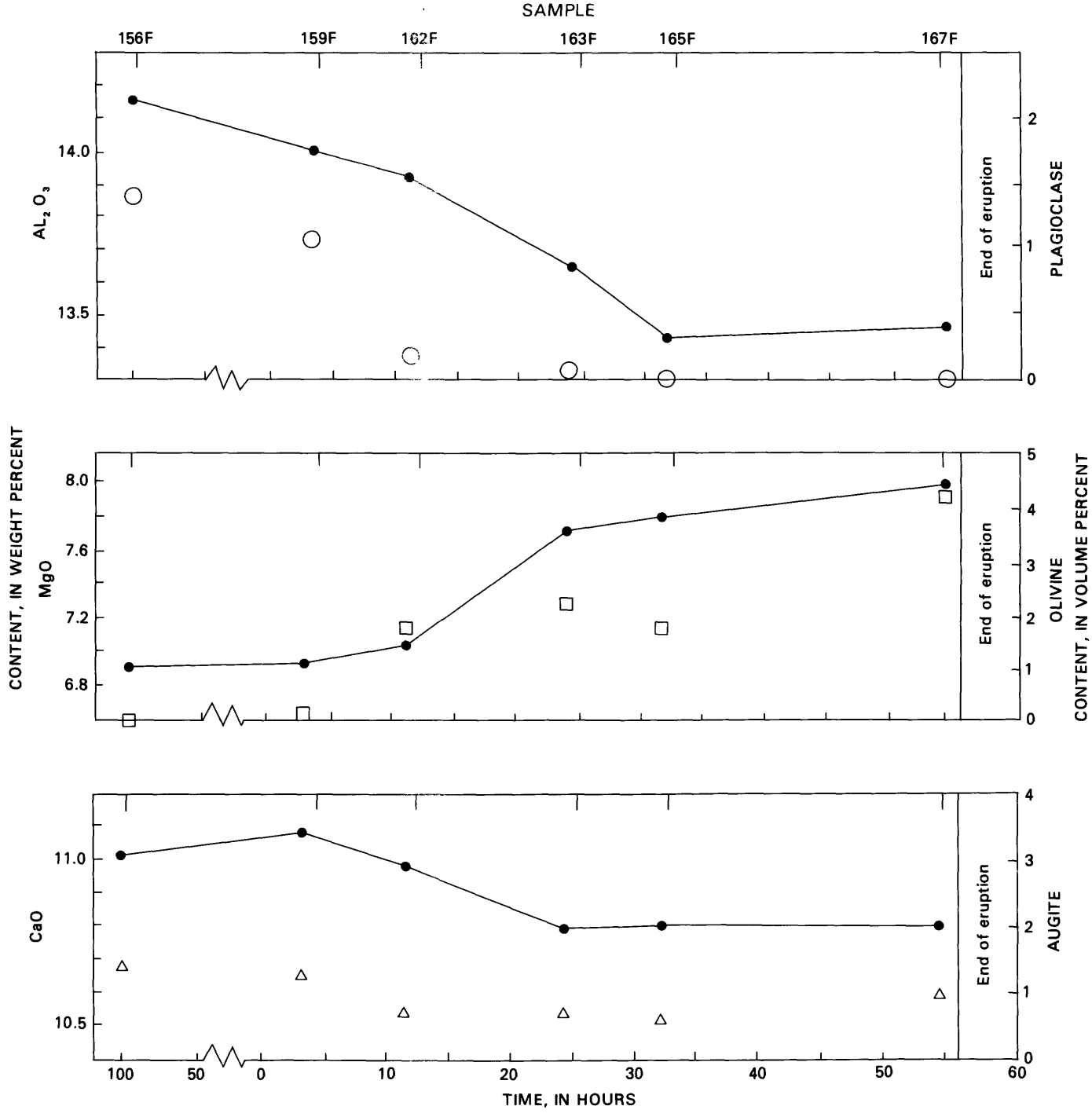

FIGURE 3.8.—Modal mineralogy and compositional variation over time for lava erupted within the Puu Oo Crater before the beginning of episode 7 (hours less than 0) and discharged from the crater during episode 7 (hours greater than 0). Open symbols refer to phenocryst abundance based on 1,000 points per sample: circles, plagioclase; squares, olivine; triangles, augite. Connected dots are compositions based on microprobe analyses of whole-rock samples fused to glass (table 3.3). Modal compositions from table 3.1.

tents in the Puu Oo lava. Between eruptions at Puu Oo, the hybrid magma, in a reservoir beneath the vent, evolved by fractionation of a few percent of olivine and augite to produce a limited volume of magma depleted in MgO. The magma thus fractionated was extruded during the early part of some episodes and throughout other episodes when the erupted volume was less than that of the MgO-depleted volume in the Puu Oo reservoir. This process was certainly established by episode 5.

Alternatively, changing melting processes in the mantle may have caused the observed compositional variation. The lava of episodes 11 through 20, as well as some of the lava of episodes 5 through 10, is nearly aphyric (less than 1 volume percent olivine; fig. 3.4; table 3.1) and contains more than 7.0 weight percent MgO. Thus, it may have undergone only olivine (plus minor chromite) fractionation at crustal depths (Wright, 1971). To remove the effect of varying degrees of olivine fractionation for the following discussion, we have adjusted compositions for olivine control to 12 weight percent MgO. Following Wright (1971), we made these adjustments with a mixture of 98.5 weight percent olivine (fo_{82}) and 1.5 weight percent chromite.

Hofmann and others (1984) also normalized lava compositions from the 1969–71 Mauna Ulu eruption to 12.0 weight percent MgO. Plotting the normalized values against time, they noted a progressive decrease in the content of incompatible minor (Na, Ti, K, P) and trace elements. They related this decrease to an increase of approximately 20 percent in the degree of partial melting of the source during the eruption.

Normalized compositions of olivine-controlled samples of lava from episodes 5 through 20 also show progressive compositional changes (fig. 3.10). The contents of incompatible minor elements (Na, Ti, K, P) decrease, and that of Ca increases; Si and Al contents do not vary systematically. These results are consistent with a melting model requiring an 8- to 10-percent increase in melting of the source, leading to an increase in the contribution of clinopyroxene to the melt.

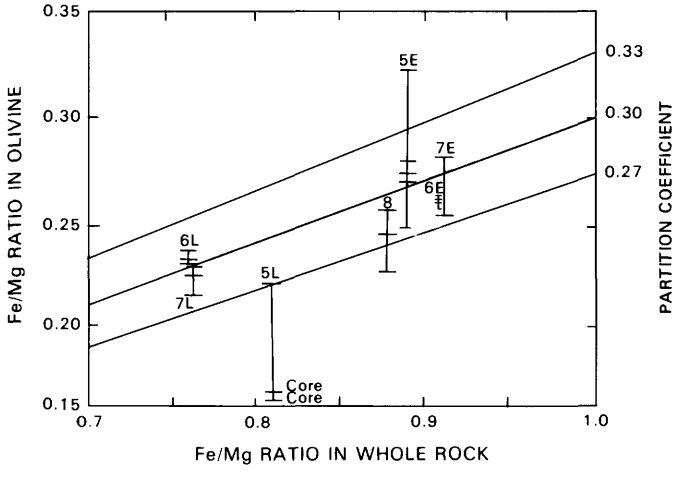

FIGURE 3.9.—Fe/Mg molecular ratio of olivine phenocrysts versus whole rock for lava from episodes 5 through 8 (numbered); E, early; L, late. Horizontal lines indicate average analyses (3-4 points) for individual grains; vertical bars indicate range in composition for each sample. Partition coefficient (Fe/Mg in olivine)/(Fe/Mg in rock).

Trace-element and isotopic analyses of the Puu Oo lavas are now in progress (J.M. Rhodes and A.W. Hofmann, written commun., 1985). These data will allow us to interpret the relative importance of each of these processes in controlling the long-term compositional variation of Puu Oo lava.

SUMMARY

The Puu Oo eruption is one of the most important historical eruptions of Kilauea Volcano because: (1) it is one of the longest (2½ years and continuing as of July 1985), (2) it is the most voluminous historical eruption of the volcano, and (3) the compositional variation of the lava is large. This compositional variation probably reflects several processes, including crystal fractionation with magma mixing, and/or a progressive increase in the degree of partial melting of the mantle. Compositional variation during episodes 1 through 3 probably resulted from eruption of pockets of magma that had differentiated to varying degrees during storage in the rift zone. Significant compositional variation between the lava erupted in the early and late parts of episodes 5 through 10 may reflect fractionation of olivine and a lesser amount of augite in a shallow magma chamber beneath Puu Oo. An overall progressive increase in CaO and MgO contents, and a decrease in FeO_t, TiO_2, Na_2O, K_2O, and P_2O_5 contents, may be due to: (1) progressive increase in the proportion of summit magma mixed with rift-zone magma; (2) progressive increase in the degree of partial melting of the mantle, involving an increase in the contribution of clinopyroxene to the melt; or (3) a combination of both these processes.

REFERENCES CITED

Dzurisin, Daniel, Koyanagi, R.Y., and English, T.T., 1984, Magma supply at Kilauea Volcano, Hawaii, 1956–83: Journal of Volcanology and Geothermal Research, v. 21, p. 177–206.

Hofmann, A.W., Feigenson, M.D., and Raczek, Ingrid, 1984, Case studies on the origin of basalt: III. Petrogenesis of the Mauna Ulu eruption, Kilauea, 1969–1971: Contributions to Mineralogy and Petrology, v. 88, no. 1-2, p. 24–35.

Jezek, P.A., Sinton, J.M., Jarosewich, Eugene, and Obermeyer, C.R., 1979, Fusion of rock and mineral powders for electron microprobe analysis, *in* Fudali, R.F., ed., Mineral sciences investigations, 1976–1977: Smithsonian Contributions to the Earth Sciences, no. 22, p. 46–52.

Moore, R.B., 1983, Distribution of differentiated tholeiitic basalts on the lower east rift zone of Kilauea Volcano, Hawaii: A possible guide to geothermal exploration: Geology, v. 11, no. 3, p. 136-140.

Moore, R.B., Helz, R.T., Dzurisin, Daniel, Eaton, G.P., Koyanagi, R.Y., Lipman, P.W., Lockwood, J.P., and Puniwai, G.S., 1980, The 1977 eruption of Kilauea Volcano, Hawaii: Journal of Volcanology and Geothermal Research, v. 7, p. 189-210.

Peck, L.C., 1964, Systematic analysis of silicates: U.S. Geological Survey Bulletin 1170, 89 p.

Roeder, P.L., and Emslie, R.F., 1970, Olivine-liquid equilibrium: Con-

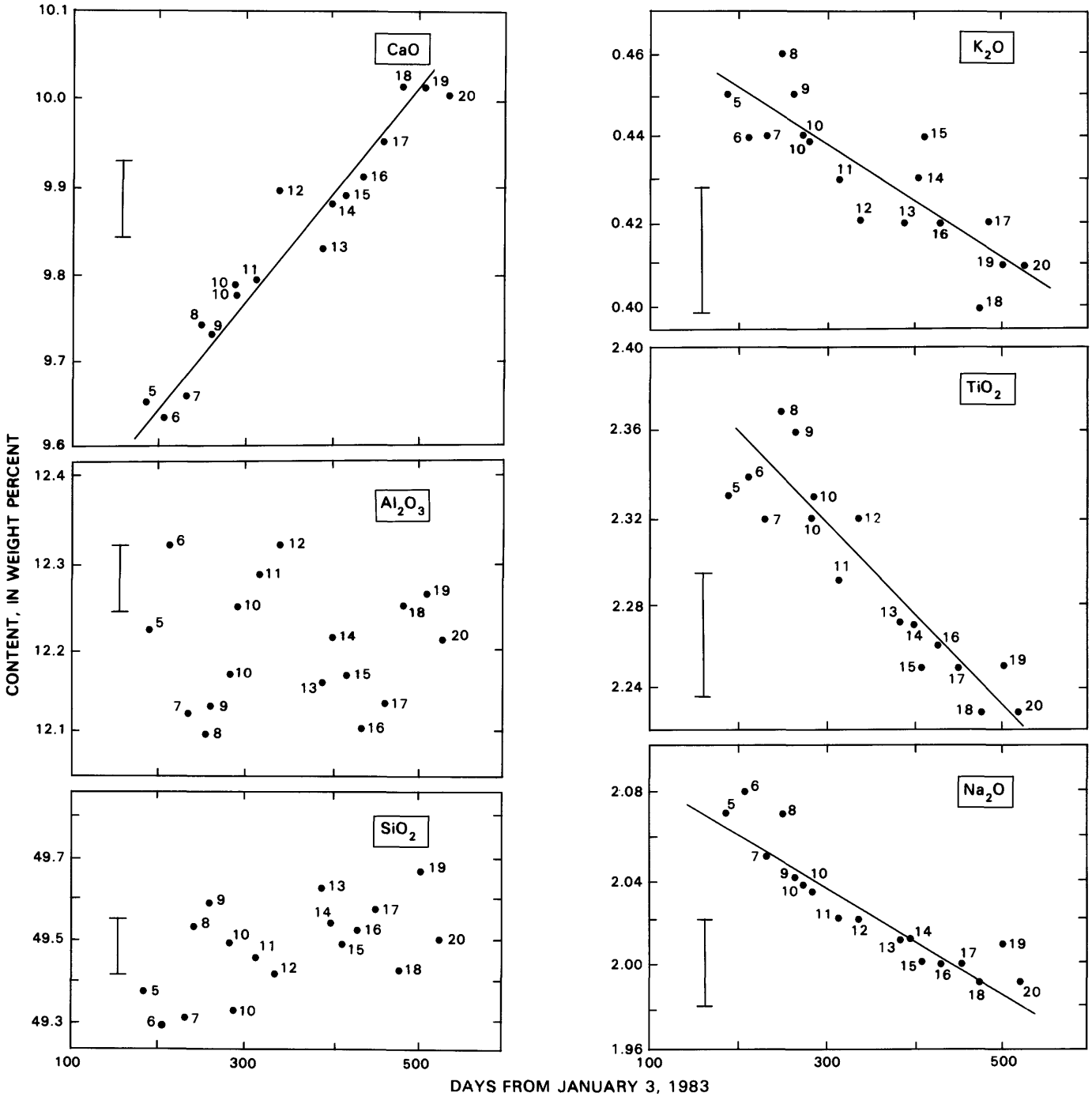

FIGURE 3.10.—Compositional variation versus day of eruption for selected samples of olivine-controlled lava from episodes 5 through 20. Compositions normalized for olivine control to 12 weight percent MgO, following the procedure of Hofmann and others (1984). Scale bars indicate precision of analyses (Wright, 1971). Diagonal line indicates trend of variation in composition over time.

tributions to Mineralogy and Petrology, v. 29, no. 4, p. 275–289.
Ryan, M.P., Koyanagi, R.Y., and Fiske, R.S., 1981, Modeling the three-dimensional structure of macroscopic magma transport systems: Applications to Kilauea Volcano, Hawaii: Journal of Geophysical Research, v. 86, no. 8, p. 7111–7129.
Wolfe, E.W., Garcia, M.O., Jackson, D.B., Koyanagi, R.Y., Neal, C.A., and Okamura, A.T., 1987, The Puu Oo eruption of Kilauea Volcano, episodes 1–20, January 3, 1983, to June 8, 1984, chap. 17 *of* Decker, R.W., Wright, T.L., and Stauffer, P.H., eds., Volcanism in Hawaii: U.S. Geological Survey Professional Paper 1350, v. 1, p. 471–508.
Wright, T.L., 1971, Chemistry of Kilauea and Mauna Loa lava in space and time: U.S. Geological Survey Professional Paper 735, 40 p.
—— 1984, Origin of Hawaiian tholeiite: A metasomatic model: Journal of Geophysical Research, v. 89, no. B5, p. 3233–3252.
Wright, T.L., and Fiske, R.S., 1971, Origin of the differentiated and hybrid lavas of Kilauea volcano, Hawaii: Journal of Petrology, v. 12, no. 1, p. 1–65.
Wright, T.L, Swanson, D.A., and Duffield, W.A., 1975, Chemical composition of Kilauea east rift lava, 1968–1971: Journal of Petrology, v. 16, no. 1, p. 110–133.
Wright, T.L., and Tilling, R.I., 1980, Chemical variation in Kilauea eruptions 1971–1974: American Journal of Science, v. 280–A (Jackson volume), pt. 2, p. 777–793.

4. GASES FROM THE 1983–84 EAST-RIFT ERUPTION

By L.P. GREENLAND

CONTENTS

ABSTRACT

Gases emitted during the January 1983-March 1984 eruptive period of the east rift of Kilauea Volcano had a very low C/S atomic ratio (0.17). This low atomic ratio is attributable to preeruptive degassing in the shallow summit storage reservoir before transport of the magma to the east rift zone. The varying water content, whether total or equilibrated, is the major source of variation in gas compositions; it induces variation in the other species through the constant-sum condition. The variation in water content of the gases is suggested to be due to pressure and temperature conditions at the point where the gases became separated from the magma, and to the chemical kinetics of degassing eruptive magma. Recalculated to an equilibrium assemblage, the gases follow a ($\log p O_2$)–T relation very close to that directly measured in a Kilauean lava lake. The volatile contents (in weight percent) of the eruptive magma are estimated at: H_2O, 0.42; S, 0.11; and CO_2, 0.02.

INTRODUCTION

Sampling and analysis of eruptive gases from Kilauea Volcano began in 1912 and continued through the now-classic collections of 1917, 1918, and 1919. These samples, all from Halemaumau pit crater, were summarized by Jaggar (1940) and have been the subject of many subsequent studies (Matsuo, 1962; Nordlie, 1971; Gerlach, 1980). Eruptive-gas collections since 1919, however, have been few, sporadic, and of only limited usefulness; these collections were summarized and evaluated by Gerlach (1980). With the installation of gas-analysis laboratory facilities at the Hawaiian Volcano Observatory (HVO) in 1980 and the continuing, intermittent eruptive activity on Kilauea's east rift zone since January 1983, a thorough sampling and analysis of eruptive gases from Kilauea Volcano has again been possible. This chapter discusses the results of analyses of gas samples collected over the first 14 months of the current eruption.

The most recent east-rift eruption began in Napau Crater on January 3, 1983, and was continuing as of May 1985. During the first 5 days of this eruption, the vent system gradually extended about 8 km discontinuously to the northeastward. During January and February 1983, sites of gas emission from eruptive vents and associated ground cracks were scattered along the full length of the fissure; these sites decreased in number until July 1983, when magmatic-gas emissions became localized to a main vent at Puu Oo (see chap. 1). Since that time, gas collections have been possible only on the rare occasions when magma rises to the top of the conduit and forms a crusted lava pond within the cone, with small vents emitting gas, spatter, and occasional small lava flows. Full details of the geologic aspects of the eruption are given in chapter 1.

EXPERIMENTAL

SAMPLING SITES

Two general classes of sampling sites are distinguished here: (1) noneruptive vents where magma was not visible, and (2) eruptive vents where magma was actively erupting. Noneruptive sites consisted of posteruptive vents that had emitted lava and (or) spatter in the fissure system (and that occasionally erupted again after sampling), and of ground cracks. Although these ground cracks commonly were immediately adjacent to eruptive vents, some were as much as 200 m distant. Gases from such noneruptive sites presumably represent degassing of the feeder dike (or dike plexus) at some unknown (presumably, less than 500 m) depth. These emissions have not occurred since July 1983, when all activity became localized at the main Puu Oo vent.

At eruptive vents, gases were collected within a few meters (or even centimeters) of actively erupting (flowing, spattering) lava. In the period January–April 1983, vigorously fountaining vents could occasionally be sampled through cracks in the spatter cone. Such samples invariably were highly oxidized, presumably owing to sucking of air into the vent by the chimney effect; none of these analyses are reported here.

Since July 1983, the only source of magmatic gases has been the main Puu Oo Crater. Eruptions of Puu Oo have

been uniformly preceded by a rising of magma in the conduit to form a lava lake (10–100 m diam) on the crater floor that persists for a few hours to a few days before active fountaining begins. Occasionally, this lava lake has become temporarily crusted over while one or more small vents continue jetting gases, spatter, and small lava flows; these vents provided all the samples described here as being from eruptive vents.

SAMPLING TECHNIQUE

Gas samples were collected in evacuated bottles, using 1- to 2-m-long lead-in tubes of titanium, stainless steel, or mullite, 1 to 4 cm in diameter. The lead-in tubes were inserted as much as two-thirds of their length into the vent and left for several minutes for the natural gas flow to flush residual air from them. On first usage, the metal tubes were inserted into a vent for as long as 30 minutes to develop an equilibrated corrosion layer that prevented further reaction between tube and gases; no samples were taken during this conditioning process. My experience has shown that 1 to 2 minutes of flushing is adequate before sampling, whereas more than 10 to 15 minutes of flushing of stainless-steel or titanium tubing at temperatures above 1,000 °C results in samples with increased H_2 contents, presumably reflecting reduction of water by the metal; all the samples reported here were collected within 5 minutes of tube insertion when stainless-steel or titanium tubing was used. Some samples were collected through mullite lead-in tubes, which are much less reactive than the metals; however, such tubes are discouragingly fragile under rough field conditions. With the sampling technique used here, there appear to be no differences in sample composition related to lead-in-tube composition.

The evacuated bottles used for gas collection were similar to those described by Giggenbach (1975). Gases were collected by covering the exit of the lead-in tube with a metal washer to reduce air contamination, inserting the stem of the inverted bottle, and opening the stopcock, whereby the gases bubbled through an aqueous solution. Through July 1983, two collection bottles were used for each sample: (1) one containing 0.05 *M* As_2O_3 in 6 *M* HCl, in which H_2S immediately precipitated as As_2S_3; CO_2, CO, and H_2 were determined in the headspace, and H_2O was determined by the weight gain of the bottle; and (2) one containing 6 *M* NaOH, in which acidic gases (CO_2, SO_2, HCl, and HF) were absorbed for subsequent determination by wet chemistry; CO and H_2 were again determined in the headspace; and H_2O was again determined by the weight gain of the bottle. Results from the two bottles were combined to provide a complete analysis. Then, in July 1983, T.M. Gerlach (oral commun., 1983) suggested the much simpler technique of using a single bottle containing an ammonia-Cd solution. Thereafter, single samples were collected with a bottle containing a solution of 3 *M* NH_4OH, 0.1 *M* $NH_4CH_3CO_2$, and 0.04 *M* CdO in which H_2S was determined as CdS, acidic gases by wet chemistry in the aqueous solution, CO and H_2 in the headspace, and H_2O by the weight gain of the bottle. Direct comparison of these two techniques showed no significant differences in the analytical results.

Temperatures were measured with a Chromel-Alumel thermocouple. Because of the difficult experimental conditions, measured temperatures at the eruptive vents may have been as much as 25 to 50 °C lower than the actual magma temperatures.

Extreme precautions to exclude air from the sample bottles were not taken. Experiments have shown that gas collections made in this way are stable for 4 to 6 hours, even in the presence of 95 percent air; however, left overnight before analysis, such samples are useless owing to oxidation effects. Because of the proximity of laboratory facilities and the availability of helicopter transport, gas-chromatographic analyses could ordinarily be completed within 5 hours of collection; on the few occasions when analyses were impossible, the samples were discarded. Aqueous solutions of acidic gases are unaffected by air contamination, except for possible oxidation of SO_3^{2-} to SO_4^{2-}; all the S in these solutions was calculated as SO_2, and these analyses could be performed at leisure.

CHEMICAL ANALYSIS

CO_2, CO, and H_2 in the headspace of the acidic-solution evacuated bottles, and CO and H_2 in the headspace of the alkaline-solution evacuated bottles, were determined by gas chromatography. Instrumental details are described elsewhere (Greenland, in press).

CO_2, SO_2, HCl, and HF were determined in aliquants of aqueous alkaline solutions of the evacuated-bottle gases by wet chemical procedures described elsewhere (Greenland, in press). H_2S was determined by the weight of As_2S_3 precipitate in the As_2O_3-HCl solutions. In the ammonia-CdO solutions, Cd remaining in the supernatant liquid was determined by atomic-absorption spectrometry; the difference from that originally present was attributed to CdS and thus identified with the amount of H_2S.

RESULTS AND DISCUSSION

ANALYSES OF GAS COLLECTIONS

Analyses of the evacuated-bottle gas collections are listed in table 4.1; the three analyses from January 1983 have been reported previously (Greenland, 1984). The

TABLE 4.1.—*Analyses of eruptive-gas samples from Kilauea Volcano, 1983–84*

[All values in mole percent]

Date	H_2O	H_2	CO_2	CO	SO_2	H_2S	HCl	HF
Noneruptive vents								
1/17/83	85.2	0.85	3.16	0.068	9.58	0.53	0.32	0.26
1/18/83	84.8	.62	2.33	.078	11.30	.39	.21	.26
1/18/83	82.9	.86	2.94	.084	12.30	.49	.20	.26
2/04/83	84.1	.05	2.27	.002	12.63	.65	.22	.09
2/10/83	89.3	.03	1.36	.001	8.16	.83	.22	.10
2/12/83	87.8	.02	1.91	.002	9.32	.62	.21	.14
2/17/83	89.0	.03	1.76	.004	8.50	.60	.08	.08
2/17/83	89.9	.01	.98	.001	8.61	.01	.30	.15
2/17/83	86.3	.26	1.61	.036	11.20	.24	.19	.13
2/23/83	80.3	.39	1.96	.019	16.90	.05	.23	.13
2/23/83	85.3	.02	2.16	.002	11.85	.38	.23	.05
2/24/83	75.9	.39	3.14	.029	19.80	.55	.15	.07
2/24/83	87.8	.02	1.82	.003	9.81	.00	.31	.23
2/27/83	86.4	.05	1.85	.011	11.39	.12	.12	.05
3/01/83	89.7	.02	1.26	.003	8.44	.04	.31	.22
3/01/83	79.7	.10	3.80	.032	16.20	.01	.12	.02
3/05/83	85.1	.00	3.44	.013	10.50	.00	.85	.06
3/05/83	85.8	.00	2.51	.007	11.30	.00	.35	.02
3/08/83	76.3	.00	2.46	.004	20.80	.00	.46	.02
3/08/83	83.6	.00	3.11	.004	12.50	.00	.69	.05
3/08/83	86.8	.03	1.85	.002	10.57	.28	.25	.22
3/22/83	89.4	.00	2.07	.001	8.46	.00	.03	.04
3/22/83	74.9	.03	2.11	.025	22.70	.00	.11	.06
3/22/83	83.3	.05	2.08	.005	14.30	.04	.10	.12
3/28/83	86.9	.01	1.80	.001	10.73	.11	.25	.18
3/28/83	83.9	.02	2.01	.001	13.61	.29	.08	.08
3/29/83	79.6	.07	2.52	.005	17.67	.00	.03	.08
3/30/83	82.4	.03	2.20	.002	15.16	.01	.07	.08
3/31/83	87.9	.02	1.50	.001	10.52	.00	.04	.04
4/01/83	87.9	.04	1.52	.001	10.40	.01	.02	.06
4/04/83	83.8	.03	2.07	.001	13.88	.00	.11	.10
4/05/83	82.4	.03	2.18	.001	15.18	.00	.08	.09
4/09/83	86.0	.03	1.74	.001	11.74	.18	.18	.16
4/09/83	88.1	.00	1.60	.000	9.96	.00	.16	.17
4/11/83	84.2	.03	1.98	.001	13.03	.24	.26	.24
4/13/83	82.7	.04	2.11	.001	14.60	.15	.18	.19
4/19/83	90.3	.01	1.72	.001	7.86	.00	.07	.08
4/21/83	93.5	.00	1.19	.001	5.24	.00	.03	.05
4/28/83	96.3	.00	.70	.001	2.95	.00	.04	.03
4/29/83	93.8	.00	1.03	.000	4.97	.00	.10	.06
4/29/83	96.0	.00	.80	.001	3.14	.00	.05	.04
5/04/83	74.8	.00	1.22	.004	23.77	.00	.16	.07
5/06/83	82.8	.03	2.06	.002	15.00	.00	.06	.02
5/06/83	90.2	.00	.32	.003	9.39	.00	.00	.00
5/13/83	89.5	.00	.69	.004	9.74	.00	.00	.02
Noneruptive vents--Continued								
5/16/83	87.8	.25	1.84	.007	8.96	.65	.34	.20
5/20/83	87.6	.14	1.70	.009	9.07	.53	.72	.26
5/24/83	87.4	.24	1.84	.005	9.37	.51	.40	.24
6/08/83	95.4	.00	.35	.005	4.20	.00	.02	.01
6/08/83	99.6	.00	.35	.000	.00	.00	.00	.01
6/13/83	98.4	.00	.15	.002	1.45	.00	.00	.00
6/14/83	99.6	.00	.34	.001	.00	.00	.00	.01
6/15/83	98.8	.00	.17	.000	.99	.00	.01	.02
6/29/83	99.5	.00	.09	.001	.43	.00	.00	.00
6/29/83	99.6	.00	.38	.003	.00	.00	.01	.00
6/30/83	99.9	.00	.03	.000	.10	.00	.00	.00
Eruptive vents								
8/13/83	89.4	0.51	1.46	0.030	8.32	0.31	0.00	0.02
8/13/83	91.1	.36	1.33	.021	7.00	.14	.01	.05
8/14/83	84.5	.38	2.58	.025	12.40	.08	.01	.03
8/14/83	87.1	.56	1.13	.031	10.80	.31	.01	.04
8/13/83	82.7	1.76	1.75	.073	12.70	.72	.10	.21
8/13/83	88.2	.43	1.05	.058	9.68	.43	.05	.14
8/14/83	83.4	1.54	2.78	.086	11.10	1.02	.01	.03
8/14/83	84.0	1.51	2.10	.103	11.80	.43	.02	.06
8/14/83	84.7	2.08	1.36	.089	11.20	.21	.09	.29
9/02/83	91.0	.53	1.24	.014	6.44	.49	.11	.14
9/02/83	86.3	1.18	1.16	.010	10.50	.53	.10	.15
9/02/83	92.4	1.23	1.16	.043	4.43	.44	.13	.15
9/02/83	83.5	.59	1.71	.028	14.10	.01	.04	.08
9/02/83	88.9	.64	1.29	.010	8.22	.64	.10	.16
9/02/83	69.2	.50	1.72	.021	27.10	.72	.15	.55
9/02/83	90.8	.93	1.18	.027	6.63	.22	.11	.15
9/03/83	89.5	1.82	1.18	.056	6.04	1.20	.08	.12
9/03/83	83.5	.56	1.20	.019	13.10	1.38	.12	.15
9/04/83	88.0	1.24	1.38	.044	8.80	.33	.11	.14
9/04/83	91.0	.98	1.39	.031	6.06	.23	.15	.14
9/04/83	90.6	1.24	1.32	.041	6.15	.35	.13	.13
9/04/83	83.3	1.44	1.37	.053	13.40	.26	.11	.12
1/30/84	90.3	1.29	1.62	.065	6.20	.25	.19	.12
1/30/84	89.3	1.35	1.80	.077	6.80	.32	.19	.13
1/30/84	89.4	1.01	1.58	.062	7.23	.43	.16	.14
1/30/84	89.5	1.41	1.53	.074	6.91	.28	.18	.13
1/30/84	87.7	1.39	1.81	.073	8.30	.30	.20	.21
3/02/84	89.6	1.23	1.59	.083	6.74	.45	.11	.22
3/02/84	90.4	1.10	1.46	.078	6.43	.33	.06	.15

large variations in the reduced species H_2, CO, and H_2S reflect variations in both the temperature and the oxygen partial pressure at which the gases were last in equilibrium. Many of the samples from noneruptive vents had ample opportunity to react with air and thus be oxidized in the vent system before collection. These sources of variation can be eliminated by considering only the atomic composition of the gases (table 4.2).

Much of the variation in major species can be attributed to the constant-sum condition, whereby a variation in water content induces variation in the contents of other gases (Chayes, 1960). The significance of water-content variation in these analyses can be illustrated by a ternary H-C-S atomic diagram (fig. 4.1): In such a plot, points will lie along a straight line extending from the respective apex if all the variation is due to any one of the constituents H_2O, CO_2, or SO_2, which are the major contributors of atomic H, C, and S. The data from the 1983–84 eruption (table 4.2) adhere fairly closely to an H_2O-control line, with a constant C/S atomic ratio of about 0.17. This result accords with previous suggestions that Hawaiian volcanic gases are commonly admixed with meteoric water (Heald and others, 1963; Nordlie, 1971; Gerlach, 1980). Thus, the variation in the molecular proportions of the gases (table 4.1) is compatible with representation of the samples by a single gas composition that has undergone mixing with varying amounts of meteoric water and atmospheric oxygen and equilibration over a range of temperatures.

EQUILIBRIUM CONSIDERATIONS

A simple technique for studying equilibrium in volcanic gases is described in detail elsewhere (Greenland, in press). Estimations of apparent equilibrium temperatures from the oxidation reactions of H_2, CO, and H_2S show that many of the samples listed in table 4.1 approach equilibrium assemblages, whereas others are far from equilibrium. Divergence of volcanic-gas analyses from

TABLE 4.2.—*Atomic composition of eruptive-gas samples from Kilauea Volcano, 1983-84*

[Values for Cl and F exaggerated x1,000]

Date	H	O	C	S	Cl	F
Noneruptive vents						
1/17/83	174	111	3.23	10.11	320	260
1/18/83	172	112	2.41	11.69	210	260
1/18/83	169	113	3.02	12.79	200	260
2/04/83	170	114	2.27	13.28	220	90
2/10/83	181	108	1.36	8.99	220	100
2/12/83	177	110	1.91	9.94	210	140
2/17/83	179	110	1.76	9.10	80	80
2/17/83	180	109	.98	8.62	300	150
2/17/83	174	112	1.65	11.44	190	130
2/23/83	162	118	1.98	16.95	230	130
2/23/83	172	113	2.16	12.23	230	50
2/24/83	154	122	3.17	20.35	150	70
2/24/83	176	111	1.82	9.81	310	230
2/27/83	173	113	1.86	11.51	120	50
3/01/83	180	109	1.26	8.48	310	220
3/01/83	160	120	3.83	16.21	120	20
3/05/83	171	113	3.45	10.50	850	60
3/05/83	172	113	2.52	11.30	350	20
3/08/83	153	123	2.46	20.80	460	20
3/08/83	168	115	3.11	12.50	690	50
3/08/83	175	112	1.85	10.85	250	220
3/22/83	179	110	2.07	8.46	30	40
3/22/83	150	125	2.13	22.70	110	60
3/22/83	167	116	2.09	14.34	100	120
3/28/83	174	112	1.80	10.84	250	180
3/28/83	169	115	2.01	13.90	80	80
3/29/83	159	120	2.53	17.67	30	80
3/30/83	165	117	2.20	15.17	70	80
3/31/83	176	112	1.50	10.52	40	40
4/01/83	176	112	1.52	10.41	20	60
4/04/83	168	116	2.07	13.88	110	100
4/05/83	165	117	2.18	15.18	80	90
4/09/83	173	113	1.74	11.92	180	160
4/09/83	177	111	1.60	9.96	160	170
4/11/83	169	114	1.98	13.27	260	240
4/13/83	166	116	2.11	14.75	180	190
4/19/83	181	109	1.72	7.86	70	80
4/21/83	187	106	1.19	5.24	30	50
4/28/83	193	104	.70	2.95	40	30
4/29/83	188	106	1.03	4.97	100	60
4/29/83	192	104	.80	3.14	50	40
5/04/83	150	125	1.22	23.77	160	70
5/06/83	166	117	2.06	15.00	60	20
5/06/83	180	110	.32	9.39	0	0
5/13/83	179	110	.69	9.74	0	20
Noneruptive vents--Continued						
5/16/83	178	109	1.85	9.61	340	200
5/20/83	178	109	1.71	9.60	720	260
5/24/83	177	110	1.85	9.88	400	240
6/08/83	191	105	.35	4.20	20	10
6/08/83	199	100	.35	.00	0	10
6/13/83	197	102	.15	1.45	0	0
6/14/83	199	100	.34	.00	0	10
6/15/83	198	101	.17	.99	10	20
6/29/83	199	101	.09	.43	0	0
6/29/83	199	100	.38	.00	10	0
6/30/83	200	100	.03	.10	0	0
Eruptive vents						
8/13/83	180	109	1.49	8.63	0	20
8/13/83	183	108	1.35	7.14	10	50
8/14/83	170	114	2.61	12.48	10	30
8/14/83	176	111	1.16	11.11	10	40
8/13/83	171	112	1.82	13.42	100	210
8/13/83	178	110	1.11	10.11	50	140
8/14/83	172	111	2.87	12.12	10	30
8/14/83	172	112	2.20	12.23	20	60
8/14/83	174	110	1.45	11.41	90	290
9/02/83	184	106	1.25	6.93	110	140
9/02/83	176	110	1.17	11.03	100	150
9/02/83	188	104	1.20	4.87	130	150
9/02/83	168	115	1.74	14.11	40	80
9/02/83	181	108	1.30	8.86	100	160
9/02/83	142	127	1.74	27.82	150	550
9/02/83	184	106	1.21	6.85	110	150
9/03/83	185	104	1.24	7.24	80	120
9/03/83	171	112	1.22	14.48	120	150
9/04/83	179	108	1.42	9.13	110	140
9/04/83	185	106	1.42	6.29	150	140
9/04/83	185	106	1.36	6.50	130	130
9/04/83	170	113	1.42	13.66	110	120
1/30/84	184	106	1.68	6.45	190	120
1/30/84	182	107	1.88	7.12	190	130
1/30/84	182	107	1.64	7.66	160	140
1/30/84	183	106	1.60	7.19	180	130
1/30/84	179	108	1.88	8.60	200	210
3/02/84	183	106	1.67	7.19	110	220
3/02/84	184	106	1.54	6.76	60	150

equilibrium can generally be attributed to excess, meteoric water in the sample and (or) oxidation of the gases, either in the vent or during storage before analysis (Gerlach, 1980; Greenland, in press).

Listed in table 4.3 are the results of adjusting the analyses in table 4.1 to equilibrium assemblages, under the assumptions that all disequilibrium is due solely to (1) excess water or (2) oxidation of H_2. Nonetheless, about a third of the samples listed in table 4.1 cannot be adjusted to equilibrium by this procedure because: (1) one or more of the gases H_2, CO, and H_2S were not detected in the analysis, a result suggestive of a highly oxidized sample and (or) a very low temperature of equilibration; (2) estimated equilibrium temperatures were higher than 1,200 °C, above the magmatic temperature (see chap. 2), a result suggestive of a poor analysis and (or) contamination of the sample by pyrolysis of organic matter; or (3) estimated water content was less than 30 mol percent, suggestive of a high degree of oxidation of H_2 in the sample. The remaining two-thirds of the samples, amenable to this procedure, indicate that most of the samples from eruptive vents and many of those from noneruptive vents (table 4.3) require very small corrections in water content, probably within analytical uncertainty, to be adjusted to

equilibrium assemblages. Attributing all disequilibrium in the samples to oxidation of H_2 requires larger relative corrections to H_2 than to water content (table 4.3), but the changes, particularly at eruptive vents, are mostly small.

Apparent equilibrium temperatures and oxygen partial pressures from the water correction are about the same as from the H_2 correction (table 4.3). Oxygen partial pressure versus temperature for these samples relative to the quartz-fayalite-magnetite (QMF) buffer are compared in figure 4.2. The gas samples follow a buffer relation that is very close to that of QMF at temperatures above 1,000 °C and that becomes more oxidized at lower temperatures. Fitting a least-squares line to the analytical data yields

$$\log pO_2 = (-1.80 \times 10^4)/T + 3.66,$$

which is very close to the buffer relation observed (Greenland, in press) for Mauna Loa eruptive gases:

$$\log pO_2 = (-1.93 \times 10^4)/T + 4.46.$$

Exclusion of the few points in figure 4.2 that deviate markedly from the others would make the degree of correspondence of the Kilauea and Mauna Loa buffers even greater. Sato and Wright (1966) also observed that oxygen fugacity in a cooling lava lake is buffered according to the relation

$$\log fO_2 = (-1.86 \times 10^4)/T + 3.73,$$

and so the oxidation state of the eruptive gases is apparently controlled by a lava-buffer system.

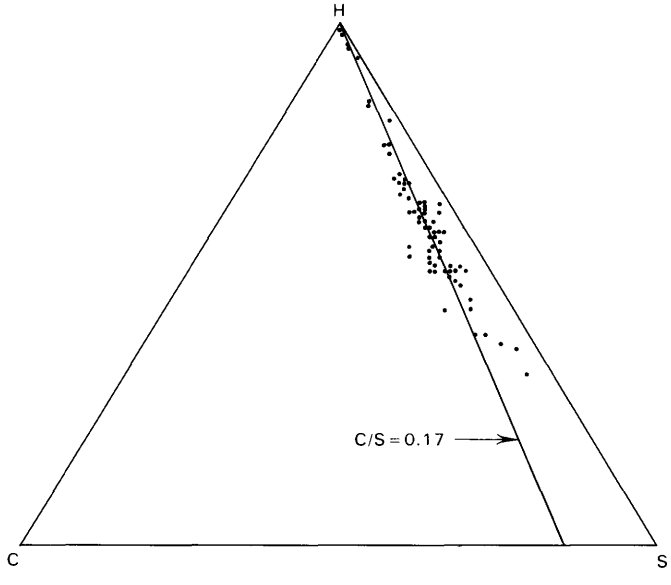

FIGURE 4.1.—Ternary plot of H-C-S composition in evacuated-bottle samples (data from table 4.2). Atomic H has been scaled by a factor of 0.1 for clarity of plotting. Water-control line has a C/S atomic ratio of 0.17.

WATER CONTENT

Of the 29 eruptive vent samples listed in table 4.3, 26 require a less than 10 percent relative change in observed water content to match an equilibrium composition; thus, these samples represent equilibrium assemblages, within experimental uncertainties. In contrast, only 7 of the 25 samples from noneruptive vents (table 4.3) meet this constraint and thus can be considered approximate equilibrium assemblages; the remaining 18 have been altered by contamination with water and (or) by oxidation. Gases from noneruptive vents have separated from magma at some considerable depth and traversed an unknown length of country rock, and thus had ample opportunity for contamination by meteoric water and ambient oxygen in the vent system, before collection. If oxidation has affected these samples, then the actual equilibrium water content is greater than that (64.0 mol percent) obtained by averaging the estimates from water contamination in table 4.3; similarly, if water contamination has been important, then the actual equilibrium water content is less than that (78.9 mol percent) obtained by averaging the seven samples observed to be in approximate equilibrium.

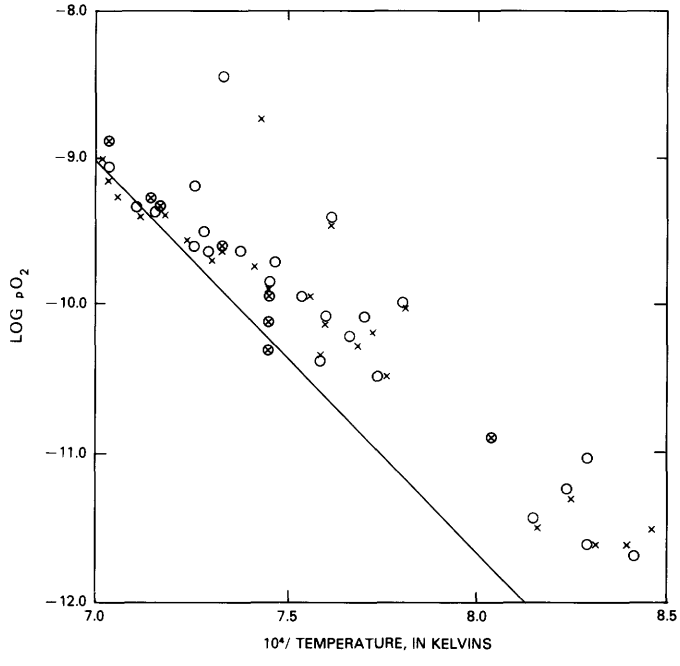

FIGURE 4.2.—Oxygen partial pressure versus temperature for equilibrated compositions of gas samples listed in table 4.3. Circles, deviation from equilibrium due solely to water content; X's, deviation from equilibrium due solely to oxidation of H_2. Line indicates quartz-magnetite-fayalite buffer.

TABLE 4.3.—*Apparent equilibrium values in eruptive-gas samples, assuming excess H_2O or oxidation of H_2*

[Dashes, samples for which the assumption of oxidation of H_2 does not yield an apparent equilibrium]

Sample	Excess H_2O				Oxidation of H_2			
	Temperature (°C)	pO_2	H_2O (mol percent)		Temperature (°C)	pO_2	H_2 (mol percent)	
			Estimated	Observed			Estimated	Observed
Noneruptive vents								
1	1,016	10.48	82.40	85.20	1,018	10.46	1.04	0.85
2	1,090	9.63	71.60	84.80	1,099	9.50	1.35	.62
3	1,066	9.89	77.60	82.90	1,068	9.84	1.20	.86
4	705	14.99	69.80	84.10	709	14.85	.11	.05
5	675	15.77	68.60	89.30	681	15.57	.11	.03
6	703	15.19	50.20	87.80	717	14.77	.14	.02
7	761	14.17	49.40	89.00	777	13.73	.23	.03
8	809	12.21	48.40	89.90	828	11.75	.09	.01
9	1,050	9.94	61.60	86.30	1,065	9.69	.99	.26
10	1,038	9.42	79.00	80.30	1,038	9.41	.42	.39
11	712	14.82	49.60	85.30	725	14.41	.11	.02
12	937	11.25	71.40	75.90	939	11.20	.49	.39
14	907	11.48	44.80	86.40	931	10.99	.37	.05
15	843	12.12	46.80	89.70	864	11.63	.19	.02
16	1,072	8.73	53.80	79.70	1,090	8.43	.32	.10
21	733	14.31	60.60	86.80	743	14.04	.12	.03
24	869	11.53	59.40	83.30	880	11.28	.17	.05
25	700	14.73	46.60	86.90	716	14.25	.07	.01
26	681	15.24	59.40	83.90	689	14.98	.07	.02
28	825	11.72	65.60	82.40	832	11.55	.07	.03
30	791	12.28	82.00	87.90	793	12.23	.06	.04
33	703	14.67	70.60	86.00	708	14.52	.08	.03
35	689	14.99	69.60	84.20	694	14.85	.07	.03
36	700	14.58	75.60	82.70	703	14.51	.06	.04
46	820	13.07	84.40	87.80	821	13.05	.33	.25
Eruptive vents								
47	853	12.59	70.40	87.60	860	12.43	0.41	0.14
48	800	13.30	86.80	87.40	800	13.30	.25	.24
57	1,026	10.27	80.80	89.40	1,031	10.19	1.01	.51
58	1,019	10.16	81.80	91.10	1,024	10.08	.81	.36
59	1,005	9.99	81.20	84.50	1,007	9.96	.48	.38
60	1,074	9.72	76.00	87.10	1,080	9.62	1.18	.56
61	1,106	9.57	84.00	82.70	1,105	9.59	1.61	1.76
62	1,144	9.25	60.40	88.20	---	---	---	---
63	1,043	10.34	84.80	83.40	1,042	10.36	1.39	1.54
64	1,151	9.04	81.80	84.00	---	---	---	---
66	930	11.57	88.00	91.00	931	11.55	.73	.53
67	916	11.61	93.00	86.30	914	11.65	.56	1.18
68	1,066	10.10	89.60	92.40	1,067	10.09	1.74	1.23
70	889	12.10	90.20	88.90	889	12.10	.55	.64
71	969	10.87	67.40	69.20	969	10.85	.54	.50
72	1,050	9.95	89.40	90.80	1,051	9.94	1.10	.93
73	1,067	10.30	87.80	89.50	1,068	10.29	2.15	1.82
74	950	11.46	76.00	83.50	953	11.39	.89	.56
75	1,089	9.61	87.00	88.00	1,089	9.60	1.36	1.24
76	1,041	10.09	90.00	91.00	1,041	10.08	1.09	.98
77	1,068	9.93	89.40	90.60	1,068	9.93	1.43	1.24
78	1,148	8.88	83.80	83.30	1,148	8.88	1.38	1.44
79	1,120	9.33	88.00	90.30	1,120	9.32	1.64	1.29
80	1,120	9.38	86.60	89.30	1,122	9.35	1.73	1.35
81	1,095	9.69	83.60	89.40	1,098	9.65	1.67	1.01
82	1,147	9.09	86.60	89.50	1,148	9.07	1.85	1.41
83	1,125	9.26	86.20	87.70	1,125	9.25	1.59	1.39
84	1,131	9.39	83.60	89.60	1,134	9.34	2.06	1.23
85	1,148	9.15	83.40	90.40	---	---	---	---

In view of the common meteoric-water contamination of Hawaiian eruptive gases (Gerlach, 1980), the equilibrium water content of noneruptive-vent gases is evidently less than that (85.0 mol percent) of equilibrated eruptive-vent gases; this difference most probably reflects the depth of degassing of the magma (see chap. 5).

Comparison of these results with those of other studies of Hawaiian eruptive gases shows this 1983–84 east-rift magma to be water rich. The equilibrium compositions estimated by Gerlach (1980) for the 1918–19 eruption of Halemaumau yield an average water content of 52 mol percent; the equilibrium water content of 1984 Mauna Loa eruptive-vent gases is 56 mol percent (Greenland, in press). However, the Mauna Loa gases from eruptive vents contained 73 mol percent total water; Greenland (in press) attributes the difference between equilibrated and total water at Mauna Loa to the rate of degassing, and so the difference between Mauna Loa and Kilauea magmas may be less than implied by the comparison of equilibrated water contents. The high water content of Kilauea magma may have originated during formation in the mantle. Kyser and O'Neil (1984), however, showed that most submarine basalt erupted from Kilauea's east rift contains a substantial fraction of assimilated crustal water, and so the high water content of these gas samples may reflect only the shallow storage and transport of the 1983–84 eruptive magma.

C/S ATOMIC RATIO

The C/S atomic ratio of these gas samples is approximately constant (fig. 4.1). Averaging the data from table 4.2 yields C/S atomic ratios of 0.172 and 0.176 for gases from noneruptive and eruptive vents, respectively; thus, unlike water content, noneruptive and eruptive vents are indistinguishable in C/S atomic ratio. The observation that the C/S atomic ratio is independent of the depth of degassing as represented by these samples implies that CO_2 and SO_2 are nearly completely exsolved from the magma at a depth where H_2O is only beginning to appear in the gas phase. This conclusion is consistent with suggestions that CO_2 and SO_2 are saturated in the magma at the pressure of Kilauea's summit storage reservoir (Greenland and others, 1984), whereas H_2O is considerably undersaturated (Moore, 1965).

The very low C/S atomic ratio of this eruptive gas markedly contrasts with that of most basaltic gases, in which carbon is generally more abundant than sulfur (Gerlach, 1982). Gerlach (1982) emphasized the importance of shallow degassing for controlling the C/S atomic ratio of volcanic gases, and Greenland (1984) and Greenland and others (1985) attributed the low ratio in these east-rift gases to prior degassing during storage of the magma in the summit reservoir of Kilauea. The absence of any appreciable change in the C/S atomic ratio of the gases over the 14-month course of the Puu Oo eruption is consistent with degassing of the magma to equilibrium in the summit reservoir before its transport to the east rift zone.

HALOGEN CONTENTS

Halogens are unaffected by oxidation and temperature effects, and statistical tests of the data in table 4.1 show no correlation of halogen with water content. Thus, the observed variation in halogen content reflects a real compositional variation among these gas samples. HCl and HF are highly correlated with each other (99-percent-confidence level) but are uncorrelated with other gas species, a relation suggesting that their variation may be due to magmatic degassing rather than to changes in magmatic composition. The data of Greenland and others (1985) imply that less than 15 mol percent of the Cl and F in the magma is volatilized on eruption, and so very small changes in the efficiency of the degassing process could yield large relative changes in the halogen content of the eruptive gas. The significance of this degassing process is shown by the large difference in Cl/F atomic ratio between samples collected from eruptive vents (mean Cl/F atomic ratio, 0.68) and from vents degassing magma at some shallow depth (mean Cl/F atomic ratio, 2.8). The highest Cl/F atomic ratios from noneruptive vents (max 30) were excluded from figure 4.3, but the noneruptive vents still have much higher Cl/F atomic ratios than the eruptive vents. This change in ratio is due to increasing emission of HF from the eruptive vents. Little change in the Cl/S atomic ratio between noneruptive and eruptive vents is shown (fig. 4.4), whereas the F/S atomic ratio is much greater at eruptive than at noneruptive vents. (Ratios with sulfur are used in figure 4.4 to exclude variations induced by changes in the water content of these samples.) From the data in figure 4.4, HCl, like CO_2 and SO_2, apparently is degassed from the magma early in its ascent, whereas HF, like H_2O, is mostly degassed near the surface.

GAS CONTENT OF THE MAGMA

Greenland and others (1985) estimated 0.022 and 0.016 weight percent CO_2 degassed from the eruptive magma, from measurements of CO_2 emission in the plume during two episodes of the current eruption. Assuming 85 mol percent H_2O in the eruptive gases (as in the equilibrated eruptive-gas samples), a C/S atomic ratio of 0.17 (see above) yields an H_2O/CO_2 weight ratio of 16. Combining this ratio with 0.02 weight percent CO_2 degassed

yields 0.32 weight percent H_2O degassed on eruption. The water contents of lava spatter and flowing lava from this eruption are typically less than 0.1 weight percent (see chap. 2). Adding 0.1 weight percent H_2O retained by the lava to the volatilized water yields an estimate of the H_2O content of the eruptive magma of 0.42 weight percent, comparable to Moore's (1965) estimate of 0.45 ± 0.15 weight percent H_2O for submarine basalt.

The S content of the magma can be similarly estimated. Combining 0.02 weight percent CO_2 degassed on eruption with a C/S atomic ratio of 0.17 yields 0.086 weight percent S degassed on eruption. Assuming 0.02 weight percent S retained by the lava (Moore and Fabbi, 1971; Swanson and Fabbi, 1973; Fornari and others, 1979) yields a preeruptive S content for the magma of 0.11 weight percent. Summing the amounts of H_2O, CO_2, and S degassed on eruption and retained by the lava gives a total volatile content of the magma of 0.55 weight percent.

Although the weight fraction of gases in the magma is small, their significance is great. With 0.43 weight percent of gases exsolved from the melt on eruption, an average molecular weight for the gases of 24, and a magma density of 2.8 g/cm^3, we obtain 497 moles of gas per cubic meter of magma. At 1,130 °C and 1 atm pressure, this volatile content equals 57 m^3 of gas per cubic meter of magma, corresponding to a system (gas + liquid) density of 0.05 g/cm^3 on eruption. Therefore, it is apparent both that lava constitutes a volumetrically insignificant fraction of a volcanic eruption and that this fiftyfold change in system volume must be the overwhelming force in fountaining dynamics.

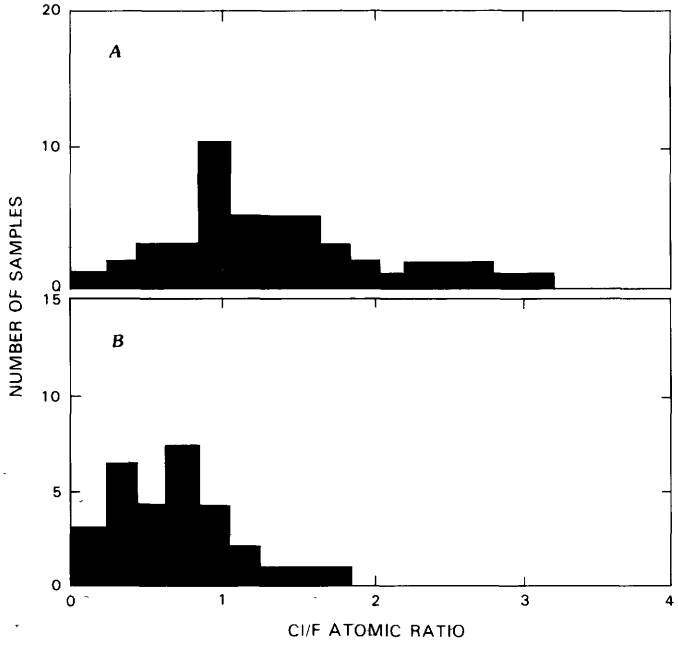

FIGURE 4.3.—Cl/F atomic ratio in gases from noneruptive vents (*A*) and eruptive vents (*B*). Data from table 4.2.

CONCLUSIONS

The differing gas compositions found between eruptive and noneruptive vents suggest that degassing of the magma proceeds in stages: At the depth represented by the noneruptive vents, most of the volatilizable CO_2, SO_2, and HCl have exsolved, whereas some of the water and most of the halogens remain in the melt; continuing ex-

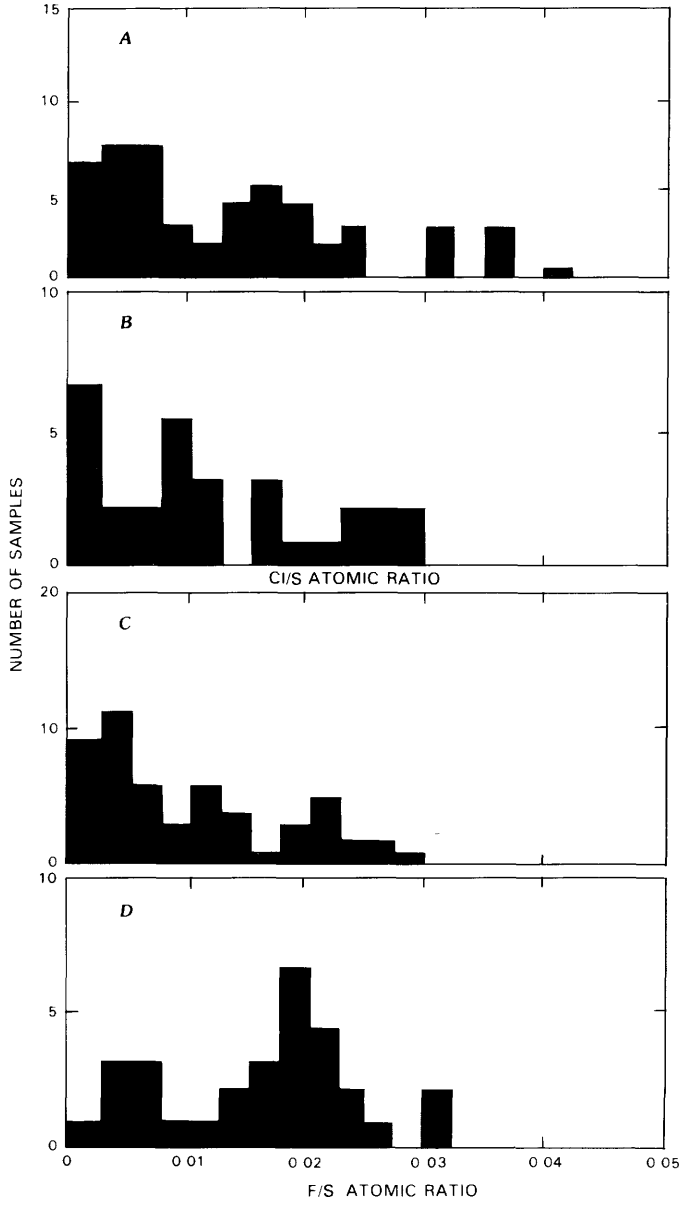

FIGURE 4.4.—Halogen/sulfur atomic ratios in gases from noneruptive vents (*A*, *C*) and eruptive vents (*B*, *D*). Data from table 4.2.

solution of dissolved H_2O and HF during final rise in the eruptive conduit yields a continuously changing composition of the eruptive-gas phase. Therefore, there is probably no need to invoke major changes in magmatic composition, meteoric-water contamination, or atmospheric oxidation to account for most of the observed chemical variation of these gas samples: The highly dynamic, nonequilibrium, eruptive degassing process necessarily leads to a varying composition of the gas phase. This conclusion completely accords with Shepherd's (1921, p. 87) statement about the 1918–19 gas collections from Halemaumau: "We are not here dealing with a mixture of gas which is definite in composition and given off steadily by the magma. Each bubble has its own composition * * *."

Nevertheless, these analyses and those of gases from other volcanoes (Gerlach, 1982; Greenland, in press) show that eruptive gases generally do approximate equilibrium assemblages (except, commonly, for water content). In particular, the oxidation state of Hawaiian gases appears to be controlled by a common, natural buffer system: Both these Kilauea gases and the Mauna Loa eruptive gases (Greenland, in press) follow oxygen-temperature curves very close to those directly measured (Sato and Wright, 1966) in a Kilauean lava lake. It would be of some interest to determine what this system is and how general its applicability might be.

These results have implications for any future collections of Kilauea (and, possibly, other) eruptive gases. (1) C/S atomic ratios in the gases, which are controlled by degassing of the magma to equilibrium in the summit reservoir, can be expected to be similar to those reported here; an exception would be a long Halemaumau eruption, when summit degassing would coincide with eruptive degassing. (2) The contents of water and halogens, which are unsaturated in the magma at the temperature and pressure of the reservoir, may vary among eruptions, owing to assimilation of crustal water by the magma and to differing compositions of the initial magmas formed in the mantle. (3) Because very little of the halogen content is volatilized on eruption, their variations are better studied in lavas rather than in gas collections. (4) Large variations in the water content of the gases can be expected both within and among eruptions, owing primarily to the depth at which gases separate from the magma before sampling, to the rate of magma effusion, to the amount of assimilated crustal water in the magma, and to possible incorporation of meteoric water into the sample. (5) During fissure eruptions, useful gas samples can be collected from low-temperature ground cracks far removed from the actual eruptive site. Many of these collections will be found to have quenched at around 1,000 °C, but the depth of degassing must also be considered when evaluating their water content. (6) Because degassing is a dynamic, nonequilibrium process, samples must be collected from as many sites and at as many different times as possible. The usual practice of collecting an abundance of samples from a single site within a brief period is expected to result in misleading interpretations.

REFERENCES CITED

Chayes, Felix, 1960, On correlation between variables of constant sum: Journal of Geophysical Research, v. 65, no. 12, p. 4185–4193.

Fornari, D.J., Moore, J.G., and Calk, L.C., 1979, A large submarine sand-rubble flow on Kilauea Volcano, Hawaii: Journal of Volcanology and Geothermal Research, v. 5, no. 3-4, p. 239-195.

Gerlach, T.M., 1980, Evaluation of volcanic gas analyses from Kilauea volcano: Journal of Volcanology and Geothermal Research, v. 7, no. 3, p. 295–317.

—— 1982, The interpretation of volcanic gas data from tholeiitic and alkaline mafic lavas: Bulletin Volcanologique, v. 45, no. 3, p. 235–244.

Giggenbach, W.F., 1975, A simple method for the collection and analysis of volcanic gas samples: Bulletin Volcanologique, v. 39, no. 1, p. 132–145.

Greenland, L.P., 1984, Gas composition of the January 1983 eruption of Kilauea Volcano, Hawaii: Geochimica et Cosmochimica Acta, v. 48, no. 1, p. 193–195.

—— 1987, Composition of gases from the 1984 eruption of Mauna Loa Volcano, chap. 30 *of* Decker, R.W., Wright, T.L., and Stauffer, P.H., eds., Volcanism in Hawaii: U.S. Geological Survey Professional Paper 1350, v. 1, p. 781–790.

Greenland, L.P., Rose, W.I., and Stokes, J.B., 1985, An estimate of magmatic gas content and gas emissions from Kilauea volcano, Hawaii: Geochimica et Cosmochimica Acta, v. 49, no. 1, p. 125–129.

Heald, E.F., Naughton, J.J., and Barnes, I.L., Jr., 1963, The chemistry of volcanic gases. 2. Use of equilibrium calculations in the interpretation of volcanic gas samples: Journal of Geophysical Research, v. 68, no. 2, p. 545–557.

Jagger, T.A., 1940, Magmatic gases: American Journal of Science, v. 238, no. 5, p. 313–353.

Kyser, T.K., and O'Neil, J.R., 1984, Hydrogen isotope systematics of submarine basalts: Geochimica et Cosmochimica Acta, v. 48, no. 10, p. 2123–2133.

Matsuo, Sadao, 1962, Establishment of chemical equilibrium in the volcanic gas obtained from the lava lake of Kilauea, Hawaii: Bulletin Volcanologique, v. 24, p. 59–71.

Moore, J.G., 1965, Petrology of deep-sea basalt near Hawaii: American Journal of Science, v. 263, no. 1, p. 40–52.

Moore, J.G., and Fabbi, B.P., 1971, An estimate of the juvenile sulfur content of basalt: Contributions to Mineralogy and Petrology, v. 33, no. 2, p. 118–127.

Nordlie, B.E., 1971, The composition of the magmatic gas of Kilauea and its behavior in the near surface environment: American Journal of Science, v. 271, no. 5, p. 417–463.

Sato, Motoaki, and Wright, T.L., 1966, Oxygen fugacities directly measured in magmatic gases: Science, v. 153, no. 3740, p. 1103–1105.

Shepherd, E.S., 1921, Kilauea gases, 1919: Hawaiian Volcano Observatory Monthly Bulletin, v. 9, p. 83–88.

Swanson, D.A., and Fabbi, B.P., 1973, Loss of volatiles during fountaining and flowage of basaltic lava at Kilauea Volcano, Hawaii: U.S. Geological Survey Journal of Research, v. 1, no. 6, p. 649–658.

5. CONSTRAINTS ON THE MECHANICS OF THE ERUPTION

By L.P. GREENLAND, ARNOLD T. OKAMURA, and J.B. STOKES

CONTENTS

ABSTRACT

We have combined the data from gas emissions and inflation/deflation of Kilauea's summit to estimate the gas content and rise rate of magma at Puu Oo, the vertical gradients of pressure and density in the magma column, and the conduit diameter. Eruptive magma rises through the conduit, estimated at about 50 m in diameter, from the summit reservoir at an estimated rate of about 0.1 m/s. Most degassing of the magma occurs in the depth interval 500–900 m of the conduit; above 540 m, less than 10 percent of the conduit volume is occupied by melt during episodes of high fountaining. The base of the lava fountain, where the magma column becomes disrupted into a spray of gas and liquid droplets, occurs at a depth of about 500 m. Because of the depth at which fountaining of the column begins, effusive flow of magma from the vent is impossible during major fountaining events: All the main Puu Oo lava flows during high fountaining are derived from molten droplets coalescing in the crater. The height and vigor of fountaining is controlled by the extent of drainback of degassed magma from the overlying pond and by the rise rate of the eruptive magma; thus, the crater-basin volume, the magma-supply rate, and the conduit dimensions determine the physical appearance of fountaining activity. Repose-period gas emissions represent previously exsolved gases migrating upward; these emissions may be the source of continuous repose-period tremor. The magma column is under less than lithostatic pressure at any depth down to the summit reservoir; the difference is greater than 7.5 MPa at any depth between 350 and 2,500 m.

INTRODUCTION

The physical mechanics of eruptions has been widely studied (Shaw and Swanson, 1970; Sparks, 1978; Wilson and others, 1980; Wilson and Head, 1981). These studies show the critical importance of conduit diameter, magma rise rate, and magmatic gas content on eruption dynamics—parameters that generally can be only guessed at. Because of the many uncertainties, such studies necessarily are highly general and of only limited applicability to individual eruptions. The recent series of episodic eruptions of Puu Oo have provided an opportunity to estimate these parameters and thus to lay a foundation for understanding why and how eruptions take place at one particular basaltic volcano. Our discussion of Puu Oo is restricted to eruptive episodes 15 through 24 and, within each episode, to major high fountaining activity.

The sequence of eruptions that have built the massive cone of Puu Oo is fully described in chapter 1. In summary, the magma conduit beneath Puu Oo is connected hydrostatically to the summit reservoir of Kilauea. During the eruptive episodes studied here, the conduit opened into the basinlike Puu Oo crater at a height of about 100 m above the preeruptive (1982) ground surface. At the surface, the conduit during these episodes was typically about 20 m in diameter. At the end of a given episode, degassed magma in the crater drained back into the conduit. During a repose period, magma slowly rose in the Puu Oo conduit as Kilauea's summit gradually reinflated, and eventually reached the surface and ponded in the crater. With continuing magma inflow into the conduit, the pond overflowed through a spillway, and full-scale fountaining began several hours to a few days later. Data for the eruptive periods studied here are listed in table 5.1.

DEGASSING OF MAGMA

Although the weight fraction of gases in the magma is small, their significance to the eruption dynamics is very great. In chapter 4, it is estimated that the gas content of the magma at 1 atm pressure and 1,130 °C is 48 m^3/m^3, which corresponds to a system density of 0.06 g/cm^3 on eruption. This fiftyfold increase in system volume apparently is the overwhelming force in fountain dynamics. In this section, we derive curves for the variations of pressure, density, and gas composition in the Puu Oo magma as a function of depth in the conduit.

DENSITY OF THE GAS-MAGMA SYSTEM

The current east-rift magma degasses 0.02 weight percent CO_2, 0.172 weight percent SO_2, and 0.23 weight percent H_2O on eruption (see chap. 4). Assuming a nonvesicular magma density of 2.8 g/cm^3, these values correspond to 12.7, 75.3, and 358 mol CO_2, SO_2, and H_2O, respectively, per cubic meter of magma. CO_2 and SO_2

TABLE 5.1.—*Puu Oo eruption data*

[Data for episodes 15 through 20 from chapter 1; data for episodes 21 through 24 from George Ulrich (written commun., 1985). Deflation measurements represent the east-west tilt component recorded at Uwekahuna]

Episode	Repose period (d)	Eruption length (h)	Lava-emission rate (10^3 m^3/h)	Total summit deflation (μrad)	Deflation period (h)	Deflation rate (μrad/h)
15	14	19	421	11.6	44	0.26
16	17	31.5	375	14.8	33	.45
17	26	22	436	10.5	51	.21
18	18	59.5	430	19.5	67.5	.29
19	25	7	314	5.7	51	.11
20	20	9	467	10.3	29	.36
21	22	8	713	9.4	39	.24
22	8	15	513	13.0	28	.47
23	19	18	528	12.9	24	.55
24	21	20	585	14.3	22	.65

are supersaturated in the magma arriving at the summit reservoir and are rapidly degassed through summit fumaroles; their exsolution leaves the magma saturated in CO_2 and SO_2 at the temperature and pressure of the reservoir (Greenland and others, 1984). At any lower pressure, CO_2 and SO_2 exsolve to form a separate phase in the magma; we take this saturation pressure to be 55 MPa (at 2- to 3-km depth, depending on the assumed density). From data on submarine basalt, Moore (1965) estimated the saturation pressure of H_2O to be 8 MPa. With these values, and assuming a linear solubility curve over this pressure range, we calculate the number of moles n of these gases exsolved as a function of pressure P (in megapascals):

$$n(CO_2) = -0.23P + 12.7 \quad (1)$$
$$n(SO_2) = -1.37P + 75.4 \quad (2)$$
$$n(H_2O) = -45.3P + 362 \quad (3)$$

Sparks (1978) concluded that if magma becomes even slightly supersaturated, nucleation of bubbles is an inevitable consequence. Thus, these equations yield a realistic estimate of the amount of separate gas phase present in the magma as a function of pressure.

From the ideal-gas law, the total volume V (in cubic meters) of gas at 1,130 °C exsolved as a function of pressure (P<8 MPa) is given by

$$V = (450 - 46.9P)(0.115/P). \quad (4)$$

With a negligible mass of gas and a nonvesicular-magma density of 2.8 t/m^3 (=g/cm^3), the density ρ of the melt-gas system is given by

$$\rho = 2.8/(V + 1). \quad (5)$$

Substituting equation 4 yields the density as a function of pressure:

$$\rho = (2.8P)/(5.17 + 0.46P). \quad (6)$$

Thus, the pressure as a function of depth D (in meters) in the conduit is given by

$$P = (0.98\rho D) + 1. \quad (7)$$

The density required by equation 7 is the mean density of the overlying column. We computed equation 6 at 0.02-MPa increments of pressure and calculated the increments of column height represented by that pressure change from equation 7. Summing the height increments yielded the pressure-density-depth data listed in table 5.2 and plotted in figure 5.1. The mean density of the overlying column at any depth was obtained from equation 7 by using the pressure-depth curve of figure 5.1. Note that this procedure considers only the exsolution and expansion of gas bubbles as a function of pressure; though appropriate for the magma column, it provides a completely unrealistic description of the physical state of the lava fountain. Our discussion concerns the properties of the magma column and refers to the fountain only for its mass.

BASE OF THE ERUPTIVE FOUNTAIN

The mean densities of the overlying column as a function of depth are listed in table 5.2. These data indicate that at 940-m depth, where H_2O begins to exsolve (8-MPa pressure), the mean density of the overlying column during eruptions is only about a third that of the undegassed

TABLE 5.2.—*Magma-column properties*

Depth (m)	Pressure (MPa)	Density (g/cm^3)	Overlying mean density (g/cm^3)	H_2O/SO_2 mole ratio
129	0.2	0.10	0.08	4.70
261	.4	.20	.12	4.60
339	.6	.30	.15	4.49
395	.8	.40	.18	4.39
440	1.0	.49	.20	4.28
477	1.2	.58	.23	4.18
508	1.4	.67	.26	4.07
536	1.6	.75	.28	3.96
561	1.8	.84	.30	3.85
584	2.0	.92	.32	3.74
605	2.2	.99	.35	3.63
624	2.4	1.07	.37	3.52
642	2.6	1.14	.39	3.40
659	2.8	1.21	.41	3.29
675	3.0	1.28	.43	3.18
691	3.2	1.35	.45	3.06
705	3.4	1.41	.47	2.95
719	3.6	1.47	.49	2.83
732	3.8	1.53	.50	2.71
745	4.0	1.60	.52	2.59
757	4.2	1.65	.54	2.47
769	4.4	1.71	.56	2.35
781	4.6	1.76	.58	2.23
792	4.8	1.82	.59	2.11
803	5.0	1.87	.61	1.98
813	5.2	1.92	.63	1.86
823	5.4	1.97	.64	1.73
833	5.6	2.02	.66	1.61
843	5.8	2.07	.68	1.48
853	6.0	2.12	.69	1.35
862	6.2	2.16	.71	1.22
871	6.4	2.21	.72	1.09
880	6.6	2.25	.74	.96
889	6.8	2.29	.75	.82
898	7.0	2.33	.77	.69
906	7.2	2.38	.78	.55
914	7.4	2.41	.80	.42
923	7.6	2.45	.81	.28
931	7.8	2.49	.83	.14
939	8.0	2.53	.84	.00

magma; thus, melt constitutes only about 30 percent of the volume of the conduit above 940 m. Sparks (1978) showed that magma becomes disrupted into a spray of liquid droplets when gas amounts to about 75 percent of the total volume. From table 5.2, this gas fraction, corresponding to a mean density of 0.7 g/cm^3, occurs at a depth of 520 m. This depth, at which magma becomes converted to spray, can be taken as the base of the fountain. The highest fountain heights at Puu Oo are about 400 m above the local surface; at Puu Oo the actual fountain height is apparently more than double the observed height.

A consequence of locating the base of the fountain so far below the surface is that simple effusion of magma from such a vent becomes impossible; the magma is converted to spray long before it can reach the surface. Therefore, during major fountaining episodes at Puu Oo, the lava pond (and flows therefrom) is formed by coalescence of liquid droplets falling out of the fountain. Thus, the distinction between main flows and spatter-fed flows at Puu Oo depends on the greater extent of coalescence/mixing of droplets falling in the crater relative to those falling on the outer, steep slopes of the cone.

EFFECT OF DRAINBACK

We assume that melt and exsolved gas do not separate in the conduit during eruption (fig. 5.1). The rise of gas bubbles through magma is a complex process (Sparks, 1978), difficult to evaluate. We suggest a magma rise rate in the conduit of about 0.1 m/s during active eruption of lava, a rate that may be sufficiently rapid to prevent rising of bubbles through the melt; the presence of continuous fountains, rather than sporadic gas bursts, at Puu Oo suggests this to be the case. In the fountain, where gas becomes the predominant component, some of the degassed melt will probably fall back into the magma column rather than being ejected, and so the densities calculated from equation 6 would increase. Furthermore, expected drainback of some of the degassed magma from the overlying pond into the conduit would further increase the densities calculated from equation 6.

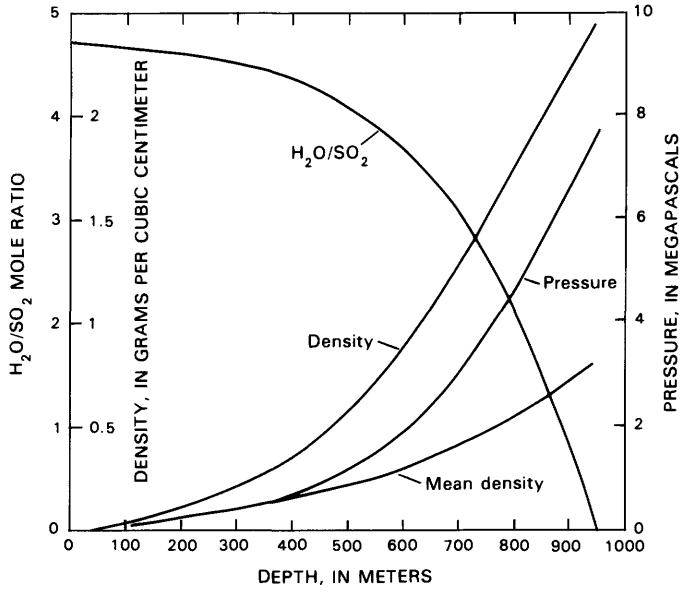

FIGURE 5.1.—Pressure, density, mean density of overlying magma column, and H_2O/SO_2 mole ratio in the gas phase, as a function of depth in the conduit.

If some fraction f of the eruptive magma is degassed, drains back into the conduit, and mixes with rising, new magma, the density given by equation 5 is increased:

$$\rho = (2.8 + 2.8f)/(V + 1 + f), \quad (8)$$

and equation 6 for the variation of density with pressure becomes

$$\rho = (2.8(f + 1)P)/[5.17 + (0.46 + f)P]. \quad (9)$$

These equations yield the density of eruptive magma when supply of new magma, mixing of new magma with a constant fraction of degassed drainback magma, and fountaining represent a continuous process. Repeating the calculations above, using equation 9 in place of equation 6, yields a series of curves, depending on the chosen fraction of drainback. The effect of drainback can then be seen by plotting (fig. 5.2) the fraction of drainback against the depth of the base of the fountain, that is, where the system density falls below 0.7 g/cm^3 and magma disruption begins. Even if all the eruptive magma returns to the conduit after degassing (100-percent drainback), the base of the fountain is raised less than 300 m, within the conduit 210 m below the surface. This analysis suggests that, regardless of the extent of drainback of degassed magma into the conduit, (1) actual fountain heights are much greater than observed, and (2) main lava flows from Puu Oo during full-fountain episodes are derived from droplets of magma coalescing in the crater, rather than representing simple effusion of magma from a vent.

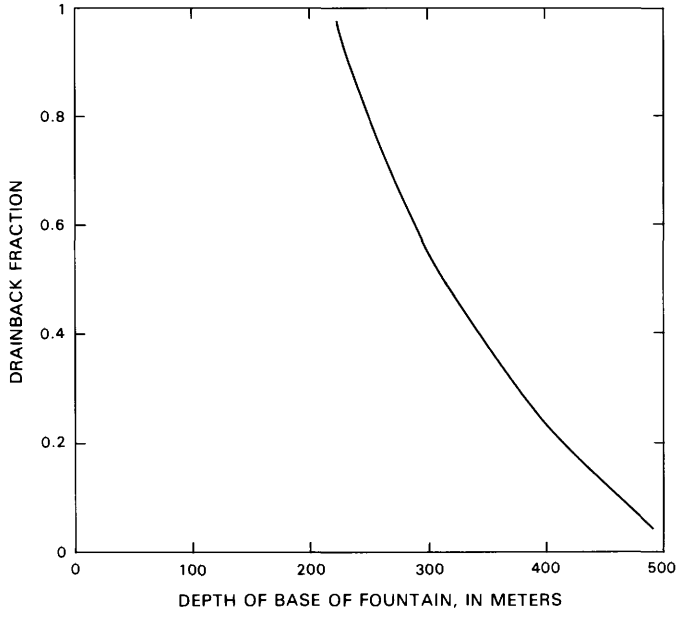

FIGURE 5.2.—Depth in column at which magma becomes disrupted into spray (forming base of lava fountain), as a function of the fraction of eruptive magma that drains back into the conduit.

Equations 8 and 9 depend on the assumption that the degassed drainback magma mixes completely with incoming, new magma. More realistically, we expect sinking and mixing of the dense drainback liquid to be slow relative to the influx rate of new magma; thus, an inverse density gradient would be expected to form at the top of the column. Such a gradient would raise the base of the fountain in the conduit above that calculated from equations 8 and 9. In the extreme case, formation of a dense plug at the top of the column would prevent fountaining altogether when the pressure at the base of the plug reached 1.5 MPa (table 5.2). We suggest that a density gradient is the major cause of the observed great variation in fountaining height and style at Puu Oo. For the eruptive episodes of Puu Oo studied here, extruded lava volumes are generally comparable to estimates of magma-supply rate, a result suggesting that relatively little of the degassed magma drains back into the conduit. Nevertheless, our conclusions about the depth of the fountain and the impossibility of effusive flows from Puu Oo depend on the assumption that drainback of degassed magma into the eruptive column is either negligibly small or well mixed; thus, we insist on them only for the periods of full-scale, high-fountaining activity.

ERUPTIVE-GAS COMPOSITION

Using the pressure-depth curve (fig. 5.1), the H_2O/SO_2 mole ratio of the gas can be estimated from equations 2 and 3. This estimation is important in interpreting gas collections because, although gases in the fountain can only rarely be directly sampled, nearby vents commonly can provide gas samples. Fountain gas changes composition very rapidly as a function of depth (fig. 5.1), and so the composition of gas samples from adjacent noneruptive vents depends on the depth at which the gas separated from the magma. Gases from nearby vents during this eruption typically have H_2O/SO_2 mole ratios only half those of gases from eruptive vents (see chap. 4). Therefore, nearby vent gases appear to be escaping from the magma at a depth of 760 m, only about 200 m above the point where H_2O begins to exsolve (fig. 5.1). We note that equations 1 and 2 yield a constant CO_2/SO_2 mole ratio independent of pressure, as has been observed at this eruption (see chap. 4).

REPOSE-PERIOD DEGASSING

The density at any point in the eruptive-magma column is controlled by the mass of melt in the overlying column.

When an eruption ends, collapse of the fountain adds a layer of relatively cold and dense material to the top of the magma column. If this material were to sink through the underlying lighter magma, the head pressure on the column would decrease, gases would exsolve and expand, and fountaining would ensue. This fountaining would cause more dense material to sink through the column, inducing more fountaining, and so on. In principle, this process could degas the column all the way to the summit reservoir. Both direct observation and monitoring of seismic activity indicate that, in fact, fountains cease fairly abruptly and only very rarely recommence. This observation is possible only if the dense material falling out of the collapsing fountain is floated by the froth at the top of the column, forming a plug that maintains the head pressure on the column. However, sinking of this dense plug through the underlying magma may provide an explanation for those rare occasions when fountaining activity is sporadic.

If all of the fountain mass remains at the top of the magma column, the pressure everywhere in the column (which is due to the mass of overlying material) remains the same after as during eruption. Taking the top of the column when eruption ceases as the base of the previous fountain, the top of the column occurs at 520-m depth and has a pressure of 1.5 MPa (table 5.2). At a density of 2.8 for the degassed fountain material, this pressure implies a 50-m-thick plug (equation 7) overlying the column; thus, the top of the posteruption column (now including the plug) occurs at a depth of 470 m. At the end of eruption, the overlying lava pond also drains back into the conduit, adding to the plug thickness. Because pond dimensions vary for different eruptions of Puu Oo, and because the relative contribution of the pond to the thickness of the fountain plug depends on the diameter of the conduit, we can somewhat arbitrarily assume a less-than-70-m additional thickness of the plug due to pond drainback, and take the magma surface to be at a depth of 400 to 470 m (corresponding to an 80,000-m^3 pond draining into a 40-m-diameter conduit, values expected to overestimate the pond contribution). We note that any drainback of the pond adds mass to the top of the column and thus increases the pressure on the column above that during eruption. During a repose period, the magma column rises in the conduit but this rise does not affect the mass distribution, and so the head pressure on the column remains constant. Because no mechanism exists for reducing pressure on the column, no gases exsolve from the magma during repose periods. Therefore, the gas emissions observed during repose periods must be the result of already-exsolved gases (and gases from new magma injected into the rift) migrating upward. Degassing and, thus, fountaining can begin only after the column is raised to the surface and the head pressure is reduced by spreading of the top of the column; the extent of spreading required depends on the thickness of the degassed plug and thus on the volume of the preceding eruptive pond.

A problem arises if the top of the magma column is more than 400 m below the surface at the start of a repose period. Using 0.085 MPa/μrad for the change in pressure with summit inflation (Decker and others, 1983), a 15-μrad summit inflation (typical total repose-period inflation) raises the column only 50 m (equation 7), which is completely inadequate to start a new eruptive episode if the head of the column is at a depth of 400 m. Observation as well as calculation, however, has shown the column head to lie deeper than 50 m. Therefore, because the summit-pressure change during a repose period is inadequate to renew eruption at Puu Oo, the pressure of the summit reservoir must always be greater than required to lift the magma column to the surface. However, because eruptions of Puu Oo are episodic rather than continuous, the connection between the conduit and the reservoir must be only intermittently open, as suggested by Dvorak and Okamura (1984). If magma is injected into the conduit only sporadically, the only source of continuous motion in the conduit during repose periods is the rise and escape of gas bubbles from the magma. The observation that low-level seismic tremor is continuous during repose periods (see chap. 7) suggests that repose-period tremor reflects the migration of gases in the column, and so tremor magnitude should be related to the volume of gas and the rate of bubble rise.

CONDUIT PROPERTIES

LITHOSTATIC VERSUS CONDUIT PRESSURE

The calculations for figure 5.1 extend only to 8 MPa, the saturation pressure for water. Similar calculations can be made for higher pressures by excluding water from the gases, but in table 5.2 the density of the magma at 8 MPa is about 2.5 g/cm^3. Thus, for depths greater than 940 m, it is probably adequate to average this value with an unvesiculated-magma density of 2.8 g/cm^3 and to assume a constant density of 2.65 g/cm^3. The pressure-depth (P-D) curve below 940 m becomes

$$P = 0.265(D - 940) + 80. \quad (10)$$

Although the pressure in an eruptive conduit is commonly taken as lithostatic (for example, Wilson and Head, 1981), at 940 m, where water begins to exsolve, the pressure in the conduit is only 8 MPa (fig. 5.1), whereas lithostatic pressure at that depth is 22 MPa. Taking the mean magma density below 940 m as 2.65 g/cm^3 (as

above) and the overlying lava density as 2.3 (Kinoshita and others, 1963), the ratio of conduit pressure P_c to lithostatic pressure P_l below 940 m is given by

$$P_c/P_l = (0.265D - 169)/(0.23D + 1), \quad (11)$$

and the difference between lithostatic and conduit pressures by

$$P_l - P_c = 170 - 0.035D, \quad (12)$$

where D is the depth (in meters). This relation (fig. 5.3) and the pressure-depth data from table 5.2 indicate that the pressure in the conduit is less than lithostatic at any depth down to the summit reservoir. Excess lithostatic pressure is greatest at 900-m depth, amounting to 14 MPa, and is greater than 7.5 MPa at any depth between 350 and 2,500 m; only the strength of the wallrock prevents collapse of the conduit.

CONDUIT DIAMETER

SO_2 emissions during eight repose periods (table 5.3) were measured by a correlation-spectrometer (COSPEC) technique (Stoiber and Jepson, 1973; Casadevall and others, 1981). From these data, we estimate a repose-period degassing rate of magma that leads to a volume estimate and, thus, the diameter required for a cylindrical conduit. These estimates depend on extrapolating 1 to 3 days of SO_2 emission data over an entire repose period, even though we would expect emissions to show a rapid initial decline followed by a longer slow decline. Our measurements were generally made in the middle to late part of a repose period and thus lead to minimum estimates of degassing rates and conduit diameters.

The degassing rate R during a repose period (in cubic meters of magma degassed per hour) can be obtained by dividing the observed number of moles of SO_2 emitted per hour, N, by equation 2:

$$R = N/(75.4 - 0.137P). \quad (13)$$

Magma at pressures above 40 MPa can contribute very little to repose-period SO_2 emissions (equation 13, plotted as fig. 5.4). Magma at pressures below 1.5 MPa represents the degassed plug at the top of the column (ignoring pond drainback) and thus contributes nothing to repose-period SO_2 emissions. Computing equation 13 at 0.02-MPa increments and averaging these increments over the range 1.5–40 MPa yields the magma-degassing rates for each of the repose periods listed in table 5.3.

These degassing rates put constraints on the conduit geometry. Assuming a mean density of 2.65 g/cm^3 for the column below 940 m, a pressure of 40 MPa occurs at a depth of 1,700 m below the top of the column (2,170 m below the surface); allowing for 50 m of degassed magma at the top of the column gives a column length of 1,650 m. The diameter of a cylindrical column calculated from these degassing rates is listed (table 5.3) under the assumptions

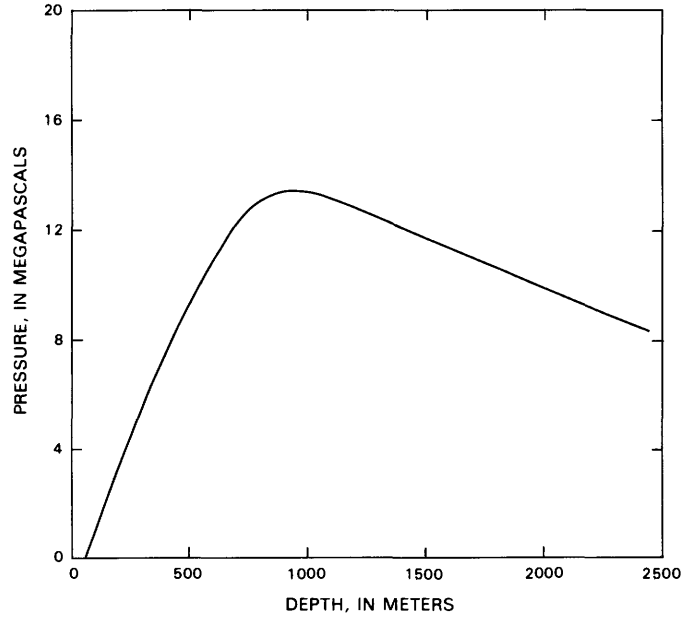

FIGURE 5.3.—Excess pressure (lithostatic minus conduit) on magma column as a function of depth in conduit.

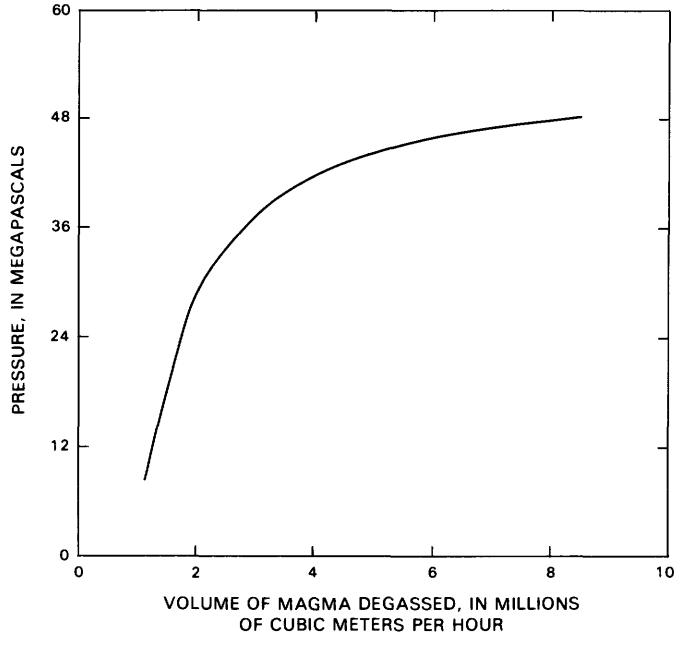

FIGURE 5.4.—Volume of magma that must be degassed at any pressure to yield 100 t/d (65×10^3 mol/h) SO_2.

TABLE 5.3.—*Estimates of conduit diameter*

[Conduit diameter from gas emissions calculated on basis of 100- and 30-percent gas escape. Dashes indicate a negative result]

Repose period (episodes)	Gas emissions					Magma supply			
	SO_2 (mol/h)	R (m^3/h)	Volume (10^6 m^3)	Diameter (m)		Inflation (μrad)		Magma loss (10^6 m^3)	Diameter (m)
				100 pct	30 pct	Observed	Calculated		
14-15	77,469	1,865	0.63	22	40	7.05	9.94	1.12	60
15-16	37,107	894	.36	17	31	10.47	12.56	.84	52
16-17	59,892	1,442	.90	26	48	9.30	18.94	3.86	111
19-20	51,429	1,240	.60	21	39	9.20	15.84	2.66	92
20-21	65,100	1,568	.90	25	46	7.56	15.60	3.22	101
21-22	19,530	470	.091	8.4	15	5.89	5.53	---	---
22-23	123,690	2,978	1.36	32	59	12.67	14.06	.56	42
23-24	97,650	2,351	1.18	30	55	10.51	16.12	2.25	85

that (1) all the gas escapes from the column during the repose period and (2) only 30 percent of the gas escapes to be measured by COSPEC. Because the actual fraction of gas that escapes to the atmosphere during a repose period is certainly less than 100 percent (gas emissions never cease), the conduit diameter based on 100-percent escape can be taken as a lower limit.

An independent estimate of the conduit diameter can be based on the summit tilt record. Taking 1.0 μrad of inflation of the summit as equivalent to 0.4×10^6 m^3 of magma (Dvorak and Okamura, 1984) and assuming that the annual supply of magma to the summit reservoir (110×10^6 m^3; Swanson, 1972) is constant over time yields an expected daily tilt change of 0.75 μrad at the summit during a repose period. The difference between the observed and expected summit-inflation rates during a repose period provides an estimate of the maximum volume of magma injected into the east-rift conduit (table 5.3). We showed above that the top of the magma column is at least 400 m below the surface at the start of the repose period and must be raised to the surface before an eruption can start. Combining the volume of magma injected into the conduit with the required rise of the column provides the estimate for the diameter of a cylindrical conduit listed in the last column of table 5.3.

Both the estimate of the conduit diameter based on gas emissions and that based on summit inflation apparently have large uncertainties. At best, gas emissions provide a lower limit, and summit inflation an upper limit, for this diameter. Furthermore, the estimate from summit inflation refers to the upper 400 m of conduit, whereas the estimate from gas emissions refers to the depth interval 500–2,200 m. Nevertheless, the agreement of these two estimates is sufficiently close for each repose period that the overall average diameter of 50 ± 30 m provides a realistic constraint on the conduit geometry. This estimate is barely compatible, however, with the observed opening of the conduit in the crater (typically, approx 20 m diameter); the conduit probably becomes constricted near the surface, possibly throughout the new Puu Oo spatter cone.

The conduit diameter for repose period 21–22 could not be estimated from the summit-inflation data because the observed inflation was greater than that expected from assuming of a constant magma-supply rate. This discrepancy may indicate a surge of magma from the mantle into the summit reservoir: Repose period 21–22 was among the shortest observed for 25 eruptive episodes. This repose period was also anomalous for very low SO_2 emissions, leading to a very low estimate of conduit diameter from repose-period gas emissions; the SO_2 measurement listed in table 5.3 is the median of 63 determinations made 3 days after the end of episode 21, and so we have no reason to discount it.

RISE RATE OF MAGMA

From the estimates of conduit diameter given above, we can estimate the rise rate of magma in the conduit during eruption. We assume 20-percent vesicularity for the lava to convert lava-emission rate (table 5.1) to magma-effusion rate. Combining this rate with the minimum conduit diameter estimated from gas emissions yields a maximum rise rate for the eruptive magma. We obtain a minimum rise rate estimate by combining the measured summit-deflation rate during eruption (table 5.4) with the conduit diameter estimated above from summit tilt. The use of independent estimates for conduit diameter and magma-effusion rate assures independence of the two rise-rate estimates listed in table 5.4. The magma-effusion rate estimated from summit deflation is generally less

TABLE 5.4.—*Estimates of the rise rate of eruptive magma*

[---, negative number calculated]

Episode	Gas emissions		Magma supply	
	Magma-effusion rate (m^3/s)	Rise rate (m/s)	Deflation volume (m^3/s)	Rise rate (m/s)
15	93.6	0.25	74.4	0.026
16	83.3	.38	86.7	.041
17	96.9	.18	77.8	.008
20	104	.29	123.3	.019
21	158	.32	100.0	.012
22	114	2.1	---	---
23	117	.14	94.4	.068
24	130	.18	111.1	.020

than that from extruded lava and thus emphasizes the difference in diameter estimates. Therefore, the order-of-magnitude difference in the rise-rate estimates listed in table 5.4 is not unreasonable, and these estimates can be taken as realistic limits. We have some confidence that the rise rate of the magma in the conduit (to the point where fountaining begins) during eruptions is within a factor of 3 of 0.1 m/s. In contrast, the rise rate during a typical repose period (400 m in 20 days, 0.8 m/h) is more than 100 times less than this eruptive rate.

One constraint on our estimates of rise rates is that the rate must be sufficiently great to prevent the magma from solidifying in place. Wilson and Head (1981), following Fedotov (1977), showed that this limiting rate U (in meters per hour) is given by

$$U = 4.5 \times 10^{-3} D/r^2, \quad (14)$$

where D is the depth from which the magma rises and r is the radius of the conduit. Taking D as 2,500 m, about the depth to the top of the summit reservoir, and r as 25 m (estimated above) gives a limiting rise rate of 0.018 m/h, more than 10 times less than our inferred typical repose-period rise rate and 10,000 times less than our estimated eruptive-episode rise rate. Equation 14 can also be used to derive a limiting diameter for the conduit. Setting U equal to the repose-period rise rate at Puu Oo (0.8 m/h), it can be shown that the magma column would solidify during a repose period if the conduit diameter were less than 8 m. We note that reducing our estimate of the depth to the top of the column at the end of an eruptive episode increases the diameter of the column required to prevent solidification; for example, if the magma column rises only 100 m during a repose period, the column diameter must be at least 15 m to prevent solidification. Therefore, our estimate of neither conduit diameter nor magma rise rate is incompatible with magma remaining molten in the conduit throughout a repose period.

Another constraint on our estimate of eruptive rise rate derives from the requirement that fire fountains, rather than discrete gas bursts, be produced at Puu Oo. With a sufficiently slow rise rate of magma, gas bubbles can coalesce and grow to fill the conduit; discrete gas bursts occur as these large bubbles reach the surface (the probable origin of the "gas pistoning" frequently observed at Puu Oo late in repose periods). Wilson and Head (1981), studying bubble coalescence in magmas, concluded that only discrete gas bursts will be produced if eruptive rise rates of less than 0.1 m/s are maintained; thus, our estimated rise rate seems barely compatible with the occurrence of continuous fire fountains at Puu Oo. Wilson and Head's analysis, however, was restricted to very small vents (less than 6 m diam) and high water contents (more than 1 weight percent H_2O). Study of their graph suggests that extrapolation to Puu Oo conditions would reduce their limiting rise rate for continuous fountains by at least a factor of 10 and make our estimate entirely compatible with continuous fountaining activity.

Finally, we note that combining our estimated eruptive rise rate, 0.1 m/s, with our estimated diameter, 50 m, yields an eruptive magma-effusion rate of 0.7×10^6 m^3/h; this value is within a factor of 2 of observed lava-emission rates (table 5.1) and within the uncertainties of our estimates. Thus, our estimated rise rates probably are at least within the range of physical possibility.

CONCLUSIONS

Although CO_2 and SO_2 begin to exsolve from the magma as soon as the pressure in the magma falls below that in the summit reservoir, rapid degassing does not begin until the magma rises to within 940 m of the surface and water begins to exsolve. Within the next 400 m, gas comes to constitute 90 percent of the conduit volume. This near-explosive transition from predominantly liquid to predominantly gas is the source of the eruptive fountain. Because fountain heights are easily measured and have great physical significance for understanding eruptive mechanisms (Wilson and Head, 1981), it is significant that much, possibly most, of the fountain occurs within the conduit below the ground surface.

An important consequence of locating the base of the fountain so far below the surface during full-scale fountaining events is that main lava flows from Puu Oo at these times must be supplied by coalescence of molten droplets in the crater, rather than representing simple effusion of magma. Indeed, with the eruptive rise rate inferred here (approx 0.1 m/s), 2.6 hours are required from the point where water begins to exsolve to the point where

magma would overflow the vent; rapid exsolution of water and expansion of gases effectively prevent the passive effusion of magma. Therefore, the lava in flows has been largely degassed during its transit as molten droplets in the fountain, and so the gases observed in lava flows represent plume gases and air that have been trapped and mixed with the coalescing droplets.

Our conclusions about the depth of the fountain and the source of the lava in flows depend on the assumptions that drainback of degassed melt into the conduit is negligible and (or) well mixed with the rising, new magma. Thus, these conclusions apply only to those (frequent) eruptive episodes characterized by very high fountaining activity. If drainback becomes extensive, an inverse density gradient probably forms at the top of the column. Adding a dense, degassed layer to the top of the eruptive column both suppresses expression of the fountain (by absorbing kinetic energy from the expanding gas) and raises the depth in the column at which magma becomes disrupted into spray, even to the extent that simple effusion of melt from the vent becomes possible.

We suggest that the volume of the overlying pond, which controls the extent of drainback, is one of the major factors governing the height, volume, and type of lava fountains. This factor may also account for short-period fluctuations in fountain behavior, because the effect of drainback is sensitive to the extent to which the degassed drainback magma mixes with rising, new magma. Another major factor controlling fountain activity is the rise rate of eruptive magma in the conduit, which is a function of the magma-supply rate and the diameter of the conduit. If the rise rate is sufficiently slow that bubbles can coalesce to fill the conduit, fountain activity becomes reduced to sporadic release of large gas bursts (Wilson and Head, 1981). The effects of pond drainback and magma rise rate apparently can account for all the variations in fountain appearance during the course of this 1983–84 east-rift eruption, without recourse to variation in the gas content of the magma, in accord with the conclusion by Greenland and others (1984) that all Kilauea magmas have about the same gas content, and with the observation (see chap. 4) that gas composition has been constant over the first 14 months of the eruption.

Closing of the connection between the conduit and the summit reservoir (Dvorak and Okamura, 1984) seems the probable cause for the ending of individual eruptive episodes. Whatever the cause, however, the degassed melt in the fountaining part of the conduit then falls back to the head of the magma column. Because the head pressure on the eruptive-magma column is due to the mass of material in the fountain within the conduit, fallback of this material results in the head pressure of the column being the same during repose periods as during an eruption. (Drainback of the degassed surface lava pond also adds to the head pressure on the column.) Thus, no gases exsolve from the magma during repose periods, and the gas emissions observed during those periods represent previously exsolved gases rising through, and escaping from, near-stagnant magma. This migration of gases is probably the source of the continous seismic tremor observed during repose periods. Because the head pressure on the column is due to the mass of the overlying degassed plug, rise of the column in the conduit by injection of new magma does not alter the pressure at any point in the column: Pressure release, thus degassing, thus fountaining, can recommence only when the magma column regains the surface, where its top can spill off.

The pressure within the magma column is a function of the density of the overlying column, which, in turn, is related to the volume of gases exsolved from the melt. Lithostatic pressure, however, is governed by a near-constant density. This contrast results in a pressure differential, between magma in the conduit and the wallrock, of greater than 7.5 MPa at depths between 350 and 2,500 m. This pressure differential, acting to close off the conduit, makes continuing eruption susceptible to seismic activity and consequent rock failure.

The dynamics of the eruptive fountain are generated within a 100- to 200-m interval of the column within which gases rapidly exsolve, expand, and coalesce to transform a largely liquid system into one of largely gas. Understanding eruptive dynamics entails understanding this transformation process, which has been extensively studied (for example, Sparks, 1978; Wilson and Head, 1981). Critical factors in the process are the gas content of the melt, the diameter of the conduit, and the rise rate of magma in the conduit. Previous studies have largely considered only cases in which the gas content is much higher, the eruptive conduits much smaller, and the magma rise rates much greater than seem plausible at Puu Oo. Relating these studies to Puu Oo eruptions—a nontrivial task—will require the constraints derived above.

REFERENCES CITED

Casadevall, T.J., Johnston, D.A., Harris, D.M., Rose, W.I., Jr., Williams, S.M., Woodruff, Laurel, and Thompson, J.M., 1981, SO_2 emission rates at Mount St. Helens from March 29 through December, 1980, *in* Lipman, P.W., and Mullineaux, D.R., eds., The 1980 eruptions of Mount St. Helens, Washington: U.S. Geological Survey Professional Paper 1250, p. 193–200.

Decker, R.W., Okamura, A.T., and Dvorak, J.J., 1983, Pressure changes in the magma reservoir beneath Kilauea Volcano, Hawaii [abs.]: Eos (American Geophysical Union Transactions), v. 64, no. 45, p. 901.

Dvorak, J.J., and Okamura, A.T., in press, Variations in tilt rate and harmonic tremor amplitude during the January–August 1983 east rift eruptions of Kilauea Volcano, Hawaii: Journal of Volcanology and Geothermal Research.

Fedotov, S.A., 1977, Ascent of basic magmas in the crust and the mechanism of basaltic fissure eruptions: International Geology Review, v. 20, no. 1, p. 33-48.

Greenland, L.P., Rose, W.I., and Stokes, J.B., 1985, An estimate of gas emissions and magmatic gas content from Kilauea Volcano: Geochimica et Cosmochimica Acta, v. 49, no. 1, p. 125-129.

Kinoshita, W.T., Krivoy, H.L., Mabey, D.R., and MacDonald, R.R., 1963, Gravity survey of the island of Hawaii, art. 89 *of* Short papers in geology and hydrology: U.S. Geological Survey Professional Paper 475-C, p. C114-C116.

Moore, J.G., 1965, Petrology of deep-sea basalt near Hawaii: American Journal of Science, v. 263, no. 1, p. 40-52.

Shaw, H.R., and Swanson, D.A., 1970, Eruption and flow rates of flood basalts, *in* Gilmour, E.H., and Stradling,, Dale, eds., Columbia River Basalt Symposium, 2d, Cheney, Wash., 1969, Proceedings: Cheney, Wash., EWSC Press, p. 271-299.

Sparks, R.S.J., 1978, The dynamics of bubble formation and growth in magmas: A review and analysis: Journal of Volcanology and Geothermal Research, v. 3, no. 1-2, p. 1-37.

Stoiber, R.E., and Jepson, Anders, 1973, Sulfur dioxide contributions to the atmosphere by volcanoes: Science, v. 182, no. 4112, p. 577-578.

Swanson, D.A., 1972, Magma supply rate at Kilauea Volcano, 1952-1971: Science, v. 175, no. 4018, p. 169-170.

Wilson, Lionel, and Head, J.W., III, 1981, Ascent and eruption of basaltic magma on the earth and moon: Journal of Geophysical Research, v. 86, no. B4, p. 2971-3001.

Wilson, Lionel, Sparks, R.S.J., and Walker, G.P.L., 1980, Explosive volcanic eruptions, IV, The control of magma properties and conduit geometry on eruption column behavior: Royal Astronomical Society Geophysical Journal, v. 63, p. 117-148.

6. SURFACE DEFORMATION DURING DIKE PROPAGATION

By ARNOLD T. OKAMURA, JOHN J. DVORAK, ROBERT Y. KOYANAGI, and WILFRED R. TANIGAWA

CONTENTS

ABSTRACT

Emplacement of a dike in the vicinity of four electronic tiltmeters at the start of the 1983 Puu Oo eruption provided a unique set of surface-deformation data. The tiltmeter data were analyzed with a simple three-dimensional elastic model of a thin rectangular dike. The intrusion began at 2100 H.s.t. January 1 in the area near Makaopuhi Crater from a depth of 2.5 km to the dike top. The dike propagated laterally at about 550 m/h and vertically at about 70 m/h, and its final size is estimated at 15 km long, 2.5 km high, and 3.5 m wide. The model also predicts that reversals in tilt direction would occur as the dike tip passed a station or as the dike top ascended above a critical depth, and these reversals in tilt direction were observed in the data.

The temporal relation between the Kilauea summit-region deformation and the rift-zone deformation was recorded for the first time on a real-time basis. In nearly all instances, deformation on the rift zone preceded summit changes.

The probable presence of a large rift-zone magma-storage body is indicated by the preeruption inflationary-tilt pattern, by diffusion of the migrating earthquake swarm, and by anomalously early deformation at the Kalalua tiltmeter station. The magma-storage area outlined by the data extends from Napau Crater to beyond Kalalua, possibly as far as Heiheiahulu.

INTRODUCTION

Rapid tilt changes immediately preceding and accompanying the 1983 east-rift-zone eruption of Kilauea Volcano, Hawaii, provided a unique opportunity to study surface deformation during emplacement of a dike, because the path of intrusion was in the vicinity of four continuously recording electronic tiltmeters. In this chapter we document the tilt changes recorded during intrusion of the dike, analyze those changes with simple elastic models, and compare the temporal relation between tilt changes and the locations of seismic activity. The scope of our study is limited to the surface deformation and seismicity that occurred immediately before and during the initial episode of the 1983 Puu Oo eruption.

Kilauea Volcano, one of five volcanoes that form the Island of Hawaii, is situated in the southeastern section of the island on the slopes of the larger volcano, Mauna Loa. A caldera dominates the summit region, and two conspicuous rift zones, the southwest rift zone and the east rift zone, radiate outward from the summit (fig. 6.1). Seismic and surface-deformation data suggest that magma of mantle origin accumulates at a shallow (2–6 km) depth beneath the summit region and may be emplaced laterally into the rift zones as long, steeply dipping dikes.

The surface deformation associated with intrusions and eruptions of Kilauea Volcano has been documented and analyzed by earlier investigators, who helped to develop an understanding of the magma storage and conduit system of the volcano (Mogi, 1958; Eaton, 1962; Fiske and Kinoshita, 1969; Dieterich and Decker, 1975; Jackson and others, 1975; Swanson and others, 1976; Duffield and others, 1982; Dvorak and others, 1983; Pollard and others, 1983; Ryan and others, 1983). Because of the extensive geodetic data available for the summit region of the volcano, most previous work focused on modeling the central summit magma chamber, generally with a simple point source. Jackson and others (1975), using the plane-strain, finite-element models of Dieterich and Decker (1975), were the first to model the surface deformation associated with an eruptive fissure. A comprehensive analysis of dike emplacement on Kilauea was included in the study by Pollard and others (1983), who utilized cross-sectional displacement curves derived from models of large planar sheets generated by pressurizing a fluid-filled crack. In this chapter, we develop a method that incorporates the constant temporal growth of a dike, to analyze the continuous tiltmeter data obtained during emplacement of a dike along the east rift zone on January 2 and 3, 1983.

Acknowledgments.—We are deeply indebted to the staff of the U.S. Geological Survey's Hawaiian Volcano Observatory for all their help and patience during preparation

of the manuscript. The manuscript was greatly enhanced from informative discussions with David Pollard and James Dieterich.

TILTMETER NETWORK AND INSTRUMENTATION

Changes in the slope of the ground, commonly called tilt, were recognized by Jaggar and Finch (1926) to be directly related to changes in the volume or location of magma within the volcano. By carefully measuring changes in tilt in the summit region and rift-zone areas of Kilauea, the staff of the Hawaiian Volcano Observatory monitors the state of inflation of the summit magma chamber and the movement of magma within the volcano. The method of measurement has evolved through the years, and the latest technique employed is by electronic tiltmeters, which detect changes in the slope of the ground and produce an analog output signal whose magnitude corresponds to the amplitude of the tilt change. Eight electronic-tiltmeter stations are located in the summit region and along the east rift zone of Kilauea (fig. 6.2), and except for the Uwekahuna (UWE) station, all stations are equipped with biaxial, resistance-type, borehole tiltmeters with digital radio telemetry. Station UWE, located in an underground vault, has a uniaxial, mercury-pool, capacitance tiltmeter with analog telemetry. The station UWE tiltmeter data are recorded continuously on a strip-chart recorder, but the digitally telemetered output signals from the borehole instruments are recorded on microcomputer at 10-minute intervals. The Kilauea borehole-tiltmeter stations are patterned after those used

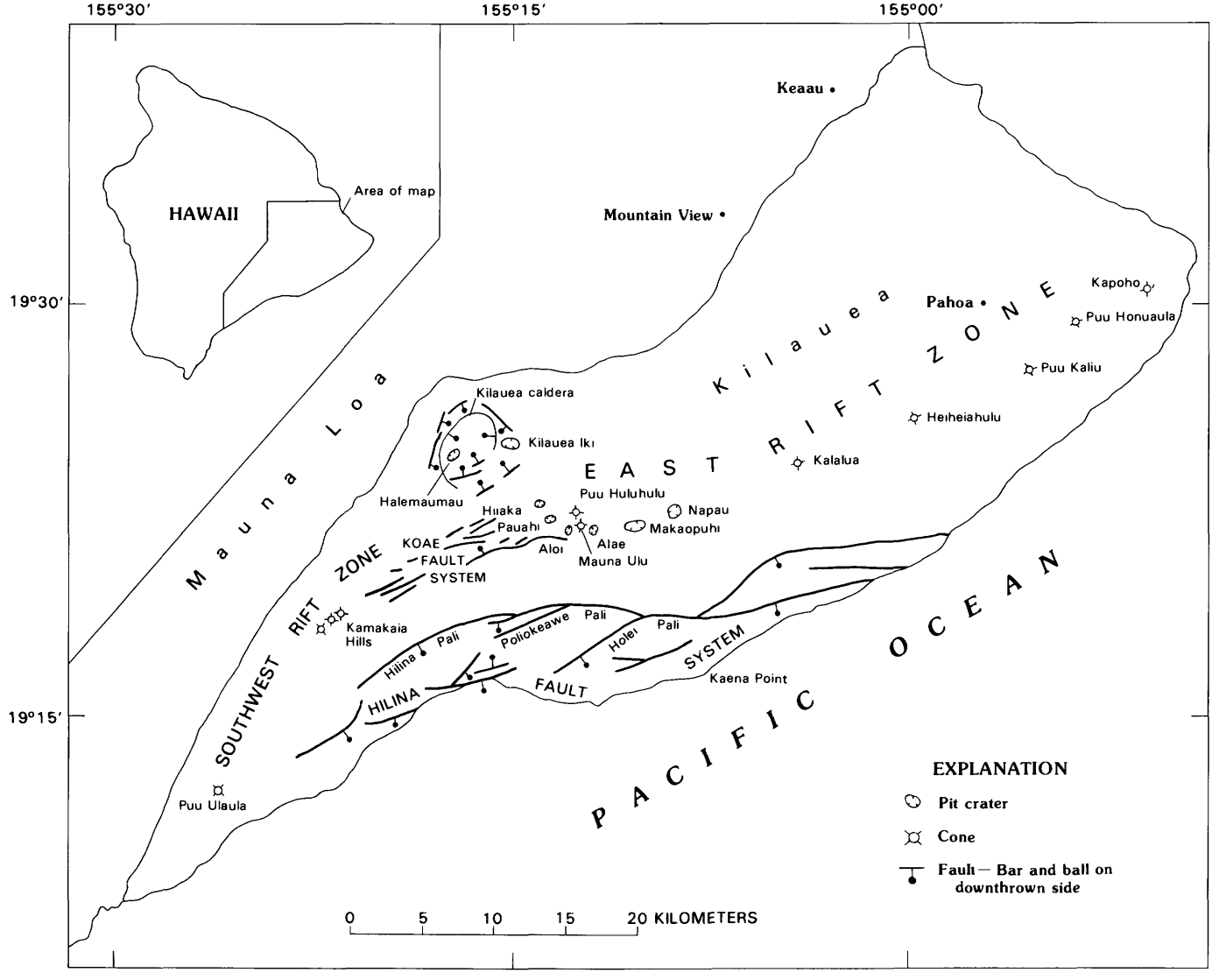

FIGURE 6.1.—Kilauea Volcano, showing main structural features. From Swanson and others (1979, fig. 1).

in California by the U.S. Geological Survey for premonitory earthquake events (Mortensen and others, 1977).

The borehole tiltmeters used at Kilauea have an output of 20 to 40 mV/μrad and are extremely stable for rapid tilt changes, with less than 0.01 μrad drift over a 24-hour period (Johnston, 1976). However, owing to the short baseline of the tiltmeters, diurnal variations of several microradians related to environmental conditions are common. The 12-bit digital telemetry system has a resolution of 0.1 μrad over a range of 500 μrad and a timing accuracy of 10 minutes. Tiltmeter data are commonly displayed either as vectors on a map, with the direction indicating downward movement of the ground, or as a time-series graph, with the direction labels showing the relative downward movement of the ground.

The electronic-tiltmeter stations along the east rift zone of Kilauea were favorably located (fig. 6.3) to record the surface deformation as the dike propagated eastward down the rift. The Puu Kamoamoa (KMM) station was located 600 m north of an eruptive fissure, and the Kalalua (KLU) station was along strike of the dike and within 25 m of tensional cracks that formed during emplacement of the dike. The results from these two stations provided the primary data for this chapter.

METHOD OF ANALYSIS

Analysis of the continuous tilt measurements recorded as the dike was emplaced in the rift zone requires a method whereby growth of the intrusive body is allowed. Earlier investigators utilized methods that analyzed deformation data obtained after the dike was emplaced, but those methods are not suited to analyze data recorded by electronic tiltmeters. The method of analysis described here permits simulation of the continuous, real-time tilt pattern associated with emplacement of a dike.

A simple, three-dimensional elastic model is proposed to explain the tilt pattern recorded by the Kamoamoa tiltmeter during the 24 hours between the start of the earthquake swarm and the onset of eruptive activity along the middle east rift zone. Our model is an extension of earlier studies on Kilauea dikes reported by Dieterich and Decker (1975), Jackson and others (1975), and Pollard and

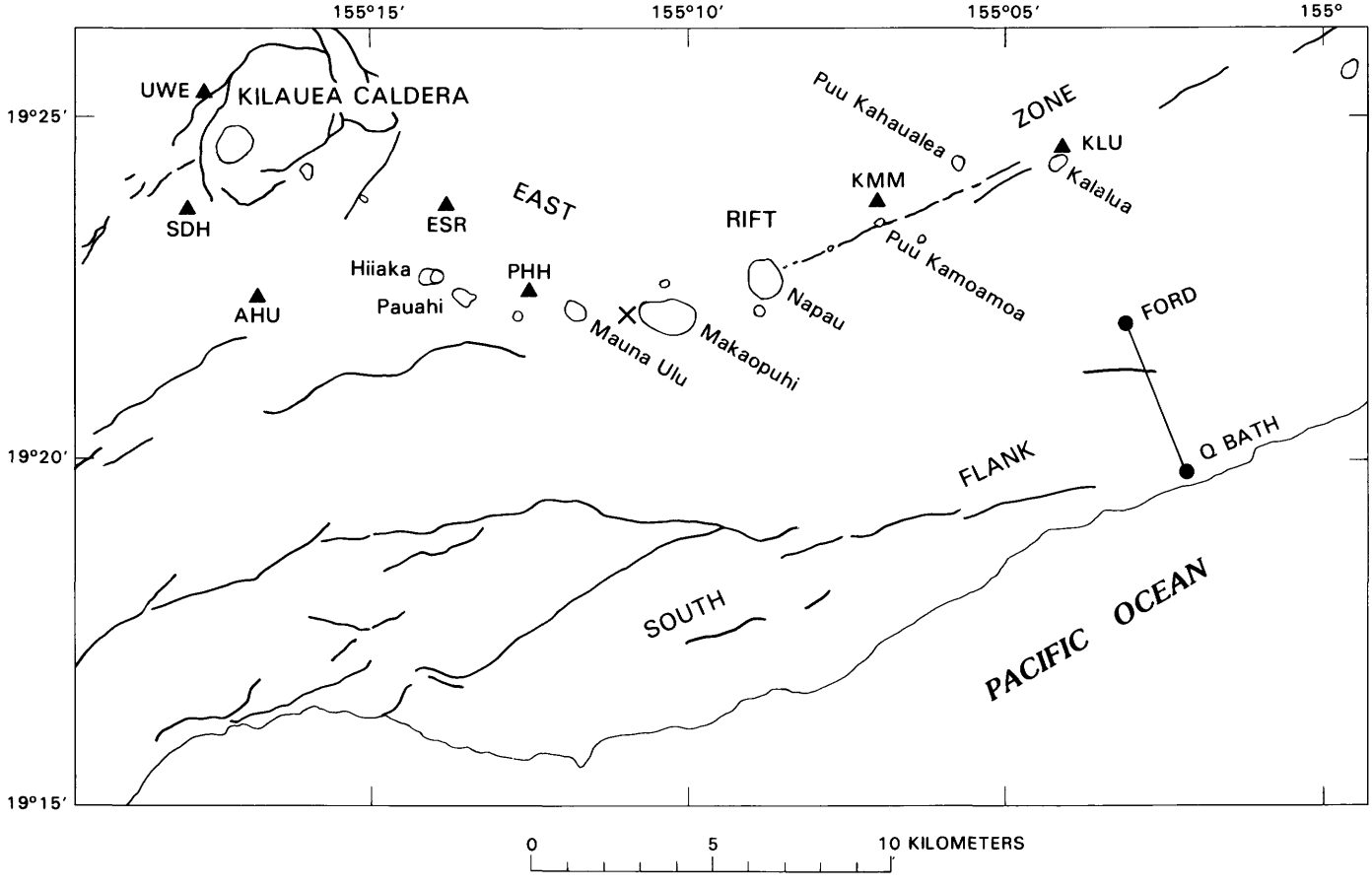

FIGURE 6.2.—East rift zone, showing locations of electronic-tiltmeter stations (triangles), south-flank EDM monitoring line (connected dots), and assumed starting point of dike emplacement (X). Fault traces, solid lines. Major craters are labeled.

others (1983). They utilized leveling data across the axes of the rift zones to show that the elevation changes were consistent with a thin, steeply dipping, planar body modeled as a pressurized sheet of finite vertical dimension. Their analyses were limited to plane-strain approximations and applied only to measurements of ground displacement taken after emplacement of the magma body. Analysis of nearly continuously recorded electronic-tiltmeter data requires that we adopt a three-dimensional model and consider the growth of the magma body.

The simplest three-dimensional model that approximates a dike is a vertical, rectangular sheet. In our model, the dike begins at a point in the X_2X_3 plane at $X_2=0$ and $X_3=D$ as the initial conditions (fig. 6.4). The length (L) and height (H) of the dike are allowed to increase at constant rates, but the width (W) remains unchanged. The vertical surface displacement is U_3, and the horizontal surface displacements parallel and perpendicular to the dike are U_2 and U_1, respectively. Boundary conditions at the sheet require a constant displacement (Δu_1) perpendicular to the plane of the sheet. The medium surrounding the body is assumed to be a homogeneous, isotropic, elastic half-space with free-surface boundary conditions. We further assume that the medium is always in equilibrium during growth of the magma body, so that the static equations of equilibrium may be used.

The analytic solution for the vertical displacement at the free surface in our model at any time (t) during growth of the magmatic sheet is given by (Maruyama, 1964, p. 345):

$$\frac{4\pi u_3(t)}{\Delta u_1}=\left(\frac{x_2-\xi_2}{p+\xi_3}\right)-\left(\frac{2x_1^2(x_2-\xi_2)}{p(x_1^2+\xi_3^2)}\right)// \qquad (1)$$

where $$p=\sqrt{x_1^2+(x_2-\xi_2)^2+\xi_3^2};$$

and we use the notation

$$f(\xi_2,\ \xi_3)//=f(0,D-H)-f(0,D)-f(L,D-H)+f(L,D)$$

to mean that the expression is evaluated at the four pairs of values of ξ_2 and ξ_3. Equation 1 may be differentiated along x_2 to yield the tilt at any point along the free surface parallel to the plane of the sheet:

$$\frac{4\pi(t)\delta u_3}{\Delta u_1 \delta x_2}=$$

$$\left(\frac{1}{p+\xi_3}-\frac{(x_2-\xi_2)^2}{p(p+\xi_3)^2}-\frac{2x_1^2}{p(x_1^2+\xi_3^2)}+\frac{2x_1^2(x_2-\xi_2)^2}{p^3(x_1^2+\xi_3^2)}\right)//, \qquad (2)$$

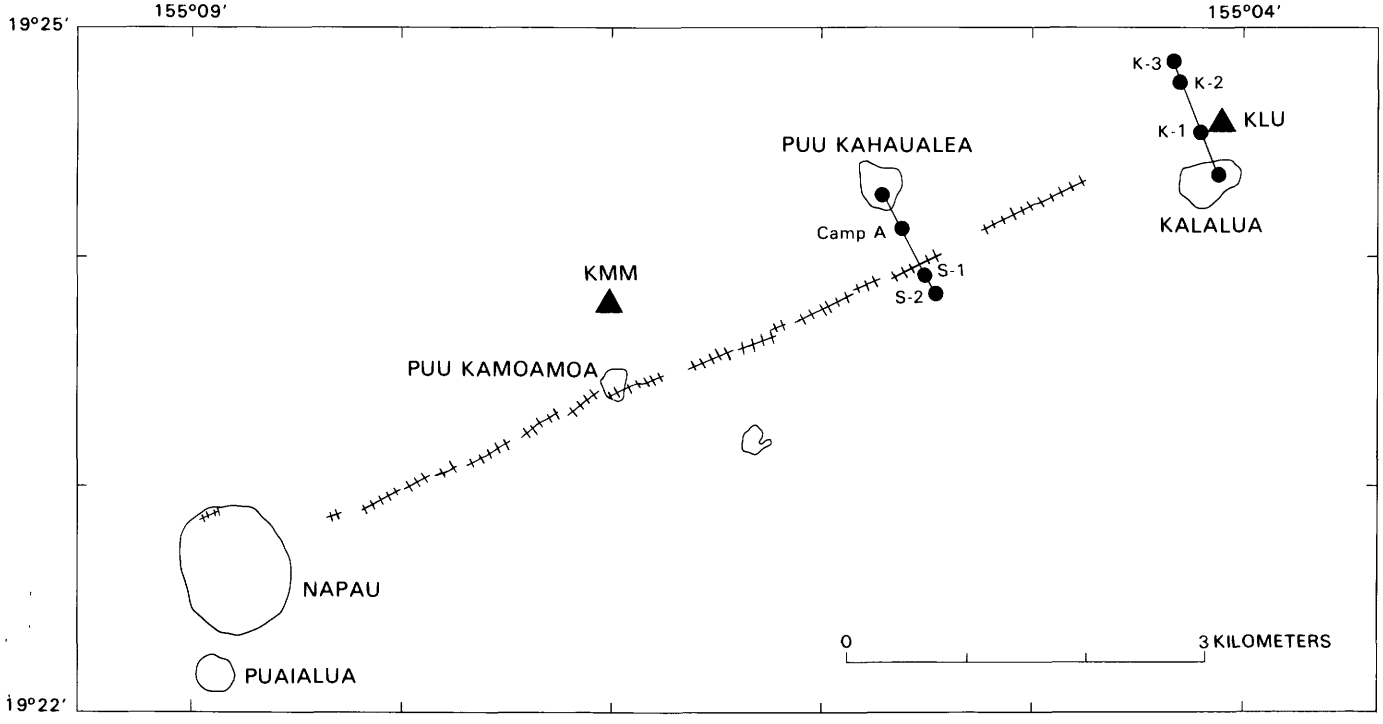

FIGURE 6.3.—East rift zone, showing locations of 1983 eruptive vents (hachured lines), electronic-tiltmeter stations KMM (Puu Kamoamoa) and KLU (Kalalua) (triangles), and crossrift EDM monitoring lines (connected dots). Major craters are labeled.

and along x_1 for the tilt perpendicular to the plane of the sheet:

$$\frac{4\pi(t)\delta u_3}{\Delta u_1 \delta x_1} =$$

$$\left(\frac{2x_1{}^3(x_2-\xi_2)}{p^3(x_1{}^2+\xi_3{}^2)} - \frac{x_1(x_2-\xi_2)}{p(p+\xi_3)^2} - \frac{4x_1(x_2-\xi_2)}{p(x_1{}^2+\xi_3{}^2)} + \frac{4x_1{}^3(x_2-\xi_2)}{p(x_1{}^2+\xi_3{}^2)^2}\right)//. \quad (3)$$

The six parameters in our model are: the initial location (0,D) and beginning (t_0) of dike propagation; the width (W), length (L), and height (H) of the dike; and the distance (x_1) between the plane of the dike and the recording tiltmeter.

Results of our calculations indicate that the tilt component parallel to the direction of dike propagation is most sensitive to lengthening of the dike. The initial tilt is downward away from the origin and in the direction of horizontal propagation as the dike approaches the station. When the dike tip passes the station, the tilt direction reverses and remains downward toward the origin until there is no tilt change in the direction parallel to the strike of the dike. The theoretical tilt curve for a tiltmeter station located 0.6 km away from the axis of a rectangular dike of given height and width but increasing length is plotted in figure 6.5*A*. The model parameters include a

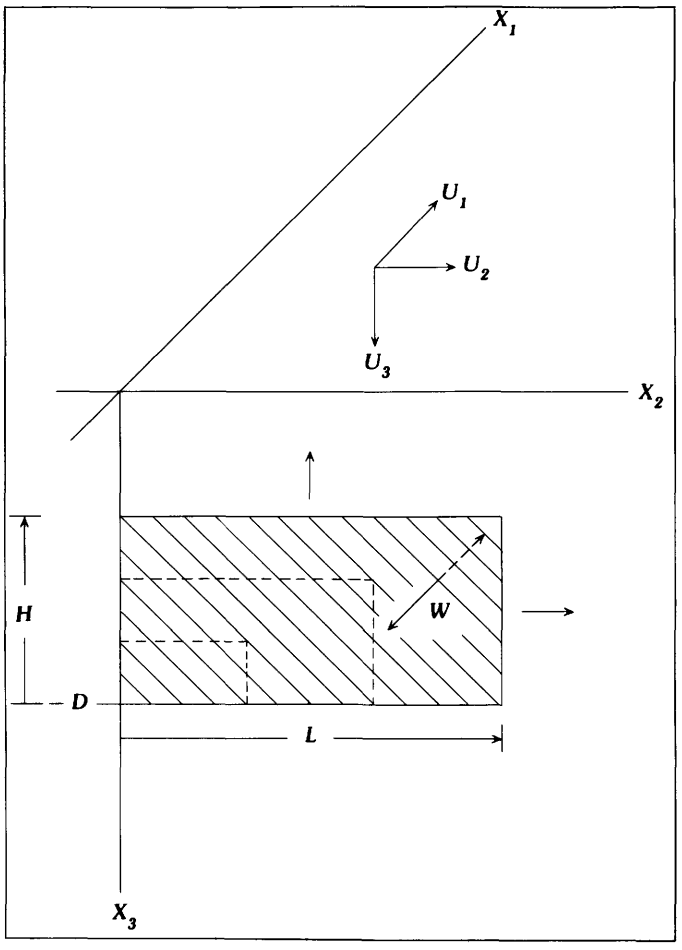

FIGURE 6.4.—Model of a rectangular dike embedded in a homogeneous, isotropic, elastic half-space. Model parameters include depth (D) to bottom of dike, height (H), length (L), and width (W) in a cartesian coordinate system (X_1, X_2, and X_3). Displacements are labeled U_1, U_2, and U_3. Dashed lines and arrows indicate propagation directions.

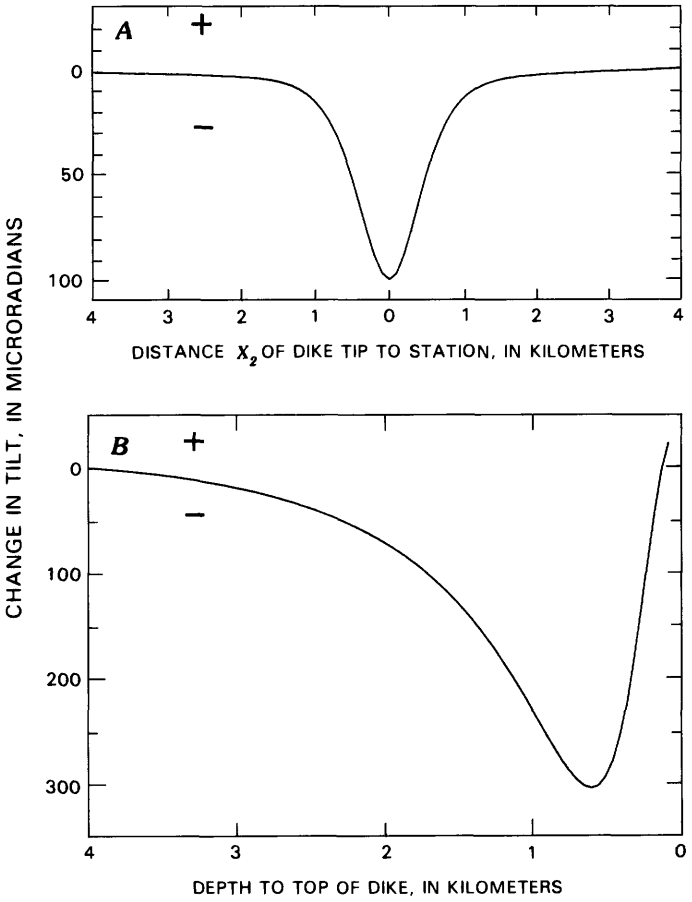

FIGURE 6.5.—Theoretical tilt. See model (fig. 6.4). *A*, Tilt that is created parallel to plane of a model dike of fixed width and height but increasing length. Width (W) of dike is set at 1.5 m, height (H) is 2.5 km, and top is 0.5 km below ground surface; length (L) is allowed to increase from 0 to 8 km. Tiltmeter station is located 4 km (X_2) from origin of dike and 0.6 km (X_1) from axis of dike. Positive (+) tilt indicates a downward slope toward origin of dike and away from direction of propagation; negative (−) tilt indicates a downward slope in direction of dike propagation and away from origin of dike. Reversal in tilt direction occurs when dike tip passes station. *B*, Tilt that is created perpendicular to plane of a model dike of fixed length and width but increasing height. Length (L) and width (W) of dike are set at 8 km and 2.5 m, respectively; bottom (D) of dike is at 4 km, and height (H) is allowed to increase until dike intersects ground surface. Tiltmeter station is located at midpoint of dike in X_2 direction and 0.6 km away in X_1 direction. Positive (+) tilt indicates a downward slope in direction away from axis of dike; negative (−) tilt indicates a downward slope in toward axis of dike. Reversal in tilt direction occurs when dike top rises to a depth equal to or less than X_1 distance.

1.5-m width and a 2.5-km height, with the dike top 0.5 km below the surface of the ground. The dike starts lengthening at 4 km away from the station and grows to a length of 8 km.

The tilt component perpendicular to the plane of the dike is most sensitive to vertical growth of the dike. The initial tilt direction is downward toward the axis of the plane of the dike if the depth to the top of the dike is greater than the distance from the axis to the tiltmeter (X_1). As the dike top nears the surface, the perpendicular tilt component reverses direction and tilts away from the plane of the dike. Pollard and others (1983) found this tilt reversal to occur at dike-top depths ranging from 0.5 to 1.0 X_1. The theoretical tilt curve for a tiltmeter station located 0.6 km away from the axis of a rectangular dike of set length and width but increasing height is plotted in figure 6.5*B*. The model parameters include a length of 8 km and a width of 2.5 m. The dike top starts at a depth of 4 km and moves upward until the surface is breached. The tilt reversal occurs when the dike top is slightly less than 600 m deep.

PREERUPTION EVENTS

The setting for the 1983 eruption can be traced back to the Kalapana $M=7.2$ earthquake of November 27, 1975, when the regional compressive-stress field of Kilauea was relaxed by seaward movement of the south flank. This release of stress allowed intrusions, rather than eruptions, to become the more frequent type of magmatic activity. With a south-flank region that was still mobile because of the large earthquake, the Kilauea summit region and rift zones were able to accommodate a larger volume of magma in storage, as forecast by Ando (1979) in his analysis of the 1975 earthquake. If the south flank were unyielding, eruptions would be the dominant type of magmatic activity, and a smaller volume of magma would be stored. In the period December 1975–April 1982, this larger storage capacity was indicated by an increase in the number of intrusive relative to eruptive events. A total of 13 intrusions and only 1 major and 2 minor east-rift-zone eruptions (Dzurisin and others, 1984) occurred during this post-1975-earthquake period. In contrast, 27 eruptions and only 9 intrusions occurred during the 15-year period before the 1975 south-flank earthquake. Spirit-level tilt surveys in 1981 detected significant uplift of the east rift zone between Makaopuhi Crater and Heiheiahulu (fig. 6.6). This inflation of the rift zone indicated that most of the magma that entered the volcano intruded and was stored in that area.

Two summit eruptions in 1982, one in April and another in September, signaled a change in the regional stress field of Kilauea. These eruptions indicated that the south flank was resisting seaward displacement and further accommodation of the distending magma-storage systems, and because the constantly increasing volume of magma had to be accommodated somewhere, it moved vertically and erupted. The south flank, however, was not totally unyielding because a major intrusion occurred in the southwest rift zone during June 1982.

Gradual tilt changes in the upper and middle east rift zone after the September 1982 summit eruption indicated that magma was moving in those areas while the summit was slowly inflating. Ten days after the September 25, 1982, summit eruption, the Escape Road (ESR) and Puu Huluhulu (PHH) tiltmeters, located in the upper east rift zone (fig. 6.2), recorded a similar, gradual southwesterly tilt (fig. 6.7*A*) of the ground that continued for a month. The station KMM tiltmeter, about 12 km downrift of the station ESR and PHH tiltmeters, also recorded a tilt change in early November. These tilt changes suggest a downrift movement of magma stored within the rift zone. Probably, no more magma was added from the summit storage system to the rift-zone storage system, because the summit tiltmeters continued to record gradual inflation during October (fig. 6.7*B*). An earthquake swarm in the upper east rift zone on December 9, 1982, had no effect on the tiltmeters in that area. Two weeks later, however, the station ESR and PHH tiltmeters began to record a southwesterly tilt of the ground, but no increase in earthquake activity accompanied these tilt changes. The tilt changes indicated that magma was again moving in the rift-zone storage system.

INTRUSION AND ERUPTION OF JANUARY 1983

SEISMIC DATA

A series of shallow earthquakes beginning at 0030 H.s.t. January 2, 1983, in the vicinity of Makaopuhi Crater marked the start of seismic activity associated with the dike emplacement that led to the onset of eruptive activity 24 hours later (see chap. 7). As the dike was emplaced, hundreds of shallow earthquakes were generated by fracturing of the crustal rocks that formed cracks which accommodated the added mass.

An outline of the dike is inferred from the distribution of earthquakes that accompanied the dike emplacement. An epicentral plot of earthquake activity during the period of dike emplacement is shown in figure 6.8. In longitudinal section *A-A'* (fig. 6.9), a cluster of hypocenters is plotted in the 2- to 4-km depth range and extends from the area between Mauna Ulu and Makaopuhi to 2 km beyond Kalalua, a distance of slightly more than 15 km. In cross section *B-B'* (fig. 6.10), hypocenters are concentrated in a 2-km-wide band slightly offset to the south of the trace of the eruptive fissures (arrow, fig. 6.10). A diffuse group

of earthquakes was also located in the south flank region, where 0.15 m of contraction was measured across an electronic-distance-measurement (EDM) line after the dike was emplaced. The earthquakes beneath the rift zone outline a zone 4 km deep and 15 km long (figs. 6.9, 6.10) that was affected by the dike emplacement.

Both seismic and geodetic data indicate that the 15-km length of the dike was emplaced in two phases. The initial dike emplacement on January 2 was from Makaopuhi to Kahaualea, and on January 7 the dike lengthened from Kahaualea to beyond Kalalua. The earthquake-distribution pattern before (fig. 6.11*A*) and after (fig. 6.11*B*) January 7 outlines the shift in eruptive activity with extension of the dike. Before January 7, no earthquakes were located in the vicinity of Kalalua, whereas after January 7, nearly all the located rift-zone earthquakes were in that area. The number of located shallow earthquakes diminished significantly after the dike was emplaced.

Because emplacement of the dike and the distribution of earthquake epicenters are closely related, the rate of dike propagation can be inferred from the rate of migration of the earthquakes. A distance-time plot of the earthquakes on January 2 suggests an average rate of nearly 0.7 km/h (fig. 6.12) for the initial dike emplacement, in agreement with the rate determined from tiltmeter data (see subsection below entitled "Electronic-Tiltmeter Data").

ELECTRONIC-DISTANCE-MEASUREMENT DATA

Several linear arrays of permanently mounted reflectors were located across the east rift zone and along the south flank to quickly monitor horizontal distance changes with an EDM instrument. An array in the Kamoamoa area was destroyed by the eruption on January 3 before it could be monitored, but the array from Kalalua (fig. 6.3) was left intact, and the lines were measured 7 times in January. The south-flank monitoring line from Q BATH to FORD (fig. 6.2) was remeasured eight times during January, and a new monitoring array across the eruptive fissures (fig. 6.3) was established in late January.

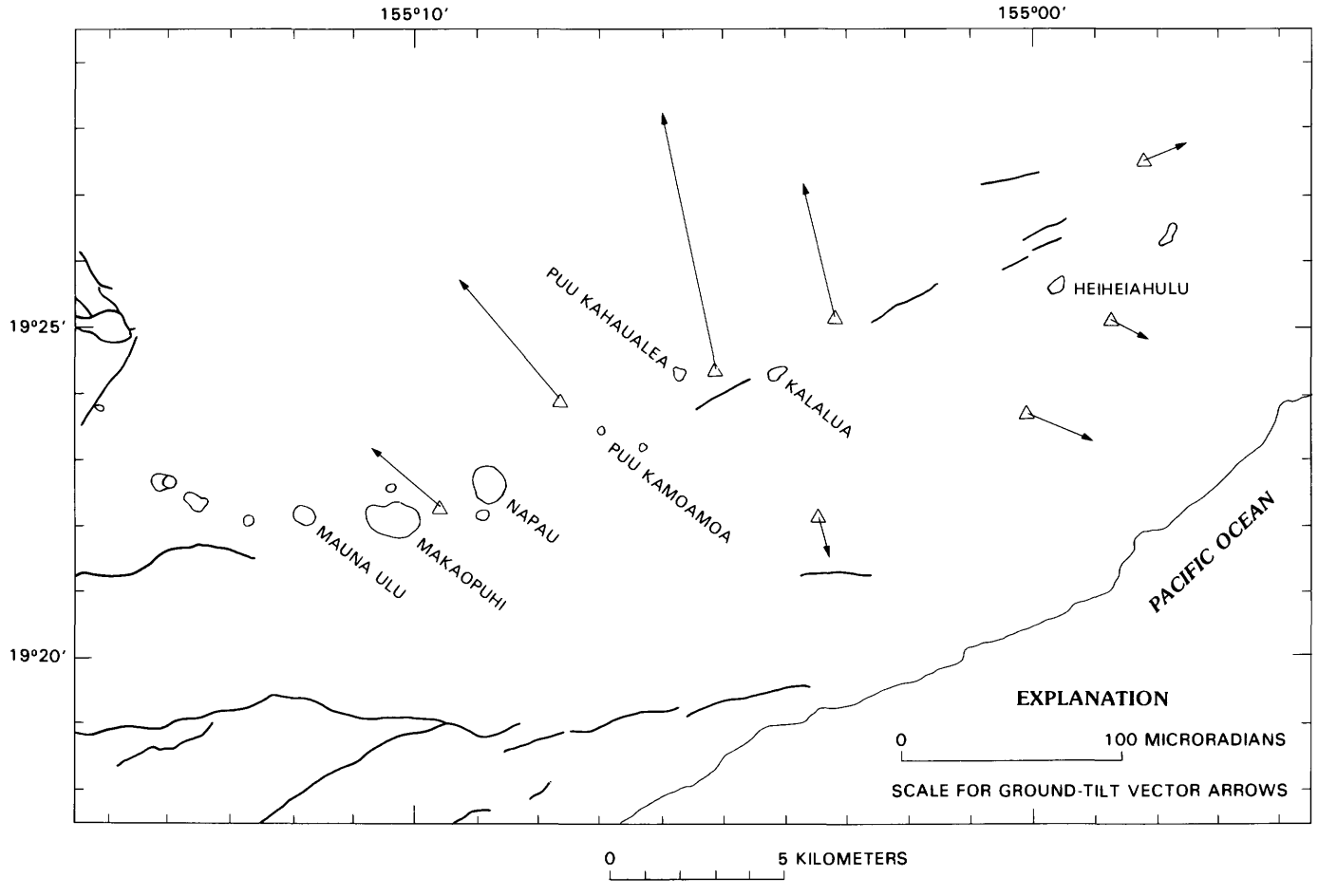

FIGURE 6.6.—Middle east rift zone, showing ground-tilt vectors (arrows) indicating rift-zone inflation during the period January 1978-March 1981. Vectors point in downslope direction. Triangles, spirit-level-tilt stations; solid lines, fault traces. Major craters are labeled.

The EDM data (fig. 6.13) indicate that the initial dike emplacement on January 2 did not reach Kalalua, because there were no changes in the horizontal distances of the lines across the rift zone from late 1982 to January 5, 1983. Changes in the length of these lines between January 5 and 7 indicated that the dike extended into that area during the 2-day interval between measurements. Although no eruptive fissures in the area positively demonstrated the presence of a dike, a fresh set of parallel cracks that extended beyond Kalalua were found on strike with the eruptive fissures uprift (see pl. 1). The cracks were situated between reflectors K-1 and K-2, where line-length changes totaled 2.6 m. The displacement measured between these two reflectors indicates a minimum width of 2.6 m for the dike. As the dike intruded the Kalalua area of the rift zone, the EDM monitoring line in the south flank of Kilauea shortened by 0.15 m (fig. 6.13). After January 11, no significant changes in line length were measured along the Kalalua array, although minor extension occurred on the south-flank monitoring array.

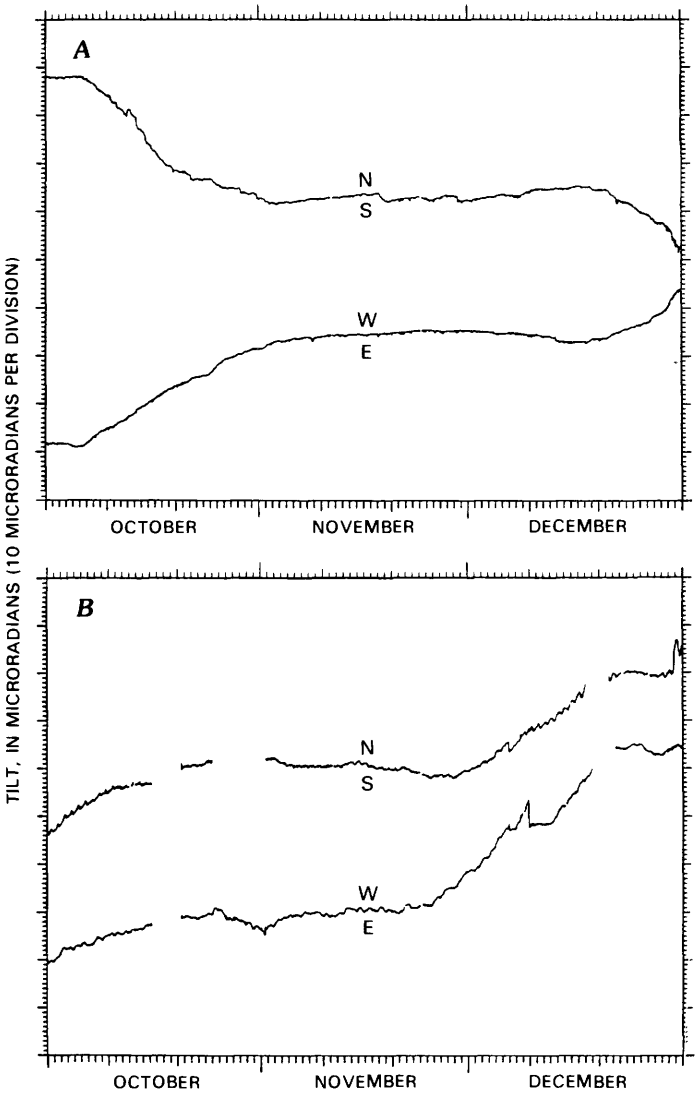

FIGURE 6.7.—Tiltmeter records from October 1 to December 31, 1982. *A*, Puu Huluhulu (PHH) station. Cardinal points indicate downslope direction of tilt. Southwestward tilt throughout October and late December suggests movement of magma in the station area. *B*, Sandhill (SDH) station, located in summit region. Northwestward tilt in early October and throughout December denotes inflation of summit region. Small, sharp eastward tilt on December 9 was due to minor collapse of summit region in response to a minor intrusion into upper east rift zone. Breaks in record are periods of no data.

Shortly after the start of the eruption, a linear array of three EDM lines from the Kahaualea area was established across the eruptive vents, with two reflector stations bracketing the fissures (fig. 6.3). Changes along these lines were small but consistently displayed lengthening to indicate that the rift was continuing to widen in the area of the eruptive fissures (fig. 6.14). Lava flows destroyed this array, and when a new array was established in April, the line-length changes had diminished in amplitude but continued to show minor extension.

ELECTRONIC-TILTMETER DATA

ONSET OF TILT CHANGES

Within 10 to 20 minutes after the start of earthquake activity at 0030 H.s.t. January 2, the station PHH and ESR tiltmeters began to record an abrupt tilt change in response to magma movement in the upper east rift zone (fig. 6.15). As the dike propagated downrift, the large surface-displacement field created by the growing dike also moved downrift in advance of the dike tip. This deformation was recorded by the station KMM tiltmeter at 0430 H.s.t., and by the station KLU tiltmeter at 0630 H.s.t. The onset of tilt changes in the rift zone was fairly sharp at the four tiltmeter stations along the rift, whereas the summit subsidence began gradually about 90 minutes after the onset of earthquake activity. The reason for the small tilt change at station KMM coincident with the changes at stations PHH and ESR is unknown.

SUMMIT-REGION/RIFT-ZONE RELATION

A comparison of the tilt changes that occurred at the summit and at the eruption site (fig. 6.16) demonstrates the connection between the summit magma chamber and the feeder dike through a conduit system. The station UWE west-east component of tilt is sensitive to vertical movement of the summit region in response to addition or withdrawal of magma from the shallow summit reservoir. The station KMM north-south tilt component, which was nearly perpendicular to the strike of the eruptive fissure, is sensitive to vertical movement of the dike.

Subsidence of the summit region started gradually at about 0200 H.s.t. on January 2; the tilt rate increased slightly at 1100 H.s.t. There was no significant change in tilt rate when eruptive activity began (line A, fig. 6.16); however, when the activity stopped (line B, fig. 6.16), the tilt direction immediately reversed. The west-side-down tilt at station UWE (to right of line B, fig. 6.16) indicated that the summit was reinflating, and inflation continued until 0300 H.s.t. January 5, when subsidence was reinitiated. The eruption resumed (line C, fig. 6.16) nearly 9 hours after the summit started to collapse, and again there was no significant change in the slope of the summit tilt with the onset of eruptive activity. The shape of the station UWE deflationary-tilt curve for January 5 and 6 resembles a typical subsidence curve for the Kilauea summit, in which tilt rate decreases over time. However, this gradually decreasing tilt-rate trend changed when the rate of subsidence increased at 2200 H.s.t. January 6 (line D, fig. 6.16). The increasing rate of subsidence coincided with renewed downrift lateral propagation of the dike and followed an abrupt tilt change at station KLU (line D, fig. 6.17).

While the summit was gradually subsiding on January 2, the ground at Puu Kamoamoa was tilting southward (fig. 6.16). The initial south-side-down tilt at station KMM continued for 13 hours until 1730 H.s.t., before the tilt direction reversed to north side down. This north-side-down tilt persisted for several hours, except for a brief period of no tilt change between 2100 and 2300 H.s.t. shortly before eruptive activity started 4 km uprift of station KMM, when northward tilt quickly resumed at an even higher rate. The rate of tilt slowed significantly, however, when the eruptive fissure moved downrift and closer to Puu Kamoamoa; and the tilt direction reversed from north to south side down immediately before the eruption stopped. This sharp southward tilt continued for

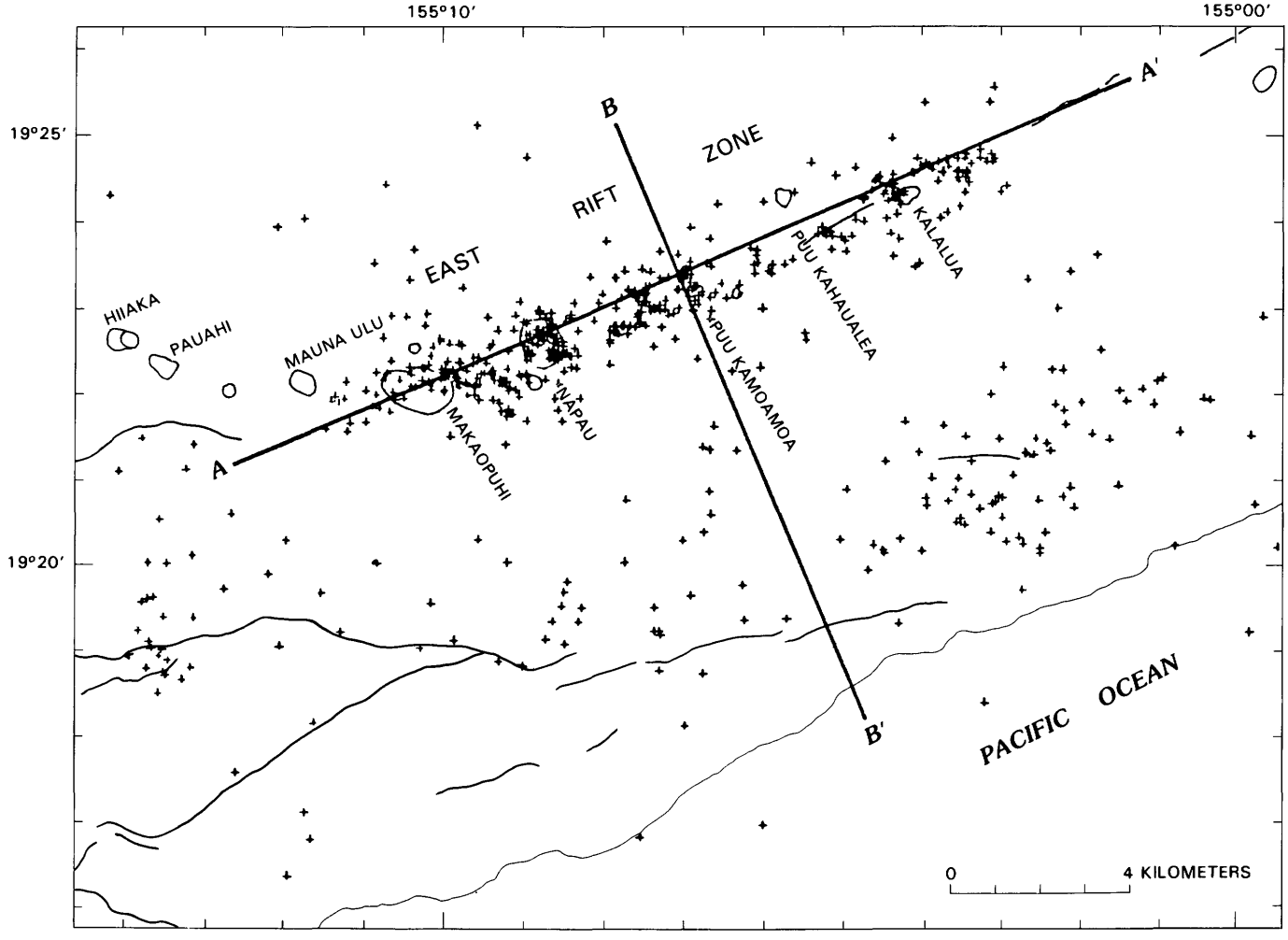

FIGURE 6.8.—East rift zone, showing epicenters of earthquakes (crosses) occurring between 0000 H.s.t. January 2 and 0000 H.s.t. January 9. *A-A′* and *B-B′* are sections used in figures 6.9 and 6.10, respectively. Fault traces (solid lines) and craters (labeled) are shown for location reference.

a few hours until 1400 H.s.t.; then, there was no significant tilt change until 0600 H.s.t. January 5. Three hours after the summit started to subside on January 5, rapid

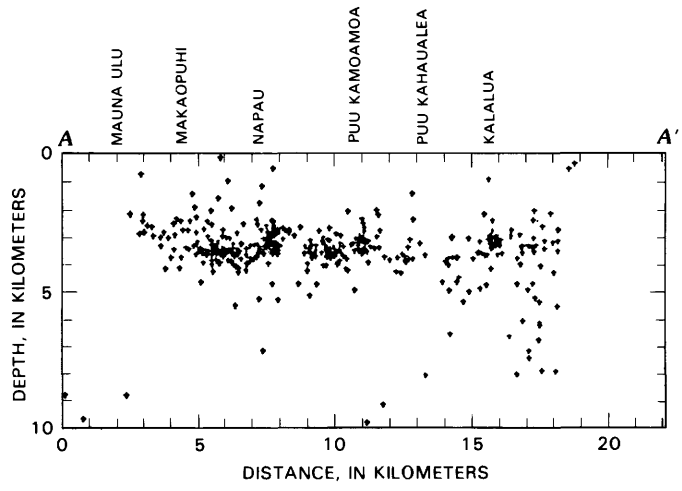

FIGURE 6.9.—Longitudinal section *A-A'* (see fig. 6.8 for location) of earthquake hypocenters located within 3 km of plane of eruptive dike. Hypocenter cluster between 2- and 4-km depth extends for nearly 15 km along rift. A group of deeper earthquakes located east of Kalalua may indicate distal end and vertical extent of dike.

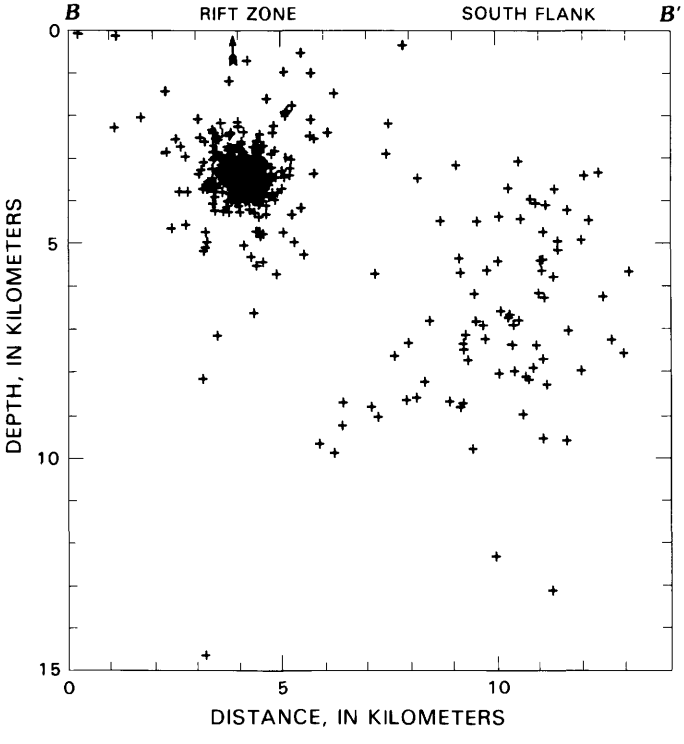

FIGURE 6.10.—Transverse section *B-B'* (see fig. 6.8 for location) of earthquake hypocenters located in rift zone and south flank. Earthquakes outline a core beneath and slightly to south of eruptive fissures (arrow). Deeper south-flank earthquakes are probably due to increased compression caused by intrusion of dike into rift zone.

southward tilt was again recorded at station KMM. The tilt direction reversed to north side down shortly before the eruption resumed downrift of Puu Kamoamoa (line C, fig. 6.16). The small, short-period aberrations in the station KMM tiltmeter record after 1200 H.s.t. January 5 corresponded to the intermittency of the eruptive activity and possibly reflected pressure changes in the dike. Except for diurnal tilt changes, no further significant tilt changes occurred at station KMM until early April 1983.

KALALUA TILT CHANGES

After the first tilt change at Kalalua at 0630 H.s.t. January 2, no significant ground movement occurred at that station for nearly 3 days. The start and stop (lines A and B, fig. 6.17) of the eruption only minimally affected the tiltmeter at station KLU, but shortly before the eruption resumed 3 km uprift of the station on January 5 (line C, fig. 6.17), the ground started slowly to tilt northeastward. This movement continued until 1800 H.s.t. January 6, when the tilt rate suddenly accelerated, and the tilt direction shifted to the northwest. This large and rapid tilt change persisted into the night and exceeded the dynamic range of the instrument. The next morning, we found that the station was situated in the midst of a set of parallel tensional cracks that had formed during the night. Two remeasurements of a segmented EDM line that crosses the rift zone from Kalalua (fig. 6.3) showed that 2 m of extension occurred between January 5 and January 7, and another 0.6 m between January 7 and January 11 (fig. 6.13). At 1030 H.s.t. January 7, a new fissure 1 km uprift of station KLU started to erupt vigorously (see chap. 1).

ANALYSIS AND DISCUSSION

PUU KAMOAMOA TILT CHANGES

As shown by our model (fig. 6.5*B*), the station KMM north-south tilt component, which was nearly perpendicular to the strike of the January eruptive fissure, is sensitive to the vertical movement of the dike top. We interpret the initial south-side-down tilt direction on January 2 at the station KMM, located 600 m north of the eruptive fissure, to be caused by elastic drawdown over an ascending dike. Pollard and others (1983) found that a bimodal ridge-trough-ridge form, with the trough located over the axial plane of the dike, to be the typical cross-sectional profile of the vertical-surface-displacement field over a steeply dipping ascending dike. This form causes tilt toward the dike in the area between the crest and the trough, and tilt away from the dike in the area beyond the crest. As the top of the dike approaches the

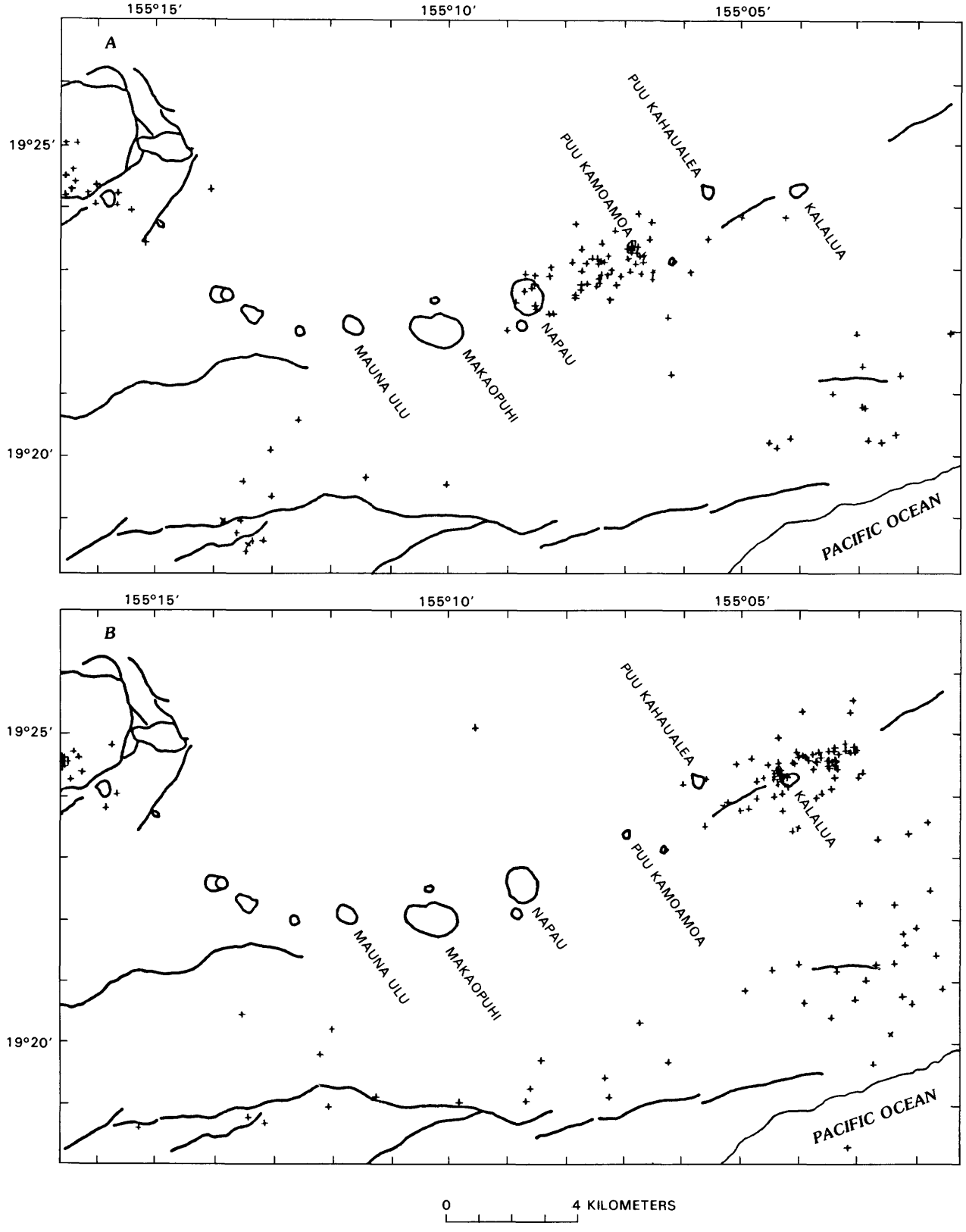

FIGURE 6.11.—East rift zone, showing epicenters of earthquakes. Fault traces, solid lines; major craters labeled. *A*, Between 0000 H.s.t. January 5 and 0000 H.s.t. January 7. Note scarcity of earthquakes in vicinity of Kalalua. *B*, Between 0000 H.s.t. January 7 and 0000 H.s.t. January 9. Note shift in earthquake activity to Kalalua area.

ground surface, the ridge crests move toward the dike axis, and this movement causes the tilt direction to reverse in the areas passed by the inward-moving crests. The ratio of the depth of the dike top to the distance between the ridge crest and the dike axis decreases from 1.0 to 0.5 as the dike top nears the surface. Thus, the reversal in tilt direction from south side down (toward the dike axis) to north side down at station KMM at 1730 H.s.t. January 2 indicated that the dike top was between 300 and 600 m of the surface.

The reversal of station KMM tilt direction from north to south side down just before the eruption first stopped (line B, fig. 6.16) may have been due to deflation of the area caused by depletion of the available magma supply. This depletion of the rift-zone magma volume resulted from either a rate of effusion higher than the rate of resupply from the summit reservoir or from blockage of the magma-conduit system between the summit region and the rift-zone eruptive area. The immediate reinflation of the summit region shown by the station UWE tiltmeter record (fig. 6.16) suggests that the conduit system between the summit region and the rift zone was temporarily blocked.

On January 5, a rapid southward tilt recorded at station KMM again indicated upward movement of the dike top. As the magma approached the surface and the eruption resumed (C, fig. 6.16), the tilt direction reversed to north side down.

PUU KAMOAMOA TILT CHANGES AND MODEL FOR DIKE PROPAGATION

To derive a propagating dike model that would recreate the tilt changes recorded at station KMM, several parameters were held fixed, and others were allowed to vary. The site near Makaopuhi where the earthquake swarm began (7 km uprift of station KMM) was fixed as the starting point of dike propagation. The starting time was allowed to vary, but only earlier and not later than 0030 H.s.t. January 2. The width of the dike was allowed to be at least 2.6 m, the amount of extension measured from Kalalua on EDM lines across the newly formed cracks on January 7 and 9. From seismic data, the length of the dike was set at 15 km, and the depth was varied between 2 and 4 km.

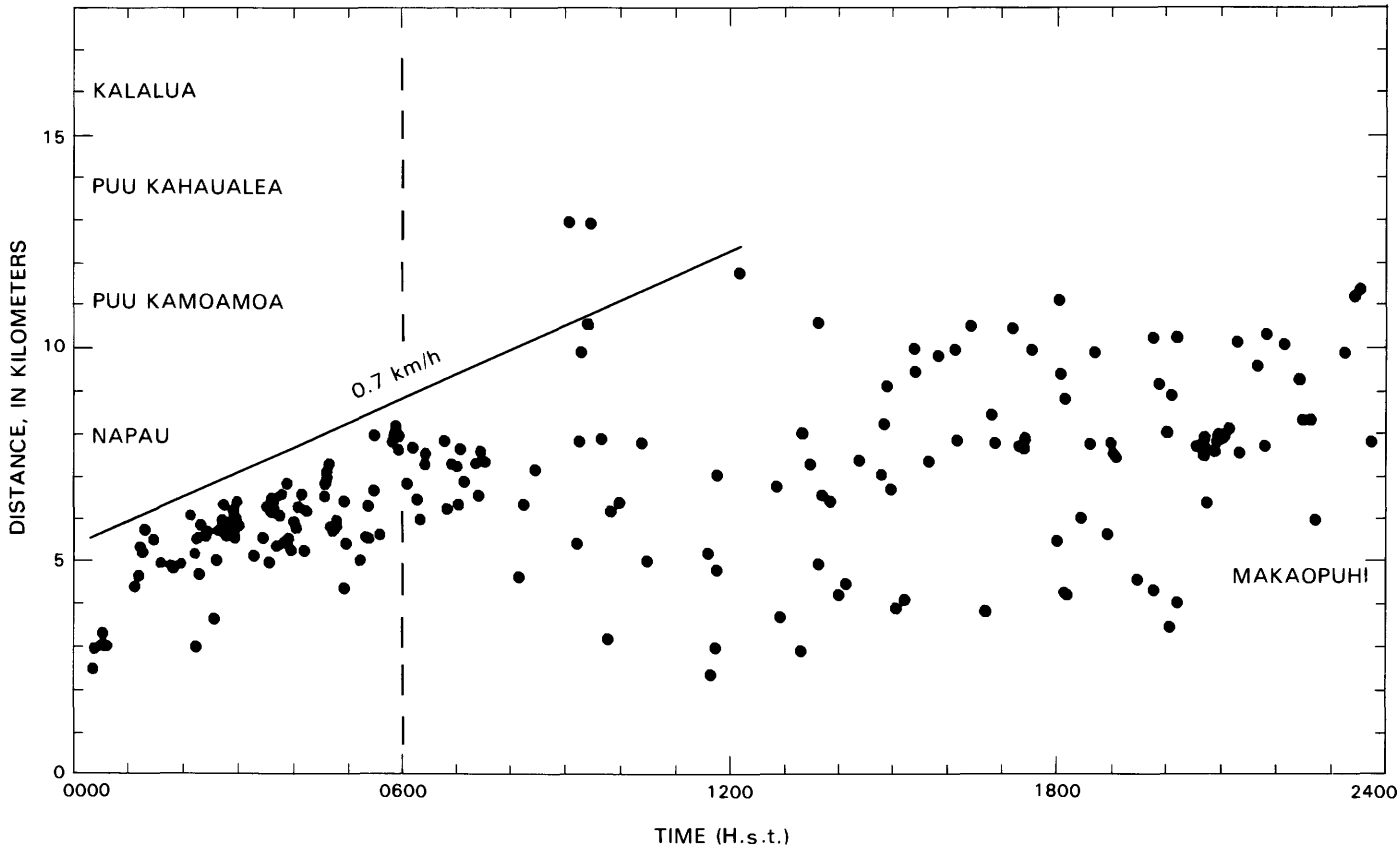

FIGURE 6.12.—Earthquake-epicenter migration on January 2, 1983. Note dispersal of leading edge of earthquake pattern after 0600 H.s.t. (dashed line) in area just beyond Napau Crater. Solid line indicates average rate of downrift migration of earthquakes.

The tilt changes recorded on both components of the station KMM record (fig. 6.18) fit the theoretical displacement curves that we derived from Maruyama (1964) for a model dike 3.50 m wide, propagating both vertically and horizontally at a constant rate. The origin of the model is 7 km uprift of station KMM in the area of Makaopuhi Crater, and the dike top starts from a depth of 2.5 km. Although earthquakes began at 0030 H.s.t. January 2, our model suggests that dike emplacement started at 2100 H.s.t. January 1. This discrepancy may be due to the limitations of our model because the propagation rates are held constant, or it may be similar to the situation on January 6 when the dike started to grow hours before seismic activity increased near Kalalua. The varying rate of upward dike growth is evident in the perpendicular (north-south) tilt component monitoring the vertical ascent of the dike. Several breaks in slope of the recorded tilt curve cause the data to diverge from the constant theoretical propagation rate.

The reversal in tilt direction of the east-west component at 1030 H.s.t. January 2 (fig. 6.18) marks the time at which the distal end of the growing dike passed station KMM. If the start of earthquake activity at 0030 H.s.t. is taken as the probable start of dike emplacement, a 0.7-km/h average rate of dike progagation is calculated from the east-west tilt reversal at station KMM, which is located approximately 7 km from the seismically determined point of origin (X, fig. 6.2). The downrift-migration rate of the earthquake swarm (fig. 6.12) also is nearly 0.7 km/h. In contrast, our model produces an average horizontal propagation rate of 0.55 km/h, because the origin time is taken to be 2100 H.s.t. January 1.

As mentioned earlier, the reversal in tilt direction of the north-south component at station KMM indicates that the top of the dike was between 300 and 600 m below the ground surface at 1730 H.s.t. January 2. The dike did not breach the surface at Puu Kamoamoa until about 0230 H.s.t. January 3 (see chap. 1), a timespan of 9 hours to rise a vertical distance of 300 to 600 m, or a rate of ascent of 33 to 66 m/h. This rate of ascent for the dike top is nearly consistent with our model, which gives an average rate of 70 m/h of vertical propagation. However, the model does not perfectly fit the data, because the recorded tilt rate varied and the ground probably did not behave elastically as surface tension cracks developed. The constancy of the station KMM north-south tilt component for 2 hours at the end of January 2 suggests that the dike stopped ascending. It is not unusual for the top of a dike to approach the ground surface and stop without producing an eruption (Pollard and others, 1983). Another estimate of the average rate of upward propagation for the dike top can be calculated from seismic data by the 24-hour timespan between the start of earthquake activity and the eruption. The earthquake data (fig. 6.10) suggest an origin between 2- and 4-km depth, which yields an average upward-propagation rate of about 125 m/h.

KALALUA TILT CHANGES

The meaning of the tilt changes at station KLU on January 6 (fig. 6.17) cannot be interpreted fully because the tiltmeter was positioned over the axis of the dike, although the reversal of tilt direction from east to west side down could mark the passing of the dike tip or simply be due to inelastic brittle failure of the rock as tension cracks formed. However, a review of the earthquake activity from 0000 H.s.t. January 5 to 0000 H.s.t. January 9 (figs. 6.11*A*, 6.11*B*) indicates that brittle failure in the Kalalua area occurred hours after the rapid tilt change began. Thus, the dike tip may have passed station KLU at about 1800 H.s.t. January 6, when the tilt of the east-west component parallel to the strike of the fissures

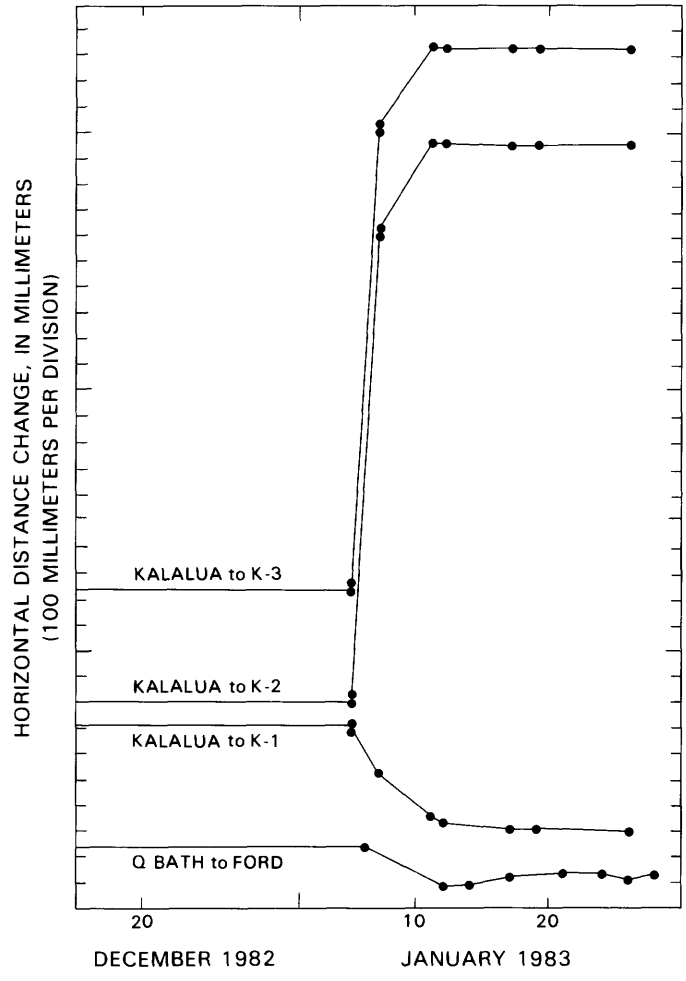

FIGURE 6.13.—Changes in horizontal distances across axis of rift zone (Kalalua to K-1, K-2, and K-3) and in south flank (Q BATH to FORD, fig. 6.2). Positive changes indicate lengthening, and negative changes shortening. Dike intruded between station K-1 and K-2 (fig. 6.3).

reversed direction. The time delay between the start of seismic activity in the Kalalua area and repropagation of the dike can explain the 3-hour difference between the starting time of our model and the start of earthquakes on January 2.

RIFT-ZONE MAGMA STORAGE

The initial change in tilt on January 2 at station KLU (fig. 6.15), which is located 5.4 km downrift of the Puu Kamoamoa tiltmeter site, occurred 2 hours after a tilt change was recorded at station KMM (fig. 6.15). This initial tilt change at station KLU is not caused by the surface-displacement field produced by the dike tip. The surface-displacement field moved downrift at the same rate (0.55–0.7 km/h) as the dike tip, but the observed rate of horizontal movement between stations KMM and KLU was 2.7 km/h. One possible explanation for the apparent high rate of horizontal movement is that shortly before 0630 H.s.t., when the dike tip was slightly beyond Napau Crater, it intersected a body of magma stored in the rift zone and caused a pressure pulse to travel through the magma body and affect the tiltmeter at station KLU. The seismic data lend support to this assumption. At about 0600 H.s.t. January 2, downrift migration of the earthquake swarm (fig. 6.12) terminated in an area just beyond Napau Crater. The preeruption surface-deformation data also suggest accumulation of magma in the rift zone, and petrologic evidence calls for magma-storage bodies in the rift zone for eruption of lava of differentiated composition (see chap. 3).

SUMMARY AND CONCLUSIONS

Electronic-tiltmeter measurements, previously utilized only in the summit region of Kilauea to monitor the inflationary state of the volcano, provided invaluable information about the surface deformation associated with emplacement of a dike into the east rift zone at the start of the Puu Oo eruption. The timing of the onset of initial tilt changes on January 2 indicated that magma first started to move within the rift zone and that the summit later responded at a gradual rate while the dike propagated downrift. When the dike again began to move downrift toward Kalalua on January 6, tilt changes were recorded first at Kalalua, then at the summit 4 hours later. This is the first time that magmatic activity has been demonstrated to occur independently on the middle east rift zone, possibly analogous to lower-east-rift activity in 1955 and 1960. In 1960, during the Kapoho eruption, nearly 50 km away from the summit of Kilauea, 4 days elapsed between onset of the eruption and the start of

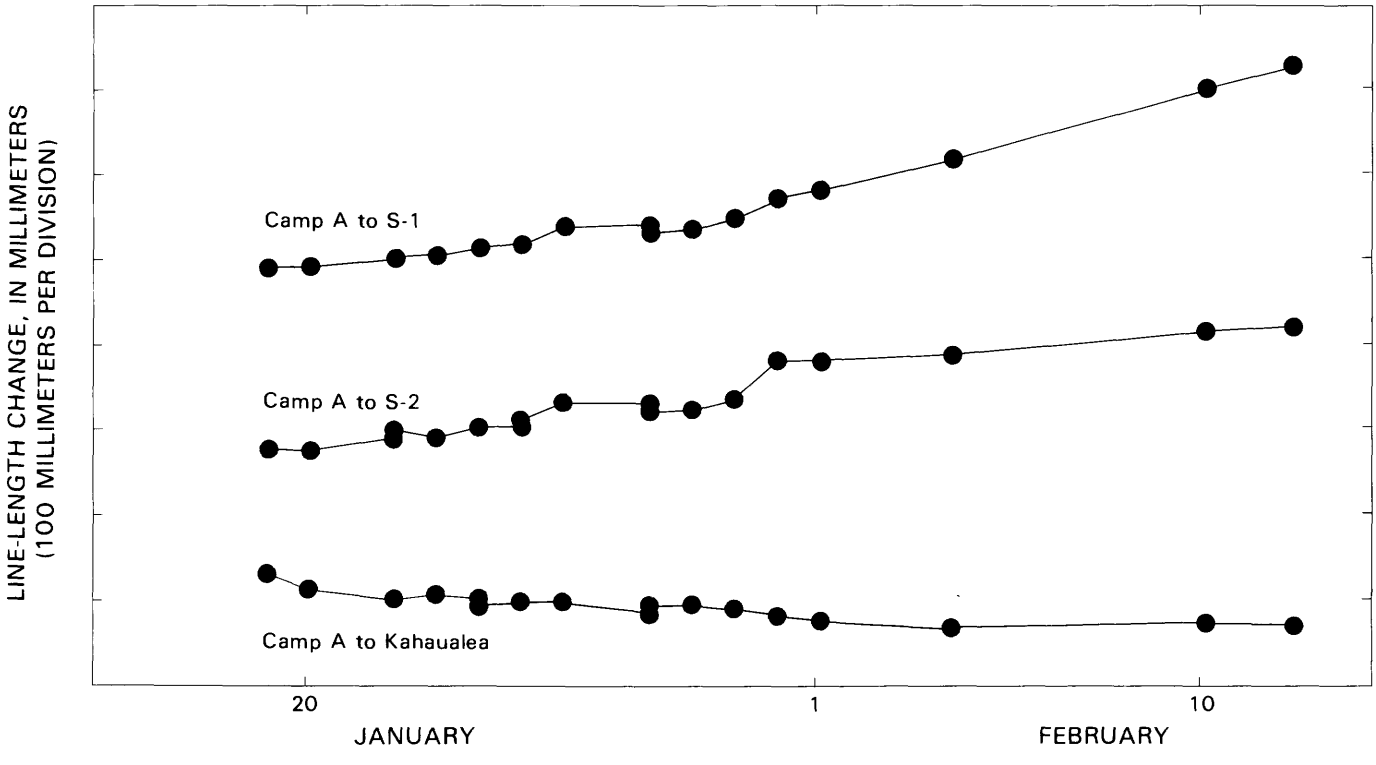

FIGURE 6.14.—Line-length changes during January and February 1983, across eruptive fissures situated between linear-array EDM stations Camp A and S-1 (fig. 6.3).

summit subsidence (Eaton and Murata, 1960). However, the summit started to subside within 2 hours of the 1983 dike emplacement, situated about 15 km away from the summit. These observations imply that rift-zone magmatic activity can be initiated independently of summit influence, and the response time of the summit primarily depends on the distance from the summit and the degree to which the conduit system between the summit and the site of rift-zone activity is filled with magma. Since 1975, the many east-rift-zone intrusions, the last one only 23 days before the January 3 eruption, probably kept the conduit system between the summit region and the rift-zone eruption site filled with magma and clear of any blockages, so that response of the summit was fairly rapid.

The high rate of horizontal movement for the surface-displacement field between Puu Kamoamoa and Kalalua strongly suggests interaction between the propagating dike and a rift-zone magma-storage body. When station KLU recorded the tilt change, the dike tip was just beyond Napau Crater in the area where the migrating seismic swarm became diffuse. As the dike intersected the magma body, a pressure pulse was probably generated. This pressure pulse was transmitted through the magma body, traveled downrift to the Kalalua area, and caused a significant change in the perpendicular component of the station KLU tiltmeter. The size of this storage body, extending from Napau Crater to at least Kalalua, is considerable but not unrealistic. The preeruption tilt measurements outline an area of inflation from Napau Crater east to Heiheiahulu, a distance of approximately 18 km; and Dzurisin and others (1983) calculated the volume of magma stored in the east rift zone since 1956 to be greater than 1 km^3.

An elastic model was developed to analyze the real-time tiltmeter data. This model provides displacement curves that fit the data but, more importantly, demonstrates the possibility of monitoring the movement of the dike by using tilt-direction reversals. Pollard and others (1983) first proposed the possible use of tilt reversals as a predictive tool, and the results of our study have shown that a well-designed array of tiltmeters parallel and orthogonal

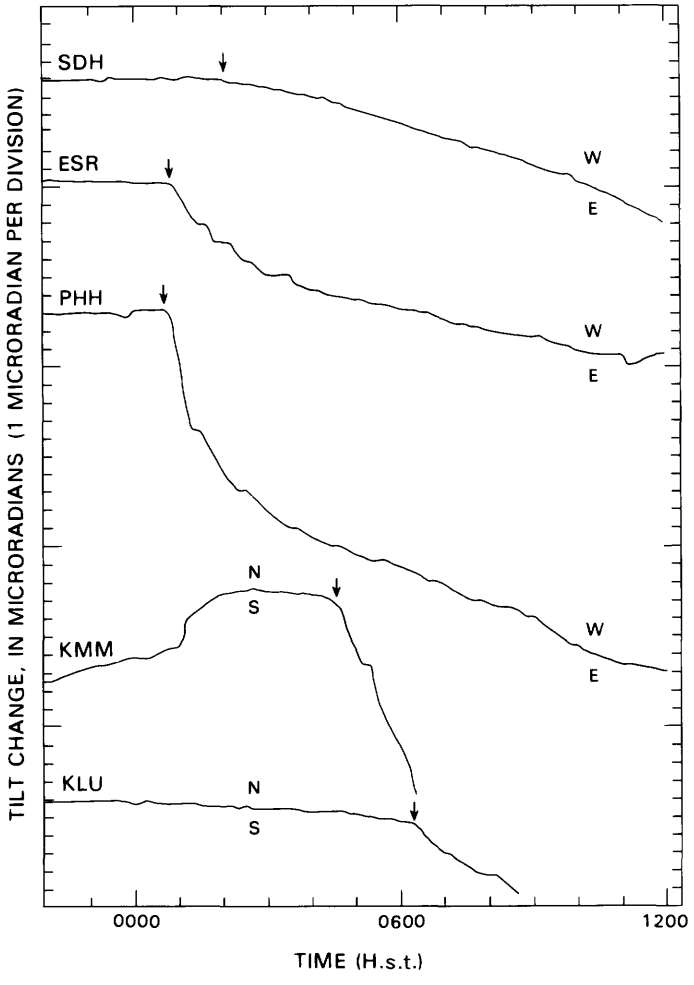

FIGURE 6.15.—Initial tilt changes (arrows) on January 2, 1983, at four east-rift-zone tiltmeter stations (ESR, PHH, KMM, KLU) and one summit station (SDH). Note that displacement starts (arrows) in upper east rift zone (stas. PHH, ESR) before it does at summit (sta. SDH). Cardinal points indicate direction of downslope tilt.

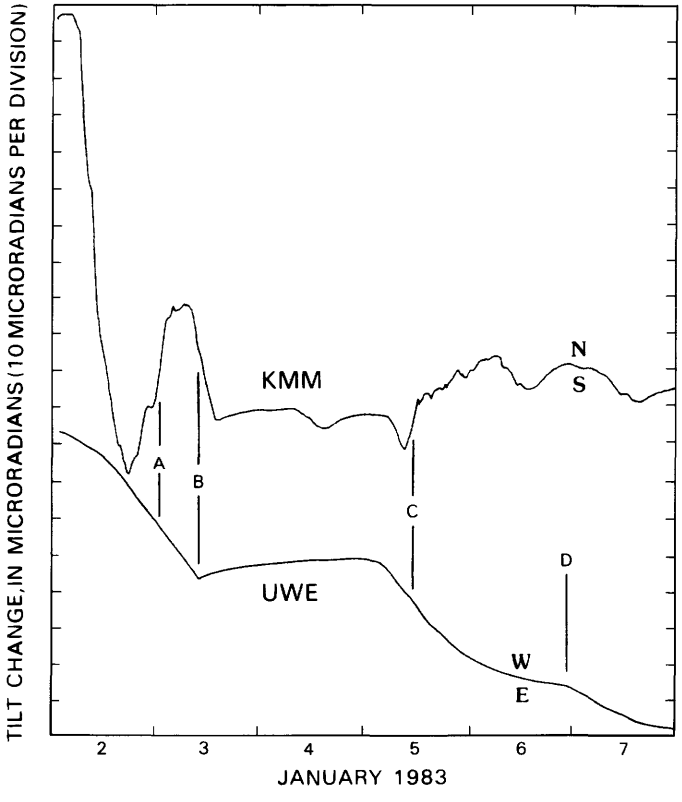

FIGURE 6.16.—Tilt changes in summit region (sta. UWE, lower curve) and at eruption site (sta. KMM, upper curve). A, start of eruption; B, temporary end of eruptive activity; C, resumption of eruption; D, increase in rate of subsidence in summit region. Cardinal points indicate direction of downslope tilt.

to the rift zone can provide the necessary information on movement of a dike. The tilt reversals on the station KMM record marked both passing of the dike tip at the station and ascent of the dike top. The lateral rate of propagation (550–700 m/h) was slower than the 1,700-m/h rate determined by Jackson and others (1975) for the October 1968, east-rift eruption, but our rate agreed with the observed rate (600 m/h) of ground cracking reported by Duffield and others (1982) for the September 1971, southwest-rift eruption. The average rate of ascent for the dike top was determined to be 70 m/h from our model, but the tilt data suggest that this rate varies. As the dike nears the surface, the model becomes ineffective because brittle failure of the ground probably occurs.

The movement of large, planar, vertical magma bodies can be monitored with a large network of tiltmeters arranged parallel and perpendicular to the strike of the rift zone. The tilt data must be collected on a real-time basis, and recognition of tilt-direction reversals is critical.

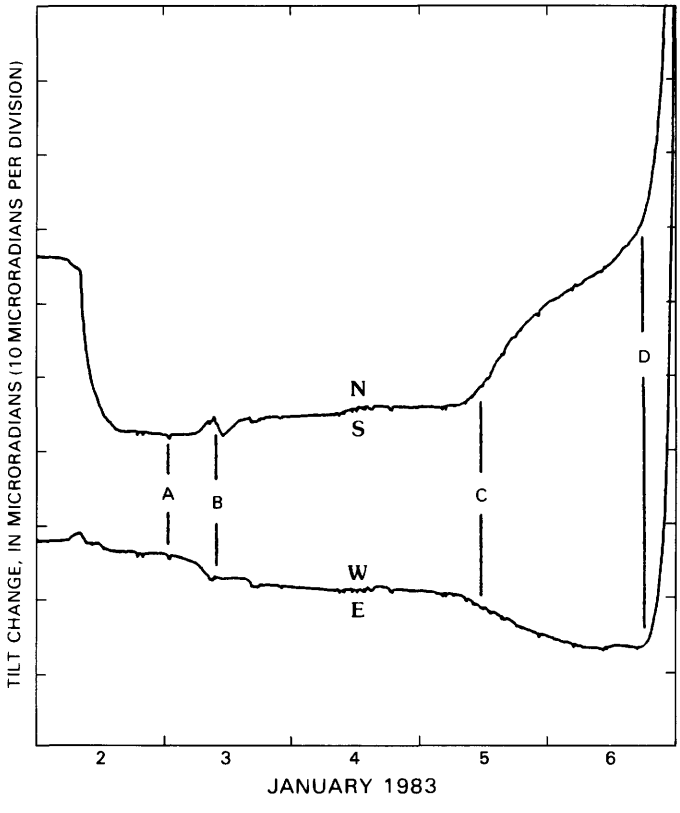

FIGURE 6.17.—Tiltmeter record from Kalalua (KLU) station. A, start of eruption; B, temporary end of eruptive activity; C, resumption of eruption; D, start of a large, rapid tilt change that exceeded dynamic range of instrument. Cardinal points indicate direction of downslope tilt.

REFERENCES CITED

Ando, Masataka, 1979, The Hawaii earthquake of November 29, 1975: Low dip angle faulting due to forceful injection of magma: Journal of Geophysical Research, v. 84, no. B13, p. 7616–7626.

Dieterich, J.H., and Decker, R.W., 1975, Finite element modeling of surface deformation associated with volcanism: Journal of Geophysical Research, v. 80, no. 29, p. 4094–4102.

Duffield, W.A., Christiansen, R.L., Koyanagi, R.Y., and Peterson, D.W., 1982, Storage, migration, and eruption of magma at Kilauea volcano, Hawaii, 1971–1972: Journal of Volcanology and Geothermal Research, v. 13, no. 3–4, p. 273–307.

Dvorak, J.J., Okamura, A.T., and Dieterich, J.H., 1983, Analysis of surface deformation data, Kilauea volcano, Hawaii: October 1966 to September 1970: Journal of Geophysical Research, v. 88, no. B11, p. 9295–9304.

Dzurisin, Daniel, Koyanagi, R.Y., and English, T.T., 1984, Magma supply and storage at Kilauea volcano, Hawaii, 1956–1983: Journal of Volcanology and Geothermal Research, v. 21, p. 177–206.

Eaton, J.P., 1962, Crustal structure and volcanism in Hawaii, *in* Macdonald, G.A., and Kuno, Hisashi, eds., The crust of the Pacific basin: American Geophysical Union Geophysical Monograph 6, p. 13–29.

Eaton, J.P., and Murata, K.J., 1960, How volcanoes grow: Science, v. 132, no. 3432, p. 925–938.

Fiske, R.S., and Kinoshita, W.T., 1969, Inflation of Kilauea volcano prior to its 1967–1968 eruption: Science, v. 165, no. 3891, p. 341–349.

Jackson, D.B., Swanson, D.A., Koyanagi, R.Y., Wright, T.L., 1975, The August and October 1968 east rift eruptions of Kilauea Volcano, Hawaii: U.S. Geological Survey Professional Paper 890, 33 p.

Jaggar, T.A., and Finch, R.H., 1926, Tilting and level changes at Pacific volcanoes: Pan-Pacific Science Congress, 3d, Tokyo, 1926, Proceedings, p. 672–686.

Johnston, M.J.S., 1976, Testing the physical parameters of short baseline tiltmeters intended for earthquake prediction: U.S. Geological Survey Open-File Report 76-556, 11 p.

Maruyama, Takuo, 1964, Statical elastic dislocations in an infinite and semi-infinite medium: University of Tokyo, Earthquake Research Institute Bulletin, v. 42, no. 2, p. 289–368.

Mogi, Kiyoo, 1958, Relations between the eruptions of various volcanoes and the deformations of the ground surfaces around them: University of Tokyo, Earthquake Research Institute Bulletin, v. 36, no. 2, p. 99–134.

Mortensen, C.E., Iwatsubo, E.Y., Johnston, M.J.S., Myren, G.D., Keller, V.G., and Murray, T.L., 1977, U.S.G.S. tiltmeter networks, operation and maintenance: U.S. Geological Survey Open-File Report 77-655, 18 p.

Pollard, D.D., Delaney, P.T., Duffield, W.A., Endo, E.T., and Okamura, A.T., 1983, Surface deformation in volcanic rift zones, *in* Morgan, Paul, and Baker, B.H., eds., Processes of continental rifting: Tectonophysics, v. 94, no. 1–4 (special issue), p. 541–584.

Ryan, M.P., Blevins, J.Y.K., Okamura, A.T., and Koyanagi, R.Y., 1983, Magma reservoir subsidence mechanics: Theoretical summary and application to Kilauea volcano, Hawaii: Journal of Geophysical Research, v. 88, no. B5, p. 4147–4181.

Swanson, D.A., Jackson, D.B., Koyanagi, R.Y., and Wright, T.L., 1976, The February 1969 east rift eruption of Kilauea volcano, Hawaii: U.S. Geological Survey Professional Paper 891, 30 p.

Swanson, D.A., Duffield, W.A., Jackson, D.B., and Peterson, D.W., 1979, Chronological narrative of the 1969–71 Mauna Ulu eruption of Kilauea Volcano, Hawaii: U.S. Geological Survey Professional Paper 1056, 55 p.

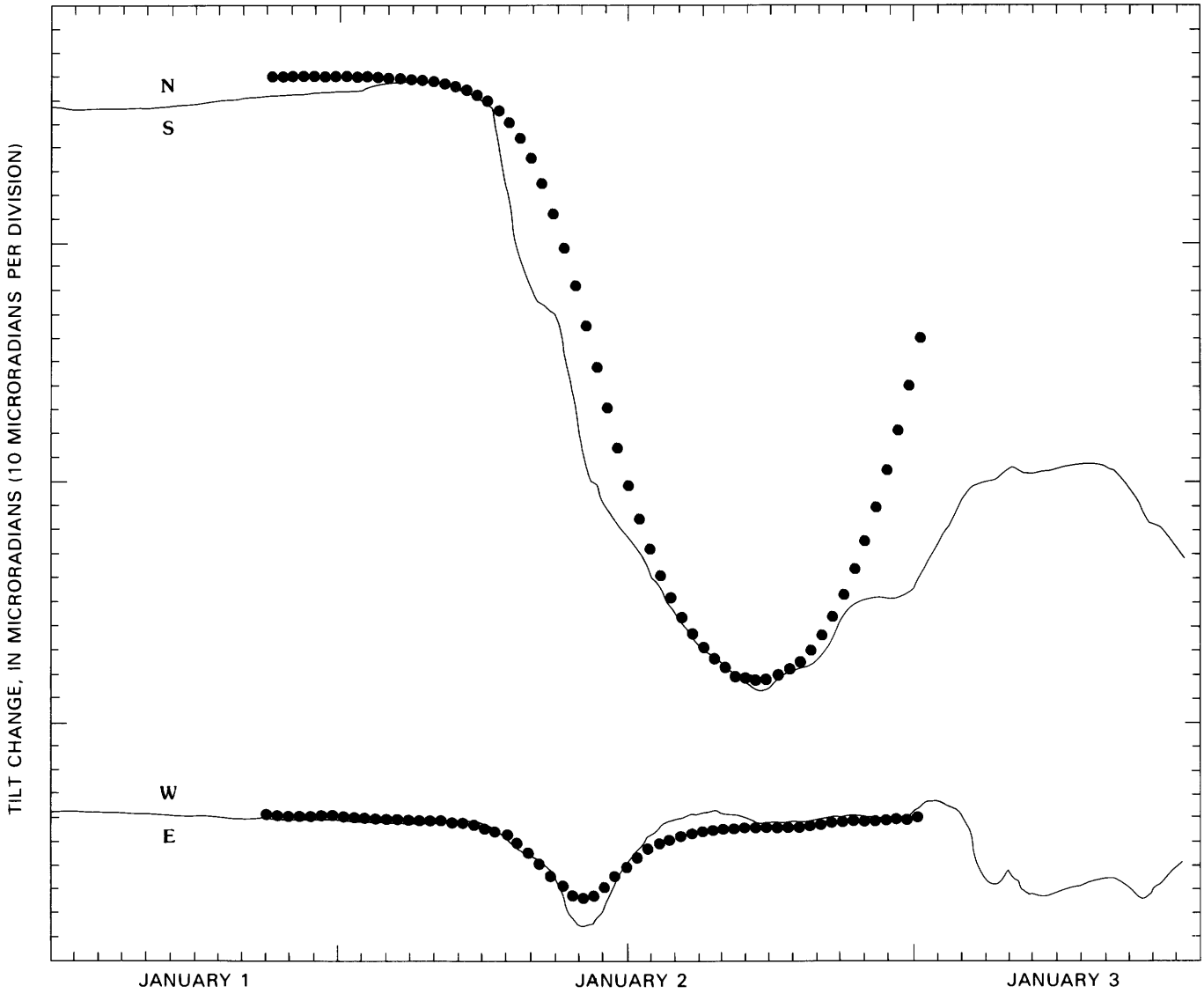

FIGURE 6.18.—Tiltmeter record from Puu Kamoamoa (KMM) station (January 1983), in comparison with theoretical tilt curves (dots) derived from an analytical model of a dike propagating both horizontally and vertically. Dike originates 7 km uprift from station and moves laterally at a rate of 550 m/h and vertically at a rate of 70 m/h. With a width of 3.5 m, dike is allowed to breach surface when eruption starts. Final length of dike is 15 km and height is 2.5 km. Movement of model dike starts at 2100 H.s.t. January 1. Cardinal points indicate direction of downslope tilt.

7. SEISMICITY ASSOCIATED WITH THE ERUPTION

By Robert Y. Koyanagi, Wilfred R. Tanigawa, and Jennifer S. Nakata

CONTENTS

ABSTRACT

Downrift migration of the shallow earthquake swarms that occurred episodically for many months before the east-rift eruption of January 1983 reflected the process of magma movement from the summit to the east-rift storage complex as a preliminary stage to the eruption. Migration of earthquakes at a rate of 0.6 to 0.7 km/h during the final intrusion before the eruption provided a seismic measure for the rate of downrift propagation of magmatic pressure. The spatial distribution of summit, rift-zone, and south-flank earthquakes delineated the magma-transport system.

This progression of earthquakes in time, as well as the distribution of earthquakes in space, supports and quantifies earlier concepts of (1) the pattern of magma movement and (2) the structure of the magma-transport system that feeds eruptions at Kilauea. Initially, magma rising from the mantle builds pressure in a small storage complex within a few kilometers beneath the summit. Dictated by the strength of the retaining caprock and by stress conditions in the east rift zone, the overload of fluid pressure beneath the summit may be tapped along the reservoir and its vertical conduit within a 10-km-deep structural feature, and directed laterally beneath the east rift in a conduit complex no more than a few kilometers wide. Magma transferred in this rift conduit, in turn, rises nearly vertically through a relatively confined system of fissures to feed the eruptive vents.

After the preeruption intrusion or dike emplacement and the early stages of eruption, earthquakes dissipate, and tremor becomes localized. Magma movement is aseismic along certain parts of the vertical conduit beneath the summit storage system and, eventually, along an extensive length of the lateral transport system linking the summit and the middle-east-rift eruption zone. This decrease and localization of the seismicity, reflecting the increasing efficiency of the magma movement, becomes increasingly apparent during later eruptive episodes. The prolonged eruption is characterized by episodic transfer of magma batches from the summit to the east rift, presumably controlled by fluctuations of pressure above and below critical levels in the expanded summit-rift system.

Continuation of the episodic eruption is indicated by the persistence of tremor localized near the eruptive vents. The tremor signal is intense during active lava output and decreases to a low level during repose times, when amplitudes vary mainly according to minor movement of lava and degassing activity from within the vent. The amplitude of harmonic tremor provides a measure of the vigor of the eruption and the rate of magma movement. Attenuation of tremor as a function of distance identifies the eruptive vent in the east rift as the principal source of radiation, and the summit as a secondary source. The east-rift source of tremor is many times more energetic than the summit source at the height of eruptive episodes. The amplitude of east-rift tremor during vigorous eruption is also influenced by noise generated from high fountaining.

INTRODUCTION

This chapter summarizes observations of changing seismicity both preceding and accompanying the 1983 east-rift eruption of Kilauea Volcano. We begin our summary with a review of concepts of the seismicity of Kilauea and an account of the aftermath of the summit eruption in September 1982; seismic and ground-deformation signatures of critical intrusive events are listed in table 7.1.

A long history of instrumental observations in Hawaii relates ground deformation and shallow earthquakes to magma pressure and eruptions (Eaton, 1962; Decker and others, 1983). At Kilauea and Mauna Loa Volcanoes, gradual inflation of the summit, accompanied by an increasing number of earthquakes, commonly leads either to a summit eruption or to rapid deflation of the inflated summit, accompanied by swarms of shallow earthquakes along a rift zone and followed by a flank eruption. Interpreted in terms of magmatic loading, the seismic data, substantiated by the pattern of ground deformation, outline a dynamic magma-transport system (Koyanagi and others, 1974; Ryan and others, 1981). The relative absence of earthquakes beneath deformational centers that are bounded by seismic zones may be interpreted as regions of low rigidity and concentrations of active magma.

The response to magma pressure from the summit reservoir system that generally starts in the south-caldera locality extends episodically into the upper parts of the rift zone bounded by the Koae fault system to the south (Klein and others, 1987). The activity may occasionally extend farther along either rift zone as the earthquake-propagation paths are reoriented northeastward along the east rift zone and southwestward along the southwest rift zone. The Koae faults form the structural boundary that separates the summit region, responding to the movement

TABLE 7.1.—*Minor intrusions of magma at Kilauea, indicated by seismic and tilt data from September to December 1982*

[Magma volumes from A.T. Okamura (oral commun., 1985)]

Time interval	Regions intruded by magma, as inferred from the seismicity pattern	Volume of intruding magma, as estimated from summit tilt (10^6 m^3)
Sept. 26-Nov. 3	Summit to upper east rift zone on September 26; sustained in upper east rift zone from late September to about October 20; migration into middle east rift zone from October 21 to November 3.	Approx 1
Dec. 9-31	Summit to upper east rift zone from December 9 to 10; sustained in upper east rift zone from December 11 to 25; migration into middle east rift zone from December 25 to 31.	Approx 1

of magma in the central reservoir complex, from the lower rift zones, influenced by laterally extensive intrusions and tectonic events in the south flank (Duffield, 1975).

The seaward displacement of Kilauea's south flank, in response to magmatically induced dilation of the east rift, was deduced from deformational and seismic data (Swanson and others, 1976). Structural subdivisions of Kilauea into summit region, east rift zone, and south flank are based on the geologic classifications proposed by Swanson and others (1976) and augmented with spatial- and temporal-distribution patterns of earthquakes. The unstable regions of Kilauea's south flank over the past few decades of high-level volcanic activity are outlined by the distribution of aftershocks from an $M=7.2$ earthquake near the south coast in November 1975. These aftershocks, concentrated at a depth of about 5 to 10 km, extended laterally over a distance of about 40 km in an elongate zone parallel to the rift system and offset to the south. Tectonic models for the seaward displacement of the south flank, derived primarily from aftershocks of this earthquake, were summarized and refined by Crosson and Endo (1982). Fault-plane solutions of earthquakes and the distribution of aftershocks imply block displacement of the south flank seaward and away from the rift along a subhorizontal zone extending southward from a depth of about 10 km. Incremental displacement is apparently induced by accumulating stresses from magma intrusion into the rift zone. The south-flank slip zone lies above the oceanic crust and dips toward the center of the island (Crosson and Endo, 1982). The increasing gravitational load and southward widening with depth to about 10 km beneath the rift axis is compensated by increasing seaward displacement.

Dvorak and others (1986) summarized the pattern of earthquake activity and deformational events associated with magma intrusion from September 1971 to January 1983. Intrusion-related, shallow (less than 5 km deep) earthquakes beneath the east rift were immediately followed by deeper (5–13 km) earthquakes beneath the adjacent part of the south flank. On the basis of their recent data, Dvorak and others pointed out that shallow rift intrusions generate compressive strain and that induced stresses from deeper within the rift zone cause extensional deformation of the south flank.

Volcanic tremor has been instrumentally documented in Hawaii since 1912. Shimozuru and others (1966) summarized various models for the origin of tremor proposed by early investigators, and evaluated their own seismic survey of tremor at Kilauea in 1963. Sources of tremor, influenced by patterns of volcanic activity, were classified according to spectral contents. Their results concurred with earlier findings that harmonic tremor is fundamentally related to magma movement and eruptive activity.

Aki and others (1977) developed a mathematical model for the magma-transport mechanism, based on driving of magma through a system of connecting cracks by excess fluid pressure. They applied their model to the data collected by Shimozuru and others for the brief Kilauea flank eruptions in 1963, and proposed that harmonic tremor is generated by magma movement in a succession of episodic crack extensions and by rapid opening and closing of the narrow channels connecting the fluid-filled cracks. In the

model of Aki and others, the frequency of the seismic waves is a measure of the length of an activated crack, and the signal strength indicates the rate of magma movement through the system of cracks. Using this model, Chouet (1981) obtained a complete representation of ground motion in the near field of the fluid-driven crack. His calculations show the presence of a broad peak in the ground-response spectrum, the characteristics of which depend on source geometry, the bulk modulus of the fluid, medium properties, receiver position, and the component of motion. The basic assumption underlying the models of Aki and others (1977) and Chouet (1981) is that the fluid behaves as a passive element in the source; that is, no acoustic source exists in the fluid. Because of this assumption, the source duration predicted by their theoretical models is rather short, and the spectral peaks displayed by the synthetic seismograms are broader than those generally observed for harmonic tremor at Kilauea.

Ferrick and others (1982) proposed that harmonic tremor is generated by fluctuating fluid flow. In their experiments with hydraulic systems, a disturbance in the steady state of a fluid system was found to cause flow and pressure oscillations in the fluid that would generate oscillating displacement of the conduit wall and elastic waves in the wallrock. A fluid system at rest or gradually changing fluid flow is not expected to produce tremor. Chouet (1985) used this concept to develop a seismic model in which the fluid is included as an active element in the source. In his model, the bandwidth associated with the dominant spectral peak of motion is controlled by the combined losses due to viscous attenuation in the fluid and elastic radiation in the solid. When the fluid viscosity is low, the source acts as a high-Q oscillator, and the ground motion can last a relatively long time. A more refined model of the dynamics of a fluid-driven crack was recently developed by Chouet and Julian (1985), using the same concept of active fluid participation. Our present knowledge of the origin of volcanic tremor can be found in Chouet and others (1987).

This chapter treats two distinct seismic periods in the eruption chronology. The first part describes the early period of widespread earthquake activity of a highly stressed volcano. The second part emphasizes the activity of harmonic tremor during the later stage of the eruption, when the low-stress environment was distinguished by a relative absence of significant earthquakes and by intermittently high eruption rates with strong tremor.

Acknowledgments.—We dedicate this chapter to the entire staff of the Hawaiian Volcano Observatory, each of whom has played a special part in the volcanic research that contributes to definitive interpretation of the seismic data. Bernard Chouet guided us in our treatment of volcanic tremor. To Ed Wolfe we extend special gratitude for his persistent encouragement, patience, and assistance in completing this chapter. Tina Neal and George Ulrich provided useful comments based on their many hours of field observations of the eruption.

LIMITATIONS OF THE DATA

The distribution in space and time of earthquake swarms in the shallow crust describes near-surface magmatic processes, and that of deeper crustal earthquakes outlines the surrounding region stressed by intrusive activity. The dominant frequency and signal strength of harmonic tremor were measured to within the capabilities of the Hawaiian Volcano Observatory (HVO) seismic system, to quantify the source parameters relative to the eruptive process. This compilation of data is intended to serve as a preliminary guide for future detailed analyses of the seismic data associated with the Kilauea volcanic activity in 1983 and 1984.

Shallow harmonic tremor associated with the 1983–84 eruption of the east rift of Kilauea varied in amplitude and frequency within the expected range as a function of time and distance from the source. Complex and erratic, high-frequency tremor accompanied the intrusive swarm of earthquakes during the early period of seismicity and was later replaced by constant, low-frequency tremor that persisted at varying intensity during the prolonged eruption. The principal tremor in the eruptive zone was followed by weaker tremor and long-period events at the summit. In this chapter, strength of tremor is generally described in terms of micrometers or nanometers of ground displacement, derived from amplitudes read on seismograms at the dominant frequency and reduced according to instrumental magnification and response. Station corrections obtained from amplitude differences of local earthquakes and teleseisms were used where station-to-station comparisons of tremor amplitude were made. Although measurements were fairly consistent in relative terms, instrumental noise in the seismograph system and variations in signal attenuation unique to the station site introduced inconsistencies into the reduction of tremor to actual ground motion. In Hawaii, natural ground noise is particularly high in the frequencies about and below 1 Hz, and noise of about a micrometer in amplitude is common. This noise significantly reduces the detection capability of the HVO seismographs for any tremor in the lower frequency range. The 1-s-period seismometer used in the standard HVO system also restricts detection of low-frequency signals.

Because of structural complexities in the active crustal regions of Kilauea and the feature of harmonic tremor, detailed analysis of tremor requires an extensive expansion of our instrumental capability. A network of broadband and three-component seismometer stations spaced

less than several tens of meters apart within a few kilometers of the critical source regions of the east rift and summit would add quality to our data base, and velocity information from an organized seismic-refraction program would enhance our analysis of tremor.

SEISMIC NETWORK AND DATA PROCESSING

The HVO maintains a network of 50 stations covering the Island of Hawaii (fig. 7.1); one station each on the Islands of Maui and Oahu provides additional coverage

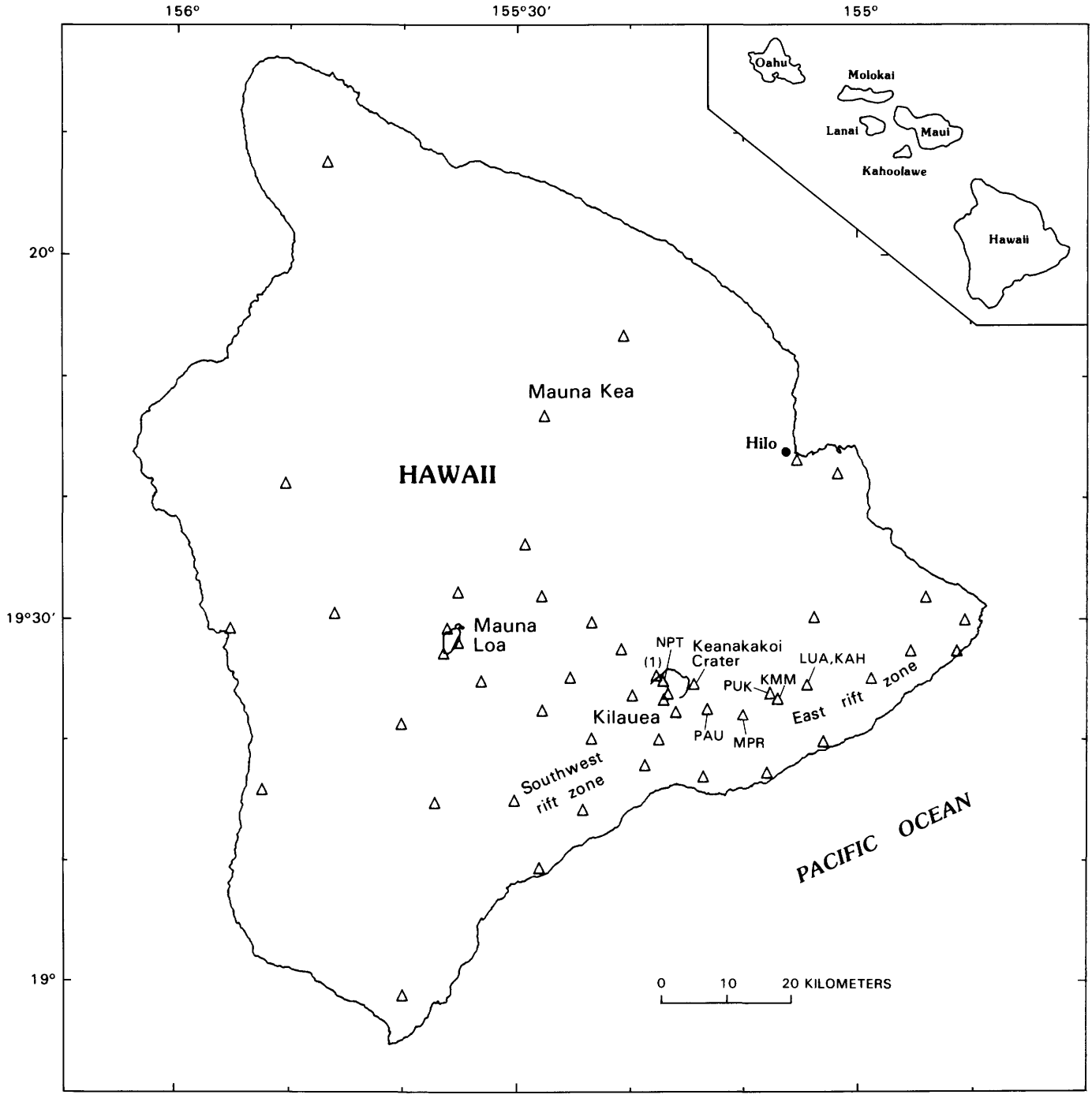

FIGURE 7.1.—Island of Hawaii, showing locations of seismic stations (triangles) operated by HVO (key stations labeled). Summit calderas are outlined for the active volcanoes Kilauea and Mauna Loa. See Tanigawa and others (1983) for details of station parameters.

on the northwestern parts of the Hawaiian Archipelago. Seismometer density is highest in the southeastern parts of the Island of Hawaii, where seismic and volcanic activity is centered. The seismometers are mainly short-period vertical instruments operated at high sensitivity to detect low-amplitude seismicity associated with volcanism (fig. 7.2). Ten of the stations have three-component seismometers, with the horizontal components operated about 12 dB below the gain of the vertical component for measurements of *S*-wave arrival times and amplitudes.

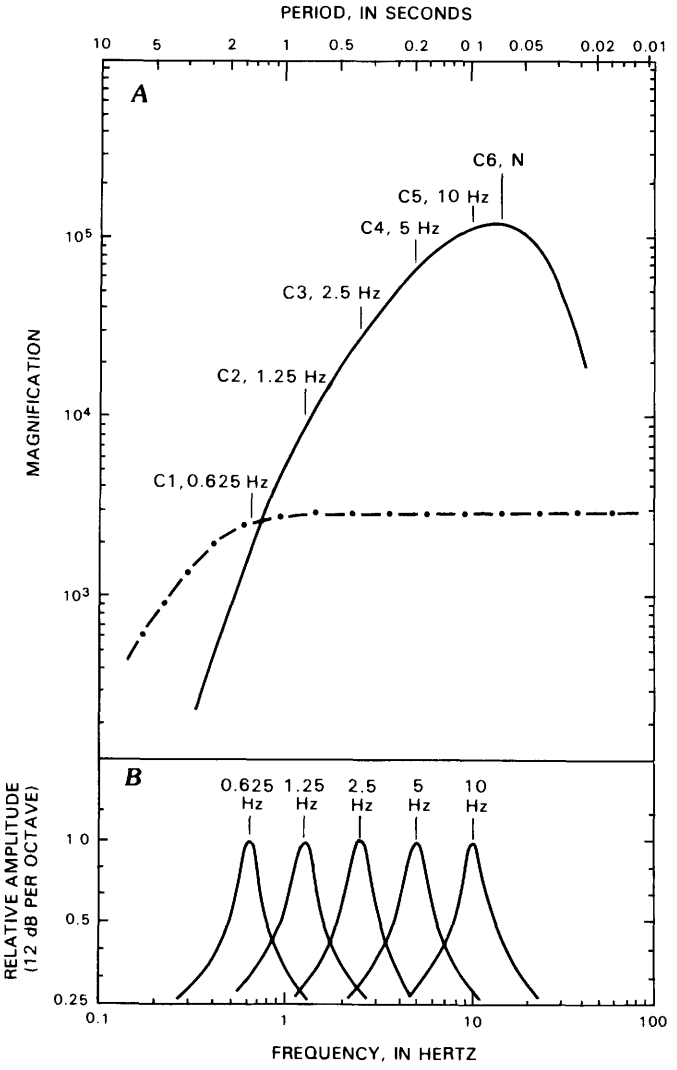

FIGURE 7.2.—System-response curves for short-period seismographs operated in Hawaii during 1983–84 eruption of Kilauea. Filtered signals from a designated station were assigned to channels 1 through 5 (C1–C5), and normal (N), unfiltered signal was recorded on channel 6 (C6). *A*, Curve for Type 1 instruments (solid line) applies to standard HVO high-gain vertical components on a Develocorder-based FM system, and curve for modified Wood-Anderson instruments (dot-dashed) applies to lower sensitivity horizontal seismometers at three-component stations. *B*, Filter system with various center frequencies as shown was designed for a six-channel chart recorder to be used for spectral analysis of specific seismic events.

All signals are telemetered by radio to the HVO and recorded on a 1-in.-magnetic-tape recorder; some signals are also recorded on 24-hour rotating-drum recorders and 16-mm-microfilm-strip recorders. Some stations located at the HVO and Hilo on the Island of Hawaii and on Maui and Oahu are maintained independently, and their signals are recorded optically on 24-hour-cycle rotating drums.

Hundreds of earthquakes with magnitudes ranging upward from a threshold of about 0.1 are detected each day on key stations near active seismic zones in the summit region and rift zones of Kilauea. These tiny events are classified into regional categories on the basis of estimated arrival and amplitude differences, and their hourly and daily numbers are documented as an index of the seismicity (and state) of the volcano. Short- and long-period events are also distinguished for the summit region. The count of shallow events near detection level is especially sensitive to instrumental magnification, background noise, and reading format and thus is highly approximate, in comparison with the more quantitatively analyzed, larger events. About 2 to 5 percent of the detected earthquakes exceed 1.0 in magnitude and are sharply recorded at a dozen or more stations. These larger events are selected for hypocenter and magnitude determination by computer (Klein, 1978), using measured arrival times of P and S waves, trace amplitude, and signal duration. Earthquakes that are timed and located total several thousand per year and form the primary data base for the quantitative definition of earthquakes and volcanic processes in Hawaii. The location, magnitude, and classification data for all processed earthquakes, as well as for other, distant seismic events, and the instrumental information and highlights of volcanic activity are published in annual summaries of the HVO (for example, Nakata and others, 1984).

Seismicity associated with the 1983 Kilauea eruption was classified into short-period (SP) earthquakes, long-period (LP) earthquakes, and harmonic tremor to provide a broad base for the seismic interpretation of volcanic processes. This classification is based on signature variations routinely relied on to differentiate seismic events at the HVO (Koyanagi, 1982):

1. SP earthquakes, the most common type, occur widely in the southeastern part of the Island of Hawaii, particularly beneath the active volcanoes Mauna Loa and Kilauea. They are heavily concentrated in the crust from about 0- to 15-km depth in tectonic regions under volcanic stress. The shallowest earthquakes, between 0- and 5-km depth, generally coincide with magmatically induced ground-deformation events; their occurrence defines the locations and times of volcanic activity. The magnitude range of SP earthquakes is

wide; correspondingly, the magnitude-frequency parameter (Richter, 1958, p. 359) is commonly low—about 0.5 to 1.5. The seismic signature has a pronounced onset of high-frequency waves that attenuate exponentially over time; the dominant frequency changes systematically from about 15 Hz at the onset to less than 1 Hz at the end of the coda. High-frequency body waves are strong for deeper SP earthquakes. Low-frequency and low-velocity surface waves are seen in the shallowest crustal and distant earthquakes, and signal envelopes for these events are generally elongate.

2. LP earthquakes occur only in places of active volcanism and suspected magma movement, such as beneath the summit region of Kilauea. They commonly accompany harmonic tremor. Their seismic signature and mode of occurrence suggest that these earthquakes may be discrete events that, in some instances, increase in number to collectively form harmonic tremor. The frequencies of the seismic waves range from about 1 to 10 Hz and do not substantially change from the start to the end of an individual event. The signal onset is emergent and elongate in comparison with typical SP earthquakes. Magnitude is low and narrow in range, and the poorly defined magnitude-frequency parameter *b* appears to be correspondingly high, ranging from about 1.5 to 2.5.
3. Harmonic tremor, which is the seismic indicator of magma movement and volcanic eruptions in Hawaii, is classified into depth categories of shallow, intermediate, and deep, depending on amplitude differences recorded on the seismic network. In general, tremor signals are sustained in duration and relatively constant in amplitude and frequency. In detail, amplitude and frequency constantly oscillate within a limited range at time intervals of a few to about 10 s. Shallow tremor (less than 5 km deep) accompanies eruptions; the recorded amplitude is highest in the active vent area and varies nearly in proportion to the lava-output rate. The frequency of the seismic waves ranges mainly from about 1 to 10 Hz and is sometimes superimposed on lower frequencies. Shallow tremor recorded within about 2 km of the eruptive vent has dominant frequencies of 2 to 5 Hz, and at more distant locations (several tens of kilometers away), 1- to 3-Hz signals are common. Bursts of tremor, ranging from minutes to days in duration, sometimes occur independently of eruptive activity. Shallow tremor may accompany intrusions recorded by ground deformation. The attenuation rate of amplitude across the seismic network distinguishes intermediate-depth tremor (mostly 6–12 km) in the lower crustal region beneath the summit from deeper tremor (mostly 30–60 km) in the upper mantle that extends broadly southwestward of Kilauea. The source of tremor in Hawaii is further described by Koyanagi and others (1987).

Earthquake *P* waves are timed to within 0.01- to 0.05-s precision, and in the Kilauea area, where seismometers are spaced about 5 km apart, calculated hypocenter accuracy for crustal earthquakes is commonly better than 1 km. Focal depth is referenced to ground elevation at the earthquake epicenter. The peaked instrument response means that amplification is strongly influenced by the spectral content of the event. The detection capability of a Type 1 system (see Nakata and others, 1984) varies and is restricted to frequencies from about 1 to 20 Hz. Irregularities in instrumental and ground noise also introduce inconsistencies into the reduction of ground motion.

For tremor, relative measurements of amplitude at specific stations are consistent to within a factor of about 2, whereas analyses dependent on absolute measurements are confined to order-of-magnitude calculations. Uncertainties in the reduction of tremor signals to actual ground motion is introduced by variations of tremor frequency from 1 to 10 Hz, particularly during eruptions, when higher frequencies are detected near the source than at locations more than several kilometers away. In our general procedure, the repeating bursts of amplitude maxima were read and averaged for 5-minute samples from Develocorder film records, and reduced according to instrumental magnification and apparent frequencies averaged for the amplitude bursts. Station-to-station differences in background noise and signal amplification were calibrated by comparisons of local-earthquake and teleseismic signals and taken into account in our reduction of tremor amplitudes.

To provide more nearly uniform detection capability for earthquakes and harmonic tremor over a wider spectral range, a system based on Wood-Anderson response was recently adapted to the horizontal components of selected stations (fig. 7.2). This system was installed in several frequency-modulated (FM) stations at Kilauea beginning in mid-1983, to improve amplitude measurements used for the determination of earthquake magnitude and tremor readings.

A filter system designed by George Kojima at the HVO to record seismic signals at frequencies centered at 10, 5, 2.5, 1.25, and 0.625 Hz was adapted to a six-channel chart recorder. This system is comparable to that used by Bernard Chouet (Chouet and others, 1978; Chouet, 1979) to collect earthquake data near Stone Canyon, Calif. Different stations were monitored at different times, and normalized with unfiltered signals from continuously recorded network stations on Develocorder films or magnetic tape. Tremor, as well as other seismic events associated with the eruption process, was monitored at various stations over different intervals of time.

DATA, 1982–84

LOCATIONS AND MIGRATION PATTERN OF EARTHQUAKES

In the past few years, frequent magma intrusions and eruptions at Kilauea have resulted in high levels of seismicity in the rift zones and adjacent flanks (Nakata and others, 1982; Tanigawa and others, 1983). Similarly, earthquakes in the southeastern part of the Island of Hawaii were numerous in the months before the 1983 eruption (fig. 7.3). Of these earthquakes, crustal events at 5- to 10-km depth in the south flank of Kilauea, believed to occur from seaward displacement of the unbuttressed flank in response to rift intrusions (Swanson and others, 1976), were most persistent. Shallow summit and rift earthquakes at 0- to 5-km depth occurred during times of sustained inflation and intrusions (fig. 7.4; table 7.1). On the basis of earlier findings (Koyanagi and others, 1974), the shallow events from 0- to 5-km depth delineate an inflation center at the summit and outline linear intrusion zones projecting southward, southwestward, and southeastward into the rift zones. The deep crustal earthquakes from September to December 1982 were mainly concentrated in a 20-km-long zone adjacent to the intrusive area in the east rift. The sequence of shallow earthquakes plotted in the summit region indicates the progressive shift to and increase of activity in the upper east rift zone from September to December 1982 (fig. 7.5). The combined plots present an arcuate alignment of hypocenters, with linear zones radiating from the south edge of the caldera near Keanakakoi Crater to the south

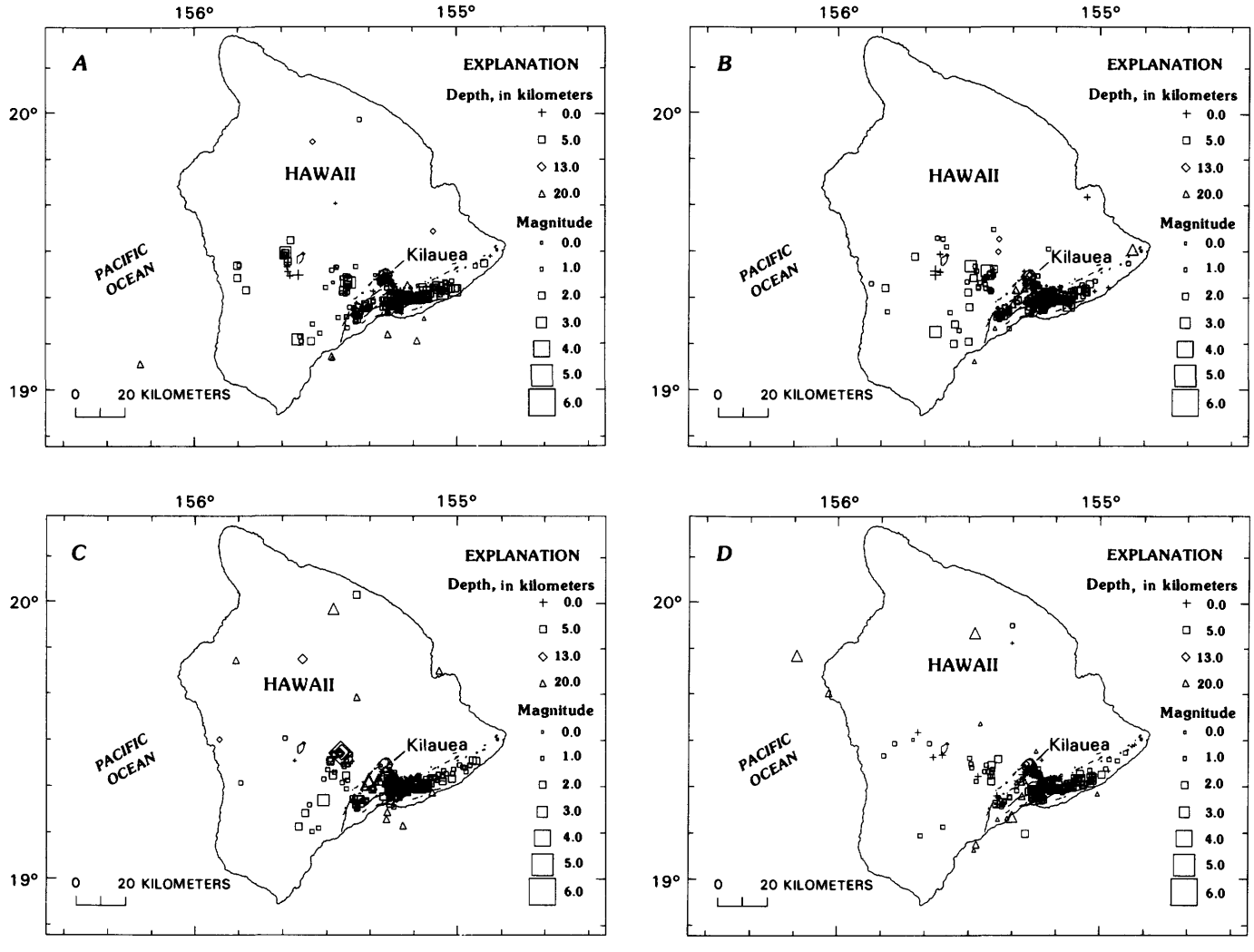

FIGURE 7.3.—Locations of earthquakes on the Island of Hawaii for September (*A*), October (*B*), November (*C*), and December (*D*) 1982. Solid lines, fault traces.

that trends into the southwest rift zone, and to the southeast along the upper east rift zone. The increasing rate of earthquakes before and during the early eruption period in January 1983 broadened the seismic zone along the east rift (fig. 7.6). The earthquakes associated with shallow intrusion along a linear 15-km increment of the east rift, the earthquakes associated with shallow collapse at the summit, and the deep crustal earthquakes that are broadly elongate in the south flank are distinguished in this widened seismic zone.

The hypocentral distribution of earthquakes from the successive intrusions that outlined the dynamic regions during September 1982 to January 1983 is expanded in map and depth views (figs. 7.7, 7.8). Shallow swarms of earthquakes were concentrated at the summit and along the axis of the east rift. The shallow seismicity beneath the southern caldera area radiated laterally to feed a 3-km-long protrusion to the south and an 8-km-long alignment to the southeast that connects with a 17-km-long extension along the axis of the east rift. The shallow earthquake swarm formed a 2- by 25-km zone centered from 2 to 4 km in depth. Nearly parallel to the rift was a broad zone of deep crustal earthquakes in the adjacent south flank of the volcano. The 30-km-long and 5-km-wide belt of earthquakes were concentrated at depths between 5 and 10 km; the lower limit was near the crustal boundary. The elongate seismic zone that parallels the summit-rift axis is formed by a multiclustered distribution of earthquakes. Regions of decreasing numbers of crustal earthquakes (0–13 km deep) extended obliquely to the major axis of the east-rift and south-flank seismic zone (fig. 7.7). Some of the noticeable gaps occurred across (1) the middle upper east rift, (2) the bend in the east rift, and (3) the middle east rift south of Puu Kahaualea.

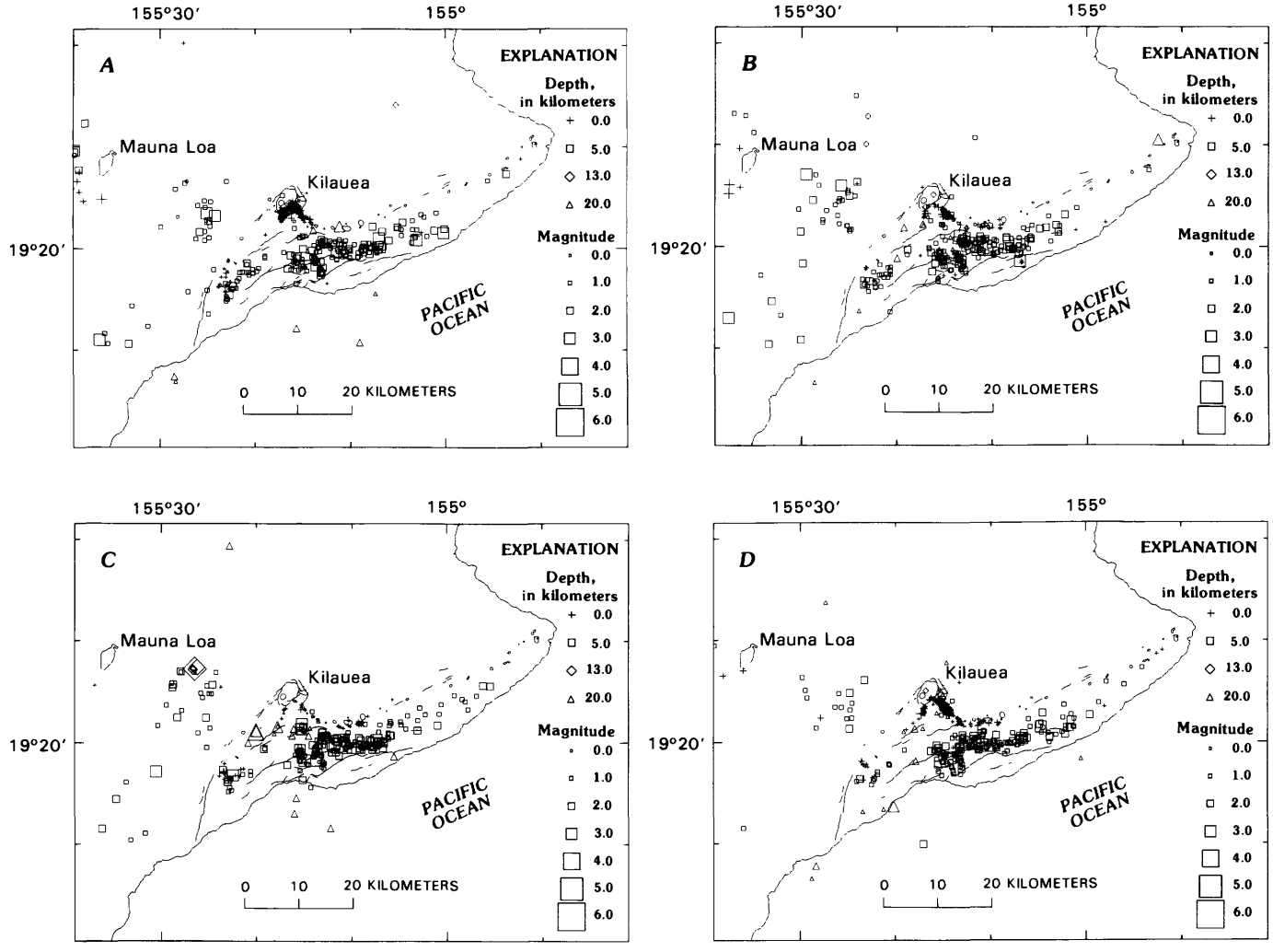

FIGURE 7.4.—Locations of earthquakes in the Kilauea area, southeastern part of the Island of Hawaii, for September (*A*), October (*B*), November (*C*), and December (*D*) 1982. Solid lines, fault traces.

The January swarm of east-rift earthquakes migrated downrift, initially at a rate of about 0.6 to 0.7 km/h and episodically thereafter (fig. 7.9). The well-defined linearity formed by the concentration of earthquakes along the leading edge of the space-time diagram during the early morning hours of January 2 defined the downrift migration and rate. The earthquakes then moved farther downrift erratically until midday. The earthquakes continued within the seismic zone for about a day after the initial migration. From about the middle of January 3, earthquakes were scattered even farther downrift almost to Kalalua, and then were sustained along a zone between Puu Kahaualea and Napau Crater, assuming a slow, uprift migration pattern at a rate of about 0.06 to 0.07 km/h until the middle of January 6. The final swarm on January 7 extended farther downrift to about 2 km east of Kalalua, again at a rate of about 0.6 to 0.7 km/h.

DEPTH AND MAGNITUDE OF EARTHQUAKES

From September 1982 to January 1983, earthquakes located beneath the Island of Hawaii were mainly confined to depths of less than 20 km and had magnitudes of less than 4.2 (fig. 7.10). The 5- to 10-km-deep zone, most noticeably on the south flank, persisted throughout this time interval as the major source of seismic-energy release. These earthquakes increased in number above the already-high background mostly during the early period of eruption from January 2 to 8. Many strong earthquakes, as large as about $M=4.2$, fell in this depth category at seemingly random intervals.

Earthquakes shallower than 5 km were abundant beneath the summit and east rift during intrusions in the months before the eruption, as well as in the early eruption period. The east-rift intrusions in late September,

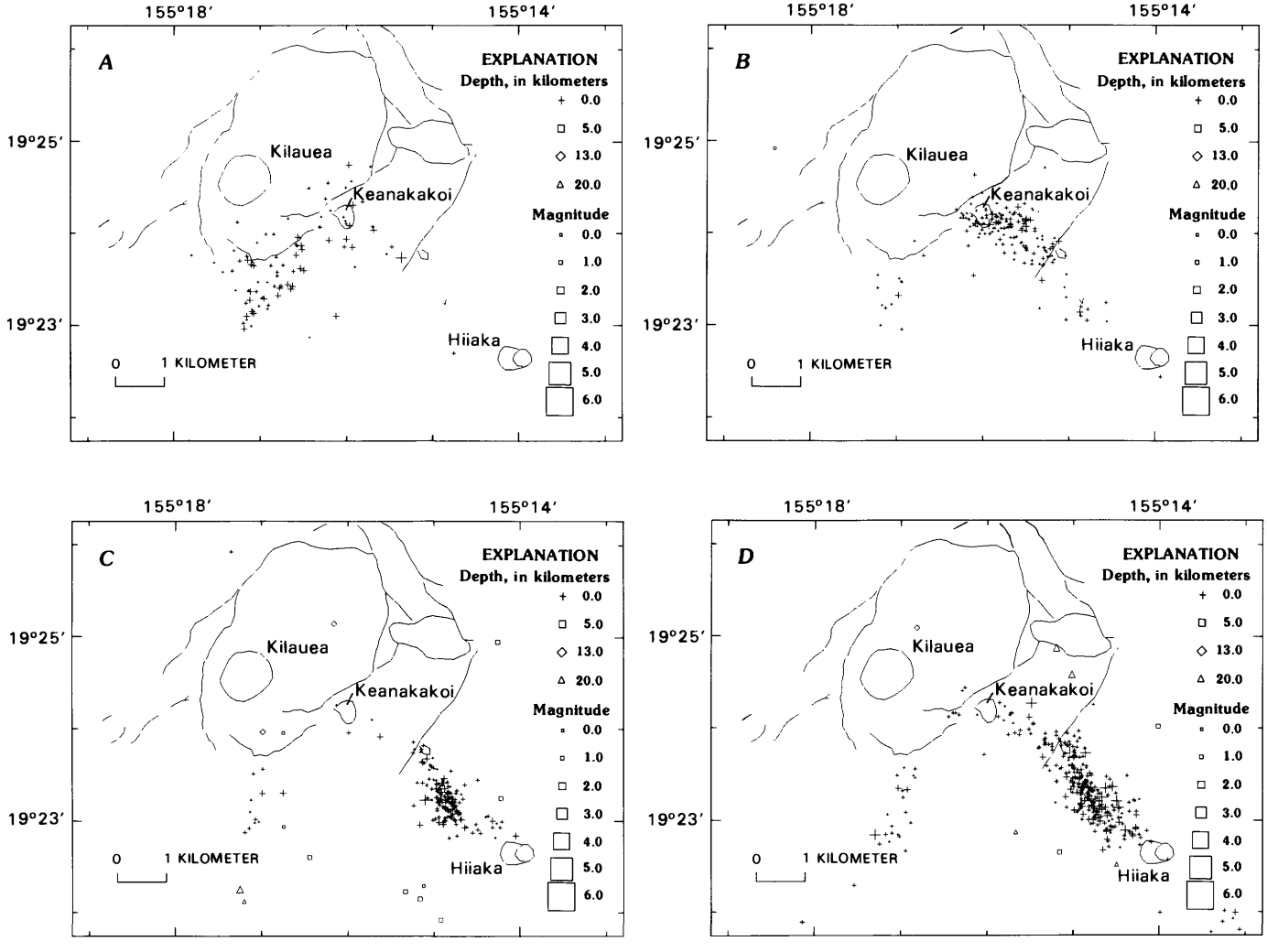

FIGURE 7.5.—Locations of earthquakes beneath the summit region of Kilauea for 1982. *A*, 1650 to 1845 H.s.t. September 25. *B*, 1845 H.s.t. September 25 to 1500 H.s.t. September 26. *C*, October. *D*, December. Solid lines, fault traces.

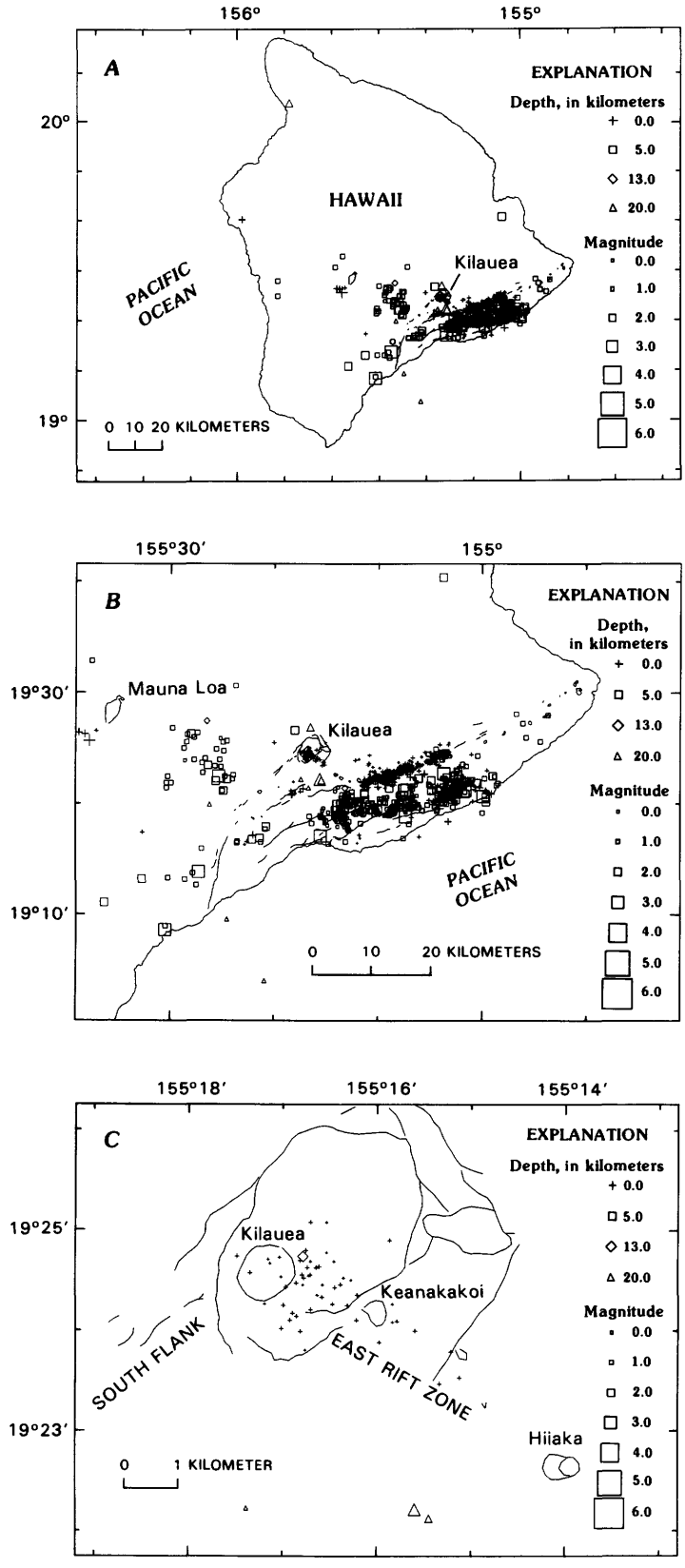

FIGURE 7.6.—Locations of earthquakes on the Island of Hawaii for January 1983. *A*, Entire island. *B*, In the Kilauea area. *C*, Beneath the summit region of Kilauea. Solid lines, fault traces.

December, and early January, marked by swarms of shallow earthquakes, were followed within a few days by more subtle increases in the number of deeper crustal earthquakes.

RATE AND FREQUENCY OF EARTHQUAKES

The cumulative numbers of timed and located earthquakes larger than $M = 1.5$ are plotted in figure 7.11. Shallow summit and rift earthquakes at 0- to 5-km depth selectively are concentrated at times of sustained summit inflation, summit collapse, rapid rift intrusions, and eruptions. The number of shallow summit and rift earthquakes of $M > 1.5$ appreciably decreased after the eruption in January 1983. Changes in volcanic activity during the later eruptive episodes were reflected seismically only by changes in the number of very small earthquakes, and by variations in the amplitude of shallow harmonic tremor. The rate of deeper south-flank earthquakes, however, was contrastingly high and constant. The relatively high rate during the period of episodic intrusions from September to December 1982 led to a short acceleration in rate in January during the early eruption period, followed by a constant lower rate during the prolonged eruption period in 1983. The number of earthquakes in the south flank decreased further after January 1984.

The daily number of small and shallow earthquakes counted in the summit and east rift zone generally responded to the volcanic activity associated with the

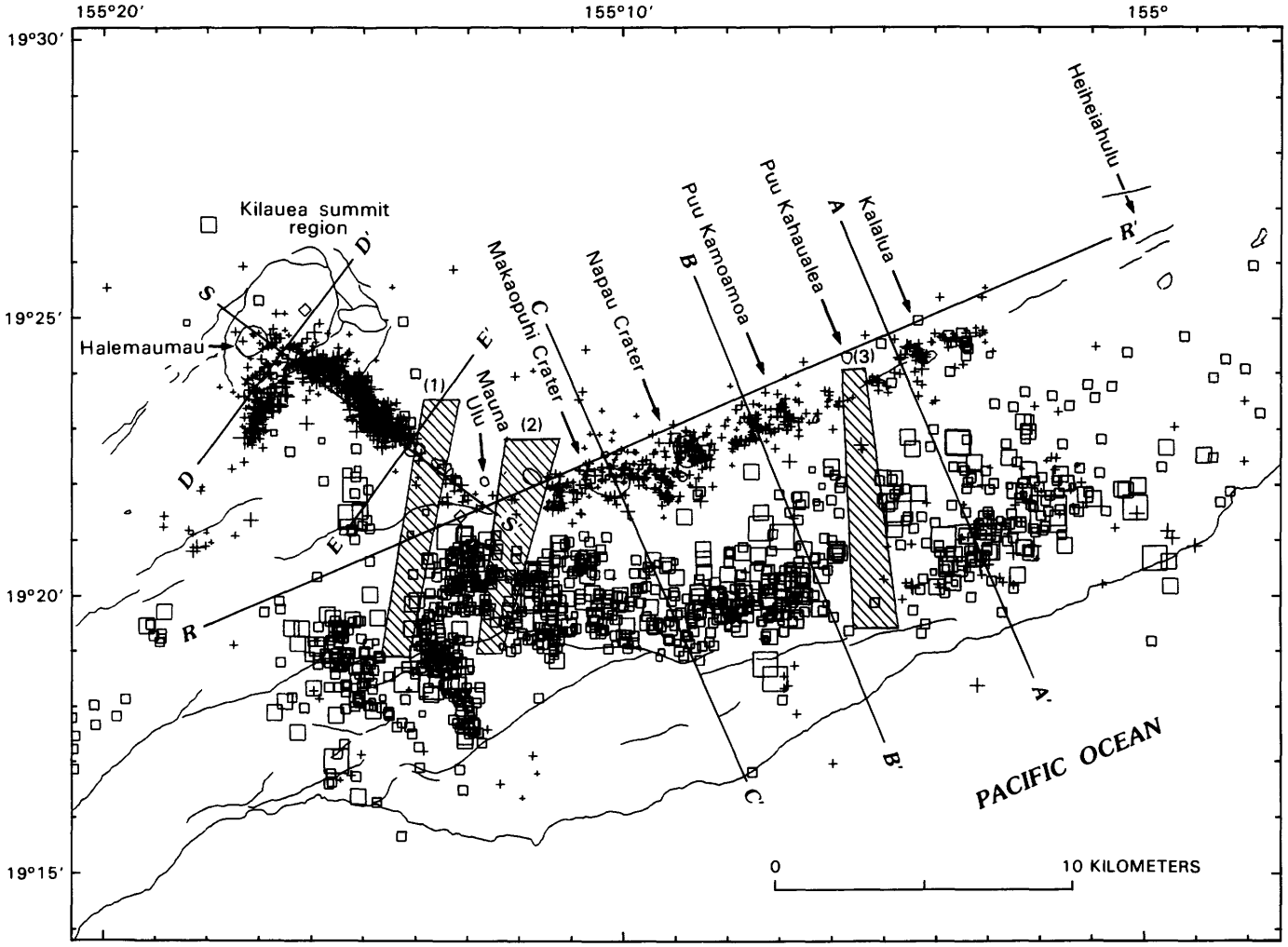

FIGURE 7.7.—Summit region and eruption area along east rift zone of Kilauea, showing earthquakes less than 15 km deep located with horizontal and vertical standard errors of less than 2 km (see fig. 7.3 for explanation of symbols) and aseismic regions (crosshatched areas) for period September 1982 to January 1983. East rift zone was sometimes separable into upper and middle parts, according to the structural classification of Swanson and others (1976); upper part extends from southeast of the summit region to about Makaopuhi Crater, and middle part includes area from Makaopuhi Crater to Heiheiahulu. Lines *A-A′*, *B-B′*, and *C-C′* refer to cross sections normal to middle east rift zone, lines *D-D′* and *E-E′* to cross sections normal to southeastward trend of summit to upper east rift zone, and lines *R-R′* and *S-S′* to cross sections along east rift zone and summit to east rift zone, respectively (see fig 7.8). Solid lines, fault traces. Major craters are labeled.

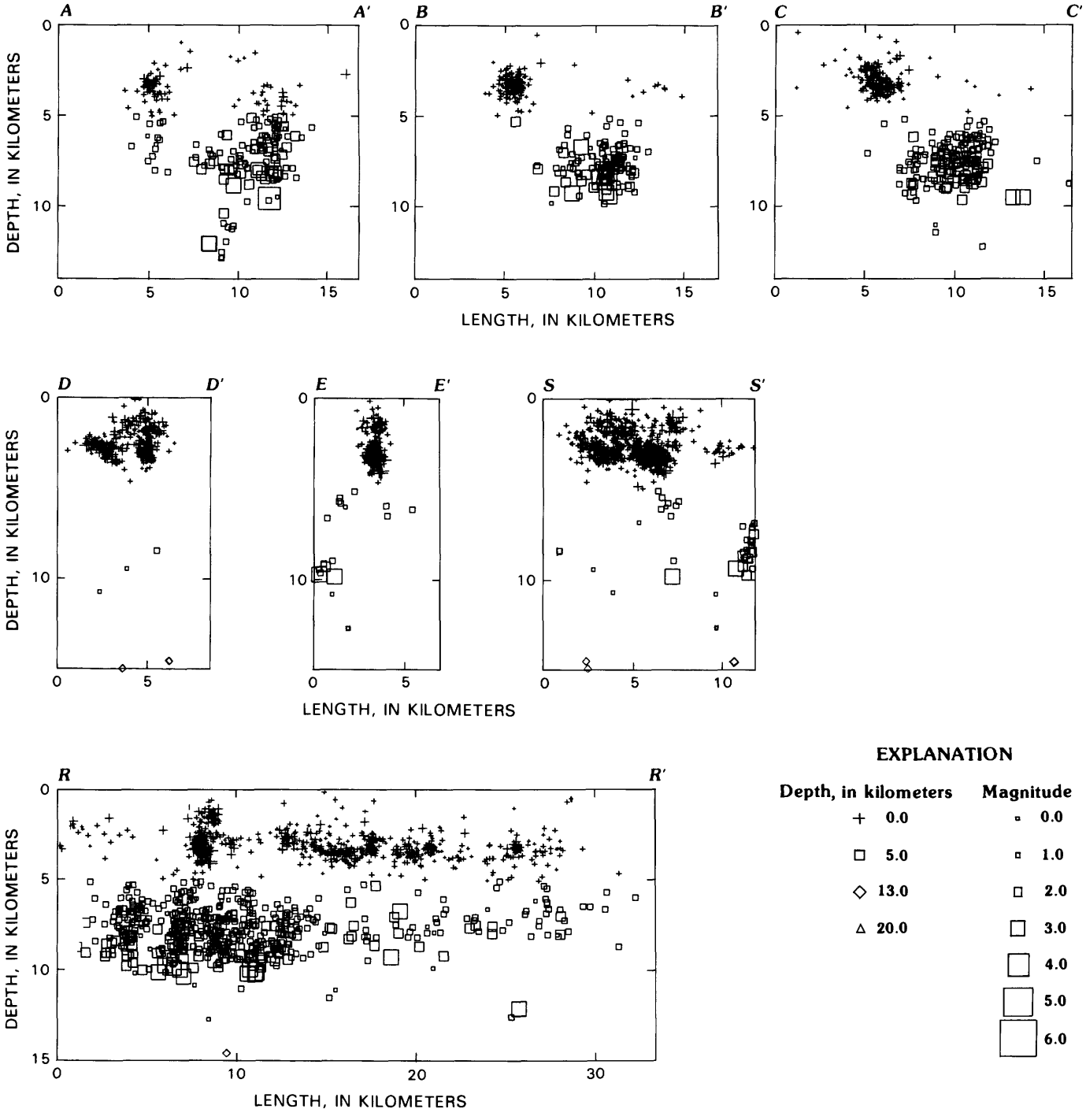

FIGURE 7.8.—Depth sections of earthquake locations in summit region and east rift zone (see fig. 7.7 for locations of section lines). Each section represents a volume of length and depth as indicated and of the following widths: sections *A-A'*, *B-B'*, *C-C'*, and *S-S'*, 5 km; sections *D-D'* and *E-E'*, 4 km; and section *R-R'*, 10 km.

major eruption that started in 1983 (fig. 7.12). The rate of shallow SP earthquakes that delineate the level of stresses around the summit storage system increased to more than a thousand per day during the summit eruption and intrusion in September 1982 and before the east-rift intrusion in December. Later, during the eruption period in 1983 and 1984, the rate of these events ranged from less than a hundred to several hundred per day. The increases coincided with sustained summit inflations or large, eruption-related deflations; alternating decreases occurred after relatively small deflation events between eruptive episodes. The rate of shallow SP earthquakes delineates the level of stress around the summit storage system. LP caldera earthquakes followed eruption-related deflation of the summit. These events emerged from continuous, intermediate-amplitude harmonic tremor that began during large and (or) rapid deflations; the variation in rate partly reflected the level of continuous tremor at the station NPT. LP events and (or) summit tremor more consistently responded to the amount and increasingly rapid rate of summit deflation associated with eruptive episodes after the first half-year of activity. The pattern of summit tremor and LP events is further described below in the subsection entitled "Seismic Events at the Summit."

During the period before the 1983 eruption, the daily number of east-rift earthquakes dominated by swarms of shallow rift earthquakes marked the intrusions in September and December. The total counts have been affected by scattered larger earthquakes in the south flank. After January 1983, many small shocks occurred from various thermal and structural anomalies at the eruptive vent, including degassing and cooling of fresh lava flows.

After the summit eruption in September 1982, the number of shallow earthquakes increased in the upper east rift zone, and minor swarms occurred in September-October and December. In both swarms, shallow earthquakes moved from the summit caldera rapidly into the uppermost east rift zone between Puhimau and Kokoolau Craters. The activity remained in the upper east rift for 2 to 3 weeks and was followed by farther-downrift spreading at a gradual migration rate of about 0.7 km/d (fig. 7.13). The episodic intrusions of magma indicated by the pattern of seismicity extended from the summit to beyond Makaopuhi Crater.

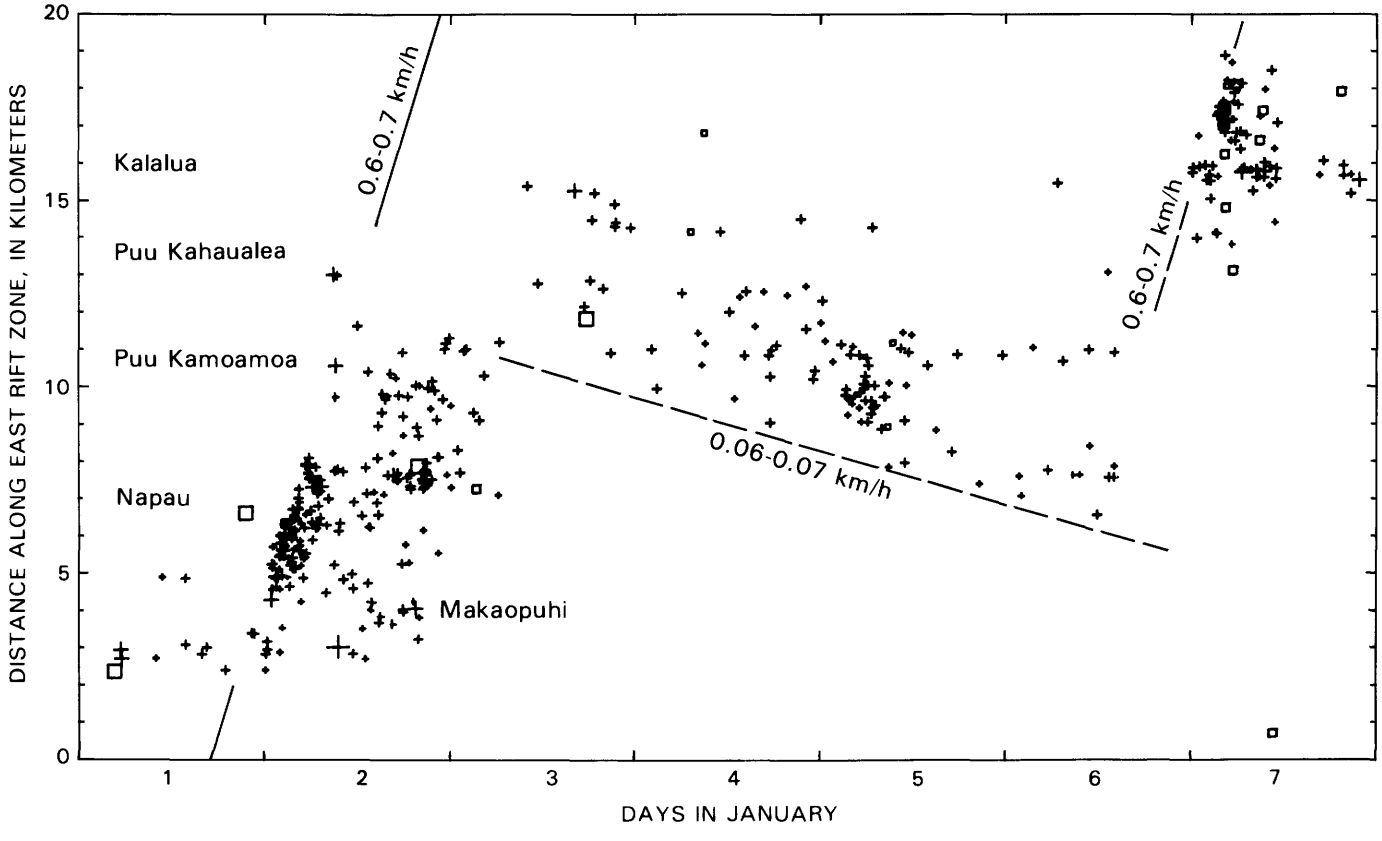

FIGURE 7.9.—Earthquake locations (see fig. 7.3 for explanation of symbols) along a west-to-east profile of east rift zone of Kilauea as a function of time for the period January 1–7, 1983. Distribution of shallow earthquakes during swarm on January 2 indicates a downrift migration rate of 0.6 to 0.7 km/h (solid line). Thereafter until January 7, distribution implies uprift and, subsequently, downrift movement (dashed lines). Major craters are labeled.

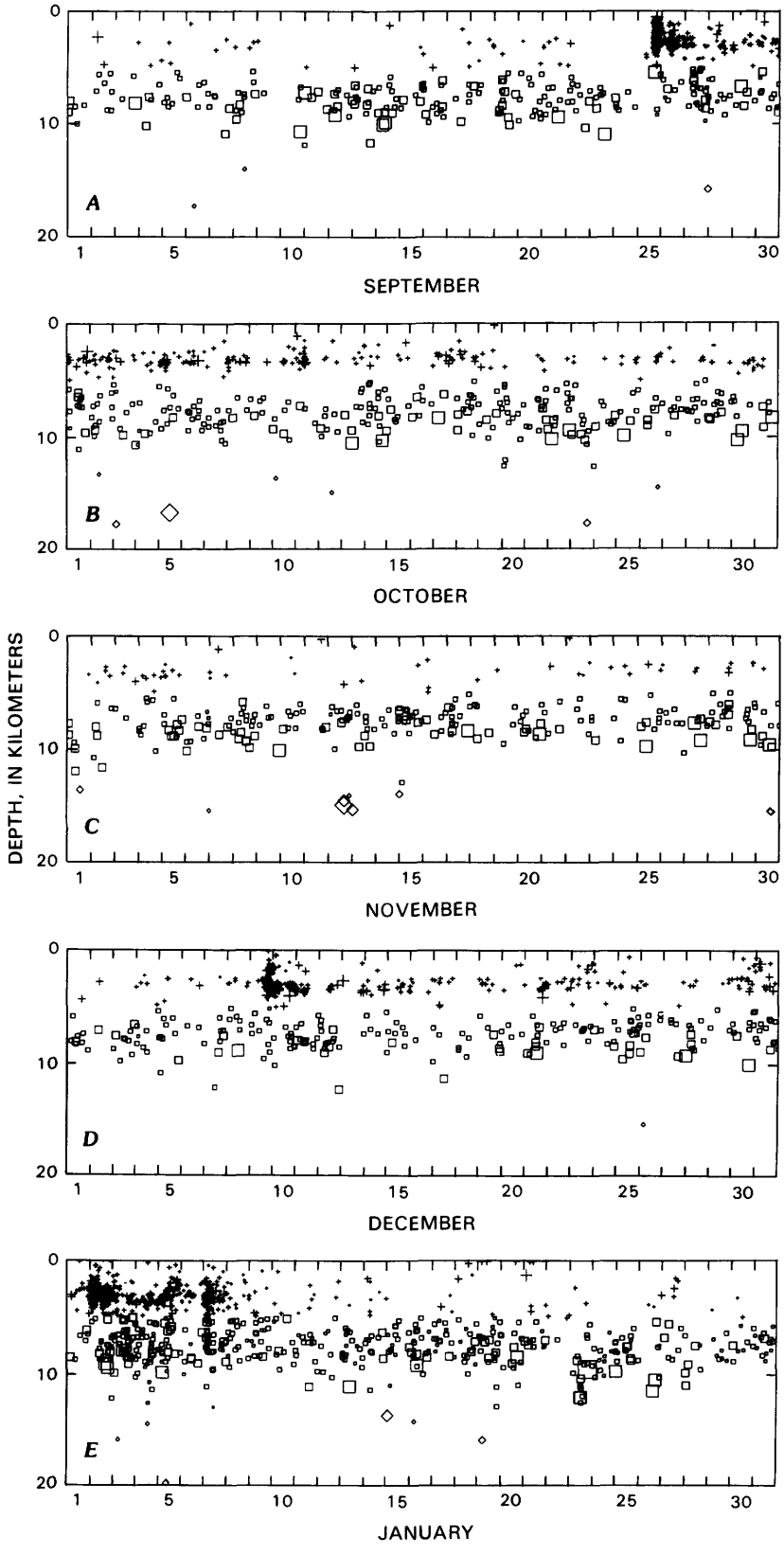

FIGURE 7.10.—Chronologic sequence of earthquake hypocenters beneath the Island of Hawaii in terms of focal depth and magnitude (see fig. 7.3 for explanation of symbols). *A*, September 1982. *B*, October 1982. *C*, November 1982. *D*, December 1982. *E*, January 1983.

The large summit collapse accompanying the January 1983 intrusion produced an anomalous increase in the number of shallow summit earthquakes. In contrast, deep crustal earthquakes were separated randomly in the south flank, except for slight postintrusion increases adjacent to the downrift margins of the intruded zone.

STRONG TREMOR IN THE EAST RIFT ZONE DURING ERUPTIVE EPISODES

The continuous tremor recorded during magmatic intrusions and eruptions varied in amplitude according to the apparent rate of magmatic movement and the vigor of the eruption. During the first week of activity in January 1983, high-frequency (5–10 Hz) tremor was very strong beneath the extensive fissure system. The center of maximum tremor accompanying the downrift movement of eruptive activity is shown (fig. 7.14) by the relatively larger amplitude of tremor at station MPR on January 2 and, later, downrift at station LUA on January 7–8. Tremor was strongest during this interval, and the amplitudes recorded during subsequent major episodes were considerably lower. For most of the rest of January, tremor was highest at station PUK, and amplitudes varied generally with changes in eruption activity. The downrift migration of earthquakes, as described previously, is indicated by the hourly count of shallow earthquakes (fig. 7.14).

As the eruption continued and lava emission became confined to a single vent system, tremor responded more obviously to the eruption itself and accompanying summit deflation, and less to underground movement of magma between the summit and the site of eruption. During episodes of high lava output, the tremor level increased by a factor of at least 10 over that defined by weak background tremor between periods of vigorous eruptive activity (fig. 7.15). The hourly variations in the amplitude of increasing tremor at the east-rift eruptive site and summit region, the times of major lava outbreaks, and the pattern of rapid summit deflation during eruptive episodes 2 through 23 are plotted in figure 7.16. Amplitude changes of the east-rift tremor were generally more gradual during the early episodes of the eruption than during the later ones. From episode 7 on, changes in amplitude were more abrupt, especially at the start and end of eruptive episodes. Amplitude changes ranged from a slow rate of several percent per hour to rapid changes exceeding an order of magnitude within a few minutes. The pattern of tremor amplitude and duration changed approximately from a continuously long duration of low amplitude, as in episodes 2 and 3, to shorter durations of higher amplitude in later episodes.

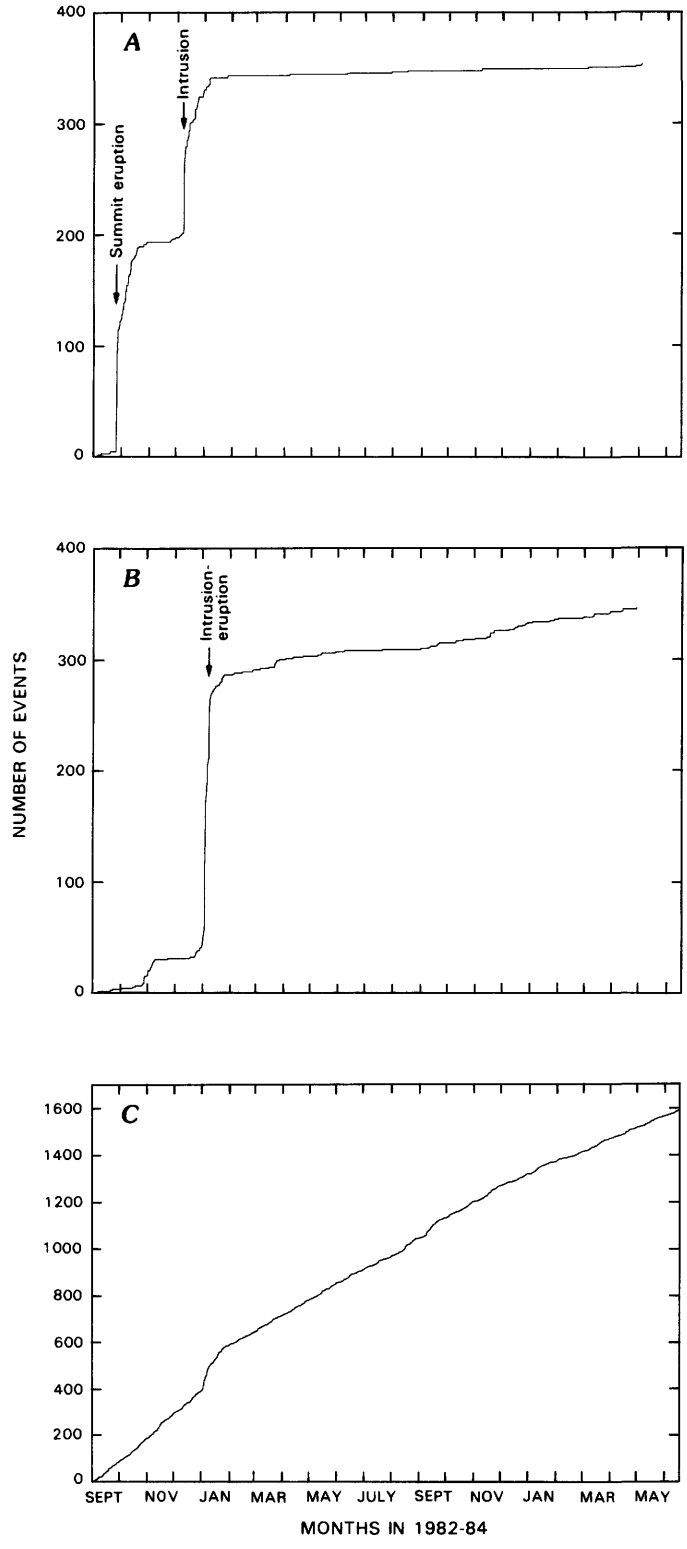

FIGURE 7.11.—Cumulative number of $M>1.5$ earthquakes beneath Kilauea from September 1, 1982, to June 15, 1984. *A*, Shallow (0–5 km deep) summit and east-rift earthquakes, recorded between lat 19°22′–19°28′ N. and long 155°14′–155°19′ W. *B*, Shallow (0–5 km deep) east-rift and south-flank earthquakes, recorded between lat 19°16′–19°28′ N. and long 154°57′–155°14′ W. *C*, Deep (5–15 km) east-rift and south-flank earthquakes, recorded between lat 19°16′–19°28′ N. and long 154°57′–155°14′ W.

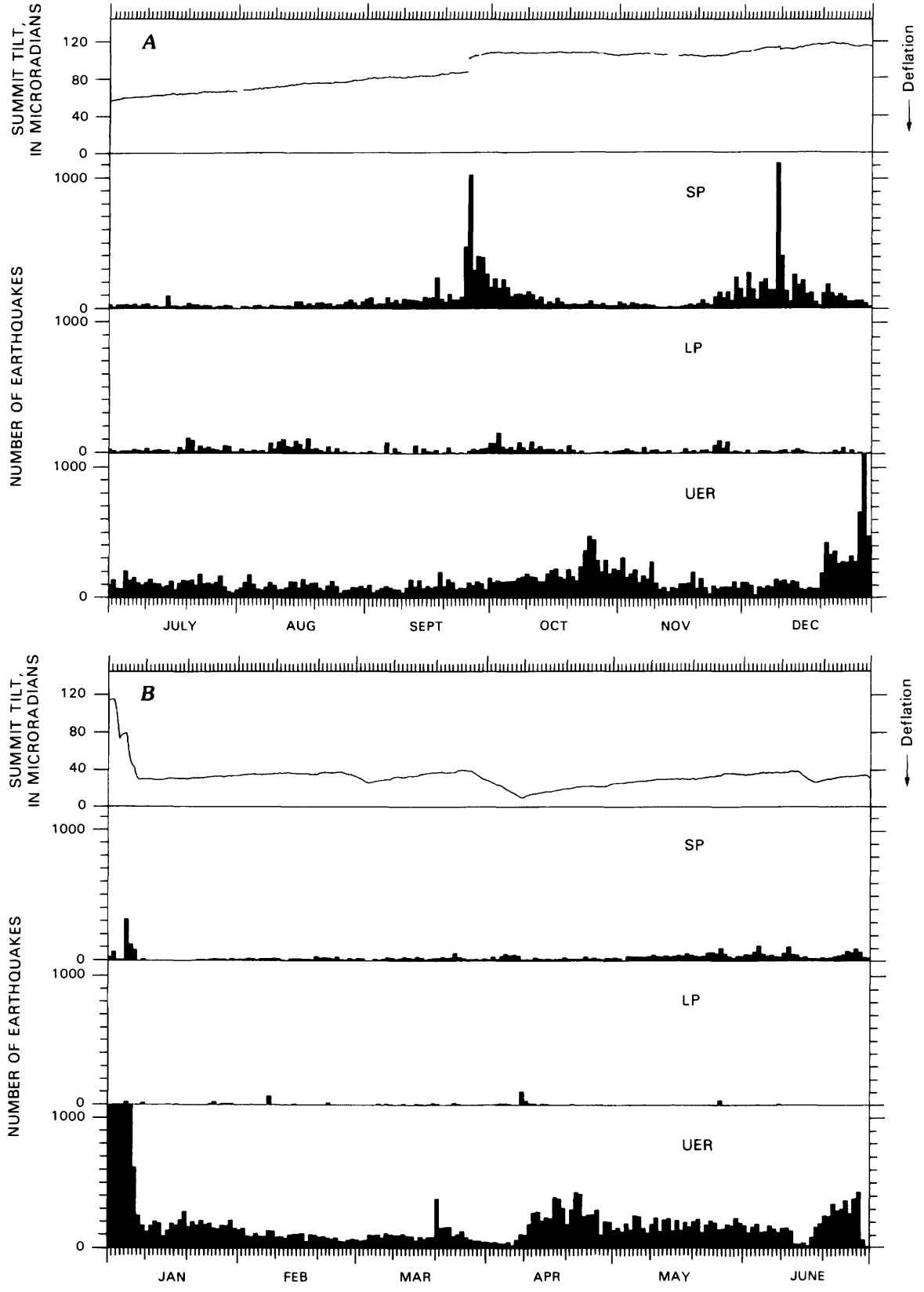

FIGURE 7.12.—Daily number of crustal earthquakes in summit region and upper east rift (UER) zone of Kilauea, referenced to summit tilt. *A*, July-December 1982. *B*, January-June 1983. *C*, July-December 1983. *D*, January-June 1984. Shallow summit earthquakes, recorded mainly at station NPT, were classified into short-period (SP) and long-period (LP) events, according to their characteristic signatures. UER earthquakes, recorded at stations KMM, MPR, or PAU, were shallow rifting events west of Kalalua and deeper crustal events in adjacent parts of the south flank. Earthquakes as small as $M \sim 0.1$ were detected and included in counts. At this level of detection, counts are sensitive to variations

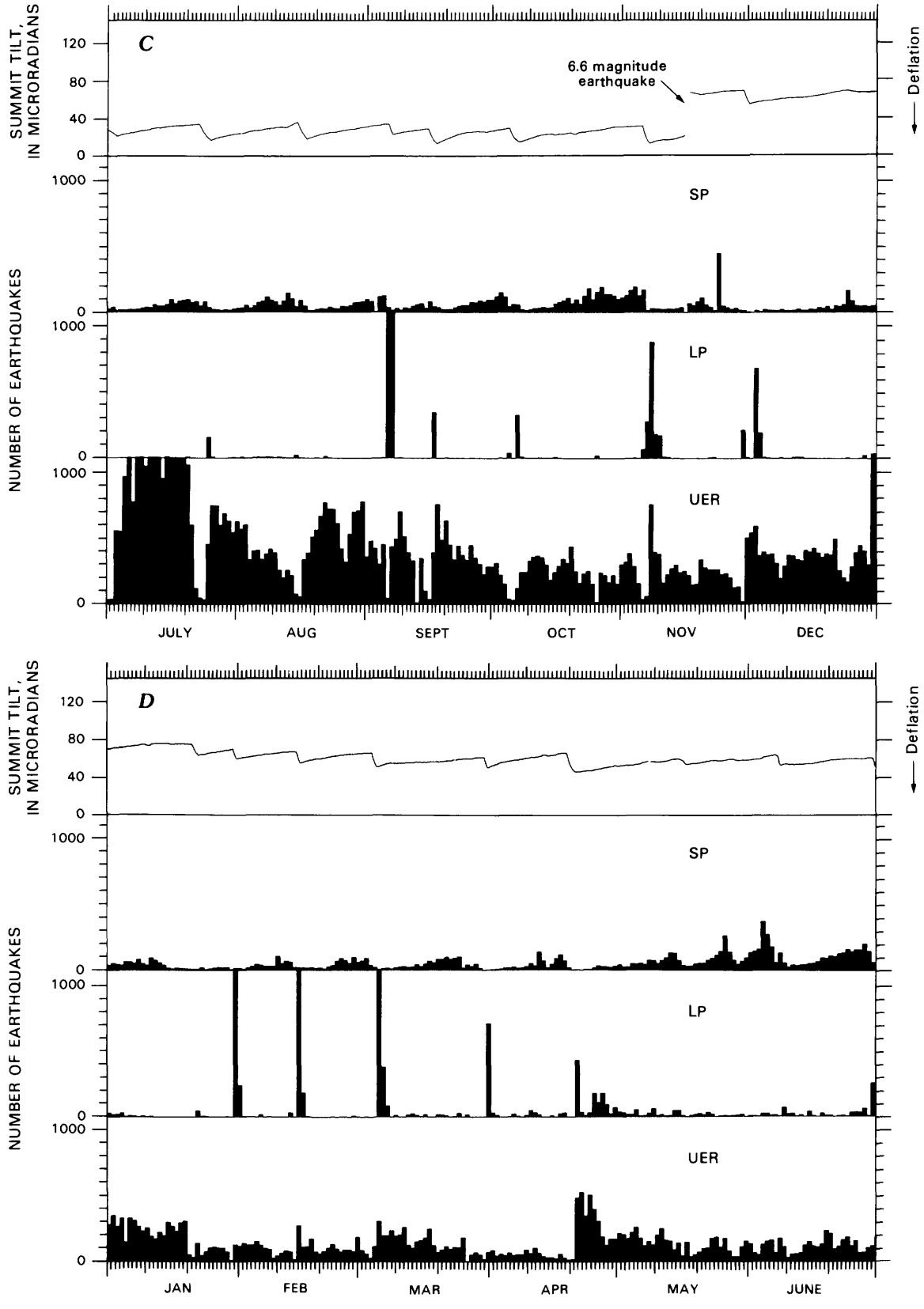

in noise levels caused by weather conditions and volcanic activity. The generally lower number of earthquakes counted during major eruptive episodes is partly attributed to the locally higher seismic background from harmonic tremor. Seismic record was sometimes interrupted by instrumental failure, high winds, and heavy rains. Summit tilt derived from hourly readings of the Ideal Aerosmith east-west-component tiltmeter at Uwekahuna is approximately due to such effects as instrumental drift, climatic interference, and strong earthquakes (Arnold Okamura, written commun., 1986).

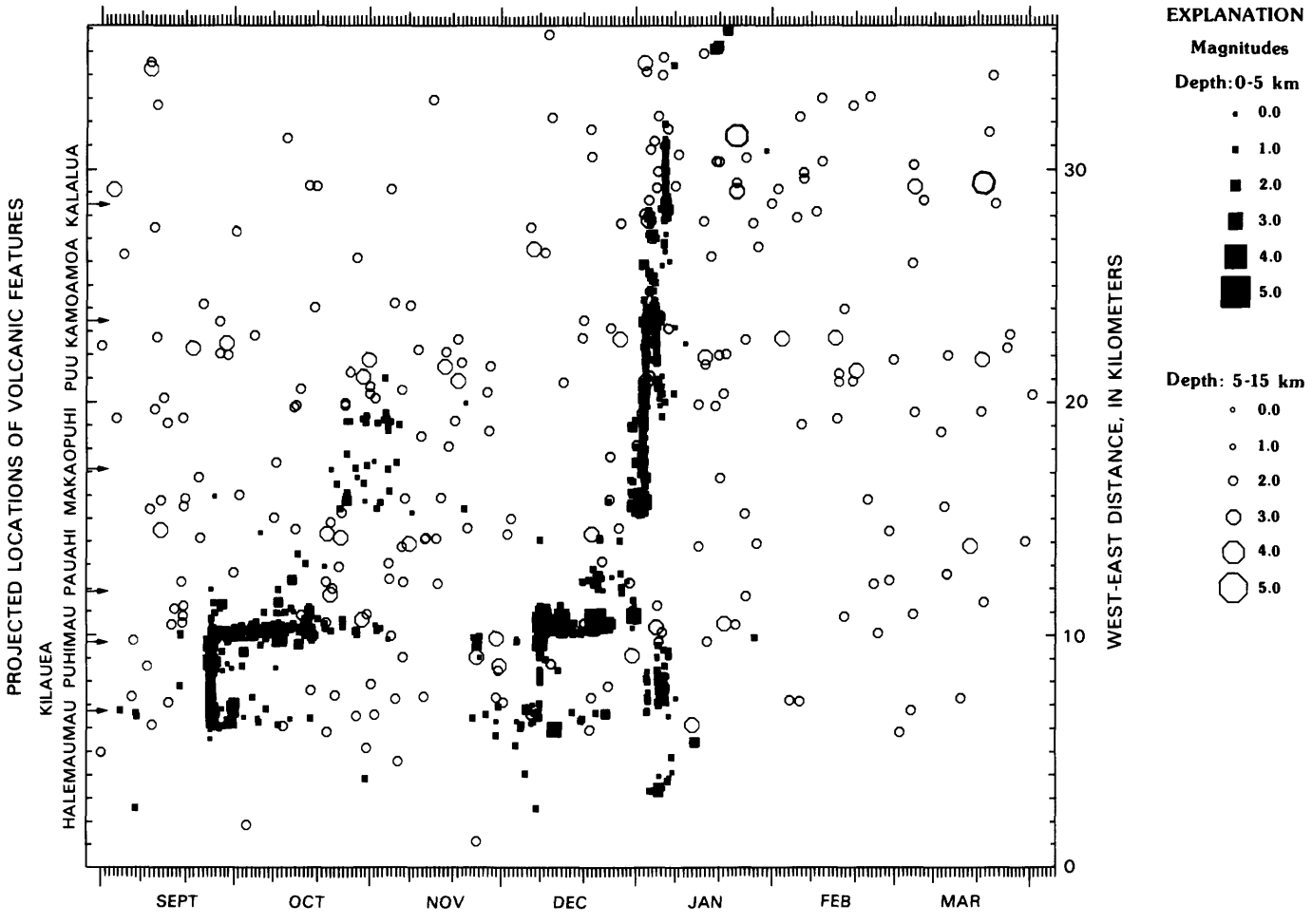

FIGURE 7.13.—Earthquake locations along west-to-east profile from summit region to east rift zone of Kilauea within area of figure 7.7 during the period September 1, 1982, to March 31, 1983.

The gradual changes in the amplitude of east-rift tremor during early eruptive episodes were accompanied by comparatively slow changes in tilt and an absence of summit tremor. This pattern advanced to more abrupt and vigorous tremor and tilt activity. Increases in summit tremor were more conspicuous during later eruptive episodes, characterized by rapid deflation events. These summit events are further discussed below in the subsection entitled "Seismic Events at the Summit."

Erratic high-frequency tremor during the intrusion and early eruption period changed to more nearly consistent tremor during later eruptive episodes, when the dominant frequencies constantly alternated from about 1 to 10 Hz at short increments of time ranging from about 1 to 10 s. This pattern of repeated changes in frequency is similarly observed for deep tremor episodes that are not associated with eruptive activity. The absence of correlation between recurring amplitude bursts recorded at different frequencies, particularly at 2.5 and 5.0 Hz (fig. 7.17), indicates that the tremor is constantly changing in frequency within at least a limited bandwidth. The resulting chain of amplitude bursts most obviously recorded at 2.5 Hz resembles the behavior of high lava fountains, which consists of similarly repeated pulses.

Amplitudes read from the bandpass signals at stations MPR and PUK for two selected 5-s intervals, corrected

FIGURE 7.14.—Seismic activity and eruptive events from January 1 to 11, 1983. *A*, Summit tilt recorded on east-west component of Ideal-Aerosmith tiltmeter at Uwekahuna station (see fig. 7.12). *B*, Tremor amplitude at stations NPT, MPR, PUK (clipping level, 3.0), and LUA (clipping level, 3.8). Tremor amplitudes were measured and earthquakes counted for hourly intervals. Tremor amplitudes were reduced to approximate units of micrometers, according to instrumental response for recorded frequency of tremor. *C*, Number of earthquakes in summit region, along east rift zone from Makaopuhi Crater to Puu Kamoamoa, and along east rift zone from Puu Kamoamoa to Heiheiahulu. Most earthquakes were shallow (less than 5 km deep), small ($M \gtrsim 0.5$) events. *D*, Duration of increased eruptive activity.

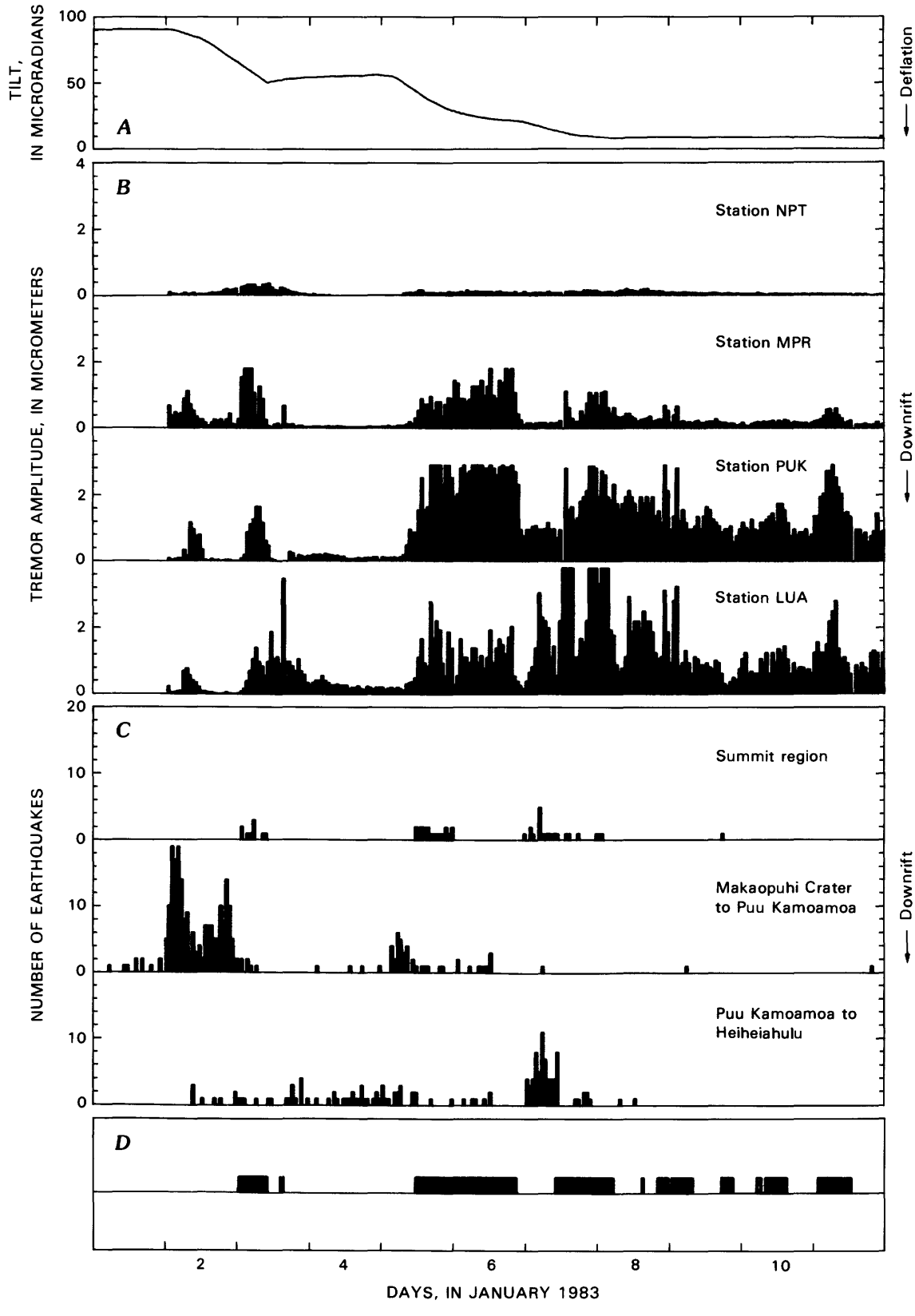
TILT, IN MICRORADIANS
100
50
0
A
Deflation
TREMOR AMPLITUDE, IN MICROMETERS
4
2
0
B
Station NPT
Station MPR
Station PUK
Station LUA
Downrift
NUMBER OF EARTHQUAKES
20
10
0
C
Summit region
Makaopuhi Crater to Puu Kamoamoa
Puu Kamoamoa to Heiheiahulu
Downrift
D
2
4
6
8
10
DAYS, IN JANUARY 1983

for instrumental magnification and background noise, indicated varying amplitudes at 0.625, 1.25, 2.5, 5.0, and 10.0 Hz (fig. 7.18). High-frequency signals at 2.5 and 5.0 Hz were strong at station PUK, located within 1 km of the eruptive vent, whereas lower frequency signals (max 2.5 Hz) were more significant at station MPR, located 6 km away. Such measurements represent partial short-term variations in tremor frequency that collectively produce a wider, multipeaked spectrum of frequencies. Spectral analysis of tremor sampled about 1 km from the eruptive vent on August 20, 1984, showed varyingly peaked frequencies from at least 1 to 10 Hz (Chouet and others, 1987). Between major episodes of fountaining, the commonly recorded signal at 2.5 Hz on the vertical-component seismometer at station PUK or KMM served to differentiate weak tremor from background noise created by lower frequency ocean surf and higher frequency wind.

In addition to changes in tremor amplitude resulting from variations in intrusion and eruption rates, tremor amplitude decreased as a function of distance from the eruptive vent (fig. 7.19). High-frequency signals were strong in a wide area during the intrusion and early eruption period, but during the later period of centralized eruption, tremor amplitude decreased more with distance, owing to the shallowness of the source and intense fountaining of the lava.

Amplitude readings used to determine distance attenuation of tremor were first corrected for instrumental magnification, background microseismic noise, and variations in signal level attributed to local ground conditions and instrumental installation at each station. Teleseismic signals from a sufficiently distant source that would normally be recorded with equal strength across the entire HVO seismic network, and deep local earthquakes, were chosen to calculate station corrections. The amplitude of background microseisms for each station was subtracted. The station-to-station differences in amplitude from the teleseismic and deep events remaining after reduction of background microseisms and instrumental magnification

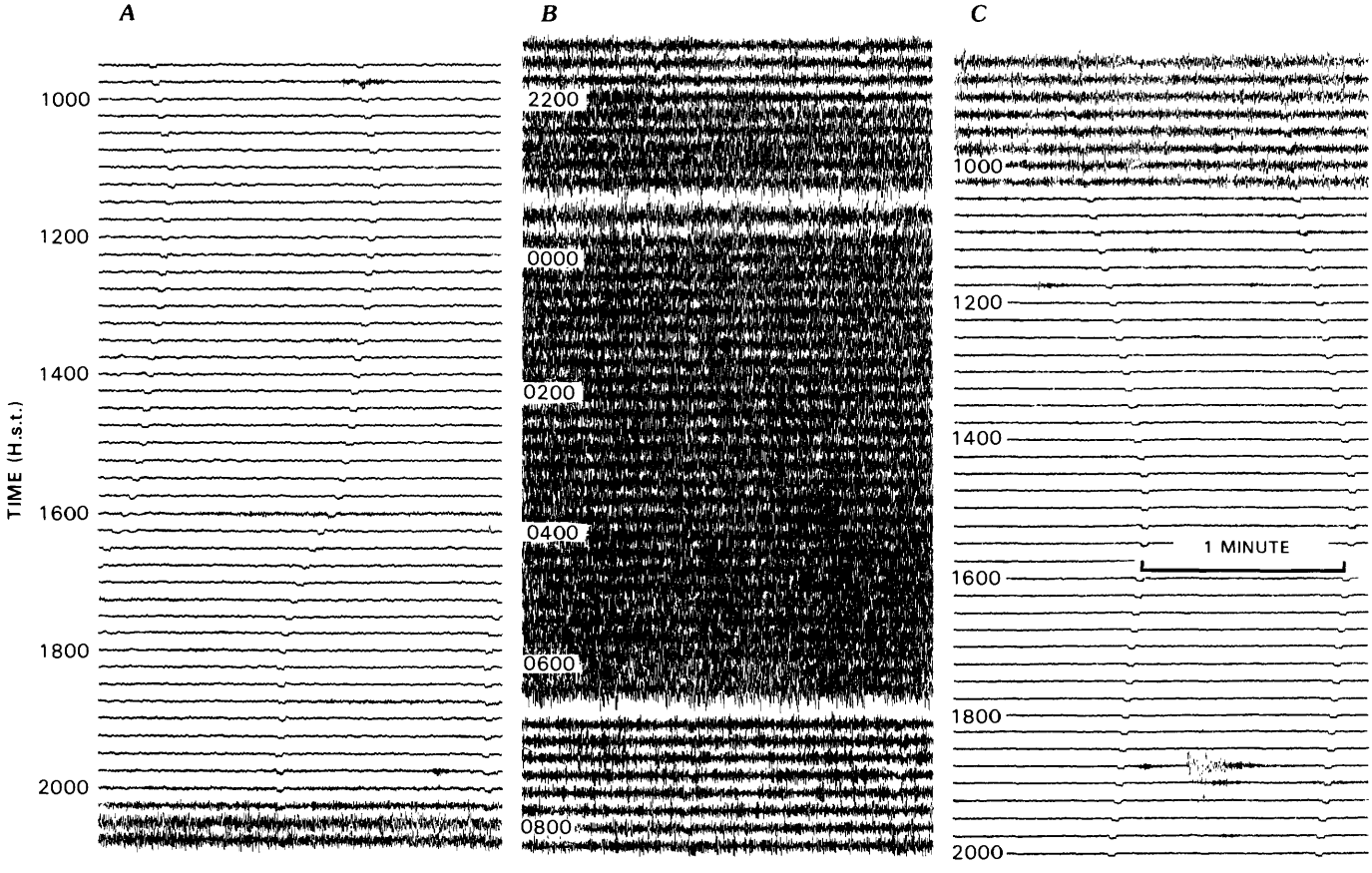

FIGURE 7.15.—Parts of seismograms from rotating-drum recorder at station KAH, located 5 km downrift of active Puu Oo vent, showing changes in tremor amplitude during episode 22 on July 8–9, 1984, at constant instrumental sensitivity. *A*, Tremor amplitude increases after 2000 H.s.t. July 8, at onset of high lava output. *B*, High-level tremor continues during period of high fountaining and lava production. *C*, Tremor amplitude decreases to background level after 1000 H.s.t. July 9, at end of eruptive episode.

were attributed to variations in signal level inherent to local ground conditions and instrumental installation at each station. The station-correction and instrumental-magnification factors were applied in reducing the tremor amplitude read at each station, and the normalized measurements were used to determine attenuation patterns and rates as a function of increasing distance from the source. Tremor signals during high-level activity were read from 30- to 120-s samples of digitized magnetic-tape records and from analyses of Develocorder films. Measurements from portable seismographs, normalized to readings from permanent stations located nearby, were used for additional coverage in critical areas near the eruptive vent. Amplitudes for each station measured at the dominant frequency were averaged for the sample interval, normalized according to instrumental magnification and station correction, and mapped in units of micrometers or nanometers of ground movement. Contour intervals were drawn relative to the station of maximum intensity to outline the areal pattern of attenuation (fig. 7.20). The amplitude pattern may be slightly biased by the seismic-network geometry. The contours indicate that the principal source of tremor is centered near the eruption site, where attenuation outward is radially symmetrical. Beyond a distance of about 5 km, contours are elongate toward the secondary source near the summit. Tremor was recorded at greater distances in early January 1983 than later in June 1984. The amplitude decayed exponentially with distance at rates that appear to increase as a function of time (fig. 7.21). These decay rates are about comparable to those of crustal earthquakes less than 10 km deep in this region.

Tremor was also monitored with a single-component portable system near the eruption area. Such readings as those taken on April 4, 1983, during a period of low and constant eruptive activity, were normalized with readings from a continuously recording permanent station at Puu Kamoamoa; the results are plotted in figure 7.22. The data similarly fit an exponential-decay pattern with a higher rate than that for stronger activity covered on the permanent network stations.

Varying rates of signal attenuation with distance were also determined from strong tremor monitored in real time on a filtered system sequentially at about 5-minute intervals for each station in the network. Data were normalized for instrumental magnification and station corrections, as well as any changes in tremor intensity during the sampling interval, by comparison with a continuously recording standard station, such as MPR or KAH (fig. 7.23). Peak amplitudes, read several seconds apart, were averaged over 3 to 5 minutes of chart record for the signals with center frequencies at 0.625, 1.25, 2.5, 5.0, and 10.0 Hz. Normalized amplitudes at the various stations attenuated with distance exponentially and at decreasing rates for the lower frequencies. Microseismic noise was appreciably higher in the lower frequencies, and at the 0.625-Hz center frequency the signal-to-noise ratio was essentially too low to determine its attenuation rate. The analysis was repeated for samples taken earlier during episode 10 on October 7, 1983, and during episode 16 on March 4, 1984; the results remained reasonably consistent.

Hourly readings of tremor amplitude previously made from station MPR seismograms were translated to a directly proportional unit termed "reduced displacement," introduced by Aki and Koyanagi (1981) and used as a basic index of seismic energy generated from deep tremor beneath Kilauea.[1] The product of reduced displacement and duration of shallow tremor, summit deflation, and the volume of lava extrusion (see chap. 1) during eruptive episodes in 1983 and the first half of 1984 are plotted cumulatively (fig. 7.24). These quantities are closely related, as seen by their parallel rates over most of the time interval. The cause of the slightly lower rates of tremor and lava extrusion relative to the rate of tilt in May-July 1984 is uncertain; it may be partly due simply to the approximateness of the measurements. The short-term, reduced displacement rates of shallow tremor during this continuing eruption until July 1984 measured about 80 times higher than the long-term rate of deep tremor beneath Hawaii determined by Aki and Koyanagi (1981).

The height of lava fountains commonly associated with eruptive rate was a partial measure of tremor intensity. Obvious correlations existed during large changes in eruptive activity, as observed consistently at the start and end of eruptive episodes. Fountaining and tremor were both characterized by constant repetitions of amplitude bursts at intervals of a few seconds apart, but many of the minor relative changes in amplitude over longer intervals of minutes or hours did not correlate. This discrepancy suggests the involvement of additional factor(s) that we cannot clearly identify, separating the source of tremor and the driving force of lava fountaining.

---

[1]Reduced displacement (RD) is a function of tremor amplitude corrected for geometric spreading:

$$RD = \frac{A}{2\sqrt{2}} \cdot \frac{r}{M},$$

where A is the peak-to-peak amplitude, r is the station-to-source distance, and M is the instrumental magnification. This formula is based on deep tremor recorded at relatively short epicentral distances and dominated by body waves. For shallow tremor recorded at relatively large epicentral distances, where Raleigh waves predominate, the calculation for reduced displacement was slightly revised by Fehler to accommodate Raleigh waves rather than body waves (Fehler, 1983). The records used in this chapter to determine reduced displacement were taken from stations near the epicentral region, and so Aki's original formula was applied (Aki and Koyanagi, 1981). If source amplitude is extrapolated from the exponential-decay pattern as expressed in figure 7.21, the reduced displacement determined from the record of station MPR at a distance of 6 km would be about double. In any case, the choice of equations should not seriously affect our aim in determining relative time patterns for the tremor generated.

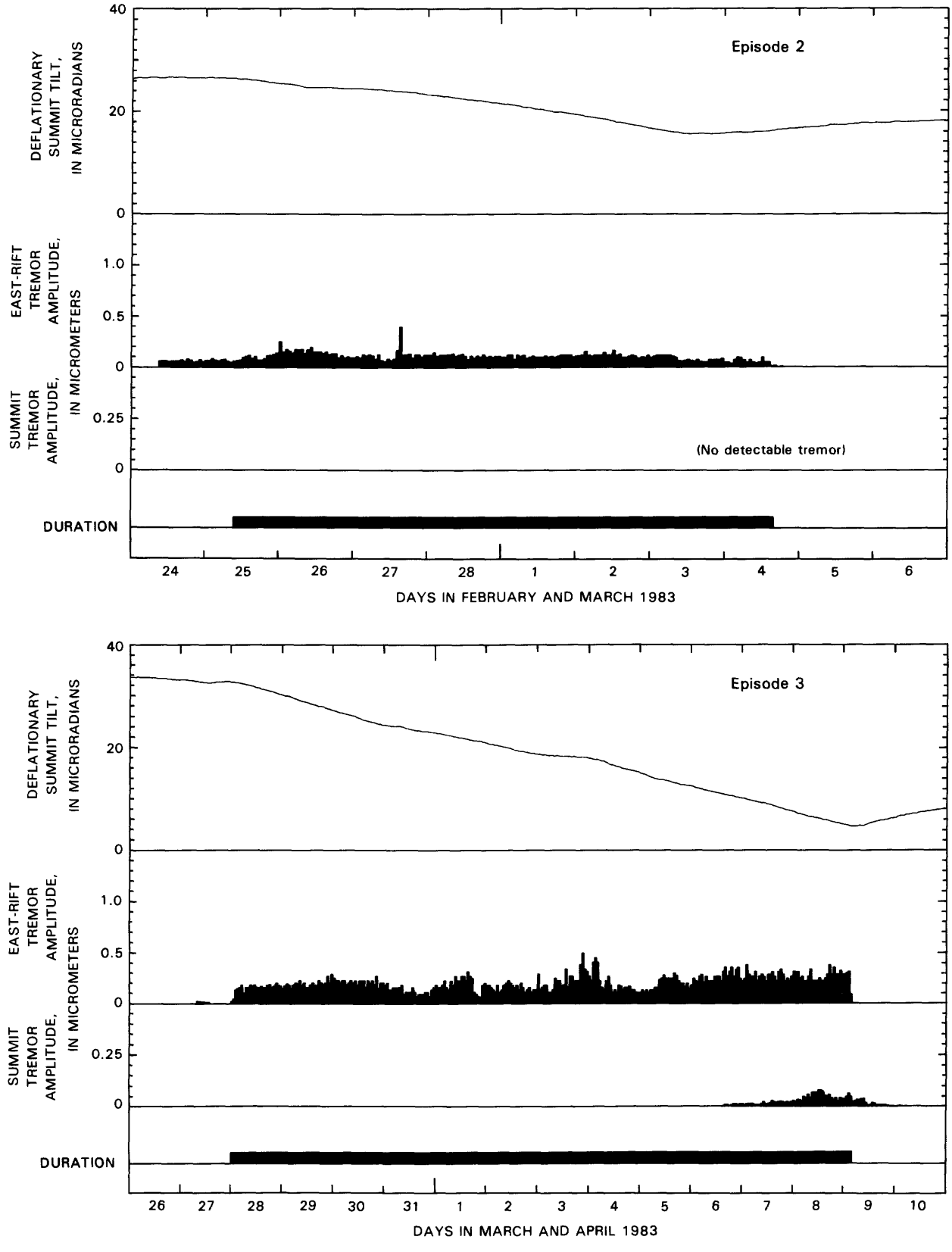

FIGURE 7.16.—Deflationary summit tilt, amplitudes of east rift tremor at station MPR, amplitudes of summit tremor at station NPT, and duration of eruptive episodes 2 to 23. Summit tilt was measured from hourly readings on east-west component of the Ideal-Aerosmith tiltmeter at Uwekahuna (see fig. 7.12). Tremor amplitudes and apparent frequencies on Develocorder seismograms from stations MPR and NPT were averaged for several consecutive minutes at hourly intervals for times of significant-

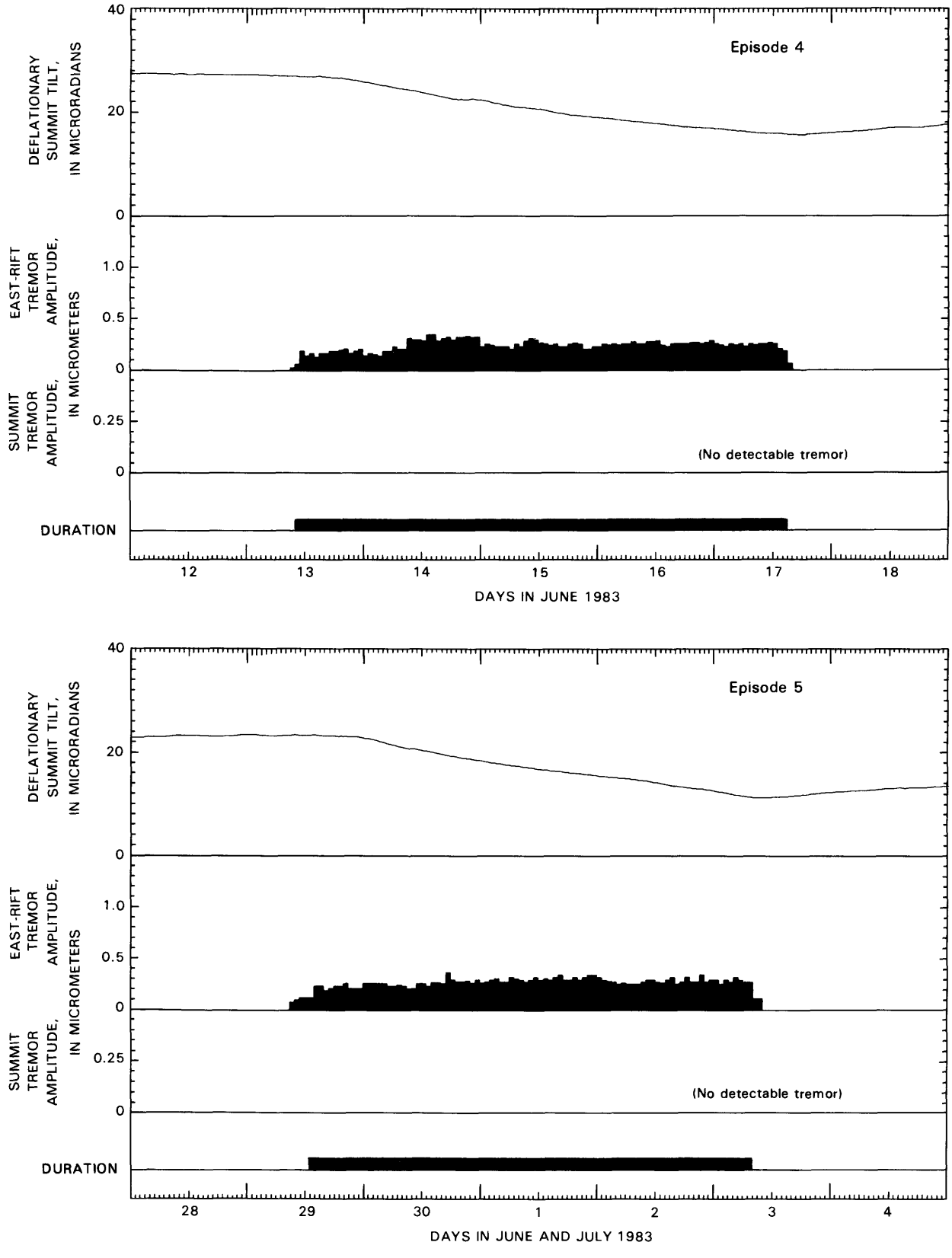

ly higher than background tremor, and reduced to ground displacement according to instrumental response at recorded frequency of the signal. Note difference in vertical scale to accommodate generally lower amplitudes of summit tremor. Horizontal (time) scale was varied to accommodate the generally shorter and more rapid changes in activity during later episodes. Times of eruptive episodes, defined by horizontal bars at bottom of the plots, correspond to those in chapter 1.

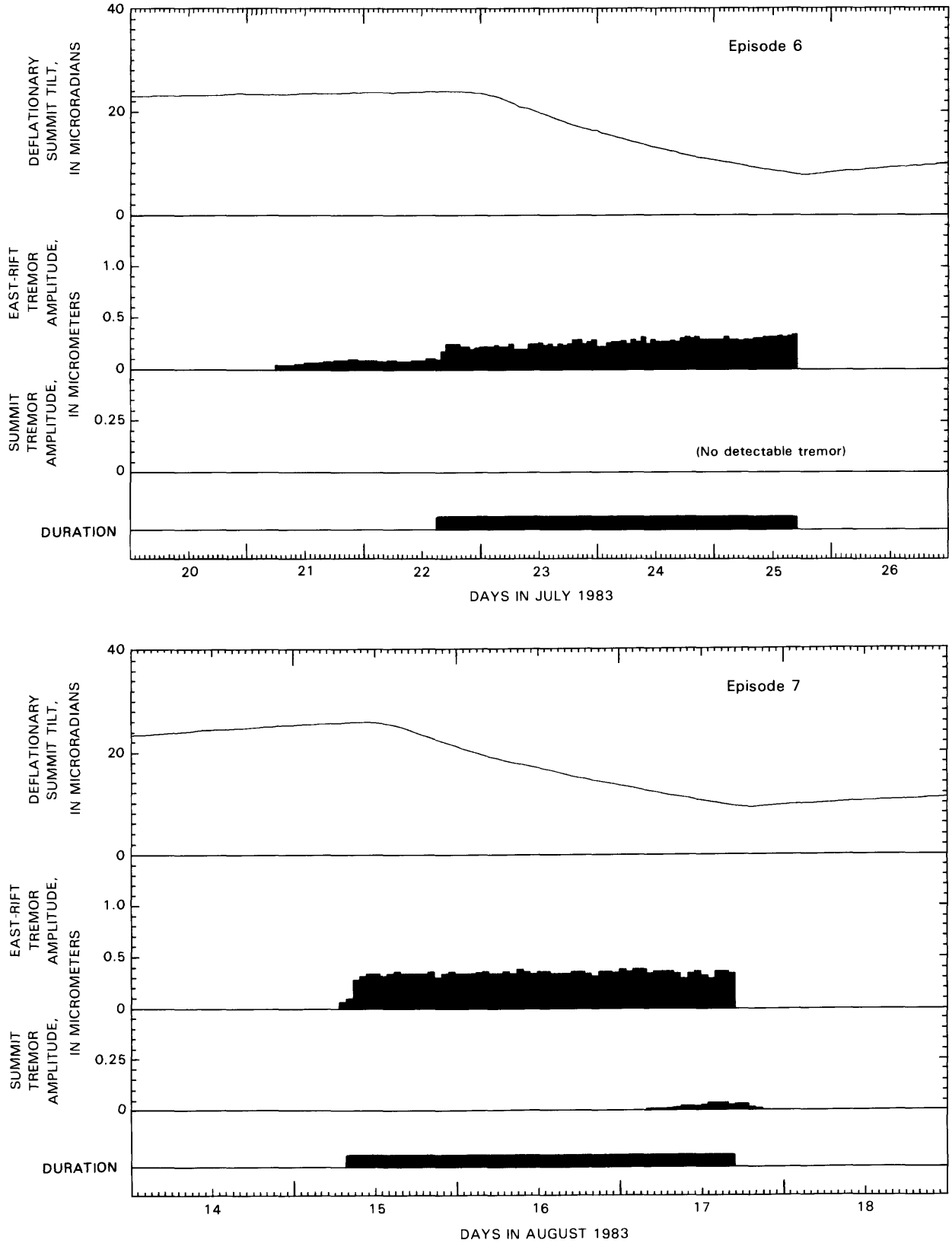

FIGURE 7.16.—Continued

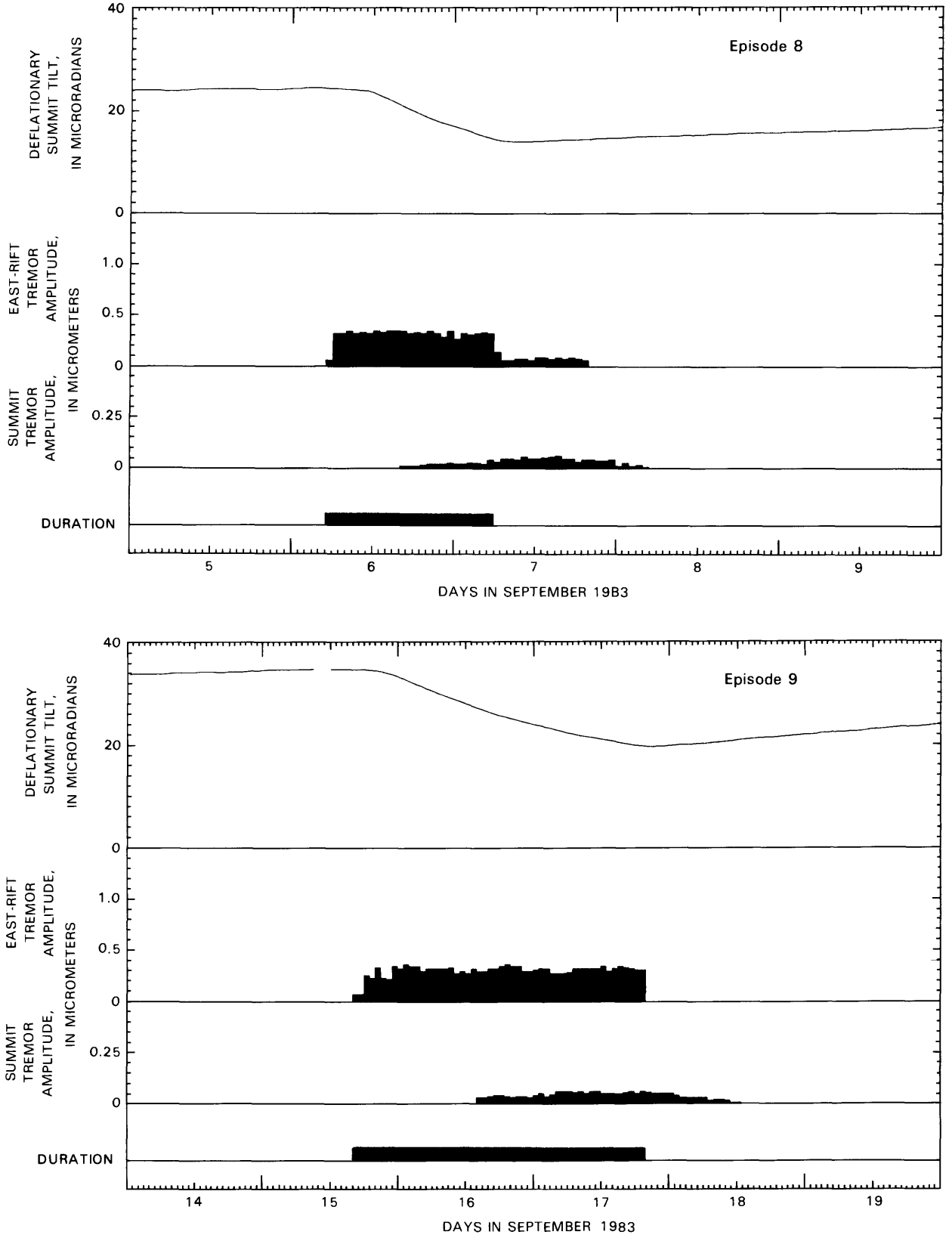

FIGURE 7.16.—Continued

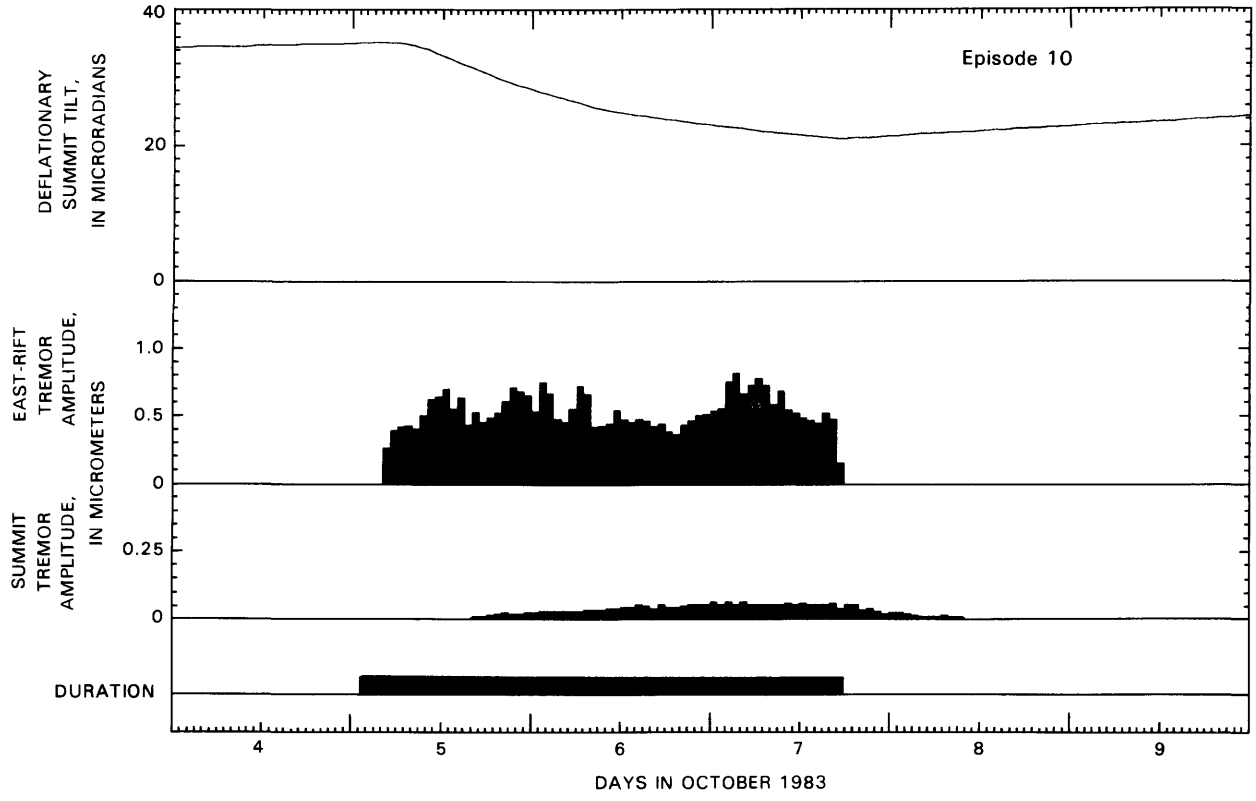

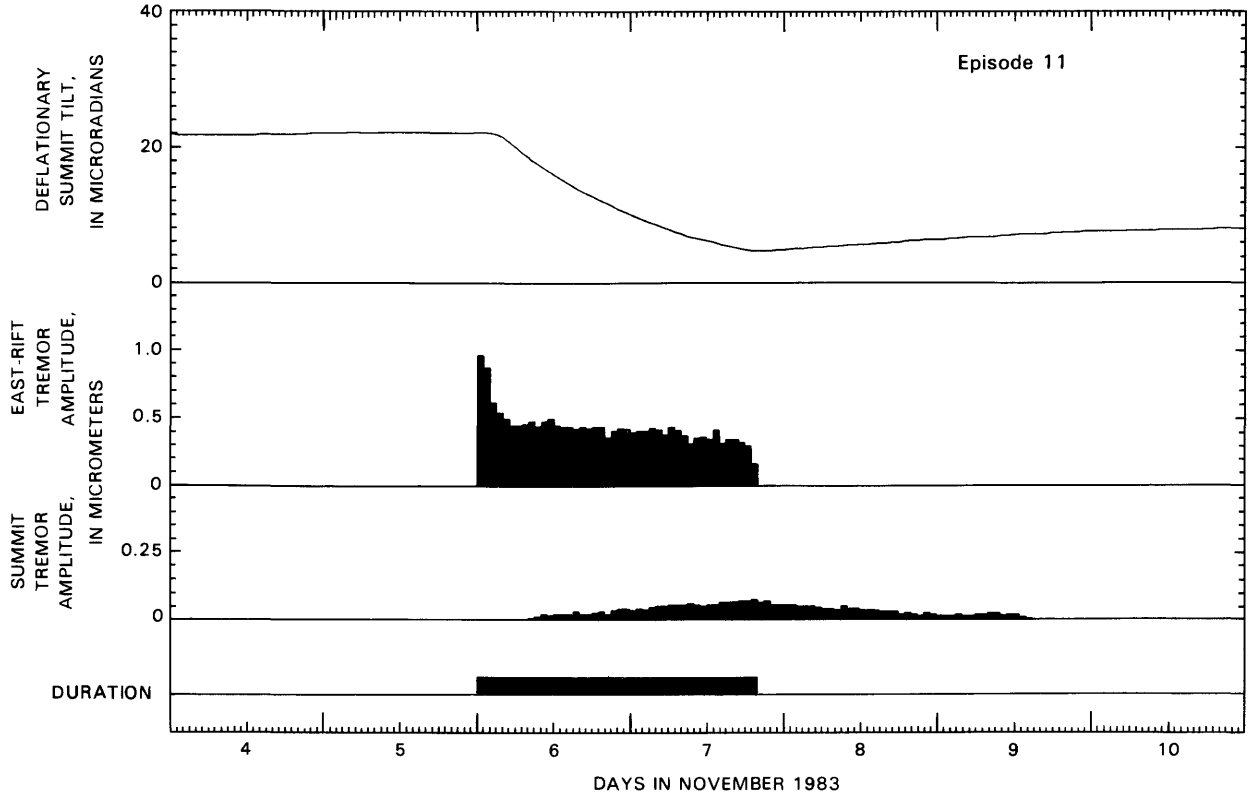

FIGURE 7.16.—Continued

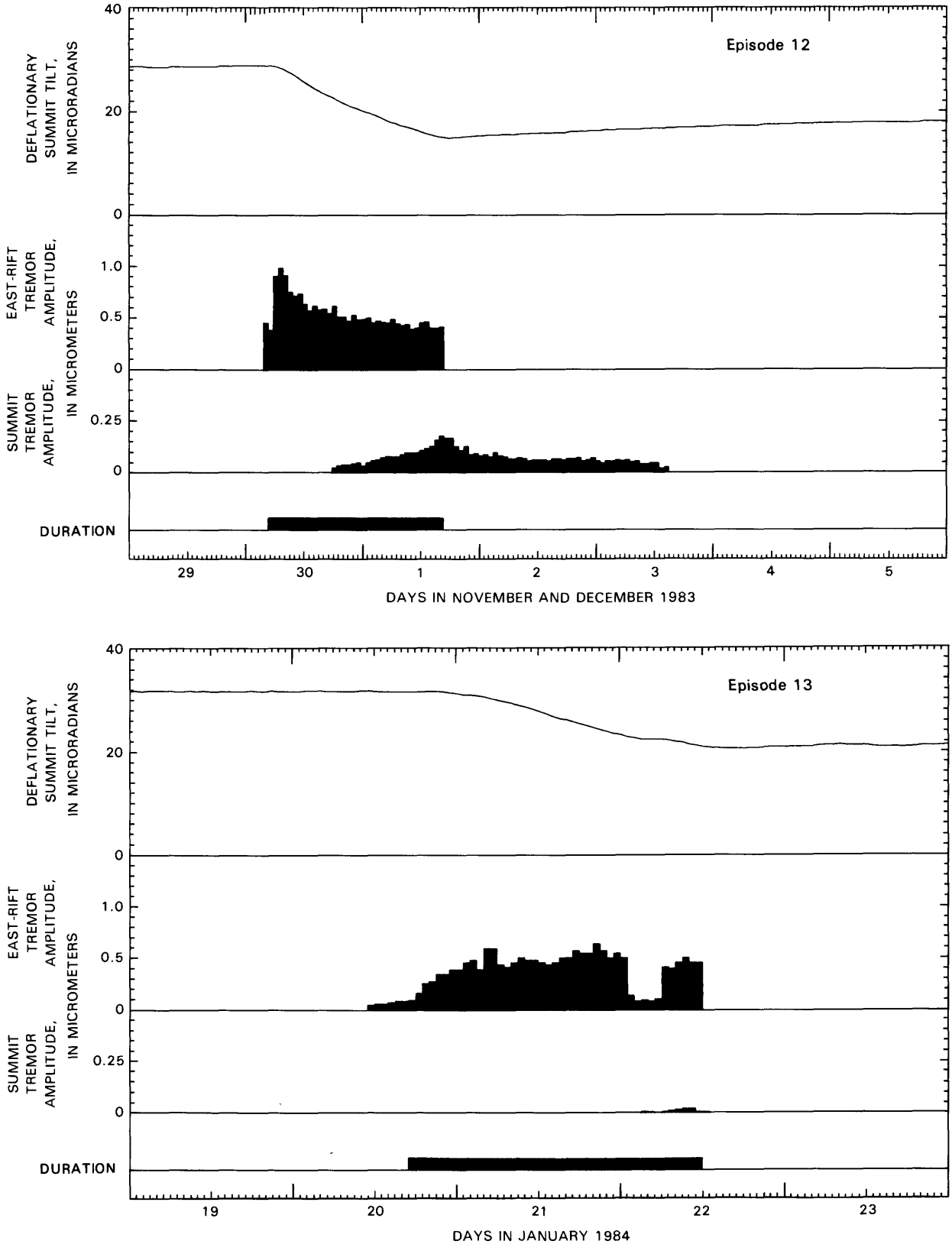

FIGURE 7.16.—Continued

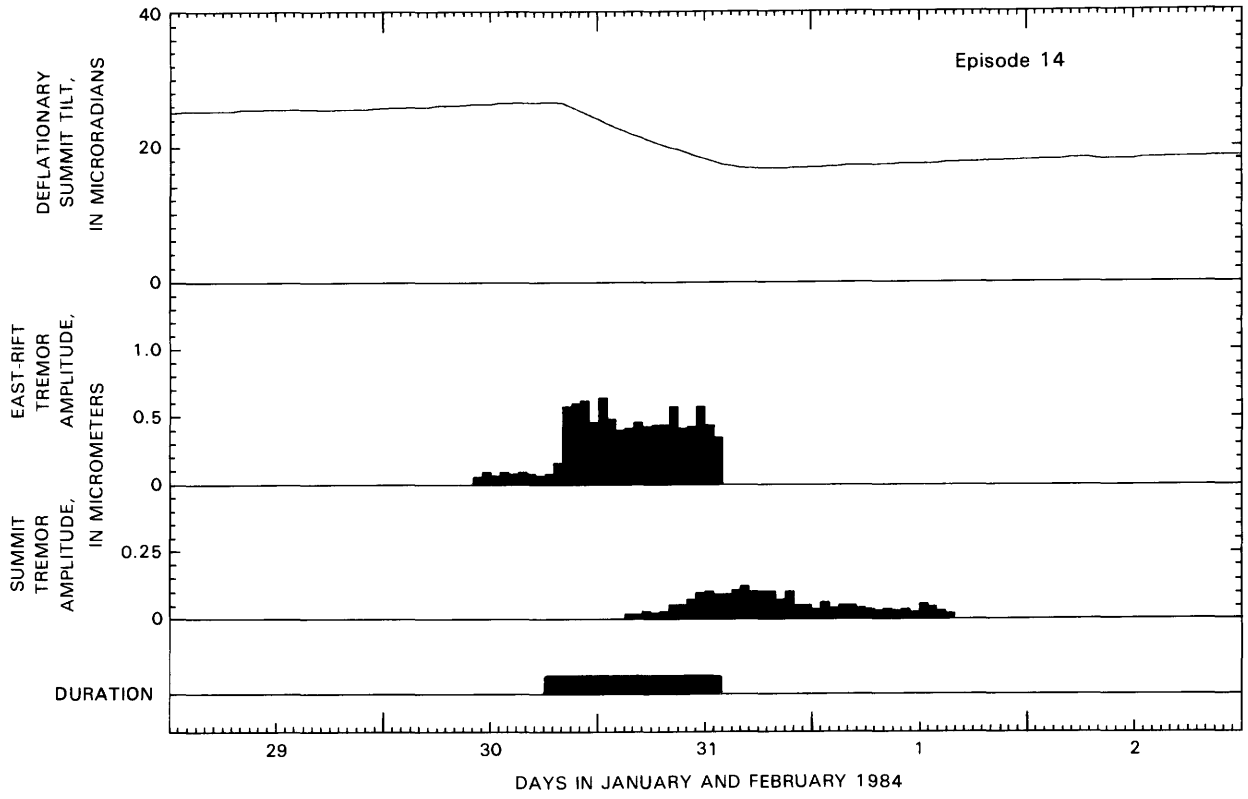

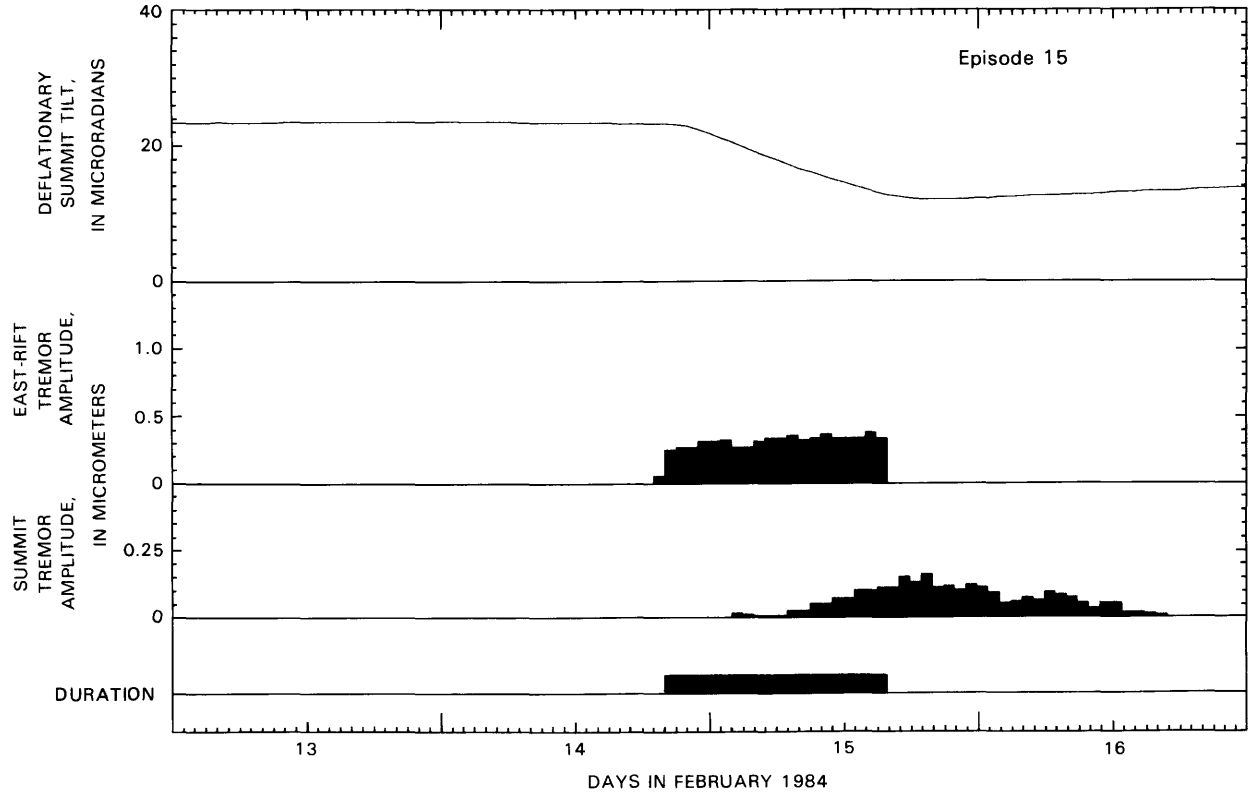

FIGURE 7.16.—Continued

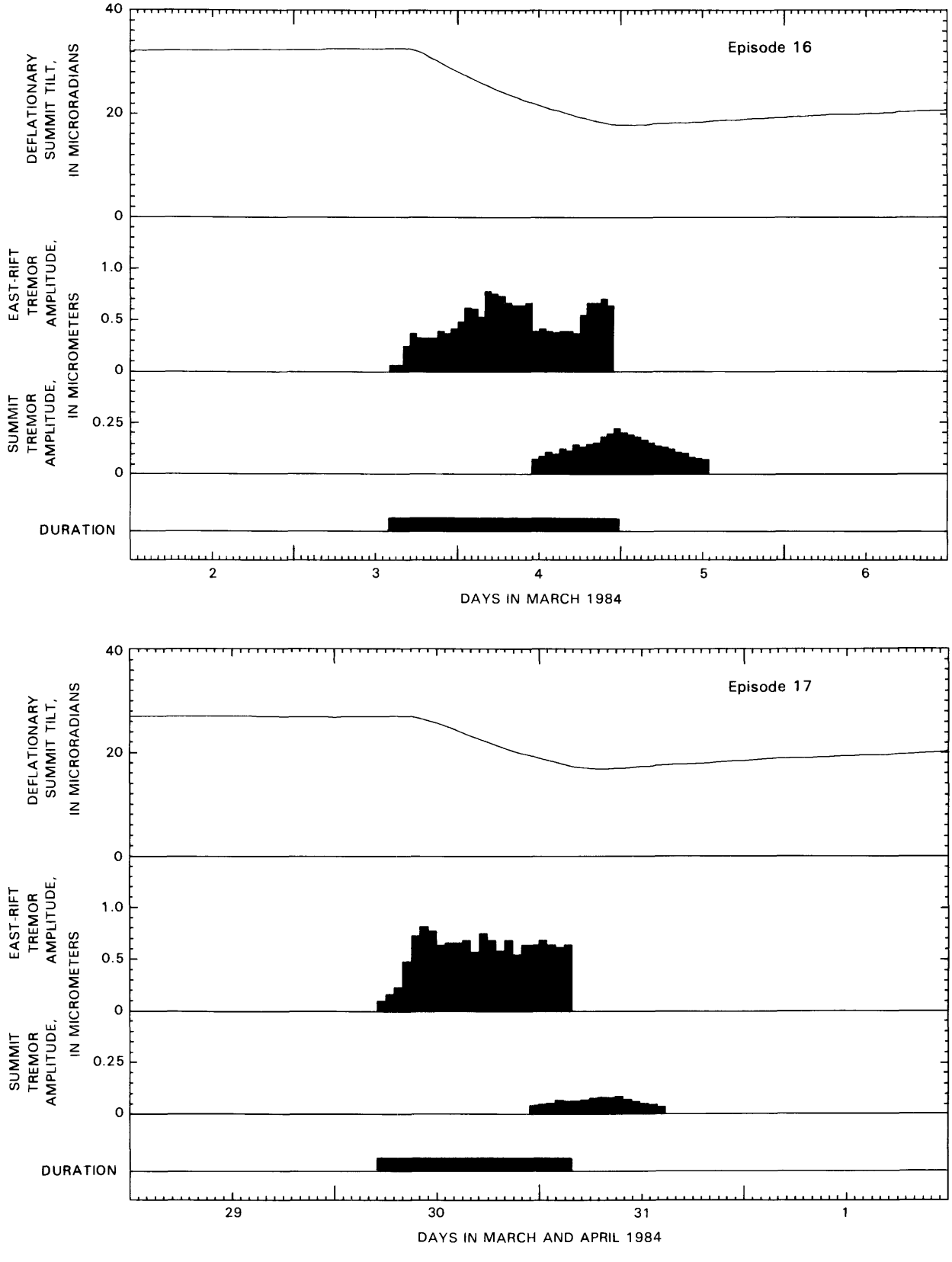

FIGURE 7.16.—Continued

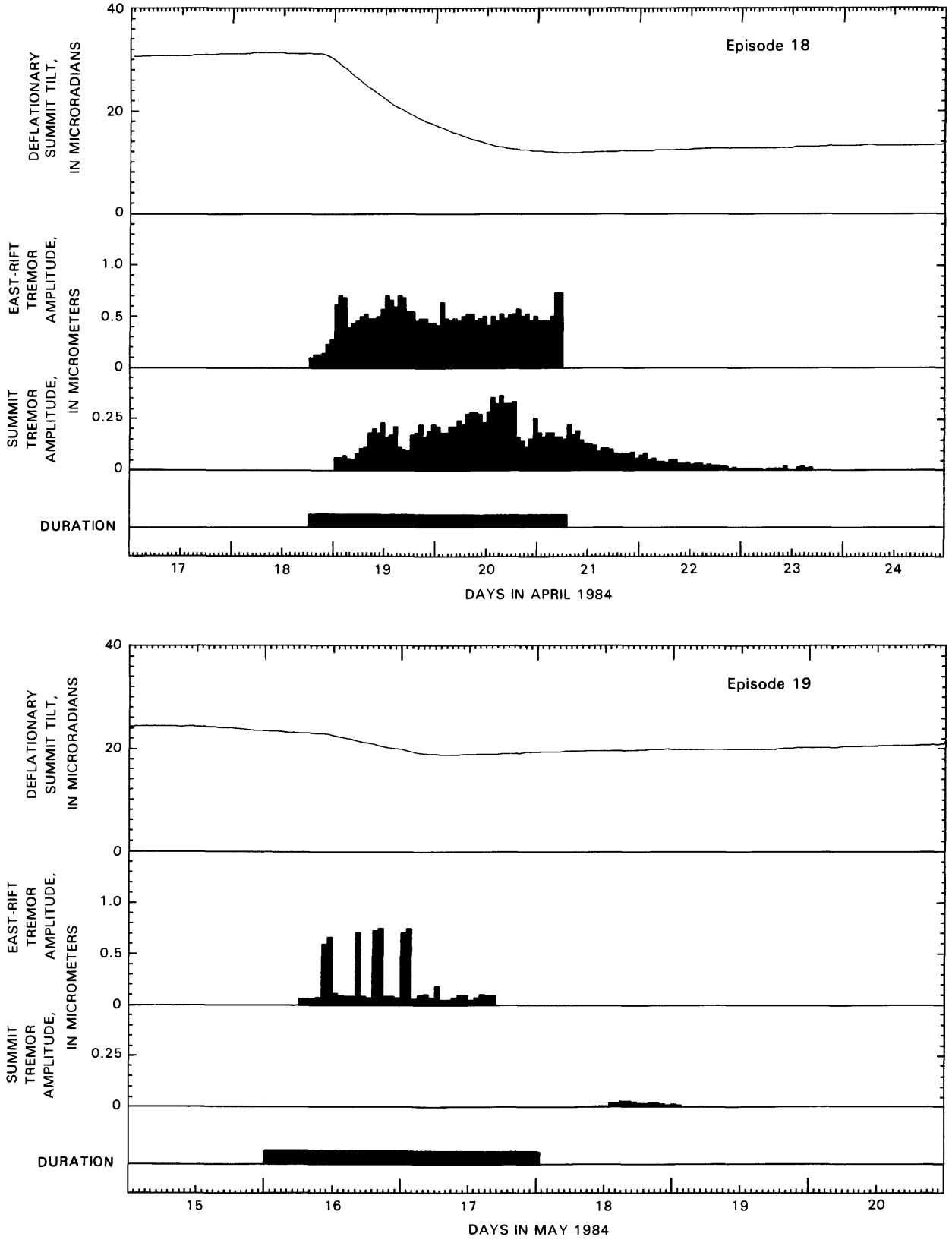

FIGURE 7.16.—Continued

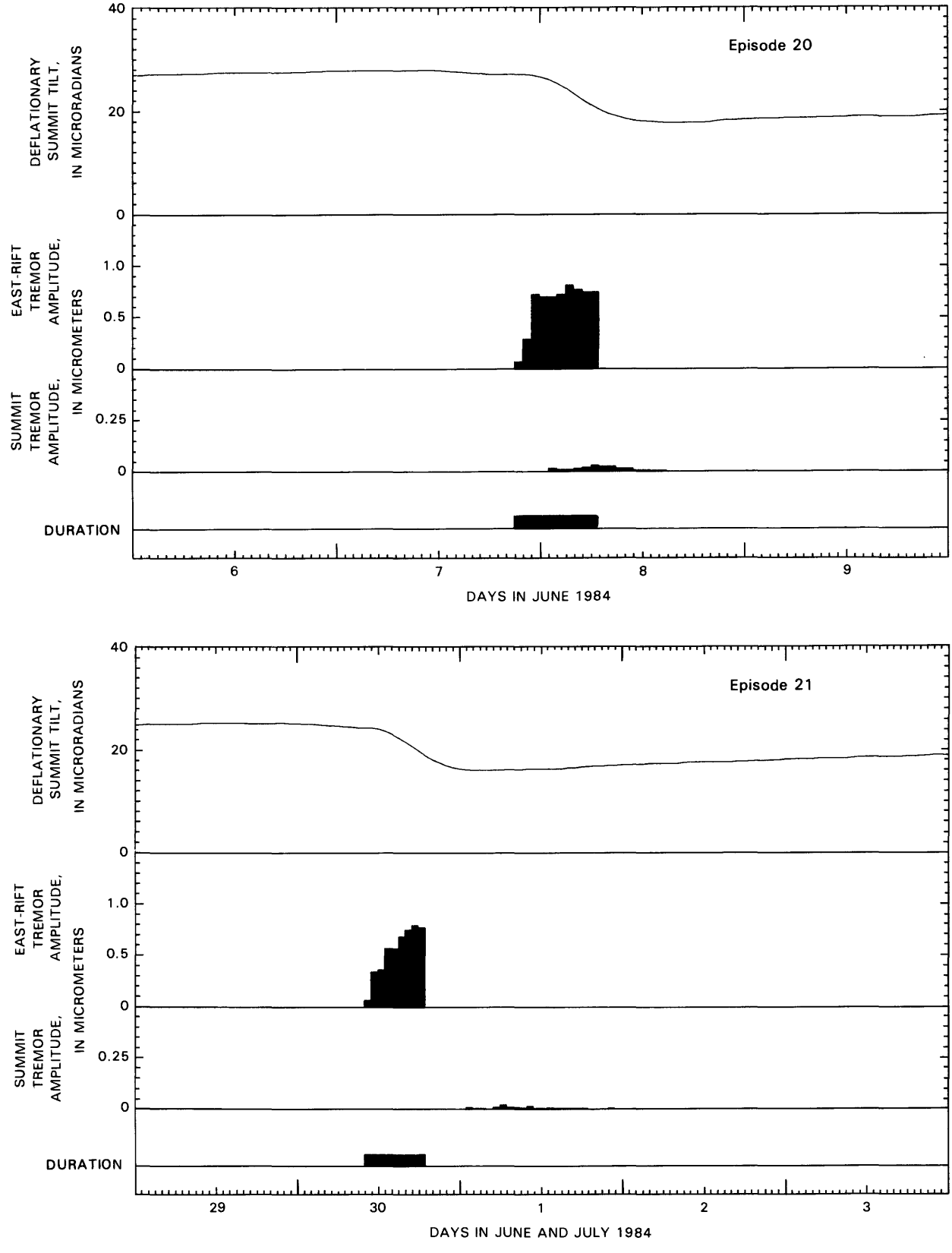

FIGURE 7.16.—Continued

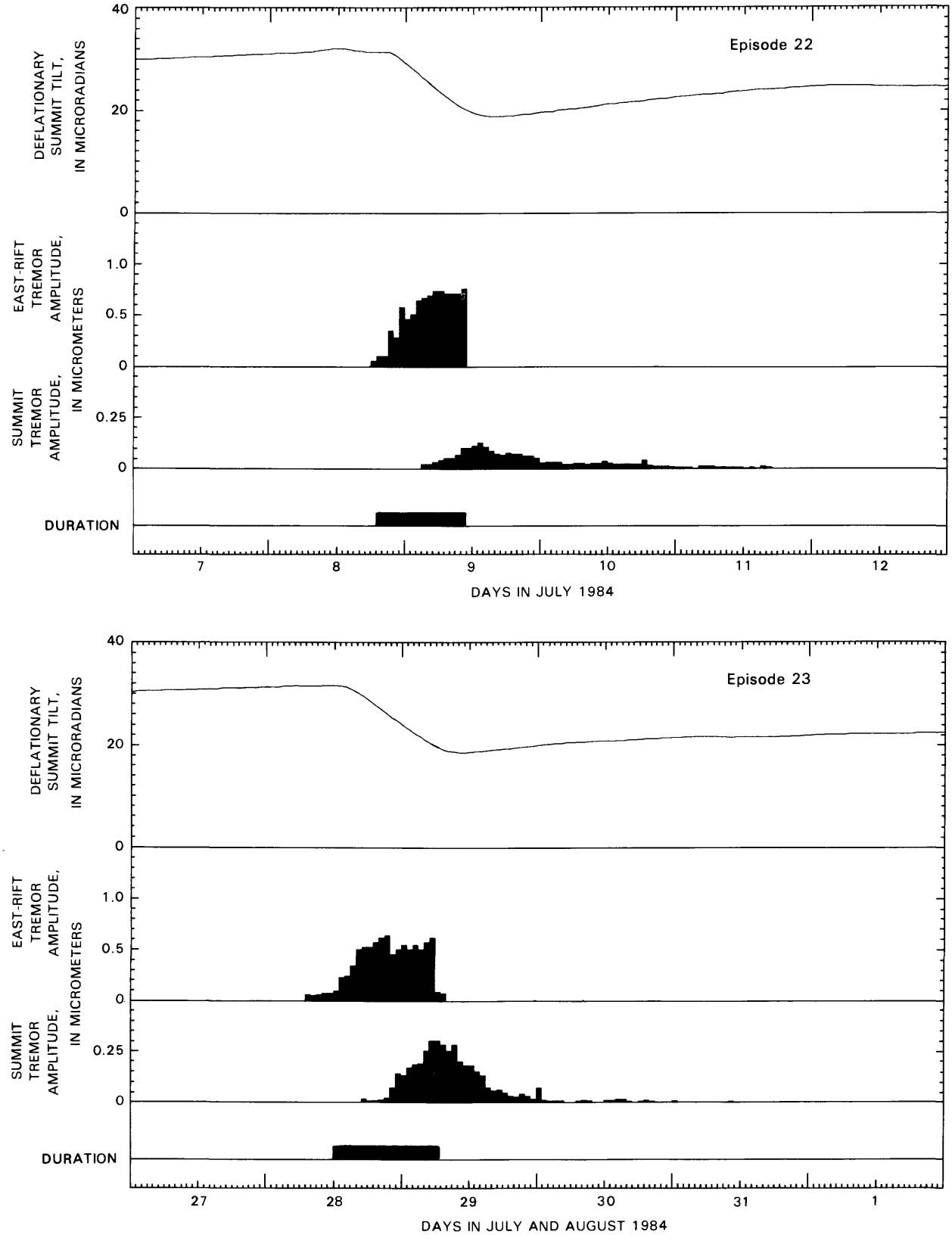

FIGURE 7.16.—Continued

SEISMIC EVENTS IN THE EAST RIFT ZONE BETWEEN ERUPTIVE EPISODES

Low-level harmonic tremor continued in the east-rift eruption area between eruptive episodes. As detected at station KMM (or PUK), less than 1 km from the principal vent, this background tremor at about 3 Hz was at least one-tenth that of the intense tremor connected with times of major lava outbreaks. Tremor amplitude could be constant and sustained for many days, varying at intervals of many minutes to several hours, or fluctuate with 1-minute bursts at intervals of a few to about 15 minutes (fig. 7.25). Amplitude changes of the weak tremor between eruptive episodes were typically minor, ranging from barely detectable to nearly 10 times larger. Also recorded above the low-level background tremor were high-frequency (higher than approx 5 Hz) events associated with rockfalls and degassing explosions at the active vent, and with fracturing from contraction during the cooling of fresh lava flows. These events generally numbered from several tens to many hundreds per day on station KMM seismograms. The sequence of low-level activity leading to eruptive episodes varied, and no consistent precursory seismic pattern could be identified. The gradual increase in the frequency of microearthquakes that accompany inflationary tilt at the summit (see next subsection) provided limited indication for eruption probability based on the state of stress within the summit storage system. In a few cases, relatively constant, low tremor at the eruptive vent developed erratic changes in amplitude before a rapid increase marking the onset of a new outbreak (fig. 7.26).

The 1-minute bursts of tremor at intervals of a few minutes to about 15 minutes sometimes continued for many days. These bursts correlated with the pattern of minor lava movement within the active vent, at times when the system was open and visible. A gradual rise of the magma column accompanied by very low tremor was periodically disrupted, presumably at a critical state of pressure, by relatively vigorous spattering, degassing, and drop of the magma column during about a minute of increased tremor. The tremor developed and decayed symmetrically in amplitude. These bursts of tremor, recorded with signals filtered from the nearby station KMM instrument, peaked on the 2.5-Hz channel and were as much as several times above the background amplitude (fig. 7.27). The "cyclic" pattern of low lava oscillations in the active vent, also observed during the 1969–72 Mauna Ulu eruption, was appropriately termed "gas piston" activity (Swanson and others, 1979). The seismic tremor associated with this type of activity is further described by Koyanagi and others (1987).

SEISMIC EVENTS AT THE SUMMIT

In addition to the occasional deep tremor and LP events tracing the magma source to the mantle, shallow seismic events reflected ground-deformation changes at the summit during the ongoing eruption in the east rift. Normal, high-frequency microearthquakes gradually increased in number during the inflationary tilt before eruptive episodes, as indicated by the daily count of SP earthquakes in figure 7.10. Summit seismicity ranged from less than 50 shocks per day after an eruptive episode to about 100 to 200 events per day at critically inflated stages of the summit before outbreaks. This pattern became pronounced after about June 1983. The numbers of SP events dropped after the sharp deflations that accompanied eruptive episodes.

The summit station NPT recorded a conspicuously independent pattern of tremor from that of east-rift stations closer to the eruption site (fig. 7.16). A moderate increase in tremor amplitude was detected repeatedly after a continuing high rate of summit deflation during eruptive episodes in the east-rift zone. Typically, the signal increased gradually and peaked several to many hours after the start of high rates of lava output and summit subsidence. Tremor amplitude decayed to background levels at a rate equal to or more gradual than the rate of its onset. Many eruptive episodes started with a slow increase of discrete LP events that developed into higher amplitude and continuous harmonic tremor. This continuous tremor evolved into a succession of LP events as the signal decreased to background levels, and smaller LP events occurred at increasingly wider intervals of time (fig. 7.28). This evolution accounts for the repeated high count of LP earthquakes after eruptive episodes, as shown in figure 7.12.

This tremor and LP events peak around 2.5 Hz from filtered signals at station NPT, after allowances are made for instrumental magnification and a naturally high background of microseisms in the lower frequencies near 1 Hz (fig. 7.29). The tremor lasts from about 1 to many days, and amplitudes range from about a detectable level of 0.05 to a peak of 0.35 μm, as indicated in figure 7.16. Locations calculated for a few adequately recorded LP events that were associated with tremor indicate a source region a few kilometers beneath the inflation/deflation epicenter in the southern caldera region. Summit tremor generally reached a detectable level after a rapid deflation event sustained for a few to many hours. The duration and amplitude of tremor increase with the amount and rate of deflation. This relation, to within about an order of magnitude, can be shown by plotting square roots of the product of reduced displacement and duration of

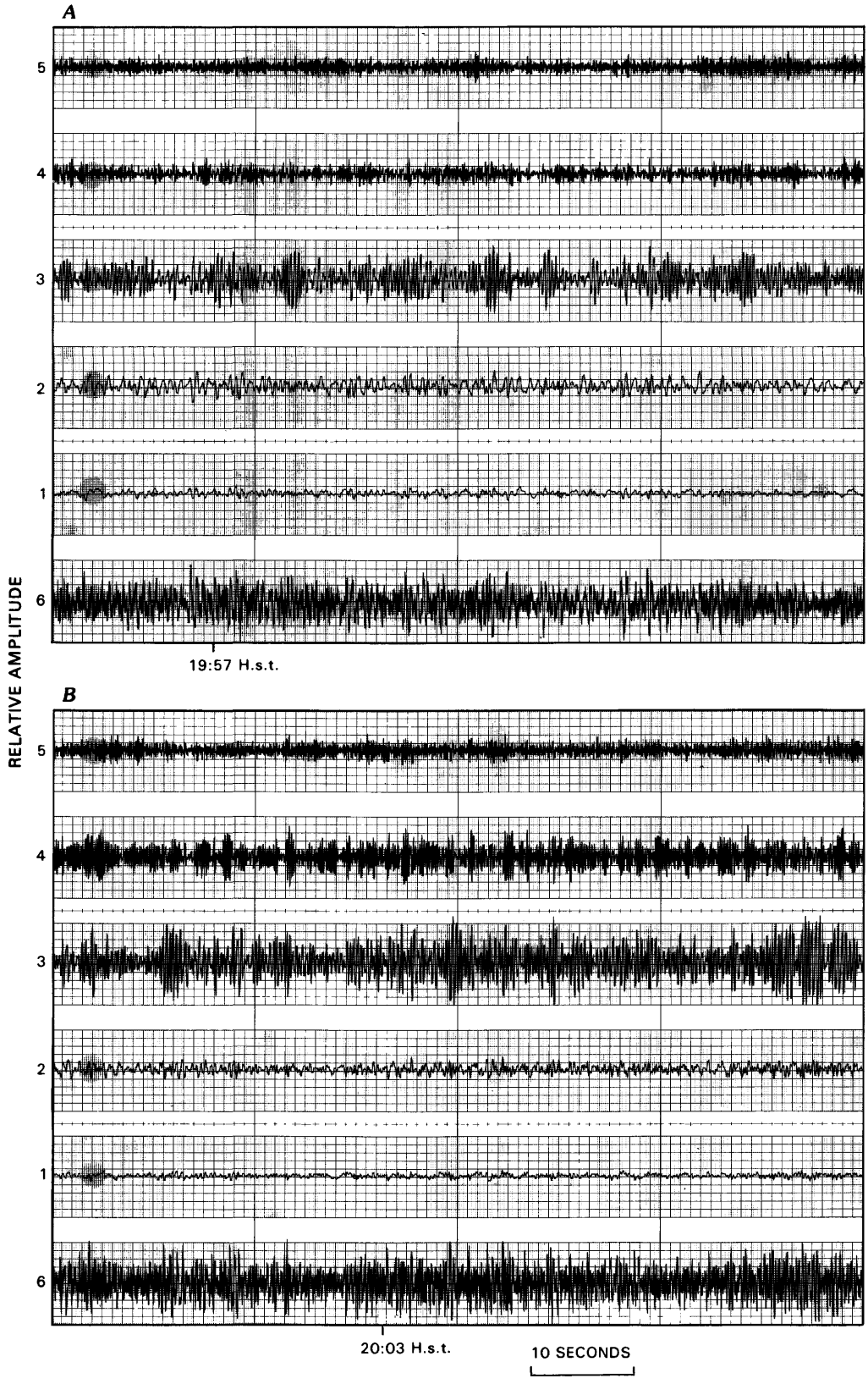

FIGURE 7.17.—East-rift tremor recorded during episode 23 on July 28, 1984, at station MPR (*A*), located 6 km uprift of eruptive vent; station KAH (*B*), located 5 km downrift of vent; and stations KMME (*C*) and (*D*) KMMN (east-west and north-south components, respectively, of station KMM), located within 1 km of vent. Signal on channel 6 in figures 7.17*A* and 7.17*B* is unfiltered HVO Type 1 system, and in figures 7.17*C* and 7.17*D* is unfiltered Wood-Anderson type; signals on channels 1 through

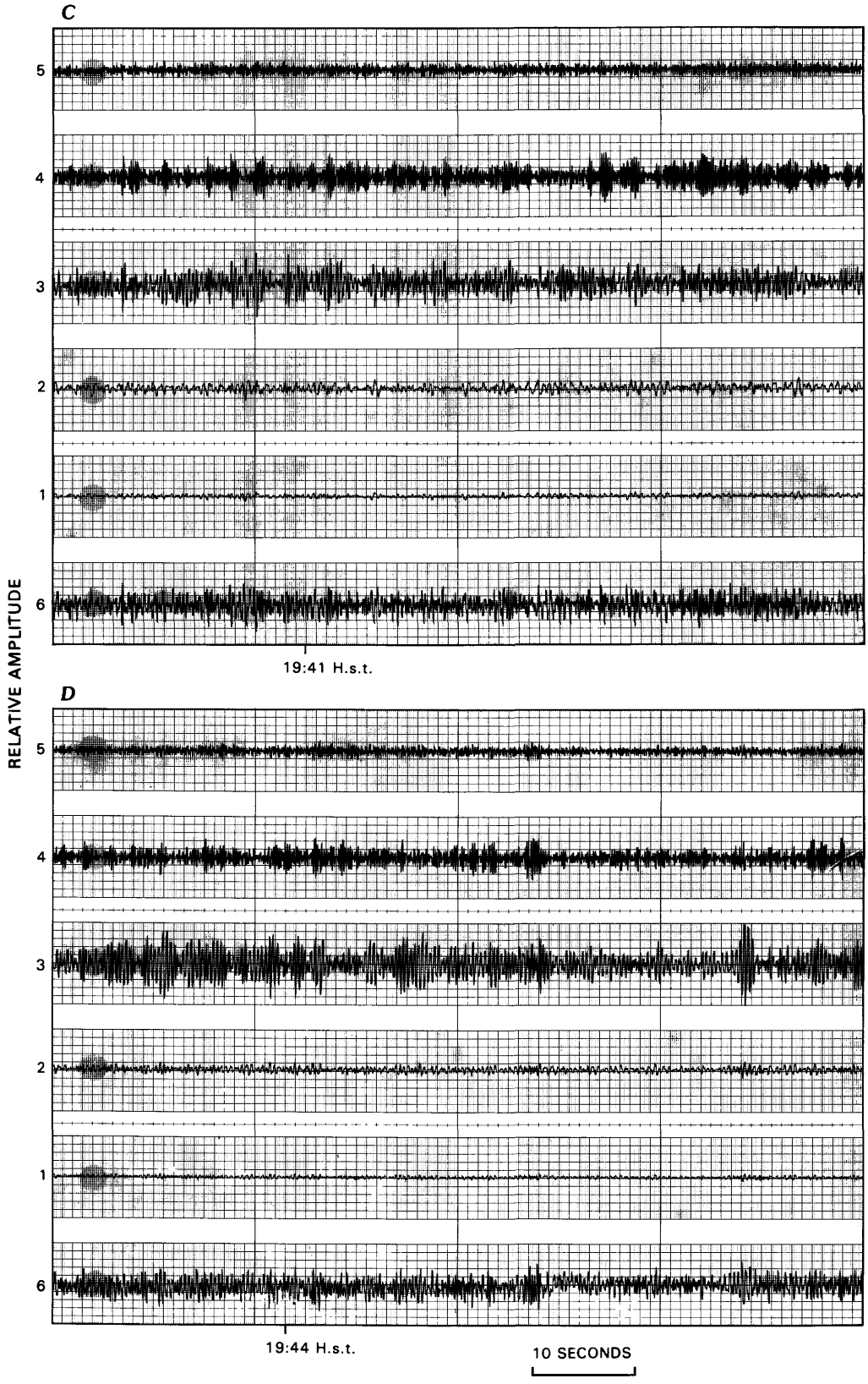

5 are filtered. Peak responses and relative magnifications for filtered channels in figures 7.17*A* and 7.17*B*: 1, 0.625 Hz at ×2; 2, 1.25 Hz at ×10; 3, 2.5 Hz at ×26; 4, 5.0 Hz at ×60; and 5, 10.0 Hz at ×100. Peak responses and relative magnifications of filtered channels in figure 7.17*C* and 7.17*D*: 1, 0.625 Hz at ×1; 2, 1.25 Hz at ×1; 3, 2.5 Hz at ×1; 4, 5.0 Hz at ×1; and 5, 10.0 Hz at ×1.

tremor against that of the product of amount and rate of tilt (fig. 7.30). The tremor source was estimated to be a few kilometers beneath the southern caldera region, and the signal recorded at station NPT, located about a kilometer from the epicenter, was assumed to be dominated by body waves. Therefore, reduced displacement for the summit tremor was calculated from the same formula that Aki and Koyanagi (1981) used for reduction of deep Kilauea tremor.

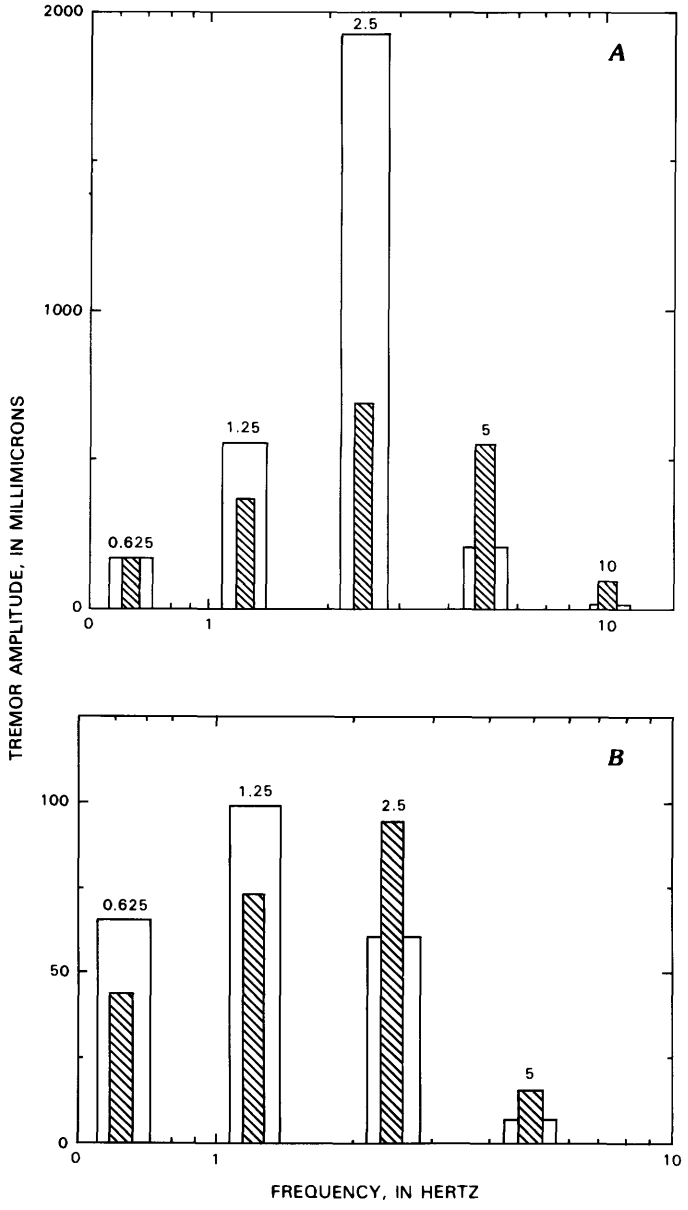

FIGURE 7.18.—Tremor amplitude normalized from two selected 5-s samples (open bar, hachured bar) of filtered signals at various center frequencies as indicated. *A*, Station PUK, 0655 H.s.t. October 7, 1983. *B*, Station MPR, 0658 H.s.t. October 7, 1983.

This relation between tremor amplitude and summit tilt is simply described in the common units of measurements here, and further reduction to quantitatively related units will be left to future analysis. Conversion of east-west tilt to vertical ground displacement at the deflation epicenter, averaged at 9 mm/microradian from data collected between 1983 and mid-1984 (Ronald Hanatani, oral commun., 1986), could initiate a quantitative comparison of tremor and tilt at the summit. Shifting of the center of tilt over time that changes the tilt/vertical-displacement ratio must be considered in processing the data.

CHRONOLOGY OF EVENTS, 1978–83

A concentration of earthquakes less than 5 km deep in the middle east rift zone near Puu Kamoamoa became increasingly apparent after November 1978 (Wolfe and others, 1987). The locus of this increasing activity was uprift from the major eruption site at and near Puu Kiai in September 1977 (Moore and others, 1980). Between April and August 1980, a series of minor swarms of shallow earthquakes, centered in the east rift near Puu Kamoamoa, increased in number and alternated with bursts of shallow, inflation-related summit earthquakes. This pattern of seismicity, in combination with the cumulative inflation of the middle east rift zone indicated by field tilt surveys, was interpreted by Dzurisin and others (1984) as discrete pulses of deep magma rising to feed the shallow summit storage system, and subsequent transfer of melt into the plumbing connecting the summit region and the east rift zone. This pattern was interrupted on January 20, 1981, by a swarm of shallow earthquakes and changes in ground deformation that indicated magma intrusion into the southwest rift zone. This event marked the beginning of a series of at least three definable intrusions into the southwest rift zone that lasted until August 1981. Two short summit eruptions occurred on April 30 and September 25, 1982. During the second eruption, shallow earthquakes migrated from the eruption area in the caldera to the upper east rift zone. Over the next 3 months, oscillations in seismicity and ground deformation implied resumption of intrusive activity in the east rift. During the episodic, intrusion-related seismicity in the middle east rift zone after the September 1977 eruption until the outbreak in January 1983, no significant swarms of shallow earthquakes were reported east of the Puu Kamoamoa-Puu Kahaualea locality.

Daily counts of earthquakes reached several hundred to more than a thousand per day during intrusive events in September-October and again in December 1982. In both sequences, the peak of summit seismicity was followed by migration of shallow (0–5 km deep) earthquakes from the summit into the east rift. The activity in

December developed into an intense swarm of upper-east-rift earthquakes that, early on January 2, 1983, moved progressively downrift and farther into the east rift.

At 0030 H.s.t. January 2, 1983, the seismicity beneath Kilauea's east rift zone was augmented by a marked increase in the number of earthquakes and an emerging background of low-level tremor. The final preeruption seismic swarm, which started near Mauna Ulu, increased and migrated 6 km downrift to beyond Napau Crater at a maximum rate of about 0.7 km/h. Beginning with 3 to 5 small earthquakes per minute, the seismic intensity increased at 0040 H.s.t. By 0600 H.s.t., several earthquakes of $M = 2.0$-2.7 were felt in the nearby Volcano and Hawaii Volcanoes National Park housing areas, about 1 and 5 km north of Kilauea caldera, respectively.

From about 0600 to 1300 H.s.t. January 2, the seismic zone spread farther downrift to beyond Puu Kamoamoa. From then until the onset of the first outbreak, the rate of small and shallow earthquakes was nearly constant, mainly beneath a zone between Napau Crater and Puu Kamoamoa. Low-level harmonic tremor persisted during this interval. At 0031 H.s.t. on January 3, lava was sighted at Napau Crater, and seismographs recorded increasing harmonic tremor, especially at the Makaopuhi station (MPR) about 2 km west of Napau Crater. The eruption advanced downrift, and the locus of highest tremor shifted from station MPR to the station near Puu Kamoamoa (PUK). At 1000 H.s.t., the eruption momentarily subsided, and tremor decreased. Low-level tremor continued, and small earthquakes increased in number east of Puu Kamoamoa. Tremor intensity increased sharply at the Kalalua station (LUA) when eruptive activity renewed its vigor at 1425 H.s.t. at a site downrift of Puu Kamoamoa, but subsided an hour later as lava output ended. Low-level tremor continued for more than a day.

The number of small earthquakes and the amplitude of harmonic tremor slowly increased near the eruptive fissures east of Puu Kamoamoa, and then activity gradually migrated uprift to the vicinity of Napau Crater until the afternoon of January 6. An increase in the number of earthquakes on the morning of January 5 was followed by resumption of lava fountaining and high-level tremor at 1123 H.s.t. The change in activity from the middle of January 3 to early January 5, characterized by a temporary cessation of eruption, uprift migration of earthquakes, and tilt reversals indicating reinflation of the summit (figs. 7.9, 7.14), has been interpreted as due to a temporary blockage in the conduit system beneath the

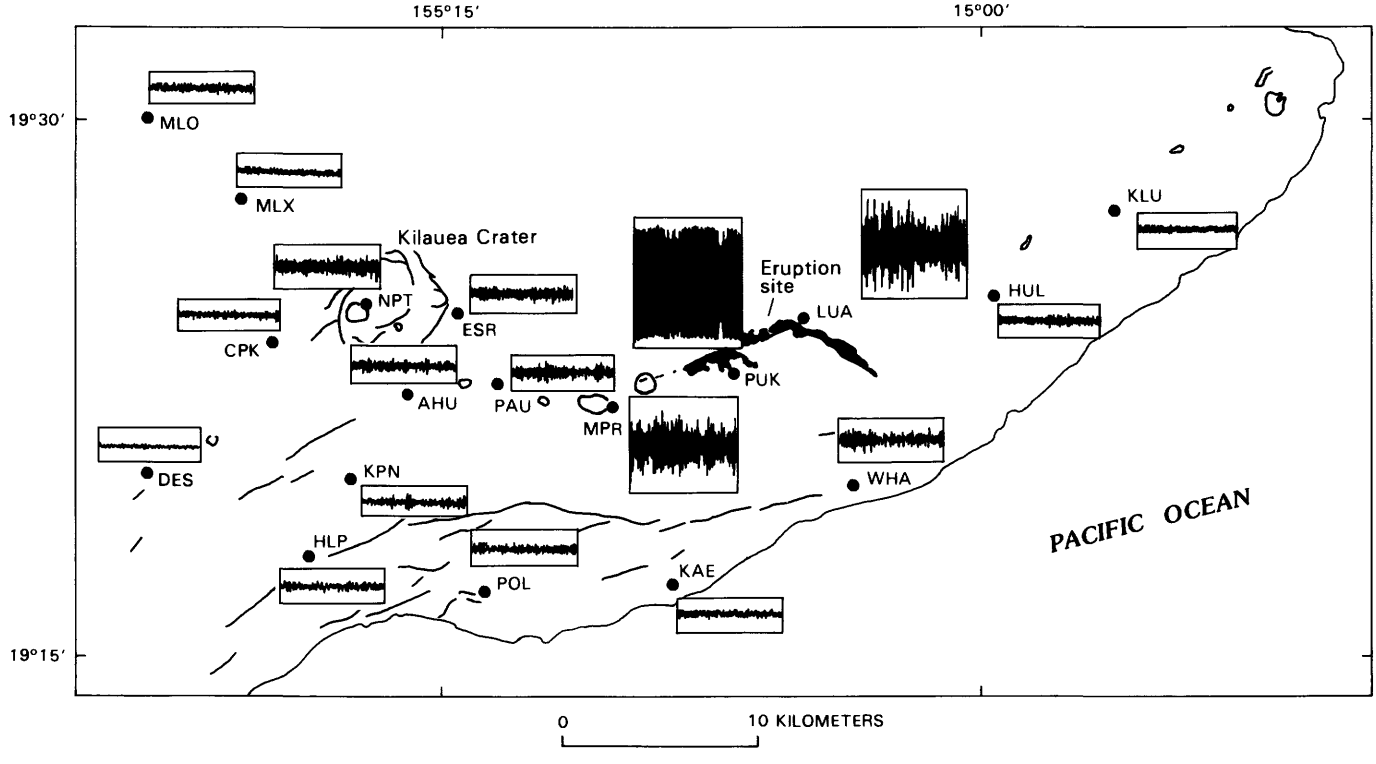

FIGURE 7.19.—Kilauea area, southeastern part of the Island of Hawaii, showing 30-s samples of seismograms of digitized recordings of harmonic tremor at HVO stations (dots) surrounding area of eruptive activity at 1500 H.s.t. January 6, 1983. Records are uncorrected for instrumental magnification. Shaded areas show lava flows produced during initial days of eruption. Major craters and faults are labeled.

area between Puu Kamoamoa and Napau Crater (see chap. 6). Tremor amplitude remained generally high during the eruptive activity on January 5 to 6; it heightened during high fountaining and relatively dropped during low fountaining. After January 6, as the eruption temporarily waned, shallow earthquakes in the middle east rift zone increased in number and migrated downrift to about 2 km east of Kalalua; the microearthquake swarm accompanied ground cracking near Kalalua. Lava emission then resumed from fissures extending southeast of Puu Kahaualea. High-level tremor, now centered at station LUA, correlated with high lava output from the easternmost vents on January 7 and 8.

Shallow earthquake swarms related to the principal rift intrusion and summit collapse had essentially ended by January 8. Shallow earthquakes on the east rift associated with subsequent period of the eruption were limited to small events ($M<1.0$) caused by locally induced thermal and gravitational stresses near the active vents and by fresh lava flows. Seismicity at the summit varied, and minor but periodic inflation-deflation intervals were associated with further eruptive episodes. Major lava production during episodes 2 through 23 was accompanied by locally recorded tremor, and there were no precursory earthquake swarms as observed before the outbreak of a new eruption. Magma movement within the summit-rift conduit system appeared unrestricted, a behavior that we interpret as defining an open, magma-filled conduit connecting the base of the summit reservoir to the dike intrusion beneath the eruptive vent. Dvorak and Okamura (1985) attribute the increases in the rate of deflation at the summit and in tremor amplitude within the east rift with each sequential outbreak between episodes 2 and 7 to an increasing rate of magma flow from the summit to the east rift. The reduction of flow resistance in the conduit system that accommodated the increased flow rate was considered to be caused by the repeated movement of magma. Seismic parameters for January 1983, the initial month of activity, are outlined for more than 800 earthquakes (table 7.2) and for a continuous record of tremor (table 7.3). The sequence of shallow earthquakes, tremor, summit tilt changes, and eruptive events during the initial 11 days of intense seismicity is summarized in figure 7.14. The progressive downrift movement of shallow earthquakes and tremor was completed during this interval.

The timing of and changes in summit deflation, east-rift tremor, summit tremor, and eruptive events for episodes 2 through 23 are plotted in figure 7.16. Tremor in the east rift increases to many orders of magnitude above background during major lava outbreaks. Rapid and sustained deflation was frequently followed by low-level tremor at the summit that reached several times above background level. The early eruptive episodes (2–5) were characterized by gradual changes in low-level east-rift tremor, lava outbreaks that lasted many days, a low rate of summit deflation, and weak (to undetectable) summit tremor. The later eruptive episodes (6–23) featured contrastingly abrupt and larger changes in these parameters.

SUMMARY AND DISCUSSION

Seismographs at the HVO continuously monitored the seismicity associated with the 1983 eruption of Kilauea. From the islandwide network of 50 continuously operating stations, the area of volcanic activity was monitored by at least 20 stations spaced about 5 km apart. The nearest station to the eruption site was less than 1 km away.

During the interval from September 1982 to June 1984, several hundred thousand earthquakes were detected in the magnitude range from about 0.1 to 4.2. A total of 4,163 earthquakes of $M \gtrsim 0.5$ from beneath the Kilauea area were computer processed for location and magnitude. The Kilauea selection numbered 876 events in the shallow summit region at 0- to 5-km depth, 73 in the deep summit region between 5- and 40-km depth, 720 in the shallow east rift zone at 0- to 5-km depth, and 2,494 in the south flank region, mainly at 5- to 13-km depth. These earthquakes, in combination with ground-deformation data, describe the process of magma transport from the summit storage complex, through the rift-zone conduit system, to the eruptive vents in the east rift zone.

Earthquakes in three distinct hypocentral groups that progressively responded to the volcanic process outlined the magma-conduit system. Shallow summit earthquakes monitored the state of the dynamic summit storage complex, shallow swarms of rift earthquakes indicated the summit-to-rift extent of magma intrusion, and deep crustal earthquakes in the adjacent south flank reflected the translation of compressional stresses to Kilauea's unstable south flank. The spatial distribution of summit,

FIGURE 7.20.—Kilauea area, showing contours of tremor amplitude mapped from 30-s samples of seismograms from permanent stations (circles), supplemented by records from temporary stations (dots) monitored by portable seismographs. *A*, 1500 H.s.t. January 6, 1983. *B*, 0300 H.s.t. June 8, 1984. Peak-to-trough amplitude readings subtracted from background noise were reduced to micrometers of ground displacement, according to instrumental response at the signal frequency. Intermittent tremor readings from portable seismographs were normalized with continuous records from permanent stations; amplitude distribution was then used to approximate contours at intervals of micrometers to proportional fractions of a micrometer, varied to accommodate map scale.

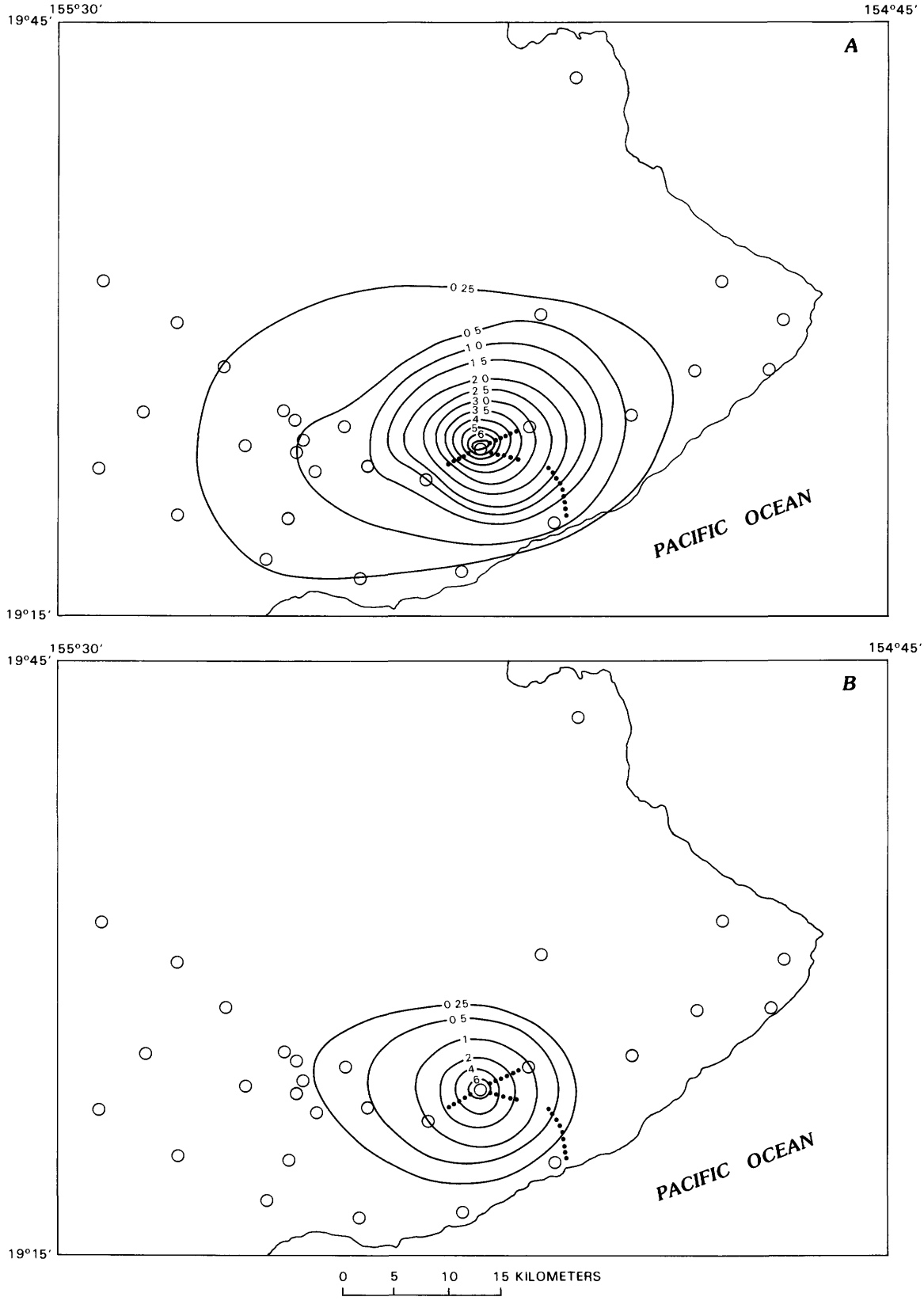
155°30′
154°45′
19°45′
19°15′
A
0 25
0 5
1 0
1 5
2 0
2 5
3 0
3 5
4
5
6
PACIFIC OCEAN
155°30′
154°45′
19°45′
19°15′
B
0 25
0 5
1
2
4
6
PACIFIC OCEAN
0 5 10 15 KILOMETERS

TABLE 7.2.—*Outline of seismic parameters for microearthquakes in the east-rift eruption of Kilauea, January 1983*

Principal source	Type of activity	Number of events processed	Magnitude range (M)	Magnitude-frequency parameter b	Focal depth (km)	Seismic-energy release (10^6 J)	Location	Dimensions	Time and duration of peak activity
East rift zone.	Intrusion-related swarm at shallow depth.	410	0.5–2.6	2.0	0–5	500	Mauna Ulu to east of Kalalua.	2 km wide by 16 km long by 4 km deep.	0300 H.s.t. Jan. 2 to 2400 H.s.t. Jan. 7; 144 hours. Downrift migration from Mauna Ulu to Puu Kamoamoa at 0.6–0.7 km/h from 0300 to 1300 H.s.t. Jan. 2.
Summit-------	Deflation-related flurries at shallow depth.	50	.6–1.6	---	0–5	10	South caldera---	2 km wide by 3 km long by 4 km deep.	0100 H.s.t. Jan. 3 to 0100 H.s.t. Jan. 8; intermittent for 144 hours.
South flank---	Relative increase in isolated earthquakes and aftershock sequences at intermediate depth, believed to be caused by tectonic response to magma intrusion into east rift.	350	.6–4.2	.9	5–13	16,000	South of east rift zone, between the Koae faults and Kalalua.	5 km wide by 25 km long by 8 km deep.	Persistent through January.

rift, and south-flank earthquakes delineated a magma-conduit complex whose maximum dimensions are 3 by 5 by 25 km.

Our model for the magma-transport system along the east rift zone based on an interpretation of seismic and corroborating data, as partly shown in a profile perpendicular to the strike of the rift zone in figure 7.31, is consistent with the structure and dynamics proposed by Crosson and Endo (1982). The magmatic-conduit complex within the rift, as inferred in the cross section, is no more than 4 km wide at its 10-km-depth base, and about 1 km wide near the surface. The lateral extent at the base is constrained by the zone of 5- to 10-km-deep earthquakes in the adjacent south flank. The top of the principal conduit is outlined by the narrower zone of earthquakes at 2- to 4-km depth that occur in swarms as the system opens

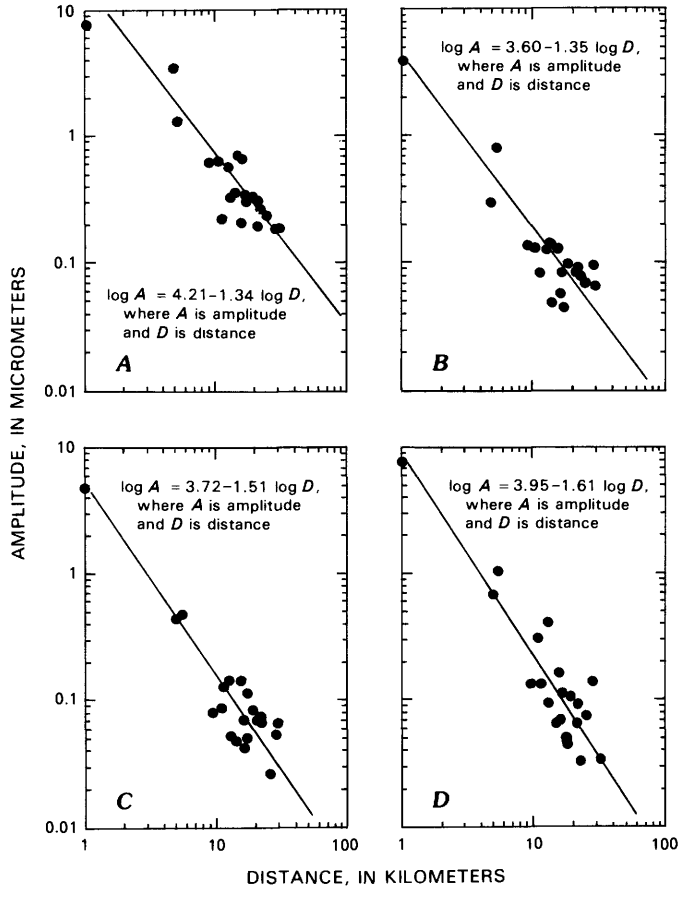

FIGURE 7.21.—Tremor amplitude as a function of distance from station PUK in eruption area that registered highest intensity. *A*, 1500 H.s.t. January 6, 1983. *B*, 1500 H.s.t. August 17, 1983. *C*, 0300 H.s.t. October 7, 1983. *D*, 0300 H.s.t. June 8, 1984. Amplitudes were reduced from signals recorded simultaneously during high-level activity at network stations 1 to 30 km away. Data points (circles) approximately fit an exponential-decay pattern, as described by equations for lines (diagonal line) of best fit.

TABLE 7.3.—*Outline of seismic parameters for harmonic tremor in the east-rift eruption of Kilauea, January 1983*

Principal source	Nearest station	Epicentral distance of station from source (km)		Time and duration	Maximum peak-to-peak amplitude reduced to actual ground motion (μm) (station)	Time of maximum amplitude	Frequency range (Hz) (predominant range)
		Summit	East rift				
East rift zone from Napau to Kalalua Crater.	Puu Kamoamoa (PUK).	17	1-5	0100 H.s.t. Jan. 2 to 2400 H.s.t. Jan. 31; 719 hours (continuous).	Clipping level (PUK). 2.0 (MPR)[1]	Jan. 5-12	1-10 (2-4)
Summit caldera------	North Pit (NPT).	1	14-21	0100 H.s.t. Jan. 2 to 0900 H.s.t. Jan. 15; 320 hours (intermittent).	.2 (NPT)	Jan. 3-8	1-5 (2-4)

[1]Station MPR was located 2 to 10 km from east-rift tremor source.

to the surface to accommodate eruptions. Magma from the mantle thus rises steeply to within a few kilometers beneath the summit caldera for temporary storage. Magma is then tapped from the summit reservoir and subvertical conduit below, and directed along the east rift zone. The zone of concentrated earthquakes at 2- to 4-km depth beneath the rift zone outlines the region of active structural changes that accommodate dike emplacements from lateral and vertical movement of magma during rift intrusions. The zone directly beneath this region that lies adjacent to a concentration of 5- to 10-km-deep south-flank earthquakes is relatively aseismic except at the downrift end of the intrusion zone, where rift earthquakes deepen to at least 8 km below the surface. This region may be a relatively passive, semirigid zone that acts as a medium for transfer of magma pressure. Lateral pressure exerted from this 5- to 10-km-deep zone may induce compressive stresses and strain release in the adjacent wallrocks along the south flank and in deep barriers within the rift conduit during intrusions. The top of this zone subjected to less confining stresses would more actively participate in the lateral transfer of relatively fluid and degassed magma. This region may constitute a relatively persistent conduit complex that upon overpressurization would episodically feed dike emplacements above.

A nearly vertical alignment of eruptive vents above the rift conduit is indicated by the concentric pattern of tremor attenuation from the eruptive vent to distances of about 5 km (fig. 7.20). Although this pattern could also be observed if the seismic source was isolated in a very shallow vent system, part of the energy is probably radiated from at least a few kilometers beneath the vent. Evidence for this interpretation is (1) the constant supply of magma to a deeper magma-transport system and (2) the incomplete harmony between fountain activity and tremor amplitude. The spectrum of peaked frequencies, ranging from at least 1 to 10 Hz, recorded near the active vent during the height of eruptive activity (Koyanagi and others, 1987) may also be due to variations in source properties that require an extended region beneath the vent.

Along the rift zones affected by vigorous magma movement, swarms of shallow earthquakes at about 2- to 4-km depth occur in short episodes (fig. 7.10) to accommodate the rapidly accumulating local stresses. Earthquake activity in the upper kilometer of the summit and rift zones—an isolated region of low velocity and low stress outlined by Hill (1969) and Zucca and Hill (1980) that is highly fractured and constantly deforming—is confined to small events that are generally recorded at an insufficient number of stations to permit standard processing for hypocenter determination. The increasing number of small seismic events in the east rift zone during the eruption is mainly attributed to surface and near-surface activity local to the eruption site. Such events include microfracturing and rockfalls along the unstable vent walls, explosive degassing of the magma in the vent, and explosive combustion of methane gas from buried organic material adjacent to active lava flows. Microfracturing from thermally related contractions of fresh lava flows near the monitoring stations also contributed to the increasing number of east-rift earthquakes.

The clustering of earthquakes indicates variations in stress, probably dictated by nearby magma movement and influenced by regional stresses. Places of few earthquakes along the rift zone may be interpreted as regions where magma passage is unrestricted. Zones of increasing numbers of earthquakes may be constricted localities where magma pressure induces compressional stresses in the host rocks, vertically causing earthquakes in the caprock above the magma-transport system, and laterally causing earthquakes within the unstable south flank. The numerous earthquakes in the south flank that occur along a subhorizontal zone, 5 to 10 km deep, in combination with analysis of focal mechanisms, indicate that large blocks of the south flank respond by moving away from the rift axis and slipping southeastward along the prevolcanic ocean floor (Crosson and Endo, 1982). Such relief of stress will allow a temporary accommodation of further rift dilation, and a decrease in south-flank seismic activity, until tensions once more build up in the south flank, owing to continuing intrusion. The earthquake distribution may thus be interpreted in terms of magma pressure and stresses in the country rock that are relieved to accommodate the resulting pattern of magma movement.

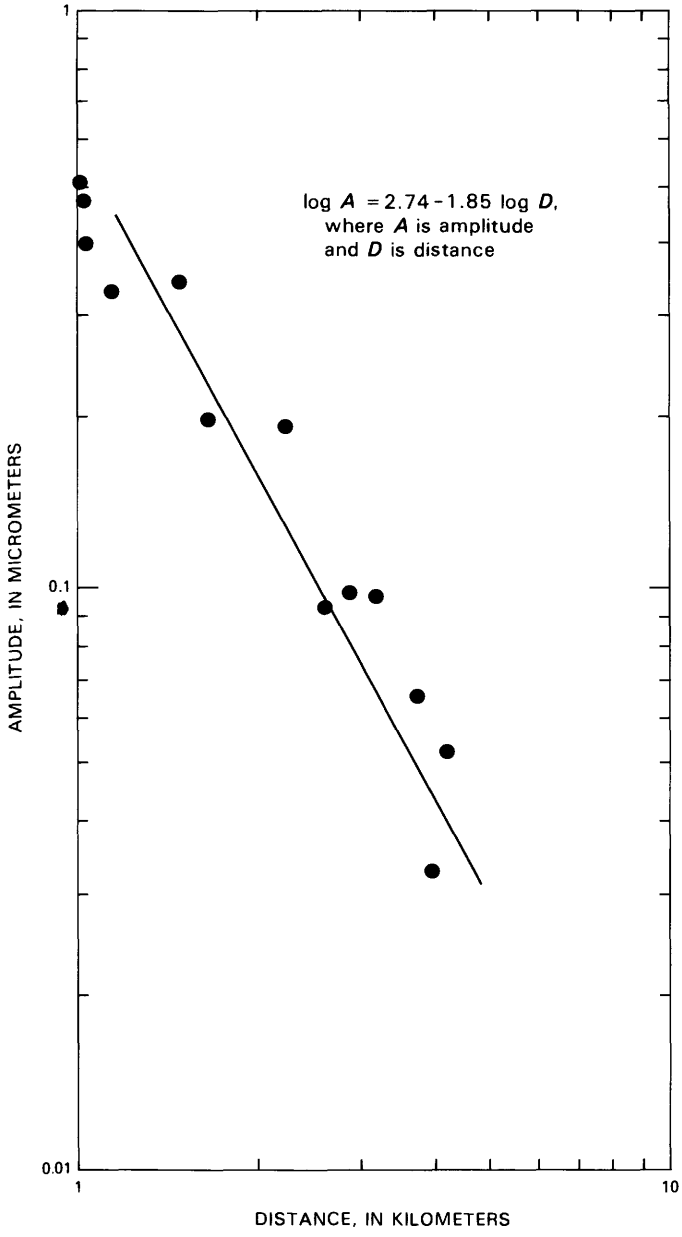

FIGURE 7.22.—Tremor amplitude as a function of distance from eruptive vent during low and localized activity at 1100 to 1535 H.s.t. April 4, 1983. Amplitudes were reduced from signals recorded on a portable seismograph and normalized with signals from continuously recording, permanent station at Puu Kamoamoa. Data points (circles) approximately fit an exponential-decay pattern, as described by equations for lines (diagonal lines) of best fit.

The episodic bursts of shallow earthquakes concentrated in the Puu Kamoamoa area since 1977 are believed to be associated with disruptions in the conduit system, and in combination with a pattern of rift inflation (Dzurisin and others, 1984) was interpreted to be caused by localization of magma supplied by intrusions. The absence of intrusion-related swarms and inflation farther downrift marked the locality between Puu Kamoamoa and Puu Kahaualea to be the easternmost extent of intrusive activity. Consequently, the relatively few earthquakes in this specific locality during the early January 1983 activity may have been due to preexisting dike emplacement. Locations of low seismicity along the active rift conduit are interpreted to be regions where magma movement is relatively free, and complementing zones of low-level seismicity extending normal to the rift axis are believed to be due to variations in stress translated tectonically, rather than to injection of magma into the south flank. Isolated earthquakes and aftershock sequences characterize the seismic activity in the south flank. The absence of localized earthquake swarms and harmonic tremor around aseismic zones in the south flank suggests that these parts are not dynamic regions of magma intrusion comparable to the active regions beneath the axis of the east rift. Irregularities in the spatial distribution of the south-flank earthquakes that accompany major rift intrusions suggest differences in the rate of seaward displacement or, alternatively, aseismic movement of some components of the south flank (Crosson and Endo, 1982). Some inconsistencies in the detection of small earthquakes, especially those of $M<1.0$, are otherwise caused by sustained episodes of high-level tremor that mask earthquake signals.

The pattern in overall spatial distribution of the earthquakes, which extends from the volcanic regime along the rift zone through its tectonic counterpart along the south

flank, also suggests the influence of regional stresses in addition to the expected local stresses induced by magma intrusion. The aseismic pockets along the east rift zone that continue deep into the adjacent south flank, forming elongate zones normal to the orientation of the rift, may be due to neutralized stress conditions developed as a consequence of variations in stress orientation in the surrounding regions. These regions also appear to produce structural accommodations conducive to the development of magma-storage zones in complementary parts of the rift zone. The magma pockets formed and maintained in these rift-zone anomalies before rapid intrusions, in turn, would tend to interrupt the spatial and temporal distribution of earthquake swarms. Magma pressure would be transmitted freely through these zones of low rigidity, and only a few earthquakes would be generated.

At times when downrift movement of magma is effectively restricted in the middle east rift zone, uprift propagation of pressure may cause earthquakes to also migrate uprift as the existing dike system tends to widen, or upward diversion of magma by a relative increase of magmatic over gravitational force at the blockage may supply lava to an east-rift eruption. In January 1983, the initial pressure causing earthquakes along the dike system propagated downrift at a rate of about 0.6 to 0.7 km/h before reaching the surface adjacent to the blockage in the conduit. During the subsequent intermittent swarms, earthquakes migrated uprift at a slow rate of about 0.06 to 0.07 km/h and reversed downrift again at a rate of 0.6 to 0.7 km/h, ending east of Kalalua by January 8.

Tremor is apparently generated by magma flow in particular localities where pressure either fluctuates or increases near conduit constrictions. It intensifies near the surface upon eruption as relatively free flow of impulsively degassing magma impacts the vent walls. Ascending magma is subject to rapid volume increase from depressurization and release of volatile materials.

Thus, the normalization of pressure at the distal end of the intrusion is accommodated laterally by overcoming downrift barriers along the preexisting conduit system, upward as dikes extend to shallower zones that are more accessible owing to lower stress conditions, or backward uprift along the active conduit system. If the rate of magma flow into the rift zone is low relative to the strength of downrift barriers and the caprock, the pressure buildup at the terminus would have time to be normalized within the existing fluid system by propagating back uprift. This normalization would tend to widen the dike system progressively uprift and cause earthquakes to slowly migrate uprift. As the rate of in-

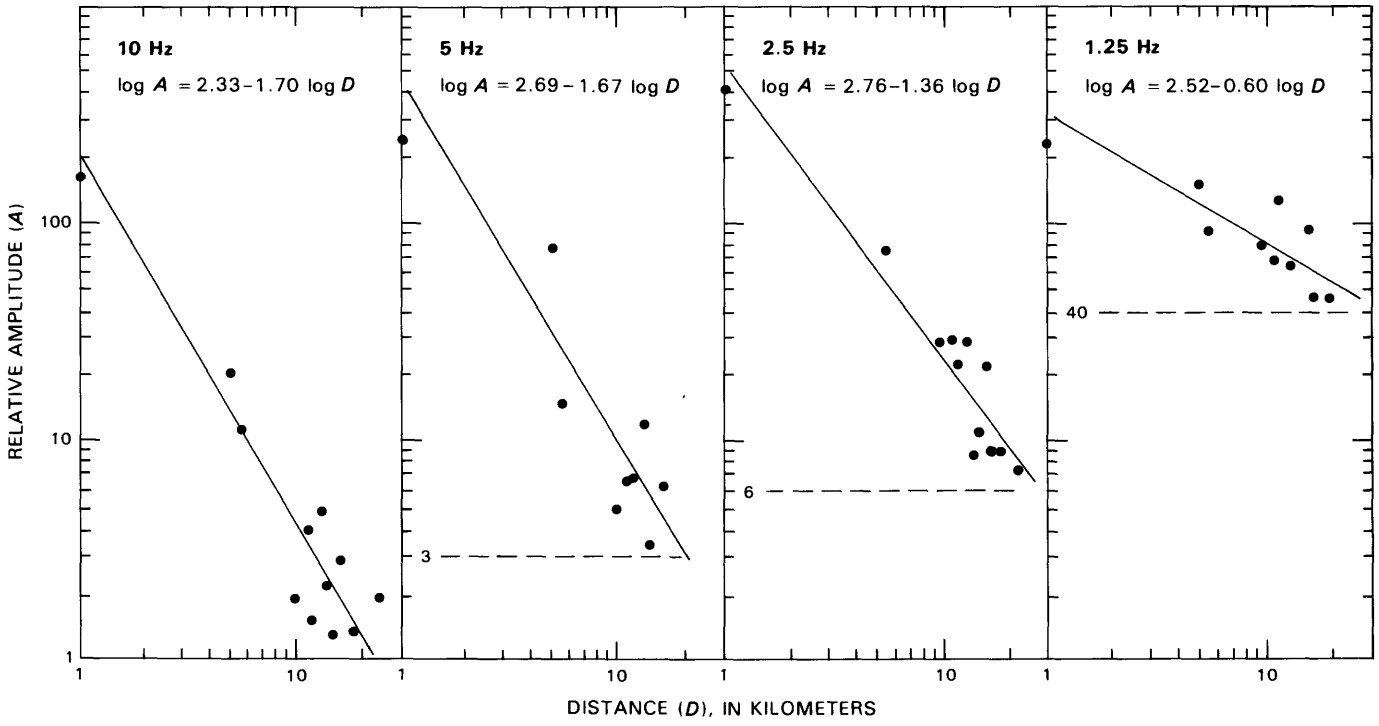

FIGURE 7.23.—Tremor amplitude from filtered signals recorded at various stations and times during episode 23 on July 28, 1984,as a function of distance from Puu Kamoamoa station (KMM), located within 1 km of eruptive vent. Data points (circles) approximately fit an exponential-decay pattern for frequencies centered at 10, 5, 2.5, and 1.25 Hz. Equations describe lines (diagonal line) of best fit. Dashed horizontal lines denote noise level at various frequencies.

trusion increases, however, rapid buildup of pressure at the intrusion front would tend to be rapidly normalized by inducing stress relief in the immediate region, and dike emplacement would extend upward and downrift. The relative strength of downrift barriers or a slight decrease in flow rate may reduce the momentum in lateral movement downrift and emphasize dilation upward to the surface.

Upon eruption, pressure is further reduced near the surface as a result of conduit enlargement and lava discharge. The drop in fluid pressure at the vent induces vesiculation and accelerates expansion of the rising magma, and the resulting increase in buoyancy also increases the eruptive intensity, until magma pressure deeper in the conduit system drops to a critical level. When a sufficient balance in magma pressure remains in the rift conduit after an eruptive episode, a seismically open system is maintained, characterized by persistent low-level harmonic tremor. This condition facilitates more eruptive episodes from the same vent system upon a minimal increase in internal pressure. Swarms of earthquakes typical of new eruptions are not required when there is no need for new dikes to form. At the summit, SP earthquakes increase in frequency with inflation, and harmonic tremor and LP events are correlated with sustained high rates of deflation after the onset of intense eruptive episodes. The tremor activity that accompanies the accelerated summit deflation probably reflects adjustments attendant on decompression of magma leaving the summit, and (or) interaction with ground water introduced into the depressurized magma system (Pollard, 1981; L.P. Greenland, oral commun., 1985).

The absence of widespread intrusion-related swarms of earthquakes preceding eruptive episodes after the initial dike emplacement and fissure outbreaks, and the generally shorter intervals and abrupt changes in tremor amplitude in the middle east rift zone responding immediately to changes in eruptive vigor during later eruptive episodes, are attributed to the development of an increasingly efficient summit-to-rift transport system. The

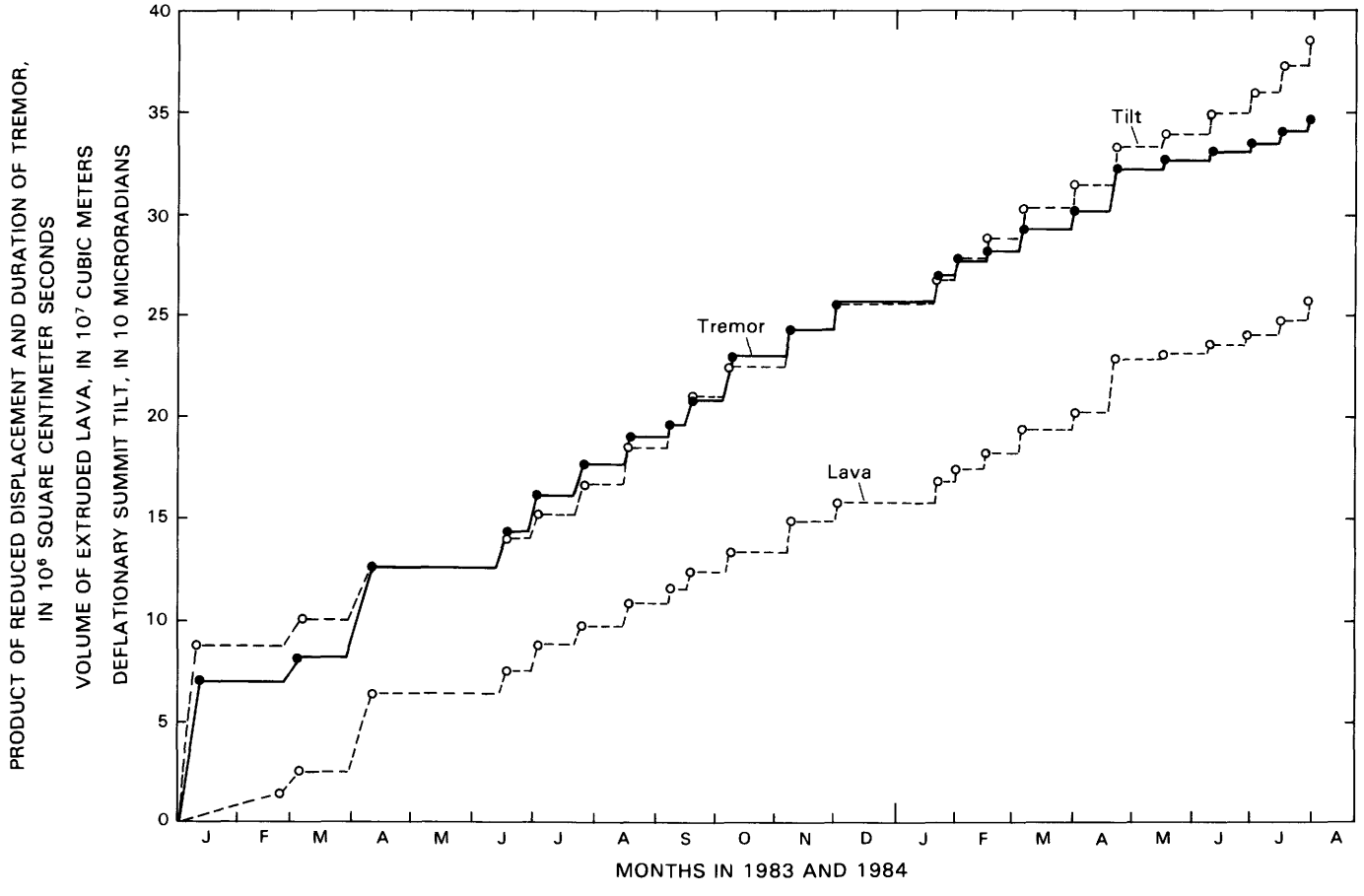

FIGURE 7.24.—Cumulative product of reduced displacement and duration of tremor, cumulative volume of extruded lava, and cumulative deflationary summit tilt for periods of high lava production during episodes 1 through 23 as a function of time. Tremor was reduced from station MPR record, assuming a 6-km hypocentral distance. Lava-volume and summit-tilt data from chapters 1 and 6.

localized tremor that persisted between eruptive episodes is attributed to the continuity maintained in the magma-transport system and the active vent. The amplitude of low-level tremor near the vent between eruptive episodes varied according to the relative vigor and pattern of lava movement or degassing in the vent.

The location of the eruption site initially appears to be dictated by the strength of the retaining roofrock and the

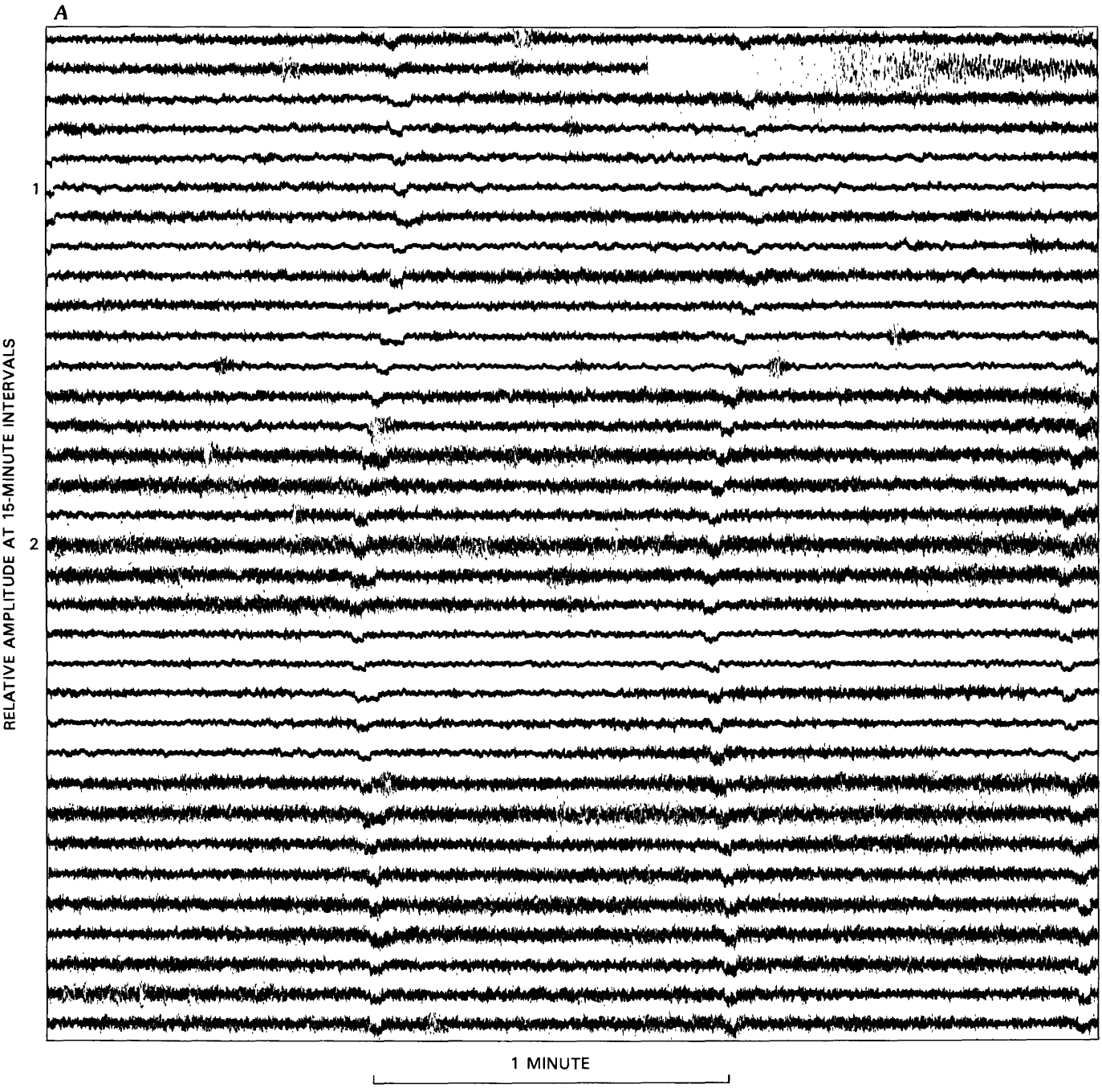

FIGURE 7.25.—Seismograms from a rotating-drum recorder at station KMM, located within 1 km uprift of Puu Oo. *A*, Variations in amplitude of low-level tremor between eruptive episodes on April 28-29, 1984. Tremor at nearly background level (1) and amplitude increases of 3 to 5 times (2) alternate at intervals of several or more hours. *B*, Various seismic events during gas-piston lava activity at Puu Oo vent on May 5, 1984: 1, high-frequency microearthquake; 2, rockfall; 3, associated tremor.

distribution of fluid pressure, which frequently vary in time and space along the summit and rift magma system. The locus of eruptions along the summit-rift alignment may either shift for successively new outbreaks or remain the same for prolonged eruptions, as with such persistent episodes as the Puu Oo and early Mauna Ulu sequences. Repeated eruptions from the same vent system seem to be controlled by changes in the critically balanced pressure system. The sequence of events from gradual inflation of the summit, through impulsive eruption, to rapid summit deflation implies that, once the major outbreak is started by critical depressurization of the system, the connecting fluid complex serves as a medium for pressure transfer from the overpressurized summit reser-

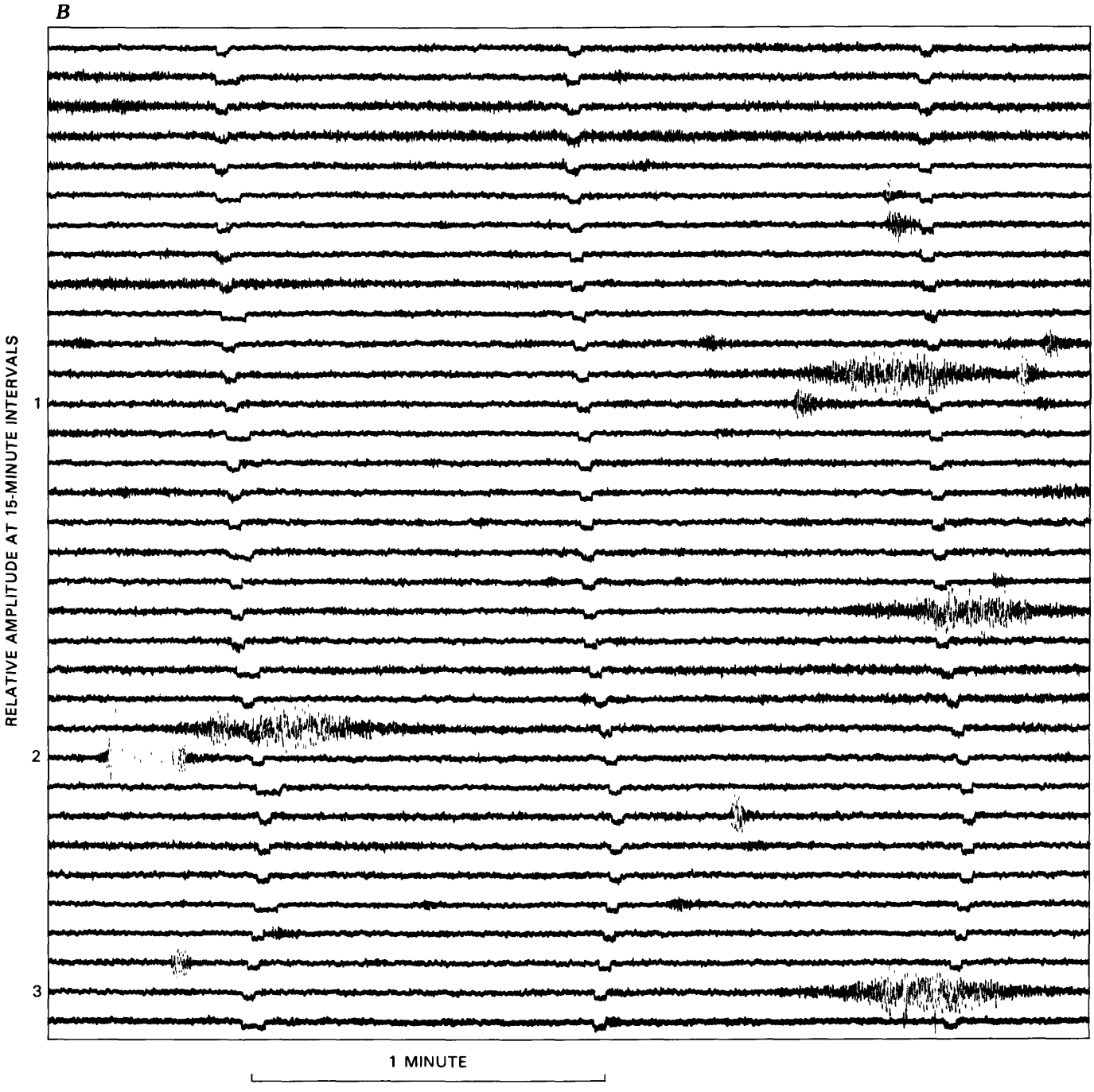

FIGURE 7.25.—Continued

voir to the relatively underpressurized conduit region beneath the east-rift vent. A relatively steady and critically lower velocity of magma movement through a wider central part of the rift conduit, once the connection is made, would help to explain the absence of tremor in the active part of the transport system connecting the summit and eruptive vent. Development of an increasingly continuous conduit system may alternatively generate uniquely longer period tremor beyond our instrumental system's detection capability.

Harmonic tremor, at frequencies between about 1 and 10 Hz, varied in amplitude according to the rate of magma flow and the intensity of eruption. The higher frequencies dominated near the vent, where tremor was most intense. Tremor amplitude attenuated exponentially with distance from the source, and at decreasing rates for lower frequencies. Rapid changes in tremor occurred during the start and end of most eruptive episodes. Order-of-magnitude changes in tremor amplitude occurred within one to several minutes at these times. Alternatively, summit tremor and LP events that occurred after a substantial collapse were much more gradual in buildup and decay, and many times less energetic, than the rift tremor during eruptive peaks.

Tremor signals consisting of constant fluctuations over a limited range of dominant frequencies that appeared as amplitude bursts separated seconds apart on the seismograms, corresponded to the pulsations of intense lava

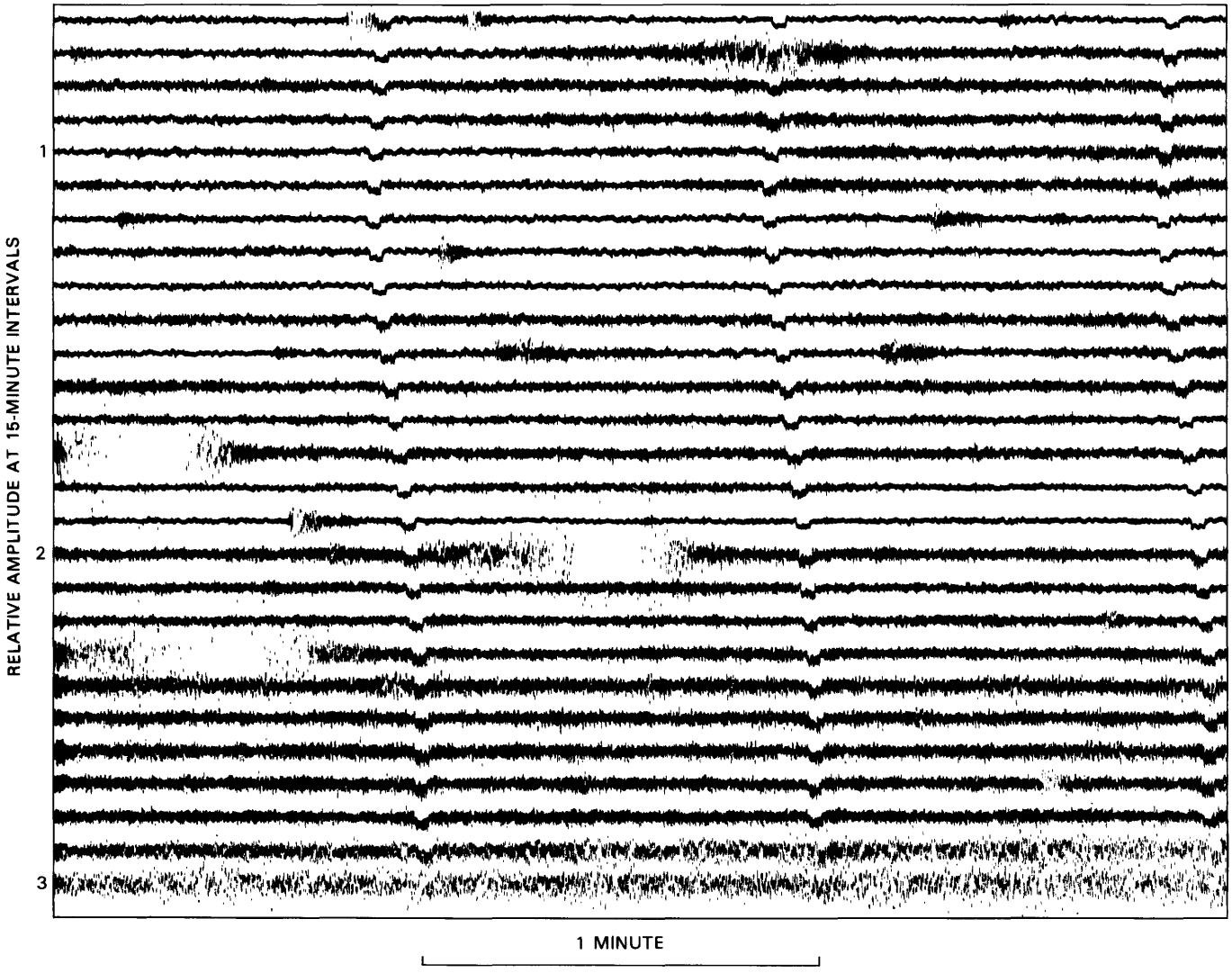

FIGURE 7.26.—Seismograms from a rotating-drum recorder at station KMM, located within 1 km uprift of Puu Oo, showing various low-level tremor events between major outbreaks of lava at the vent on May 15–16, 1984: 1, constant low-amplitude tremor; 2, tremor burst associated with intermittent lava spattering and degassing; 3, sustained increase in tremor amplitude coinciding with onset of lava fountaining.

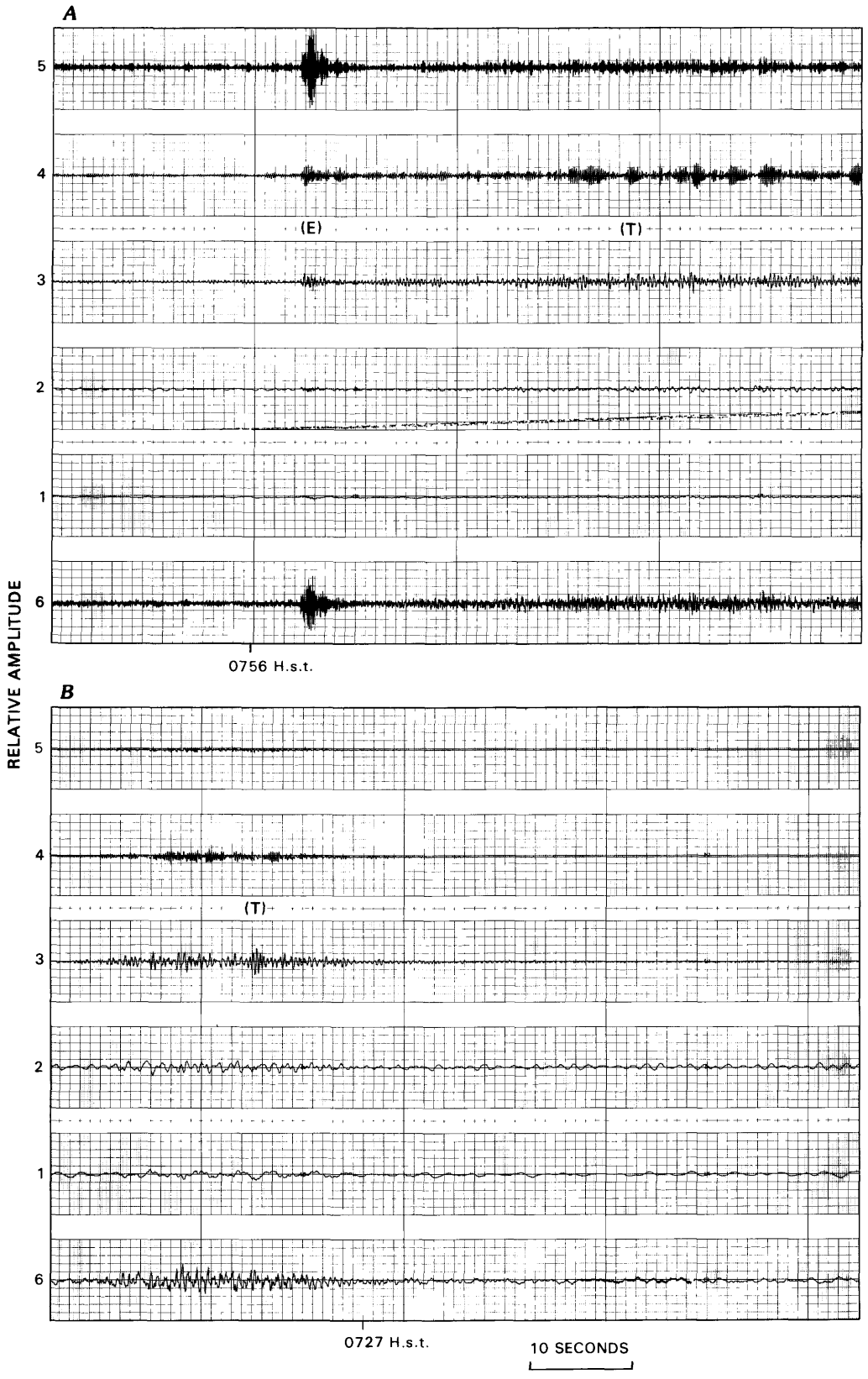

FIGURE 7.27.—Low-level tremor burst (T) associated with gas-piston lava activity in eruptive vent, recorded after episode 23 on August 7, 1984. Signal on channel 6 is unfiltered HVO Type 1, and signals on channels 1 through 5 are filtered. *A*, 0756 H.s.t., station KMM, located within 1 km of the vent. Burst

fountaining. This pulsating behavior, which is characteristic of both eruption and noneruption tremor, appears to be fundamentally related to the mechanism that drives the movement of magma. The recognizable pulses in lava fountaining and seismograms of tremor average about 5 s apart.

A subtle increase in the number of deep-tremor episodes and LP events in 1984 (Koyanagi and others, 1987) suggests an accelerated rate of magma supply from the mantle during the Puu Oo eruption. Calculations based on the volume of extruded lava support this inferred increase in supply rate (Wolfe and others, 1987). The SO_2 emission in the summit area, indicative of magma influx from depth, rapidly increased early during the intrusive period and remained at a constant high rate thereafter (Greenland and others, 1984). Apparently, the accelerated rate of magma flow that accommodated a decrease in pressure, translated vertically along the transport system, eventually reached the mantle source region more than 50 km beneath the southern part of the Island of Hawaii in early 1984. A similar correlation of increase in deep tremor and high lava production during the prolonged eruption at Mauna Ulu in 1969–74 was noted by Aki and Koyanagi (1981) and later emphasized by Dzurisin and others (1984). The increase in deep tremor associated with the 1983–84 eruption was not evident until many months after the onset of eruptive activity. This delay in deep tremor activity suggests that the inferred increase in supply rate of magma from the mantle was induced by a pressure decrease in the upper conduit system, an interpretation that favors one of the mechanisms proposed by Dzurisin and others (1984). They suggested that the time-related increase in deep tremor with high lava-production rates, and the relatively rapid reinflation of the summit after large deflation events, can be explained by a process whereby rapid removal of magma from the shallow summit reservoir relieves the load on the hydraulically linked plumbing system to accelerate the rate of magma supply

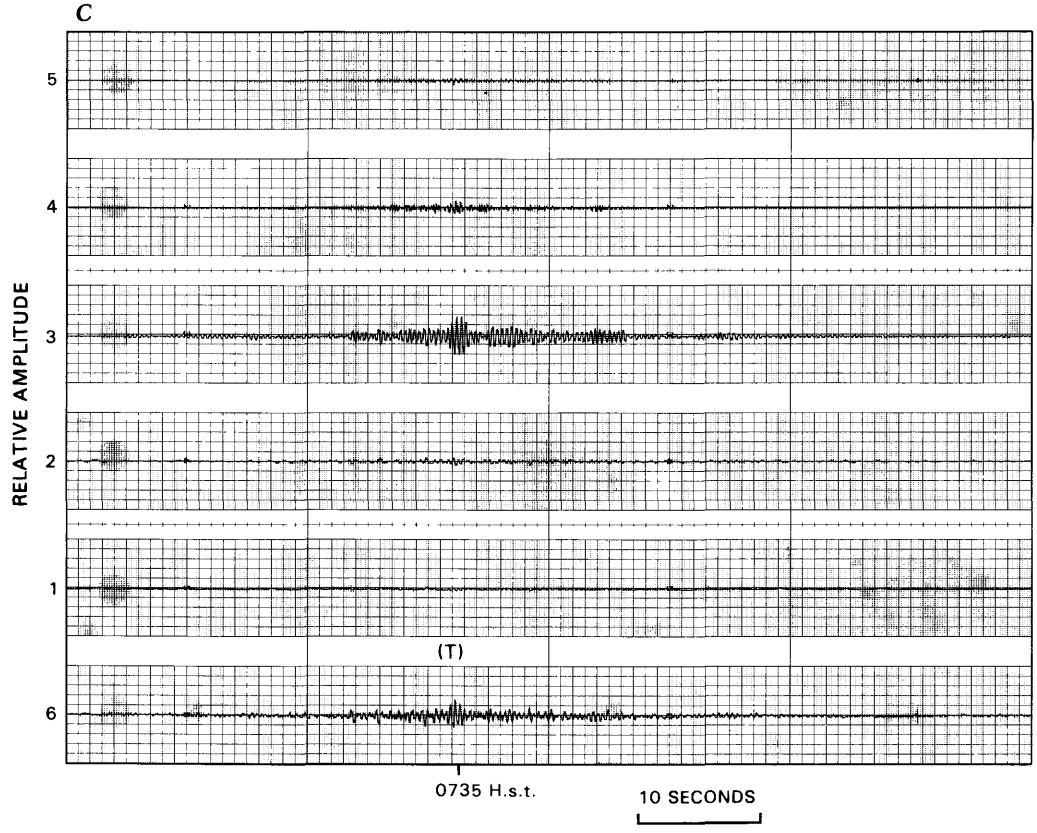

was preceded by a high-frequency microearthquake (E). *B*, 0727 H.s.t., station KMME (east-west component), located within 1 km of the vent. *C*, 0735 H.s.t., station KMMN (north-south component), located within 1 km of the vent. Peak responses and relative magnifications for filtered channels in figure 7.27*A*: 1, 0.625 Hz at ×2; 2, 1.25 Hz at ×10; 3, 2.5 Hz at ×26; 4, 5.0 Hz at ×60; and 5, 10.0 Hz at ×100. Peak responses and relative magnifications for filtered channels in figures 7.27B and 7.27*C*: 1, 0.625 Hz at ×1; 2, 1.25 Hz at ×1; 3, 2.5 Hz at ×1; 4, 5.0 Hz at ×1; and 5, 10.0 Hz at ×1.

from the mantle. Episodically varying rates of magma supply from the mantle and a close connection between eruptive events, rates of magma supply at depth, and, ultimately, rates of melting were inferred by Wright (1984), on the basis of the petrologic evolution of Hawaiian basalt. In view of how efficiently the summit reservoir and an eruptive vent 20 km away could be magmatically linked, thermal and density gradients that continually drive magma from the mantle to the surface could also develop an increasingly efficient and sensitively balanced hydraulic system that would be readily affected by remotely induced pressure variations.

The amplitude of continuous tremor during the Puu Oo eruption thus far has varied according to the rate of magma movement implied by the pattern of summit tilt and eruptive activity. The seismic data indicate episodic behavior, ranging from monthlong separations of eruptive episodes to shorter recurrences minutes apart during gas-piston activity. Such repetitious activity, also noted in hydraulic systems elsewhere (Keiffer, 1984), is believed to occur during a relatively steady state of stress in a temporarily isolated and regularly perturbed pressure regime. The seismicity and ground deformation accompanying eruptive episodes are localized near the magma

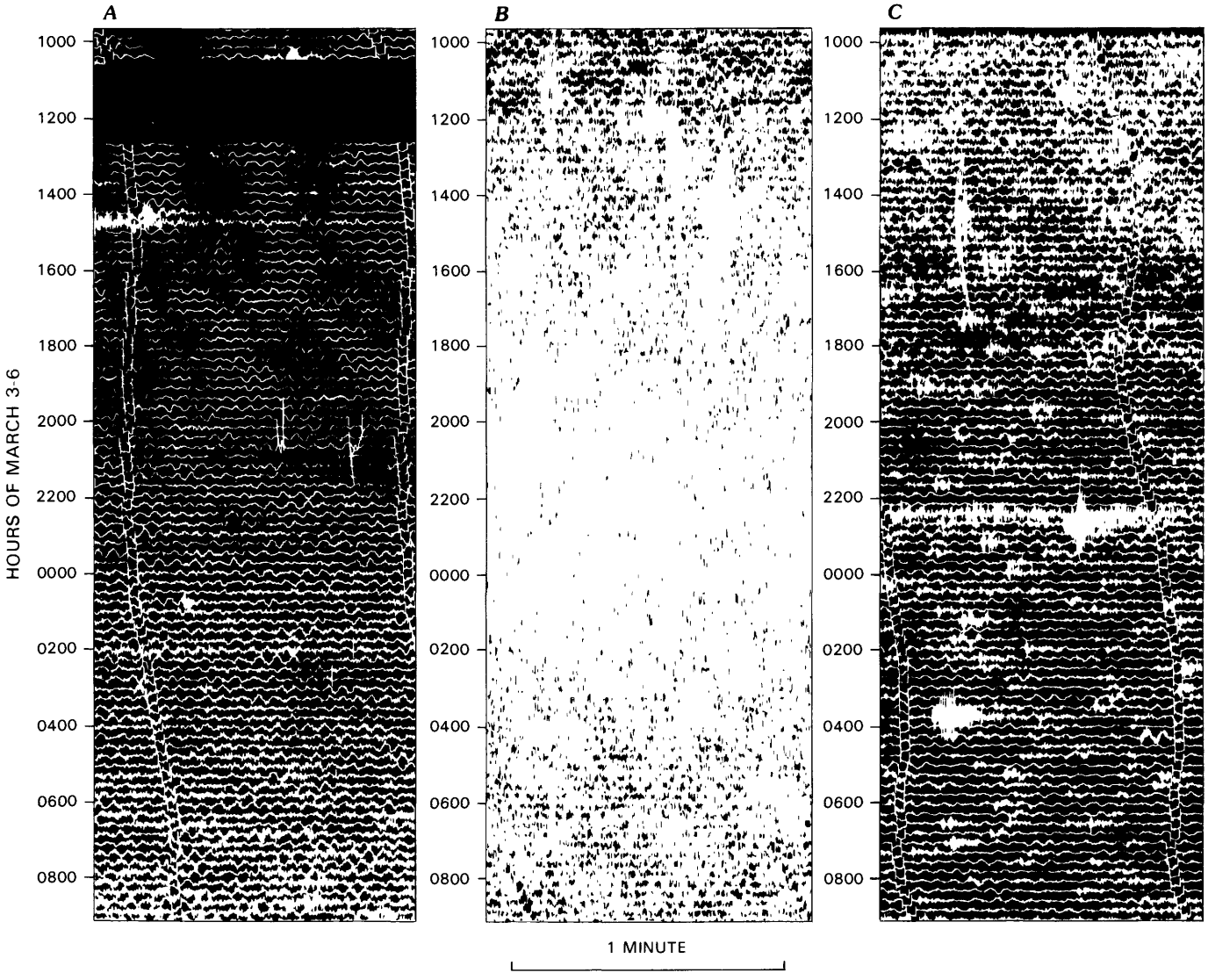

FIGURE 7.28.—Parts of 24-hour seismograms from a rotating-drum recorder at station NPT, showing changes in tremor amplitude and number of long-period (LP) events at summit during and after episode 16 on March 3–6, 1984 (see fig. 7.16). *A*, Tremor amplitude gradually increases at about 2300 H.s.t. during period of rapid deflation of summit. *B*, Tremor amplitude and number of LP events increase, peak at about 0000 H.s.t., and gradually decay during and after period of rapid deflation of summit. *C*, Tremor amplitude and number of more conspicuous LP events very gradually decrease throughout the day during period of gradual inflation of summit.

system beneath the summit and eruptive zone. No significant activity is generated along the flanks to suggest any rapid change in the volcano's regional stress condition. We speculate that this quasi-steady state is controlled by a critically balanced pressure system which gradually increases and rapidly decreases in pressure at time intervals dictated by the size of the hydraulically connected system. The stage of depressurization that induces exsolution of volatile materials and vesiculation of the magma accordingly occurs at a higher and more vigorous rate, and is complemented by high-level tremor. The eruptive episodes are characterized by strong tremor with a maximum amplitude of, at least, an order of magnitude above background that (1) generally lasts a day to several days during high lava production, (2) recurs at intervals of about a month and maintains the pattern in terms of years, and (3) indicates involvement of a 20-km-long fluid system which extends from the summit to the east-rift eruptive zone. The contrastingly minor repetitions of gas-piston activity are characterized by weak tremor with a maximum amplitude of, at least, several times above background that (1) lasts about a minute during vigorous collapse of the magma column in the vent, (2) recurs at intervals about 5 to 15 minutes apart and maintains the pattern for several to many days, and (3) is confined to within several kilometers beneath the active vent.

The repetition of eruptive episodes, characterized by a pattern of lava outbreak and high-level tremor followed by summit deflation, suggests that these outbreaks are initiated near the eruptive vent. Depressurization is translated along the rift conduit and back to the summit reservoir during the eruptive process. High lava production ends when magma pressure drops to a critically low level. The subsequent buildup of magma pressure to a critical level before an eruptive episode involves the summit reservoir, as well as the entire length of the rift conduit system that supplies the eruption. The eruptive interval and the volume of lava produced episodically should therefore be dictated by the volumetric capacity of the summit and rift storage system. Where the summit storage capacity may be relatively fixed, the capacity of the active part of the rift conduit system that feeds the

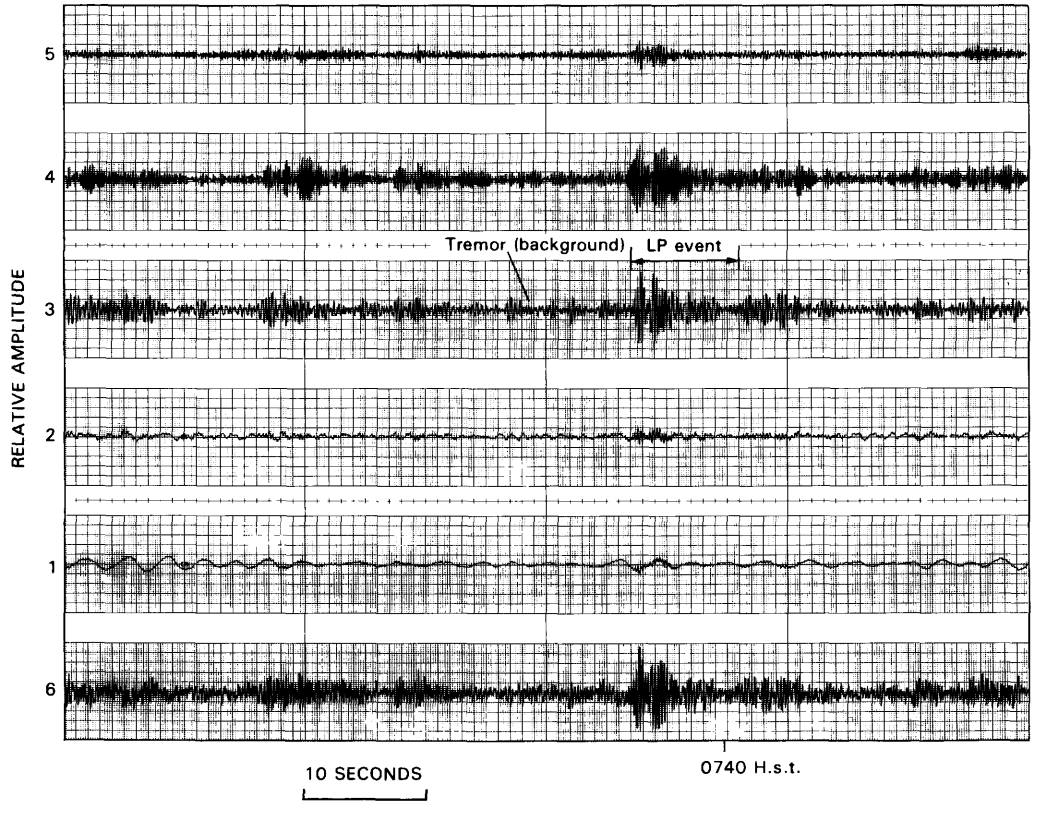

FIGURE 7.29.—Summit tremor and long-period (LP) events recorded at station NPT after episode 16 at 0740 H.s.t. March 5, 1984. Signal on channel 6 is unfiltered HVO Type 1, and signals on channels 1 to 5 are filtered. Peak responses and relative magnifications for filtered channels: 1, 0.625 Hz at ×2; 2, 1.25 Hz at ×10; 3, 2.5 Hz at ×26; 4, 5.0 Hz at ×60; and 5, 10.0 Hz at ×100.

eruption would depend on the distance between the eruptive vent and the summit inflation center. The progressively longer average intervals and durations of eruptive episodes for Puu Oo, in comparison with the upper-east-rift Mauna Ulu sequence in 1969 (Swanson and others, 1979) and the earlier summit sequence at Halemaumau in 1967–68 (Kinoshita and others, 1969), may be controlled by the difference in the length of the active conduit and in the consequent volume of the pressure regime. The length of the conduit system indicated by the distance from the inflation center at the summit to the eruptive vent is 20 km for Puu Oo, 8 km for Mauna Ulu, and 2 km for Halemaumau.

REFERENCES CITED

Aki, Keiiti, Fehler, Michael, and Das, Shamita, 1977, Source mechanism of volcanic tremor: Fluid-driven crack models and their application to the 1963 Kilauea eruption: Journal of Volcanology and Geothermal Research, v. 2, p. 259–287.

Aki, Keiiti, and Koyanagi, R.Y., 1981, Deep volcanic tremor and magma ascent mechanism under Kilauea, Hawaii: Journal of Geophysical Research, v. 86, no. B8, p. 7095–7109.

Chouet, Bernard, 1979, Temporal variation in the attenuation of earthquake coda near Stone Canyon, California: Geophysical Research Letters, v. 6, no. 3, p. 143–146.

——— 1981, Ground motion in the near field of a fluid-driven crack and its interpretation in the study of shallow volcanic tremor: Journal of Geophysical Research, v. 86, no. B7, p. 5985–6016.

——— 1985, Excitation of a buried magmatic pipe: A seismic source model for volcanic tremor: Journal of Geophysical Research, v. 90, no. B2, p. 1881–1893.

Chouet, Bernard, Aki, Keiiti, and Tsujiura, Masaru, 1978, Regional variation of the scaling law of earthquake source spectra: Seismological Society of America Bulletin, v. 68, no. 1, p. 49–79.

Chouet, Bernard, and Julian, B.R., 1985, Dynamics of an expanding fluid filled crack: Journal of Geophysical Research, v. 90, p. 11187–11198.

Chouet, Bernard, Koyanagi, R.Y., and Aki, Keiiti, 1987, Theory and discussion, pt. 2 *of* Origin of volcanic tremor in Hawaii, chap. 45 *of* Decker, R.W., Wright, T.L., and Stauffer, P.H., eds., Volcanism in Hawaii: U.S. Geological Survey Professional Paper 1350, v. 2, p. 1259–1280.

Crosson, R.S., and Endo, E.T., 1982, Focal mechanisms and locations of earthquakes in the vicinity of the 1975 Kalapana earthquake aftershock zone 1970–1979: Implications for tectonics of the south flank of Kilauea volcano, island of Hawaii: Tectonics, v. 1, no. 6, p. 495–542.

Decker, R.W., Koyanagi, R.Y., Dvorak, J.J., Lockwood, J.P., Okamura, A.T., Yamashita, K.M., and Tanigawa, W.R., 1983, Seismicity and surface deformation of Mauna Loa Volcano, Hawaii: Eos (American Geophysical Union Transactions), v. 64, no. 37, p. 545–547.

Duffield, W.A., 1975, Structure and origin of the Koae fault system, Kilauea Volcano, Hawaii: U.S. Geological Survey Professional Paper 856, 12 p.

Dvorak, J.J., and Okamura, A.T., 1985, Variations in tilt rate and harmonic tremor amplitude during January–August 1983 east rift erup-

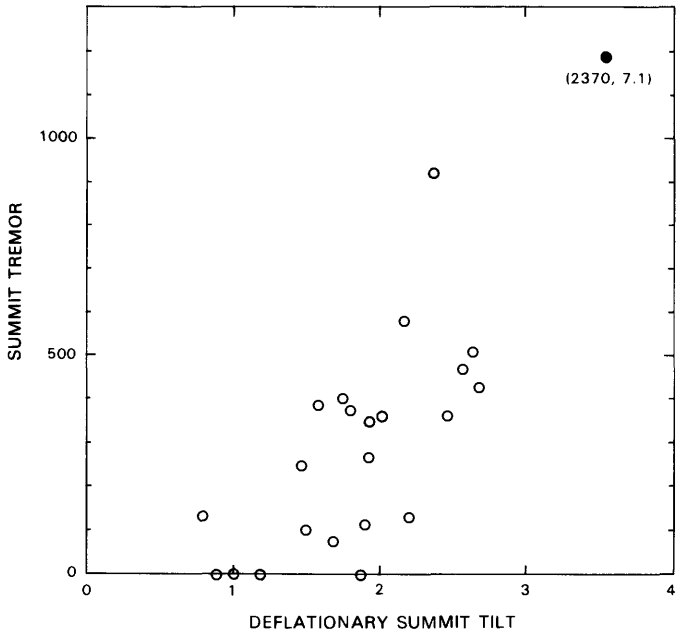

FIGURE 7.30.—Harmonic tremor versus deflationary tilt at summit after each eruptive episode (1-23) in east rift zone from January 1983 to July 1984. Dot denotes data point for exceptionally vigorous first episode, scaled down by half to accommodate rest of plot (actual values, 2,370 and 7.1).

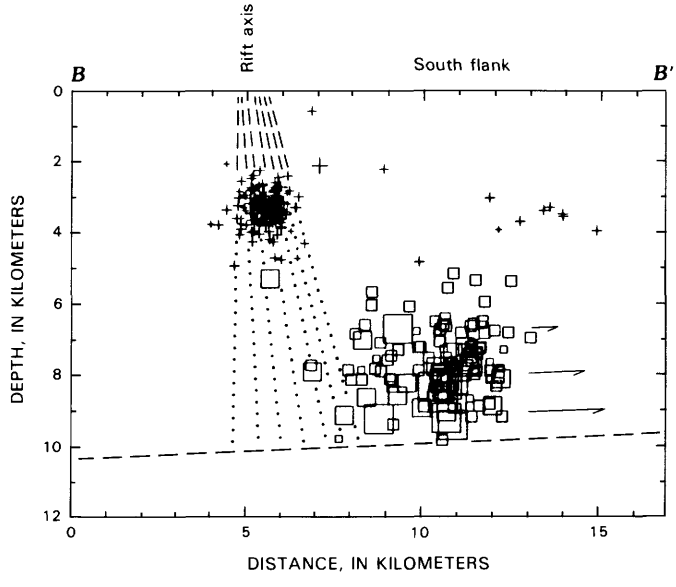

FIGURE 7.31.—Characterization of east-rift dike complex in and above 2- to 4-km-deep zone of rift earthquakes and in ductile zone below, laterally constrained by distribution of 5- to 10-km-deep south-flank earthquakes. Line *B-B'* (see figs. 7.7, 7.8) is normal to rift axis. Vertical dashed lines outline shallow region in and above earthquake swarms that actively deforms during magma intrusions; dotted region below outlines relatively passive zone of low rigidity. Entire complex is about 4 km wide at base at about 10-km depth and tapers to about 1 km wide when projected to surface above retaining zone marked by earthquake swarms at 2- to 4-km depth. Subhorizontal dashed line denotes principal slip zone dipping toward center of the island, and arrows indicate direction of relative movement of south flank. See figure 7.6 for explanation of symbols.

tions of Kilauea Volcano, Hawaii: Journal of Volcanology and Geothermal Research, v. 25, p. 249–258.

Dvorak, J.J., Okamura, A.T., English, T.T., Koyanagi, R.Y., Nakata, J.S., Sako, M.K., Tanigawa, W.T., and Yamashita, K.M., 1986, Mechanical response of the south flank of Kilauea Volcano, Hawaii, to intrusive events along the rift systems: Tectonophysics, v. 124, p. 193–209.

Dzurisin, Daniel, Koyanagi, R.Y., and English, T.T., 1984, Magma supply and storage at Kilauea Volcano, Hawaii, 1956–1983: Journal of Volcanology and Geothermal Research, v. 21, p. 177–206.

Eaton, J.P., 1962, Crustal structure and volcanism in Hawaii, *in* Macdonald, G.A., and Kuno, Hisashi, eds., The crust of the Pacific basin: American Geophysical Union Geophysical Monograph 6, p. 13–29.

Fehler, Michael, 1983, Observations of volcanic tremor at Mount St. Helens Volcano: Journal of Geophysical Research, v. 88, no. 4, p. 3476–3484.

Ferrick, M.G., Qamar, Anthony, and St. Lawrence, W.F., 1982, Source mechanism of volcanic tremor: Journal of Geophysical Research, v. 87, no. 10, p. 8675–8683.

Greenland, L.P., Rose, W.I., and Stokes, J.B., 1984, An estimate of gas emission and magmatic gas content from Kilauea Volcano: Geochimica et Cosmochimica Acta, v. 49, p. 125–129.

Hill, D.P., 1969, Crustal structure of the island of Hawaii from seismic-refraction measurements: Seismological Society of America Bulletin, v. 59, no. 1, p. 101–130.

Kieffer, S.W., 1984, Seismicity at Old Faithful Geyser: An isolated source of geothermal noise and possible analogue of volcanic seismicity: Journal of Volcanology and Geothermal Research, v. 22, p. 59–95.

Klein, F.W., 1978, Hypocenter location program HYPOINVERSE: U.S. Geological Survey Open-File Report 78–694, 113 p.

Klein, F.W., Koyanagi, R.Y., Nakata, J.S., and Tanigawa, W.R., 1987, The seismicity of Kilauea's magma system, chap. 43 of Decker, R.W., Wright, T.L., and Stauffer, P.H., eds., Volcanism in Hawaii: U.S. Geological Survey Professional Paper 1350, v. 2, p. 1019–1185.

Kinoshita, W.T., Koyanagi, R.Y., Wright, T.L., and Fiske, R.S., 1969, Kilauea volcano: The 1967–1968 summit eruption: Science, v. 166, no. 3904, p. 459–468.

Koyanagi, R.Y., 1982, Precedure for routine analyses and classification of seismic events at the Hawaiian Volcano Observatory, part 1: U.S. Geological Survey Open-File Report 82–1036, 18 p.

Koyanagi, R.Y., Chouet, Bernard, and Aki, Keiiti, 1987, Data from the Hawaiian Volcano Observatory 1969–1985, pt. 1 *of* Origin of volcanic tremor in Hawaii, chap. 45 *of* Decker, R.W., Wright, T.L., and Stauffer, P.H., eds., Volcanism in Hawaii: U.S. Geological Survey Professional Paper 1350, v. 2, p. 1221–1258.

Koyanagi, R.Y., Unger, J.D., Endo, E.T., and Okamura, A.T., 1974, Shallow earthquakes associated with inflation episodes at the summit of Kilauea Volcano, Hawaii, *in* Gonzáles Ferrán, O., ed., Symposium on Andean and Antarctic Volcanology Problems, Santiago, Chile, 1974, Proceedings: Naples, International Association of Volcanology and Chemistry of the Earth's Interior, p. 621–631.

Moore, R.B., Helz, R.T., Dzurisin, Daniel, Eaton, G.P., Koyanagi, R.Y., Lipman, P.W., Lockwood, J.P., and Puniwai, G.S., 1980, The eruption of Kilauea Volcano, Hawaii: Journal of Volcanology and Geothermal Research, v. 7, p. 189–210.

Nakata, J.S., Tanigawa, W.R., and Klein, F.W., 1982, Hawaiian Volcano Observatory summary 81, part 1, seismic data, January to December 1981: U.S. Geological Survey report, 77 p.

Nakata, J.S., Tomori, A.H., Koyanagi, R.Y., and Tanigawa, W.R., 1984, Hawaiian Volcano Observatory summary 83, seismic data, January to December 1983: U.S. Geological Survey report, 86 p.

Pollard, D.D., and Aki, Keiiti, 1981, A new source mechanism for volcanic tremor [abs.]: Eos (American Geophysical Union Transactions), v. 62, no. 17, p. 400.

Richter, C.F., 1958, Elementary seismology: San Francisco, W.H. Freeman and Co., 768 p.

Ryan, M.P., Koyanagi, R.Y., and Fiske, R.S., 1981, Modeling of the three-dimensional structure of macroscopic magma transport systems: Application to Kilauea Volcano, Hawaii: Journal of Geophysical Research, v. 86, no. B8, p. 7111–7129.

Shimozuru, Daisuke, Kamo, Kosuke, and Kinoshita, W.T., 1966, Volcanic tremor of Kilauea Volcano, Hawaii, during July–December, 1963: University of Tokyo, Earthquake Research Institute Bulletin, v. 44, no. 3, p. 1093–1133.

Swanson, D.A., Duffield, W.A., and Fiske, R.S., 1976, Displacement of the south flank of Kilauea Volcano: The result of forceful intrusion of magma into the rift zones: U.S. Geological Survey Professional Paper 963, 39 p.

Swanson, D.A., Duffield, W.A., Jackson, D.B., and Peterson, D.W., 1979, Chronological narrative of the 1969–71 Mauna Ulu eruption of Kilauea Volcano, Hawaii: U.S. Geological Survey Professional Paper 1056, 55 p.

Tanigawa, W.R., Nakata, J.S., and Tomori, A.H., 1983, Hawaiian Volcano Observatory summary 82, seismic data, January to December 1982: U.S. Geological Survey report, 91 p.

Wolfe, E.W., Garcia, M.O., Jackson, D.B., Koyanagi, R.Y., Neal, C.A., and Okamura, A.T., 1987, The Puu Oo eruption of Kilauea Volcano, episodes 1–20, January 3, 1983, to June 8, 1984, chap. 17 *of* Decker, R.W., Wright, T.L., and Stauffer, P.H., eds., Volcanism in Hawaii: U.S. Geological Survey Professional Paper 1350, v. 1, p. 471–508.

Wright, T.L., 1984, Origin of Hawaiian tholeiite: A metasomatic model: Journal of Geophysical Research, v. 89, no. B5, p. 3233–3252.

Zucca, J.J., and Hill, D.P., 1980, Crustal structure of the southeast flank of Kilauea Volcano, Hawaii, from seismic refraction measurements: Seismological Society of America Bulletin, v. 70, no. 4, p. 1149–1159.

8. GEOELECTRIC OBSERVATIONS (INCLUDING THE SEPTEMBER 1982 SUMMIT ERUPTION)

By DALLAS B. JACKSON

CONTENTS

ABSTRACT

Self-potential (SP), controlled-source electromagnetic (CSEM), and very low frequency (VLF) electromagnetic data were used to study the September 25, 1982, summit eruption and the first year of the Puu Oo east-rift-zone (ERZ) eruption. Four intrusions into the middle and upper ERZ closely preceded the onset of the January 1983 eruption. The first intrusion, on September 25, 1982, accompanied the summit eruption; it was detected in the ERZ by earthquake-epicenter locations along most of its length, but near its distal end (7 km from the summit) only by an SP monitor. The second, a slow intrusion into the upper ERZ, lasted from the first week of October through mid-November 1982; it was detected by SP changes across the ERZ 7 km from the summit, and by CSEM resistivity changes measured in the summit area. The third and fourth intrusions, on December 9–10, 1982, and January 2, 1983, immediately preceded the onset of the Puu Oo eruption on January 3; they were not detected by any geoelectric monitors. This failure to detect the December and January intrusions is interpreted to mean that little or no fracture continuity existed from the zone of magma transport to the shallow depths measurable by the SP system, and that magma transport was deeper (greater than 2 km) in the near-summit area than was detectable by the CSEM system. The near-coincidence of the January eruptive fissure at the future site of Puu Oo with a major (879 mV) preeruption SP anomaly suggests that fracture continuity to a heat source at depth existed before the eruption. SP increases along a monitoring line near Kalalua, 2 km downrift of the most northeasterly erupting fissure, between December 18, 1982, and January 3, 1983 (15 days), suggest that downrift intrusion had proceeded at least as far as Kalalua by January 3. A small (68 mV), transient SP increase along an electric-field line at Kalalua on January 5 may have been a precursor to an intrusion near the electric-field array about a day later.

INTRODUCTION

At 0031 H.s.t. January 3, 1983, an eruption on Kilauea's east rift zone (ERZ) began in Napau Crater; within 5 days it had propagated along a line of fissures that stretched downrift nearly 8 km to within 0.5 km of Kalalua (fig. 8.1). The 1983 eruption events appeared to be primed by upper- and middle-ERZ intrusions that were detected geophysically (that is, geoelectrically, seismically, and geodetically) during and after the September 25, 1982, summit eruption. This chapter discusses qualitative interpretations of self-potential (SP), controlled-source electromagnetic (CSEM), and very low frequency (VLF) electromagnetic measurements made between September 1982 and the end of the first year of the 1983 middle-ERZ eruption.

SELF-POTENTIAL MEASUREMENTS

APPLICATION TO VOLCANIC STUDIES

SP measurements were begun on Kilauea in 1972 by Zablocki (1980), who observed that all large positive SP anomalies on Kilauea are related to subsurface localizations of heat and that after an intrusion or eruption, SP-anomaly amplitudes decay slowly while maintaining their characteristic wavelengths. Zablocki attributed this slow SP decrease over time to cooling of an emplaced heat source (for example, a dike). L.A. Anderson (in Dzurisin and others, 1980) concluded from repeated profile measurements across the Escape Road on the upper ERZ that "* * * significant SP increases were recorded near recently active fissures after the June 1976, July 1976, and February 1977 intrusive events and after the September 1977 eruption." These transient SP anomalies, generally about 1 week long, were interpreted to be related to magma moving beneath Escape Road at depths of 1 to 5 km, on the basis of earthquake-hypocenter locations. These SP changes observed by Anderson were evidently related to magma movement beneath the measured profiles; however, because of the short anomaly wavelengths (never more than several hundred meters), the magma itself at depths greater than a few

hundred meters probably could not have contributed directly to the SP changes. Although the exact cause of the transient SP excursions observed in the Kilauea geoelectric studies is unknown, the short-term excursions may be related to short-lived magmatic surges and ensuing adjustments in the conduit system.

GEOLOGIC SP SOURCES

Mechanisms for the generation of large SP anomalies (as much as several hundred millivolts) are probably related to either electrokinetic (streaming potential) or thermoelectric effects. Electrokinetic potentials are generated by fluid flow through a porous medium in response to differential pressures, such as those caused by convection in a geothermal cell, or by steam and, possibly, magma flow in fractures. Thermoelectric potentials are generated by temperature gradients across a section of rock, such as might exist at the boundary between an intrusion and the adjacent wallrock. The ultimate source that drives these mechanisms is subsurface heat, a quantity in plentiful supply at Kilauea. Either thermoelectric or electrokinetic mechanisms can generate the types of positive, monopolar SP anomalies typically associated with intrusions and eruptive fissures at Kilauea. A general discussion of thermoelectric and electrokinetic processes in relation to geothermal areas was presented by Corwin and Hoover (1979), a detailed discussion of thermoelectric SP anomalies produced by dikelike bodies by Fitterman (1983), and a detailed discussion of electrokinetic SP anomalies in relation to dikelike bodies by Sill (1984). General discussions of SP effects and anomaly shapes on the Island of Hawaii were presented by Zablocki (1976, 1978b) and Jackson and Sako (1982).

PROCEDURE AND EQUIPMENT

Two types of SP measurements are made on Kilauea—profiling and monitoring. Profiling measurements are made by advancing a measuring electrode to successive positions along a traverse and reading the electrical potentials relative to a stationary reference electrode. SP-monitoring arrays use electrodes permanently sited along a traverse, and electrical potentials are measured relative to a permanently sited reference electrode.

The equipment used for SP measurements is simple and requires only a high-impedance millivoltmeter (so that reliable readings can be made where contact resistance to earth ground may be as high as 100–200 kΩ) and nonpolarizing electrodes. Two types of nonpolarizing electrodes are used—either copper-copper sulfate for profiling or lead-lead chloride for monitoring. The copper-copper sulfate electrodes consist of a copper strip immersed in supersaturated copper-sulfate solution in a porous ceramic cup. This type of electrode is rugged, but because it must be refilled with solution periodically, it is unsatisfactory for monitoring studies. Lead-lead chloride electrodes consist of a lead strip in a solid plaster matrix made by mixing plaster of paris with a supersaturated solution of lead chloride. Although lead-lead chloride electrodes are too soft to use for robust profiling unless the plaster matrix is protected with a ceramic cup, they are ideal for monitoring studies because they do not need to be recharged with a solution.

When measuring profiles, it is desirable to space the reference electrode positions as far apart as practical to keep cumulative errors to a minimum. Measurements are made at smaller intervals between reference electrodes. For example, measurements are commonly made at 100-m intervals, but reference electrode positions are established only every 1.5 km. In the field, first a reference-electrode position is established, and then a second electrode is moved to each measurement site. Readings are made by placing the electrode on the ground and rotating it to make contact with the soil-moisture layer that is generally present a few millimeters beneath the surface. If a reading is not repeatable to within 1 or 2 mV, or is unstable, then contact resistance is probably very high, and readings are discontinued at that site. Errors related to profiling were discussed by Jackson and Kauahikaua (1987), who found that the largest closure errors that have appeared in SP mapping on Kilauea are less than 10 mV/km.

SP-monitoring arrays, where the electrodes are permanently sited, are read by using the same equipment as for profiling. Measurement errors for fixed arrays are related to electrode drift (long term) as the electrodes age and, possibly, to electrode deterioration (see subsection below entitled "SP Changes on the ESR Array Associated with the January 3, 1983, Eruption"). Electrode drift is relatively unimportant for lead-lead chloride electrodes—only about 1 mV/mo (Petiau and Dupis, 1980).

SP PROFILES AND MONITORING ARRAYS ON KILAUEA

Numerous SP profiles have been established on Kilauea and Mauna Loa, where electrode positions are carefully marked for reoccupation. Only two of these profiles (fig. 8.1), near Puu Kamoamoa (KAM) and Kalalua (KAL) on the middle ERZ, are discussed in this chapter. Profile KAM is 3.5 km long and crosses the ERZ under what is now the edifice of Puu Oo. Profile KAL is 1 km long and crosses the ERZ approximately 1.5 km downrift of the most northeasterly eruptive vents (not shown) of the Puu Oo eruption.

Only one fixed-array monitor is in operation on Kilauea—on the Escape Road profile (ESR) in the ERZ (fig. 8.1). The ESR array consists of five lead-lead chloride, nonpolarizing electrodes sited along profile ESR (fig. 8.2); voltages relative to a sixth electrode are read at irregular time intervals. Four of these electrodes (68, 69, 73, and 79, respectively, in fig. 8.2) are located adjacent to fissures that erupted in 1968, 1969, 1973, and 1979. The reference electrode (REF) is located in a relatively stable geoelectric zone; the nearest historical eruptive fissures are 0.5 km to the northwest and southeast. This array has shown changes related to both intrusions and eruptions (Dzurisin and others, 1980; D.B. Jackson, unpub. data, 1979).

ELECTROMAGNETIC MEASUREMENTS

APPLICATION TO VOLCANIC STUDIES

A CSEM monitoring experiment has been run at Kilauea since 1979. The phase and amplitude of the electromagnetic field generated by a transmitter loop is monitored in the summit region and upper ERZ on receiver loops (fig. 8.1). Thus far, all the significant CSEM changes observed at Kilauea (more than a few percent amplitude or a few degrees phase change) have been correlated with intrusions and are interpreted to represent shallow dike emplacement near the receiver loops (Jackson and others, 1985).

VLF tilt-angle measurements, which are sensitive to shallow conductivity contrasts in the Earth, have been used at Kilauea since 1970 to map in detail melt-filled lava tubes, to delineate the boundaries of buried lava lakes (Anderson and others, 1971; Jackson and Zablocki, 1981), and to study the relations between SP and VLF anomalies over low-resistivity tabular bodies, such as high-angle dikes and lava lakes (Zablocki, 1978a). On Kilauea, a low-resistivity zone associated with a cooling dike can be identified to about 100-m depth because of its contrast with the more resistant country rock (Zablocki, 1978a).

PROCEDURE AND EQUIPMENT

Both CSEM and VLF methods use controlled electromagnetic sources (as opposed to natural electromagnetic fields); the CSEM system operates in the frequency range 0.1–10 Hz, whereas the VLF system operates in the frequency range near 20 kHz. The depth to which a buried low-resistivity body may be identified is primarily a function of the frequency used and of the resistivity of the Earth surrounding the body. As the frequency of the elec-

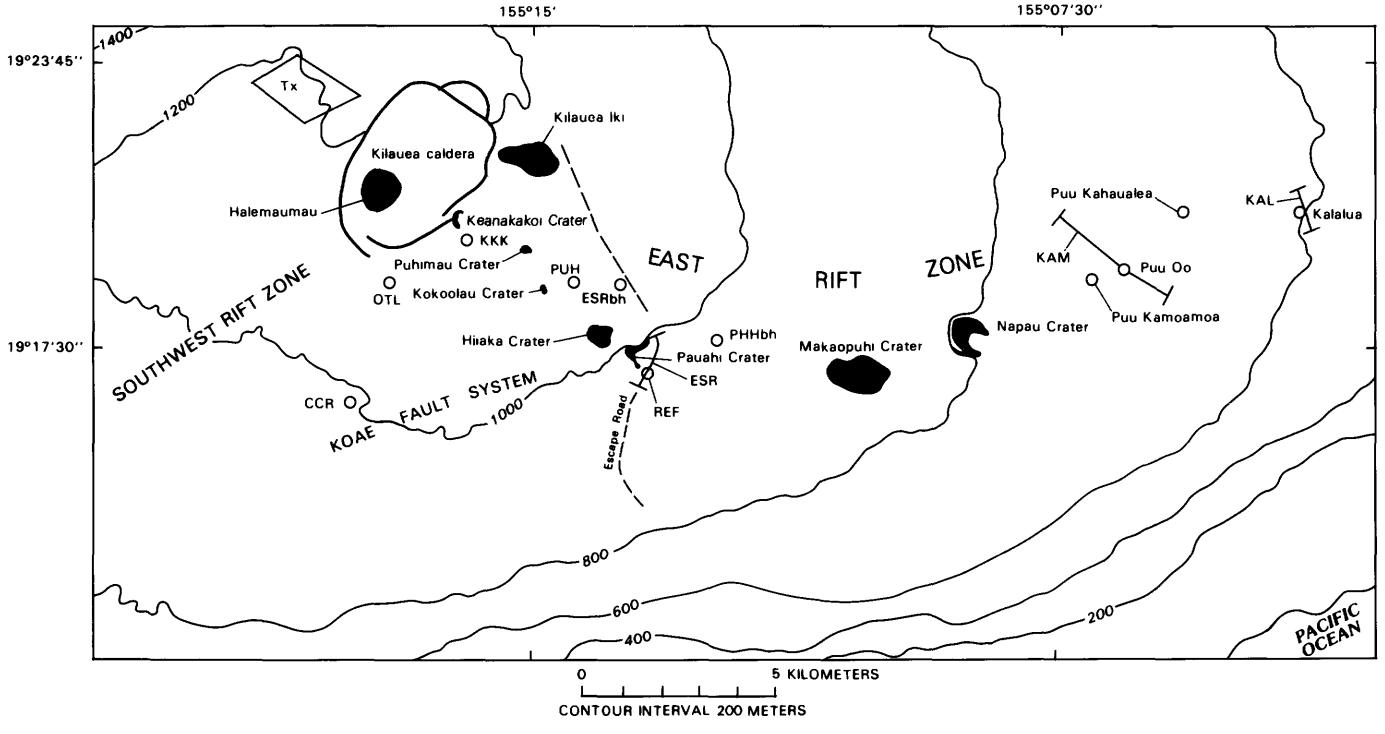

FIGURE 8.1.—Summit and east rift zone of Kilauea, southeastern Island of Hawaii, showing locations of geoelectric monitors and topographic contours. ESR, SP array on Escape Road; REF, reference electrode. SP profiles: KAL, Kalalua; KAM, Puu Kamoamoa. Tx, CSEM transmitter loop. CSEM receiver loops: CCR, Cone Crater; KKK, Keanakakoi Crater; OTL, Outlet vault; PUH, Puhimau Crater. ESRbh and PHHbh, borehole tiltmeters.

tromagnetic field decreases and (or) the resistivity of the Earth increases, the depth of investigation increases. The VLF system is shallow looking, investigating depths of tens of meters, whereas the CSEM system is deep looking, investigating depths of several kilometers.

The CSEM monitoring system at Kilauea uses an extremely low frequency (ELF) loop-loop system[1] to measure the amplitude and phase of a transmitted vertical electromagnetic field (Jackson and others, 1985) generated by a large (1.5 km on a side) horizontal, quasi-square-wire loop located about 1 km northwest of Kilauea caldera (fig. 8.1). Five frequencies from 0.4 to 8 Hz are transmitted sequentially, using the transmitter loop (Tx, fig. 8.1). Phases and normalized amplitudes relative to this transmitter are recorded at the receiver coils (for a detailed discussion of CSEM instrumentation, see Cooke and others, 1983).

Although several parameters can be measured with the VLF technique, only the inclination (tilt angle) of the electromagnetic field radiated by a 24.8-kHz military-radio transmitter at Seattle, Wash., is discussed in this chapter. Tilt-angle anomalies associated with steeply dipping, low-resistivity tabular bodies are easily recognized by the antisymmetric deflections produced on either side of the body and by their smooth, nearly straight line gradients through the zero point (zero crossover) from the positive and negative peaks (see inset, fig. 8.10).

Numerous VLF profiles exist on Kilauea because it is common practice to make tilt-angle readings so as to iden-

[1]Horizontal coils of wire form both the transmitter and receiver loops.

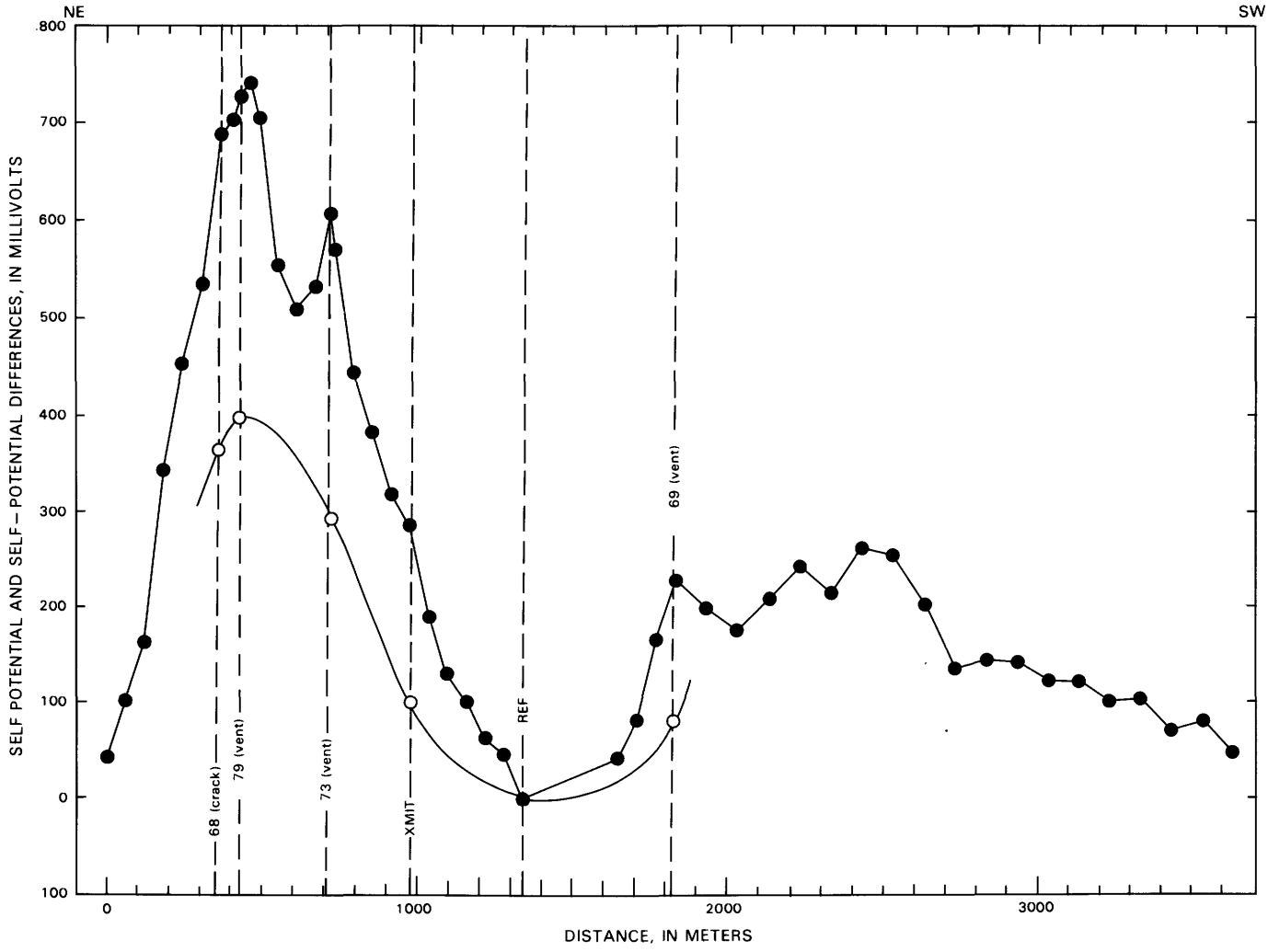

FIGURE 8.2.—Typical self-potential (SP) profile (dots) along Escape Road, showing locations of electrodes (69, REF, XMIT, 73, 79, 68) in ESR array. Open circles show SP differences (increases) between 0935 H.s.t. September 22 and 2225 H.s.t. September 25, 1982. See figure 8.1 for location of profile.

tify shallow conductors when SP profiles are first read. Only the Puu Kamoamoa line was read after the start of the Puu Oo eruption.

GEOELECTRIC CHANGES IN THE SUMMIT REGION AND UPPER ERZ

SP CHANGES ON THE ESR ARRAY ASSOCIATED WITH THE SEPTEMBER 25, 1982, ERUPTION

The last SP measurements made on the ESR array (fig. 8.1) before the September 25, 1982, eruption were at 0930 H.s.t. September 22. No unusual SP changes were measured before the eruption; array readings are made only about once every 3 days, and so short-term precursors would be recognized only by chance. The eruption began in the southern summit area at 1845 H.s.t., and the ESR array, more than 7 km downrift from the eruption site, was read at 2221 H.s.t. and again at 2228 H.s.t. that evening; both data sets were essentially identical. SP changes of 82, 102, 294, 399, and 361 mV were noted on electrodes 69, XMIT, 73, 79, and 68, respectively; the SP increases are plotted in figure 8.2 beneath a typical SP profile at the ESR. The following morning, the array was read at 1130 H.s.t., 5.5 hours after the summit eruption had stopped; all potentials were once again within 2 mV of their values 2 days before the eruption.

SP CHANGES ON THE ESR ARRAY ASSOCIATED WITH THE JANUARY 3, 1983, ERUPTION

In early October 1982, SP increases began to be noticeable on electrodes 68, 73, and 79 (fig. 8.3). Except for a brief but sharp SP decrease in late October, this trend continued until about November 3, when a rapid SP decrease was recorded on these electrodes, as well as at electrode XMIT. This rapid SP decrease lasted until November 10, after which more a gradual decrease continued until early January 1983. These increasing SP's in early October coincided closely with slow, nearly aseismic ground displacements in the vicinity of Kokoolau Crater to Escape Road that began on October 6 and continued into early November (see chap. 6, fig. 6.7*A*).

Between the beginning of the eruption on January 3 until mid-March, just before episode 3 that began on March 28, SP changes on the ESR array were near zero (fig. 8.3). Although all voltages on the ESR array began to increase on about March 13, just before episode 3, the increase was most noticeable at electrode 65. The SP peaked during episode 3 and then began to slowly decline.

After July 1983, no SP changes occurred that were obviously related to the eruption, and those changes that did occur may have been related to electrode deterioration. In mid-August, a 40-mV offset occurred between two measurements on electrode 73. An SP profile run along the array line several days later, in comparison with another in February 1983, showed no offset at electrode 73; thus, this rapid SP shift was presumably caused by electrode deterioration as the electrode aged. Beginning in late November 1983, similar SP changes also occurred on electrodes XMIT, 68, and 79; therefore, even though the array data are presented to the end of the year, they are highly suspect after mid-August. In January 1984, all the electrodes were replaced (they were 3 years old); and as of the time of this writing (June 1985), no similar offsets have been observed in the array data.

CSEM MONITORING CHANGES, SEPTEMBER 1982 TO MID-JULY 1983

On September 27, 36 hours after the September 25 eruption ended, CSEM monitoring data at two frequencies (1.0 and 4.0 Hz) were being collected at the OTL, KKK, and PUH receiver loops in the south caldera and upper ERZ. Previously, the equipment had been under repair. Although no baseline data were available before the September eruption, conspicuous CSEM amplitude changes occurred at these monitoring stations at 1.0 and 4.0 Hz (fig. 8.4); station CCR was not in operation at that time. Amplitude changes continued between early October and mid-November, at least in the southern summit area near stations OTL and KKK (the only stations at which data were collected in October).

In November, the CCR monitor coil in the southwest rift zone (fig. 8.1) was added to the CSEM array, and smoothly varying amplitude changes over several data points were recorded at 1.0 and 4.0 Hz on the CCR coil into early December. Although the data are noisy, CSEM-amplitude changes on the other monitor coils seem to track those from the CCR coil. It is unclear what these changes may represent.

A large (109 μrad) summit deflation that began on January 2, 1983, 1 day before the eruption, caused no significant CSEM changes at any of the monitoring stations.

Two notable CSEM changes are evident in the data set between early May and mid-July 1984. The first excursion in early May, between episodes 3 and 4, appeared most strongly as amplitude and phase changes at stations KKK and PUH (fig. 8.4). Station OTL also showed some change, though less pronounced than those at stations PUH and KKK. There are insufficient data at station CCR to define any changes. The second excursion, before and during episode 5, occurred in late June and early July, when both CSEM amplitude and phase changes were recorded at all four monitoring stations.

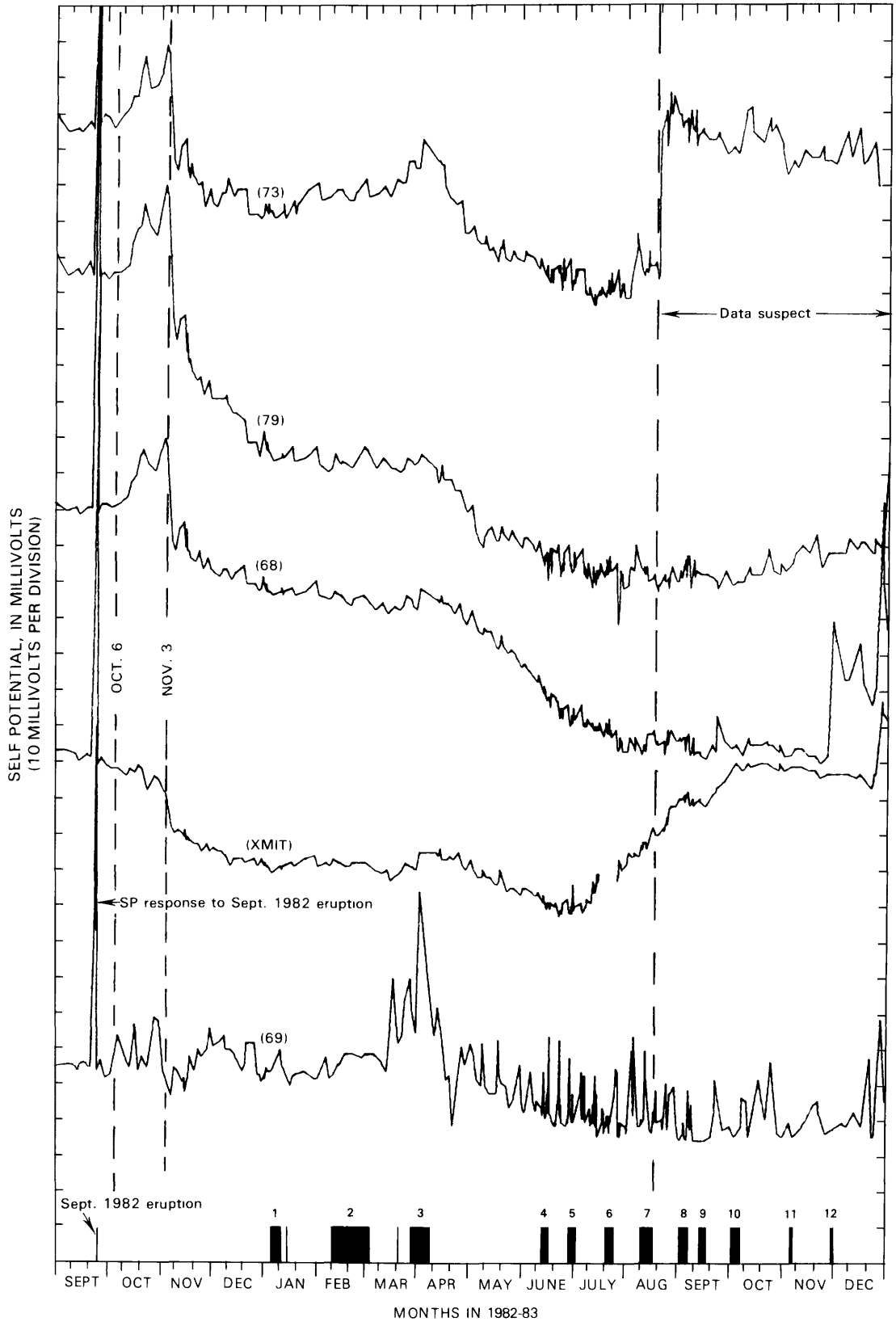

FIGURE 8.3.—Data at five measuring electrodes (69, XMIT, 73, 79, 68) of ESR array from September 15, 1982, to January 1, 1984. Numbered bars, eruptive events. Dashed vertical lines (October 6 and November 3) show beginning and end of SP excursion correlated with tiltmeter changes near Escape Road (see fig. 6.7A).

GEOELECTRICAL CHANGES NEAR THE 1983 ERUPTION SITES

Two SP profiles in the middle ERZ, one near Kalalua and another near Puu Kamoamoa (fig. 8.1), were reoccupied after the January 1983 eruption. Each profile had been measured previously and had electrode positions marked for reoccupation.

KALALUA SP PROFILE

An SP profile was established near Kalalua (fig. 8.1) in January 1979. The southeast end of this profile crosses a 1977 eruptive fissure, and the northwest end passes just a few tens of meters downrift of a 1963 eruptive fissure. The approximate trend of the 1963 fissure as projected across the profile, and the location of the 1977 fissure on the profile, are shown in figure 8.5. The profile had been

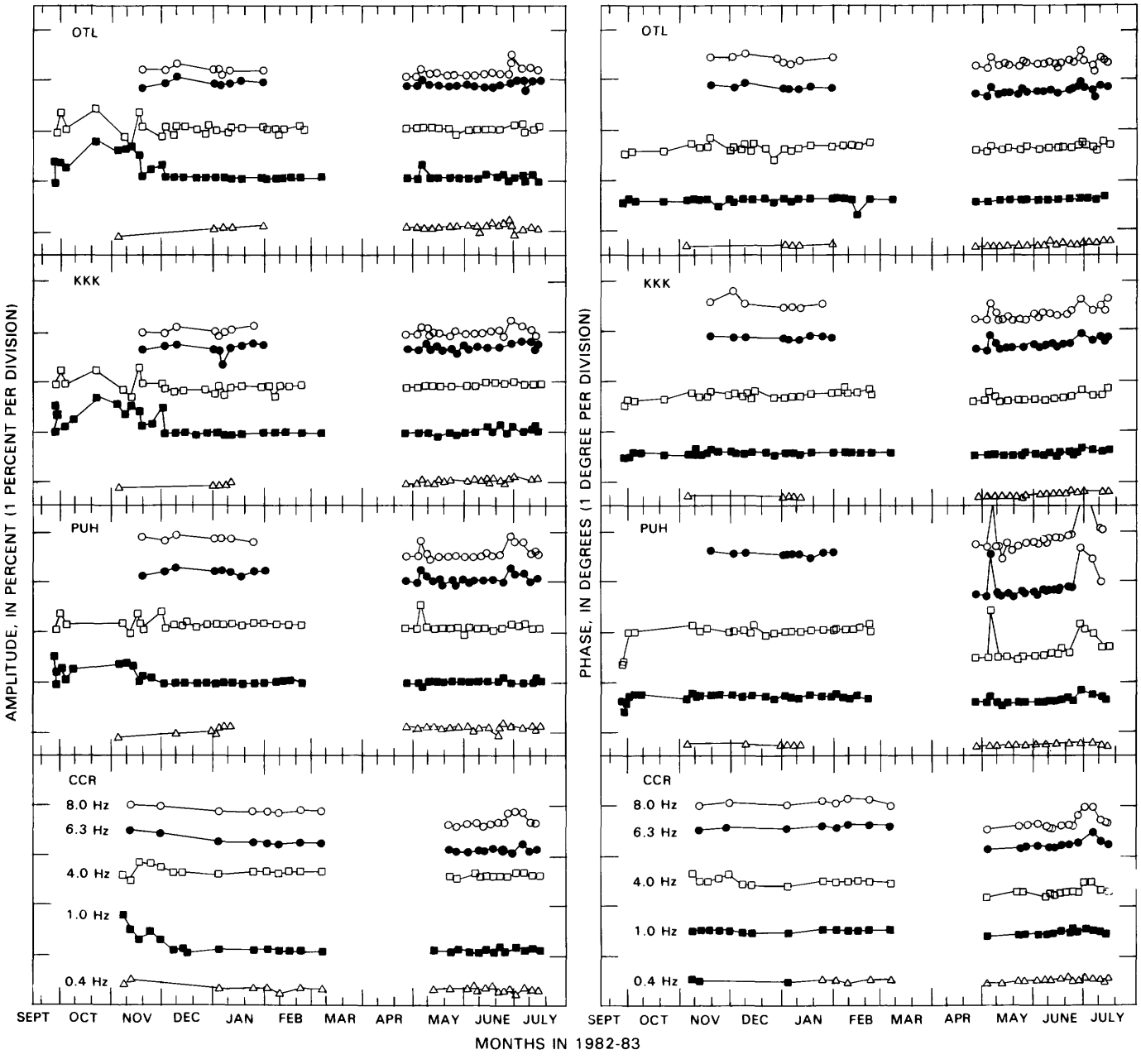

FIGURE 8.4.—CSEM data, showing amplitude and phase, at five frequencies, for monitors at Outlet vault (OTL), Keanakakoi Crater (KKK), Puhimau Crater (PUH), and Cone Crater (CCR) (see fig. 8.1 for locations). CCR monitor was inoperative in September and October 1982. Gaps in records are periods of no data. Numbers (0.4-8.0 Hz) labeled for CCR apply to all graphs.

measured five times before the January 3, 1983, eruption. Although some positive SP changes were measured near the 1977 vents on this profile during known periods of middle-ERZ intrusion, changes over the long term had been mostly negative, presumably reflecting cooling of the 1963 and 1977 intrusions.

On January 3, 1983, 13 hours after the eruption began and when eruptive fissures had migrated downrift to within 3 km of the SP line, the profile was remeasured. A December 18 profile (the last occupation of the profile before the January eruption) and the January 3 profile, and their differences, are shown in figure 8.5. Between December 18, 1982 and January 3, 1983, SP increases of 12 and 24 mV were measured at data points southeast of the 1963 vent and at the 1977 vent, respectively.

In an attempt to record subsequent SP changes on the Kalalua profile, a three-electrode array was installed on January 5, with the reference electrode near the center of the profile and the recording electrodes near the 1963 and 1977 vents (see fig. 8.8 for electrode locations). Although the recorders were not operable until 2 days later, readings on the two SP lines were made by using a high-impedance electrometer, with an input filtered to reject radio frequencies, for about 4 hours on January 5. At 1510 H.s.t. January 5, a positive SP excursion began on the electrode near the 1977 vent and peaked at 1543 H.s.t. after increasing by 68 mV (fig. 8.6). By 1600 H.s.t., the SP had returned to its base level and then began to increase again (measurements were stopped because of helicopter scheduling). A mirror image of the 68-mV ex-

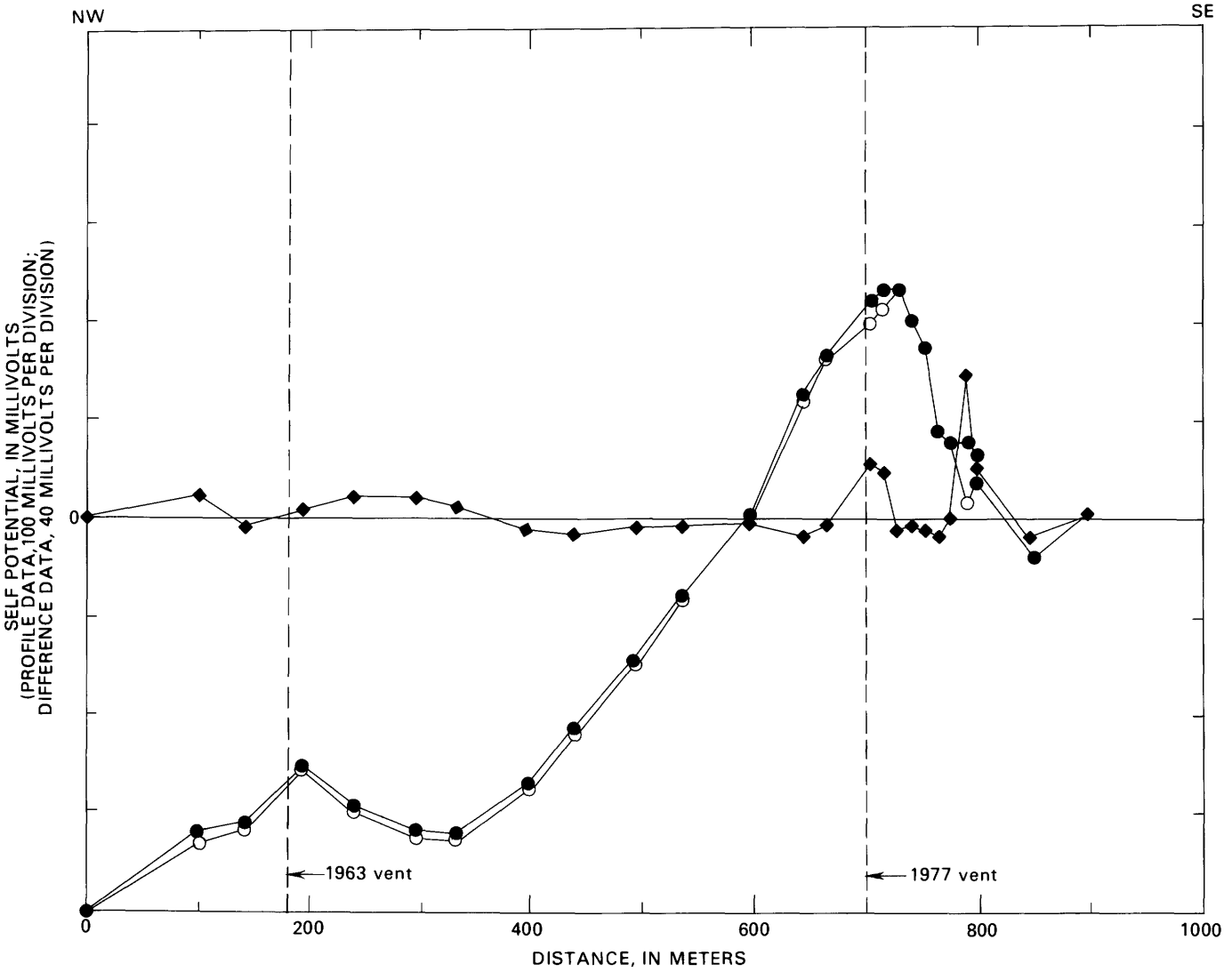

FIGURE 8.5.—SP data along Kalalua profile for December 18, 1982 (circles), and January 3, 1983 (dots), and differences between data (diamonds) for January 1983 minus December 1982. Dashed vertical lines show projected positions of 1963 and 1977 eruptive fissures. See figure 8.1 for location of profile.

cursion, though smaller in amplitude (approx 12 mV) and negative going (a potential change in the negative sense), is visible on the trace of the 1963 vent electrode.

At 1700 H.s.t. January 7, analog SP recording from the 1963 and 1977 electrode arrays was begun, and nearly equal, positive SP changes of about 80 mV on the 1963 and 1977 vent electrodes were detected (fig. 8.7). By January 16, potentials at the 1963 and 1977 vent electrodes appear to have decayed to a stable level.

Between January 5 and 7, a large (70 mV) SP increase was detected at 140 m on the Kalalua profile (fig. 8.8) that may have been coincident with the SP changes on the 1963 and 1977 vent electrodes discussed above. This large SP increase was essentially restricted to one data point on the profile at 140 m, as was a 44-mV SP decrease measured on a profile on January 10 (data not shown), and caused no changes at the 1963 vent electrode, only 100 m distant.

PUU KAMOAMOA SP PROFILE

The Puu Kamoamoa area was a locus of intrusions from November 1978 through 1980, as indicated by tilt changes and numerous earthquake swarms (Dzurisin and others, 1984). A leveling line that crossed what was to become the January 3 eruptive fissure, about ½ km northeast of Puu Kamoamoa, was occupied three times between March 1979 and December 1980. During that period, it showed approximately 82 mm of uplift across the zone in which the January 3 vents formed (Hawaiian Volcano Observatory, unpub. data, 1980).

In November 1980, a 3.5-km-long SP line was run across the middle ERZ (fig. 8.1), close to the Kamoamoa leveling line. Two modest SP highs were identified (fig. 8.9) that can be matched to an 1840 fissure covered by 1969 lava and to a mapped fissure (Moore and Koyanagi, 1969, pl. 1), also buried by 1969 lava, where steam was being emitted. By far the largest SP anomaly on the profile, positive 879 mV relative to the reference electrode, occurred over an area at 2,300 m on the profile that showed no surface cracking or steaming but was within approximately 100 m of what would become part of the January 3, 1983, fissure system and the location of Puu Oo. On January 28 (25 days after the eruption began), as much of the SP line as could be relocated was reoccupied (fig. 8.9). The January 3 fissure opened about 100 m northwest of the location of the previous SP high, and the peak SP amplitude was 73 mV greater than the previous high 100 m away; however, because it was shifted northwestward from the previous peak, it was actually 200 mV more positive than the SP measured at that point in 1980 (fig. 8.9).

Complex SP changes also were measured in the vicinity of the 1840 fissure, where three positive peaks formed (fig. 8.9).

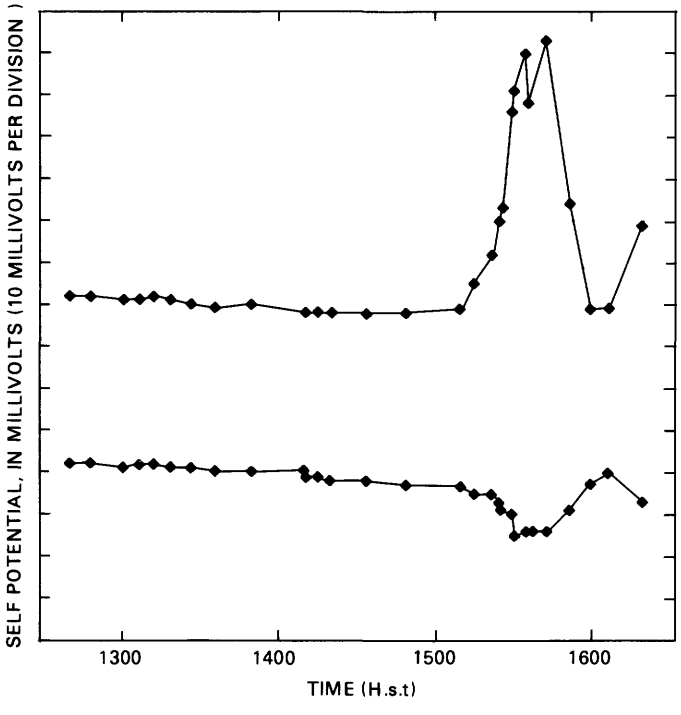

FIGURE 8.6.—Transient 68-mV SP anomaly recorded at 1977 vent (upper curve) and 1963 vent (lower curve) along Kalalua profile at about 1543 H.s.t. January 5.

PUU KAMOAMOA VLF PROFILE

Before the January 1983 eruption, two VLF tilt-angle anomalies were apparent on the Puu Kamoamoa VLF pro-

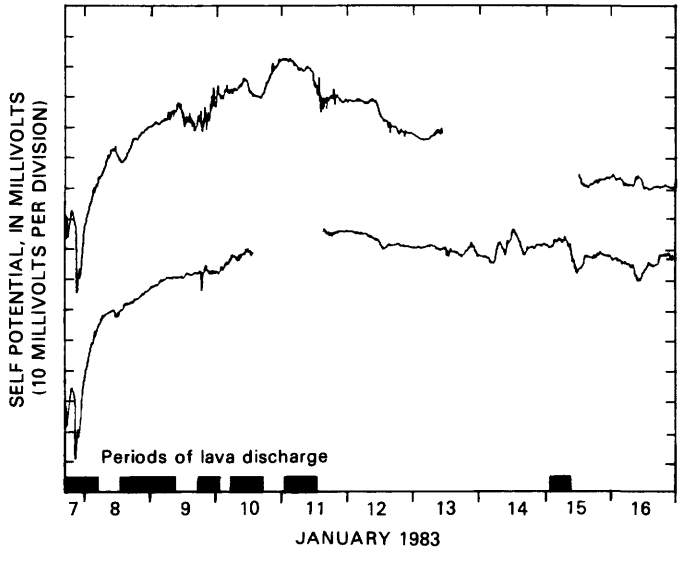

FIGURE 8.7.—SP data recorded at 1977 vent (upper curve) and 1963 vent (lower curve) along Kalalua profile between 1700 H.s.t. January 7 and 2400 H.s.t. January 16. Gaps in records are periods of no data.

file (fig. 8.10). One anomaly was associated with the buried 1840 fissure, and the other with the zone of steaming ground between 1.9 to 2.0 km from the northwest end of the profile; however, no tilt-angle anomaly was associated with the preeruption SP maximum. After the January 3 eruption, a high-amplitude VLF tilt-angle anomaly developed over the January 3 eruptive fissure (fig. 8.11) where copious steam was being emitted, and the amplitude of the SP anomaly coincident with the zone of steaming ground also increased. The signature of the preexisting tilt-angle anomaly over the steaming ground also became more complex from interaction with the new high-amplitude tilt-angle anomaly over the eruptive fissure. However, no VLF tilt-angle anomalies accompanied the positive SP changes in the vicinity of the 1840 fissure.

DISCUSSION

The SP, CSEM, and VLF electromagnetic measurements before and during the first year of the 1983 eruption can be used to infer some interesting structural relations when combined with complementary seismic and deformation data. Furthermore, viewed in hindsight, they illustrate several instances of phenomena that were apparently precursory to intrusive or eruptive events.

The very large SP increases at the ESR array associated with the September 25 summit eruption (figs. 8.2, 8.3) were 7 km from the erupting fissures and at least 1.2 km downrift from the nearest located earthquake at Hiiaka. The migration of earthquakes downrift from the summit during the eruption was related to intrusion. The SP changes that were noted at Escape Road 3 hours and 40 minutes after the eruption onset indicate that a pressure increase, probably related to intrusion, within the magma conduits must have propagated at least as far downrift as Escape Road and suggest that the summit magma plexus was in fluid continuity with the upper ERZ. This pressure increase within the conduit system may have been relieved by intrusion uprift of Escape Road because the SP anomaly had decayed to preeruption levels when the SP arrays were read at 1130 H.s.t. September 26 (5.5 hours after the eruption stopped). The concept of an open fluid core to the upper ERZ in continuity with the summit is not new; it was proposed earlier by Swanson and others (1976).

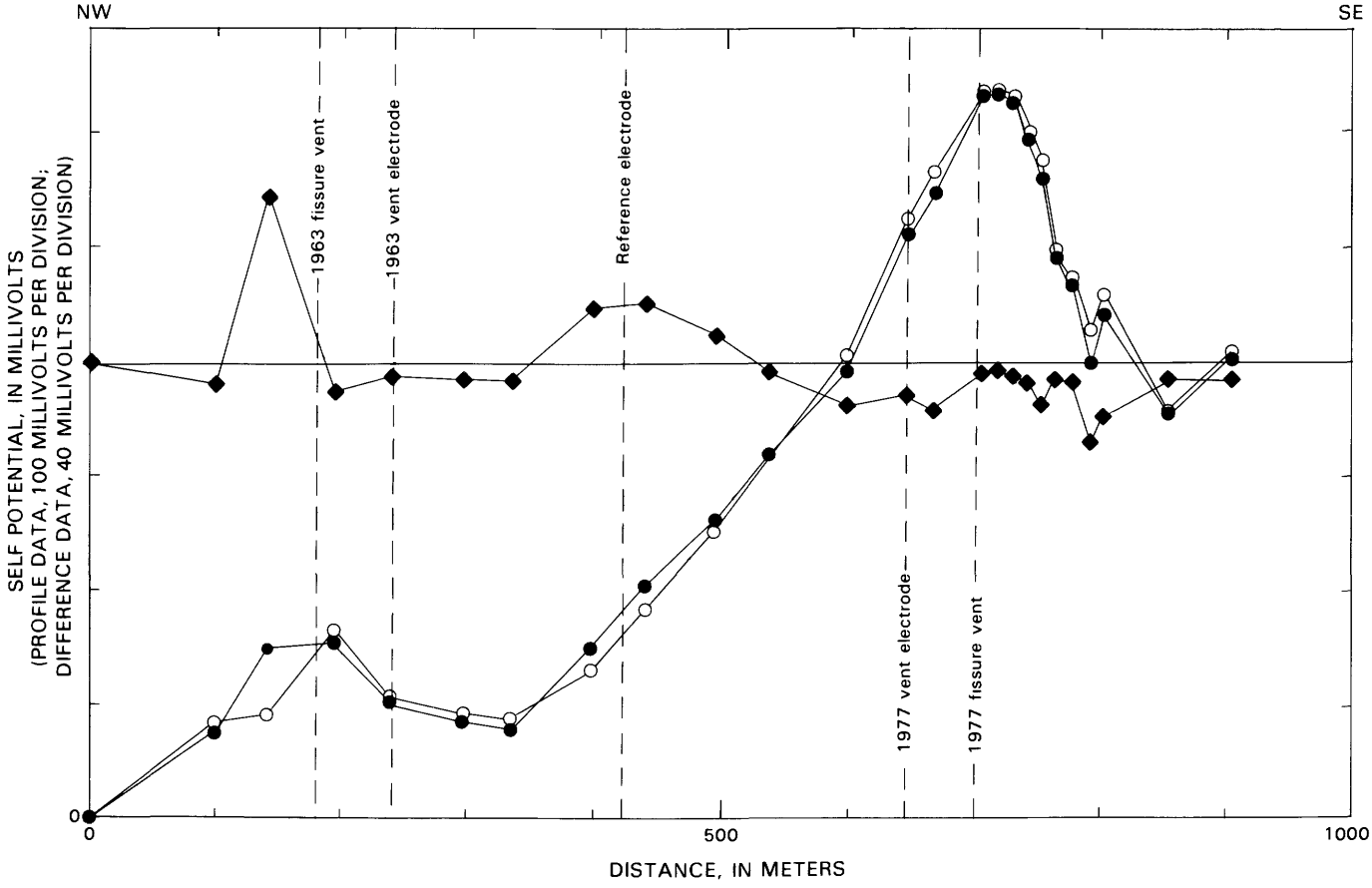

FIGURE 8.8.—SP data recorded along Kalalua profile on January 5 (circles) and January 7 (dots), 1983, before and after a small graben-forming event (near center of profile) that occurred late on January 6, 1983. Diamonds, differences between data for January 7 minus January 5. See figure 8.1 for location of profile.

The spatial form of the transient SP changes (fig. 8.2) mimics the shape of the static SP anomalies on Escape Road so closely that it appears that no new shallow intrusions were emplaced but rather that the SP sources were temporarily strengthened. A pressure increase in the volcanic plumbing system, with very little magma movement, might generate electrokinetic changes (possibly from increased evolution of steam) that could cause the observed changes. For rapid SP variations as these, temporary enhancement of preexisting SP sources is a likely mechanism. Pressure changes accompanied by very little magma movement in the vicinity of Escape Road are also compatible with four other observations relevant to this event. (1) By 1130 H.s.t. on September 26, 5.5 hours after the eruption ceased, no residual SP anomaly remained that was not already present before the eruption began. Unless magma was immediately removed from possible intrusions, the SP increases should have persisted. (2) No earthquakes (which commonly accompany intrusions) were located as far downrift as Escape Road; the nearest earthquakes were located about 1.2 km uprift, near Hiiaka Crater. (3) Failure of the ESR tiltmeter to respond to any event other than the summit inflation that immediately preceded the eruption (see chap. 6) is evidence that little, if any, new space could have opened to accommodate intrusion in the vicinity of Escape Road during the summit eruption. (4) The striking similarity between the preexisting SP anomalies at Escape Road and the transient anomalies produced during the eruption suggests temporary enhancement of preexisting SP sources without any major changes in the source geometries.

On or about October 3, 1982 (1–2 weeks after the September eruption), SP's began to increase on three of the ESR array electrodes (68, 79, 73, fig. 8.3). Simultaneously, seismicity increased near Puhimau (see chap. 7), and tiltmeters ESRbh and PHHbh abruptly began to register upper-ERZ deformation located approximately between Pauahi and Puhimau Craters (see chap. 6). The close correlation in time between the SP increase on ESR array electrode 79 (the largest change at Escape Road) and the tilt rates measured at tiltmeters ESRbh and PHHbh is shown in figure 8.12. The SP increases measured at Escape Road suggest that the intrusion uprift, inferred

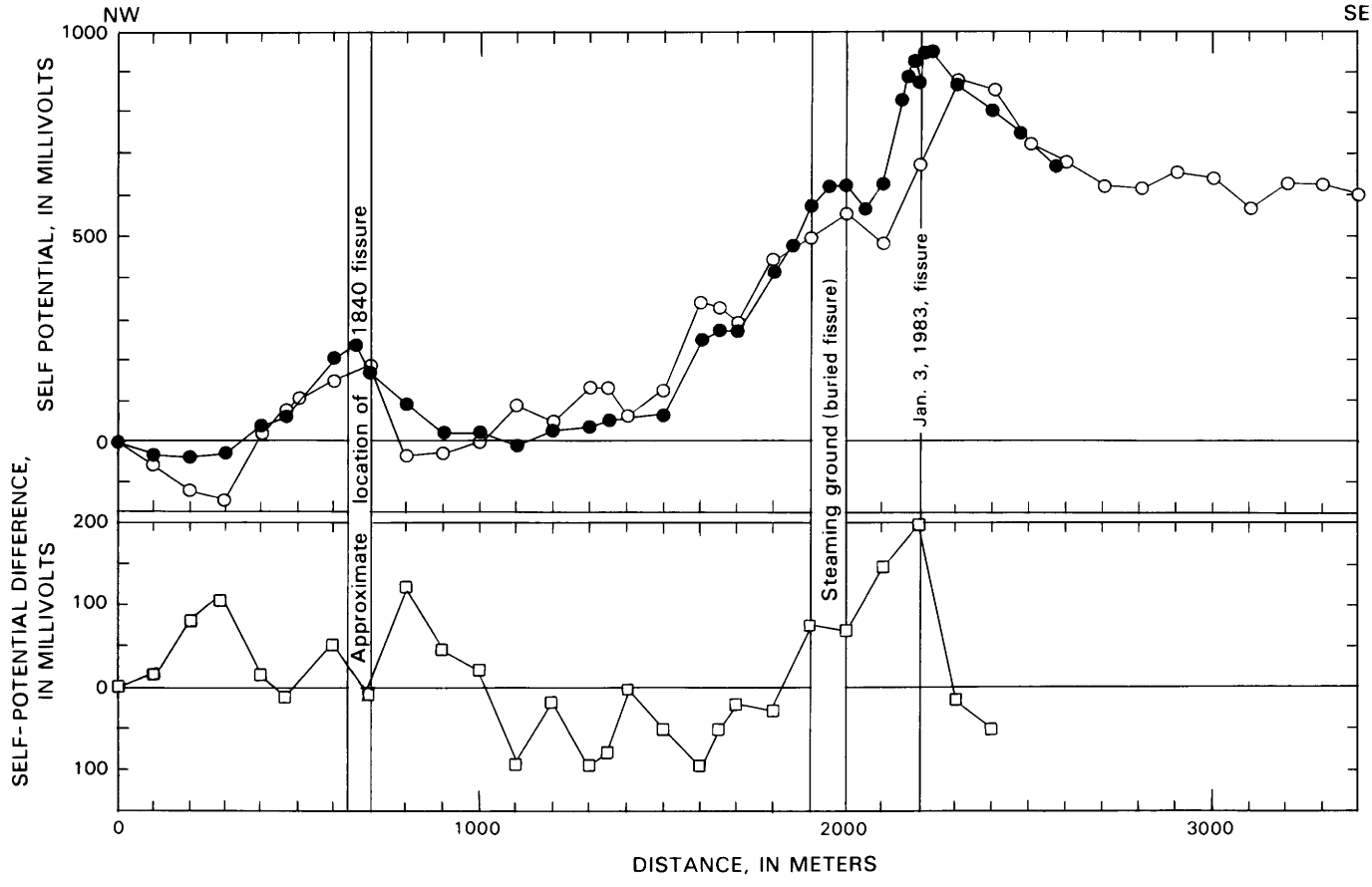

FIGURE 8.9.—SP data along Puu Kamoamoa profile for April 11, 1980 (circles), and January 28, 1983 (dots). Diamonds, differences between data for January 1983 minus April 1980. January 28 profile, at and southeast of January 3, 1983, eruptive fissure, was on 1983 lava. See figure 8.1 for location of profile.

from the seismic and deformation data, was supplying magma elsewhere farther downrift. During the first and second weeks of November, the tilt rates measured at tiltmeters ESRbh and PHHbh approached zero, and the SP's at Escape Road began an abrupt decline (fig. 8.3) that lasted until about January 1, 1983. This decline suggests that the slow intrusion (or transport) of magma beneath the array probably stopped during the first week of November. In late October, earthquakes near Puhimau decreased, and some earthquakes began to be recorded near Napau. During the first week of November (simultaneously with the SP decrease at Escape Road), the earthquakes near Napau peaked and then declined abruptly (see chap. 7)—behavior implying that the magma which had been moving beneath the ESR intruded to near Napau and then stopped.

Accompanying the upper-ERZ deformation in October and early November, amplitude changes by as much as 9 percent at the CSEM monitoring coils (fig. 8.4) suggest that magma was also being transported at shallow depths in the summit region near the OTL and KKK monitor coils, as well as at Puhimau (PUH).

Although there were no accompanying earthquake swarms and no obvious correlation with the ongoing ERZ eruption, the CSEM data for May and July 1983 suggest that an intrusion took place in both the summit region and upper parts of the rift zones. These were the last significant SP changes at the ESR array monitor or on the CSEM monitors that can be correlated with events either preceding or during the first year of the January 1983 eruption.

The absence of CSEM response to the 109-μrad summit deflation that began on January 2, 1984, is probably related to a deep conductive zone at approximately 2 km depth or deeper in the summit region and upper ERZ, identified in an electromagnetic sounding survey of these areas (Kauahikaua and others, 1986). Scale-model studies (D.B. Jackson and J.P. Kauahikaua, unpub. data, 1983) suggest that this conductive zone acts as a screening layer which masks the effects of conductivity changes at the monitors if these changes occur below the top of the conductive horizon. Accordingly, the depth of magma transport to the middle-ERZ eruption site that began on January 2, 1983, was apparently greater than 2 km at

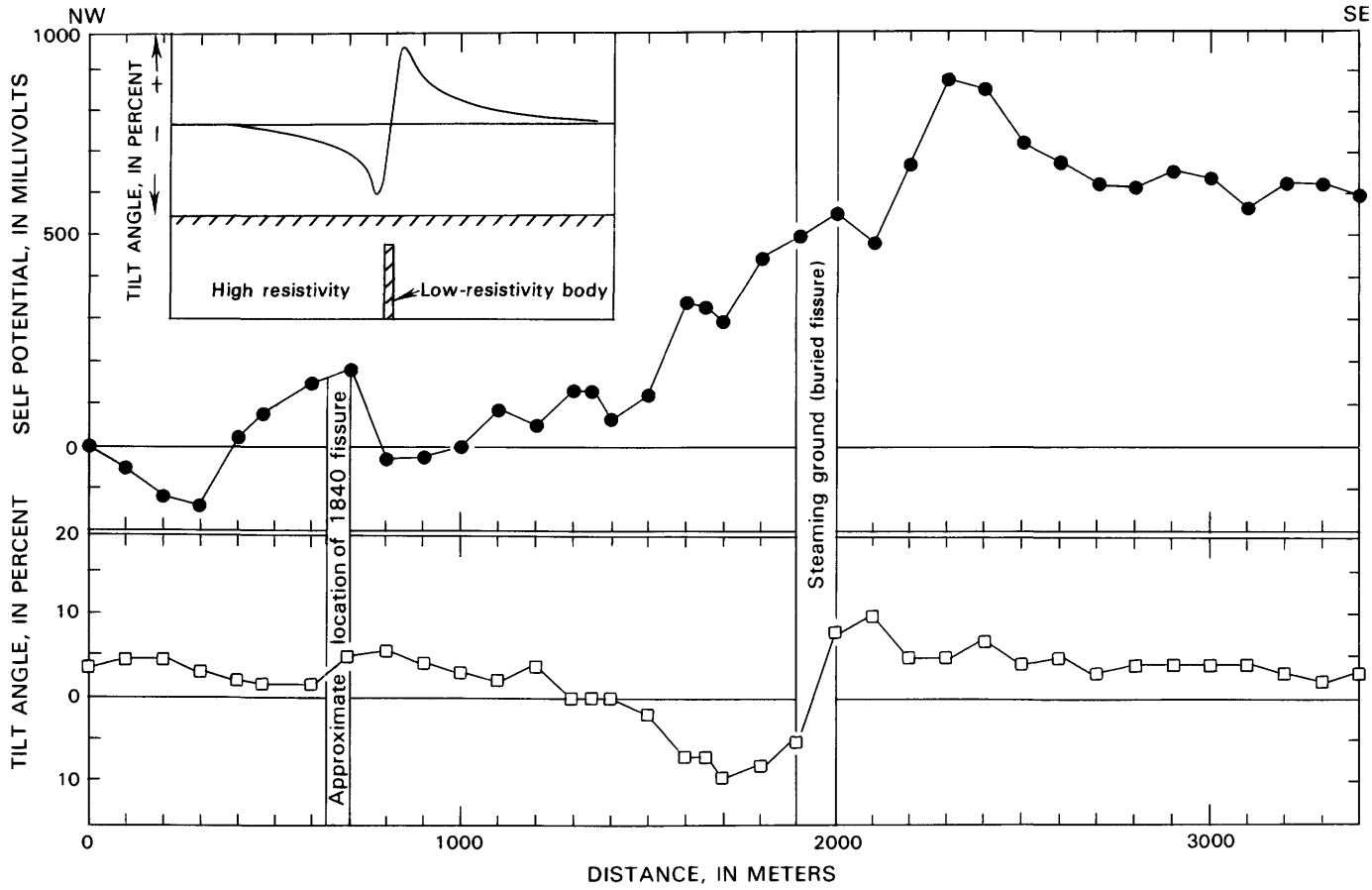

FIGURE 8.10.—SP data (dots) and VLF tilt-angle data (squares) recorded along Puu Kamoamoa profile on December 11, 1980. See figure 8.1 for location of profile. Inset shows typical VLF tilt-angle response over a vertical, two-dimensional, low-resistivity body (hachured) in a high-resistivity half-space at shallow depth.

least as far as the position of the CSEM monitor just downrift of Puhimau Crater, and occupied a conduit that was relatively unrestricted at least as far as Mauna Ulu, where the first seismic swarm began on January 2.

As with the CSEM monitor, no identifiable SP event on the ESR array could be correlated with the onset of the 109-μrad summit deflation and the beginning of ERZ intrusion on January 2, 1983. I interpret this absence of correlation to mean that magma transport was through conduits deeper than 2 km (deeper than the slow intrusion of October-November 1982) beneath the PUH monitor coil and without continuity to the surface at the ESR array. This may have been the same conduit system that fed an intrusion near Pauahi Crater on December 9–10, 1982 (see chap. 7), which also was not detected on the ESR array or the CSEM monitors because it was apparently too deep.

SP changes between December 18, 1982, and January 3, 1983 (the start of the eruption, with eruptive fissures as far downrift as Puu Kahaualea), on the Kalalua profile (fig. 8.5) suggest that a magma-filled conduit extended as far as the Kalalua area during the early hours of the eruptive activity farther uprift.[2] The SP increases may actually have been related to intrusion or, at least, to the magmatic-pressure changes, inferred from borehole-tiltmeter data (see chap. 6), that occurred before the eruption began on January 3. A borehole tiltmeter located

[2]No earthquakes were located near Kalalua at this time, although tremor levels were high and would have masked small events.

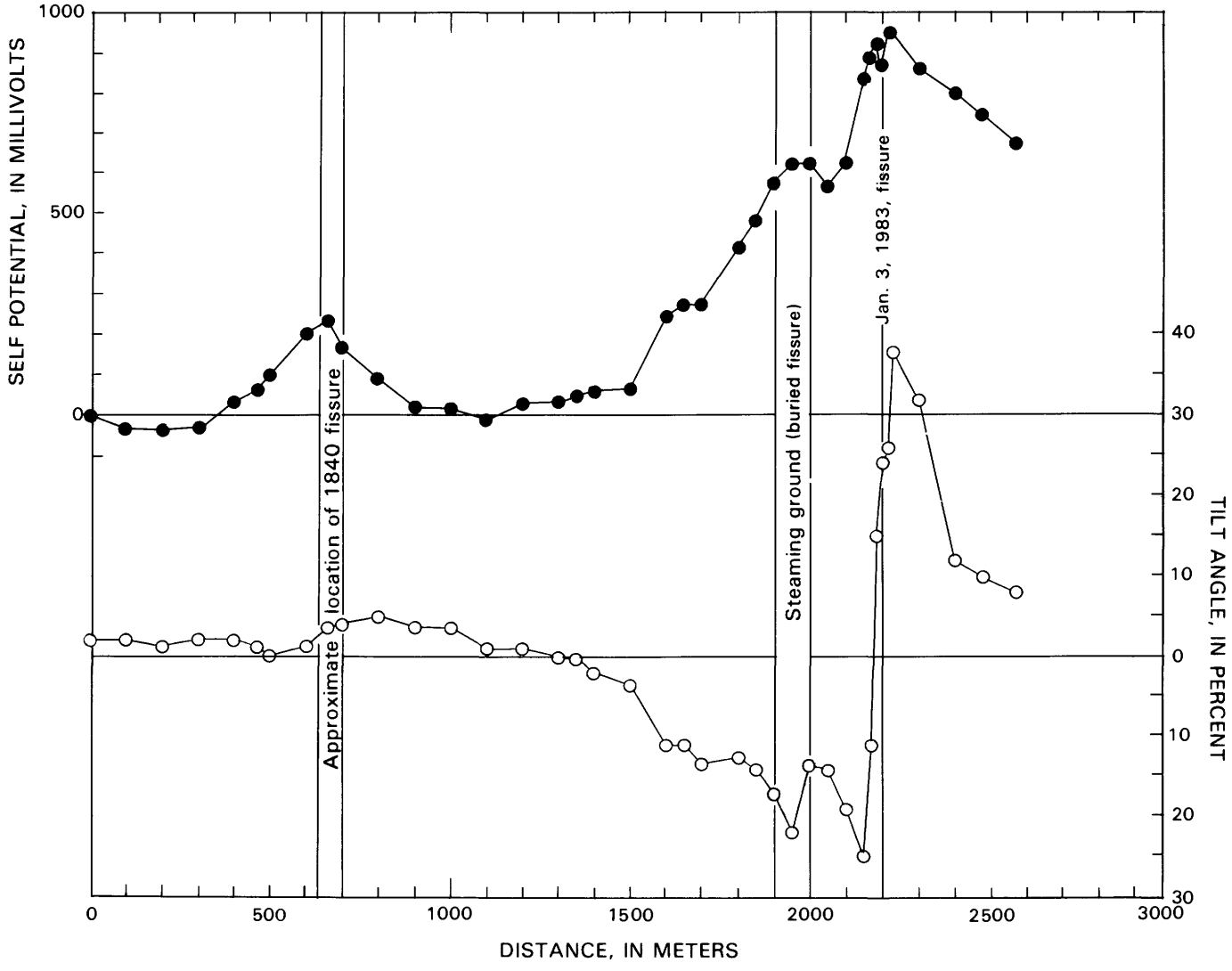

FIGURE 8.11.—SP data (dots) and VLF title-angle data (circles) along Puu Kamoamoa profile on January 28, 1983. See figure 8.1 for location of profile.

about 400 m uprift of the SP profile registered tilting, down to the south, of about 22 μrad at 0840 H.s.t. January 2. At about 1500 H.s.t. January 5, an SP excursion (positive 68 mV) was noted at the 1977 vent electrode (fig. 8.7) located between the center of the Kalalua profile and the 1977 fissure (fig. 8.8). A mirror image of this excursion that appeared at the 1963 vent electrode suggests that the source for this event was close enough to the reference electrode to affect it also (a positive potential that affects the reference will subtract from the potential at a measuring electrode). The excursion lasted about an hour and preceded an episode of ground cracking and formation of a shallow graben that apparently reflected emplacement of a dike during the night of January 6–7.

At about 1900 H.s.t. January 6, a borehole tiltmeter 400 m uprift of the Kalalua SP profile went off scale. Daylight on January 7 showed that a shallow graben had formed near the tiltmeter, and new ground cracks extended northeastward, passing within a few meters of the reference electrode for the KAL array. A horizontal-distance measurement indicated that 2.6 m of extension had occurred perpendicular to the strike of the graben and cracks (see chap. 6, fig. 6.13) between January 5 and 7. Apparently, these events recorded shallow intrusion of magma to form a dike north of Kalalua during the night of January 6–7, and eruption from this new feeder dike began a short distance uprift at 1030 H.s.t. January 7 (see chap. 1). SP differences for data obtained between January 5 and 7 (fig. 8.8) on the Kalalua profile show an SP high (approx 250 m wide) related to the January 6 intrusion (graben) that is nearly centered on the reference electrode. Because the SP source was nearly beneath the array reference electrode, what seem to be nearly equal, positive-80-mV SP changes on the 1963 and 1977 electrodes (fig. 8.7) are actually due to a decay of the SP high generated near the reference electrode between January 5 and 7; that is, an SP decrease at the reference electrode appears as an SP increase at the measuring electrodes. The small amount of ground cracking near the reference electrode, in comparison with distinct graben formation only 400 m uprift, may indicate that the dike did not quite reach the SP array. If so, then the rapidly decaying SP anomaly may simply have been caused by a short-lived emission of steam downrift, along the small fractures propagating from the dike tip.

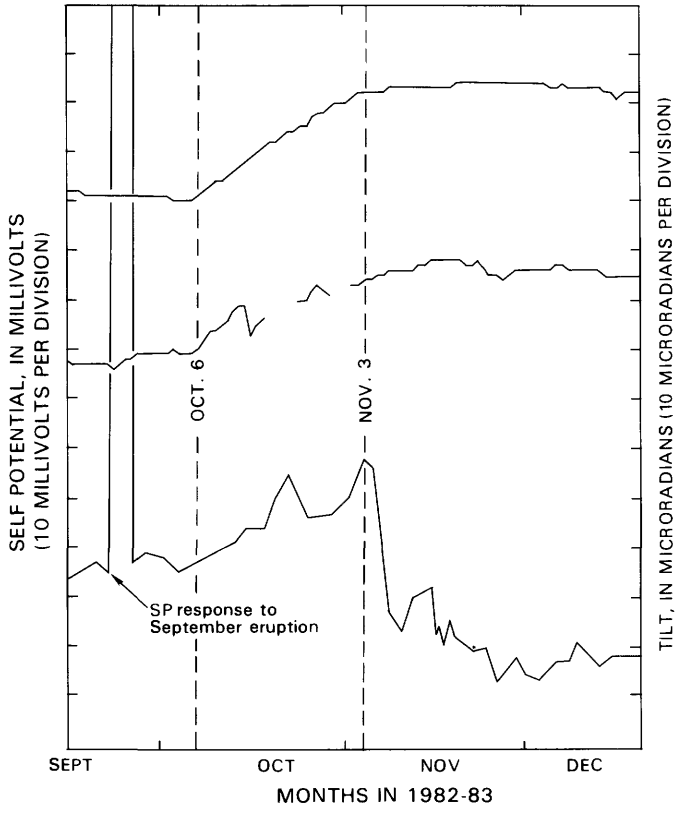

FIGURE 8.12.—East-west components of borehole tiltmeters ESRbh (middle curve) and PHHbh (upper curve) records, and SP data (lower curve) recorded at electrode 79 on ESR array, during a gradual tilt change in vicinity of Puhimau to Hiiaka Craters from approximately October 6 to November 3, 1982. Gaps in records are periods of no data.

SP's remeasured on January 28 on a profile (fig. 8.9) about 700 m northeast of Puu Kamoamoa (very close to what later became Puu Oo) showed that the January 3, 1983, fissure opened within 100 m of a major (879 mV) preexisting SP anomaly that did not coincide with any known structural feature. The relatively small SP increase near the SP profile maximum (200 mV), and the close coincidence of the existing SP anomaly with the location of the January 3, fissure, suggest that the eruptive fissure at Kamoamoa probably opened within a fracture zone which had continuity with a heat source within the ERZ before the eruption. A similar relation exists between a large preexisting SP high and ground fracturing on the first day of the 1984 northeast-rift-zone eruption of Mauna Loa (Lockwood and others, 1985). Areas of shallow conductivity along the SP profile, probably related to hot water (condensed steam) in fractures, are clearly marked by changes in shallow-looking (to approx 100-m depth) VLF tilt-angle measurements at the 1840 fissure, the steamin' ; ground (fig. 8.10), and the January 3 fissure (fig. 8.11). N) VLF tilt-angle anomaly was associated with the preeru.ptive 879-mV SP high (fig. 8.10) near the January 3 fissure. Presumably, any preeruptive conductive zone related to the SP source must have been deeper than 100 m.

CONCLUSIONS

The January 1983 eruption was preceded by an intrusion into the upper ERZ during the September 25

eruption, a slow, nearly aseismic intrusion in October-November, and a third intrusion again in December. The October-November and December intrusions apparently set the stage for the January eruption by emplacing magma downright of Escape Road. The site of vent opening, near Kamoamoa at least, was already defined by a high-amplitude SP anomaly. The rapid decay of the SP anomaly at ESR during the September eruption, the nearly aseismic October-November intrusion, and the two SP events at Kalalua several days before a dike was emplaced there on January 6–7 all suggest that the conduit down the ERZ was open before the onset of the eruption in January 1983. After the eruption began, the conduit system was continuous to about 0.5 km beyond Kalalua. The absence of CSEM or SP changes that correlate definitively with any eruptive episodes during 1983 suggests that the path of magma transport was at least 2 km deep in the upper ERZ (CSEM data) and, probably, within a conduit system that had little, if any, continuity to the surface beneath Escape Road (SP data).

REFERENCES CITED

Anderson, L.A., Jackson, D.B., and Frischknecht, F.C., 1971, Kilauea: Detection of shallow magma bodies using VLF and ULF induction methods [abs.]: Eos (American Geophysical Union Transactions), v. 52, no. 4, p. 383.

Cooke, James, Bradley, Jerry, Mitchell, Charles, and Lescelius, Rodger, 1983, A description of an extremely low-frequency loop-loop geophysical system: U.S. Geological Survey Open-File Report 81-1130, 63 p.

Corwin, R.F., and Hoover, D.B., 1979, The self-potential method in geothermal exploration: Geophysics, v. 44, no. 2, p. 226–245.

Dzurisin, Daniel, Anderson, L.A., Eaton, G.P., Koyanagi, R.Y., Lipman, P.W., Lockwood, J.P., Okamura, R.T., Puniwai, G.S., Sako, M.K., and Yamashita, K.M., 1980, Geophysical observations of Kilauea Volcano, Hawaii, 2. Constraints on the magma supply during November 1975–September 1977: Journal of Volcanology and Geothermal Research, v. 7, no. 3-4, p. 241-269.

Dzurisin, Daniel, Koyanagi, R.Y., and English, T.T., 1984, Magma supply and storage at Kilauea Volcano, Hawaii, 1956–1983: Journal of Volcanology and Geothermal Research, v. 21, no. 3-4, p. 177-206.

Fitterman, D.V., 1983, Modeling of self-potential anomalies near vertical dikes: Geophysics, v. 48, no. 2, p. 171–180.

Jackson, D.B., Kauahikaua, J.P., and Zablocki, C.J., 1985, Resistivity monitoring of an active volcano using the controlled-source electromagnetic technique: Kilauea, Hawaii: Journal of Geophysical Research, v. 90, no. B14, p. 12545–12555.

Jackson, D.B., and Sako, M.K., 1982, Self-potential surveys related to probable geothermal anomalies, Hualalai volcano, Hawaii: U.S. Geological Survey Open-File Report 82-127, 10 p.

Jackson, D.B., and Zablocki, C.J., 1981, Interpretation of D.C. resistivity, VLF, and total magnetic field intensity measurements on Kilauea Iki lava lake, 1979–1980: U.S. Geological Survey Open-File Report 81-256, 12 p.

Kauahikaua, J.P., Jackson, D.B., and Zablocki, C.J., 1986, Resistivity structure to a depth of 5 km beneath Kilauea volcano, Hawaii, from large-loop-source electromagnetic measurements (0.04–8 Hz): Journal of Geophysical Research, v. 91, no. B8, p. 8267–8283.

Lockwood, J.P., Banks, N.G., English, T.T., Greenland, L.P., Jackson, D.B., Johnson, D.J., Koyanagi, R.Y., Rhodes, J.M., and Sato, Motoaki, 1985, The 1984 eruption of Mauna Loa volcano, Hawaii: American Geophysical Union Transactions, v. 66, no. 16, p. 169–171.

Moore, J.G., and Koyanagi, R.Y., 1969, The October 1963 eruption of Kilauea Volcano, Hawaii: U.S. Geological Survey Professional Paper 614-C, p. C1–C13.

Petiau, G., and Dupis, André, 1980, Noise, temperature coefficient, and long time stability of electrodes for telluric observations: Geophysical Prospecting, v. 28, no. 5, p. 792–804.

Sill, W.R., 1984, Self-potential effects due to hydrothermal convection-velocity cross coupling: Salt Lake City, University of Utah, Department of Geology and Geophysics report DOE/ID/12079-68, 15 p.

Swanson, D.A., Jackson, D.B., Koyanagi, R.Y., and Wright, T.L., 1976, The February 1969 east rift eruption of Kilauea Volcano, Hawaii: U.S. Geological Survey Professional Paper 891, 30 p.

Zablocki, C.J., 1976, Mapping thermal anomalies on an active volcano by the self-potential method, Kilauea, Hawaii: United Nations Symposium on the Development and Use of Geothermal Resources, 2d, San Francisco, 1975, Proceedings, v. 2, p. 1299–1309.

—— 1978a, Applications of VLF induction method for studying some volcanic processes of Kilauea volcano, Hawaii: Journal of Volcanology and Geothermal Research, v. 3, p. 155–195.

—— 1978b, Streaming potentials resulting from the descent of meteoric water—a possible source mechanism for Kilauean self-potential anomalies, *in* Geothermal energy: A novelty becomes a resource [abs.]: Geothermal Resources Council Transactions, v. 2, sec. 2, p. 747–748.